

The Design, Synthesis, and Pharmacological Evaluation of Bifunctional Mu-/Delta-Selective Opioid Receptor Ligands for the Treatment of Pain

by

Anthony F. Nastase

A dissertation submitted in partial fulfillment
of the requirements for the degree of
Doctor of Philosophy
(Medicinal Chemistry)
in the University of Michigan
2018

Doctoral Committee:

Professor Henry I. Mosberg, Chair
Assistant Professor Amanda L. Garner
Professor Scott D. Larsen
Associate Professor Peter J. H. Scott
Professor John. R. Traynor

Anthony F. Nastase

nastase@med.umich.edu

ORCID iD: 0000-0003-4520-2215

© Anthony F. Nastase 2018

Acknowledgements

First, I would like to thank my parents for recognizing and promoting the value of education. Their experience as a teacher and a nurse impacted my relationship with school in ways I could not fully appreciate as a child. However, their emphasis on curiosity and diligent study has persisted throughout my graduate work, having laid a solid foundation upon which I was able to build under the guidance of Drs. Henry Mosberg, Aubrie Harland, and Aaron Bender.

I would also like to thank Dr. Mosberg for being a magnificent mentor under whose guidance I have studied for the past five years. His even-keeled demeanor has been a stabilizing force when graduate school has seemed overwhelming. Additionally, I would like to thank Kate Kojiro whose tireless effort has kept the laboratory functioning throughout my time at Michigan. Furthermore, Kate provided crucial assistance in the development and attempted synthesis of a glucoserine peptidomimetic conjugate. I'd like to thank Sean and Deanna, fellow Mosberg lab members who have provided support synthetically, intellectually, and conversationally for past three years. Their presence in the lab has made an enormous impact on my grad school experience. Additionally, our collaborators John Traynor and Emily Jutkiewicz, along with Nick Griggs and Jessica Anand, have provided major contributions to the work presented in this dissertation. Without the work of Nick and Jess, the work done by the chemists of the Mosberg lab would be virtually meaningless. There is no way to acknowledge and thank these collaborators enough for their time and effort. That appreciation is extended to the countless others in those labs who have also contributed to this work.

To those that made the last several years of graduate school so memorable—Ahmed, Fred, Dalia, and Lorraine—thank you for everything. I will miss you all and expect to keep in touch for life. I am so thankful that (fellow IUPUI alum and fraternity brother) Ahmed Malik came to Michigan for his MD/PhD, providing irreplaceable friendship over the past decade and introducing me to some lifelong friends in the process.

Jeff, Brandt, and Erin—you've been some of my closest friends throughout graduate school, and I can't imagine surviving through it all without you. You are some of the brightest people I know. I fully expect to remain friends for life and truly hope that in the future we might work together again. Jeff, I cannot thank you enough for your constant insights in research, climbing, and life. Likewise, Max Stefan, your friendship and counseling when school has seemed overwhelming (essentially the entire time) has been monumental. I hope to maintain contact with you all, wherever you go.

Lastly, I'd like to acknowledge the lab family that predated me in the Mosberg lab—Larisa, Aubrie, and Aaron. Larisa has been an unrivaled boss/friend, helping me deal with the stresses of grad school, lab dynamics, and NMR duties. You're one of the kindest people I've met and thankful to have been your friend/NMR minion. Aaron and Aubrie, you were the reasons I joined the Mosberg lab (well, also the research). I don't believe I would have survived first and second year of grad school without your friendship and mentorship. I have missed our lab lunch trips to Ashley's and the Brown Jug ever since your departure, but very much look forward to reuniting with Aaron in Nashville. Thank you both for the impact you've made on me and my experience at Michigan. I could never fully articulate how helpful and beneficial you both have been.

Thank you to all who have supported me in more ways than can be articulated here. This has been one of the most challenging yet rewarding chapters of my life, and it has all been made possible by the support from those individuals listed above and many, many others.

TABLE OF CONTENTS

Acknowledgments	ii
List of Figures	vii
List of Tables	ix
List of Schemes	xi
List of Abbreviations	xii
Abstract	xviii
Chapter 1. Introduction	1
1.1 The History of Opioids	1
1.2 The Opioid Receptors	3
1.3 Opioid Receptor Signaling	6
1.4 Bifunctional Opioid Ligands	11
Chapter 2. Exploration of the THQ Core at the C-8 Position	17
2.1 Introduction	17
2.2 Translocation of the Phe ⁴ Pharmacophore	19
2.3 Design and Synthesis of C-8 Substituted Analogues	20
2.4 <i>In Vitro</i> Pharmacology and SAR Analysis	27
2.5 <i>In Vivo</i> Pharmacology	34

2.6	Conclusions	37
2.7	Experimental Procedures	41
Chapter 3. Dual Pharmacophores Explored via SAR Matrix		123
3.1	Introduction	123
3.2	Rationale & Approach	128
3.3	Synthesis of Analogues 39-69	130
3.4	<i>In Vitro</i> Pharmacology of Dual-Pharmacophore Ligands	133
3.5	<i>In Vivo</i> Pharmacology	142
3.6	SAR of the Thiochromane Analogues of the Bicyclic Series	146
3.7	Conclusions	148
3.8	Experimental Procedures	151
Chapter 4: Additional Projects		233
4.1	Bicyclic/C-8 Hybrid Peptidomimetics	233
4.2	<i>N</i> -Acetyl/C-8 Hybrid Peptidomimetics	238
4.3	Scaled Syntheses of <i>In Vivo</i> Candidates & Radiosynthetic Approaches	243
4.4	Experimental Procedures	251
Chapter 5: Conclusions & Future Directions		270
5.1	Observations at C-8	270
5.2	Future Directions for C-8 Utilization	273
5.3	C-8 Conclusions	280
5.4	Observations Based on Combined Bicyclic C-6 and <i>N</i> -1 or C-8 Motifs	281
5.5	Future Directions of the Bicyclic C-6 Chemotype	284
5.6	Bicyclic C-6 Conclusions	288
5.7	Concluding Remarks	289
REFERENCES		291

List of Figures

Figure 1. SAR of the Morphinan Scaffold Adapted from Pert and Snyder, 1973	5
Figure 2. Active- and Inactive-State Water-Mediated Polar Networks of Opioid Receptors	7
Figure 3. GPCR-Stimulated G Protein Activation and Signaling	9
Figure 4. Downstream Effectors Following GPCR Activation of Inhibitory G Protein	10
Figure 5. Acute Morphine Tolerance Following a Single Injection of Morphine Sulfate	12
Figure 6. Chronic Morphine Tolerance Following Subcutaneous Implantation of Morphine Sulfate Pellet after 3 Days	12
Figure 7. Active 3D Conformation of the Opioid Peptide Agonist DAMGO and Comparison to the THQ Lead 1	14
Figure 8. Leads for the Design of Mixed-Efficacy MOR Agonist/DOR Antagonist Ligands	18
Figure 9. Suzuki-Type Palladium-Catalyzed Carbonylation Mechanism	23
Figure 10. Final C-8 R Groups of Analogues 8-31	26
Fig. 11. Crystallographic Models of MOR and DOR in Active and Inactive States with Partial DOR Agonist 12 (DOR Active) and Antagonist 26 (DOR Inactive) Computationally Docked	32
Figure 12. Agonist-Bound GPCR Models Indicate Contiguous Solvation Through the Core of the Receptor While Antagonist-Bound Models Display Primarily Extracellular Solvation	33
Figure 13. Summary Profiles of MOR Agonist/DOR Antagonist Analogues 20 and 26	40
Figure 14. Abbreviated Catalogue of C-6 Substitutions Probing the Phe ⁴	124

Binding Pocket

Figure 15. Substitutions at the 1-Position of the Peptidomimetic Core	125
Figure 16. SAR Matrices Highlight Trends in Potency & Efficacy at MOR & DOR	140
Figure 17. <i>In Vivo</i> SAR Matrix Indicates Lower ClogP is Favorable for Bioavailability	144
Figure 18. Plotting ClogP Against <i>In Vivo</i> Activity	146
Figure 19. Summary Profiles of 2 nd Generation Lead 43 and Optimized Analogue 56	149
Figure 20. Profile Summary of Bicyclic/C-8 Hybrid Peptidomimetic 70	237
Figure 21. <i>In Vivo</i> Candidates and Amounts of Compound Synthesized	243
Figure 22. Chronic Antinociceptive Tolerance Evaluation of 43 , 45 , and morphine	245
Figure 23. Compounds 43 and 64 Show No Physical Dependence; Only 43 Shows No CPP ^a	246
Figure 24. Structures of Analogues 32 , 70-77 Discussed in Chapter 4	251
Figure 25. Summary Profiles of Top C-8 <i>In Vivo</i> Candidates 20 and 26 Compared to Lead 1	272
Figure 26. Structures of Proposed Compound 79 and its Radiolabeled Analogue [¹¹ C] 79	274
Figure 27. Structures of the Unglycosylated Peptide KSK-103 , the Bioavailable VRP-26 , and 80	276
Figure 28. Bicyclic Leads Displaying MOR Agonism/DOR Antagonism with <10:1 MOR/DOR Selectivity & >10:1 MOR/KOR Selectivity	283
Figure 29. Proposed Bicyclic Analogues 81-86	285

List of Tables

Table 1. Probing the Effects of Translocating the Phe ⁴ Aryl Pharmacophore to C-7 and C-8 of the THQ Core	19
Table 2. Alkyl and Halogen Substituted C-8 Analogues are MOR Agonists/DOR Partial Agonists	27
Table 3. Increasing Size of C-8 Substitution Moderately Decreases DOR Efficacy	29
Table 4. Carbonyl Substituted C-8 Analogues Consistently Display Desired MOR Agonist/DOR Antagonist Profile	30
Table 5. Antinociceptive Activity in Mouse WWTW Assay Following Intraperitoneal Administration	35
Table 6. Duration of Antinociceptive Action for C-8 Analogues	36
Table 7. <i>N</i> -Acyl Analogues with Improved MOR/DOR Affinity Balance, MOR Agonism/DOR Partial Agonism	126
Table 8. Bicyclic C-6 Pendant with Unsubstituted <i>N</i> -1 Affords a MOR-Selective, MOR Agonist/DOR Antagonist Profile	133
Table 9. <i>N</i> -1 Acetylation Reduces MOR Selectivity, Achieves Sub-Nanomolar DOR Affinity with Modest DOR Efficacy	134
Table 10. Cyclopropyl Acyl <i>N</i> -1 Substitution Further Improves MOR and DOR Affinity, Increases DOR Efficacy & Potency	135
Table 11. Sulfonyl <i>N</i> -1 Moiety Increases MOR Selectivity, MOR Potency & MOR Efficacy; Regains DOR Antagonism	137
Table 12. Benzoyl <i>N</i> -1 Substitution Maintains DOR Antagonism, Reduces MOR Efficacy & Potency	138
Table 13. Antinociceptive Activity of C-6/ <i>N</i> -1 Analogues in WWTW Assay Following Intraperitoneal Administration	143

Table 14. Thiochromane and <i>Gem</i> -Dimethyl Tetrahydro-naphthalene Analogues Show High MOR Selectivity	147
Table 15. Chapter 3 Compound Numbering and Literature References	151
Table 16. Bicyclic/C-8 Hybrid Peptidomimetic 70 Compared to Parent Analogues 20 & 43	236
Table 17. <i>N</i> -Acetyl/C-8 Hybrid Peptidomimetics 71-77 Mimic Parent <i>N</i> -Acetyl Analogue 32	239
Table 18. Investigating the Effect of <i>N</i> -Acetylation on Bioavailability for C-8 Substituted Ligands	241
Table 19. Large, Hydrophilic C-8 Substitution Show Limited Impact on Binding Affinity	277
Table 20. <i>N</i> -1 Methyl Carbamate Leads 32 , 87 , & 88 , and Proposed C-6 Heterocyclic Analogues 81-83	286

List of Schemes

Scheme 1. Synthesis of C-8 Alkyl and Trifluoromethyl Analogue Intermediates from Anilines	21
Scheme 2. Synthesis of C-8 Ethyl and Fluoro Analogue Intermediates from 6-Bromo Anilines	21
Scheme 3. Synthesis of C-8 Bromo, Aryl, and Carbonyl Analogue Intermediates from 6-Benzyl Aniline	22
Scheme 4. Synthesis of C-8 Amine Analogue Intermediates from 6-Bromo-8-Methyl THQ	24
Scheme 5. Completing the Synthesis of Analogues 8-31	25
Scheme 6. Condensed Synthetic Scheme of C-6/N-1 Dual Pharmacophore Ligands	130
Scheme 7. Synthesis of <i>Gem</i> -Dimethyl Analogue 69	131
Scheme 8. Synthesis of Thiochromane Analogues 65-68	132
Scheme 9. <i>De Novo</i> Synthesis of Analogue 70	235
Scheme 10. Attempted Radiolabeling of [¹¹ C] 43	249
Scheme 11. Proposed radiosynthesis of [¹¹ C] 79	275
Scheme 12. Full Synthetic Scheme of Glucoserine Conjugated Peptidomimetic 80	278

List of Abbreviations

2D: two-dimensional

6Cl-HOBt: 1-hydroxy-6-chloro-benzotriazole

[³⁵S]GTP γ S: [³⁵S]guanosine 5'-O-[γ -thio]triphosphate

β -FNA: beta-funaltrexamine

μ mol: micromoles

Ac₂O: acetic anhydride

Å: ångströms

A^{1,3}: allylic strain

A.A.H.: Aubrie H. Harland, Ph.D.

A.F.N.: Anthony F. Nastase, the author of this dissertation

A.M.B.: Aaron M. Bender, Ph.D.

Ar: argon

BBB: blood brain barrier

BL: baseline

BPO: benozyl peroxide

Boc: tert-butyloxycarbonyl

Boc₂O: di-tert-butyl dicarbonate

Br: bromine, bromo

BRET: bioluminescence resonance energy transfer

cAMP: cyclic adenosine monophosphate

°C: degrees Celsius

C: carbon

Ca²⁺: calcium ion

CCl₄: carbon tetrachloride.

CD₃OD: deuterated methanol

CDCl₃: deuterated chloroform

CF₃: trifluoromethyl

CHO: Chinese hamster ovary

ClogP: calculated logarithm of octanol/water coefficient

CNS: central nervous system

CO: carbon monoxide

CPP: conditioned place preference

Cryo-EM: electron cryomicroscopy

D: Asp, aspartate

DAMGO: D-Ala²,N-MePhe⁴,Gly-ol]enkephalin DCE: 1,2-dichloroethane

DCM: dichloromethane

DCE: dichloroethane

D.J.M.: Deanna J. Montgomery

diBoc-Dmt: di-boc protected 2,6-dimethyl-L-tyrosine

DIPEA: N,N-diisopropylethylamine

DMAP: 4-dimethylaminopyridine

DMF: dimethylformamide

Dmt: 2,6-dimethyl-L-tyrosine

dns: does not stimulate

DOR: δ-opioid receptor, delta opioid receptor

DPDPE: D-Pen^{2,5}-enkephalin

EC₅₀: concentration of a drug that gives half-maximal response

Et₃N: triethylamine

EtOH: ethanol

FRET: fluorescence resonance energy transfer

G protein: guanine nucleotide-binding protein

G α : alpha-subunit of a G protein

G $\beta\gamma$: beta-gamma subunit of a G protein

GDP: guanosine diphosphate

GIRK: G protein inwardly rectifying potassium channels

Gly: glycine

GPCR: G protein-coupled receptor

GTP: guanosine triphosphate

h: hours

H₂SO₄: sulfuric acid

HCl: hydrochloric acid

HPLC: high pressure liquid chromatography

HSQC: heteronuclear single quantum correlation

icv: intracerebroventricular, i.c.v.

in situ: in place, used as produced without isolation or purification

in vitro: in glass, using proteins or receptors removed from a cell

in vivo: in a live animal

in vacuo: under vacuum, or under reduced atmospheric pressure

ip: intraperitoneal, i.p.

IPA: isopropanol

J.P.A.: Jessica P. Anand, Ph.D.

K₂CO₃: potassium carbonate

K: Lys, lysine

K⁺: potassium ion

K_i: inhibitory constant

K_e: equilibrium constant

KOR: κ-opioid receptor, kappa opioid receptor

LCMS: liquid chromatography mass spectrometry

Leu: leucine

LiOH: lithium hydroxide

L.Y.M.: Larisa Yeomans, Ph.D.

MeOH: methanol

Met: methionine

mg: milligrams

mg/kg: milligrams of compound per kilogram of body weight

MgSO₄: magnesium sulfate

min: minutes

MOR: μ-opioid receptor, mu opioid receptor

MPE: maximal possible effect

Ms: mesyl, methanesulfonyl

N: nitrogen

N: Asp, asparagine

N/A: not available

NaBH₄: sodium borohydride

NaOH: sodium hydroxide

NaHCO₃: sodium bicarbonate

NaOtBu: sodium tert-butoxide

NBS: N-bromosuccinimide

NH₄Cl: ammonium chloride

NLX: naloxone

nM: nanomolar

NMR: nuclear magnetic resonance

NTI: naltrindole

NTX: naltrexone

N.W.G.: Nicholas W. Griggs

p. somniferum: Papaver somniferum, opium poppy

Pd(dppf)Cl₂: bis(diphenylphosphino)ferrocene]palladium(II) dichloride

PET: positron emission tomography

PGP: P-glycoprotein.

Phe: phenylalanine

pmol: picomoles

PyBOP: (benzotriazol-1-yl-oxytripyrrolidinophosphonium hexafluorophosphate)

r.t.: room temperature

s: seconds

sc: subcutaneous, s.c.

SAR: Structure-Activity Relationship

S.E.M.: standard error of the mean

SNC80: (+)-4-[(α R)- α -((2S,5R)-4-Allyl-2,5-dimethyl-1-piperazinyl)-3-methoxybenzyl]-N,N-diethylbenzamide

stim: stimulation

TFA: trifluoroacetic acid

TfOH: trifluoromethanesulfonic acid, triflic acid

Ti(OEt)₄: titanium (IV) ethoxide

THF: tetrahydrofuran

THIQ: tetrahydroisoquinoline

THN: tetrahydronaphthalene

THQ: tetrahydroquinoline

TLC: thin-layer chromatography

Tyr: tyrosine

WWTW: warm water tail withdrawal

U69,593: (+)-(5 α ,7 α ,8 β)-N-Methyl-N-[7-(1-pyrrolidiny)-1-oxaspiro[4.5]dec-8-yl]-benzeneacetamide

UV: ultraviolet

Abstract

Opioid-mediated pain relief, currently the gold standard treatment for many types of pain, has been inextricably associated with negative side effects including analgesic tolerance and physical dependence. These side effects have perpetuated the rising rates of opioid addiction across the United States. Several investigators have shown that activating the mu opioid receptor (MOR) while blocking the delta opioid receptor (DOR) can provide pain relief devoid of tolerance or dependence, laying the foundation for the work presented here. This dissertation is focused on the design and synthesis of bifunctional ligands that both activate MOR and block DOR while binding to both targets with equal affinity. Specifically, this work investigates how substitutions at the *N*-1, C-6, and C-8 positions of the tetrahydroquinoline (THQ) scaffold impact pharmacological activity. Through these investigations, we have identified two distinct chemical motifs that produce the desired MOR agonist/DOR antagonist efficacy profile. Furthermore, multiple analogues bearing this advantageous efficacy profile also display similar affinity for both targets, improve drug-like properties such as ClogP, and effectively block pain responses in mice after peripheral administration. Additionally, combining those chemical motifs in a hybrid ligand achieved optimal *in vitro* binding and efficacy, laying a foundation for further exploration. The work discussed herein has yielded 13 novel ligands displaying robust antinociceptive activity; evaluation of tolerance and dependence for select compounds is ongoing.

Chapter 1: Introduction

1.1 The History of Opioids

“Here was a panacea, a pharmakon nepenthes, for all human woes. Here was the secret of happiness, about which philosophers had disputed for so many ages, at once discovered.”

— Thomas de Quincey

“The Pleasures of Opium” in Confessions of an English Opium-Eater, 1856.

The earliest evidence of human cultivation of the opium poppy, *Papaver somniferum*, was discovered in the submerged Neolithic settlement of La Marmotta near modern-day Rome, dating back to 5,700 BCE.^{1,2} The opium poppy appears to have been known throughout the eastern Mediterranean, as the Sumerian civilization of modern-day Iraq provides the first written example of opium preparation as early as the third millennium BCE. *P. somniferum* was depicted in the ancient Sumerian cuneiform script as “hul gil” or the “joy plant,” though this translation is the subject of some debate.^{3,4} The use of the opium poppy has appeared repeatedly throughout the history of the eastern Mediterranean civilizations.^{1,5,6} Spreading north from La Marmotta, over 33 settlements in Switzerland and nearby France and Germany indicate cultivation of *P. somniferum*, dating back to the Neolithic, Copper, and Bronze Ages, as has been documented in a thorough review by ethnobotanist Mark Merlin in 2003.¹

Galen (130 – 210 CE), in his writing *De Compositione Medicamentorum Localium*, described the “antidote of Hippocrates,” an opium-containing elixir, as a “panacea” or a cure for all that ails.⁷ Experimenting in the 16th century, the Swiss physician Paracelsus discovered that the active alkaloids in opium can be extracted much more effectively with alcohol than previous warm-water preparations described by the Greeks. This tincture of opium he named “laudanum” was described as an effective analgesic, which was modified and popularized by English physician Thomas Sydenham in the 1660s in his seminal work *Medical Observations Concerning the History and Cure of Acute Diseases*. Laudanum became a popular drug of abuse in the Romantic and Victorian eras among both the working and artistic classes.⁸ Some notable opium users of this era include Samuel Taylor Coleridge, Thomas de Quincey, Charles Dickens, and Percy Shelley among others.^{8,9} It was around this time that opium first appeared as a public health threat, though orally ingested opium lacked many of the risk factors associated with modern intravenous opioid use.

The early 1800s saw the isolation of a major active alkaloid from opium by the German pharmacist Friedrich Sertürner, which he named *morphine* after Morpheus, the Greek god of dreams. The isolation of morphine allowed for more standardized and predictable dosing, as laudanum preparations varied widely in potency.¹⁰ Sertürner’s crystallization of morphine is recognized as the first isolation of an active plant alkaloid. Following the invention of the hypodermic syringe and hollow needle in the 1850s, morphine use expanded to operating rooms across Europe.³ However, the advent of the hypodermic needle combined with the discovery of diacetylmorphine (heroin) in the late 1800s set the stage for the opioid crisis that is presently devastating large swaths of the United States. Other technological, legal, and cultural changes connecting morphine of the 1800s to the opioid crisis of 2018 are examined in depth in Johann

Hari's *Chasing the Scream* (2015),¹¹ Sam Quinones' *Dreamland* (2015),¹² and Beth Macy's *Dopesick* (2018).¹³

1.2 The Opioid Receptors

“Pharmacological evidence for the existence of a specific opiate receptor is compelling, but heretofore it has not been directly demonstrated biochemically. We report here a direct demonstration of opiate receptor binding, its localization in nervous tissue, and a close parallel between the pharmacologic potency of opiates and their affinity for receptor binding.”

— Candace B. Pert & Solomon H. Snyder

“Opiate Receptor: Demonstration in Nervous Tissue” in *Science*, 1973.

Throughout the 19th and 20th centuries, the library of known opioid ligands expanded significantly. With an increasing number of known opioid ligands, it had become apparent that changes in chemical structure and stereochemistry could modulate the pharmacological responses to these ligands. The existence of a structure-activity relationship (SAR) among the morphinan ligands suggested a specific binding site upon which these ligands must act.¹⁴⁻¹⁷ As early as the 1950s, it had been proposed that one or multiple opioid receptors must exist,¹⁴ though they were not demonstrated experimentally until 1973.¹⁶⁻²⁰ Due to the low concentration of opioid receptors in the brain and limited sensitivity for low specific activity radioligands, early [¹⁴C]-based probes failed to identify specific opioid binding sites.¹⁷ The implementation of [³H]naloxone by Pert and

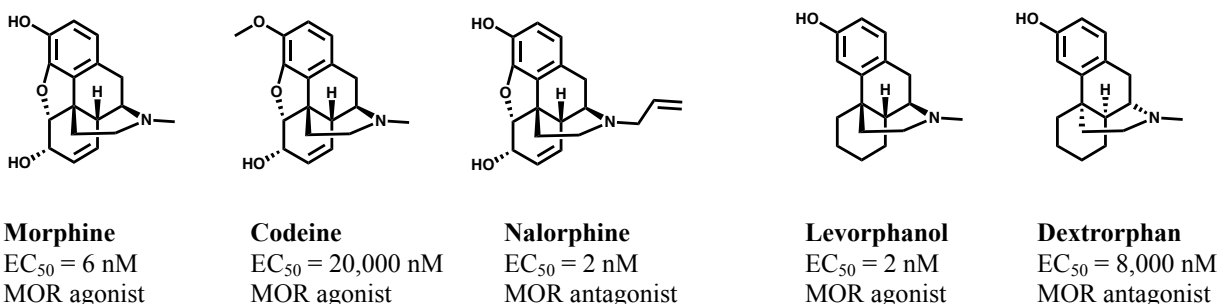
Snyder,¹⁸ [³H]dihydromorphine by Terenius,^{19,20} and [³H]etorphine by Simon et al,²¹ enabled three laboratories to almost simultaneously identify what would later be termed the mu opioid receptor.

Shortly after the discovery of the opioid receptors, some of the endogenous peptides for the opioid receptors, enkephalins and endorphins, were discovered.^{22,23} By the 1990s, three types of opioid receptors had been cloned—the mu opioid receptor (MOR),^{24,25} delta opioid receptor (DOR),^{26,27} and kappa opioid receptor (KOR).^{28,29} MOR is the most widely studied of the three and is the primary binding site of morphine and the endorphins. DOR is known to bind the endogenous enkephalin peptides and the prototypical DOR agonist SNC-80 is known to stimulate antinociception as well as antidepressant and anxiolytic effects.^{30,31} Unfortunately, SNC-80 is also associated with epileptic seizures in mice, limiting the therapeutic potential of selective DOR agonists.³² KOR, named after the synthetic benzomorphan derivative ketazocine, binds endogenous peptides known as dynorphins.³³ Activation of KOR is associated with hallucinations and dysphoria, as is induced by the exogenous KOR agonist salvinorin A, found in the *Salvia divinorum* plant.^{34,35} The endorphins, enkephalins, and dynorphins all feature a conserved N-terminal Tyr¹-Gly²-Gly³-Phe⁴-X⁵ sequence, with the phenol and amine of Tyr¹ participating in crucial H-bonds and ionic interactions. Most morphinan, peptide, and peptidomimetic ligands feature similar phenol and amine moieties, taking advantage of these endogenous H-bond partners.

It is of note that the morphinan ligands such as morphine achieve high binding affinity by conformationally restricting the Tyr¹ pharmacophore into a bridged phenanthrene ring system while truncating other pharmacophore elements of the endogenous peptides completely. The added rigidity of morphinan ligands reduces the entropic loss associated with binding, necessitating fewer receptor-ligand interactions to achieve similar affinity. Due to the conformational restriction and

rigidity of the morphinan scaffold, small changes often result in dramatic shifts in affinity or activity. Depicted in **Fig. 1** are the structures, potencies, and functional activities of the highly homologous morphinan ligands morphine, codeine, and nalorphine as well as the enantiomeric pair levorphanol and dextrorphan. These data were reported by Pert and Snyder in the seminal work that described the first characterization of the opioid receptors.¹⁸

Figure 1. SAR of the Morphinan Scaffold Adapted from Pert and Snyder, 1973^a



^a Relative potencies of drugs in reducing [³H]naloxone binding to rat brain homogenate and guinea pig intestine.

As demonstrated by the drastic reduction in potency induced by phenolic methylation of morphine (see codeine, **Fig. 1**), modification of the Tyr¹ pharmacophore—especially at sites of critical H-bonds—is poorly tolerated. Additionally, extending the N-methyl group of morphine to an allyl substitution converts the opioid agonist activity of morphine to an antagonist profile in nalorphine. Other modifications to the stereochemistry of the Tyr¹ moiety, as demonstrated by the pair of enantiomers levorphanol and dextrorphan, provides further validation that the receptors show preference for the endogenous tyrosine-like stereochemical orientation of levorphanol over the inverted orientation of the phenol and amine found in dextrorphan. This stereospecific binding provided some of the first concrete evidence of a specific opiate (opioid) receptor.

1.3 Opioid Receptor Signaling

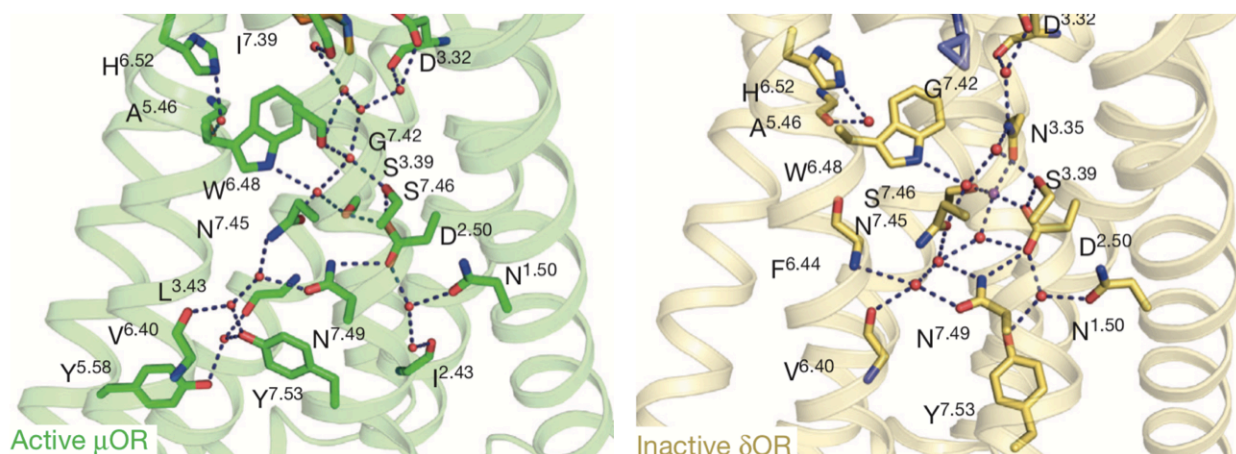
The opioid receptors belong to the Class A (rhodopsin-like) family of G protein-coupled receptors (GPCRs). GPCRs feature seven transmembrane alpha-helices and associate with a G protein at the intracellular surface. The opioid peptides and exogenous ligands bind to a large, solvent-exposed³⁶⁻³⁸ extracellular pocket and stabilize a particular conformation of the receptor. These are typically classified into the “inactive” and “active” states in relation to whether or not they stimulate the dissociation of a G protein, though there are nearly infinite conformations that a receptor might sample.^{39,40} Multiple investigators have engaged in molecular dynamics, NMR, and spectroscopic studies to probe the nature of events that relate the binding of an agonist to the dissociation of a heterotrimeric G protein from the membrane-bound GPCR.³⁸⁻⁴⁵ The shift from an inactive to an active state entails multiple translocations and rotations in domains, hydrogen bond network rearrangements, and ion cofactor and substrate exchanges. Simplistically speaking, binding of an agonist stabilizes a series of changes in the receptor that promotes G protein binding and subsequent dissociation of its $G\alpha$ and its $G\beta\gamma$ subunits.

Classical ligand binding models consider two primary factors: the ligand and the receptor. An emerging concept in GPCR modeling and structural biology is that of a highly conserved water network as a third major factor (or cofactor) in ligand binding and receptor activation.^{40,46-52} The groups of Bryan Roth and Brian Kobilka, who combined have solved the crystal structures of MOR, DOR, and KOR at high resolution in both active and inactive states, have noted the

significance of water networks and their importance to GPCR activation, both in the orthosteric site and through the core of the receptor (see **Fig. 2**).^{40,46,47} Quoting the Kobilka group in 2018:

*The [high-resolution crystal structures] highlight the contribution of many hydrogen bonds in stabilizing both the inactive and active states of opioid receptors. These hydrogen bonds represent many low-energy molecular switches that have to be broken and reformed in a concerted manner to achieve the active conformation.*⁴⁶

Figure 2. Active- and Inactive-State Water-Mediated Polar Networks of Opioid Receptors^a



^a Distinct networks of polar interactions extending through the transmembrane domains of the active- and inactive-state crystal structures from Kobilka et al.⁴⁶(Left) MOR 2.1 Å, PDB ID: 5C1M. (right) DOR 1.8 Å, PDB ID: 4N6H.

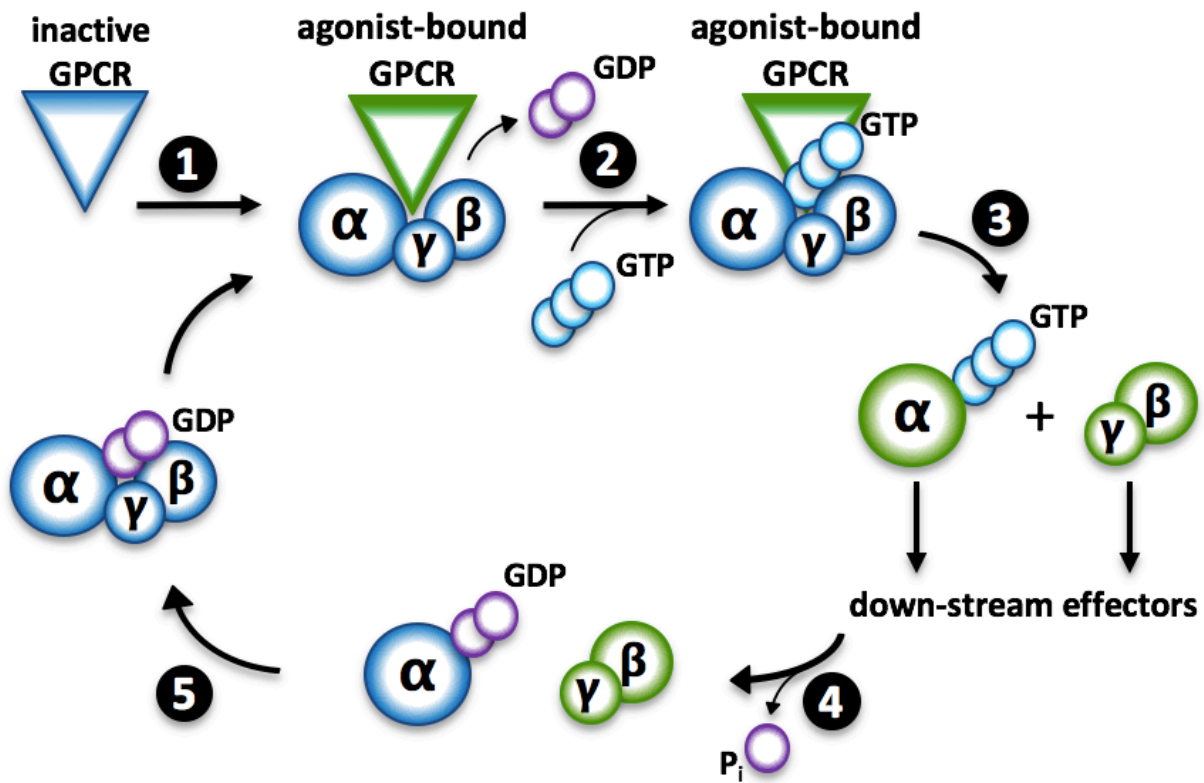
The emerging structural biology studies in this area continue to add layers of detail to our understanding of how small modifications to ligands that bind at the extracellular orthosteric (ligand-binding) site can propagate through the transmembrane domains, facilitated by a membrane-spanning polar network, to modulate intracellular G protein interactions.^{40,46,52–54} Crystallographic, spectroscopic, and computational investigations into receptor activation indicate a critical role for an allosteric sodium ion in the inactive state,^{40,54} whereas the active state is more

solvated and features a continuous channel of waters extending through the core of the GPCR.^{52,53} At present, computational models of GPCRs lack a comprehensive understanding and incorporation of the many factors involved in the transmission of a signal from the orthosteric binding site to the intracellular G protein interface. Thus, a reliable *in silico* determination of the efficacy or affinity of a ligand, especially when probing minor structural changes, still eludes computational models. Therefore, we rely primarily on radioligand assays to accurately report a compound's *in vitro* affinity, potency, and efficacy, which can be further explained in some instances through computational modeling of the active or inactive states of the opioid receptors. These assays measure affinity through competitive displacement of an orthosteric radioligand, [³H]diprenorphine, and measure potency and efficacy via incorporation of a radiolabeled GTP analogue, [³⁵S]GTP γ S into G α proteins.

As depicted in **Fig 3-1** the inactive-state G protein, which holds a GDP molecule between its G α and its G $\beta\gamma$ subunits, binds to an active-state GPCR intracellularly. GDP is displaced from the G protein when the active-state GPCR allosterically disrupts the G protein's nucleotide-binding site (**Fig. 3-2**).^{38,42,45,55} A high intracellular GTP concentration drives the binding of GTP to the nucleotide-free binding site on the G α subunit of the G protein.⁵⁶ With GTP bound, the G $\beta\gamma$ subunits dissociate from G α (**Fig. 3-3**) and both subunits go on to promote intracellular signaling.^{56,57} The GTP is hydrolyzed following activation of downstream effectors (**Fig. 3-4**), shifting G α to an inactive GDP-bound state. The G $\beta\gamma$ subunits then re-associate with G α (**Fig. 3-5**), recycled for further intracellular signaling. In the [³⁵S]GTP γ S assay, the hydrolysis step (**Fig. 3-4**) is blocked by replacement of an oxygen on the terminal phosphate with ³⁵S, causing an

accumulation of radioactivity in the membrane connected to G α activation that can be quantified by scintillation counting.

Figure 3. GPCR-Stimulated G Protein Activation and Signaling^a

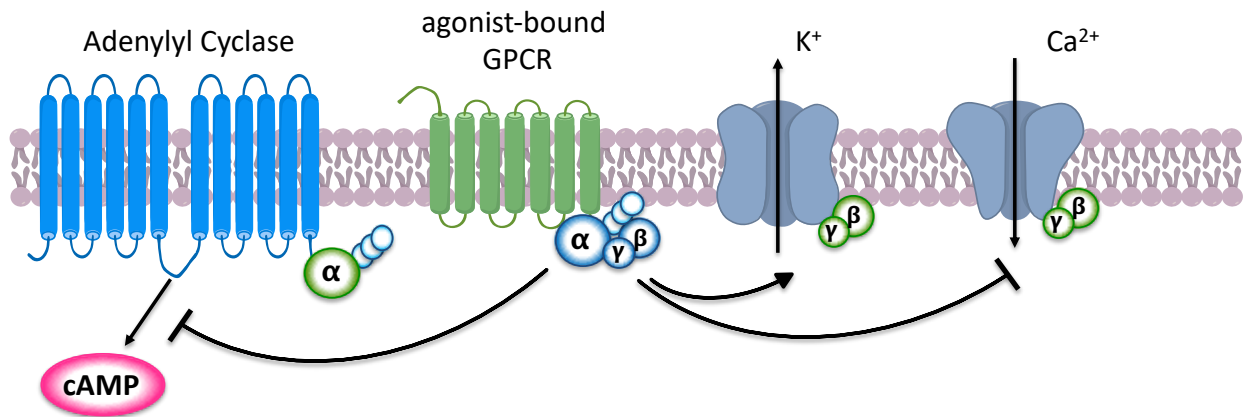


^a Green outline indicates an activated G protein or GPCR, while blue indicates an inactive state. GDP is depicted as purple and GTP is shown in light blue. **1.** Agonist binds to the GPCR, recruiting GDP-bound heterotrimeric G protein; GPCR-binding promotes dissociation of GDP from the nucleotide-binding site. **2.** GTP binds the G protein nucleotide-binding site. **3.** G α and its G $\beta\gamma$ subunits dissociate in activated form and interact with downstream effectors such as cAMP, GIRK, and Ca²⁺ channels **4.** GTP is hydrolyzed to GDP + P_i, inactivating G α **5.** GDP-bound G α and G $\beta\gamma$ re-associate.

Of the G protein subtypes, the opioid receptors selectively interact with the inhibitory G protein family. The G $\alpha_{i/o}$ subunit inhibits adenylyl cyclase and production of cAMP. Meanwhile,

the $G\beta\gamma$ subunit activates G protein-coupled inwardly-rectifying potassium channels (see **Fig. 4**), allowing outward K^+ diffusion and inducing a hyperpolarized state in the neuron.⁵⁶⁻⁵⁹ Additionally, the dissociated $G\beta\gamma$ subunit interacts with Ca^{2+} channels following GPCR activation, reducing the voltage-gated pore opening of Ca^{2+} channels thereby decreasing the Ca^{2+} concentration within the cell. The hyperpolarizing effects of decreased intracellular K^+ , paired with the decreased Ca^{2+} signaling, serves to further reduce neural firing.^{56,57} Through these mechanisms depicted in **Fig. 4**, as well as other downstream effectors, the opioid receptors act to quiet neural transmission.

Figure 4. Downstream Effectors Following GPCR Activation of Inhibitory G Protein^a



^a Inhibitory $G\alpha$, following GPCR activation, GTP binding, and dissociation from $G\beta\gamma$, activates K^+ channels while inhibiting adenylyl cyclase and its downstream product cAMP. $G\beta\gamma$ acts on Ca^{2+} channels to reduce influx of Ca^{2+} .

Because the opioid receptors are often found in cell populations responsible for pain transmission, opioid agonists (especially MOR agonists such as morphine) function to decrease the afferent pain signaling, resulting in analgesia. Of note, while agonism at MOR, DOR, and KOR all induce some antinociception, the euphoric and rewarding effects of MOR agonists such as morphine are not observed for agonists of DOR and KOR. In fact, DOR agonists are established

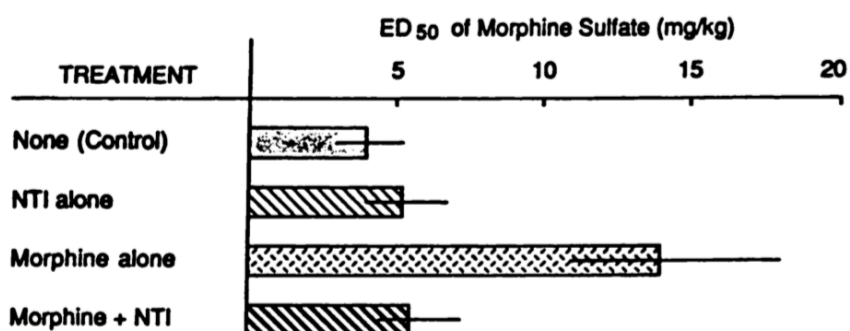
to be non-rewarding and non-euphoric whereas KOR agonists are known to be aversive and dysphoric. As such, it may be possible to combine these differential opioid effects to mitigate some negative side effects associated with MOR agonists, including tolerance and dependence.

1.4 Bifunctional Opioid Ligands

The idea that the opioid receptors may interact and modulate the activities of one another has been a subject of interest to many researchers aiming to improve opioid treatments. Of particular interest in the field of pain and analgesia is the observation that DOR agonists have been shown to potentiate the analgesic activity of MOR agonists⁶⁰⁻⁶³ while DOR antagonists are associated with a reduction in tolerance and dependence toward MOR agonists including morphine.⁶⁴⁻⁶⁶ In 1991, a landmark study by Abdelhamid, Sultana, Portoghese and Takemori demonstrated that the selective DOR antagonist naltrindole (NTI) reduced both tolerance and dependence toward morphine in mice.⁶⁴

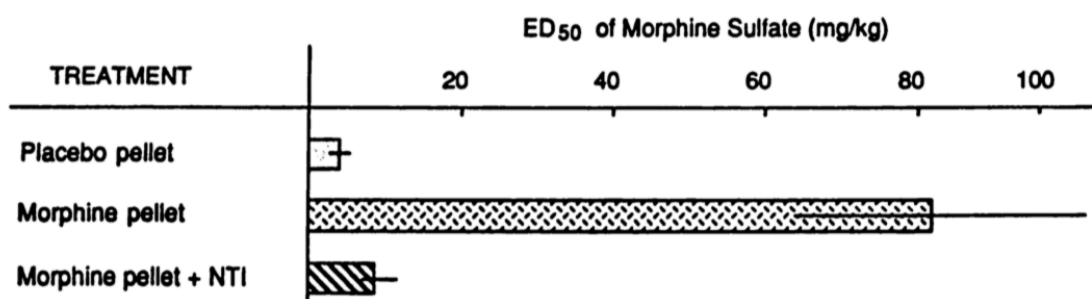
Following a single subcutaneous (s.c.) injection of morphine (100 mg/kg), mice show acute antinociceptive tolerance, indicated by an increase in the effective dose (ED₅₀) of morphine, meaning more of the drug must be administered to elicit the same antinociceptive effect. Abdelhamid et al. demonstrated that when mice are pretreated with NTI intracerebroventricularly (i.c.v.), morphine tolerance is suppressed as illustrated in **Fig. 5**. Furthermore, a subcutaneous implantation of a morphine pellet caused a dramatic increase in chronic tolerance, which was similarly suppressed by once-daily injections of NTI (**Fig. 6**).

Figure 5. Acute Morphine Tolerance Following a Single Injection of Morphine Sulfate^{a, b}



^a Figure taken from Abdelhamid, Sultana, Portoghese and Takemori, 1991 (reference ⁶⁴). ^b Effect of naltrindole (NTI) on morphine tolerance. NTI was administered i.c.v. 5.5 hr prior and immediately preceding anti-nociceptive testing. Morphine (100 mg/kg) was administered 4 hr prior to testing. Bars represent 95% CI of the values.

Figure 6. Chronic Morphine Tolerance Following Subcutaneous Implantation of Morphine Sulfate Pellet after 3 Days^{a, b}



^a Figure taken from Abdelhamid, Sultana, Portoghese and Takemori, 1991 (reference ⁶⁴). ^b Effect of NTI on chronic morphine tolerance. Mice were implanted with placebo or morphine pellet (75 mg free base) for 3 days. NTI (10 pmol) was administered i.c.v. 1.5 hr before, 24 hr after, and 48 hr after pellet implantation. Bars represent 95% CI of the values.

In this same study, the amount of naloxone (NLX), an opioid antagonist, required to precipitate withdrawal was measured under various conditions. Mice given a single s.c. injection (100 mg/kg) of morphine needed only 2 μ mol/kg NLX to precipitate withdrawal jumping, whereas opioid-naïve mice demonstrated no withdrawal after 250 μ mol/kg NLX. When pre-treated with

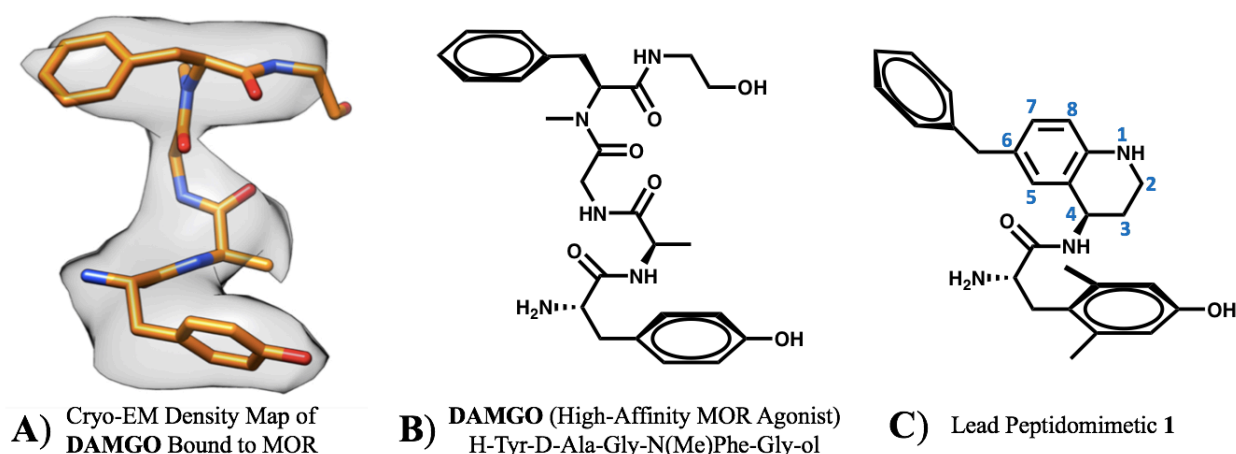
NTI (10 pmol, i.c.v.) 90 min before, then co-treated with morphine (100 mg/kg) and NTI again (10 pmol, i.c.v.), these mice showed a 45-fold increase in NLX (90 μ mol/kg) required to induce withdrawal, suggesting a dramatic decrease in acute physical dependence. These results were further substantiated by studies in rats,⁶⁵ with DOR-1 antisense oligonucleotides,⁶⁷ and DOR-1 knockout mice,⁶⁶ implicating a role for DOR in the development of tolerance and dependence toward MOR agonists.

Based on the DOR antagonist co-administration and DOR-1 knockout studies discussed above, much interest has been focused on the development of a single agent that can achieve both the MOR agonist and DOR antagonist components.⁶⁸⁻⁸⁵ Some labs have used a bivalent ligand approach, predicated on the existence of MOR/DOR heterodimers, which link a MOR agonist and DOR antagonist through a flexible linker.^{72-76,86,87} While work in this area has shown some promise, a single-agent approach features a ligand that can reproduce the MOR agonist/DOR antagonist profile independent of whether or not MOR/DOR heterodimers exist in a meaningful context *in vivo*—a subject that is still contested within the field of opioid pharmacology.⁸⁸ Our lab has been interested in developing ligands that bind to both MOR and DOR with high affinity, and act as an agonists at MOR and antagonists at DOR. Early work in the Mosberg lab focused on peptides and pseudopeptides,^{82,84,85,89-91} though recent work has seen the development of several peptidomimetic series exploring the MOR agonist/DOR antagonist profile.^{80,83,92-100} These peptidomimetic series primarily build around a tetrahydroquinoline (THQ) core, which replaces the cyclic peptide scaffold that was initially used to develop the structure-activity relationship (SAR) and pharmacophore models for the MOR agonist/DOR antagonist profile. Both series take key pharmacophore elements from the endogenous opioid peptides which feature the previously described Tyr¹-Gly²-Gly³-Phe⁴-X⁵ sequence. It was determined through SAR studies and

computational modeling that the Tyr¹ and Phe⁴ residues (separated by a flexible di-glycine spacer) are important pharmacophores to achieve high opioid affinity for flexible, peptide-like ligands. In contrast to the rigid morphinan scaffold, the relatively flexible peptide/peptidomimetic scaffold is less responsive to minute structural modifications, allowing us to fine-tune our desired pharmacological profile.

In 2018, the Kobilka lab obtained a cryo-EM structure of the high-affinity, MOR selective peptide DAMGO (H-Tyr¹-D-Ala²-Gly³-N(Me)Phe⁴-Gly⁵-ol) bound to MOR with a resolution of 3.5Å.³⁸ They reported the active 3D conformation for the peptide depicted in **Fig. 7A**. Comparison between the structures of DAMGO (**Fig. 7B**) and our lead THQ-based peptidomimetic **1** (**Fig. 7C**) suggests our small-molecule scaffold can position the key pharmacophores—Tyr¹ and Phe⁴—similarly to the opioid peptides while reducing flexibility and rotatable bonds through conformational restriction.

Figure 7. Active 3D Conformation of the Opioid Peptide Agonist DAMGO and Comparison to the THQ Lead **1**



One minor difference between DAMGO (and the endogenous peptides) and the peptidomimetic series is the replacement of the Tyr¹ residue with a 2',6'-dimethyl-L-tyrosine residue (Dmt) shown at bottom in **Fig. 7C**. Since its introduction in 1985,¹⁰¹ Dmt has been widely used as a mimetic of the endogenous Tyr¹ residue across the field of opioid ligand design.^{78,97,102,103} The Dmt residue maintains the critical phenolic H-bond donor and has demonstrated widespread bioavailability, and in many contexts displays superior MOR affinity relative to unsubstituted tyrosine. As can be seen in **Fig. 7A**, the bioactive conformation of the Tyr¹ residue shows the ring to be out-of-plane with the peptide backbone, with the phenol and amine pointing in opposite directions. The steric influence of the methyl groups on Dmt favor this anti-planar orientation, reducing the entropic loss associated with binding and thus decreasing the binding energy. The compounds presented in this work have held constant the Dmt section of the THQ scaffold constant while probing modifications around the THQ core.

Initial exploration of the peptidomimetic series focused primarily on modifications to the 1- and 6-positions. Chapter 2 departs from past SAR campaigns and explores the effects of substitutions at the 8-position of the THQ core. This previously unexplored chemical space is probed with a diverse set of substitutions, leading to unique *in vitro* SAR observations as well as several novel analogues displaying antinociceptive activity *in vivo*. Chapter 3 returns to the past 1- and 6-position SAR campaigns, taking advantageous substitutions from both positions and combining them in a series of dually-substituted analogues with fine-tuned *in vitro* profiles. Trends from this campaign are visualized via a two-dimensional matrix, providing novel insights into the effects of various pharmacophore elements on binding and efficacy. In Chapter 4, a collection of short series and side-projects are presented, with concluding remarks and future direction presented in Chapter 5. The following chapters represent the collaborative efforts of several

chemists and pharmacologists spanning several years of work. In some cases, analogues designed and synthesized by other chemists will be presented to provide context for the novel chemical exploration done in this dissertation. Unless otherwise noted, compounds presented here are the work of the author of this dissertation.

Chapter 2: Exploration of the THQ Core at the C-8 Position

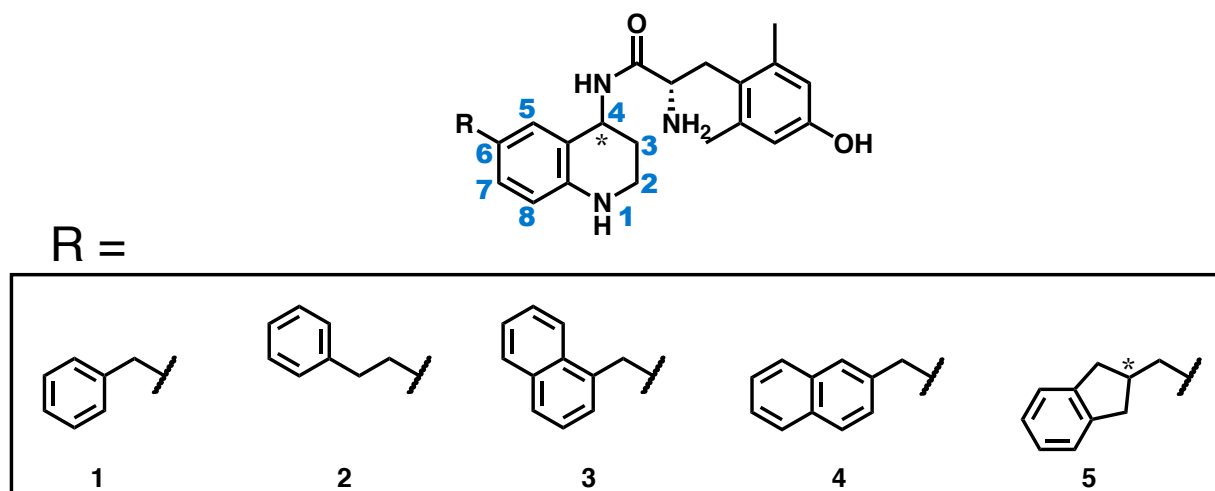
2.1 Introduction

Research on opioid peptides performed by the Mosberg lab and others led to the development of pharmacophore models highlighting the importance of two key pharmacophores—a tyrosine and an aryl ring—separated by an appropriate linker region.^{89,93} As discussed previously, modifications to the tyrosine functionality caused significant changes in pharmacology, though conversion to the Dmt analogue was well-tolerated. The second aryl pharmacophore was more tolerant to modification, and much peptide work went into probing the effects of various unnatural amino acids in the Phe⁴ position.^{82,84,85,89} To increase metabolic stability and restrict rotational freedom, the peptide core was cyclized through disulfide and di-thioether bridges. This peptide scaffold was later replaced with a more drug-like tetrahydroquinoline (THQ) core, resulting in the first peptidomimetic small molecule developed by our lab based on the aforementioned series of peptide ligands.⁹³ Subsequent development of small molecules, which largely mirror the changes initially probed in the peptide series, was explored with renewed interest in 2013.⁸³ Some of these early analogues showed selectivity for MOR and DOR over KOR, and these were carried forward for further development with the MOR agonist/DOR antagonist profile in mind.

In vitro pharmacology data obtained by Nicholas Griggs, Thomas Fernandez, Tyler Trask, Jessica Anand, and others in the lab of John Traynor. *In vivo* data were obtained by Jessica Anand and others in the lab of Emily Jutkiewicz.

Computational models and ligand overlays indicated that placement of the benzyl pendant at the C-6 position of the THQ ring (see **Fig. 8** compound **1**) offered optimal overlay with the Phe⁴ residue of the peptide series of ligands that showed high affinity for MOR and DOR.^{83,93} Our lab then went on to probe the effects of linker length (**Fig. 8** compound **2**), ring fusion (**3**), connection point (**4**), and saturation (**5**) with regard to the C-6 aryl pharmacophore, providing some of our first leads for THQ-based SAR development of MOR and DOR selective ligands.⁸³

Figure 8. Leads for the Design of Mixed-Efficacy MOR Agonist/DOR Antagonist Ligands^a



^a Figure adapted from reference ⁸³. Synthesis of analogues **1-5** was performed by L.Y.M., A.A.H., and A.M.B.

These ligands displayed high MOR efficacy and little to no DOR efficacy, however all five ligands in **Fig. 8** showed 8- to 120-fold binding selectivity for MOR over DOR. As such, further development of the MOR agonist/DOR antagonist profile required optimization in reducing MOR selectivity while optimizing MOR and DOR efficacy profiles (compounds **1** and **3** displayed some DOR efficacy whereas **2** was only a partial MOR agonist). Furthermore, only compound **1** displayed full antinociceptive activity *in vivo* after peripheral administration in mice. In order to determine what degree of MOR selectivity is tolerable while maintaining the favorable profile

established by prior DOR blocking studies,^{64–67} it was important to develop a library of *in vivo* active MOR agonist/DOR antagonist analogues with varying degrees of selectivity. With this goal in mind, further exploration about the THQ core was undertaken with the aim of maintaining bioavailability while varying MOR selectivity. The results of this chapter were described in part in a 2018 manuscript published by the journal *ACS Chemical Neuroscience*.⁹⁶

2.2 Translocation of the Phe⁴ Pharmacophore

While prior pharmacophore and computational models suggested that the C-6 position offered optimal overlap with the Phe⁴ position of the peptide series, empirical evidence of such a conclusion had not yet been established. To test this hypothesis, the C-6 benzyl pendant of our lead peptidomimetic **1** (Table 1) was translocated to C-7 and C-8 in analogues **6** and **7** respectively.

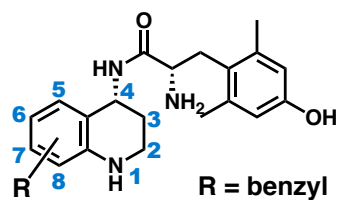


Table 1. Probing the Effects of Translocating the Phe⁴ Aryl Pharmacophore to C-7 and C-8 of the THQ Core^a

#	R position	K _i (nM)				EC ₅₀ (nM)			% stim		
		MOR	DOR	KOR	DOR K _i /MOR K _i	MOR	DOR	KOR	MOR	DOR	KOR
1	C-6	0.22 (0.02)	9.4 (0.8)	68 (2)	43	1.6 (0.3)	110 (6)	>500 (70)	81 (2)	16 (2)	22 (2)
6	C-7	0.8 (0.3)	26 (2)	92 (n=1)	33	25 (20)	dns	---	18 (5)	dns	---
7	C-8	48 (9)	360 (60)	1500 (400)	7.5	1200 (300)	dns	dns	37 (4)	dns	dns
8	C-6 & C-8	1.0 (0.1)	1.6 (0.4)	23 (5)	1.6	4 (2)	380 (80)	dns	96 (4)	42 (7)	dns

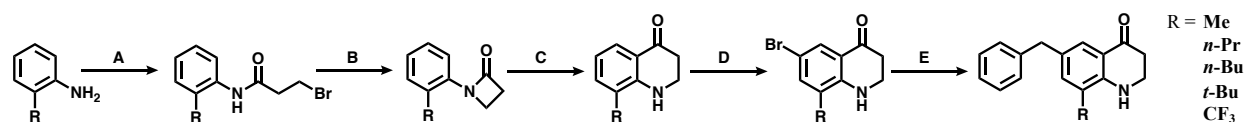
^a Binding affinities (K_i) were obtained by competitive displacement of radiolabeled [³H]-diprenorphine in membrane preparations. Functional data were obtained using agonist induced stimulation of [³⁵S]-GTPγS binding. Potency is represented as EC₅₀ (nM) and efficacy as percent maximal stimulation relative to standard agonist DAMGO (MOR), DPDPE (DOR), or U69,593 (KOR) at 10 μM. All values are expressed as the mean of three separate assays performed in duplicate with standard error of the mean in parentheses. “dns” = does not stimulate (<10% stim). “---” = not tested. Analogue **6** was synthesized by A.A.H..

Both analogues **6** (C-7 benzyl) and **7** (C-8 benzyl) showed significant decreases in efficacy at MOR, while compound **7** showed a 100-fold decrease in MOR potency and affinity at both MOR and DOR (**Table 1**). We then questioned whether this reduction in MOR activity was due to the loss of the C-6 pharmacophore, or to unfavorable ligand-receptor interactions at C-8. To examine this, we incorporated both the C-6 and C-8 benzyl substitutions in compound **8**. The binding affinity as well as potency and efficacy of **8** at MOR were restored ($K_i = 1$ nM; $EC_{50} = 4$ nM; 96% stimulation), while the DOR binding affinity increased 6-fold compared to **1**, not only validating the importance of the C-6 pharmacophore for MOR activity, but also identifying a key role for the C-8 position in modulating DOR affinity. The moderate loss in MOR affinity and increase in DOR affinity for **8** shifted the MOR/DOR binding ratio (DOR K_i /MOR K_i) from 43 for compound **1** to a more balanced 1.6 for compound **8** (**Table 1**). Consequently, this 6-,8-disubstituted THQ analogue **8** established C-8 as a region of interest for future SAR.

2.3 Design and Synthesis of C-8 Substituted Analogues

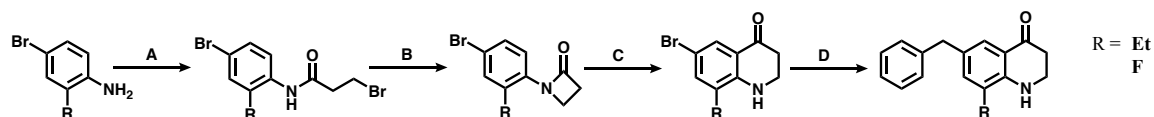
The synthesis of final compounds **8-31** began with the aniline derivatives depicted in **Schemes 1** and **2**, which differ only by R-group and the presence or absence of an aryl bromide at C-6 (THQ numbering depicted in **Table 1** is used throughout this synthesis for consistency). Likewise, **Scheme 3** follows many of the same steps but features a benzyl C-6 substitution in the starting aniline.

Scheme 1. Synthesis of C-8 Alkyl and Trifluoromethyl Analogue Intermediates from Anilines



^a (A) 3-bromopropionyl chloride & K₂CO₃ in DCM. (B) NaOtBu in DMF. (C) TfOH in DCE. (D) NBS in DCM. (E) benzyl boronic acid pinacol ester, Pd(dppf)Cl₂ & K₂CO₃ in 3:1 acetone/H₂O, 80°C.

Scheme 2. Synthesis of C-8 Ethyl and Fluoro Analogue Intermediates from 6-Bromo Anilines

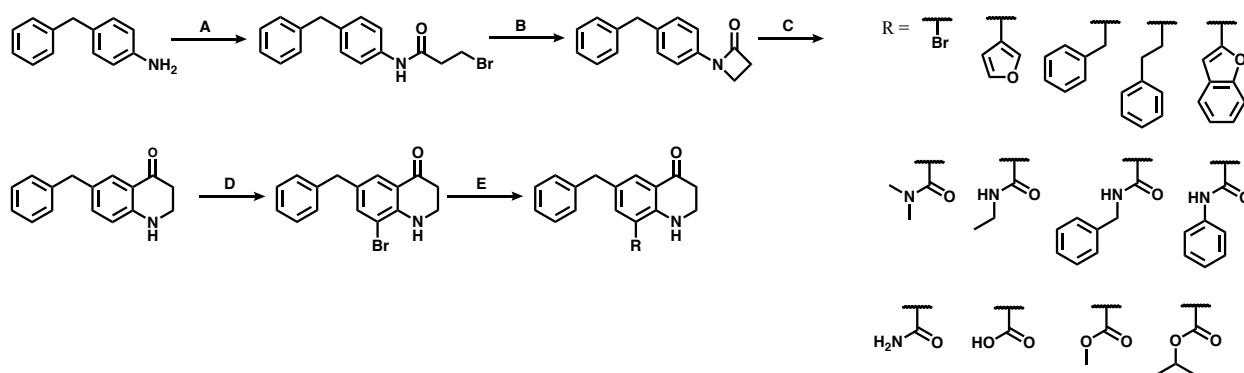


^a (A) 3-bromopropionyl chloride & K₂CO₃ in DCM. (B) NaOtBu in DMF. (C) TfOH in DCE. (D) benzyl boronic acid pinacol ester, Pd(dppf)Cl₂ & K₂CO₃ in 3:1 acetone/H₂O, 80°C.

The synthesis of the THQ core in three steps—A, B, and C in Schemes 1-3—was developed by Dr. Larisa Yeomans, though these transformations had been previously reported in the literature independently. In step A, the aniline is substituted in a simple, high-yielding amide formation reaction with the acid chloride 3-bromopropionyl chloride. Step B involves an intramolecular β -lactam cyclization, catalyzed by the powerful base sodium *tert*-butoxide.¹⁰⁴ In step C, this β -lactam intermediate undergoes an intramolecular Friedel-Crafts-like acylation (Fries rearrangement) facilitated by the ring strain of the 4-membered β -lactam in the presence of the superacid trifluoromethanesulfonic (triflic) acid, which is proposed to both protonate the amide while also coordinating the carbonyl to promote acylium ion formation.¹⁰⁵ Though breaking

aromaticity is energetically unfavorable, the establishment of a more conjugated, less-strained bicyclic 6-membered ring system (the THQ core) makes this reaction exergonic. If not already present as in **Scheme 2**, an aryl bromide was next installed with *N*-bromosuccinimide in a highly regioselective addition at the C-6 (**Scheme 1**) or C-8 (**Scheme 3**) positions, directed by the *ortho*/*para*-directing aniline and *meta*-directing ketone. The final step in **Schemes 1-3** (step **E** in **1** and **2**, **D** in **Scheme 3**) involves palladium-catalyzed functionalization of the aryl bromide. In **Schemes 1** and **2**, this involves a simple Suzuki cross-coupling with a benzyl boronic acid pinacol ester in the presence of potassium carbonate and heat.

Scheme 3. Synthesis of C-8 Bromo, Aryl, and Carbonyl Analogue Intermediates from 6-Benzyl Aniline

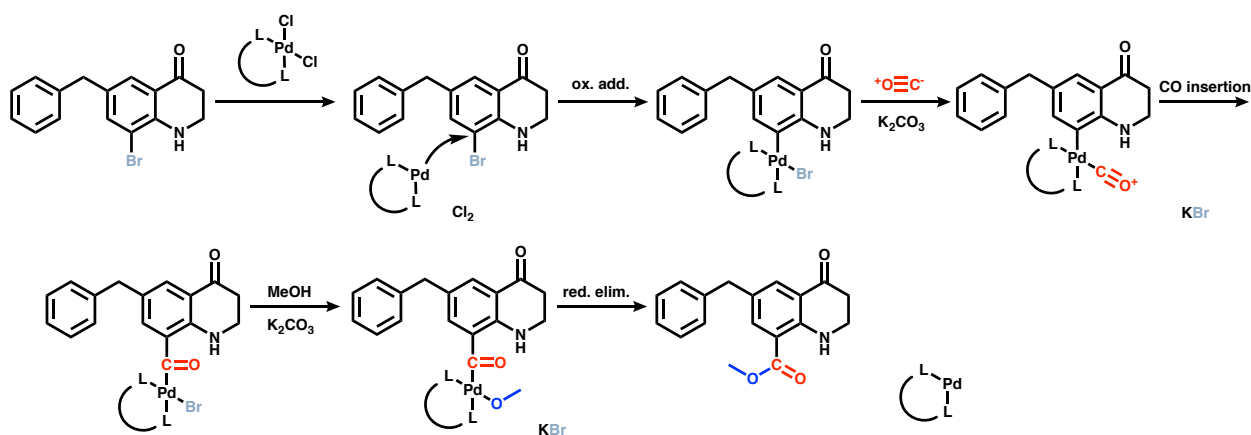


^a (A) 3-bromopropionyl chloride & K₂CO₃ in DCM. (B) NaOtBu in DMF. (C) TfOH in DCE. (D) NBS in DCM. (E) *Suzuki conditions*: 3-furyl, benzyl, ethylphenyl, or 2-benzofuranyl boronic acid pinacol ester, Pd(dppf)Cl₂ & K₂CO₃ in 3:1 acetone/H₂O, 80°C. *Carbonylation conditions*: carbon monoxide gas, Pd(dppf)Cl₂ & K₂CO₃ in 3:1 DMF/H₂O, MeOH, or IPA, 80°C. *Amide coupling conditions*: amine, PyBOP & DIPEA in DMF.

In **Scheme 3**, Suzuki conditions could be used to install the 3-furan, 2-benzofuran, benzyl, or ethylphenyl substitutions. However, different functionalization was required to further diversify

the SAR at the C-8 position beyond simple aryl modifications. Heretofore unreported on a heterocyclic substrate, a method was developed for aryl carbonylation at the C-8 position using carbon monoxide generated *in situ* from the decomposition of oxalyl chloride in 2M sodium hydroxide. The decomposition side products carbon dioxide and hydrochloric acid are readily absorbed in the degassed aqueous media while carbon monoxide is liberated as a gas. CO is cannulated or balloon-transferred to a mixture of aryl bromide, Pd(dppf)Cl₂, and potassium carbonate in an argon-sparged solution of DMF and water or alcohol. Through a proposed Suzuki-type mechanism shown in **Fig. 9**, the carboxylic acid or ester (corresponding to which alcohol is used) can be installed at C-8. The carboxylic acid could then be substituted with amide coupling conditions (using DIPEA and the peptide coupling reagent PyBOP) to achieve the carboxamide as well as the dimethyl, ethyl, benzyl, and phenyl amides in modest yields (**Scheme 3** step **E**).

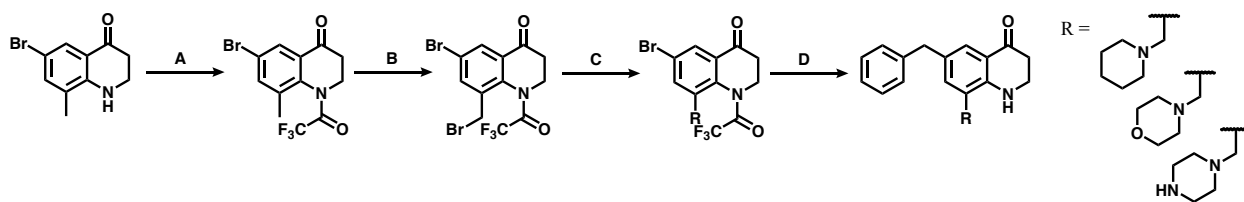
Figure 9. Suzuki-Type Palladium-Catalyzed Carbonylation Mechanism



In addition to alkyl, halo, aryl and carbonyl substitutions at C-8, a series of basic amine heterocycles were also explored. These ligands started with a 6-bromo-8-methyl THQ intermediate, the synthesis of which can be found in **Scheme 1** prior to Suzuki coupling. As laid

out in **Scheme 4**, the THQ amine was first substituted with a trifluoroacetyl group in step **A**. This protecting group was selected as it would be least likely to sterically inhibit subsequent benzylic bromination at the C-8 methyl position, yet also offered facile removal under mild conditions compared to the fairly robust acetyl alternative. Unprotected amines are poorly tolerated in the subsequent radical bromination reaction. In step **B** of **Scheme 4**, benzylic bromine insertion was catalyzed by the radical initiator benzoyl peroxide and heat. The benzylic bromide could then be substituted with a secondary amine such as piperidine, morpholine, or mono-Boc piperazine. Due to the use of potassium carbonate as a base, some loss of the trifluoroacetyl group was observed. However, the unprotected amine was sterically hindered by the C-8 substitution and caused no adverse side-reactions during subsequent Suzuki coupling. With the C-8 amine installed, the C-6 aryl bromide underwent Suzuki coupling as described previously. The use of potassium carbonate in aqueous solvent during Suzuki coupling, heated at 80°C for several hours, provided full trifluoroacetyl removal affording the 6-benzyl-8-R THQ intermediate desired to begin **Scheme 5**.

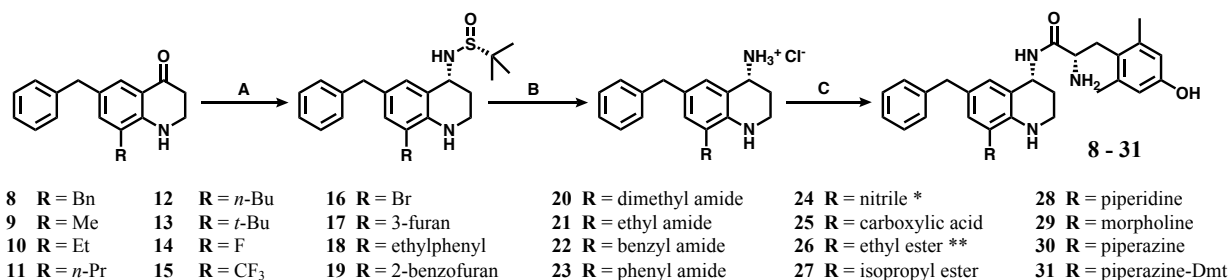
Scheme 4. Synthesis of C-8 Amine Analogue Intermediates from 6-Bromo-8-Methyl THQ



^a **(A)** Trifluoroacetic acid anhydride in DCM. **(B)** NBS & benzoyl peroxide in CCl₄, 80°C. **(C)** amine & K₂CO₃ in DMF. **(D)** benzyl boronic acid pinacol ester, Pd(dppf)Cl₂ & K₂CO₃ in 3:1 acetone/H₂O, 80°C.

To complete the synthesis of analogues **8-31** as shown in **Scheme 5**, the 6-benzyl-8-R THQ intermediates underwent reductive amination in step **A** to install the desired stereochemistry at the C-4 position. Using the chiral Ellman auxiliary (R)-(+)-2-methyl-2-propanesulfonamide and $\text{Ti}(\text{OEt})_4$, the ketone was converted to an *N*-sulfinyl imine, which was then reduced stereoselectively *in situ* with sodium borohydride to provide the (R) sulfonamide at C-4. During this reaction, it was observed that methyl, isopropyl, and phenyl esters were all converted to an ethyl ester. The excess titanium, which is used to coordinate the ketone to facilitate transamination, could also coordinate the ester functionality. The ester coordination catalyzed nucleophilic attack by excess ethoxide liberated from $\text{Ti}(\text{OEt})_4$ during the 48-hour reaction. To synthesize the isopropyl analogue **27**, $\text{Ti}(\text{O}i\text{Pr})_4$ was used instead of $\text{Ti}(\text{OEt})_4$. The methyl and phenyl esters were not re-synthesized, though use of TiCl_4 or another suitable Lewis acid would likely achieve transamination without the unwanted nucleophilic attack. Additionally, NMR indicated conversion of the carboxamide to a nitrile under reductive amination conditions, demonstrated by a downfield shift in ^{13}C -NMR and loss of 18 mass units for the major peak by LC-MS.

Scheme 5. Completing the Synthesis of Analogues **8-31**^a

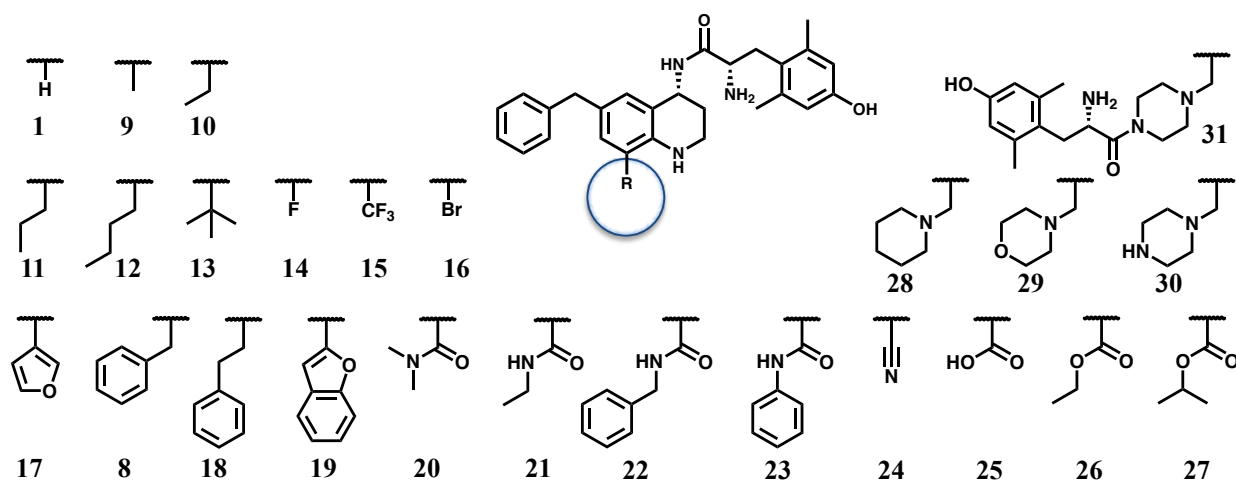


*carboxamide was unintentionally converted to a nitrile in step B under reductive amination conditions. **methyl ester was converted to an ethyl ester during step A via nucleophilic attack by excess ethoxide ion, catalyzed by coordination of the ester carbonyl with Ti, both effects of $\text{Ti}(\text{OEt})_4$ reagent.

^a (A) (R)-(+)-2-methyl-2-propanesulfonamide & $\text{Ti}(\text{OEt})_4$ in THF, 0°C to 70°C, then NaBH_4 in THF, -78°C to r.t. (e) HCl, 1,4-dioxane, r.t., then diBoc 2,6-dimethyl-L-tyrosine, PyBOP, DIPEA, DMF, r.t., then TFA, DCM, r.t.

In step **B** of **Scheme 5**, the sulfinamide was cleaved with hydrochloric acid giving the chiral amine salt, which was typically carried forward without characterization. Previously, this amine intermediate has been fully characterized by 1D and 2D NMR as well as X-ray crystallography, confirming that the stereoselectivity and chirality at C-4 that results from the described reductive transamination. During the synthesis of analogue **30** which featured a Boc-piperazine at C-8, the Boc group was removed during the sulfinamide cleavage of step **B**. Subsequent amide coupling to *N*-,*O*-diBoc-2',6'-dimethyl-L-tyrosine, followed by Boc deprotection with trifluoroacetic acid, gave title compounds **8-30**. In the case of analogue **30**, some double insertion of Dmt at both the C-4 and piperazine amine was observed, yielding **31** by accident. A depiction of the C-8 substitutions analyzed in analogues **8-31** is provided below in **Fig. 10**.

Figure 10. Final C-8 R Groups of Analogues **8-31**



2.4 In Vitro Pharmacology and SAR Analysis

Following the promise of the initial C-8 benzyl substituted analogue **8** for modulating MOR selectivity, the SAR around C-8 was further expanded with the diverse substitutions represented in **Fig. 10**. Subsequent compounds in the C-8 series explored the steric environment and depth of the C-8 binding pocket with various alkyl substitutions, ranging from methyl to t-butyl (**Table 2**). We extended this series to include halogens (F, CF₃, Br), which largely fit the same trend as the alkyl set.

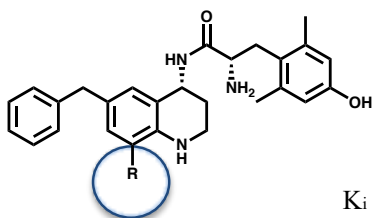


Table 2. Alkyl and Halogen Substituted C-8 Analogues are MOR Agonists/DOR Partial Agonists^a

#	C-8 R Group	K _i (nM)				EC ₅₀ (nM)			% stim		
		MOR	DOR	KOR	DOR K _i /MOR K _i	MOR	DOR	KOR	MOR	DOR	KOR
1	H	0.22 (0.02)	9.4 (0.8)	68 (2)	43	1.6 (0.3)	110 (6)	>500	81 (2)	16 (2)	22 (2)
9	Me	0.24 (0.08)	1.9 (0.4)	17 (0.7)	8	4.2 (1.6)	110 (24)	>500	91 (1)	71 (3)	52 (2)
10	Et	0.09 (0.04)	1.9 (0.4)	40 (5)	21	6.2 (2.9)	32 (10)	dns	74 (2)	45 (4)	dns
11	n-Pr	0.64 (0.08)	5.9 (1.5)	98 (18)	9	23 (7)	310 (30)	dns [†]	90 (6)	36 (3)	dns [†]
12	n-Bu	0.76 (0.28)	3.6 (0.5)	34 (5)	5	17 (4)	250 (39)	dns [†]	85 (2)	25 (4)	dns [†]
13	tert-Bu	0.47 (0.18)	3.8 (0.7)	48 (7)	8	9.9 (3.6)	240 (40)	dns [†]	83 (5)	42 (2)	dns [†]
14	F	0.11 (0.01)	3.0 (0.3)	9 (1)	27	1.6 (0.2)	97 (19)	>500	95 (2)	28 (3)	40 (1)
15	CF ₃	0.26 (0.10)	2.2 (0.7)	29 (10)	9	1.8 (0.9)	50 (14)	>500	70 (5)	42 (2)	18 (4)
16	Br	0.23 (0.14)	2.4 (0.8)	13 (1)	10	1.2 (0.5)	36 (18)	310 (95)	73 (3)	69 (4)	29 (1)

^a Binding affinities (K_i) were obtained by competitive displacement of radiolabeled [³H]-diprenorphine in membrane preparations. Functional data were obtained using agonist induced stimulation of [³⁵S]-GTPγS binding. Potency is represented as EC₅₀ (nM) and efficacy as percent maximal stimulation relative to standard agonist DAMGO (MOR), DPDPE (DOR), or U69,593 (KOR) at 10 μM. All values are expressed as the mean of three separate assays performed in duplicate with standard error of the mean in parentheses. dns = does not stimulate. † indicates n=2.

The alkyl and halogenated series generally showed potent, efficacious agonism at MOR and partial agonism at DOR. Additionally, most alkyl-substituted analogues showed no KOR activation, whereas the halogenated compounds were low-potency partial agonists at KOR. In terms of binding, the smallest C-8 substitutions (**9**, **10**, **14**, **15**, and **16**) maintained high affinity for MOR and moderately increased affinity for DOR relative to the unsubstituted lead peptidomimetic **1**. Conversely, larger C-8 substitutions (**11**, **12**, and **13**) slightly decreased MOR affinity and maintained the modest increase in DOR affinity. This alkyl/halo subset provided a range of MOR selectivity profiles between 5 and 30, though all analogues were partial DOR agonists.

Expanding upon the alkyl and halogen subsets, we synthesized a series of analogues featuring conjugated, aryl, and saturated heterocyclic substitutions, summarized in **Table 3**. The conjugated nitrile (**24**), furan (**17**), and benzofuran (**19**) analogues all favored MOR 10-fold or more, while the more flexible benzyl (**8**) and ethylphenyl (**18**) analogues displayed slightly better balance between MOR and DOR affinity. The flexible, saturated heterocycles offered little change in the MOR-selectivity profile compared to the lead compound **1**. In fact, analogues **28** and **30** were not only selective for MOR over DOR, but also displayed high affinity for KOR. Again, all analogues in this subset showed some DOR agonism, though these were generally less efficacious than the alkyl/halo subset. The lone outlier is the piperazine-Dmt analogue **31**, which showed no DOR efficacy. Generally, analogues in **Tables 2 & 3** showed only slight variation in binding affinities at MOR and DOR, yielding relatively flat SAR at the C-8 position. Even so, mild increases in DOR affinity paired with mild decreases in MOR affinity (as with compound **8**) can serve to provide promising improvements towards balancing MOR and DOR affinities.

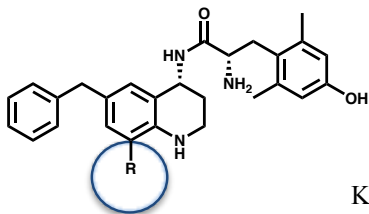


Table 3. Increasing Size of C-8 Substitution Moderately Decreases DOR Efficacy^a

#	C-8 R Group	K _i (nM)			DOR K _i /MOR K _i	EC ₅₀ (nM)			% stim		
		MOR	DOR	KOR		MOR	DOR	KOR	MOR	DOR	KOR
24	nitrile	0.16 (0.06)	2.3 (0.7)	7.3 (0.7)	14	1.3 (0.5)	188 (22)	>500 [†]	73 (6)	27 (6)	38 [†] (3)
17	3-furan	0.34 (0.08)	3.5 (0.6)	28 (6)	10	3.4 (0.3)	10 (4)	dns [†]	103 (5)	33 (5)	dns [†]
8	benzyl	1.0 (0.1)	1.6 (0.4)	23 (5)	2	4 (2)	380 (84)	dns	96 (4)	42 (7)	dns
18	ethylphenyl	0.37 (0.07)	1.4 (0.7)	27 (8)	4	44 (17)	33 (13)	dns [†]	78 (1)	15 (2)	dns [†]
19	2-benzofuran	3 (1)	71 (17)	>500	24	16 (7)	18 [†] (5)	dns [†]	101 (2)	13 [†] (2)	dns [†]
28	piperidine	0.07 (0.03)	4.4 (1.0)	0.93 (0.18)	63	2.3 (0.2)	27 (2)	100 (33)	93 (2)	31 (4)	30 (6)
29	morpholine	0.15 (0.04)	2.3 (0.7)	7.3 (1.4)	15	1.8 (0.4)	180 (47)	dns	96 (2)	29 (5)	dns
30	piperazine	0.35 (0.18)	15 (3)	1.9 (0.5)	43	8.2 (3.5)	290 (100)	170 (67)	60 (2)	18 (1)	17 (1)
31	piperazine-Dmt	0.31 (0.16)	2.6 (0.5)	7 (2)	20	5.9 (0.7)	dns [†]	dns	86 (8)	dns [†]	dns

^a Binding affinities (K_i) were obtained by competitive displacement of radiolabeled [³H]-diprenorphine in membrane preparations. Functional data were obtained using agonist induced stimulation of [³⁵S]-GTPγS binding. Potency is represented as EC₅₀ (nM) and efficacy as percent maximal stimulation relative to standard agonist DAMGO (MOR), DPDPE (DOR), or U69,593 (KOR) at 10 μM. All values are expressed as the mean of three separate assays performed in duplicate with standard error of the mean in parentheses. dns = does not stimulate. † indicates n=2.

As indicated by **18**, **19**, and **31**, it may be possible to achieve the MOR agonist/DOR antagonist profile by increasing the size of substituents at C-8. However, due to the already high polar surface area of the analogues in this subset, further increasing the size of substituents at C-8 seemed to offer diminishing returns.

It was discovered in the following subset (see **Table 4**) that incorporation of a simple carbonyl bond at C-8 achieved the desired MOR agonist/DOR antagonist functional profile.

Similar to the prior subsets, MOR selectivity persisted throughout **Table 4**. All analogues in this subset were less than 20-fold selective with four of the seven analogues displaying less than 10-fold MOR selectivity. MOR potency showed modest improvement over past subsets, with all analogues showing single-digit nanomolar EC₅₀ values. It is worth noting that the carbonyl C-8 substituents consistently reduced MOR and DOR efficacy despite having only limited effects on binding. Thus, despite the relatively flat binding SAR around C-8, modifications in this region show a distinct ability to reliably modulate efficacy at MOR and DOR.

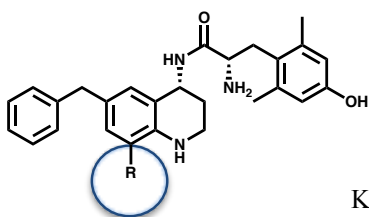


Table 4. Carbonyl Substituted C-8 Analogues Consistently Display Desired MOR Agonist/DOR Antagonist Profile^a

#	C-8 R Group	K _i (nM)			DOR K _i / MOR K _i	EC ₅₀ (nM)			% stim		
		MOR	DOR	KOR		MOR	DOR	KOR	MOR	DOR	KOR
20	dimethyl amide	0.23 (0.08)	1.3 (0.2)	80 (50)	6	9 (3)	dns	>500	58 (1)	dns	25 (4)
21	ethyl amide	0.20 (0.06)	1.8 (0.4)	25 (4)	9	2.1 (0.3)	dns	dns	56 (5)	dns	dns
22	benzyl amide	0.17 (0.03)	3.0 (0.4)	30 (2)	18	3.4 (1.4)	dns	dns	73 (5)	dns	dns
23	phenyl amide	0.32 (0.08)	5.4 (0.5)	29 (5)	17	1.2 (0.7)	dns	dns [†]	49 (4)	dns	dns [†]
25	carboxylic acid	0.47 (0.16)	2.4 (0.4)	210 (6)	5	4.4 (1.7)	dns	dns	67 (3)	dns	dns
26	ethyl ester	1.0 (0.3)	3.7 (0.3)	47 (2)	4	4.9 (0.3)	dns	dns [†]	71 (3)	dns	dns [†]
27	isopropyl ester	0.45 (0.06)	5.9 (0.6)	77 (12)	13	N/A	dns	dns	58 (1)	dns	dns

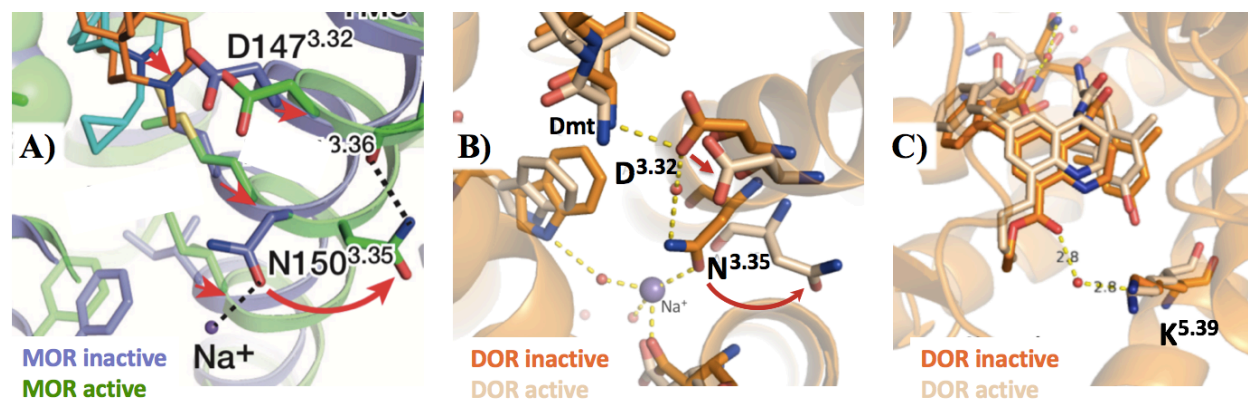
^a Binding affinities (K_i) were obtained by competitive displacement of radiolabeled [³H]-diprenorphine in membrane preparations. Functional data were obtained using agonist induced stimulation of [³⁵S]-GTPγS binding. Potency is represented as EC₅₀ (nM) and efficacy as percent maximal stimulation relative to standard agonist DAMGO (MOR), DPDPE (DOR), or U69,593 (KOR) at 10 μM. All values are expressed as the mean of three separate assays performed in duplicate with standard error of the mean in parentheses. dns = does not stimulate. † indicates n=2. The EC₅₀ of **27** is listed as N/A, as the potency values vary too widely to assert a meaningful numerical value.

Based on this diverse set of substitutions, it is apparent that the C-8 position tolerates a wide degree of variability in terms of binding. With few exceptions, most analogues display MOR affinity between 0.1 and 1.0 nM and DOR affinity ranging between 1.0 and 10 nM. KOR binding showed greater variability than MOR or DOR, with only the basic amines **28-31**, the nitrile **24**, and the fluoro analogue **14** displaying single-digit or sub-nanomolar affinity. The rigid, conjugated 2-benzofuran **19** and carboxylic acid **25** were both poorly tolerated. These results are consistent with computational models which show a non-conserved glutamate residue near C-8 in KOR which is likely to prefer nitrogenous substituents over acidic residues like **25**.

Despite the C-8 substitutions only having a minor effect on binding affinity at MOR and DOR, the carbonyl substitutions were functionally distinct from the alkyl, halo, aryl, or amino groups tested in this series. The carbonyl analogues all displayed less efficacy at MOR, DOR and KOR compared to other subsets, consistently affording the MOR agonist/DOR antagonist profile that had proven elusive in **Tables 1-3**. While insights gained from computational models are retrospective and have not been experimentally validated, the models *may* provide an indication as to why the carbonyl has proven effective at reducing efficacy across all three receptors. In **Fig. 11A** are the crystal structures of MOR bound to the antagonist β -FNA (MOR inactive, lavender) and the agonist BU72 (MOR active, green), adapted from Huang et al.⁴⁶ In **Fig. 11B** is an analogous view of DOR with the partial agonist ligand **12** (DOR active, tan) and antagonist **26** (DOR inactive, orange) docked. Labeled “Dmt” is the primary amine and carbonyl backbone of the Dmt moiety of each ligand. **Fig. 11C** shows the same ligands and coloring schemes with a face-on view of the THQ core and C-8 substitutions. The DOR models are based on agonist-bound and antagonist-bound crystal structures.^{40,106} Because of the 1.8 Å resolution of the antagonist-bound (inactive) receptor, stable water molecules were able to be placed within electron density

maps with high confidence. Some of these DOR-inactive water molecules were included in the **Fig. 11B** and **C** renderings, though these were not involved in the docking models for **12** and **26**.

Fig. 11. Crystallographic Models of MOR and DOR in Active and Inactive States with Partial DOR Agonist **12** (DOR Active) and Antagonist **26** (DOR Inactive) Computationally Docked^a

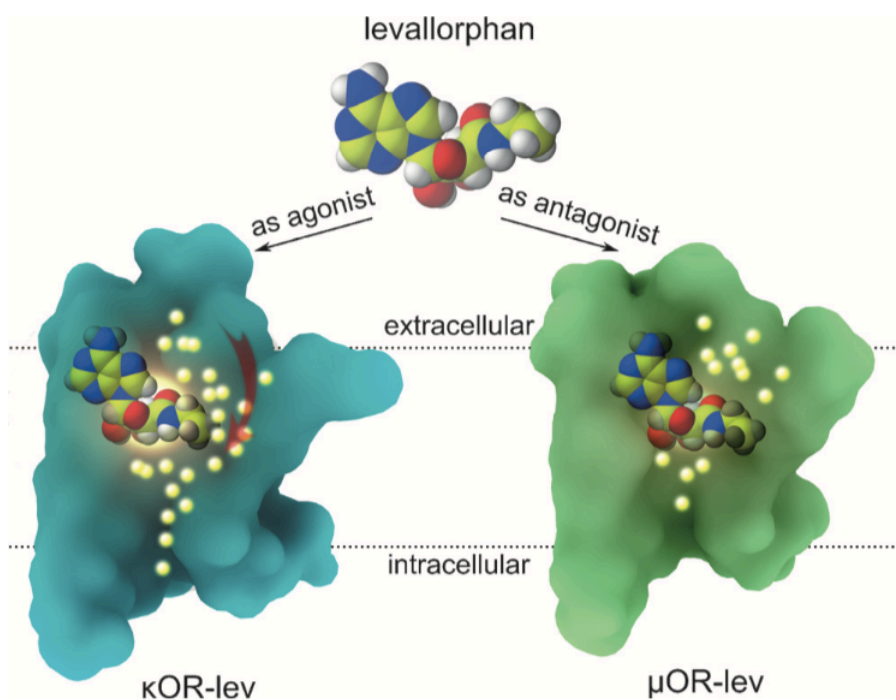


^aPanel A adapted from Huang et al, 2015. Panels B and C use models based on structures obtained by Granier et al, 2012 and Fenalti et al, 2014. Ligands **12** and **26** were docked by Ira Pogozeva.

As noted by the Kobilka group in **Fig. 11A** with a red curved arrow, the shift from the inactive (lavender) to the active (green) state involves a large rotation in residue N^{3.35} with a smaller translation of residue D^{3.32} away from the receptor core. **Fig. 11B** indicates a similar shift in residues N^{3.35} and D^{3.32} between inactive and active states. As described previously, a distinct water-mediated polar network in the core of the receptor is involved in the stabilization of either the active or inactive state for both MOR and DOR. In **Fig. 11B**, one can observe a network of hydrogen bonds that link residue D^{3.32} to N^{3.35} and a critical sodium ion, which is believed to be involved in stabilizing the inactive state of the receptor. Importantly, D^{3.32} is also critical to ligand binding. This residue forms a H-bond with the amine of morphinan ligands β -FNA and BU72 and the Dmt amine of ligands **12** and **26**. A shift in ligand binding toward helix 3 may push D^{3.32} away

from the core of the receptor, which would disrupt the water-mediated interaction with N^{3,35} and facilitate its outward swing. Through loss of this coordinating network and opening of the receptor core, the inactive-state sodium ion can more easily dissociate, allowing further solvation of the receptor's core, which is associated with the active state as proposed by Yuan et al (see **Fig. 12**).⁵²

Figure 12. Agonist-Bound GPCR Models Indicate Contiguous Solvation Through the Core of the Receptor While Antagonist-Bound Models Display Primarily Extracellular Solvation^a



^a Molecular dynamics simulation by Yuan et al. of agonist- and antagonist-bound receptor states, with water molecules depicted by yellow circles. The active-state KOR model indicates a channel of water molecules extending through the receptor core while the inactive-state MOR excludes water molecules primarily to the extracellular orthosteric site.⁵²

The view of analogues **12** and **26** in **Fig. 11C** allows one to scrutinize what effect C-8 may have in receptor activation. The *n*-butyl and ethyl ester groups are very similar in size and occupy similar positions in the binding pocket of DOR, but one can see that the partial agonist **12** sits

“higher” or more toward helix 3 than the antagonist **26**. Of note, the carbonyl in the C-8 position is predicted to bind near a conserved lysine residue in helix 5, K^{5.39}. Though it is out of range for a direct H-bond, a stable water observed in the inactive-state structure could mediate a polar interaction between the C-8 carbonyl and helix 5, preventing the “upward” shift toward helix 3 associated with activation. The decrease in efficacy across all three receptors further supports the proposal of a key interaction with a conserved residue such as K^{5.39}. Further mutagenesis studies would be needed to confirm this hypothesis, but these models suggest a potential mechanism by which ligand design could predictably modulate receptor activation.

As a caveat, it is worth noting that the changes observed in binding modes are relatively small (1.0 Å or less) and retrospective modeling is poorly suited for identifying causation. Additionally, though the carbonyl ligands are antagonists at DOR and KOR, they maintain efficacy at MOR despite the inactivating mechanism being conserved. This could be due to other minor differences in binding-site topography, but certainly merits further investigation. As such, these structural insights remain hypotheses and not experimental observations at present.

2.5 *In Vivo* Pharmacology

In addition to optimizing *in vitro* SAR, another key aim of this project was to test the effects that differing MOR selectivities had on *in vivo* tolerance and dependence. As such, only compounds that displayed an *in vivo* antinociceptive response could be evaluated in this context. To determine the antinociceptive effect of each compound following peripheral administration, compounds were tested in the mouse warm water tail withdrawal (WWTW) assay. Briefly, the WWTW assay measures the response to a noxious stimulus—submersion of part of the tail in 50°C

water—and whether latency to tail withdrawal increases in a dose-dependent manner after intraperitoneal (ip) administration of a test compound. Compounds were given at doses of 1.0, 3.2 and 10 mg/kg (cumulative) in 30-minute intervals. Fully efficacious compounds such as morphine reach the maximal possible effect (MPE) of a 20 s latency to tail withdrawal at 10 mg/kg. Compounds displaying less than a 10-second latency to tail withdrawal (<50% MPE) were considered not to stimulate an antinociceptive response *in vivo*, denoted as “dns” in **Table 5**.

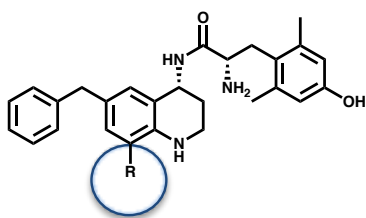


Table 5. Antinociceptive Activity in Mouse WWTW Assay Following Intraperitoneal Administration^a

Alkyl & Halo Analogues (from Table 2)			Conjugated & Cyclic Analogues (from Table 3)			Amide, Acid & Ester Analogues (from Table 4)		
#	C-8 R Group	% MPE	#	C-8 R Group	% MPE	#	C-8 R Group	% MPE
1	H	100	24	nitrile	dns	20	dimethyl amide	100
9	Me	100	17	3-furan	dns	21	ethyl amide	dns
10	Et	100	8	benzyl	dns	22	benzyl amide	dns
11	n-Pr	dns	18	ethylphenyl	dns	23	phenyl amide	---
12	n-Bu	100	19	2-benzofuran	100	25	carboxylic acid	dns
13	tert-Bu	60	28	piperidine	dns	26	ethyl ester	100
14	F	dns	29	morpholine	dns	27	isopropyl ester	100
15	CF ₃	dns	30	piperazine	---			
16	Br	50	31	piperazine-Dmt	dns			

^a Results from the mouse WWTW assay after cumulative dosing of test compound up to 10 mg/kg ip. Antinociceptive activity represented as percent maximum possible effect (% MPE), with MPE being a 20 s latency to tail withdrawal. Baseline tail withdrawal latency is ~5 s, or 25% MPE. “dns” indicates no stimulation of an antinociceptive response. “---” indicates the compound was not tested in the WWTW assay.

In the alkyl series, compounds **9**, **10** and **12** were fully efficacious, showing dose dependent antinociception and reaching the cutoff latency of 20 s at 10 mg/kg after intraperitoneal (ip) administration, whereas **11** showed no significant antinociceptive effect at the same dose. The *tert*-butyl analogue **13** was partially active *in vivo*, with a latency of 10 s at 10 mg/kg. The 2-benzofuran analogue **19** was the only analogue from **Table 3** to show any activity *in vivo*. The smaller conjugated analogues **24** and **17** as well as the larger substitutions including the cyclic amines **28** – **31** and aryl rings **8** and **18** produced no antinociception at the doses tested. Within the carbonyl series, the dimethyl amide analogue **20**, as well as the ethyl and isopropyl esters **26** and **27**, showed full antinociceptive activity. Of the bioactive analogues **9**, **10**, **12**, **19**, **20**, **26** and **27**, the duration of action for **12** and **26** proved to be the longest at 2.5 hours (**Table 6**). This is a modest improvement over the lead **1** (2 hours).

Table 6. Duration of Antinociceptive Action for C-8 Analogues^a

#	C-8 R Group	Duration (h)	#	C-8 R Group	Duration (h)
1	H	2.0	19	2-benzofuran	1.5
9	Me	1.5	20	dimethyl amide	2.0
10	Et	1.0	26	ethyl ester	2.5
12	n-Bu	2.5	27	isopropyl ester	1.5

^a Duration of action was determined by administering a 10 mg/kg bolus dose of test compound, then evaluating animals in the WWTW assay at 30-minute intervals until latency to tail withdrawal returned to baseline.

As shown in **Table 5**, most compounds in this series demonstrated no antinociceptive activity at the doses tested *in vivo*. While we cannot definitively attribute a loss of activity to any individual factor for all compounds in the series, typical physicochemical properties such as high molecular weight, lipophilicity, polar surface area, and hydrogen bond partners are likely to inhibit

membrane permeability and access to the CNS. Accordingly, our reported *in vivo* SAR was constrained to small C-8 modifications. Small alkyl and carbonyl substitutions were best correlated with *in vivo* antinociceptive activity, with **19** being a notable exception. However, the relatively small fluoro-substituted compounds (**14-16**) showed no activity *in vivo* at the doses tested, indicating pharmacokinetic obstacles besides polar surface area. Another pair of relatively low molecular weight analogues with differing *in vivo* effects, **21** and **26**, suggest other parameters affecting bioavailability. Although **21** and **26** are comparable in size, **21** features a hydrogen bond donating amide moiety, whereas **26** bears a more lipophilic ester functionality devoid of H-bond donating capacity. The added hydrogen bond donating amide may affect specific interactions with proteins that impact CNS access (e.g. active transporters, efflux proteins, metabolizing enzymes), or nonspecific parameters, including polarity, and by extension, passive membrane permeability. To test this hypothesis, the dimethylamide analogue **20** was synthesized and evaluated *in vivo*. The antinociceptive activity of **20** supported the idea that hydrogen bond donating ability and not polarity is a significant factor affecting bioavailability. Analogue **20** was the only bioavailable analogue in this series with a ClogP less than the lead compound (ClogP = 2.2 for **20** compared to 3.1 for **1**). Whether this indicates an *in vivo* preference for lipophilic ligands or is simply an artifact of the nature of the compounds explored in this series requires further exploration.

2.6 Conclusions

Comprehensive evaluation of this series of compounds suggests that C-8 carbonyl moieties block DOR activation quite effectively while bulky groups such as the 2-benzofuran, ethylphenyl, and piperazine attenuate DOR activation relative to smaller alkyl, aryl, and halogen-containing groups. We have previously shown that a bulky C-6 pendant interacts favorably with the active-

state MOR binding pocket, yet there is a steric clash between a large C-6 pendant and the analogous amino acid residues in the active-state DOR.^{83,89} We propose from our SAR analysis that the active-state binding pockets of MOR and DOR likely interact with the C-8 substitutions in a similar manner. Additionally, as previously proposed, computational models and SAR trends suggest that carbonyl moieties may participate in a conserved polar interaction with K^{5.39} which disfavors movement in the binding pocket towards transmembrane helix 3 and residue D^{3.32}, thus reducing opioid receptor activation. In MOR, this translates to reduced efficacy (between 50 and 75%) whereas DOR and KOR typically lose all activity, providing a new avenue toward the MOR agonist/DOR antagonist profile.

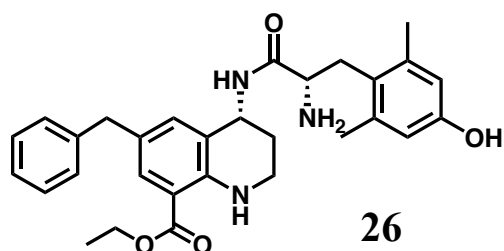
SAR at C-8 indicates that a wide range of substitutions at this position are fairly well tolerated. Though rigid substitutions such as the 2-benzofuran analogue **19** negatively impact binding affinity, modeling and SAR data suggest that flexible substitutions like the piperazine-Dmt moiety of **31** can flip into a solvent-exposed region of the receptors, leading to minimal impact on binding (see **Table 3**). Throughout this SAR campaign, we observed only slight changes in binding affinity at MOR and DOR, with most analogues binding MOR with 0.1 to 1.0 nM affinity and DOR with 1.0 to 10 nM affinity. As such, our ability to reliably modulate MOR selectivity was very limited. However, due to the fairly mild impact of C-8 substitutions on receptor binding, it was believed that solubilizing substituents such as the morpholine and piperazine rings might improve aqueous solubility and bioavailability. Those efforts were not met with the desired outcomes, as indicated by **Table 5**.

In terms of *in vivo* activity, it is apparent that C-8 can indeed be modified significantly (as with the 2-benzofuran analogue **19**) while maintaining antinociceptive activity. Seven of the

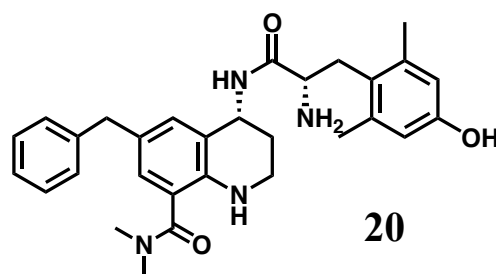
twenty-four analogues synthesized in this series displayed full antinociception, while two others were partially active. Generally speaking, small alkyl and aprotic acyl groups are best-tolerated for *in vivo* activity, whereas halogens, protic amides, and amines were less bioavailable. All of the seven analogues displaying robust antinociceptive activity were fairly short-acting, with a duration of action ranging between one and three hours. These bioavailable analogues span a range of MOR selectivity profiles—4, 5, 8, 13, 21, 22, and 24—all of which are more balanced than the lead peptidomimetic **1** with a 43-fold MOR selectivity profile. Further *in vivo* studies for tolerance and dependence are currently underway for the dimethyl amide **20**. However, despite its very poor aqueous solubility and high lipophilicity (ClogP = 4.3), the ethyl ester analogue **26** may also merit further study, as it displayed among the best potency (5 nM), lowest MOR selectivity (4-fold), longest duration of action (2.5 hours), and highest MOR efficacy (71% stimulation) within the MOR agonist/ DOR antagonist subset. Considering the propensity of esters to be hydrolyzed *in vivo*, **26** may act as a prodrug of the carboxylic acid analogue **25**. Fortunately, **25** shows an almost equally well-balanced MOR and DOR affinity profile while maintaining the MOR agonist/DOR antagonist profile. Additionally, cleavage to the carboxylic acid would boost selectivity over KOR from 50:1 to 450:1. Thus, despite the relatively unstable nature of the ester substitution, this moiety could still be useful in this specific context.

Highlights of analogues **20** and **26** are summarized in **Fig. 13**. It is worth noting the high equilibrium constant, K_e , measured for compound **26**. The K_e is used to approximate antagonist potency (the calculation for which can be found in the experimental procedures in section 2.7 of this chapter). While potency at MOR and DOR for **26** is 5- to 10-fold less than the observed affinities reported in **Table 4**, analogue **26** is still less than 10-fold selective for MOR by both affinity and potency metrics. The K_e has not yet been determined for analogue **20**.

Figure 13. Summary Profiles of MOR Agonist/DOR Antagonist Analogues **20** and **26**



MOR agonist (71% stim, $EC_{50} = 4.9$ nM)
DOR antagonist (<10% stim, $K_e = 43$ nM)
MOR/DOR selectivity: 4:1
MOR/KOR selectivity: 50:1
Full antinociceptive activity (100% MPE)
Duration of action = 2.5 h; ClogP = 4.3

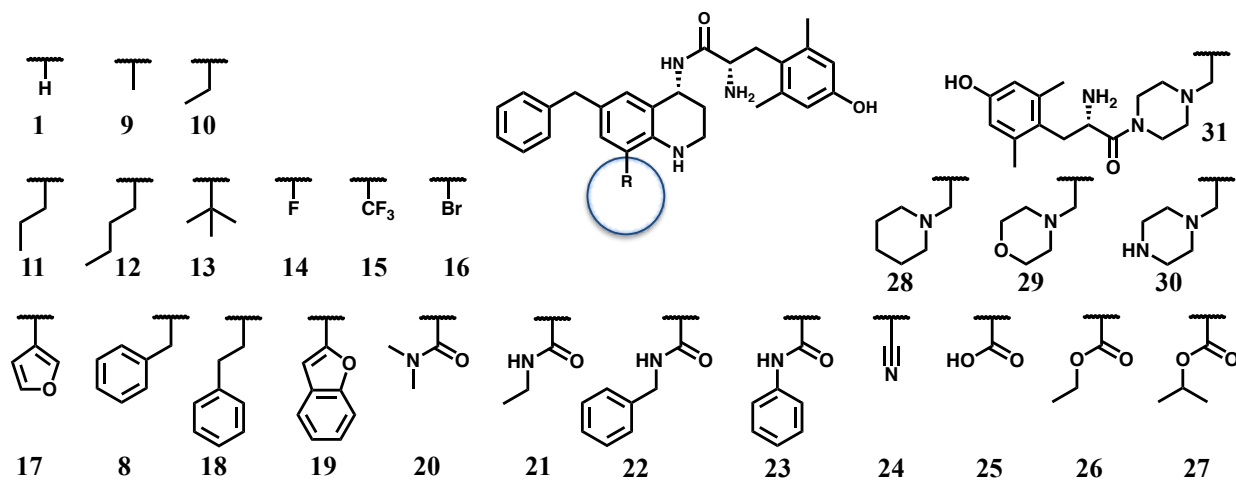


MOR agonist (58% stim, $EC_{50} = 9$ nM)
DOR antagonist (<10% stim), K_e not yet tested
MOR/DOR selectivity: 6:1
MOR/KOR selectivity: 350:1
Full antinociceptive activity (100% MPE)
Duration of action = 2.0 h; ClogP = 2.2

Going forward, the C-8 carboxylic acid could serve as a useful functionality for late-stage derivatization, facilitating further SAR exploration or probe development. Due to the limited impact on receptor binding, this position could be utilized in the development of multifunctional fluorescent probes, lysine-targeting covalent inhibitors,^{37,107} bivalent ligands,^{78,81} or receptor-mediated transport substrates.^{82,108–113} In fact, attempts were made toward developing a glucoserine-linked analogue (see Chapter 5 for further discussion); however, further methodological development is needed to bring this project to fruition. As illustrated, the C-8 position of the THQ scaffold has been instrumental in design and synthesis of bioavailable mixed-efficacy MOR agonist/DOR antagonist ligands, but also has significant room for further development. In Chapter 4, additional projects currently underway or proposed that focus on functionalizing the C-8 position (among others) will be discussed in greater detail.

2.7 Experimental Procedures

Figure 10. Final C-8 R Groups of Analogues **8-31** (replicated from above for convenience)



Materials and Methods	43
Purification & Characterization Methods	46
General Procedures	47
Compound 8 and Preceding Intermediates	53
Compound 9 and Preceding Intermediates	57
Compound 10 and Preceding Intermediates	60
Compound 11 and Preceding Intermediates	64
Compound 12 and Preceding Intermediates	68
Compound 13 and Preceding Intermediates	72
Compound 14 and Preceding Intermediates	76
Compound 15 and Preceding Intermediates	80
Compound 16 and Preceding Intermediates	84

Compound 17 and Preceding Intermediates	85
Compound 18 and Preceding Intermediates	88
Compound 19 and Preceding Intermediates	90
Compound 20 and Preceding Intermediates	92
Compound 21 and Preceding Intermediates	95
Compound 22 and Preceding Intermediates	97
Compound 23 and Preceding Intermediates	100
Compound 24 and Preceding Intermediates	102
Compound 25 and Preceding Intermediates	105
Compound 26 and Preceding Intermediates	107
Compound 27 and Preceding Intermediates	109
Compound 28 and Preceding Intermediates	112
Compound 29 and Preceding Intermediates	116
Compound 30 and Preceding Intermediates	119
Compound 31 and Preceding Intermediates	122

Cell Lines and Membrane Preparations

All tissue culture reagents were purchased from Gibco Life Sciences (Grand Island, NY, U.S.). C6-rat glioma cells stably transfected with a rat MOR (C6-MOR) or rat DOR (C6-DOR) and Chinese hamster ovary (CHO) cells stably expressing a human KOR (CHO-KOR) were used for all *in vitro* assays. Cells were grown to confluence at 37 °C in 5% CO₂ in Dulbecco's modified Eagle medium (DMEM) containing 10% fetal bovine serum and 5% penicillin/streptomycin. Membranes were prepared by washing confluent cells three times with ice cold phosphate buffered saline (0.9% NaCl, 0.61 mM Na₂HPO₄, 0.38 mM KH₂PO₄, pH 7.4). Cells were detached from the plates by incubation in warm harvesting buffer (20 mM HEPES, 150 mM NaCl, 0.68 mM EDTA, pH 7.4) and pelleted by centrifugation at 1600 rpm for 3 min. The cell pellet was suspended in ice-cold 50 mM Tris- HCl buffer, pH 7.4, and homogenized with a Tissue Tearor (Biospec Products, Inc., Bartlesville, OK, U.S.) for 20 s. The homogenate was centrifuged at 15,000 rpm for 20 min at 4°C. The pellet was rehomogenized in 50 mM Tris-HCl with a Tissue Tearor for 10 s, followed by recentrifugation. The final pellet was resuspended in 50 mM Tris-HCl and frozen in aliquots at 80°C. Protein concentration was determined via a BCA protein assay (Thermo Scientific Pierce, Waltham, MA, U.S.) using bovine serum albumin as the standard.

Radioligand Competition Binding Assays

Radiolabeled compounds were purchased from Perkin-Elmer (Waltham, MA, U.S.). Opioid ligand binding assays were performed by competitive displacement of 0.2 nM [³H]-diprenorphine (250 μCi, 1.85 TBq/mmol) by the peptidomimetic from membrane preparations containing opioid receptors as described above. The assay mixture, containing membranes (20 μg protein/tube) in 50 mM Tris-HCl buffer (pH 7.4), [³H]-diprenorphine, and various concentrations of test peptidomimetic, was incubated at room temperature on a shaker for 1 h to allow binding to reach

equilibrium. Samples were rapidly filtered through Whatman GF/C filters using a Brandel harvester (Brandel, Gaithersburg, MD, U.S.) and washed three times with 50 mM Tris-HCl buffer. Bound radioactivity on dried filters was determined by liquid scintillation counting, after saturation with EcoLume liquid scintillation cocktail, in a Wallac 1450 MicroBeta (Perkin-Elmer, Waltham, MA, U.S.). Nonspecific binding was determined using 10 μ M naloxone. The results presented are the mean \pm standard error (S.E.M.) from at least three separate assays performed in duplicate. K_i (nM) values were calculated using nonlinear regression analysis to fit a logistic equation to the competition data using GraphPad Prism, version 6.0c (GraphPad Software Inc., La Jolla, CA).

[³⁵S]-GTP γ S Binding Assays

Agonist stimulation of [³⁵S]guanosine 5'-O-[γ -thio]triphosphate [³⁵S]-GTP γ S, 1250 Ci, 46.2 TBq/mmol) binding to G protein was measured as described previously.¹¹⁴ Briefly, membranes (10–20 μ g of protein/tube) were incubated for 1 h at 25°C in GTP γ S buffer (50 mM Tris-HCl, 100 mM NaCl, 5 mM MgCl₂, pH 7.4) containing 0.1 nM [³⁵S]-GTP γ S, 30 μ M guanosine diphosphate (GDP), and varying concentrations of test peptidomimetic. G protein activation following receptor activation with peptidomimetic was compared with 10 μ M of the standard compounds [D-Ala²,N-MePhe⁴,Gly-ol]enkephalin (DAMGO) at MOR, D-Pen²,5-enkephalin (DPDPE) at DOR, or U69,593 at KOR. The reaction was terminated by vacuum filtration of GF/C filters that were washed 10 times with GTP γ S buffer. Bound radioactivity was measured as previously described. The results are presented as the mean \pm standard error (S.E.M.) from at least three separate assays performed in duplicate; potency (EC₅₀ (nM)) and percent stimulation were determined using nonlinear regression analysis with GraphPad Prism, as above.

K_e Determination

Agonist stimulation of [³⁵S]-GTPγS binding by the known standard agonist SNC80 at DOR was measured as described above. This was then compared to [³⁵S]-GTPγS binding stimulated by SNC80 in the presence of test compound (1000 nM). Both conditions produced 100% stimulation relative to SNC80. The difference between the EC₅₀ of SNC80 alone and in the presence of test antagonist is the shift in concentration response. The K_e was then calculated as $K_e = (\text{concentration of compound}) / (\text{concentration response shift} - 1)$. The results presented are the mean from at least three separate assays performed in duplicate.

In Vivo Drug Preparation

All compounds were administered by intraperitoneal (ip) injection in a volume of 10 mL/kg of body weight. Test compounds were dissolved in 5% DMSO (v/v) in sterile saline (0.9% NaCl w/v).

Animals

Male C57BL/6 wild type mice (Stock number 000664, Jackson Laboratory, Sacramento CA, USA) bred in-house from breeding pairs and weighing between 20-30 g at 8-16 weeks old, were used for behavioral experiments. Mice were group-housed with free access to food and water at all times. Experiments were conducted in the housing room, maintained on a 12 h light/dark cycle with lights on at 7:00 am; all experiments were conducted during the light cycle. Studies were performed in accordance with the University of Michigan Committee on the Use and Care of Animals and the Guide for the Care and Use of Laboratory Animals (National Research Council, 2011 publication).

Antinociception

Antinociceptive effects were evaluated in the mouse WWTW assay. Withdrawal latencies were determined by briefly placing a mouse into a cylindrical plastic restrainer and immersing 2-3 cm

of the tail tip into a water bath maintained at 50°C. The latency to tail withdrawal or rapidly flicking the tail back and forth was recorded with a maximum cutoff time of 20 s to prevent tissue damage. Antinociceptive effects were determined using a cumulative dosing procedure. Each mouse received an injection of saline *ip* and then 30 min later baseline withdrawal latencies were recorded. Following baseline determinations, cumulative doses of each test compound (1, 3.2, and 10 mg/kg) were given *ip* at 30 min intervals. Thirty min after each injection, the tail withdrawal latency was measured as described above. To determine the duration of antinociceptive action, baseline latencies were determined as described above. Thirty minutes after baseline determination, animals were given a 10 mg/kg bolus injection of test compound *ip*. Latency to tail withdrawal was then determined at 5, 15, and 30 min after injections, and every 30 min thereafter until latencies returned to baseline values.

HPLC Purification

Purification of final compounds was performed using a Waters semipreparative HPLC with a Vydac protein and peptide C18 reverse phase column, using a linear gradient of 0% solvent B (0.1% TFA in acetonitrile) in solvent A (0.1% TFA in water) to 100% solvent B in solvent A at a rate 1% per minute, monitoring UV absorbance at 230 nm.

Compound Characterization

Final compounds were characterized by ¹H NMR, electrospray ionizing mass spectrometry (ESI-MS), and HPLC retention time. ¹H NMR data for final compounds were obtained on a 500 MHz Varian spectrometer using CD₃OD as the solvent. ESI-MS was obtained using an Agilent 6130 LC-MS mass spectrometer in positive ion mode. The retention time and purity of final compounds were assessed using a Waters Alliance 2690 analytical HPLC instrument with a Vydac protein and

peptide C18 reverse phase column. Retention times were obtained by running a linear gradient starting at 0% solvent B (99.9% acetonitrile, 0.1% TFA) and 100% solvent A (99.9% water, 0.1% TFA) to 70% solvent B and 30% solvent A in 70 min, measuring UV absorbance at 230 nm. All final compounds used for testing were $\geq 95\%$ pure, as determined by analytical HPLC. Intermediate compounds were characterized by ^1H and ^{13}C NMR on a Varian 500 MHz or 400 MHz NMR instrument.

Synthesis – General Procedures

General Procedure (A): Schotten-Bauman Acylation of a Commercially Available Aniline

Starting Material. To a flame-dried round-bottom flask under Ar atmosphere was added aniline starting material (1.00 eq), followed by dichloromethane, then K_2CO_3 (1.2-3.0 eq.). After 10 minutes, 3-bromopropionyl chloride (1.05 eq) was added slowly via syringe. Reaction was monitored by TLC in 40% ethyl acetate, 60% hexanes. Ninhydrin stain was used to help monitor disappearance of aniline starting material. After 1-3 h, reaction was quenched with deionized water. Organics were separated and dried over MgSO_4 , then filtered and concentrated under vacuum. Product was purified by crystallization or, when necessary, column chromatography.

General Procedure (B): Intramolecular β -Lactam Cyclization.

To a flame-dried round-bottom flask under Ar atmosphere was added sodium *tert*-butoxide (1.05 eq) followed by anhydrous DMF, then stirred 10 min before slowly adding a solution of acyl bromide intermediate from step A (1.00 eq) dissolved in DMF at ambient temperature via syringe. Monitored reaction by TLC in 40% ethyl acetate, 60% hexanes. Desired product showed a moderate decrease in R_f relative to starting material. After stirring 1-3 h, reaction mixture was concentrated under vacuum, then resuspended in dichloromethane or ethyl acetate. Extracted reaction mixture with deionized water

and aqueous sodium bicarbonate, then separated organics and dried over MgSO₄. Filtered and reconcentrated organics onto silica, then purified by flash chromatography.

General Procedure (C): Fries Rearrangement to Synthesize the THQ Core. To a round-bottom flask containing β -lactam intermediate (1 eq) dissolved in dichloroethane under inert atmosphere was slowly added TfOH (3 eq). After 1 hour, TLC in 40% ethyl acetate, 60% hexanes showed a decrease in R_f. Reaction was quenched with deionized water and neutralized with K₂CO₃, then diluted with dichloromethane. Separated organics and dried over MgSO₄, then filtered and concentrated organics onto silica and purified by flash chromatography.

General Procedure (D): Aryl Bromination of THQ Core. To a round-bottom flask containing THQ intermediate (1.00 eq), dissolved in dichloromethane under inert atmosphere was added *N*-bromosuccinimide (1.05 eq) at ambient temperature. After 30 minutes, TLC in 40% ethyl acetate, 60% hexanes showed complete conversion. Reaction was reconcentrated onto silica and was purified by flash chromatography.

General Procedure (E): Suzuki Copuling of Aryl Bromide to Boronic Acid Pinacol Ester. To a round-bottom flask under Ar atmosphere was added 3:1 acetone/water and stirred under vacuum for 10 minutes. Next, Ar was bubbled through solvent for an additional 10 minutes before adding aryl bromide intermediate (1.0 eq), boronic acid (1.2-2.0 eq), K₂CO₃ (3 eq) and Pd(dppf)Cl₂ (0.1 eq). Reaction was heated to 80°C for 6-12 hours, after which the reaction mixture was cooled and diluted with ethyl acetate and aqueous NaHCO₃. Organics were separated and dried over MgSO₄, then filtered and concentrated *in vacuo* onto silica. Product was purified by silica chromatography.

General Procedure (F): Reductive Amination of 6-benzyl-8-R-THQ Ketone to Sulfinamide Using Ellman's Sulfinamide. To a round bottom flask already containing desiccated THQ

intermediate (1.0 eq) under Ar atmosphere was added (R)-2-methylpropane-2-sulfinamide (3.0 eq). Meanwhile, a reflux condenser was flame-dried under vacuum, and then flooded with Ar. Next, anhydrous THF (5-10 mL) was added to the reaction vessel containing starting reagents via syringe. The round bottom flask was placed in an ice bath and allowed to equilibrate to 0°C. Next, Ti(OEt)₄ (6.0 eq) was added slowly via syringe. Once addition was complete, the reaction vessel was taken out of ice bath and placed in oil bath at 70°C-75°C, affixed condenser, and stirred for 16-48 h under Ar. The reaction was monitored by TLC for loss of ketone. Once sufficient conversion to the tert-butanefulfinyl imine was observed, reaction vessel was taken out of oil bath and cooled to ambient temperature. Meanwhile, an additional round bottom flask was flame-dried under vacuum, then flooded with Ar. NaBH₄ (6.0 eq) was added quickly, and anhydrous THF was added (5-10 mL). The round bottom flask was placed in dry ice/acetone bath and allowed to equilibrate to -78°C. Contents from the round bottom flask containing the imine intermediate were transferred to round bottom flask containing NaBH₄ via cannula. Imine-containing flask was washed twice with minimal THF, which was also transferred to reducing flask via cannula under Ar. Once contents were completely added, the reaction was taken out of dry ice/acetone bath and was allowed to warm to room temperature. The reaction stirred at ambient temperature for 2-3 h. To quench, sat. NaCl solution was added. Reaction mixture was diluted with ethyl acetate and DI H₂O and separated, washing with H₂O until both layers were clear, indicating sufficient removal of titanium oxide by-product. Organics were then isolated and dried over MgSO₄ and filtered through a fritted funnel. Organic extract was then concentrated onto silica and purified by silica chromatography.

General Procedure (G): Conversion of Sulfinamide to Final Compound. Step 1: To a round bottom flask containing sulfinamide (1.0 eq) was added 1,4-dioxane, followed by conc. HCl (6.0

eq), cleaving the sulfinamide to the primary amine. The reaction stirred at r.t. for up to 3 h. Solvent was removed under reduced, and residue was re-suspended in Et₂O. The resultant white solid precipitate (the HCl salt of the amine) was isolated by decanting and washing with Et₂O up to three times. After desiccation, the solid residue was used without further purification. **Step 2:** To a pear-shaped flask under inert atmosphere containing amine salt (1.0 eq) was added di-Boc-Dmt (1.1 eq), PyBOP (1.1 eq), and, when specified, 6-Cl HOBt (1.1 eq), followed by DMF and DIPEA (10 eq) at ambient temperature. After stirring for 6 hours, solvent was removed under reduced pressure and residual oil was loaded onto silica. Boc-protected intermediate was purified by silica chromatography but was generally not characterized by NMR. **Step 3:** Boc-protected intermediate was suspended in DCM (10 mL), then TFA (3-5 mL) was added. After 1 hour, solvent was removed under vacuum. Product was resuspended in a solution of 99.9% acetonitrile, 0.1% TFA, then diluted with deionized water. Final products were purified by reverse-phase semi-preparative HPLC. Final yield not calculated.

General Procedure (H): Palladium-Catalyzed Carbonylation of Aryl Bromide. For a schematic of the apparatus, see the synthesis of **Compound 20**. To a flame-dried 2-necked round-bottom flask under Ar atmosphere was affixed a condenser to the verticle neck. Through the angled neck was added degassed, Ar-sparged 4:1 DMF/H₂O (or alcohol in place of water) and stir bar. Next, 6-benzyl-8-bromo-THQ intermediate (1 eq), K₂CO₃ (1.5 eq) and Pd(dppf)Cl₂ (0.1 eq) were added to the stirring solution. To a separate 30 mL pressure tube under Ar atmosphere was added 2M NaOH (15 mL), then evacuated, flushed with Ar, and bubbled Ar through base solution for 15 min. A cannula was added from the septum of the pressure tube leading into the reaction solution, and a vent was placed in the condenser septum. To the bottom of the tube containing stirring base solution was added, via syringe, oxalyl chloride (1 mL in aliquots of 0.1 to 0.2 mL). Carbon

monoxide generated *in situ* from the decomposition of oxalyl chloride bubbled through the vented reaction mixture 10 minutes. This process was repeated twice more at 30 minute intervals. Vent was replaced with a balloon filled with CO, and heated at 70-80°C for 6-10 hours, monitored by TLC. When TLC indicated conversion of starting material to new product, reaction was cooled to ambient temperature and reaction solvents were removed under vacuum. Residual oil was resuspended in ethyl acetate and water, and acid/base extraction was performed. Organics were isolated, dried with MgSO₄, filtered, and reconcentrated onto silica *in vacuo*. Reaction was purified by flash chromatography.

General Procedure (I): Amine Substitution of Benzylic Bromide. To a pear-shaped flask containing 6-benzyl-8-carboxylate-THQ intermediate (1.0 eq) dissolved in DMF under inert atmosphere was added PyBOP (1.2 eq), amine (1.2 eq) and DIPEA (5-10 eq), then stirred at ambient temperature. Reaction was monitored by TLC. After 3-12 hours, solvent was removed under reduced pressure and reconcentrated residue onto silica *in vacuo*. Purified by flash chromatography. Product was highly fluorescent under long-wave UV (285 nm) light.

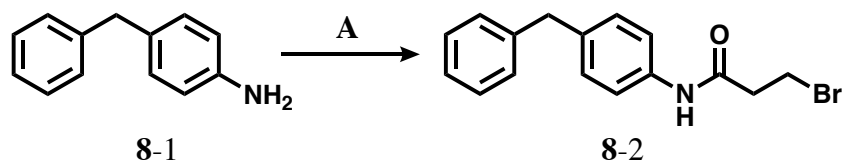
General Procedure (J): *N*-Trifluoroacetylation of the THQ core. To a round-bottom flask containing 6-bromo-8-methyl-THQ intermediate (1.0 eq) under Ar atmosphere was added DCM. Reaction flask was then cooled to 0°C before adding Et₃N (1.2 eq), followed by trifluoroacetic anhydride (1.2 eq). When starting material showed complete conversion to product by TLC, solvent was removed under reduced pressure and reaction residue was purified by silica chromatography.

General Procedure (K): Benzylic Bromination of the C-8 Methyl Group. To a round-bottom flask containing (1.00 eq) under Ar atmosphere was added degassed, Ar-sparged CCl₄, followed

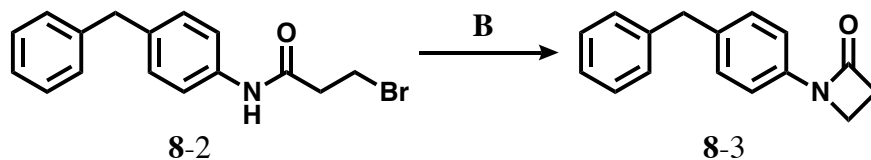
by N-bromosuccinimide (1.05 eq) and benzoyl peroxide (0.1 eq). Reaction was then heated to reflux, monitored by TLC. Quantitative conversion of starting material was generally not observed, so reaction was halted when side-product began to form. Reaction was halted by cooling to -20°C , and precipitate was filtered from solution (washing with additional cold CCl_4). Filtrate was then concentrated onto silica and purified by silica chromatography.

General Procedure (L): Substitution of Benzylic Bromide with Amine Heterocycle. To a round-bottom flask under inert atmosphere was added DMF, followed by K_2CO_3 (1.2 eq) and amine (1.2 eq), then benzylic bromide (1.0 eq) stirring at ambient temperature. After 6-12 hours, solvent was removed under reduced pressure and residual oil was resuspended in ethyl acetate and sat. NaHCO_3 . Organics were separated and dried over MgSO_4 , then filtered and concentrated *in vacuo* onto silica. Product was purified by silica chromatography.

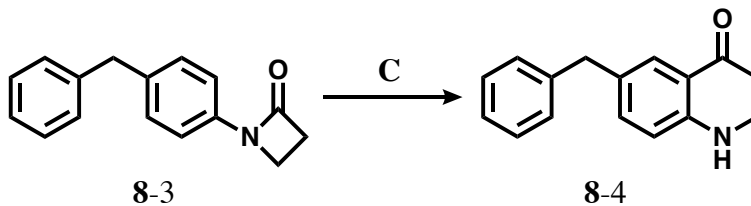
Compound 8 (Notebook name: AFN-4)



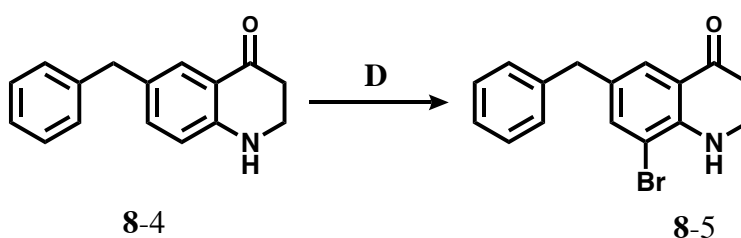
8-2. *N*-(4-benzylphenyl)-3-bromopropanamide. **8-2** was synthesized following **General Procedure (A)** from 4-benzylaniline **8-1** (3.65 g, 19.92 mmol, 1.00 eq), K_2CO_3 (3.56 g, 25.78 mmol, 1.30 eq), and 3-bromopropionyl chloride (2.11 mL, 20.91 mmol, 1.05 eq). Yield: 6.37 g, 100%. ^1H NMR (500 MHz, CDCl_3) δ 7.43 (d, $J = 8.3$ Hz, 2H), 7.29 (d, $J = 7.5$ Hz, 1H), 7.20 (d, $J = 7.3$ Hz, 1H), 7.16 (dd, $J = 7.9, 5.8$ Hz, 4H), 3.95 (s, 2H), 3.71 (t, $J = 6.6$ Hz, 2H), 2.92 (t, $J = 6.6$ Hz, 2H).



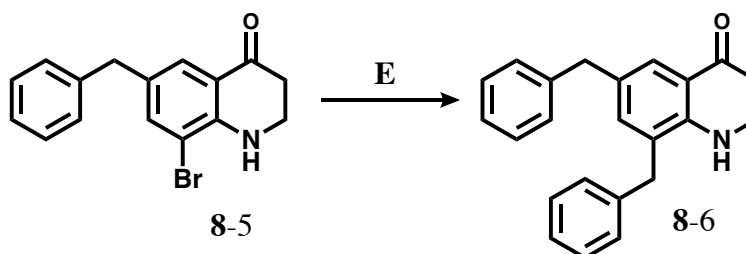
8-3. *1*-(4-benzylphenyl)azetidin-2-one. **8-3** was synthesized following **General Procedure (B)** from **8-2** (6.37g, 20.02 mmol, 1.00 eq) and NaOtBu (2.02 g, 21.02 mmol, 1.05 eq). Yield: 4.25 g, 90%. ^1H NMR (500 MHz, CDCl_3) δ 7.29 (d, $J = 8.1$ Hz, 3H), 7.20 (d, $J = 7.3$ Hz, 1H), 7.16 (d, $J = 8.0$ Hz, 4H), 3.95 (s, 2H), 3.60 (t, $J = 4.5$ Hz, 2H), 3.10 (t, $J = 4.5$ Hz, 2H).



8-4 6-benzyl-2,3-dihydroquinolin-4(1H)-one. **8-4** was synthesized following **General Procedure (C)** from **8-3** (3.75 g, 15.80 mmol, 1 eq) and TfOH (4.18 mL, 47.40 mmol, 3 eq). Yield: 3.34 g, 90%. ¹H NMR (500 MHz, CDCl₃) δ 7.72 (d, *J* = 2.1 Hz, 1H), 7.30 – 7.23 (m, 2H), 7.20 – 7.15 (m, 3H), 7.12 (dd, *J* = 8.4, 2.2 Hz, 1H), 6.60 (d, *J* = 8.4 Hz, 1H), 4.34 (s, 1H), 3.86 (s, 2H), 3.54 (td, *J* = 7.1, 2.0 Hz, 2H), 2.68 (t, *J* = 6.9 Hz, 2H). ¹³C NMR (126 MHz, CDCl₃) δ 193.92, 150.73, 141.35, 136.19, 130.89, 128.86, 128.59, 127.37, 126.18, 119.34, 116.35, 77.16, 42.53, 41.08, 38.30.

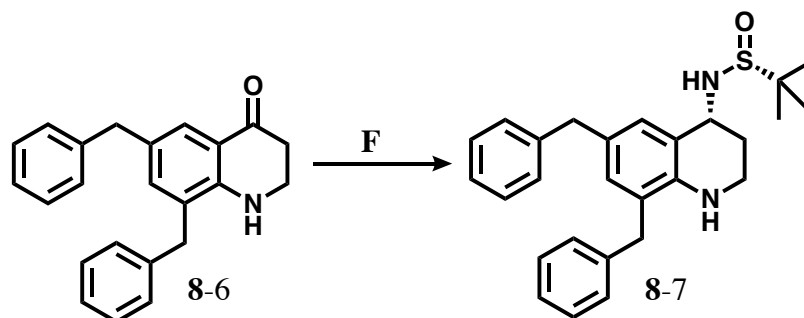


8-5 6-benzyl-8-bromo-2,3-dihydroquinolin-4(1H)-one. **8-5** was synthesized following **General Procedure (D)** from **8-4** (501 mg, 2.11 mmol, 1.00 eq) and NBS (375 mg, 2.11 mmol, 1.00 eq). Yield: 640 mg, 96%. ¹H NMR (500 MHz, CDCl₃) δ 7.70 (d, *J* = 2.0 Hz, 1H), 7.40 (d, *J* = 2.0 Hz, 1H), 7.27 (t, *J* = 7.5 Hz, 2H), 7.22 – 7.17 (m, 1H), 7.15 (d, *J* = 7.5 Hz, 2H), 4.89 (s, 1H), 3.83 (s, 2H), 3.60 (td, *J* = 7.2, 2.1 Hz, 2H), 2.69 (t, *J* = 6.9 Hz, 2H). ¹³C NMR (126 MHz, CDCl₃) δ 193.10, 147.40, 140.62, 138.57, 131.31, 128.81, 128.70, 127.07, 126.41, 120.28, 110.32, 77.16, 41.92, 40.75, 37.55.

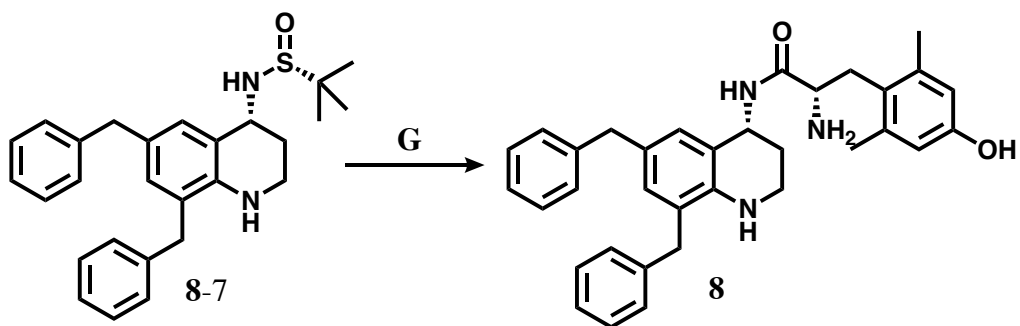


8-6 6,8-dibenzyl-2,3-dihydroquinolin-4(1H)-one. **8-6** was synthesized following **General Procedure (E)** from **8-5** (236 mg, 0.75 mmol, 1 eq), benzyl boronic acid pinacol ester (0.50 mL,

2.24 mmol, 2 eq), K₂CO₃ (310 mg, 2.24 mmol, 3 eq) and Pd(dppf)Cl₂ (55 mg, 0.08 mmol, 0.1 eq). Yield: Yield: 210 mg, 86%. ¹H NMR (500 MHz, CDCl₃) δ 7.72 (d, *J* = 2.0 Hz, 1H), 7.34 – 7.24 (m, 5H), 7.19 (dd, *J* = 7.7, 4.7 Hz, 3H), 7.14 (d, *J* = 7.5 Hz, 2H), 7.07 (d, *J* = 2.1 Hz, 1H), 4.20 (s, 1H), 3.89 (s, 2H), 3.86 (s, 2H), 3.43 (t, *J* = 7.0 Hz, 2H), 2.63 (t, *J* = 7.2 Hz, 2H). ¹³C NMR (126 MHz, CDCl₃) δ 194.17, 149.04, 141.42, 138.31, 137.54, 130.25, 128.99, 128.85, 128.60, 128.32, 126.91, 126.20, 126.16, 125.69, 119.86, 42.25, 41.13, 37.92, 37.68.

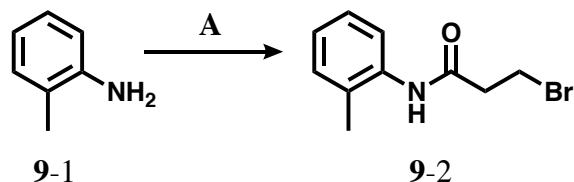


8-7. (*R*)-*N*-((*R*)-6,8-dibenzyl-1,2,3,4-tetrahydroquinolin-4-yl)-2-methylpropane-2-sulfonamide. **8-7** was synthesized following **General Procedure (F)** from **8-6** (70 mg, 0.21 mmol, 1 eq), (*R*)-2-methyl-2-propanesulfonamide (104 mg, 0.86 mmol, 4 eq), and Ti(OEt)₄ (0.27 mL, 1.28 mmol, 6 eq), then NaBH₄ (50 mg, 1.28 mmol, 6 eq). Yield: 38 mg, 41%. ¹H NMR (500 MHz, CDCl₃) δ 7.31 – 7.21 (m, 4H), 7.21 – 7.11 (m, 5H), 7.06 (d, *J* = 2.0 Hz, 1H), 6.81 (d, *J* = 2.0 Hz, 1H), 4.57 – 4.48 (m, 1H), 3.84 (d, *J* = 3.0 Hz, 2H), 3.77 (s, 2H), 3.25 (td, *J* = 11.8, 2.7 Hz, 1H), 3.15 (dt, *J* = 11.7, 3.9 Hz, 1H), 2.07 – 1.97 (m, 1H), 1.81 (tt, *J* = 13.2, 3.9 Hz, 1H), 1.19 (s, 9H). ¹³C NMR (126 MHz, CDCl₃) δ 141.97, 141.31, 139.10, 131.26, 129.81, 129.21, 128.81, 128.75, 128.53, 128.46, 126.50, 125.91, 124.70, 121.02, 77.16, 55.42, 49.86, 41.15, 37.88, 36.68, 28.28, 22.76.

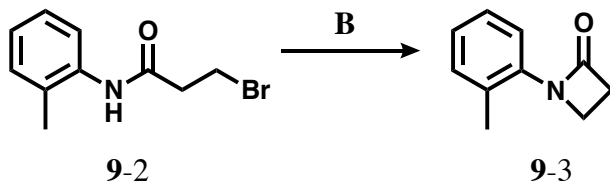


8. *(S)*-2-amino-*N*-((*R*)-6,8-dibenzyl-1,2,3,4-tetrahydroquinolin-4-yl)-3-(4-hydroxy-2,6-dimethylphenyl)propanamide. **8** was synthesized following **General Procedure (G)** from **8-7** (26 mg, 0.06 mmol, 1 eq) and concentrated HCl (0.12 mL, excess). Carried forward without further purification or characterization. **Step 2:** Performed amide coupling using **8-7** amine salt (22 mg, 0.06 mmol, 1 eq), di-Boc-Dmt (33 mg, 0.078 mmol, 1.3 eq), PyBOP (42 mg, 0.078 mmol, 1.3 eq), and 6-Cl HOBt (14 mg, 0.078 mmol, 1.3 eq), and DIPEA (0.13 mL, 0.71 mmol, 12 eq). **Step 3:** Boc-protected with TFA as described in **General Procedure (G)**. Final products were purified by reverse-phase semi-preparative HPLC. Final yield not calculated. ^1H NMR (500 MHz, Methanol- d_4) δ 8.20 (dd, $J = 8.0, 2.7$ Hz, 1H), 7.27 – 7.21 (m, 2H), 7.21 – 7.15 (m, 3H), 7.08 (ddd, $J = 23.4, 11.4, 7.1$ Hz, 5H), 6.90 (d, $J = 3.0$ Hz, 1H), 6.71 (d, $J = 2.7$ Hz, 1H), 6.47 (d, $J = 2.3$ Hz, 2H), 5.02 – 4.97 (m, 1H), 3.86 (dt, $J = 11.5, 3.6$ Hz, 1H), 3.78 (s, 2H), 3.76 (s, 2H), 3.24 (td, $J = 12.5, 11.4, 1.9$ Hz, 1H), 3.09 (dt, $J = 12.4, 4.1$ Hz, 1H), 3.02 (dt, $J = 13.9, 3.4$ Hz, 1H), 2.55 (t, $J = 12.0$ Hz, 1H), 2.26 (s, 6H), 1.75 (ddt, $J = 17.8, 10.7, 3.3$ Hz, 1H), 1.51 (dd, $J = 12.9, 5.4$ Hz, 1H). HPLC (gradient A): retention time = 44.3 min. ESI-MS 520.3[M + H] $^+$ and 542.3 [M + Na] $^+$.

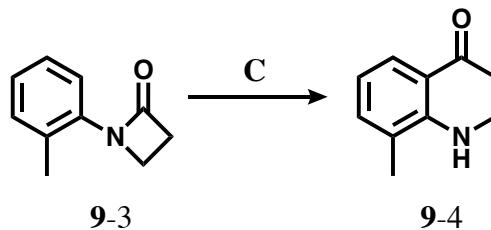
Compound 9 (Notebook reference: AFN-18 or afn-iv-75, notebook 4 p. 75)



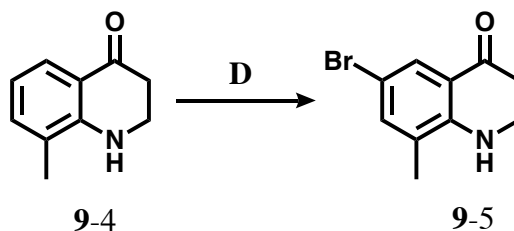
9-2. 3-bromo-N-(o-tolyl)propanamide. **9-2** was synthesized following **General Procedure (A)** from *o*-toluidine **10-1** (1.00 g, 5.38 mmol, 1.00 eq), K₂CO₃ (2.23 g, 16.14 mmol, 3.00 eq) and 3-bromopropionyl chloride (0.57 mL, 5.64 mmol, 1.05 eq). Yield: 1.72 g, 100%. ¹H NMR (500 MHz, CDCl₃) δ 7.57 (d, *J* = 7.6 Hz, 2H), 7.16 (d, *J* = 7.5 Hz, 2H), 7.08 (t, *J* = 7.5 Hz, 1H), 3.66 (t, *J* = 6.5 Hz, 2H), 2.91 (t, *J* = 6.5 Hz, 2H), 2.22 (s, 3H). ¹³C NMR(126 MHz, CDCl₃) δ 168.64, 135.16, 130.76, 130.64, 126.63, 126.03, 124.38, 40.21, 27.57, 18.02.



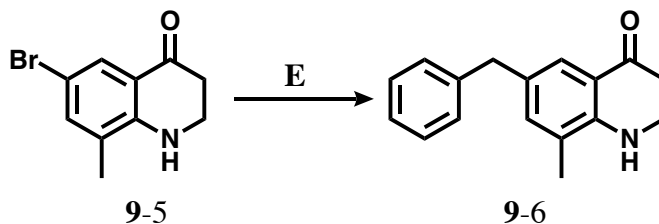
9-3. 1-(o-tolyl)azetidin-2-one. **9-3** was synthesized following **General Procedure (B)** from **9-2** (1.72 g, 5.36 mmol, 1.00 eq) and NaOtBu (540 mg, 5.63 mmol, 1.05 eq). Yield: 1.18 g, 92%. ¹H NMR (500 MHz, CDCl₃) δ 7.28 (td, *J* = 8.6, 6.9, 0.8 Hz, 1H), 7.09 (t, *J* = 6.9 Hz, 2H), 7.03 (td, *J* = 7.6, 7.2, 1.5 Hz, 1H), 3.60 (t, *J* = 4.4 Hz, 2H), 2.97 (t, *J* = 4.5 Hz, 2H), 2.28 (s, 3H). ¹³C NMR(126 MHz, CDCl₃) δ 165.27, 136.19, 131.08, 130.79, 126.06, 125.76, 125.75, 122.03, 41.04, 35.99, 18.87.



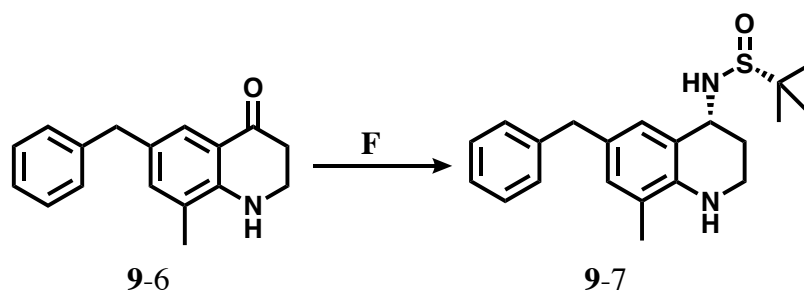
9-4. 8-methyl-2,3-dihydroquinolin-4(1H)-one. **9-4** was synthesized following General Procedure (iii) from **9-4** (1.18 g, 4.9 mmol, 1 eq) and TfOH (1.3 mL, 14.7 mmol, 3 eq). Yield: 606 mg, 52%. ^1H NMR (500 MHz, CDCl_3) δ 7.75 (d, $J = 8.0$ Hz, 1H), 7.18 (d, $J = 7.1$ Hz, 1H), 6.65 (t, $J = 7.5$ Hz, 1H), 4.40 (s, 1H), 3.60 (t, $J = 6.9$ Hz, 2H), 2.68 (t, $J = 6.9$ Hz, 2H), 2.15 (s, 3H). ^{13}C NMR(126 MHz, CDCl_3) δ 194.16, 150.47, 135.73, 125.61, 122.87, 119.10, 117.26, 77.16, 42.18, 37.92, 16.95.



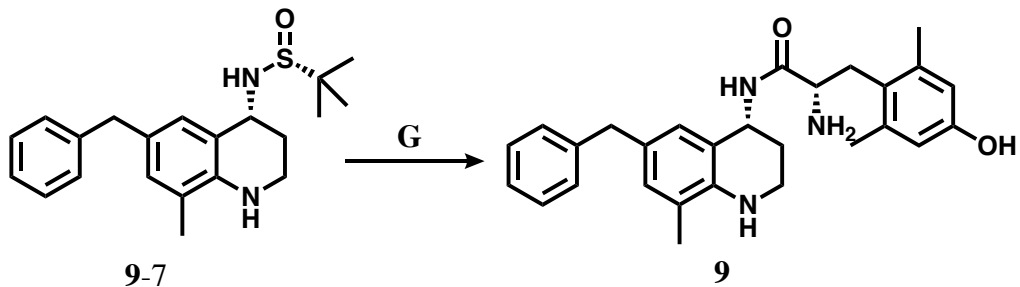
9-5. 6-bromo-8-methyl-2,3-dihydroquinolin-4(1H)-one. **9-5** was synthesized following **General Procedure (D)** from **9-4** (120 mg, 0.74 mmol, 1.00 eq) and NBS (139 mg, 0.78 mmol, 1.05 eq). Yield: 170 mg, 95%. ^1H NMR (500 MHz, CDCl_3) δ 7.85 (d, $J = 2.3$ Hz, 1H), 7.28 (dd, $J = 2.3, 1.1$ Hz, 1H), 4.34 (s, 1H), 3.61 (t, $J = 7.0$ Hz, 2H), 2.71 – 2.65 (m, 2H), 2.13 (s, 3H). ^{13}C NMR(126 MHz, CDCl_3) δ 192.79, 149.26, 137.96, 127.94, 125.36, 120.28, 109.76, 42.07, 37.60, 16.80.



9-6. *6-benzyl-8-methyl-2,3-dihydroquinolin-4(1H)-one.* **9-6** was synthesized following **General Procedure (E)** from **9-5** (300 mg, 1.25 mmol, 1 eq), benzyl boronic acid pinacol ester (0.56 mL, 2.50 mmol, 2 eq), K₂CO₃ (518 mg, 3.75 mmol, 3 eq) and Pd(dppf)Cl₂ (88 mg, 0.12 mmol, 0.1 eq). Yield: 223 mg, 71%. ¹H NMR (500 MHz, CDCl₃) δ 7.64 (d, *J* = 2.1 Hz, 1H), 7.30 – 7.23 (m, 2H), 7.20 – 7.15 (m, 3H), 7.04 – 7.02 (m, 1H), 3.84 (s, 2H), 3.59 (t, *J* = 7.0 Hz, 2H), 2.68 (t, *J* = 6.9 Hz, 2H), 2.10 (s, 3H). ¹³C NMR(126 MHz, CDCl₃) δ 194.24, 149.08, 141.53, 136.80, 130.14, 128.86, 128.59, 126.14, 125.32, 123.34, 119.11, 42.42, 41.17, 38.06, 25.00, 17.05.

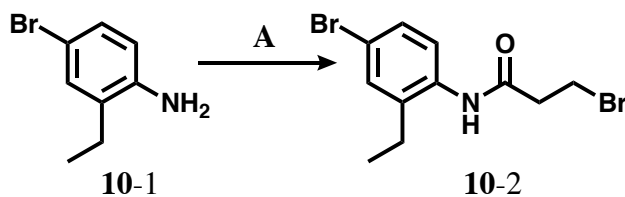


9-6. *(R)-N-((R)-6-benzyl-8-methyl-1,2,3,4-tetrahydroquinolin-4-yl)-2-methylpropane-2-sulfonamide.* **9-6** was synthesized following **General Procedure (F)** from **9-5** (75 mg, 0.30 mmol, 1 eq), (R)-2-methyl-2-propanesulfonamide (106 mg, 0.90 mmol, 3 eq), and Ti(OEt)₄ (0.38 mL, 1.80 mmol, 6 eq), then NaBH₄ (68 mg, 1.80 mmol, 6 eq). Yield: not calculated. ¹H NMR (500 MHz, CDCl₃) δ 7.29 – 7.22 (m, 1H), 7.20 – 7.12 (m, 3H), 7.00 (d, *J* = 2.0 Hz, 1H), 6.80 (d, *J* = 2.5 Hz, 1H), 4.54 (q, *J* = 3.0 Hz, 1H), 3.82 (d, *J* = 2.7 Hz, 2H), 3.40 (td, *J* = 11.8, 2.8 Hz, 1H), 3.31 (dt, *J* = 11.4, 4.0 Hz, 1H), 2.12 – 2.06 (m, 1H), 2.04 (s, 3H), 1.89 (dddd, *J* = 16.7, 8.1, 4.1, 2.1 Hz, 1H), 1.21 (s, 9H). ¹³C NMR(126 MHz, CDCl₃) δ 142.09, 141.30, 130.69, 129.79, 128.86, 128.50, 125.94, 122.12, 120.17, 116.96, 55.42, 49.71, 41.19, 36.77, 28.34, 22.80, 22.25, 17.31.

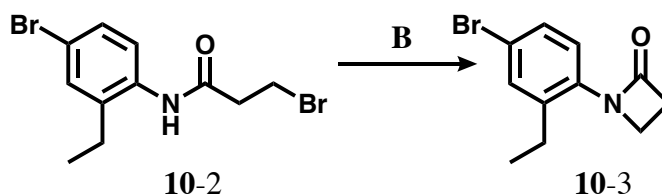


9. *(S)*-2-amino-*N*-((*R*)-6-benzyl-8-methyl-1,2,3,4-tetrahydroquinolin-4-yl)-3-(4-hydroxy-2,6-dimethylphenyl)propanamide. **9** was synthesized following **General Procedures (G)** from **9-7** (0.30 mmol, 1 eq) and concentrated HCl (0.03 mL, excess). Carried forward without characterization. **Step 2:** Performed amide coupling using **9-7** amine salt (20 mg, 0.070 mmol, 1 eq), di-Boc-Dmt (31 mg, 0.076 mmol, 1.1 eq), PyBOP (40 mg, 0.076 mmol, 1.1 eq), and 6-Cl HOBt (13 mg, 0.076 mmol, 1.1 eq), followed by DIPEA (0.12 mL, 0.70 mmol, 10 eq). **Step 3:** Boc-deprotected with TFA as described in **General Procedure (G)**. Final yield not calculated. ^1H NMR (500 MHz, Methanol- d_4) δ 7.22 (td, $J = 7.5, 2.0$ Hz, 2H), 7.13 (td, $J = 8.7, 4.2$ Hz, 3H), 7.01 (s, 1H), 6.94 (s, 1H), 6.49 (s, 2H), 4.98 (m, 1H), 3.90 – 3.82 (m, 1H), 3.83 (s, 2H), 3.26 (dd, $J = 13.6, 11.6$ Hz, 1H), 3.25 – 3.19 (m, 1H), 3.02 (dd, $J = 13.5, 5.6$ Hz, 1H), 2.76 – 2.64 (m, 1H), 2.27 (s, 6H), 2.14 (s, 3H), 1.90 – 1.78 (m, 1H), 1.63 – 1.54 (m, 1H). HPLC (gradient A): retention time = 28.4 min. ESI-MS 466.3 $[\text{M} + \text{Na}]^+$.

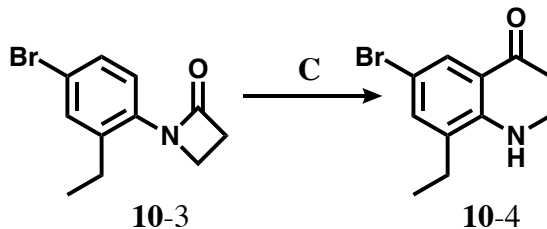
Compound 10 (Notebook reference: AFN-35 or afn-v-23, notebook 5 p. 23)



10-2. *3-bromo-N-(4-bromo-2-ethylphenyl)propanamide*. **10-2** was synthesized following **General Procedure (A)** from 4-bromo-2-ethylaniline **10-1** (1.41 g, 7.05 mmol, 1.00 eq), K₂CO₃ (1.95 g, 14.10 mmol, 2.00 eq) and 3-bromopropionyl chloride (0.75 mL, 7.35 mmol, 1.05 eq). Yield: 2.36 g, 100%. ¹H NMR (500 MHz, CDCl₃) δ 7.67 (d, *J* = 8.4 Hz, 1H), 7.37 – 7.31 (m, 2H), 7.07 (s, 1H), 3.72 (t, *J* = 5.8 Hz, 2H), 2.97 (t, *J* = 6.3 Hz, 2H), 2.60 (q, *J* = 7.5 Hz, 2H), 1.24 (t, *J* = 7.5 Hz, 3H). ¹³C NMR(126 MHz, CDCl₃) δ 168.32, 137.66, 133.70, 131.62, 129.82, 125.79, 119.24, 40.80, 27.41, 24.33, 13.93.

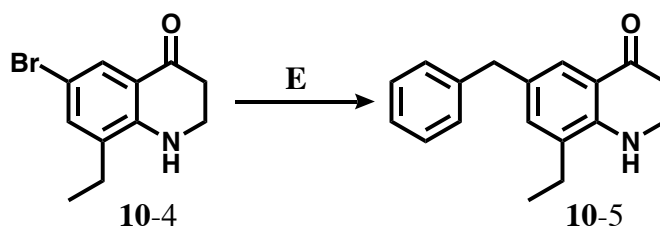


10-3. *1-(4-bromo-2-ethylphenyl)azetidin-2-one*. **10-3** was synthesized following **General Procedure (B)** from **10-2** (2.56 g, 7.64 mmol, 1.00 eq) and NaOtBu (734 mg, 7.64 mmol, 1.00 eq). Yield: 1.89 g, 97%. ¹H NMR (500 MHz, CDCl₃) δ 7.36 (d, *J* = 2.1 Hz, 1H), 7.33 – 7.29 (m, 1H), 3.75 – 3.69 (m, 2H), 3.13 (td, *J* = 4.5, 1.3 Hz, 2H), 2.71 (q, *J* = 7.5 Hz, 2H), 1.22 (td, *J* = 7.5, 1.3 Hz, 3H). ¹³C NMR(126 MHz, CDCl₃) δ 165.77, 139.73, 135.09, 132.52, 129.62, 124.88, 119.92, 42.03, 36.81, 25.12, 14.34.

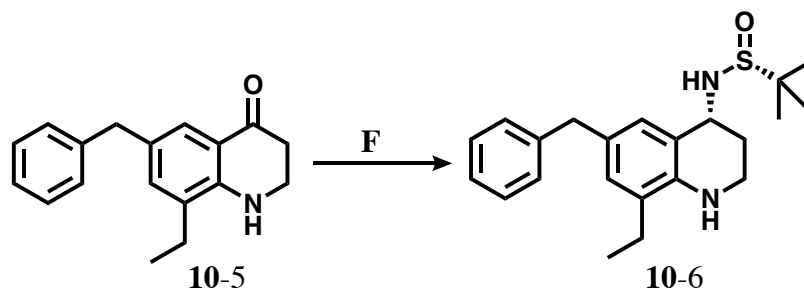


10-4. *6-bromo-8-ethyl-2,3-dihydroquinolin-4(1H)-one*. **10-4** was synthesized following **General Procedure (C)** from **10-3** (1.89 g, 7.42 mmol, 1 eq) and TfOH (1.31 mL, 14.85 mmol, 2 eq). Yield: 640 mg, 34%. ¹H NMR (500 MHz, CDCl₃) δ 7.88 (d, *J* = 2.4 Hz, 1H), 7.29 (d, *J* = 2.3 Hz,

1H), 4.40 (s, 1H), 3.61 (t, $J = 7.0$ Hz, 3H), 2.69 (t, $J = 7.1$ Hz, 3H), 2.46 (q, $J = 7.5$ Hz, 3H), 1.27 (t, $J = 7.5$ Hz, 4H). ^{13}C NMR(126 MHz, CDCl_3) δ 192.87, 148.71, 135.93, 130.97, 127.91, 120.59, 110.25, 42.13, 37.69, 23.30, 12.53.

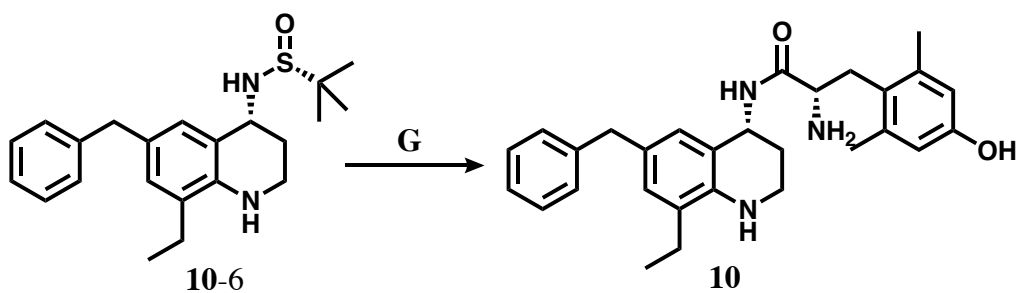


10-5. *6-benzyl-8-ethyl-2,3-dihydroquinolin-4(1H)-one*. **10-5** was synthesized following **General Procedure (E)** from **10-4** (200 mg, 0.79 mmol, 1 eq), benzyl boronic acid pinacol ester (0.35 mL, 1.57 mmol, 2 eq), K_2CO_3 (326 mg, 2.36 mmol, 3 eq) and $\text{Pd}(\text{dppf})\text{Cl}_2$ (58 mg, 0.08 mmol, 0.1 eq). Yield: 120 mg, 57%. ^1H NMR (400 MHz, CDCl_3) δ 7.64 (d, $J = 2.1$ Hz, 1H), 7.29 – 7.23 (m, 2H), 7.20 – 7.13 (m, 3H), 7.05 (d, $J = 2.1$ Hz, 1H), 4.39 – 4.31 (m, 1H), 3.86 (s, 2H), 3.57 (td, $J = 7.1$, 1.7 Hz, 2H), 2.71 – 2.64 (m, 2H), 2.44 (q, $J = 7.5$ Hz, 2H), 1.22 (t, $J = 7.5$ Hz, 3H). ^{13}C NMR (101 MHz, CDCl_3) δ 194.38, 148.55, 141.51, 134.74, 134.71, 130.14, 128.99, 128.81, 128.55, 126.09, 125.24, 125.18, 119.27, 75.12, 42.38, 41.23, 38.07, 24.98, 24.94, 23.58, 12.87, 12.85.



10-6. *(R)-N-((R)-6-benzyl-8-ethyl-1,2,3,4-tetrahydroquinolin-4-yl)-2-methylpropane-2-sulfonamide*. **10-6** was synthesized following **General Procedure (F)** from **10-5** (100 mg, 0.38

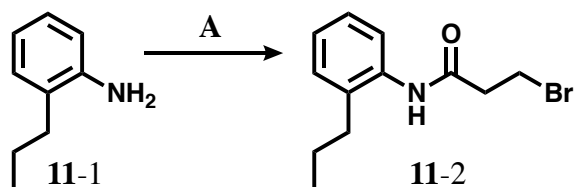
mmol, 1 eq), (R)-2-methyl-2-propanesulfonamide (137 mg, 1.13 mmol, 3 eq), and Ti(OEt)₄ (0.47 mL, 2.26 mmol, 6 eq), then NaBH₄ (85 mg, 2.26 mmol, 6 eq). Yield: not calculated. ¹H NMR (500 MHz, CDCl₃) δ 7.28 – 7.23 (m, 2H), 7.21 – 7.16 (m, 2H), 7.16 – 7.14 (m, 1H), 6.99 (d, *J* = 2.0 Hz, 1H), 6.83 (d, *J* = 2.0 Hz, 1H), 4.54 (q, *J* = 2.7, 2.2 Hz, 1H), 3.84 (d, *J* = 2.4 Hz, 2H), 3.38 (td, *J* = 11.8, 2.8 Hz, 1H), 3.33 – 3.26 (m, 1H), 2.38 (q, *J* = 7.5 Hz, 2H), 2.08 (dq, *J* = 13.6, 3.2 Hz, 1H), 1.89 (ttt, *J* = 12.1, 3.9, 1.2 Hz, 1H), 1.23 (t, *J* = 6.3 Hz, 3H), 1.20 (s, 9H). ¹³C NMR(126 MHz, CDCl₃) δ 142.10, 140.76, 129.83, 128.85, 128.52, 128.49, 128.48, 127.72, 125.92, 120.36, 55.42, 55.31, 49.81, 47.33, 41.31, 36.72, 28.35, 24.98, 23.80, 23.73, 22.80, 22.65, 12.84.



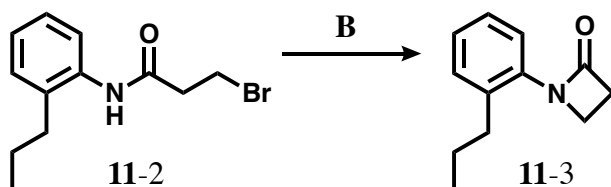
10. *(S)*-2-amino-*N*-((*R*)-6-benzyl-8-ethyl-1,2,3,4-tetrahydroquinolin-4-yl)-3-(4-hydroxy-2,6-dimethylphenyl)propanamide. **10** was synthesized following **General Procedure (G)** from **10-6** (0.38 mmol, 1 eq) and concentrated HCl (0.03 mL, excess). Carried forward without characterization following **step 2** of **General Procedure (G)** from **10-6** amine salt (45 mg, 0.15 mmol, 1 eq), di-Boc-Dmt (67 mg, 0.16 mmol, 1.1 eq), PyBOP (85 mg, 0.16 mmol, 1.1 eq), and 6-Cl HOBt (28 mg, 0.16 mmol, 1.1 eq), followed by DIPEA (0.26 mL, 1.50 mmol, 10 eq). **Step 3:** Boc-deprotected following **General Procedure (G)**. Final yield not calculated. ¹H NMR (500 MHz, Methanol-*d*₄) δ 7.21 (t, *J* = 7.5 Hz, 2H), 7.11 (t, *J* = 8.8 Hz, 3H), 6.77 (d, *J* = 6.1 Hz, 2H), 6.48 (s, 2H), 4.92 (t, *J* = 3.9 Hz, 1H), 3.84 (dd, *J* = 11.6, 5.1 Hz, 1H), 3.76 (s, 2H), 3.29 – 3.22 (m, 1H), 3.09 – 3.02 (m, 1H), 2.99 (dd, *J* = 13.7, 5.1 Hz, 1H), 2.48 (t, *J* = 11.1 Hz, 1H), 2.38 (q, *J* =

7.5 Hz, 2H), 2.27 (s, 6H), 1.70 (t, $J = 12.7$ Hz, 1H), 1.56 – 1.48 (m, 1H), 1.11 (td, $J = 7.5, 0.9$ Hz, 3H). HPLC (gradient A): retention time = 32.1. ESI-MS 480.3 [M + Na]⁺.

Compound 11 (Notebook reference: AFN-7 or afn-iii-87, notebook 3 p. 87)

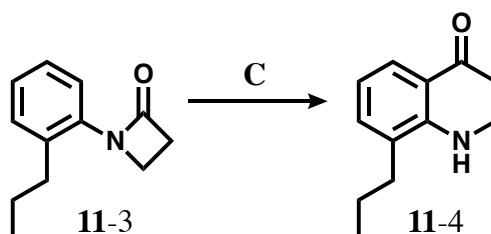


11-2. *3-bromo-N-(2-propylphenyl)propanamide*. **11-2** was synthesized following **General Procedure (A)** from 2-propylaniline **11-1** (1.00 g, 7.40 mmol, 1.00 eq), K₂CO₃ (3.07 g, 22.2 mmol, 3.00 eq) and 3-bromopropionyl chloride (0.78 mL, 7.77 mmol, 1.05 eq). Yield: 1.73 g, 86%. ¹H NMR (500 MHz, CDCl₃) δ 7.70 (q, $J = 6.9, 5.8$ Hz, 1H), 7.19 (d, $J = 7.8$ Hz, 2H), 7.13 (t, $J = 7.5$ Hz, 1H), 3.72 (td, $J = 7.0, 6.5, 3.1$ Hz, 2H), 2.96 (dq, $J = 7.1, 3.8, 3.3$ Hz, 2H), 2.56 (t, $J = 7.9$ Hz, 2H), 1.62 (h, $J = 7.6$ Hz, 3H), 0.97 (t, $J = 7.4$ Hz, 3H). ¹³C NMR(126 MHz, CDCl₃) δ 168.28, 134.56, 129.63, 126.67, 125.91, 124.54, 40.55, 33.47, 27.46, 23.12, 14.06.

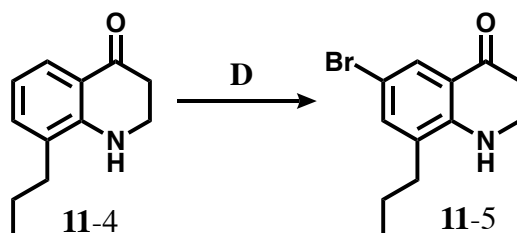


11-3. *1-(2-propylphenyl)azetidin-2-one*. **11-3** was synthesized following **General Procedure (B)** from **11-2** (1.56 g, 5.78 mmol, 1.00 eq) and NaOtBu (583 mg, 6.07 mmol, 1.05 eq). Yield: 1.10 g, 100%. ¹H NMR (500 MHz, CDCl₃) δ 7.35 (dd, $J = 7.5, 1.5$ Hz, 1H), 7.20 (td, $J = 6.2, 5.4, 2.0$ Hz,

2H), 7.16 (dd, $J = 7.2, 1.6$ Hz, 1H), 3.74 – 3.69 (m, 2H), 3.14 – 3.09 (m, 2H), 2.71 – 2.63 (m, 2H), 1.61 (h, $J = 7.4$ Hz, 2H), 0.96 (t, $J = 7.4$ Hz, 3H). ^{13}C NMR(126 MHz, CDCl_3) δ 165.86, 136.45, 136.02, 130.55, 126.64, 126.62, 123.68, 42.03, 36.59, 34.35, 23.64, 14.20.

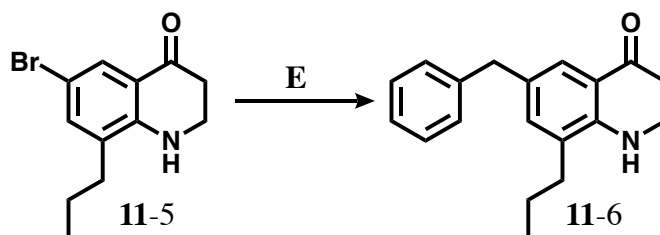


11-4. *8-propyl-2,3-dihydroquinolin-4(1H)-one*. **11-4** was synthesized following **General Procedure (C)** from **11-3** (1.10 g, 5.8 mmol, 1 eq) and TfOH (1.54 mL, 17.4 mmol, 3 eq). Yield: 1.06 g, 100%. ^1H NMR (500 MHz, CDCl_3) δ 7.77 (dd, $J = 8.0, 1.5$ Hz, 1H), 7.18 (dd, $J = 7.2, 1.5$ Hz, 1H), 6.70 (t, $J = 7.6$ Hz, 1H), 3.72 (s, 1H), 3.60 (dd, $J = 7.6, 6.3$ Hz, 2H), 2.69 (dd, $J = 7.5, 6.4$ Hz, 2H), 2.46 – 2.41 (m, 2H), 1.65 (h, $J = 7.4$ Hz, 2H), 1.01 (t, $J = 7.3$ Hz, 3H). ^{13}C NMR(126 MHz, CDCl_3) δ 194.22, 149.96, 134.78, 127.18, 125.74, 119.59, 117.47, 77.16, 42.32, 38.04, 32.84, 21.59, 14.20.

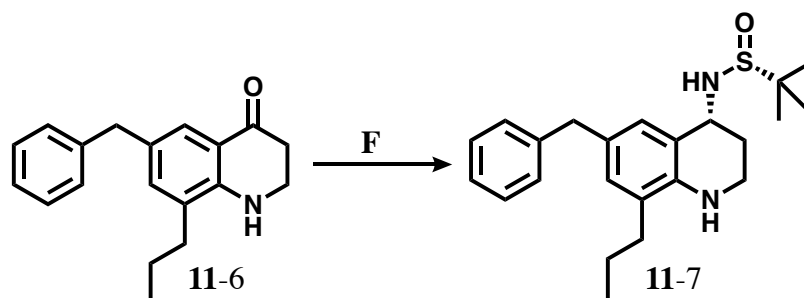


11-5. *6-bromo-8-propyl-2,3-dihydroquinolin-4(1H)-one*. **11-5** was synthesized following **General Procedure (D)** from **11-4** (294 mg, 1.55 mmol, 1.00 eq) and NBS (282 mg, 1.58 mmol, 1.02 eq). Yield: 350 mg, 84%. ^1H NMR (500 MHz, CDCl_3) δ 7.87 (d, $J = 2.3$ Hz, 1H), 7.26 (s, 1H), 4.42 (s, 1H), 3.63 – 3.56 (m, 2H), 2.68 (td, $J = 7.0, 1.1$ Hz, 2H), 2.44 – 2.37 (m, 2H), 1.70 – 1.59 (m,

2H), 1.01 (td, $J = 7.3$, 1.1 Hz, 3H). ^{13}C NMR(126 MHz, CDCl_3) δ 192.90, 148.83, 136.97, 129.68, 127.97, 120.67, 110.07, 77.16, 42.11, 37.68, 32.56, 21.40, 14.14.

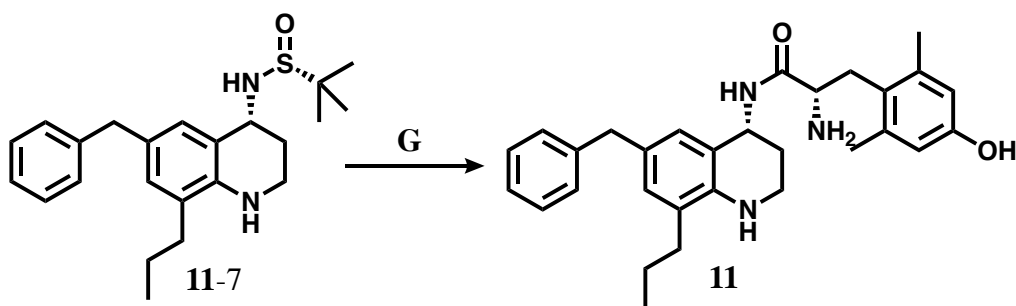


11-6. *6-benzyl-8-propyl-2,3-dihydroquinolin-4(1H)-one*. **11-6** was synthesized following **General Procedure (E)** from **11-5** (102 mg, 0.38 mmol, 1 eq), benzyl boronic acid pinacol ester (0.17 mL, 0.76 mmol, 2 eq), K_2CO_3 (157 mg, 1.14 mmol, 3 eq) and $\text{Pd}(\text{dppf})\text{Cl}_2$ (28 mg, 0.04 mmol, 0.1 eq), with the exception that the reaction was run in a microwave at 110°C for 30 minutes. Yield: 35 mg, 32%. ^1H NMR (500 MHz, CDCl_3) δ 7.65 (d, $J = 2.1$ Hz, 1H), 7.27 (dd, $J = 8.5$, 6.6 Hz, 2H), 7.20 – 7.17 (m, 3H), 7.03 (d, $J = 2.1$ Hz, 1H), 3.86 (s, 2H), 3.58 (t, $J = 7.0$ Hz, 2H), 2.68 (t, $J = 6.5$ Hz, 2H), 2.41 (t, $J = 3.9$ Hz, 2H), 1.62 (h, $J = 7.5$ Hz, 2H), 0.98 (t, $J = 7.3$ Hz, 3H).



11-7. *(R)-N-((R)-6-benzyl-8-propyl-1,2,3,4-tetrahydroquinolin-4-yl)-2-methylpropane-2-sulfonamide*. **11-7** was synthesized following **General Procedure (F)** from **11-6** (88 mg, 0.31 mmol, 1 eq), (R)-2-methyl-2-propanesulfonamide (115 mg, 0.95 mmol, 3 eq), and $\text{Ti}(\text{OEt})_4$ (0.40 mL, 1.89 mmol, 6 eq), then NaBH_4 (71 mg, 1.89 mmol, 6 eq). Yield: 20 mg, 17%. ^1H NMR (500

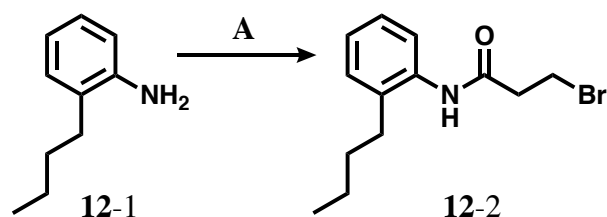
MHz, CDCl₃) δ 7.21 – 7.18 (m, 1H), 7.16 (d, J = 2.4 Hz, 2H), 7.12 – 7.08 (m, 1H), 7.00 (d, J = 2.3 Hz, 1H), 6.95 (s, 1H), 6.76 (d, J = 1.9 Hz, 1H), 4.45 (d, J = 3.0 Hz, 1H), 3.79 – 3.75 (m, 2H), 3.29 (d, J = 3.0 Hz, 1H), 3.25 (dt, J = 11.5, 4.2 Hz, 2H), 2.27 (t, J = 7.8 Hz, 4H), 2.02 (dq, J = 13.7, 3.4 Hz, 2H), 1.84 – 1.76 (m, 2H), 1.55 (qd, J = 7.2, 4.5 Hz, 3H), 1.15 (d, J = 0.9 Hz, 17H), 0.93 (t, J = 7.3 Hz, 6H). ¹³C NMR(126 MHz, CDCl₃) δ 141.26, 131.32, 130.35, 129.62, 128.78, 128.67, 128.61, 128.44, 128.35, 128.26, 128.12, 125.82, 121.94, 108.32, 55.39, 49.57, 41.12, 36.44, 32.65, 27.75, 22.64, 21.17, 14.13.



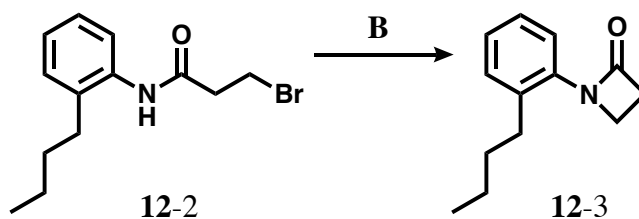
11. *(S)*-2-amino-*N*-((*R*)-6-benzyl-8-propyl-1,2,3,4-tetrahydroquinolin-4-yl)-3-(4-hydroxy-2,6-dimethylphenyl)propanamide. **11** was synthesized following **General Procedures (G)** from **11-7** (19 mg, 0.05 mmol, 1 eq) and concentrated HCl (0.02 mL, excess). Carried forward without characterization. **Step 2:** Performed amide coupling using **11-7** amine salt (16 mg, 0.050 mmol, 1 eq), di-Boc-Dmt (23 mg, 0.055 mmol, 1.1 eq), PyBOP (29 mg, 0.055 mmol, 1.1 eq), and 6-Cl HOBt (19 mg, 0.055 mmol, 1.1 eq), followed by DIPEA (0.09 mL, 0.50 mmol, 10 eq) and stirred 18 hours. **Step 3:** Boc-deprotected with TFA as described in **General Procedure (G)**. Final yield not calculated. ¹H NMR (500 MHz, Methanol-*d*₄) δ 7.21 (td, J = 7.3, 1.4 Hz, 2H), 7.16 – 7.08 (m, 3H), 6.85 (dt, J = 5.3, 2.7 Hz, 2H), 6.48 (s, 2H), 4.96 (d, J = 5.1 Hz, 1H), 3.86 (ddd, J = 11.6, 5.2, 2.3 Hz, 1H), 3.80 (d, J = 2.4 Hz, 2H), 3.25 (t, 1H), 3.11 (d, J = 4.0 Hz, 1H), 3.01 (ddd, J = 13.5, 5.3, 2.0 Hz, 1H), 2.58 (tt, J = 10.6, 2.5 Hz, 1H), 2.39 (td, J = 7.9, 3.0 Hz, 2H), 2.27 (s, 7H), 1.76

(dddd, $J = 17.9, 14.1, 9.1, 5.3$ Hz, 1H), 1.59 – 1.48 (m, 3H), 0.93 (td, $J = 7.3, 1.4$ Hz, 3H). HPLC (gradient A): retention time = 37.1 min. ESI-MS 494.3 [M + Na]⁺.

Compound 12 (Notebook reference: AFN-8 or afn-iii-91, notebook 3 p. 91)

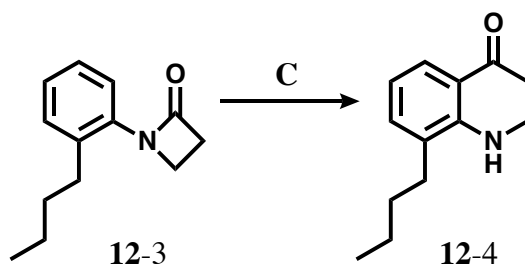


12-2. *3-bromo-N-(2-butylphenyl)propanamide*. **12-2** was synthesized following **General Procedure (A)** from 2-butylaniline **12-1** (1.00 g, 6.70 mmol, 1.00 eq), K₂CO₃ (2.78 g, 20.1 mmol, 3.00 eq) and 3-bromopropionyl chloride (0.71 mL, 7.03 mmol, 1.05 eq). Yield: 1.725 g, 91%. ¹H NMR (500 MHz, CDCl₃) δ 7.74 (d, $J = 7.9$ Hz, 1H), 7.20 (d, $J = 8.5$ Hz, 2H), 7.17 – 7.10 (m, 2H), 3.73 (t, $J = 6.5$ Hz, 2H), 2.97 (t, $J = 6.5$ Hz, 2H), 2.59 (t, $J = 7.9$ Hz, 2H), 1.57 (h, $J = 9.8, 8.7$ Hz, 2H), 1.39 (h, $J = 7.4$ Hz, 2H), 0.94 (t, $J = 7.3$ Hz, 3H). ¹³C NMR (126 MHz, CDCl₃) δ 168.13, 134.53, 134.36, 129.57, 126.67, 125.86, 124.31, 40.67, 32.10, 31.18, 27.42, 22.61, 13.96.

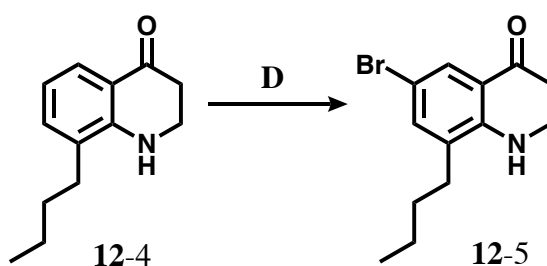


12-3. *1-(2-butylphenyl)azetidin-2-one*. **12-3** was synthesized following **General Procedure (B)** from **12-2** (1.725 g, 6.06 mmol, 1.00 eq) and NaOtBu (613 mg, 6.37 mmol, 1.05 eq). Yield: 1.23 g, 100%. ¹H NMR (500 MHz, CDCl₃) δ 7.35 (dd, $J = 7.6, 1.6$ Hz, 1H), 7.20 (td, $J = 8.4, 7.9, 2.1$

Hz, 2H), 7.17 – 7.13 (m, 2H), 3.71 (td, $J = 4.4, 0.9$ Hz, 2H), 3.11 (td, $J = 4.4, 1.0$ Hz, 2H), 2.74 – 2.65 (m, 2H), 1.56 (p, $J = 7.9, 7.5$ Hz, 2H), 1.37 (h, $J = 7.3$ Hz, 2H), 0.93 (t, $J = 7.3$ Hz, 3H). ^{13}C NMR(126 MHz, CDCl_3) δ 165.82, 136.71, 135.97, 130.49, 126.63, 126.57, 123.70, 42.02, 36.57, 32.70, 32.00, 22.71, 14.08.

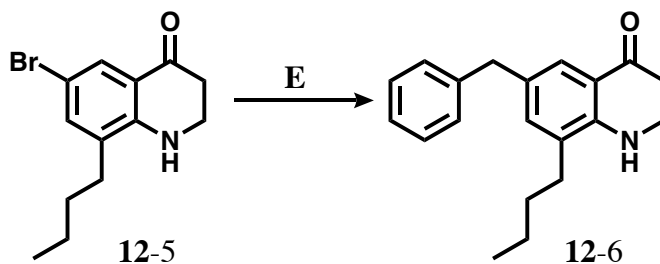


12-4. *8-butyl-2,3-dihydroquinolin-4(1H)-one*. **12-4** was synthesized following **General Procedure (C)** from **12-3** (1.23 g, 6.06 mmol, 1.00 eq) and TfOH (1.64 mL, 18.58 mmol, 3.07 eq). Yield: 1.174 g, 95%. ^1H NMR (500 MHz, CDCl_3) δ 7.80 – 7.74 (m, 1H), 7.19 (t, $J = 7.2$ Hz, 1H), 6.70 (q, $J = 7.7$ Hz, 1H), 4.44 (s, 1H), 3.61 (q, $J = 7.3$ Hz, 2H), 2.70 (q, $J = 7.3$ Hz, 2H), 2.47 (q, $J = 7.8$ Hz, 2H), 1.61 (h, $J = 7.6$ Hz, 2H), 1.42 (hept, $J = 7.5$ Hz, 2H), 0.97 (q, $J = 7.5$ Hz, 3H). ^{13}C NMR(126 MHz, CDCl_3) δ 194.23, 194.21, 149.95, 134.69, 134.67, 127.38, 125.71, 125.69, 119.59, 117.49, 42.35, 42.33, 38.06, 38.04, 30.57, 30.56, 30.52, 30.51, 22.81, 22.80, 14.08, 14.07.

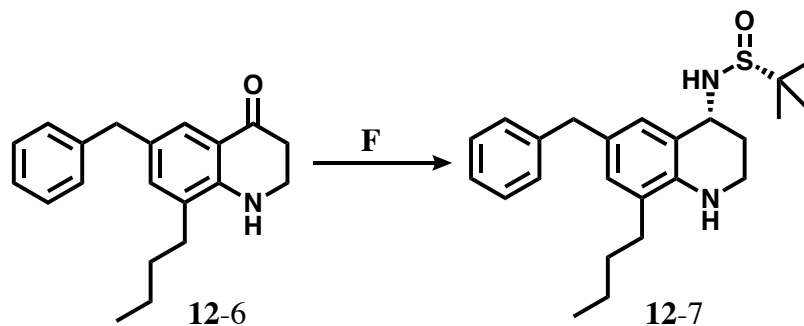


12-5. *6-bromo-8-butyl-2,3-dihydroquinolin-4(1H)-one*. **12-5** was synthesized following **General Procedure (D)** from **12-4** (485 mg, 2.46 mmol, 1.00 eq) and NBS (446 mg, 2.51 mmol, 1.05 eq). Yield: 575 mg, 85%. ^1H NMR (500 MHz, CDCl_3) δ 7.86 (dd, $J = 2.5, 1.0$ Hz, 1H), 7.26 (s, 1H),

4.44 (s, 1H), 3.63 – 3.55 (m, 2H), 2.68 (td, $J = 7.0$, 1.1 Hz, 2H), 2.47 – 2.38 (m, 2H), 1.64 – 1.54 (m, 2H), 1.41 (h, $J = 7.4$ Hz, 2H), 0.96 (td, $J = 7.3$, 1.0 Hz, 3H). ^{13}C NMR(126 MHz, CDCl_3) δ 193.15, 149.07, 137.11, 130.17, 128.14, 120.89, 110.31, 42.36, 37.92, 30.56, 30.51, 23.00, 14.29.

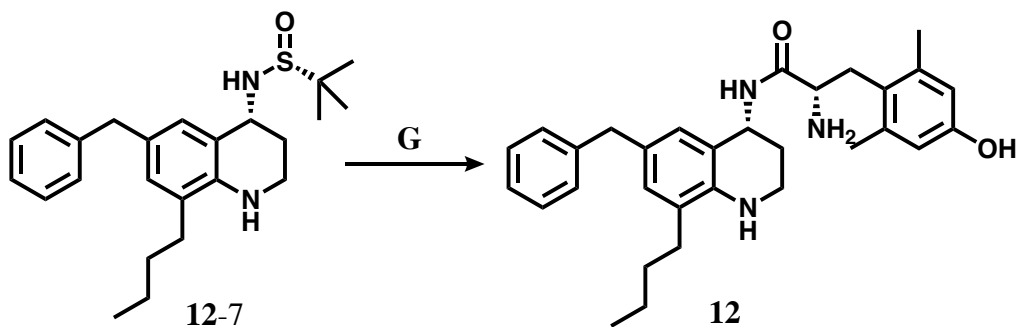


12-6. *6-benzyl-8-butyl-2,3-dihydroquinolin-4(1H)-one*. **12-6** was synthesized following **General Procedure (E)** from **12-5** (300 mg, 1.06 mmol, 1 eq), benzyl boronic acid pinacol ester (0.47 mL, 2.12 mmol, 2 eq), K_2CO_3 (440 mg, 3.18 mmol, 3 eq) and $\text{Pd}(\text{dppf})\text{Cl}_2$ (81 mg, 0.11 mmol, 0.1 eq), except reaction was run in microwave at 110°C for 30 minutes. Yield: 78 mg, 25%. ^1H NMR (500 MHz, CDCl_3) δ 7.64 (d, $J = 2.1$ Hz, 1H), 7.26 (s, 2H), 7.18 (td, $J = 8.6$, 7.8, 3.5 Hz, 3H), 7.03 (d, $J = 2.1$ Hz, 1H), 3.86 (s, 2H), 3.58 (d, $J = 7.0$ Hz, 2H), 2.70 – 2.67 (m, 2H), 2.41 (d, $J = 7.8$ Hz, 2H), 1.59 – 1.52 (m, 2H), 1.41 – 1.35 (m, 2H), 0.94 (t, $J = 7.3$ Hz, 3H). ^{13}C NMR(126 MHz, CDCl_3) δ 194.25, 141.53, 135.81, 134.70, 128.84, 128.58, 127.96, 126.55, 126.12, 125.76, 125.40, 42.52, 41.23, 38.11, 30.68, 30.64, 22.83, 14.06.



12-7. *(R)-N-((R)-6-benzyl-8-butyl-1,2,3,4-tetrahydroquinolin-4-yl)-2-methylpropane-2-sulfonamide*. **12-7** was synthesized following **General Procedure (F)** from **12-6** (78 mg, 0.27

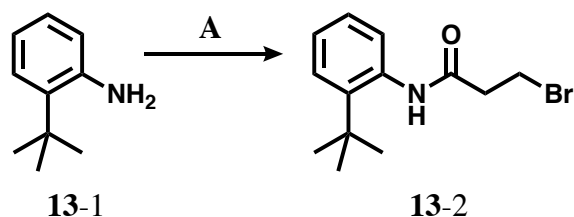
mmol, 1 eq), (R)-2-methyl-2-propanesulfonamide (97 mg, 0.80 mmol, 3 eq), and Ti(OEt)₄ (0.34 mL, 1.60 mmol, 6 eq), then NaBH₄ (61 mg, 1.60 mmol, 6 eq). Yield: 89 mg, 84%. ¹H NMR (500 MHz, CDCl₃) δ 7.20 – 7.14 (m, 1H), 7.11 (d, *J* = 7.3 Hz, 2H), 7.11 – 7.03 (m, 1H), 6.92 (d, *J* = 2.0 Hz, 1H), 6.73 (d, *J* = 2.0 Hz, 1H), 6.58 (t, *J* = 7.5 Hz, 1H), 4.47 (q, *J* = 3.8, 3.3 Hz, 1H), 3.76 (d, *J* = 2.3 Hz, 2H), 3.38 – 3.17 (m, 2H), 2.31 (dt, *J* = 21.0, 7.9 Hz, 2H), 2.02 (ddq, *J* = 13.3, 6.5, 3.2 Hz, 1H), 1.89 – 1.79 (m, 1H), 1.58 – 1.41 (m, 2H), 1.41 – 1.26 (m, 2H), 1.14 (dd, *J* = 5.0, 1.0 Hz, 9H), 0.88 (ddd, *J* = 12.4, 7.8, 6.8 Hz, 3H). ¹³C NMR(126 MHz, CDCl₃) δ 142.12, 131.41, 130.49, 129.57, 128.85, 128.81, 128.53, 128.49, 128.39, 125.92, 120.50, 117.03, 55.44, 49.88, 41.28, 36.77, 30.83, 30.67, 28.42, 23.01, 22.82, 14.11.



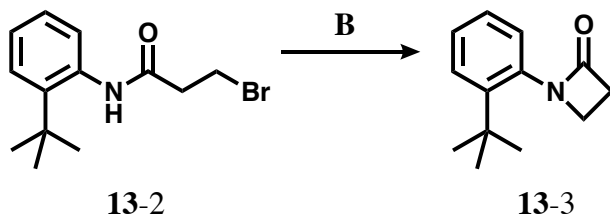
12. *(S)*-2-amino-*N*-((*R*)-6-benzyl-8-butyl-1,2,3,4-tetrahydroquinolin-4-yl)-3-(4-hydroxy-2,6-dimethylphenyl)propanamide. **12** was synthesized following General Procedure (G) from **12-7** (82 mg, 0.21 mmol, 1 eq) and concentrated HCl (0.03 mL, excess). Carried forward without characterization. **Step 2:** Performed amide coupling using **12-7** amine salt (68 mg, 0.21 mmol, 1 eq), di-Boc-Dmt (93 mg, 0.23 mmol, 1.1 eq), PyBOP (118 mg, 0.23 mmol, 1.1 eq), and 6-Cl HOBt (38 mg, 0.23 mmol, 1.1 eq), followed by DIPEA (0.40 mL, 2.1 mmol, 10 eq) and stirred 18 hours. **Step 3:** Boc-protected with TFA as described in **General Procedure (G)**. Final yield not calculated. ¹H NMR (500 MHz, Methanol-*d*₄) δ 7.23 – 7.18 (m, 2H), 7.14 – 7.08 (m, 3H), 6.82 (dq, *J* = 6.6, 2.2 Hz, 2H), 6.48 (s, 2H), 4.95 (d, *J* = 4.5 Hz, 1H), 3.86 (ddd, *J* = 11.6, 5.1, 1.9 Hz,

1H), 3.79 (d, $J = 2.3$ Hz, 2H), 3.25 (ddd, $J = 13.3, 11.6, 1.2$ Hz, 1H), 3.11 (dq, $J = 12.2, 4.0$ Hz, 1H), 3.01 (ddd, $J = 13.7, 5.2, 1.8$ Hz, 1H), 2.56 (tt, $J = 12.2, 3.0$ Hz, 1H), 2.40 (td, $J = 7.6, 2.6$ Hz, 2H), 2.27 (d, $J = 1.2$ Hz, 6H), 1.79 – 1.70 (m, 1H), 1.56 – 1.44 (m, 2H), 1.34 (hept, $J = 7.2, 6.6$ Hz, 2H), 0.91 (td, $J = 7.3, 1.2$ Hz, 3H). HPLC (gradient A): retention time = 40.9 min. ESI-MS 508.3 [M + Na]⁺.

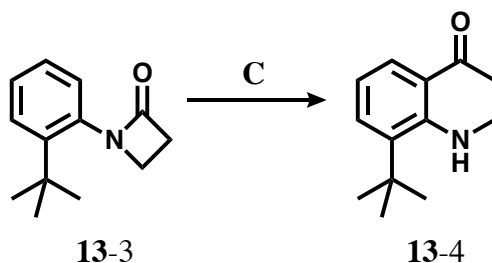
Compound 13 (Notebook reference: AFN-9 or afn-iii-93, notebook 3 p. 93)



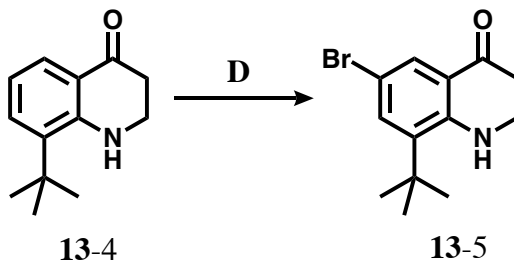
13-2. 3-bromo-N-(2-(tert-butyl)phenyl)propanamide. 13-2 was synthesized following **General Procedure (A)** from 2-(tert-butyl)aniline 13-1 (0.96 g, 6.41 mmol, 1.00 eq), K₂CO₃ (2.66 g, 19.2 mmol, 3.00 eq) and 3-bromopropionyl chloride (0.68 mL, 6.73 mmol, 1.05 eq). Yield: 1.82 g, 100%. ¹H NMR (500 MHz, CDCl₃) δ 7.54 (d, $J = 7.8$ Hz, 1H), 7.40 (d, $J = 7.8$ Hz, 1H), 7.26 – 7.16 (m, 2H), 3.75 (t, $J = 6.6$ Hz, 2H), 2.98 (t, $J = 6.5$ Hz, 2H), 1.42 (s, 13H). ¹³C NMR(126 MHz, CDCl₃) δ 168.21, 143.07, 134.64, 128.39, 127.55, 126.87, 126.65, 40.80, 34.65, 30.82, 27.24.



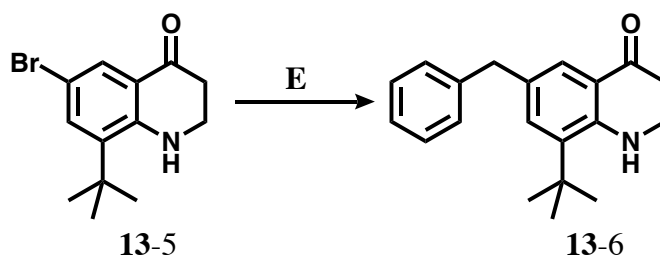
13-3. *1-(2-(tert-butyl)phenyl)azetidin-2-one*. **13-3** was synthesized following **General Procedure (B)** from **13-2** (1.90 g, 6.67 mmol, 1.00 eq) and NaOtBu (673 mg, 7.00 mmol, 1.05 eq). Yield: 1.36 g, 100%. ¹H NMR (500 MHz, CDCl₃) δ 7.46 (dd, *J* = 7.9, 1.5 Hz, 1H), 7.26 (s, 1H), 7.23 (td, *J* = 7.4, 1.5 Hz, 1H), 7.13 (dd, *J* = 7.6, 1.6 Hz, 1H), 3.64 (td, *J* = 4.3, 1.1 Hz, 2H), 3.10 (td, *J* = 4.3, 1.0 Hz, 2H), 1.41 (d, *J* = 0.9 Hz, 9H). ¹³C NMR(126 MHz, CDCl₃) δ 168.19, 148.84, 135.79, 130.22, 128.65, 127.52, 127.15, 44.52, 36.68, 35.20, 31.35.



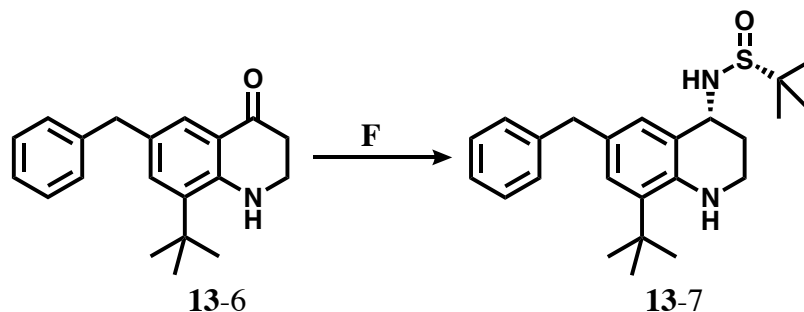
13-4. *8-(tert-butyl)-2,3-dihydroquinolin-4(1H)-one*. **13-4** was synthesized following **General Procedure (C)** from **13-3** (1.36 g, 6.71 mmol, 1.00 eq) and TfOH (1.78 mL, 20.14 mmol, 3.00 eq). Yield: 1.02 g, 75%. ¹H NMR (500 MHz, CDCl₃) δ 7.83 (ddd, *J* = 7.8, 1.6, 0.7 Hz, 1H), 7.37 (dd, *J* = 7.6, 1.7 Hz, 1H), 6.70 (td, *J* = 7.7, 1.6 Hz, 1H), 3.66 – 3.56 (m, 2H), 2.69 (ddd, *J* = 7.7, 6.8, 1.5 Hz, 2H), 1.43 (d, *J* = 1.2 Hz, 9H). ¹³C NMR(126 MHz, CDCl₃) δ 194.44, 150.68, 134.42, 132.18, 126.36, 120.68, 117.42, 42.24, 38.03, 34.28, 30.05



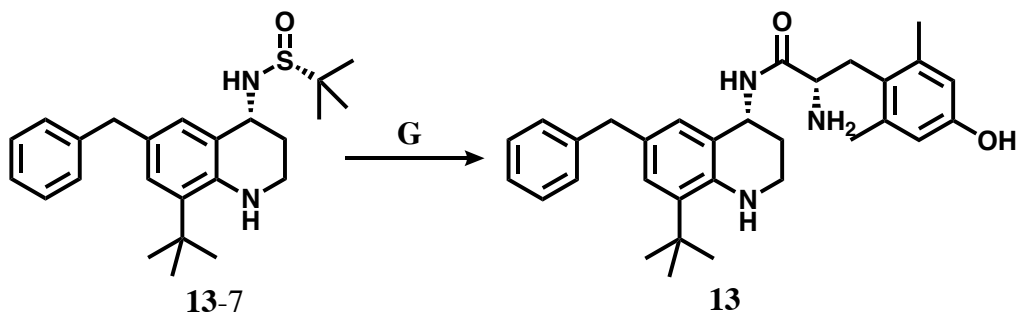
13-5. *6-bromo-8-(tert-butyl)-2,3-dihydroquinolin-4(1H)-one*. **13-5** was synthesized following **General Procedure (D)** from **13-4** (500 mg, 2.46 mmol, 1.00 eq) and NBS (460 mg, 2.58 mmol, 1.05 eq). Yield: 570 mg, 82%. ¹H NMR (500 MHz, CDCl₃) δ 7.92 (d, *J* = 2.4 Hz, 1H), 7.41 (d, *J* = 2.4 Hz, 1H), 4.73 (s, 1H), 3.61 (t, *J* = 7.0 Hz, 2H), 2.72 – 2.63 (m, 2H), 1.41 (s, 9H). ¹³C NMR(126 MHz, CDCl₃) δ 192.86, 149.20, 136.79, 134.67, 128.30, 121.49, 110.17, 77.16, 41.78, 37.37, 34.17, 29.59.



13-6. *6-benzyl-8-(tert-butyl)-2,3-dihydroquinolin-4(1H)-one*. **13-6** was synthesized following **General Procedure (E)** from **13-5** (300 mg, 1.06 mmol, 1 eq), benzyl boronic acid pinacol ester (0.47 mL, 2.12 mmol, 2 eq), K₂CO₃ (440 mg, 3.18 mmol, 3 eq) and Pd(dppf)Cl₂ (81 mg, 0.11 mmol, 0.1 eq), except reaction was run in microwave at 110°C for 2 hours. Yield: 87 mg, 28%. ¹H NMR (500 MHz, CDCl₃) δ 7.70 (d, *J* = 2.1 Hz, 1H), 7.40 – 7.37 (m, 1H), 7.30 – 7.25 (m, 2H), 7.22 (d, *J* = 2.1 Hz, 1H), 7.19 (d, *J* = 7.7 Hz, 2H), 3.87 (s, 2H), 3.62 – 3.57 (m, 2H), 2.69 – 2.65 (m, 2H), 1.39 (d, *J* = 1.0 Hz, 9H). ¹³C NMR(126 MHz, CDCl₃) δ 194.52, 149.25, 141.50, 133.32, 129.81, 128.83, 128.56, 126.08, 125.87, 120.60, 117.41, 42.34, 41.45, 38.10, 34.27, 30.06.



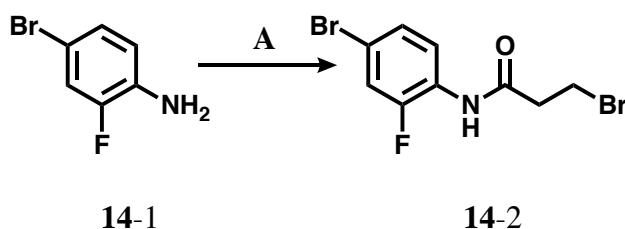
13-7. *(R)-N-((R)-6-benzyl-8-(tert-butyl)-1,2,3,4-tetrahydroquinolin-4-yl)-2-methylpropane-2-sulfonamide.* **13-7** was synthesized following **General Procedure (F)** from **13-6** (87 mg, 0.30 mmol, 1 eq), (R)-2-methyl-2-propanesulfonamide (109 mg, 0.90 mmol, 3 eq), and Ti(OEt)₄ (0.38 mL, 1.80 mmol, 6 eq), then NaBH₄ (68 mg, 1.80 mmol, 6 eq). Yield: 27 mg, 23%. ¹H NMR (500 MHz, CDCl₃) δ 7.18 (s, 1H), 7.14 – 7.10 (m, 2H), 7.10 – 7.06 (m, 1H), 6.93 (s, 2H), 6.57 (tt, *J* = 7.7, 2.1 Hz, 1H), 4.45 (d, *J* = 7.2 Hz, 1H), 3.81 – 3.72 (m, 2H), 3.34 – 3.21 (m, 2H), 2.02 – 1.95 (m, 1H), 1.81 (tdd, *J* = 16.7, 8.4, 4.1 Hz, 1H), 1.31 – 1.25 (m, 9H), 1.16 – 1.11 (m, 9H). ¹³C NMR(126 MHz, CDCl₃) δ 142.01, 141.55, 133.25, 131.16, 129.43, 129.16, 129.13, 128.92, 128.84, 128.71, 128.66, 128.45, 127.33, 127.17, 126.46, 126.34, 125.88, 121.13, 116.66, 77.16, 55.40, 50.33, 41.45, 36.56, 29.91, 29.70, 28.06, 22.80.



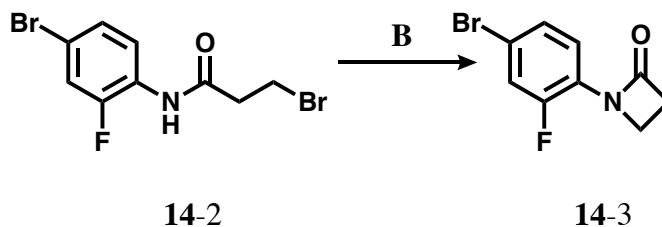
13. *(S)-2-amino-N-((R)-6-benzyl-8-(tert-butyl)-1,2,3,4-tetrahydroquinolin-4-yl)-3-(4-hydroxy-2,6-dimethylphenyl)propanamide.* **13** was synthesized following **General Procedure (G)** from **13-7** (27 mg, 0.068 mmol, 1 eq) and concentrated HCl (0.02 mL, excess). Carried forward without characterization. **Step 2:** Performed amide coupling using **13-7** amine salt (22 mg, 0.068 mmol, 1 eq), di-Boc-Dmt (31 mg, 0.074 mmol, 1.1 eq), PyBOP (39 mg, 0.074 mmol, 1.1 eq), 6-Cl HOBt (13 mg, 0.074 mmol, 1.1 eq), and DIPEA (0.12 mL, 0.67 mmol, 10 eq). **Step 3:** Boc-deprotected as described in **General Procedure (G)**. Final yield not calculated. ¹H NMR (500 MHz, Methanol-*d*₄) δ 7.23 – 7.17 (m, 2H), 7.14 – 7.07 (m, 3H), 6.91 (d, *J* = 2.2 Hz, 1H), 6.75 (d, *J* = 2.2 Hz, 1H),

6.49 (d, $J = 2.1$ Hz, 2H), 4.92 (s, 1H), 3.90 – 3.81 (m, 1H), 3.75 (s, 2H), 3.25 (ddd, $J = 13.7, 11.6, 2.3$ Hz, 1H), 3.09 (d, $J = 12.4$ Hz, 1H), 2.99 (ddd, $J = 13.8, 5.3, 2.2$ Hz, 1H), 2.48 (t, $J = 12.1$ Hz, 1H), 2.27 (d, $J = 2.2$ Hz, 6H), 1.67 (t, $J = 13.1$ Hz, 1H), 1.47 (d, $J = 13.3$ Hz, 1H), 1.29 (d, $J = 2.3$ Hz, 9H). HPLC (gradient A): retention time = 44.7 min. ESI-MS 486.3[M + H]⁺ and 508.3 [M + Na]⁺.

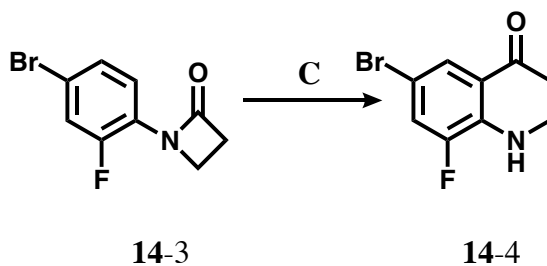
Compound 14 (Notebook name: AAH-58, synthesized by Dr. Aubrie Harland)



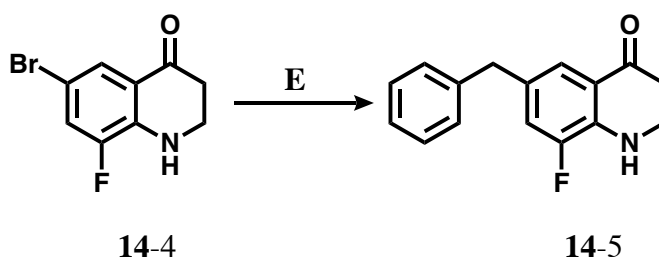
14-2. *3-bromo-N-(4-bromo-2-fluorophenyl)propanamide*. **14-2** was synthesized following **General Procedure (A)** from 4-bromo-2-fluoroaniline **14-1** (1.0 g, 5.26 mmol, 1.00 eq), K₂CO₃ (1.49 g, 10.8 mmol, 2.05 eq) and 3-bromopropionyl chloride (0.54 mL, 5.37 mmol, 1.05 eq). Yield: 1.71 g, 100%. ¹H NMR (500 MHz, CDCl₃) δ 8.18 (t, $J = 8.5$ Hz, 1H), 7.33 (s, 1H), 7.24 – 7.18 (m, 3H), 3.63 (t, $J = 6.5$ Hz, 2H), 2.93 (t, $J = 6.5$ Hz, 2H). ¹³C NMR(126 MHz, CDCl₃) δ 167.85, 152.96, 127.83, 127.80, 125.13, 122.80, 118.55, 118.37, 116.22, 40.63, 26.36.



14-3. *1-(4-bromo-2-fluorophenyl)azetidin-2-one.* **14-3** was synthesized following **General Procedure (B)** from **14-2** (1.71 g, 5.26 mmol, 1.00 eq) and NaOtBu (530 mg, 5.30 mmol, 1.05 eq). Yield: 1.00 g, 78%. ^1H NMR (500 MHz, CDCl_3) δ 7.91 (t, $J = 8.6$ Hz, 1H), 7.25 – 7.15 (m, 2H), 3.87 (q, $J = 4.4$ Hz, 2H), 3.15 (t, $J = 4.6$ Hz, 2H). ^{13}C NMR(126 MHz, CDCl_3) δ 165.40, 152.52, 150.53, 127.71, 127.68, 125.66, 125.58, 122.06, 122.03, 119.69, 119.51, 115.66, 115.59, 42.07, 42.01, 38.39, 38.38.

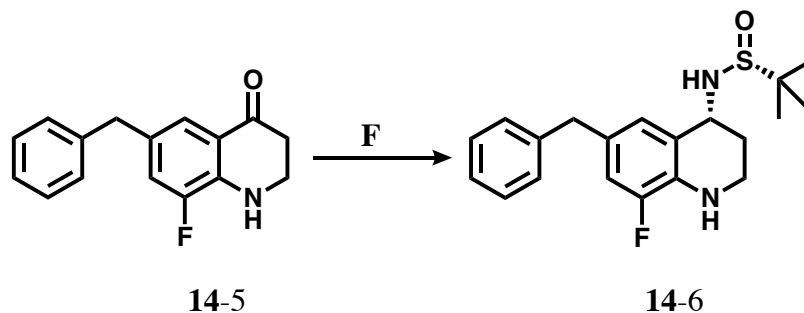


14-4. *6-bromo-8-fluoro-2,3-dihydroquinolin-4(1H)-one.* **14-4** was synthesized following **General Procedure (C)** from **14-3** (1.0 g, 4.1 mmol, 1 eq) and TfOH (1.09 mL, 12.3 mmol, 3 eq). Yield: 508 mg, 51%. ^1H NMR (500 MHz, CDCl_3) δ 7.76 (t, $J = 1.7$ Hz, 1H), 7.27 – 7.23 (m, 1H), 4.65 (s, 1H), 3.64 (td, $J = 7.5, 7.1, 2.0$ Hz, 2H), 2.73 (t, $J = 7.1$ Hz, 2H). ^{13}C NMR(126 MHz, CDCl_3) δ 191.33, 152.16, 150.20, 140.23, 140.13, 125.60, 122.79, 122.62, 121.78, 108.04, 107.97, 41.94, 37.80.

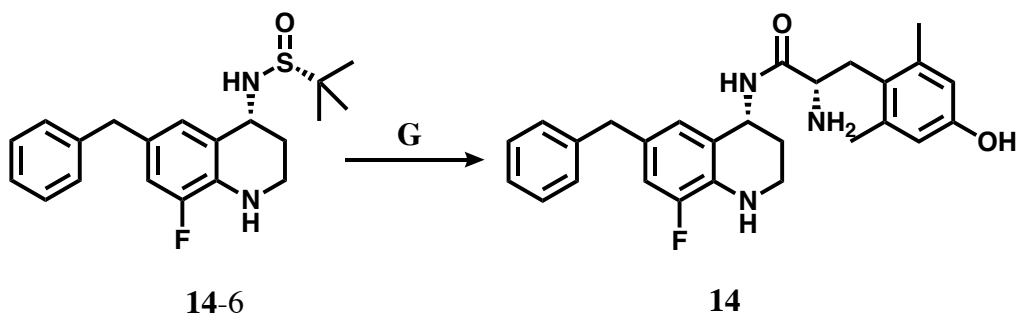


14-5. *6-benzyl-8-fluoro-2,3-dihydroquinolin-4(1H)-one.* **14-5** was synthesized following General Procedure (E) from **14-4** (75 mg, 0.31 mmol, 1 eq), benzyl boronic acid pinacol ester (0.14 mL, 0.61 mmol, 2 eq), K_2CO_3 (128 mg, 0.92 mmol, 3 eq) and $\text{Pd}(\text{dppf})\text{Cl}_2$ (23 mg, 0.03 mmol, 0.1 eq).

Yield: 29 mg, 37%. ¹H NMR (500 MHz, CDCl₃) δ 7.54 – 7.51 (m, 1H), 7.32 – 7.24 (m, 2H), 7.22 – 7.19 (m, 1H), 7.18 – 7.14 (m, 2H), 6.94 (dd, *J* = 11.7, 1.9 Hz, 1H), 4.52 (s, 1H), 3.86 (s, 2H), 3.61 (td, *J* = 7.5, 7.1, 1.8 Hz, 2H), 2.75 – 2.68 (m, 2H). ¹³C NMR(126 MHz, CDCl₃) δ 192.90, 152.40, 150.47, 140.70, 139.68, 139.57, 130.23, 128.89, 128.73, 126.45, 122.43, 120.44, 120.30, 42.29, 41.10, 38.20.

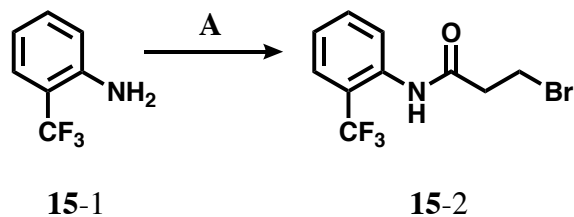


14-6. *(R)*-*N*-((*R*)-6-benzyl-8-fluoro-1,2,3,4-tetrahydroquinolin-4-yl)-2-methylpropane-2-sulfonamide. **14-6** was synthesized following **General Procedure (F)** from **14-5** (25 mg, 0.10 mmol, 1 eq), (*R*)-2-methyl-2-propanesulfonamide (36 mg, 0.30 mmol, 3 eq), and Ti(OEt)₄ (0.12 mL, 0.60 mmol, 6 eq), then NaBH₄ (23 mg, 0.60 mmol, 6 eq). Yield: 16 mg; 53%. ¹H NMR (500 MHz, CDCl₃) δ 7.27 (t, *J* = 7.6 Hz, 2H), 7.22 – 7.14 (m, 3H), 6.92 (s, 1H), 6.70 (dd, *J* = 12.0, 1.8 Hz, 1H), 4.55 (q, *J* = 3.3 Hz, 1H), 4.07 (s, 1H), 3.83 (d, *J* = 3.7 Hz, 2H), 3.36 (td, *J* = 11.6, 2.9 Hz, 1H), 3.30 (dt, *J* = 11.4, 4.2 Hz, 1H), 2.11 (dq, *J* = 13.7, 3.4 Hz, 1H), 1.97 – 1.88 (m, 1H), 1.62 (s, 1H), 1.22 (d, *J* = 0.7 Hz, 9H). ¹³C NMR(126 MHz, CDCl₃) δ 141.34, 131.91, 129.73, 128.88, 128.62, 126.23, 125.41, 122.55, 114.87, 114.73, 110.15, 55.58, 49.28, 41.10, 36.09, 28.36, 22.79.

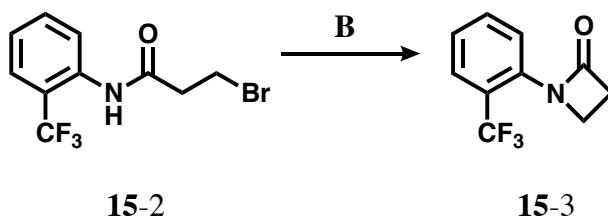


14 (*S*)-2-amino-*N*-((*R*)-6-benzyl-8-fluoro-1,2,3,4-tetrahydroquinolin-4-yl)-3-(4-hydroxy-2,6-dimethylphenyl)propanamide. **14** was synthesized following **General Procedure (G)** from **14-6** (19 mg, 0.05 mmol, 1 eq) and concentrated HCl (0.03 mL, excess). Carried forward without characterization. **Step 2:** Performed amide coupling using **14-6** amine salt (55 mg, 0.14 mmol, 1 eq), di-Boc-Dmt (60 mg, 0.15 mmol, 1.1 eq), PyBOP (73 mg, 0.15 mmol, 1.1 eq), and 6-Cl HOBt (24 mg, 0.15 mmol, 1.1 eq), followed by DIPEA (0.25 mL, 1.4 mmol, 10 eq). **Step 3:** Boc-deprotected as described in **General Procedure (G)**. Final yield not calculated. ^1H NMR (500 MHz, Methanol- d_4) δ 7.25 – 7.19 (m, 2H), 7.11 (d, $J = 7.7$ Hz, 2H), 6.70 (s, 1H), 6.63 (d, $J = 12.1$ Hz, 1H), 6.48 (s, 2H), 4.93 (s, 1H), 3.84 (dd, $J = 11.6, 4.7$ Hz, 1H), 3.75 (s, 2H), 3.25 (t, $J = 12.6$ Hz, 1H), 3.19 – 3.13 (m, 1H), 3.03 (d, $J = 8.0$ Hz, 1H), 3.00 (d, $J = 11.7$ Hz, 1H), 2.46 (t, $J = 11.7$ Hz, 1H), 2.31 – 2.23 (m, 7H), 1.68 (t, $J = 12.6$ Hz, 1H), 1.50 (d, $J = 13.4$ Hz, 1H). HPLC (gradient A): retention time = 35.2 min. ESI-MS 470.2 $[\text{M} + \text{Na}]^+$.

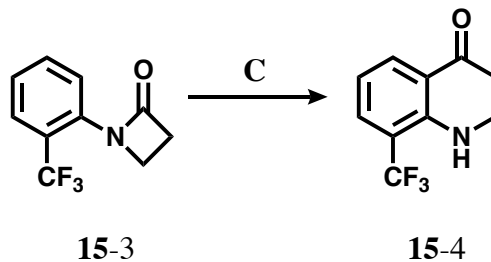
Compound 15 (Notebook reference: AFN-32 or afn-iv-285, notebook 4 p. 285)



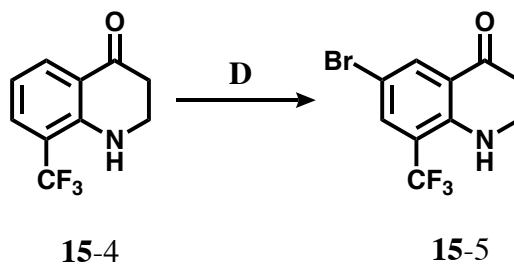
15-2. *3-bromo-N-(2-(trifluoromethyl)phenyl)propanamide*. **15-2** was synthesized following **General Procedure (A)** from 2-(trifluoromethyl)aniline **15-1** (2.00 g, 12.4 mmol, 1.00 eq), K₂CO₃ (5.14 g, 37.2 mmol, 3.00 eq) and 3-bromopropionyl chloride (1.31 mL, 13.0 mmol, 1.05 eq). Yield: 3.68 g, 100%. ¹H NMR (500 MHz, CDCl₃) δ 8.17 (d, *J* = 8.2 Hz, 1H), 7.63 (d, *J* = 8.1 Hz, 1H), 7.57 (t, *J* = 7.9 Hz, 1H), 7.43 (t, *J* = 7.7 Hz, 1H), 3.71 (t, *J* = 6.6 Hz, 2H), 2.99 (t, *J* = 6.5 Hz, 2H). ¹³C NMR(126 MHz, CDCl₃) δ 168.31, 134.75, 133.71, 133.06, 127.45, 126.26, 125.10, 40.86, 26.53.



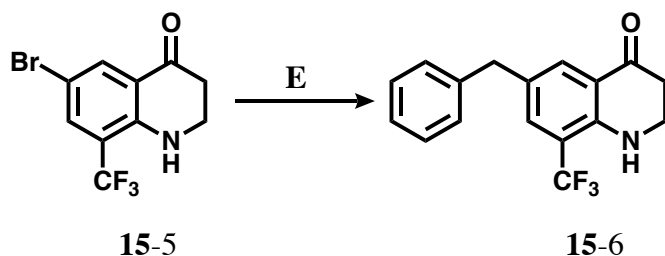
15-3. *1-(2-(trifluoromethyl)phenyl)azetidin-2-one*. **15-3** was synthesized following **General Procedure (B)** from **15-2** (3.38 g, 12.56 mmol, 1.00 eq) and NaOtBu (1.27 g, 13.19 mmol, 1.05 eq). Yield: 1.62 g, 60%. ¹H NMR (500 MHz, CDCl₃) δ 7.98 (d, *J* = 8.1 Hz, 1H), 7.64 (dd, *J* = 8.0, 1.4 Hz, 1H), 7.52 (td, *J* = 7.8, 1.5 Hz, 1H), 7.30 – 7.21 (m, 1H), 3.84 (td, *J* = 4.6, 1.2 Hz, 2H), 3.14 (t, *J* = 4.7 Hz, 2H). ¹³C NMR(126 MHz, CDCl₃) δ 166.86, 135.88, 135.87, 132.95, 132.94, 127.00, 126.95, 125.58, 125.55, 124.66, 122.49, 43.89, 43.86, 43.82, 43.79, 37.24.



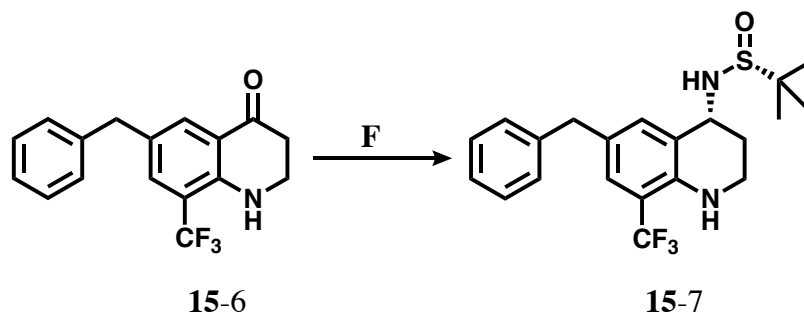
15-4. *8-(trifluoromethyl)-2,3-dihydroquinolin-4(1H)-one*. **15-4** was synthesized following **General Procedure (C)** from **15-3** (1.62 g, 7.52 mmol, 1.00 eq) and TfOH (2.00 mL, 22.56 mmol, 3.00 eq). Yield: 850 mg, 52%. ¹H NMR (500 MHz, CDCl₃) δ 8.05 (ddd, *J* = 7.9, 1.7, 0.9 Hz, 1H), 7.60 (ddd, *J* = 7.6, 1.7, 0.8 Hz, 1H), 6.77 (td, *J* = 7.7, 0.9 Hz, 1H), 5.06 (s, 1H), 3.69 – 3.63 (m, 2H), 2.77 – 2.71 (m, 2H). ¹³C NMR(126 MHz, CDCl₃) δ 192.59, 148.70, 132.75, 132.71, 132.66, 132.62, 132.22, 125.64, 123.47, 120.74, 116.46, 41.72, 37.44.



15-5. *6-bromo-8-(trifluoromethyl)-2,3-dihydroquinolin-4(1H)-one*. **15-5** was synthesized following **General Procedure (D)** from **15-4** (850 mg, 3.95 mmol, 1.00 eq) and NBS (739 mg, 4.15 mmol, 1.05 eq). Yield: 1.00 g, 86%. ¹H NMR (500 MHz, CDCl₃) δ 8.13 (d, *J* = 2.4 Hz, 1H), 7.68 (d, *J* = 2.5 Hz, 1H), 5.07 (s, 1H), 3.70 – 3.63 (m, 2H), 2.78 – 2.70 (m, 2H). ¹³C NMR(126 MHz, CDCl₃) δ 191.23, 147.36, 135.24, 135.19, 135.15, 135.10, 134.57, 124.64, 122.47, 122.03, 108.56, 41.55, 37.08.

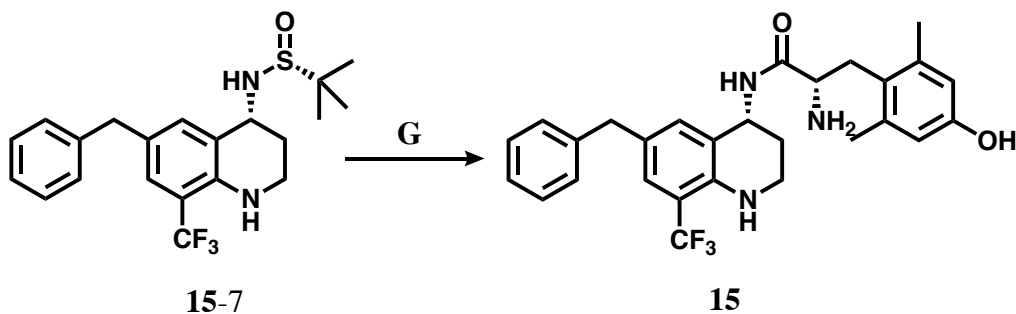


15-6. *6-benzyl-8-(trifluoromethyl)-2,3-dihydroquinolin-4(1H)-one.* **15-6** was synthesized following General Procedure (E) from **15-5** (300 mg, 1.02 mmol, 1 eq), benzyl boronic acid pinacol ester (0.45 mL, 2.04 mmol, 2 eq), K_2CO_3 (423 mg, 3.06 mmol, 3 eq) and $Pd(dppf)Cl_2$ (73 mg, 0.10 mmol, 0.1 eq). Yield: 110 mg, 35%. 1H NMR (500 MHz, $CDCl_3$) δ 7.92 (d, $J = 2.2$ Hz, 1H), 7.44 (d, $J = 2.2$ Hz, 1H), 7.29 (dd, $J = 8.2, 6.9$ Hz, 2H), 7.23 – 7.18 (m, 1H), 7.17 – 7.14 (m, 2H), 4.96 (s, 1H), 3.89 (s, 2H), 3.64 (td, $J = 7.0, 2.3$ Hz, 2H), 2.75 – 2.67 (m, 2H). ^{13}C NMR (126 MHz, $CDCl_3$) δ 192.72, 147.26, 140.45, 133.27, 132.02, 129.55, 128.81, 126.54, 120.84, 41.84, 40.82, 37.57.



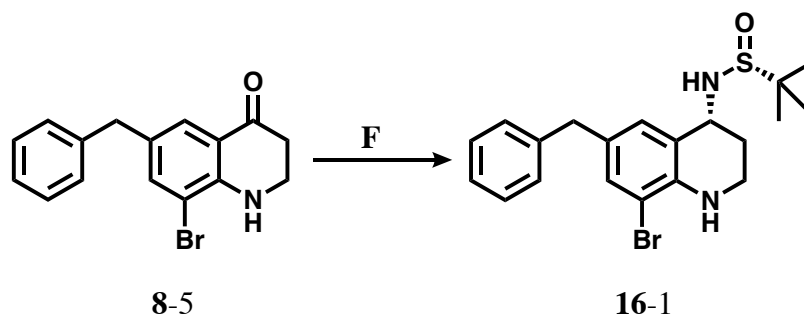
15-7. *(R)-N-((R)-6-benzyl-8-(trifluoromethyl)-1,2,3,4-tetrahydroquinolin-4-yl)-2-methylpropane-2-sulfonamide.* **15-7** was synthesized following **General Procedure (F)** from **15-6** (110 mg, 0.36 mmol, 1 eq), (R)-2-methyl-2-propanesulfonamide (132 mg, 1.08 mmol, 3 eq), and $Ti(OEt)_4$ (0.45 mL, 2.16 mmol, 6 eq), then $NaBH_4$ (82 mg, 2.16 mmol, 6 eq). Yield: 128 mg, 86%. 1H NMR (500 MHz, $CDCl_3$) δ 7.30 – 7.24 (m, 3H), 7.20 – 7.15 (m, 4H), 4.59 (s, 1H), 4.54 (q, $J = 3.3$ Hz, 1H), 3.90 – 3.79 (s, 2H), 3.41 (td, $J = 12.0, 3.1$ Hz, 1H), 3.34 (dt, $J = 7.8, 4.0$ Hz, 1H), 2.10 (dq, $J = 13.8, 3.5$ Hz, 1H), 1.88 (ddt, $J = 17.0, 12.9, 3.9$ Hz, 1H), 1.22 (s, 9H). ^{13}C NMR (126 MHz, $CDCl_3$)

δ 141.13, 140.96, 134.78, 128.80, 128.68, 127.21, 126.30, 122.16, 55.63, 49.84, 40.86, 36.30, 27.23, 22.77.

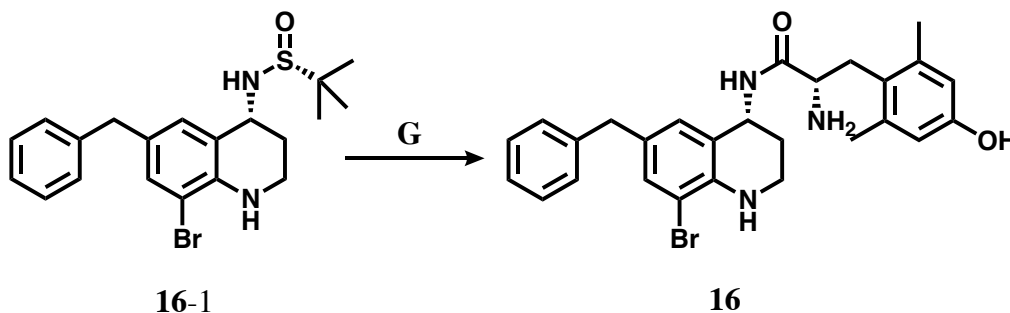


15. *(S)*-2-amino-*N*-((*R*)-6-benzyl-8-(trifluoromethyl)-1,2,3,4-tetrahydroquinolin-4-yl)-3-(4-hydroxy-2,6-dimethylphenyl)propanamide. **15** was synthesized following **General Procedure (G)** from **15-7** (128 mg, 0.31 mmol, 1 eq) and concentrated HCl (0.05 mL, excess). Carried forward without characterization. **Step 2:** Performed amide coupling using **15-7** amine salt (48 mg, 0.140 mmol, 1 eq), di-Boc-Dmt (63 mg, 0.154 mmol, 1.1 eq), PyBOP (78 mg, 0.154 mmol, 1.1 eq), and 6-Cl HOBt (26 mg, 0.154 mmol, 1.1 eq), followed by DIPEA (0.25 mL, 1.40 mmol, 10 eq). **Step 3:** Boc-protected as described in **General Procedure (G)**. Final yield not calculated. ^1H NMR (500 MHz, Methanol- d_4) δ 8.21 (d, J = 8.0 Hz, 1H), 7.26 – 7.21 (m, 2H), 7.17 – 7.13 (m, 1H), 7.13 – 7.08 (m, 3H), 7.06 (d, J = 2.1 Hz, 1H), 6.50 – 6.46 (m, 2H), 4.95 (q, J = 4.2 Hz, 1H), 3.84 (dd, J = 11.6, 5.0 Hz, 1H), 3.79 (s, 2H), 3.25 (dd, J = 13.6, 11.6 Hz, 1H), 3.08 (dtd, J = 12.6, 4.3, 1.2 Hz, 1H), 3.01 (dd, J = 13.7, 5.0 Hz, 1H), 2.50 – 2.41 (m, 1H), 1.70 – 1.60 (m, 1H), 1.50 (dq, J = 13.2, 3.7 Hz, 1H). ^{13}C NMR(126 MHz, cd_3od) δ 168.36, 157.38, 142.65, 142.38, 140.00, 135.67, 129.64, 129.48, 128.97, 127.69, 127.12, 123.27, 121.87, 116.46, 53.39, 46.76, 41.44, 37.53, 31.94, 28.05, 20.44. HPLC (gradient A): retention time = 42.1 min. ESI-MS 498.24 $[\text{M} + \text{H}]^+$.

Compound 16 (Notebook reference: AFN-31 or afn-iv-287, notebook 4 p. 287)



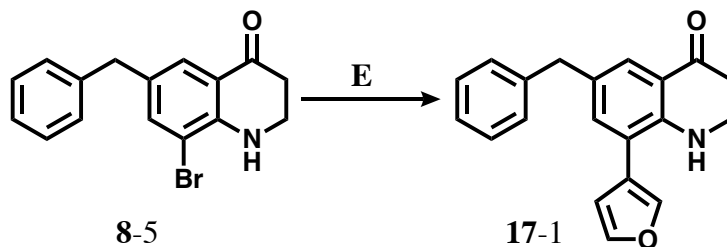
16-1. *(R)-N-((R)-6-benzyl-8-bromo-1,2,3,4-tetrahydroquinolin-4-yl)-2-methylpropane-2-sulfonamide.* **16-1** was synthesized following **General Procedure (F)** from **8-5** (80 mg, 0.25 mmol, 1 eq), (R)-2-methyl-2-propanesulfonamide (92 mg, 0.76 mmol, 3 eq), and Ti(OEt)₄ (0.32 mL, 1.52 mmol, 6 eq), then NaBH₄ (58 mg, 1.52 mmol, 6 eq). Yield: 71 mg, 67%. ¹H NMR (500 MHz, CDCl₃) δ 7.29 – 7.25 (m, 2H), 7.20 – 7.15 (m, 4H), 7.06 (d, *J* = 1.9 Hz, 1H), 4.52 (q, *J* = 3.2 Hz, 1H), 4.50 (s, 1H), 3.81 (s, 2H), 3.41 (tdd, *J* = 11.9, 3.0, 1.1 Hz, 1H), 3.37 – 3.32 (m, 1H), 2.98 (s, 1H), 2.13 – 2.06 (m, 1H), 1.93 – 1.84 (m, 1H), 1.21 (s, 9H). ¹³C NMR(126 MHz, CDCl₃) δ 141.27, 140.26, 132.57, 130.70, 129.96, 128.85, 128.62, 126.23, 121.86, 109.13, 55.58, 49.86, 40.80, 36.61, 27.91, 22.



16. *(S)-2-amino-N-((R)-6-benzyl-8-bromo-1,2,3,4-tetrahydroquinolin-4-yl)-3-(4-hydroxy-2,6-dimethylphenyl)propanamide.* **16** was synthesized following **General Procedure (G)** from **16-1**

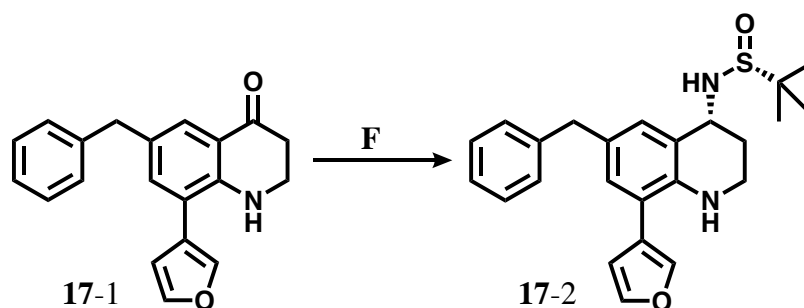
(71 mg, 0.17 mmol, 1 eq) and concentrated HCl (0.03 mL, excess). Carried forward without characterization. **Step 2:** Performed amide coupling using **16-1** amine salt (62 mg, 0.175 mmol, 1 eq), di-Boc-Dmt (78 mg, 0.192 mmol, 1.1 eq), PyBOP (99 mg, 0.192 mmol, 1.1 eq), and 6-Cl HOBt (32 mg, 0.192 mmol, 1.1 eq), followed by DIPEA (0.31 mL, 1.75 mmol, 10 eq), stirring 18 hours before Boc-deprotecting. **Step 3:** Boc-deprotected as described in **General Procedure (G)**. Final yield not calculated. ^1H NMR (500 MHz, Methanol- d_4) δ 8.16 (d, J = 8.0 Hz, 1H), 7.26 – 7.20 (m, 2H), 7.17 – 7.12 (m, 1H), 7.12 – 7.08 (m, 3H), 6.86 (d, J = 2.0 Hz, 1H), 6.48 (s, 2H), 4.91 (dt, J = 7.9, 4.1 Hz, 1H), 3.83 (dd, J = 11.6, 5.0 Hz, 1H), 3.74 (s, 2H), 3.25 (dd, J = 13.6, 11.6 Hz, 1H), 3.12 – 3.04 (m, 1H), 3.00 (dd, J = 13.7, 5.0 Hz, 1H), 2.46 (td, J = 12.0, 3.0 Hz, 1H), 2.27 (s, 6H), 1.64 (ddt, J = 13.0, 11.6, 4.1 Hz, 1H), 1.50 (dq, J = 13.3, 3.8 Hz, 1H). ^{13}C NMR(126 MHz, cd_3od) δ 168.28, 157.38, 142.79, 141.86, 139.99, 133.41, 131.24, 130.77, 129.66, 129.43, 127.06, 123.26, 121.64, 116.45, 109.56, 53.39, 46.91, 41.45, 37.96, 31.94, 28.75, 20.45. HPLC (gradient A): retention time = 39.9 min. ESI-MS 508.16[M + H] $^+$ and 510.16 [M + Na] $^+$.

Compound 17 (Notebook reference: AFN-12 or afn-iii-245, notebook 3 p. 245)

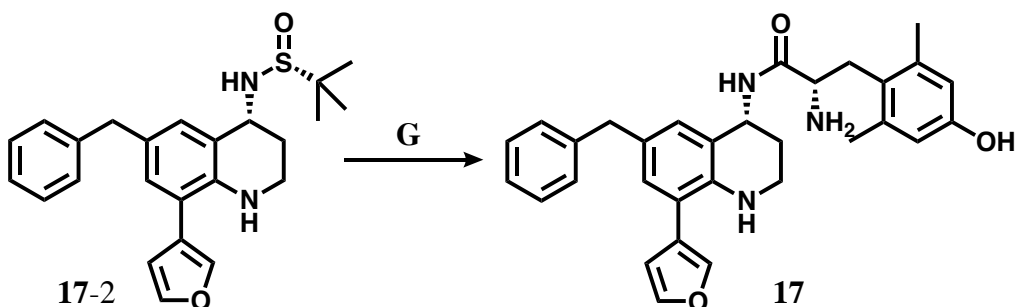


17-1. *6-benzyl-8-(furan-3-yl)-2,3-dihydroquinolin-4(1H)-one.* **17-1** was synthesized following **General Procedure (E)** from **8-5** (111 mg, 0.35 mmol, 1 eq), 3-furanylboronic acid (60 mg, 0.53 mmol, 1.5 eq), K_2CO_3 (145 mg, 1.05 mmol, 3 eq) and $\text{Pd}(\text{dppf})\text{Cl}_2$ (26 mg, 0.035 mmol, 0.1 eq).

Yield: 88 mg, 83%. ¹H NMR (500 MHz, Chloroform-*d*) δ 7.74 (d, *J* = 2.1 Hz, 1H), 7.60 – 7.56 (m, 1H), 7.52 (t, *J* = 1.5 Hz, 1H), 7.26 (t, *J* = 7.7 Hz, 2H), 7.21 – 7.16 (m, 3H), 7.17 – 7.13 (m, 1H), 6.55 – 6.52 (m, 1H), 4.75 (s, 1H), 3.88 (s, 2H), 3.50 (td, *J* = 7.5, 7.1, 2.0 Hz, 2H), 2.69 (t, *J* = 6.9 Hz, 2H). ¹³C NMR (126 MHz, cdcl₃) δ 194.00, 148.40, 143.83, 141.22, 140.26, 136.20, 130.38, 128.83, 128.62, 126.94, 126.22, 121.97, 120.04, 119.68, 111.00, 42.41, 41.09, 38.05.

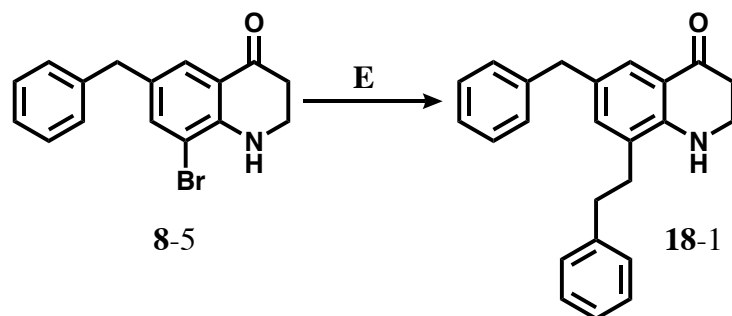


17-2. *(R)*-*N*-((*R*)-6-benzyl-8-(furan-3-yl)-1,2,3,4-tetrahydroquinolin-4-yl)-2-methylpropane-2-sulfonamide. **17-2** was synthesized following **General Procedure (F)** from **17-1** (71 mg, 0.23 mmol, 1 eq), (*R*)-2-methyl-2-propanesulfonamide (85 mg, 0.70 mmol, 3 eq), and Ti(OEt)₄ (0.29 mL, 1.40 mmol, 6 eq), then NaBH₄ (53 mg, 1.40 mmol, 6 eq). Yield: 34 mg, 35%. ¹H NMR (500 MHz, Chloroform-*d*) δ 7.49 (d, *J* = 1.7 Hz, 1H), 7.41 (q, *J* = 1.7 Hz, 1H), 7.19 (td, *J* = 7.4, 6.4, 1.6 Hz, 2H), 7.16 – 7.07 (m, 3H), 7.02 (d, *J* = 1.7 Hz, 1H), 6.85 (d, *J* = 1.8 Hz, 1H), 6.47 (d, *J* = 1.9 Hz, 1H), 4.50 (d, *J* = 4.0 Hz, 1H), 3.78 (d, *J* = 2.6 Hz, 2H), 3.25 (ddd, *J* = 14.1, 11.0, 2.5 Hz, 1H), 3.19 – 3.14 (m, 1H), 3.13 (s, 1H), 2.02 (dd, *J* = 13.6, 3.4 Hz, 1H), 1.91 – 1.80 (m, 1H), 1.14 (d, *J* = 1.5 Hz, 9H). ¹³C NMR (126 MHz, cdcl₃) δ 143.42, 141.81, 140.90, 140.08, 130.29, 130.18, 129.87, 128.86, 128.56, 126.04, 122.94, 120.89, 118.22, 111.19, 77.16, 55.49, 49.88, 41.14, 36.62, 28.27, 22.80.

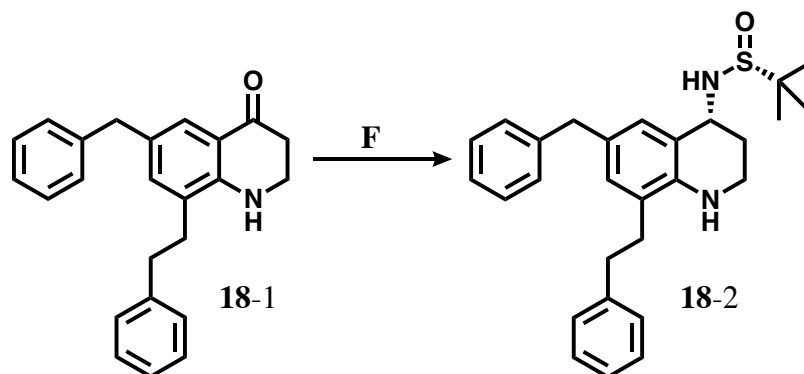


17. (*S*)-2-amino-*N*-((*R*)-6-benzyl-8-(furan-3-yl)-1,2,3,4-tetrahydroquinolin-4-yl)-3-(4-hydroxy-2,6-dimethylphenyl)propanamide. **17** was synthesized following **General Procedure (G)** from **17-2** (34 mg, 0.08 mmol, 1 eq) and concentrated HCl (0.03 mL, excess). Carried forward without characterization. **Step 2:** Performed amide coupling using **17-2** amine salt (0.08 mmol, 1 eq), di-Boc-Dmt (38 mg, 0.09 mmol, 1.1 eq), PyBOP (48 mg, 0.09 mmol, 1.1 eq), and 6-Cl HOBt (16 mg, 0.09 mmol, 1.1 eq), followed by DIPEA (0.14 mL, 0.80 mmol, 10 eq). **Step 3:** Boc-protected as described in **General Procedure (G)**. Final yield not calculated. $^1\text{H NMR}$ (500 MHz, Methanol- d_4) δ 8.19 (t, $J = 6.5$ Hz, 1H), 7.63 – 7.60 (m, 1H), 7.55 (q, $J = 1.9$ Hz, 1H), 7.25 – 7.19 (m, 2H), 7.16 – 7.10 (m, 3H), 6.93 – 6.87 (m, 2H), 6.53 (d, $J = 2.0$ Hz, 1H), 6.47 (d, $J = 1.9$ Hz, 2H), 4.96 (d, $J = 6.6$ Hz, 1H), 3.86 (ddt, $J = 11.8, 4.8, 2.0$ Hz, 1H), 3.80 (d, $J = 2.3$ Hz, 2H), 3.25 (ddd, $J = 13.6, 11.4, 2.0$ Hz, 1H), 3.07 – 2.98 (m, 2H), 2.46 (tq, $J = 11.9, 2.9, 2.0$ Hz, 1H), 2.27 (d, $J = 1.9$ Hz, 6H), 1.73 (td, $J = 12.2, 4.0$ Hz, 1H), 1.56 – 1.47 (m, 1H). $^{13}\text{C NMR}$ (126 MHz, cd_3od) δ 168.36, 157.29, 144.58, 143.13, 141.24, 140.00, 131.91, 131.16, 130.88, 129.66, 129.36, 126.92, 124.06, 123.33, 121.87, 120.62, 116.44, 111.82, 53.41, 49.00, 46.92, 41.88, 38.49, 31.92, 28.87, 20.46. HPLC (method 20 to 70%B in 50 min): retention time = 19.3 min, or approximately 39.3 minutes adjusted to gradient A. ESI-MS 496.3 $[\text{M}+\text{H}]^+$ and 518.3 $[\text{M}+\text{Na}]^+$.

Compound 18 (Notebook reference: AFN-16 or afn-iv-3, notebook 4 p. 3)

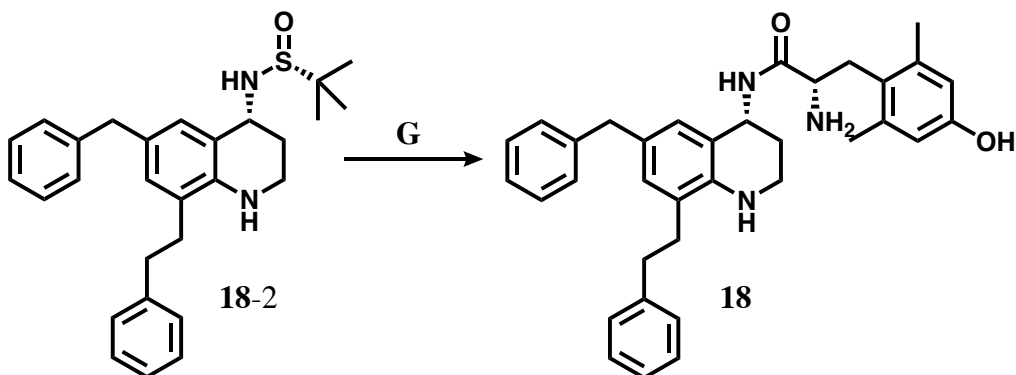


18-1. *6-benzyl-8-phenethyl-2,3-dihydroquinolin-4(1H)-one*. **18-1** was synthesized following **General Procedure (E)** from **8-5** (130 mg, 0.41 mmol, 1 eq), phenethyl boronic acid MIDA ester (161 mg, 0.62 mmol, 1.5 eq), K_2CO_3 (171 mg, 1.24 mmol, 3 eq) and $Pd(dppf)Cl_2$ (30 mg, 0.04 mmol, 0.1 eq). Yield: 65 mg, 46%. 1H NMR (500 MHz, $CDCl_3$) δ 7.67 (d, $J = 2.1$ Hz, 1H), 7.26 (s, 4H), 7.24 – 7.18 (m, 2H), 7.15 (dd, $J = 9.7, 7.7$ Hz, 4H), 7.02 (d, $J = 2.1$ Hz, 1H), 3.85 (s, 2H), 3.39 (td, $J = 7.7, 7.1, 2.1$ Hz, 2H), 2.93 – 2.87 (m, 2H), 2.73 (t, $J = 7.7$ Hz, 2H), 2.66 – 2.60 (m, 2H). ^{13}C NMR(126 MHz, $CDCl_3$) δ 194.30, 148.77, 141.43, 141.25, 136.03, 130.18, 128.79, 128.65, 128.55, 128.48, 126.93, 126.40, 126.09, 125.71, 119.56, 42.37, 41.14, 37.97, 35.30, 32.85.



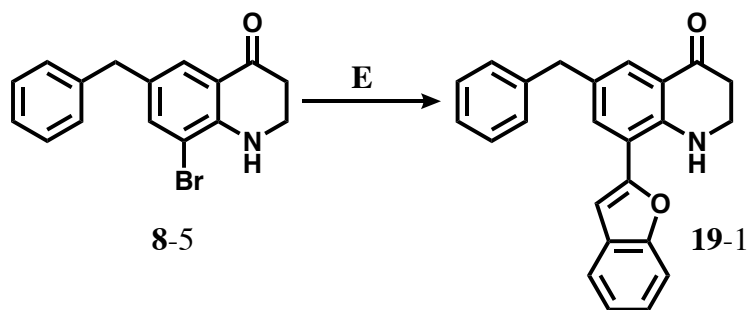
18-2. *(R)-N-((R)-6-benzyl-8-phenethyl-1,2,3,4-tetrahydroquinolin-4-yl)-2-methylpropane-2-sulfonamide*. **18-2** was synthesized following **General Procedure (F)** from **18-1** (65 mg, 0.19

mmol, 1 eq), (R)-2-methyl-2-propanesulfinamide (70 mg, 0.57 mmol, 3 eq), and Ti(OEt)₄ (0.24 mL, 1.14 mmol, 6 eq), then NaBH₄ (44 mg, 1.14 mmol, 6 eq). Yield: 61 mg, 72%. Carried forward without characterization.

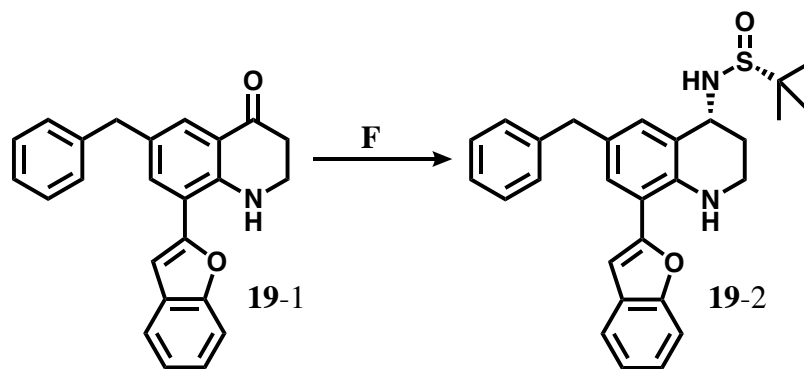


18. (*S*)-2-amino-*N*-((*R*)-6-benzyl-8-phenethyl-1,2,3,4-tetrahydroquinolin-4-yl)-3-(4-hydroxy-2,6-dimethylphenyl)propanamide. **18** was synthesized following **General Procedure (G)** from **18-2** (61 mg, 0.14 mmol, 1 eq) and concentrated HCl (0.03 mL, excess). Carried forward without characterization. **Step 2:** Performed amide coupling using **18-2** amine salt (32 mg, 0.084 mmol, 1 eq), di-Boc-Dmt (38 mg, 0.093 mmol, 1.1 eq), PyBOP (49 mg, 0.093 mmol, 1.1 eq), and 6-Cl HOBt (16 mg, 0.093 mmol, 1.1 eq), followed by DIPEA (0.15 mL, 0.84 mmol, 10 eq). **Step 3:** Boc-deprotected as described in **General Procedure (G)**. Yield after deprotection: 17 mg, 31% over 2 steps. ¹H NMR (500 MHz, Methanol-*d*₄) δ 8.12 (d, *J* = 7.9 Hz, 1H), 7.23 – 7.17 (m, 4H), 7.16 – 7.09 (m, 4H), 7.05 – 7.02 (m, 2H), 6.79 (d, *J* = 2.0 Hz, 1H), 6.70 (d, *J* = 2.0 Hz, 1H), 6.49 (s, 2H), 4.94 (q, *J* = 4.6 Hz, 1H), 3.86 (dd, *J* = 11.6, 5.0 Hz, 1H), 3.72 (s, 2H), 3.25 (dd, *J* = 13.6, 11.6 Hz, 1H), 3.06 (dt, *J* = 12.2, 4.3 Hz, 1H), 3.01 (dd, *J* = 13.6, 5.1 Hz, 1H), 2.81 (t, *J* = 7.6 Hz, 2H), 2.70 (td, *J* = 8.0, 7.5, 4.7 Hz, 2H), 2.51 (td, *J* = 11.8, 2.5 Hz, 1H), 2.28 (s, 6H), 1.76 – 1.67 (m, 1H), 1.55 – 1.47 (m, 1H). HPLC (gradient A): retention time = 45.3 min. ESI-MS 556.3 [M + Na]⁺.

Compound 19 (Notebook reference: AFN-13 or afn-iii-247, notebook 5 p. 247)

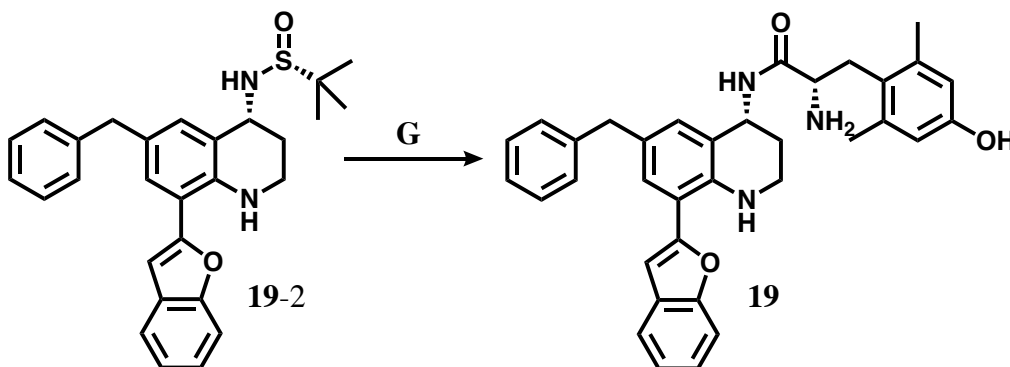


19-1. *8-(benzofuran-2-yl)-6-benzyl-2,3-dihydroquinolin-4(1H)-one.* **19-1** was synthesized following **General Procedure (E)** from **8-5** (113 mg, 0.36 mmol, 1 eq), 2-benzofuranyl boronic acid MIDA ester (146 mg, 0.54 mmol, 1.5 eq), K_2CO_3 (148 mg, 1.07 mmol, 3 eq) and $Pd(dppf)Cl_2$ (27 mg, 0.036 mmol, 0.1 eq). Yield: 116 mg, 92%. 1H NMR (500 MHz, Chloroform-*d*) δ 7.85 – 7.81 (m, 1H), 7.60 – 7.56 (m, 2H), 7.52 (d, $J = 8.1$ Hz, 1H), 7.33 – 7.23 (m, 4H), 7.19 (dd, $J = 14.5, 7.4$ Hz, 3H), 6.90 (s, 1H), 3.92 (s, 2H), 3.66 – 3.59 (m, 2H), 2.74 (t, $J = 6.9$ Hz, 2H). ^{13}C NMR (126 MHz, $cdCl_3$) δ 193.69, 154.49, 154.18, 147.86, 141.04, 135.23, 130.26, 128.98, 128.85, 128.69, 128.56, 126.32, 124.67, 123.45, 121.01, 120.48, 117.22, 111.24, 104.17, 77.16, 42.12, 41.03, 37.92.



19-2. *(R)-N-((R)-8-(benzofuran-2-yl)-6-benzyl-1,2,3,4-tetrahydroquinolin-4-yl)-2-methylpropane-2-sulfonamide.* **19-2** was synthesized following **General Procedure (F)** from **19-1**

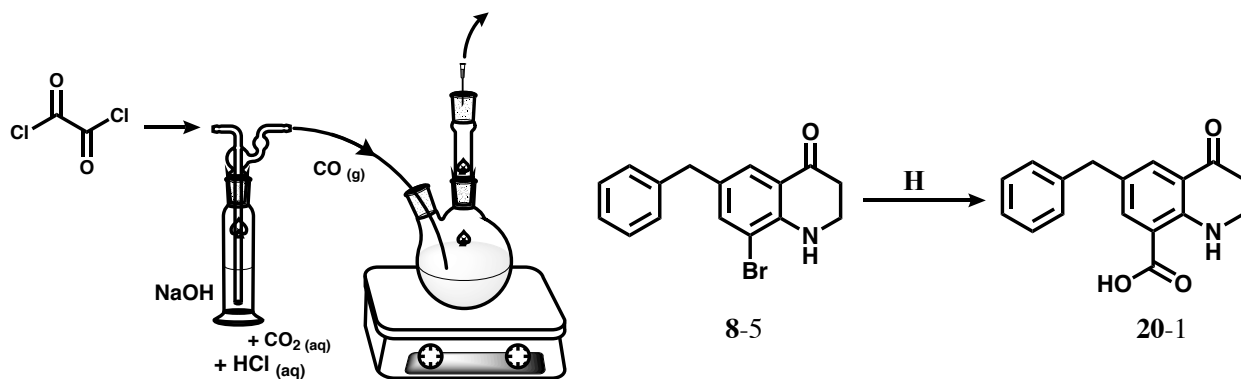
1 (97 mg, 0.27 mmol, 1 eq), (R)-2-methyl-2-propanesulfonamide (100 mg, 0.82 mmol, 3 eq), and Ti(OEt)₄ (0.35 mL, 1.65 mmol, 6 eq), then NaBH₄ (63 mg, 1.65 mmol, 6 eq). Yield: 62 mg, 52%. ¹H NMR (500 MHz, Chloroform-*d*) δ 7.50 – 7.45 (m, 1H), 7.45 – 7.40 (m, 1H), 7.27 (d, *J* = 2.2 Hz, 1H), 7.23 – 7.14 (m, 5H), 7.14 (dd, *J* = 7.2, 1.5 Hz, 2H), 7.08 (t, *J* = 3.0 Hz, 1H), 6.78 (d, *J* = 1.3 Hz, 1H), 4.51 (t, *J* = 3.0 Hz, 1H), 3.82 (s, 2H), 3.37 (td, *J* = 11.9, 3.0 Hz, 1H), 3.28 (dt, *J* = 11.6, 3.8 Hz, 1H), 2.05 (dq, *J* = 13.6, 3.2 Hz, 1H), 1.92 – 1.82 (m, 1H), 1.15 (d, *J* = 3.1 Hz, 9H). ¹³C NMR (126 MHz, cdcl₃) δ 155.55, 154.36, 141.63, 141.04, 132.05, 129.57, 129.47, 128.84, 128.58, 126.11, 124.15, 123.17, 121.70, 120.76, 115.16, 111.11, 103.46, 77.16, 55.54, 50.05, 41.05, 36.40, 27.65, 22.78, 22.64.



19. *(S)*-2-amino-*N*-((*R*)-8-(benzofuran-2-yl)-6-benzyl-1,2,3,4-tetrahydroquinolin-4-yl)-3-(4-hydroxy-2,6-dimethylphenyl)propanamide. **19** was synthesized following **General Procedure (G)** from **19-2** (62 mg, 0.14 mmol, 1 eq) and concentrated HCl (0.05 mL, excess). Carried forward without characterization. **Step 2:** Performed amide coupling using **19-2** amine salt (0.14 mmol, 1 eq), di-Boc-Dmt (61 mg, 0.15 mmol, 1.1 eq), PyBOP (78 mg, 0.15 mmol, 1.1 eq), and 6-Cl HOBt (26 mg, 0.15 mmol, 1.1 eq), followed by DIPEA (0.25 mL, 1.40 mmol, 10 eq). **Step 3:** Boc-deprotected as described in **General Procedure (G)**. Final yield not calculated. ¹H NMR (500 MHz, Methanol-*d*₄) δ 8.25 (d, *J* = 7.9 Hz, 1H), 7.59 – 7.54 (m, 1H), 7.51 – 7.46 (m, 1H), 7.38 (d,

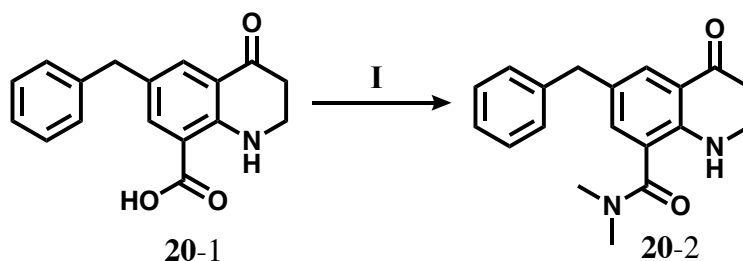
$J = 2.0$ Hz, 1H), 7.29 – 7.20 (m, 4H), 7.20 – 7.11 (m, 3H), 6.97 – 6.92 (m, 2H), 6.49 (d, $J = 1.7$ Hz, 2H), 4.97 (p, $J = 4.1$ Hz, 1H), 3.91 – 3.84 (m, 1H), 3.83 (d, $J = 1.7$ Hz, 2H), 3.26 (ddd, $J = 13.4, 11.5, 1.8$ Hz, 1H), 3.17 – 3.08 (m, 1H), 3.01 (ddd, $J = 13.5, 5.1, 1.7$ Hz, 1H), 2.56 – 2.47 (m, 1H), 2.28 (d, $J = 1.7$ Hz, 6H), 1.78 – 1.68 (m, 1H), 1.60 – 1.51 (m, 1H). ^{13}C NMR (126 MHz, cd_3od) δ 168.32, 157.33, 156.26, 155.52, 143.09, 142.03, 140.02, 132.70, 130.52, 130.30, 129.96, 129.68, 129.41, 126.98, 125.16, 124.07, 123.33, 121.76, 116.56, 116.47, 111.73, 104.17, 53.41, 49.00, 47.22, 41.83, 37.96, 31.95, 28.59, 20.47. HPLC (method 20 to 70%B in 50 min): retention time = 29.0 min, or approximately 49.0 minutes adjusted to gradient A. ESI-MS 546.3 [M+H] and 568.3 [M+Na]+.

Compound 20 (Notebook reference: AFN-54 or afn-v-295, notebook 5 p. 295)

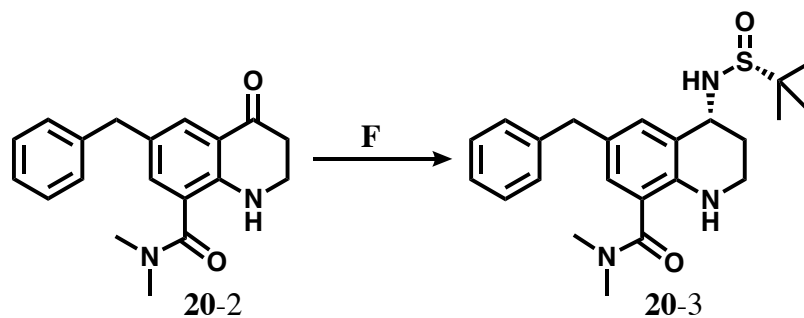


20-1. *6-benzyl-4-oxo-1,2,3,4-tetrahydroquinoline-8-carboxylic acid.* **20-1** was synthesized following **General Procedure (H)** using degassed 4:1 DMF:H₂O, intermediate **8-5** (305 mg, 0.97 mmol, 1 eq), K₂CO₃ (200 mg, 1.45 mmol, 1.5 eq), Pd(dppf)Cl₂ (71 mg, 0.097 mmol, 0.1 eq), and added oxalyl chloride (3 mL total volume). Yield: 150 mg, 55%. ^1H NMR (500 MHz, CDCl₃) δ

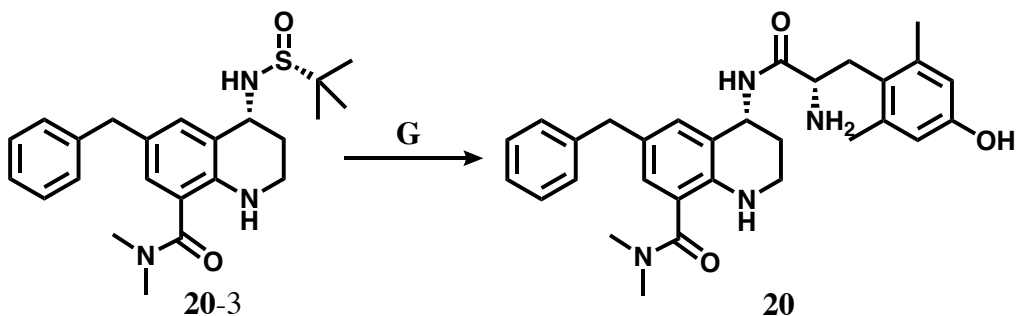
8.04 (s, 1H), 8.00 (d, $J = 2.4$ Hz, 1H), 7.98 (d, $J = 2.3$ Hz, 1H), 7.30 – 7.26 (m, 2H), 7.21 – 7.15 (m, 3H), 3.88 (s, 2H), 3.65 (t, $J = 7.1$ Hz, 2H), 2.73 – 2.68 (m, 2H), 2.12 (s, 1H). ^{13}C NMR(126 MHz, CDCl_3) δ 193.29, 172.27, 152.62, 140.82, 139.57, 134.93, 128.79, 128.75, 128.29, 126.41, 120.42, 111.83, 40.83, 37.24.



20-2. *6-benzyl-N,N-dimethyl-4-oxo-1,2,3,4-tetrahydroquinoline-8-carboxamide.* **20-2** was synthesized following **General Procedure (I)** from intermediate **20-1** (37 mg, 0.13 mmol, 1.0 eq), dimethylamine hydrochloride (22 mg, 0.26 mmol, 2.0 eq), PyBOP (75 mg, 0.20 mmol, 1.1 eq) and DIPEA (0.32 mL, 1.81 mmol, 10 eq). Yield: quantitative. ^1H NMR (500 MHz, Chloroform-*d*) δ 8.02 (s, 1H), 7.79 (d, $J = 2.1$ Hz, 1H), 7.26 (t, $J = 7.4$ Hz, 2H), 7.18 (tt, $J = 7.5, 1.4$ Hz, 1H), 7.14 (dd, $J = 8.6, 1.3$ Hz, 2H), 7.05 (d, $J = 2.2$ Hz, 1H), 3.87 (s, 2H), 3.54 (td, $J = 7.8, 7.3, 2.1$ Hz, 2H), 2.96 (s, 3H), 2.88 (s, 3H), 2.67 (t, $J = 7.0$ Hz, 2H). ^{13}C NMR (126 MHz, cdCl_3) δ 193.61, 170.12, 134.94, 129.48, 128.88, 128.70, 126.37, 77.16, 41.62, 40.85, 37.72, 36.64, 31.39.



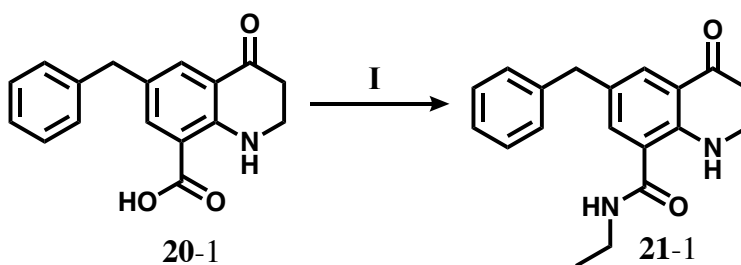
20-3. (*R*)-6-benzyl-4-(((*R*)-*tert*-butylsulfinyl)amino)-*N,N*-dimethyl-1,2,3,4-tetrahydroquinoline-8-carboxamide. **20-3** was synthesized following **General Procedure (F)** from **20-2** (55 mg, 0.18 mmol, 1 eq), (*R*)-2-methyl-2-propanesulfinamide (66 mg, 0.54 mmol, 3 eq), and Ti(OEt)₄ (0.22 mL, 1.07 mmol, 6 eq), then NaBH₄ (41 mg, 1.07 mmol, 6 eq). Yield: 51 mg, 69%. ¹H NMR (499 MHz, Chloroform-*d*) δ 7.25 (d, *J* = 7.6 Hz, 1H), 7.20 – 7.16 (m, 1H), 7.16 – 7.14 (m, 2H), 7.13 (d, *J* = 2.1 Hz, 1H), 6.98 (d, *J* = 2.2 Hz, 0H), 6.79 (d, *J* = 2.1 Hz, 1H), 4.52 (q, *J* = 3.2 Hz, 1H), 3.83 (d, *J* = 3.0 Hz, 2H), 3.36 (td, *J* = 12.1, 3.0 Hz, 1H), 3.21 (d, *J* = 11.6 Hz, 1H), 2.08 – 2.02 (m, 1H), 1.87 (tt, *J* = 12.6, 3.8 Hz, 1H), 1.27 (s, 3H), 1.21 (s, 9H). ¹³C NMR (126 MHz, cdcl₃) δ 171.06, 142.21, 141.48, 133.27, 132.22, 128.84, 128.73, 128.61, 128.52, 128.42, 128.29, 125.99, 121.89, 119.13, 55.41, 49.78, 40.74, 35.94, 27.65, 22.65, 22.12.



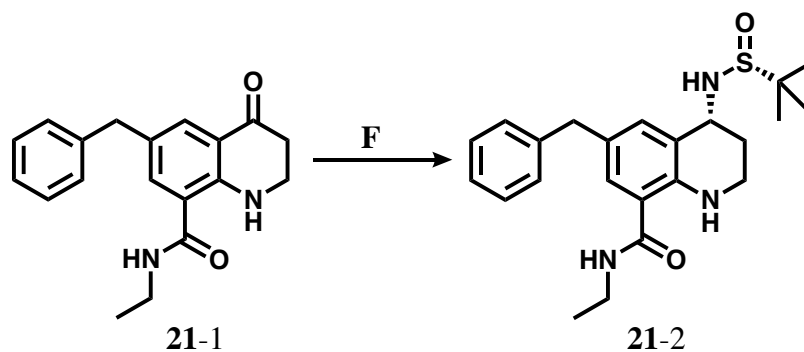
20. (*R*)-4-((*S*)-2-amino-3-(4-hydroxy-2,6-dimethylphenyl)propanamido)-6-benzyl-*N,N*-dimethyl-1,2,3,4-tetrahydroquinoline-8-carboxamide. **20** was synthesized following **General Procedure (G)** from **20-3** (51 mg, 0.12 mmol, 1 eq) and concentrated HCl (0.05 mL, excess). Carried forward without characterization. **Step 2:** Performed amide coupling using **20-3** amine salt (42 mg, 0.12 mmol, 1 eq), di-Boc-Dmt (55 mg, 0.13 mmol, 1.1 eq), PyBOP (70 mg, 0.13 mmol, 1.1 eq), and DIPEA (0.21 mL, 1.21 mmol, 10 eq). **Step 3:** Boc-deprotected as described in **General Procedure (G)**. Final yield not calculated. ¹H NMR (500 MHz, Methanol-*d*₄) δ 7.21 (dd, *J* = 8.2, 6.8 Hz, 2H), 7.12 (ddd, *J* = 8.5, 7.1, 1.5 Hz, 3H), 6.94 (d, *J* = 2.1 Hz, 1H), 6.76 (d, *J* = 2.1 Hz, 1H), 6.46 (s,

2H), 4.91 (dt, $J = 7.6, 3.9$ Hz, 1H), 3.83 (dd, $J = 11.6, 5.0$ Hz, 1H), 3.77 (s, 2H), 3.25 (dd, $J = 13.6, 11.6$ Hz, 1H), 3.02 – 2.95 (m, 3H), 2.89 (s, 3H), 2.40 (td, $J = 12.0, 2.9$ Hz, 1H), 2.27 (s, 6H), 1.68 – 1.60 (m, 1H), 1.54 – 1.46 (m, 1H). HPLC (gradient A): retention time = 34.8 min. ESI-MS 455.3[M + H]⁺ and 477.3 [M + Na]⁺.

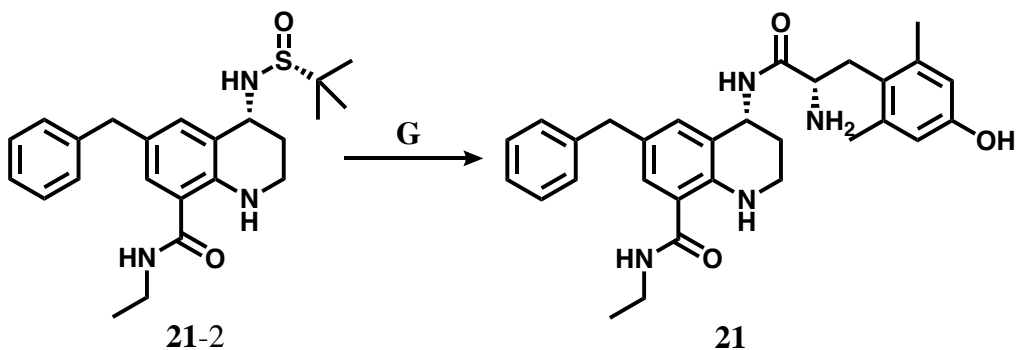
Compound 21 (Notebook reference: AFN-44 or afn-v-157, notebook 5 p. 157)



21-1. 6-benzyl-N-ethyl-4-oxo-1,2,3,4-tetrahydroquinoline-8-carboxamide. **21-1** was synthesized following **General Procedure (I)** from intermediate **20-1** (78 mg, 0.28 mmol, 1.0 eq), PyBOP (172 mg, 0.33 mmol, 1.2 eq), ethylamine hydrochloride (27 mg, 0.33 mmol, 1.2 eq) and DIPEA (0.15 mL, 0.84 mmol, 3.0 eq). Product was highly fluorescent under long-wave UV (285 nm) light. Yield: 66 mg, 77%. ¹H NMR (500 MHz, CDCl₃) δ 7.86 (d, $J = 2.0$ Hz, 1H), 7.31 – 7.27 (m, 3H), 7.21 (t, $J = 7.3$ Hz, 1H), 7.15 (d, $J = 7.5$ Hz, 2H), 3.87 (s, 2H), 3.59 (td, $J = 7.8, 7.2, 2.3$ Hz, 2H), 3.42 (p, $J = 7.1, 6.5$ Hz, 2H), 2.67 (t, $J = 7.1$ Hz, 2H), 1.23 (t, $J = 7.3$ Hz, 3H).



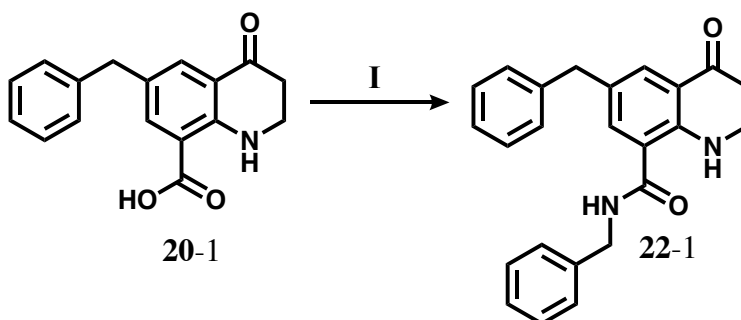
21-2. *(R)*-6-benzyl-4-(((*R*)-tert-butylsulfinyl)amino)-*N*-ethyl-1,2,3,4-tetrahydroquinoline-8-carboxamide. **21-2** was synthesized following **General Procedure (F)** from **21-1** (64 mg, 0.21 mmol, 1 eq), (*R*)-2-methyl-2-propanesulfinamide (76 mg, 0.62 mmol, 3 eq), and Ti(OEt)₄ (0.26 mL, 1.24 mmol, 6 eq), then NaBH₄ (47 mg, 1.24 mmol, 6 eq). Yield: 61 mg, 71%. ¹H NMR (500 MHz, CDCl₃) δ 7.58 (s, 1H), 7.30 – 7.22 (m, 2H), 7.19 (dd, *J* = 7.5, 1.5 Hz, 1H), 7.15 (dd, *J* = 5.6, 3.1 Hz, 3H), 7.04 (d, *J* = 2.0 Hz, 1H), 5.96 (s, 1H), 4.51 (q, *J* = 2.9 Hz, 1H), 3.83 (s, 2H), 3.39 (qd, *J* = 7.3, 4.9 Hz, 3H), 3.31 (ddd, *J* = 11.9, 5.8, 3.5 Hz, 1H), 3.09 (s, 1H), 2.07 (dt, *J* = 7.0, 3.7 Hz, 1H), 1.83 (tt, *J* = 13.2, 4.1 Hz, 1H), 1.26 (t, *J* = 7.1 Hz, 3H), 1.20 (s, 9H). ¹³C NMR (126 MHz, CDCl₃) δ 169.55, 144.90, 141.55, 134.37, 130.65, 129.68, 128.86, 128.76, 128.59, 128.49, 127.73, 126.85, 126.18, 125.96, 121.93, 115.25, 115.01, 55.53, 50.17, 40.90, 35.53, 26.92, 22.78, 22.76, 15.01.



21. *(R)*-4-(((*S*)-2-amino-3-(4-hydroxy-2,6-dimethylphenyl)propanamido)-6-benzyl-*N*-ethyl-1,2,3,4-tetrahydroquinoline-8-carboxamide. **21** was synthesized following **General Procedure**

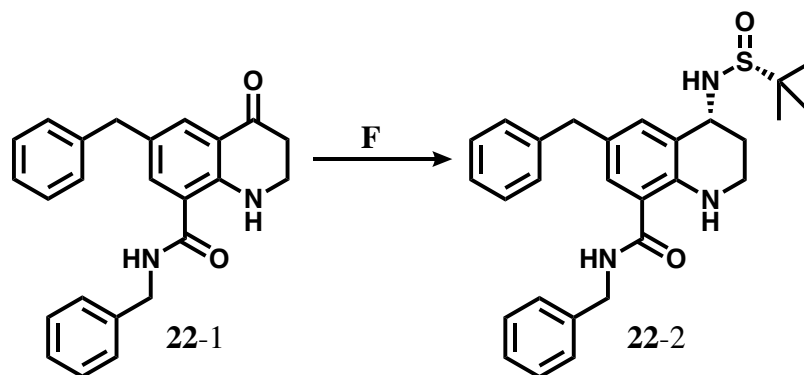
(G) from **21-2** (61 mg, 0.15 mmol, 1 eq) and concentrated HCl (0.03 mL, excess). Carried forward without characterization. **Step 2:** Performed amide coupling using **21-2** amine salt (41 mg, 0.12 mmol, 1 eq), di-Boc-Dmt (53 mg, 0.13 mmol, 1.1 eq), PyBOP (68 mg, 0.13 mmol, 1.1 eq), and DIPEA (0.21 mL, 1.19 mmol, 10 eq). **Step 3:** Boc-deprotected as described in **General Procedure (G)**. Final yield not calculated. $^1\text{H NMR}$ (500 MHz, Methanol- d_4) δ 8.21 (d, $J = 7.9$ Hz, 1H), 7.22 (t, $J = 7.5$ Hz, 2H), 7.14 (d, $J = 3.9$ Hz, 1H), 7.14 – 7.11 (m, 2H), 6.94 (d, $J = 2.0$ Hz, 1H), 6.47 (s, 2H), 4.92 – 4.87 (m, 0H), 3.82 (dd, $J = 11.6, 5.1$ Hz, 1H), 3.77 (s, 2H), 3.30 (s, 2H), 3.24 (dd, $J = 13.5, 11.6$ Hz, 1H), 2.99 (dd, $J = 13.4, 4.9$ Hz, 2H), 2.40 (td, $J = 12.0, 2.6$ Hz, 1H), 2.27 (s, 6H), 1.62 (ddt, $J = 12.5, 8.3, 4.1$ Hz, 1H), 1.50 (dd, $J = 13.3, 3.6$ Hz, 1H), 1.16 (t, $J = 7.2$ Hz, 3H). HPLC (gradient A): retention time = 32.5 min. ESI-MS 501.3[M + H] $^+$ and 523.3 [M + Na] $^+$.

Compound 22 (Notebook reference: AFN-22 or afn-iv-155, notebook 4 p. 155)

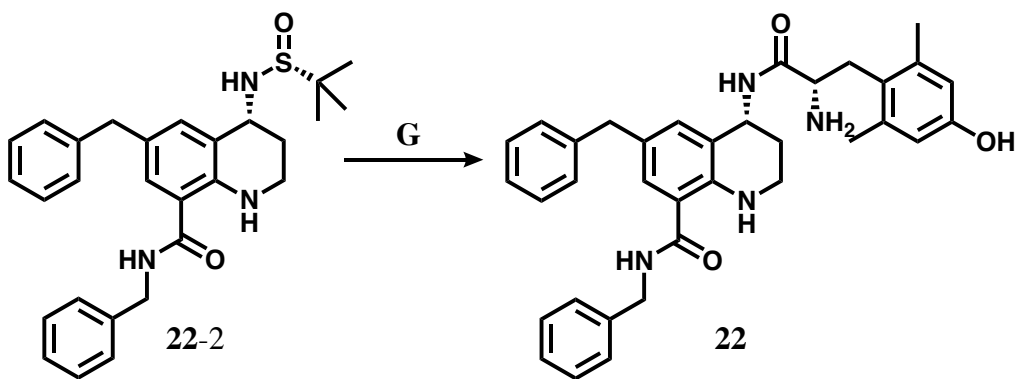


22-1. *N,N'*-dibenzyl-4-oxo-1,2,3,4-tetrahydroquinoline-8-carboxamide. **22-1** was synthesized following **General Procedure (I)** from intermediate **20-1** (43 mg, 0.15 mmol, 1.0 eq), benzylamine (0.02 mL, 0.18 mmol, 1.2 eq), PyBOP (95 mg, 0.18 mmol, 1.2 eq) and DIPEA (0.13 mL, 0.75 mmol, 5 eq). Yield: 40 mg, 70%. $^1\text{H NMR}$ (500 MHz, CDCl $_3$) δ 8.06 (s, 1H), 7.86 (d, $J = 2.1$ Hz, 1H), 7.38 – 7.30 (m, 5H), 7.29 – 7.23 (m, 2H), 7.18 (t, $J = 7.3$ Hz, 1H), 7.15 – 7.10 (m,

2H), 6.51 (t, $J = 5.9$ Hz, 1H), 4.57 (d, $J = 5.7$ Hz, 2H), 3.84 (s, 2H), 3.58 (td, $J = 7.6, 7.2, 2.3$ Hz, 2H), 2.66 (t, $J = 7.1$ Hz, 2H), 1.22 (s, 1H). ^{13}C NMR(126 MHz, CDCl_3) δ 193.62, 168.60, 151.49, 140.78, 138.05, 133.96, 132.03, 128.91, 128.74, 128.70, 127.89, 127.77, 127.73, 126.39, 120.40, 117.30, 43.88, 40.95, 40.78, 37.40, 22.22.

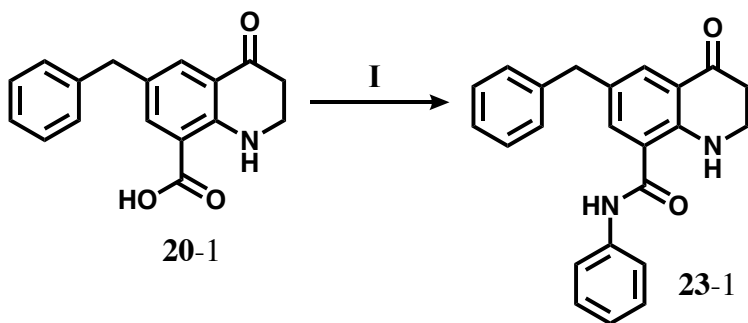


22-2. *(R)-N,6-dibenzyl-4-(((R)-tert-butylsulfinyl)amino)-1,2,3,4-tetrahydroquinoline-8-carboxamide.* **22-2** was synthesized following **General Procedure (F)** from **22-1** (40 mg, 0.11 mmol, 1 eq), (R)-2-methyl-2-propanesulfinamide (40 mg, 0.32 mmol, 3 eq), and $\text{Ti}(\text{OEt})_4$ (0.14 mL, 0.65 mmol, 6 eq), then NaBH_4 (25 mg, 0.65 mmol, 6 eq). Yield: 43 mg, 84%. ^1H NMR (500 MHz, CDCl_3) δ 7.71 – 7.65 (m, 1H), 7.38 – 7.28 (m, 5H), 7.29 – 7.23 (m, 3H), 7.18 – 7.15 (m, 2H), 7.15 – 7.11 (m, 2H), 7.07 (d, $J = 2.0$ Hz, 1H), 6.26 (s, 1H), 4.56 (dd, $J = 5.7, 2.7$ Hz, 2H), 4.52 (d, $J = 3.1$ Hz, 1H), 3.87 – 3.74 (m, 2H), 3.45 – 3.38 (m, 1H), 3.33 (dq, $J = 11.9, 4.2$ Hz, 1H), 3.09 (s, 1H), 2.11 – 2.04 (m, 1H), 1.84 (ddt, $J = 16.2, 12.7, 4.1$ Hz, 1H), 1.21 (s, 9H). ^{13}C NMR(126 MHz, CDCl_3) δ 169.48, 145.21, 141.45, 134.69, 128.89, 128.79, 128.62, 127.87, 127.76, 127.67, 126.88, 126.22, 122.10, 114.50, 55.57, 50.19, 43.81, 40.87, 35.56, 26.85, 22.78.

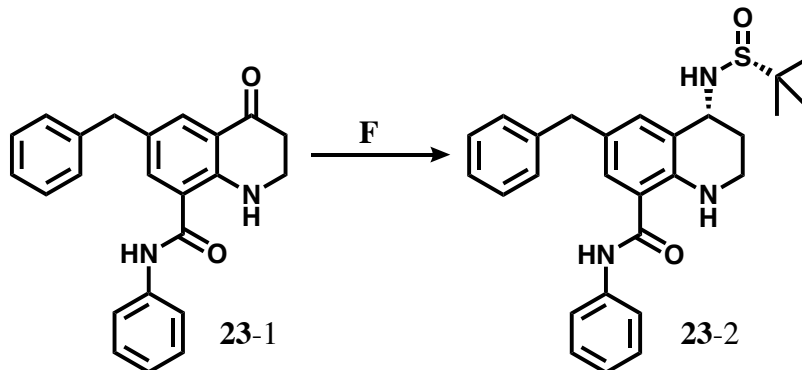


22. *(R)*-4-((*S*)-2-amino-3-(4-hydroxy-2,6-dimethylphenyl)propanamido)-*N*,6-dibenzyl-1,2,3,4-tetrahydroquinoline-8-carboxamide. **22** was synthesized following **General Procedure (G)** from **22-2** (43 mg, 0.090 mmol, 1 eq) and concentrated HCl (0.03 mL, excess). Carried forward without characterization. **Step 2:** Performed amide coupling using **22-2** amine salt (36 mg, 0.088 mmol, 1 eq), diBoc-Dmt (40 mg, 0.097 mmol, 1.1 eq), PyBOP (51 mg, 0.097 mmol, 1.1 eq), 6-Cl HOBt (17 mg, 0.097 mmol, 1.1 eq), and DIPEA (0.15 mL, 0.88 mmol, 10 eq). **Step 3:** Boc-protected as described in **General Procedure (G)**. Final yield not calculated. $^1\text{H NMR}$ (500 MHz, Methanol- d_4) δ 8.20 (d, $J = 7.8$ Hz, 1H), 7.30 (d, $J = 5.5$ Hz, 4H), 7.25 – 7.19 (m, 3H), 7.16 – 7.11 (m, 3H), 6.95 (d, $J = 2.0$ Hz, 1H), 6.47 (s, 2H), 4.90 (s, 1H), 4.52 – 4.42 (m, 2H), 3.83 (dd, $J = 11.6, 5.1$ Hz, 1H), 3.77 (s, 2H), 3.24 (dd, $J = 13.6, 11.6$ Hz, 1H), 3.01 (td, $J = 13.9, 4.7$ Hz, 2H), 2.45 – 2.36 (m, 1H), 2.27 (s, 6H), 1.63 (tt, $J = 12.4, 4.2$ Hz, 1H), 1.55 – 1.46 (m, 1H). HPLC (gradient A): retention time = 42.0 min. ESI-MS 563.3[M + H] $^+$ and 585.3 [M + Na] $^+$.

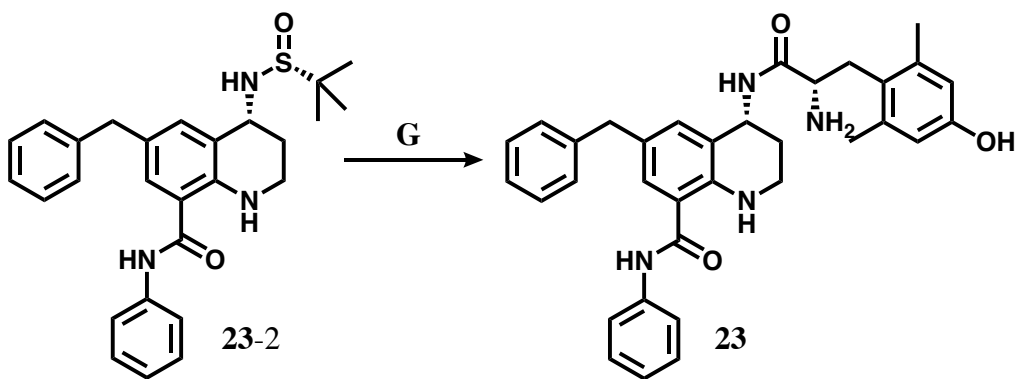
Compound 23 (Notebook reference: AFN-21 or afn-iv-153, notebook 4 p. 153)



23-1. *6-benzyl-4-oxo-N-phenyl-1,2,3,4-tetrahydroquinoline-8-carboxamide.* **23-1** was synthesized following **General Procedure (I)** from intermediate **20-1** (40 mg, 0.14 mmol, 1.0 eq), aniline (0.02 mL, 0.18 mmol, 1.2 eq), PyBOP (94 mg, 0.18 mmol, 1.2 eq) and DIPEA (0.07 mL, 0.42 mmol, 3.0 eq). Product was highly fluorescent under 385 nm light. Yield: 30 mg, 60%. ^1H NMR (500 MHz, CDCl_3) δ 7.89 (d, $J = 1.8$ Hz, 1H), 7.85 (s, 1H), 7.53 (dt, $J = 8.8, 1.8$ Hz, 2H), 7.46 (d, $J = 2.0$ Hz, 1H), 7.37 (t, $J = 7.8$ Hz, 3H), 7.27 (dd, $J = 7.6, 1.3$ Hz, 1H), 7.23 – 7.17 (m, 1H), 7.16 (d, $J = 7.1$ Hz, 3H), 3.88 (d, $J = 1.8$ Hz, 2H), 3.59 (tt, $J = 7.8, 1.8$ Hz, 2H), 2.67 (t, $J = 6.8$ Hz, 2H). ^{13}C NMR (126 MHz, CDCl_3) δ 193.52, 167.11, 151.49, 140.71, 137.50, 133.96, 132.34, 129.40, 129.21, 129.02, 128.79, 128.01, 126.51, 125.05, 120.95, 120.71, 120.51, 117.83, 77.16, 40.96, 40.85, 37.39.



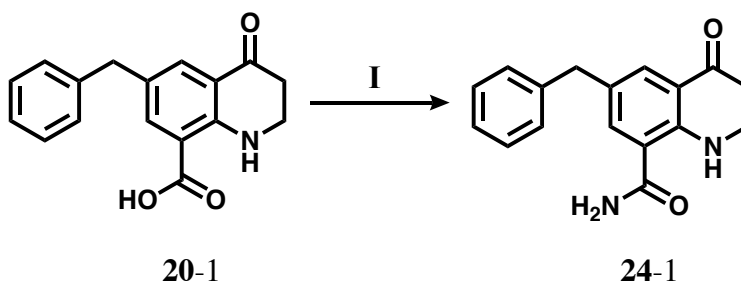
23-2. *(R)*-6-benzyl-4-(((*R*)-*tert*-butylsulfinyl)amino)-*N*-phenyl-1,2,3,4-tetrahydroquinoline-8-carboxamide. **23-2** was synthesized following **General Procedure (F)** from **23-1** (42 mg, 0.12 mmol, 1 eq), (*R*)-2-methyl-2-propanesulfinamide (43 mg, 0.36 mmol, 3 eq), and Ti(OEt)₄ (0.15 mL, 0.72 mmol, 6 eq), then NaBH₄ (28 mg, 0.72 mmol, 6 eq). Yield: 45 mg, 81%. ¹H NMR (500 MHz, CDCl₃) δ 7.52 (d, *J* = 1.3 Hz, 1H), 7.50 (t, *J* = 1.1 Hz, 1H), 7.37 – 7.32 (m, 2H), 7.29 (t, *J* = 7.5 Hz, 2H), 7.23 – 7.21 (m, 2H), 7.21 – 7.18 (m, 2H), 7.18 – 7.16 (m, 1H), 7.13 (ddt, *J* = 7.6, 6.9, 1.1 Hz, 1H), 4.53 (t, *J* = 2.8 Hz, 1H), 3.87 (d, *J* = 2.9 Hz, 2H), 3.41 (td, *J* = 12.2, 3.3 Hz, 1H), 3.33 (dq, *J* = 7.9, 4.0 Hz, 1H), 3.11 (t, *J* = 1.7 Hz, 1H), 2.08 (dd, *J* = 13.7, 3.5 Hz, 1H), 1.86 (td, *J* = 12.9, 6.5 Hz, 1H), 1.21 (s, 9H). ¹³C NMR(126 MHz, CDCl₃) δ 167.95, 145.34, 141.35, 137.90, 134.96, 129.12, 128.81, 128.68, 127.81, 127.15, 126.31, 124.62, 122.25, 120.78, 114.91, 55.60, 50.21, 40.91, 35.59, 26.80, 22.76.



23. *(R)*-4-((*S*)-2-amino-3-(4-hydroxy-2,6-dimethylphenyl)propanamido)-6-benzyl-*N*-phenyl-1,2,3,4-tetrahydroquinoline-8-carboxamide. **23** was synthesized following **General Procedure (G)** from **23-2** (45 mg, 0.097 mmol, 1 eq) and concentrated HCl (0.03 mL, excess). Carried forward without characterization. **Step 2:** Performed amide coupling using **23-2** amine salt (24 mg, 0.061 mmol, 1 eq), di-Boc-Dmt (28 mg, 0.067 mmol, 1.1 eq), PyBOP (35 mg, 0.067 mmol, 1.1 eq), 6-

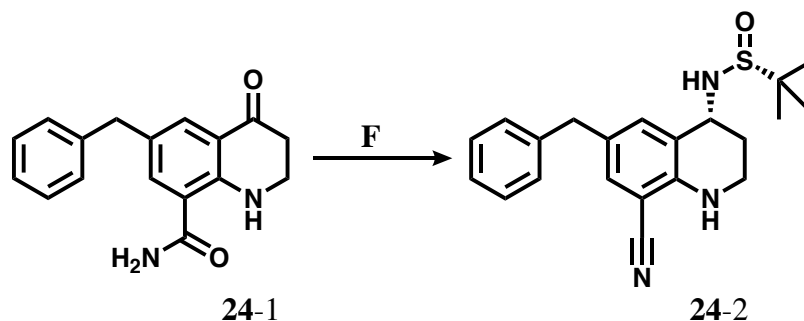
Cl HOBt (12 mg, 0.067 mmol, 1.1 eq), and DIPEA (0.10 mL, 0.61 mmol, 10 eq). **Step 3:** Boc-deprotected as described in **General Procedure (G)**. Final yield not calculated. ^1H NMR (500 MHz, Methanol- d_4) δ 8.23 (d, $J = 7.8$ Hz, 1H), 7.59 – 7.53 (m, 2H), 7.42 (d, $J = 2.1$ Hz, 1H), 7.32 (t, $J = 7.8$ Hz, 2H), 7.23 (t, $J = 7.6$ Hz, 2H), 7.19 – 7.15 (m, 2H), 7.15 – 7.09 (m, 1H), 7.00 (d, $J = 1.9$ Hz, 1H), 6.48 (s, 2H), 4.96 – 4.90 (m, 1H), 3.85 (d, $J = 5.1$ Hz, 1H), 3.82 (s, 3H), 3.25 (dd, $J = 13.6, 11.6$ Hz, 1H), 3.09 – 2.96 (m, 2H), 2.44 (t, $J = 11.7$ Hz, 1H), 2.27 (s, 6H), 1.65 (tt, $J = 12.2, 4.2$ Hz, 1H), 1.57 – 1.48 (m, 1H). HPLC (gradient A): retention time = 43.0 min. ESI-MS 549.3[M + H] $^+$ and 571.3 [M + Na] $^+$.

Compound 24 (Notebook reference: AFN-45 or afn-v-159, notebook 5 p. 159)

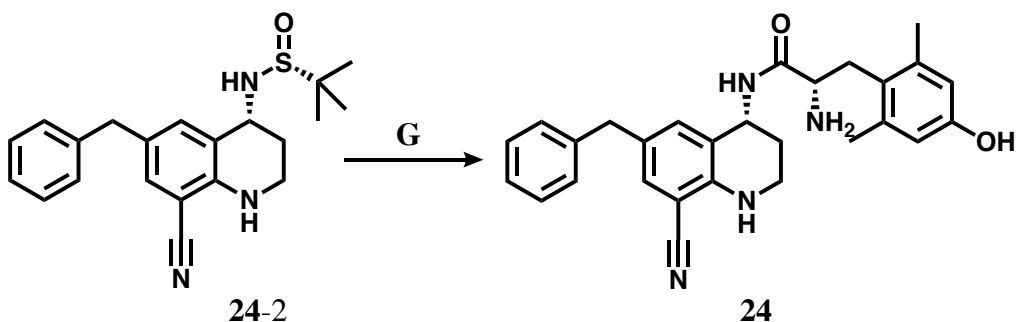


24-1. *6-benzyl-4-oxo-1,2,3,4-tetrahydroquinoline-8-carbonitrile.* **24-1** was synthesized following **General Procedure (I)** from intermediate **20-1** (51 mg, 0.18 mmol, 1.0 eq), ammonium hydroxide (1 mL, excess), PyBOP (104 mg, 0.20 mmol, 1.1 eq) and DIPEA (0.32 mL, 1.81 mmol, 10 eq). Yield: 45 mg, 89%. ^1H NMR (500 MHz, Chloroform- d) δ 8.20 (s, 1H), 7.91 (d, $J = 2.1$ Hz, 1H), 7.35 (d, $J = 2.1$ Hz, 1H), 7.31 – 7.25 (m, 2H), 7.20 (t, $J = 7.5$ Hz, 1H), 7.15 (dd, $J = 7.0, 1.3$ Hz, 2H), 3.87 (s, 2H), 3.61 (ddd, $J = 7.8, 6.7, 2.4$ Hz, 2H), 2.68 (t, $J = 7.1$ Hz, 2H). ^{13}C NMR (126 MHz,

cdcl₃) δ 193.53, 170.94, 151.84, 140.75, 134.85, 132.85, 128.83, 128.79, 127.67, 126.51, 120.56, 115.53, 40.90, 40.82, 37.39.

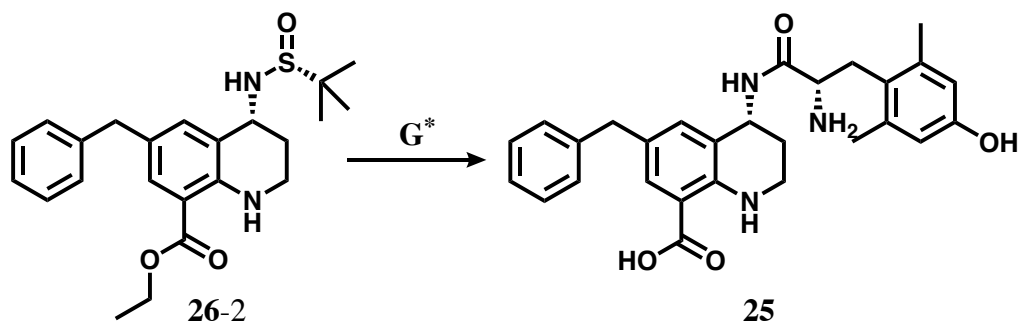


24-2. *(R)-N-((R)-6-benzyl-8-cyano-1,2,3,4-tetrahydroquinolin-4-yl)-2-methylpropane-2-sulfonamide.* **24-2** was synthesized following **General Procedure (F)** from **24-1** (45 mg, 0.16 mmol, 1 eq), (R)-2-methyl-2-propanesulfonamide (58 mg, 0.48 mmol, 3 eq), and Ti(OEt)₄ (0.20 mL, 0.96 mmol, 6 eq), then NaBH₄ (36 mg, 0.96 mmol, 6 eq). Yield: 30 mg, 50%. NMR indicated conversion of the carboxamide to a nitrile, likely promoted by titanium and/or NaBH₄ as described in Lehnert, W. *Tetrahedron Lett.* **1971**, *12*, 1501 and S. E. Ellzey, C. H. Mack and W. J. Connick. *J. Org. Chem.* **1967**, *32*, 846. Carbonyl peak at 170ppm corresponding to carboxamide of **24-1** is shifted downfield in **24-2**. ¹H NMR (500 MHz, Chloroform-*d*) δ 7.31 – 7.26 (m, 3H), 7.23 – 7.18 (m, 1H), 7.16 – 7.13 (m, 2H), 7.11 (d, *J* = 2.0 Hz, 1H), 4.81 (s, 1H), 4.51 (q, *J* = 3.4 Hz, 1H), 3.81 (s, 2H), 3.48 – 3.41 (m, 1H), 3.39 (dq, *J* = 11.9, 4.1 Hz, 1H), 3.11 (s, 1H), 2.13 (dq, *J* = 13.8, 3.6 Hz, 1H), 1.93 – 1.84 (m, 1H), 1.22 (s, 9H). ¹³C NMR (126 MHz, cdcl₃) δ 145.77, 140.59, 135.63, 132.51, 129.61, 128.85, 128.78, 126.50, 121.55, 117.77, 95.18, 55.77, 49.67, 40.61, 36.41, 27.27, 22.76.



24. *(S)*-2-amino-*N*-((*R*)-6-benzyl-8-cyano-1,2,3,4-tetrahydroquinolin-4-yl)-3-(4-hydroxy-2,6-dimethylphenyl)propanamide. **24** was synthesized following **General Procedure (G)** from **24-2** (30 mg, 0.08 mmol, 1 eq) and concentrated HCl (0.05 mL, excess). Carried forward without characterization. **Step 2:** Performed amide coupling using **24-2** amine salt (36 mg, 0.11 mmol, 1 eq), di-Boc-Dmt (44 mg, 0.14 mmol, 1.2 eq), PyBOP (70 mg, 0.14 mmol, 1.2 eq), and DIPEA (0.20 mL, 1.13 mmol, 10 eq). **Step 3:** Boc-deprotected as described in **General Procedure (G)**. Final yield not calculated. LC-MS indicated dehydration of the carboxamide to the nitrile as indicated above. ^1H NMR (500 MHz, Methanol- d_4) δ 8.17 (d, $J = 7.9$ Hz, 0H), 7.24 (t, $J = 7.4$ Hz, 2H), 7.17 – 7.13 (m, 1H), 7.13 – 7.09 (m, 2H), 7.08 (s, 2H), 6.48 (s, 2H), 4.90 (t, $J = 4.2$ Hz, 1H), 3.82 (dd, $J = 11.6, 5.0$ Hz, 1H), 3.75 (s, 2H), 3.28 – 3.21 (m, 1H), 3.10 (dt, $J = 12.7, 4.3$ Hz, 1H), 3.00 (dd, $J = 13.7, 5.1$ Hz, 1H), 2.47 (td, $J = 12.0, 3.2$ Hz, 1H), 2.26 (s, 6H), 1.68 – 1.59 (m, 1H), 1.55 – 1.47 (m, 1H). ^{13}C NMR (126 MHz, cd_3od) δ 168.42, 157.41, 149.36, 147.45, 142.32, 140.01, 136.50, 133.60, 130.01, 129.65, 129.54, 127.22, 123.24, 121.51, 118.59, 116.46, 95.50, 53.37, 46.45, 41.20, 37.61, 31.92, 27.98, 20.43, 18.71, 17.27. HPLC (gradient A): retention time = 34.8 min. ESI-MS 455.3[M + H] $^+$ and 477.3 [M + Na] $^+$.

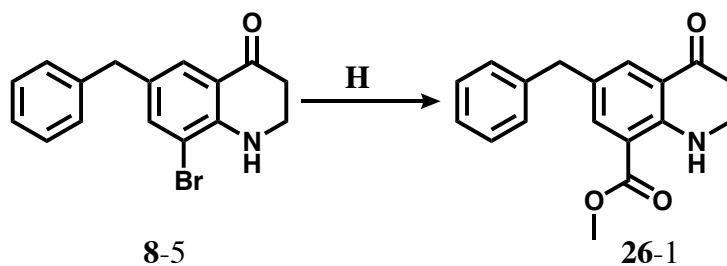
Compound 25 (Notebook name: AFN-30)



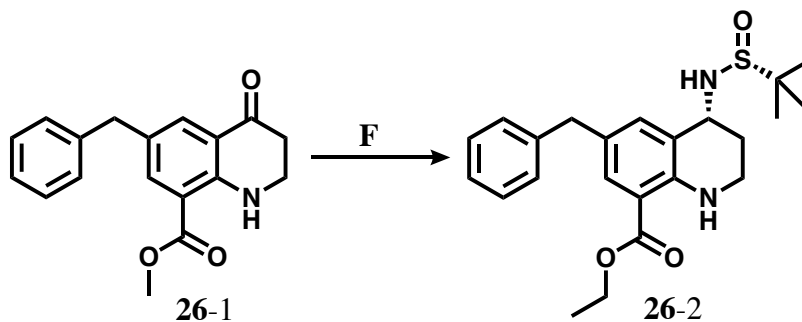
25. *(R)*-4-((*S*)-2-amino-3-(4-hydroxy-2,6-dimethylphenyl)propanamido)-6-benzyl-1,2,3,4-tetrahydroquinoline-8-carboxylic acid. **25** was synthesized following a modified version of **General Procedure (G)** from intermediate **26-2**, the synthesis of which is described below. **25** was synthesized from **26-2** (48 mg, 0.12 mmol, 1 eq) and concentrated HCl (0.03 mL, excess). Yield of amine salt: 40 mg, 99%. ^1H NMR (500 MHz, Methanol- d_4) δ 7.78 (d, $J = 2.2$ Hz, 1H), 7.29 – 7.24 (m, 3H), 7.20 – 7.14 (m, 3H), 4.48 (t, $J = 4.2$ Hz, 1H), 4.33 – 4.26 (m, 2H), 3.86 (s, 2H), 3.56 (dtd, $J = 13.1, 4.6, 1.0$ Hz, 1H), 3.45 – 3.37 (m, 1H), 2.17 – 2.10 (m, 2H), 1.34 (t, $J = 7.1$ Hz, 3H). ^{13}C NMR(126 MHz, cd_3od) δ 169.20, 147.37, 142.73, 136.75, 134.04, 129.74, 129.51, 128.39, 127.14, 117.52, 111.58, 111.41, 109.38, 61.54, 41.59, 36.22, 26.03, 14.62. Amide coupling was performed using **26-2** amine salt(30 mg, 0.086 mmol, 1 eq), di-Boc-Dmt (41 mg, 0.10 mmol, 1.15 eq), PyBOP (52 mg, 0.10 mmol, 1.15 eq), 6-Cl HOBt (17 mg, 0.10 mmol, 1.15 eq), and DIPEA (0.16 mL, 0.92 mmol, 11 eq). Boc-protected intermediate was isolated by flash chromatography. ^1H NMR (500 MHz, Chloroform- d) δ 7.56 (s, 2H), 7.27 (t, $J = 7.5$ Hz, 2H), 7.20 – 7.13 (m, 3H), 7.03 (d, $J = 2.2$ Hz, 1H), 6.84 (s, 2H), 5.67 (s, 1H), 5.41 (s, 1H), 4.98 (dt, $J = 8.8, 4.4$ Hz, 1H), 4.24 (tt, $J = 8.6, 5.3$ Hz, 1H), 4.20 – 4.10 (m, 1H), 3.78 (s, 2H), 3.23 (dt, $J = 12.9, 4.2$ Hz, 1H), 3.08 (d, $J = 9.4$ Hz, 2H), 2.55 (s, 1H), 2.38 (s, 6H), 1.72 (t, $J = 11.6$ Hz, 1H), 1.57 (s, 10H), 1.44 (s, 9H), 1.31 (t, $J = 7.1$ Hz, 2H). ^{13}C NMR (126 MHz, cdcl_3) δ 170.01, 168.52, 155.12,

152.12, 149.53, 146.47, 141.51, 138.98, 135.76, 131.62, 131.35, 128.73, 128.57, 128.55, 126.45, 126.11, 121.15, 120.57, 109.56, 83.50, 80.03, 60.44, 54.26, 45.56, 40.85, 36.43, 33.44, 28.44, 27.86, 26.85, 20.56, 14.41. This Boc-protected intermediate was then saponified as described here: To a pear-shaped flask containing diBoc-**26** (34 mg, 0.048 mmol, 1 eq) under inert atmosphere was added 1:1 THF/H₂O (6 mL), followed by LiOH (6 mg, 0.25 mmol, 5 eq) at ambient temperature, stirring for 6 hours. Solution was titrated to pH 1 with HCl, then organics were extracted with ethyl acetate. Organics were dried with MgSO₄, filtered, and concentrated *in vacuo*. ¹H NMR (499 MHz, Methanol-*d*₄) δ 7.97 (d, *J* = 8.0 Hz, 1H), 7.57 (s, 1H), 7.21 (t, *J* = 7.5 Hz, 2H), 7.15 (d, *J* = 7.4 Hz, 2H), 7.11 (d, *J* = 6.1 Hz, 2H), 6.43 (s, 2H), 4.17 (dd, *J* = 10.1, 5.9 Hz, 1H), 3.76 (s, 2H), 3.20 (dt, *J* = 11.0, 5.0 Hz, 1H), 3.04 (dd, *J* = 13.9, 10.2 Hz, 1H), 2.88 – 2.77 (m, 2H), 2.26 (s, 6H), 1.60 (d, *J* = 37.0 Hz, 2H), 1.43 (s, 9H). ¹³C NMR (126 MHz, cd₃od) δ 197.20, 172.02, 139.98, 138.40, 136.09, 131.19, 128.27, 127.92, 125.41, 124.49, 120.86, 114.63, 54.34, 45.51, 40.38, 36.33, 31.66, 27.33, 27.08, 19.16. Product was then Boc-protected and purified by HPLC as described in **General Procedure (G)**. Final yield not calculated. ¹H NMR (500 MHz, Methanol-*d*₄) δ 7.62 (d, *J* = 2.2 Hz, 1H), 7.25 – 7.20 (m, 2H), 7.16 – 7.10 (m, 3H), 7.02 (d, *J* = 2.3 Hz, 1H), 6.48 (s, 2H), 4.92 (d, *J* = 5.4 Hz, 1H), 3.83 (dd, *J* = 11.6, 5.0 Hz, 1H), 3.75 (s, 2H), 3.25 (dd, *J* = 13.6, 11.6 Hz, 1H), 3.10 (dt, *J* = 12.2, 3.9 Hz, 1H), 3.00 (dd, *J* = 13.6, 5.0 Hz, 1H), 2.50 – 2.41 (m, 1H), 2.27 (s, 6H), 1.63 (tt, *J* = 12.0, 4.2 Hz, 1H), 1.52 (dq, *J* = 13.0, 3.6 Hz, 1H). HPLC (gradient A): retention time = 31.1 min. ESI-MS 474.3[M + H]⁺ and 496.3 [M + Na]⁺.

Compound 26 (Notebook reference: AFN-20 or afn-iv-133, notebook 4 p. 133)

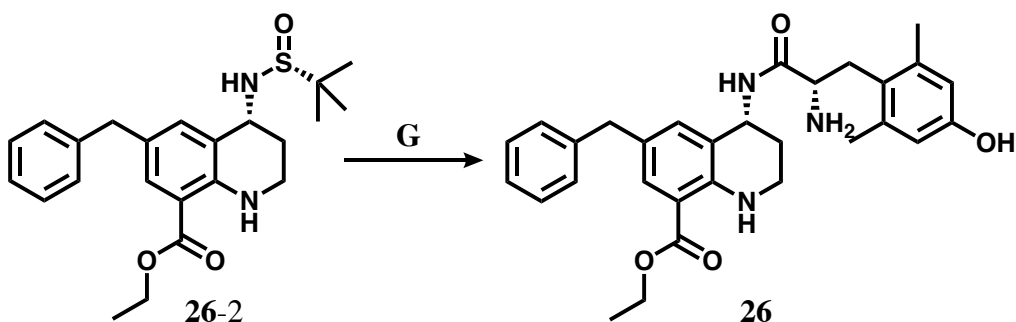


26-1. *methyl 6-benzyl-4-oxo-1,2,3,4-tetrahydroquinoline-8-carboxylate.* **26-1** was synthesized following **General Procedure (H)** from **8-5** (220 mg, 0.70 mmol, 1 eq), oxalyl chloride (1 mL, excess), K_2CO_3 (142 mg, 1.04 mmol, 1.5 eq) and $Pd(dppf)Cl_2$ (51 mg, 0.07 mmol, 0.1 eq) in 1:1 DMF:MeOH. Yield: 103 mg, 50%. 1H NMR (500 MHz, $CDCl_3$) δ 7.93 (s, 2H), 7.30 – 7.26 (m, 2H), 7.21 – 7.14 (m, 3H), 3.86 (s, 2H), 3.85 (s, 3H), 3.63 (td, $J = 7.1, 2.4$ Hz, 2H), 2.69 (t, $J = 7.1$ Hz, 2H). ^{13}C NMR(126 MHz, $CDCl_3$) δ 192.93, 167.99, 152.05, 140.82, 133.83, 128.61, 128.55, 127.84, 126.28, 120.14, 112.39, 51.81, 40.71, 40.70, 37.17.



26-2. *ethyl (R)-6-benzyl-4-(((R)-tert-butylsulfinyl)amino)-1,2,3,4-tetrahydroquinoline-8-carboxylate.* **26-2** was synthesized following **General Procedure (F)** from **26-1** (42 mg, 0.14 mmol, 1 eq), (R)-2-methyl-2-propanesulfinamide (52 mg, 0.42 mmol, 3 eq), and $Ti(OEt)_4$ (0.18 mL, 0.85 mmol, 6 eq), then $NaBH_4$ (32 mg, 0.85 mmol, 6 eq). NMR indicated conversion of **26-1** methyl ester to an ethyl ester in **26-2**. Yield: 48 mg, 83%. 1H NMR (500 MHz, $CDCl_3$) δ 7.75 (d,

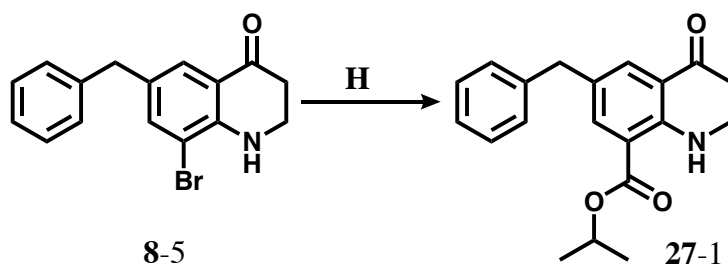
$J = 3.8$ Hz, 1H), 7.62 (d, $J = 2.2$ Hz, 1H), 7.21 – 7.16 (m, 2H), 7.15 – 7.07 (m, 4H), 4.44 (q, $J = 3.0$ Hz, 1H), 4.21 (qd, $J = 7.1, 1.5$ Hz, 2H), 3.75 (s, 2H), 3.36 (m, 1H), 3.29 (dt, $J = 12.0, 4.0$ Hz, 1H), 3.00 (s, 1H), 2.02 (dq, $J = 13.6, 3.3, 1.1$ Hz, 1H), 1.81 – 1.71 (m, 1H), 1.27 (t, $J = 7.1$ Hz, 3H), 1.12 (s, 9H). ^{13}C NMR(126 MHz, CDCl_3) δ 168.50, 146.63, 141.63, 136.18, 131.87, 128.72, 128.54, 126.63, 126.08, 121.61, 109.73, 60.37, 55.52, 50.03, 40.89, 35.53, 26.55, 22.73, 14.47.



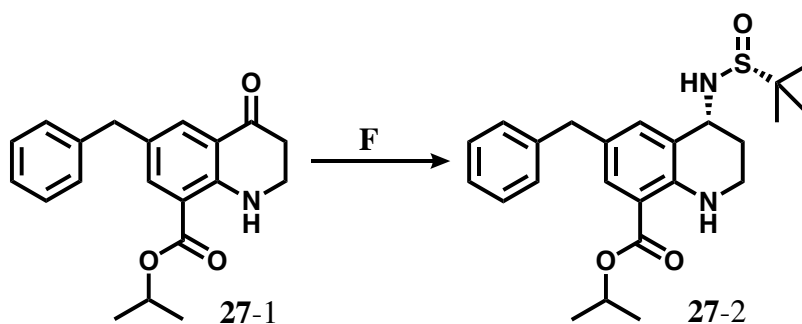
26. ethyl (R)-4-((S)-2-amino-3-(4-hydroxy-2,6-dimethylphenyl)propanamido)-6-benzyl-1,2,3,4-tetrahydroquinoline-8-carboxylate. **26** was synthesized following **General Procedure (G)** from **26-2** (48 mg, 0.12 mmol, 1 eq) and concentrated HCl (0.03 mL, excess). Yield: 40 mg, 99%. ^1H NMR (500 MHz, Methanol- d_4) δ 7.78 (d, $J = 2.2$ Hz, 1H), 7.29 – 7.24 (m, 3H), 7.20 – 7.14 (m, 3H), 4.48 (t, $J = 4.2$ Hz, 1H), 4.33 – 4.26 (m, 2H), 3.86 (s, 2H), 3.56 (dtd, $J = 13.1, 4.6, 1.0$ Hz, 1H), 3.45 – 3.37 (m, 1H), 2.17 – 2.10 (m, 2H), 1.34 (t, $J = 7.1$ Hz, 3H). ^{13}C NMR(126 MHz, cd_3od) δ 169.20, 147.37, 142.73, 136.75, 134.04, 129.74, 129.51, 128.39, 127.14, 117.52, 111.58, 111.41, 109.38, 61.54, 41.59, 36.22, 26.03, 14.62. **Step 2:** Performed amide coupling as described in **General Procedure (G)** from **26-2** amine salt (30 mg, 0.086 mmol, 1 eq), di-Boc-Dmt (41 mg, 0.10 mmol, 1.15 eq), PyBOP (52 mg, 0.10 mmol, 1.15 eq), 6-Cl HOBt (17 mg, 0.10 mmol, 1.15 eq), and DIPEA (0.16 mL, 0.92 mmol, 11 eq). ^1H NMR (500 MHz, Chloroform- d) δ 7.56 (s, 2H), 7.27 (t, $J = 7.5$ Hz, 2H), 7.20 – 7.13 (m, 3H), 7.03 (d, $J = 2.2$ Hz, 1H), 6.84 (s, 2H), 5.67 (s, 1H), 5.41 (s, 1H), 4.98 (dt, $J = 8.8, 4.4$ Hz, 1H), 4.24 (tt, $J = 8.6, 5.3$ Hz, 1H), 4.20 – 4.10 (m, 1H), 3.78

(s, 2H), 3.23 (dt, $J = 12.9, 4.2$ Hz, 1H), 3.08 (d, $J = 9.4$ Hz, 2H), 2.55 (s, 1H), 2.38 (s, 6H), 1.72 (t, $J = 11.6$ Hz, 1H), 1.57 (s, 10H), 1.44 (s, 9H), 1.31 (t, $J = 7.1$ Hz, 2H). ^{13}C NMR (126 MHz, cdCl_3) δ 170.01, 168.52, 155.12, 152.12, 149.53, 146.47, 141.51, 138.98, 135.76, 131.62, 131.35, 128.73, 128.57, 128.55, 126.45, 126.11, 121.15, 120.57, 109.56, 83.50, 80.03, 60.44, 54.26, 45.56, 40.85, 36.43, 33.44, 28.44, 27.86, 26.85, 20.56, 14.41. Boc-protected following **General Procedure (G)**. Final yield not calculated. ^1H NMR (500 MHz, Methanol- d_4) δ 7.61 (d, $J = 2.2$ Hz, 1H), 7.23 (t, $J = 7.5$ Hz, 2H), 7.15 (d, $J = 7.4$ Hz, 1H), 7.13 – 7.09 (m, 2H), 7.03 (d, $J = 2.2$ Hz, 1H), 6.48 (s, 2H), 4.92 (t, $J = 4.0$ Hz, 1H), 4.24 (qd, $J = 7.2, 1.4$ Hz, 2H), 3.83 (dd, $J = 11.6, 5.0$ Hz, 1H), 3.76 (s, 2H), 3.25 (dd, $J = 13.6, 11.6$ Hz, 1H), 3.12 (dt, $J = 12.7, 4.2$ Hz, 1H), 3.00 (dd, $J = 13.7, 5.1$ Hz, 1H), 2.47 (td, $J = 12.2, 3.2$ Hz, 1H), 2.27 (s, 6H), 1.63 (tt, $J = 11.9, 4.2$ Hz, 1H), 1.52 (dq, $J = 13.2, 3.8$ Hz, 1H), 1.31 (t, $J = 7.2$ Hz, 3H). ^{13}C NMR(126 MHz, cd_3od) δ 168.25, 157.41, 147.68, 142.95, 140.00, 137.00, 135.31, 132.61, 129.62, 129.41, 127.01, 123.26, 121.33, 116.49, 61.28, 53.35, 47.06, 36.90, 31.94, 27.77, 20.43, 14.63. HPLC (gradient A): retention time = 43.1 min. ESI-MS 525.3 $[\text{M} + \text{Na}]^+$.

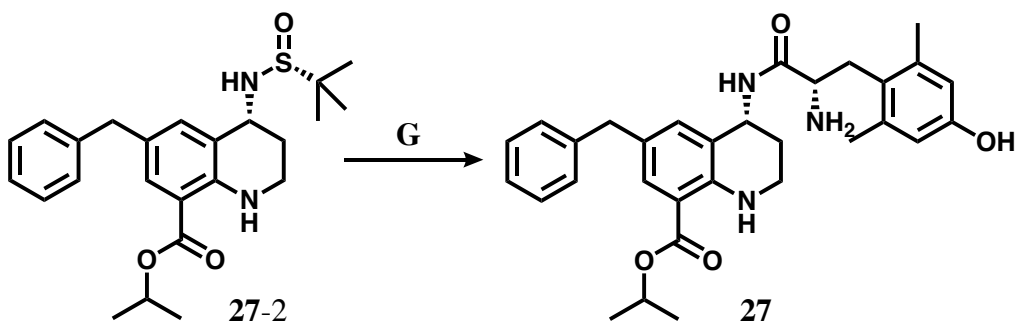
Compound 27 (Notebook name: AFN-53)



27-1. isopropyl 6-benzyl-4-oxo-1,2,3,4-tetrahydroquinoline-8-carboxylate. **27-1** was synthesized following **General Procedure (H)** from **8-5** (166 mg, 0.52 mmol, 1 eq), oxalyl chloride (1 mL, excess), K₂CO₃ (109 mg, 0.79 mmol, 1.5 eq) and Pd(dppf)Cl₂ (38 mg, 0.05 mmol, 0.1 eq) in 2:1 DMF:isopropanol. Yield: 15 mg, 9%. ¹H NMR (500 MHz, Chloroform-*d*) δ 8.11 (s, 1H), 7.93 (d, *J* = 2.4 Hz, 1H), 7.91 (d, *J* = 2.2 Hz, 1H), 7.28 (t, *J* = 7.5 Hz, 2H), 7.20 (d, *J* = 7.4 Hz, 1H), 7.17 (d, *J* = 6.9 Hz, 2H), 5.19 (hept, *J* = 6.3 Hz, 1H), 3.88 (s, 2H), 3.63 (td, *J* = 7.1, 2.4 Hz, 2H), 2.68 (t, *J* = 7.3 Hz, 2H), 1.36 (s, 3H), 1.34 (s, 3H). ¹³C NMR (126 MHz, cdcl₃) δ 167.43, 164.97, 138.57, 133.88, 128.76, 127.80, 126.33, 77.16, 40.84, 37.42, 22.07.

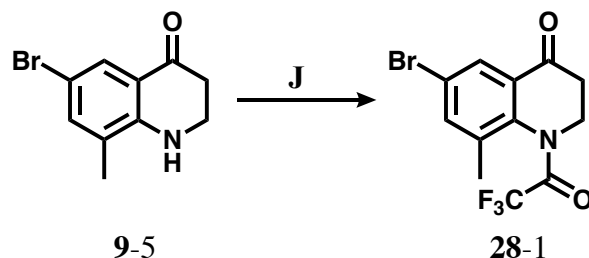


27-2. isopropyl (R)-6-benzyl-4-(((R)-tert-butylsulfinyl)amino)-1,2,3,4-tetrahydroquinoline-8-carboxylate. **27-2** was synthesized following **General Procedure (F)** from **27-1** (33 mg, 0.10 mmol, 1 eq), (R)-2-methyl-2-propanesulfinamide (38 mg, 0.31 mmol, 3 eq), and Ti(OiPr)₄ (0.18 mL, 0.61 mmol, 6 eq), then NaBH₄ (23 mg, 0.61 mmol, 6 eq). Yield: 18 mg, 41%. ¹H NMR (500 MHz, Chloroform-*d*) δ 7.86 (d, *J* = 4.8 Hz, 1H), 7.69 (d, *J* = 2.1 Hz, 1H), 7.27 (t, *J* = 7.6 Hz, 2H), 7.20 – 7.15 (m, 3H), 5.16 (hept, *J* = 6.2 Hz, 1H), 4.51 (q, *J* = 3.1 Hz, 1H), 3.84 (s, 2H), 3.44 (td, *J* = 12.2, 3.3 Hz, 1H), 3.36 (dq, *J* = 12.2, 4.2 Hz, 1H), 3.05 (s, 1H), 2.10 (dq, *J* = 13.8, 3.4 Hz, 1H), 1.83 (tt, *J* = 12.8, 4.0 Hz, 1H), 1.34 (d, *J* = 4.8 Hz, 3H), 1.32 (d, *J* = 4.9 Hz, 3H), 1.20 (s, 9H). ¹³C NMR (126 MHz, cdcl₃) δ 168.13, 146.68, 141.70, 136.13, 131.94, 128.76, 128.58, 126.56, 126.12, 121.62, 110.11, 77.16, 67.79, 55.56, 50.01, 40.91, 35.53, 26.51, 22.78, 22.13.

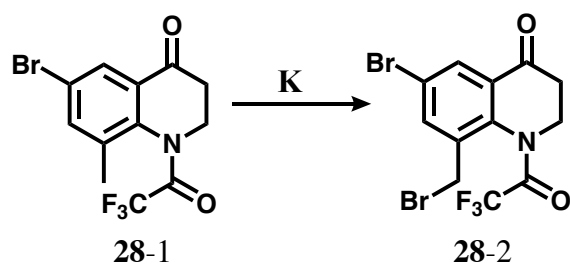


27. *isopropyl (R)-4-((S)-2-amino-3-(4-hydroxy-2,6-dimethylphenyl)propanamido)-6-benzyl-1,2,3,4-tetrahydroquinoline-8-carboxylate. 27* was synthesized following **General Procedure (G)** from **27-2** (18 mg, 0.04 mmol, 1 eq) and concentrated HCl (0.03 mL, excess). Carried forward without characterization. **Step 2:** Performed amide coupling using **27-2** amine salt (14 mg, 0.04 mmol, 1 eq), di-Boc-Dmt (18 mg, 0.04 mmol, 1.1 eq), PyBOP (22 mg, 0.04 mmol, 1.1 eq), and DIPEA (0.07 mL, 0.39 mmol, 10 eq). **Step 3:** Boc-deprotected as described in **General Procedure (G)**. Final yield not calculated. HPLC (gradient A): retention time = 45.4 min. ESI-MS 516.3[M + H]⁺ and 538.3 [M + Na]⁺. ¹H NMR (500 MHz, Methanol-*d*₄) δ 8.19 (d, *J* = 7.8 Hz, 1H), 7.58 (d, *J* = 2.2 Hz, 1H), 7.22 (dd, *J* = 8.1, 6.8 Hz, 2H), 7.14 (d, *J* = 7.5 Hz, 1H), 7.12 – 7.09 (m, 2H), 7.01 (d, *J* = 2.2 Hz, 1H), 6.48 (s, 2H), 5.11 (hept, *J* = 6.3 Hz, 1H), 4.91 (d, *J* = 6.1 Hz, 1H), 3.82 (dd, *J* = 11.6, 5.0 Hz, 1H), 3.75 (s, 2H), 3.24 (dd, *J* = 13.6, 11.6 Hz, 1H), 3.11 (dt, *J* = 12.3, 4.0 Hz, 1H), 2.99 (dd, *J* = 13.6, 5.1 Hz, 1H), 2.46 (td, *J* = 12.2, 3.3 Hz, 1H), 2.26 (s, 6H), 1.63 (tt, *J* = 12.2, 4.2 Hz, 1H), 1.55 – 1.48 (m, 1H), 1.29 (d, *J* = 2.9 Hz, 3H), 1.28 (d, *J* = 2.9 Hz, 3H). ¹³C NMR (126 MHz, cd₃od) δ 169.05, 157.40, 140.00, 136.93, 133.79, 132.56, 129.40, 127.59, 127.00, 116.48, 115.22, 110.96, 68.78, 49.00, 47.17, 41.63, 36.87, 31.93, 27.77, 22.15, 20.44.

Compound 28 (Notebook reference: AFN-15 or afn-iii-303, notebook 3 p. 303, afn-iv-5, notebook 4 p. 5, and afn-iv-81, notebook 4 p. 81)

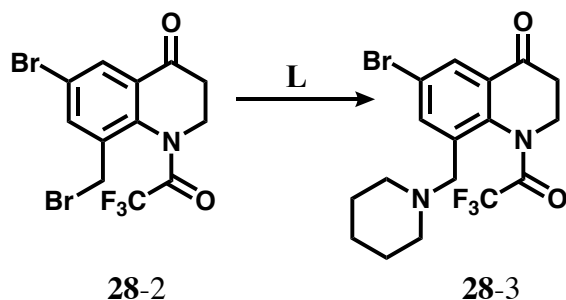


28-1. *6-bromo-8-methyl-1-(2,2,2-trifluoroacetyl)-2,3-dihydroquinolin-4(1H)-one.* **28-1** was synthesized following **General Procedure (J)** from intermediate **9-5** (1.17 g, 4.89 mmol, 1 eq) and trifluoroacetic anhydride (1.37 mL, 9.78 mmol, 2 eq). Yield: 1.54 g, 95%. ¹H NMR (400 MHz, CDCl₃) δ 7.99 (d, *J* = 2.2 Hz, 1H), 7.63 (d, *J* = 2.3 Hz, 1H), 4.52 (dd, *J* = 14.6, 5.2 Hz, 1H), 3.88 (td, *J* = 13.9, 3.9 Hz, 1H), 3.03 – 2.79 (m, 2H), 2.17 (s, 3H). ¹³C NMR (101 MHz, CDCl₃) δ 191.77, 139.79, 139.42, 139.10, 136.84, 129.86, 128.58, 128.36, 121.85, 117.65, 114.79, 77.16, 46.17, 40.13, 39.99, 18.70, 18.48.



28-2. *6-bromo-8-(bromomethyl)-1-(2,2,2-trifluoroacetyl)-2,3-dihydroquinolin-4(1H)-one.* **28-2** was synthesized following **General Procedure (K)** from **28-1** (478 mg, 1.42 mmol, 1.00 eq), NBS (266 mg, 1.49 mmol, 1.05 eq), and benzoyl peroxide (34 mg, 0.14 mmol, 0.1 eq). Reaction was then concentrated *in vacuo* onto silica and purified by manually-packed silica column

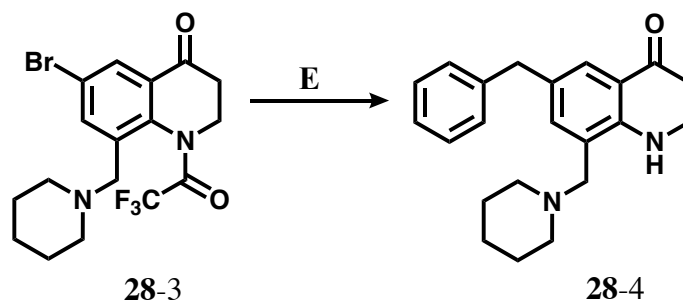
chromatography using 10% ethyl acetate, 90% hexanes, as flash chromatography did not provide sufficient separation. Yield: 232 mg, 40%. ^1H NMR (500 MHz, CDCl_3) δ 8.11 (t, $J = 2.6$ Hz, 1H), 7.82 (t, $J = 2.8$ Hz, 1H), 4.62 – 4.52 (m, 1H), 4.41 (dd, $J = 11.7, 3.0$ Hz, 1H), 4.32 (dd, $J = 11.8, 3.0$ Hz, 1H), 3.92 (tt, $J = 14.4, 3.5$ Hz, 1H), 3.00 (dddd, $J = 16.7, 13.7, 5.7, 3.0$ Hz, 1H), 2.94 – 2.85 (m, 1H). ^{13}C NMR(126 MHz, CDCl_3) δ 191.09, 138.90, 136.23, 134.42, 131.08, 130.77, 129.92, 128.99, 122.30, 77.16, 46.11, 46.08, 39.92, 28.94.



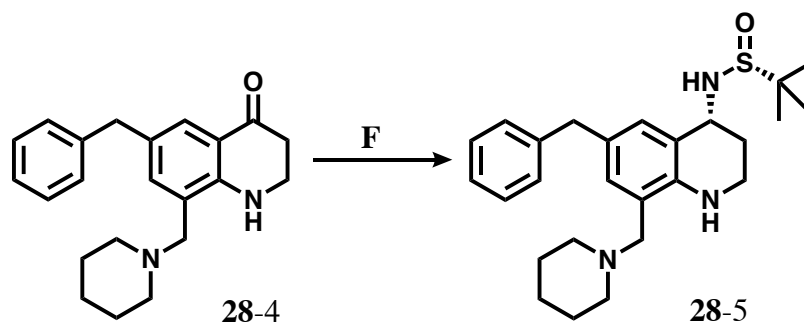
28-3 6-bromo-8-(piperidin-1-ylmethyl)-1-(2,2,2-trifluoroacetyl)-2,3-dihydroquinolin-4(1H)-one.

28-3 was synthesized following **General Procedure (L)** from **28-2** (140 mg, 0.34 mmol, 1 eq), K_2CO_3 (140 mg, 1.02 mmol, 3 eq), and piperidine (0.04 mL, 0.41 mmol, 1.2 eq). *N*-trifluoroacetyl group was partially removed during reaction, so **28-3** was carried forward as a 1:1 molar eq mixture of *N*-TFA protected (60 mg, 0.14 mmol) and deprotected (45 mg, 0.14 mmol) intermediates. Net yield: 0.28 mmol, 82%. Unprotected: ^1H NMR (500 MHz, CDCl_3) δ 7.87 (d, $J = 2.6$ Hz, 1H), 7.50 (s, 1H), 7.17 (d, $J = 2.6$ Hz, 1H), 3.54 (t, $J = 7.1$ Hz, 2H), 3.44 (s, 2H), 2.63 (t, $J = 7.1$ Hz, 2H), 2.34 (s, 4H), 1.54 (q, $J = 5.8$ Hz, 4H), 1.45 (s, 2H). ^{13}C NMR(126 MHz, CDCl_3) δ 192.97, 151.75, 137.64, 128.90, 125.72, 120.35, 108.66, 77.16, 62.11, 54.04, 41.38, 37.47, 26.23, 24.28. TFA-protected: ^1H NMR (500 MHz, CDCl_3) δ 7.97 (d, $J = 2.4$ Hz, 1H), 7.83 (s, 1H), 4.43 (dd, $J = 14.3, 5.4$ Hz, 1H), 3.77 (d, $J = 15.8$ Hz, 1H), 3.27 (dd, 2H), 2.96 – 2.72 (m, 2H), 2.17 (s, 4H), 1.54 –

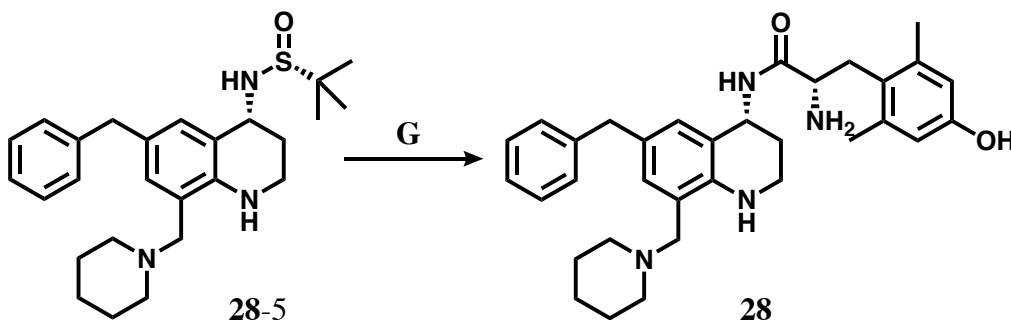
1.40 (m, 4H), 1.35 (q, $J = 6.1$ Hz, 2H). ^{13}C NMR(126 MHz, CDCl_3) δ 191.76, 182.72, 139.46, 138.55, 137.67, 129.98, 129.33, 121.93, 119.74, 117.45, 115.15, 112.87, 60.76, 54.74, 45.98, 40.04, 25.82, 24.25.



28-4. *6-benzyl-8-(piperidin-1-ylmethyl)-2,3-dihydroquinolin-4(1H)-one.* **28-4** was synthesized following **General Procedure (E)** from the mixture of **28-3** previously described (105 mg, 0.28 mmol, 1 eq), benzyl boronic acid pinacol ester (0.10 mL, 0.43 mmol, 1.5 eq), K_2CO_3 (120 mg, 0.86 mmol, 3 eq) and $\text{Pd}(\text{dppf})\text{Cl}_2$ (21 mg, 0.028 mmol, 0.1 eq). Yield: 88 mg, 92%. ^1H NMR (500 MHz, CDCl_3) δ 7.58 (d, $J = 2.1$ Hz, 1H), 7.18 (d, $J = 7.0$ Hz, 2H), 7.14 – 7.06 (m, 3H), 6.85 (d, $J = 2.1$ Hz, 1H), 3.76 (s, 2H), 3.46 (d, $J = 7.5$ Hz, 2H), 3.36 (s, 2H), 2.56 (d, $J = 7.0$ Hz, 2H), 2.29 – 2.20 (m, 4H), 1.46 (p, $J = 5.4$ Hz, 4H), 1.37 (s, 2H). ^{13}C NMR(126 MHz, CDCl_3) δ 194.42, 151.61, 141.51, 136.59, 129.02, 128.82, 128.54, 126.33, 126.09, 119.16, 75.12, 62.58, 54.09, 54.03, 41.75, 41.06, 37.90, 26.26, 24.97, 24.38.



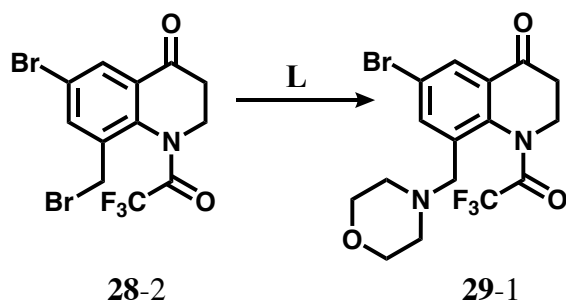
28-5. *(R)-N-((R)-6-benzyl-8-(piperidin-1-ylmethyl)-1,2,3,4-tetrahydroquinolin-4-yl)-2-methylpropane-2-sulfonamide*. **28-5** was synthesized following **General Procedure (F)** from **28-4** (88 mg, 0.26 mmol, 1 eq), *(R)*-2-methyl-2-propanesulfonamide (96 mg, 0.79 mmol, 3 eq), and $\text{Ti}(\text{OEt})_4$ (0.33 mL, 1.58 mmol, 6 eq), then NaBH_4 (60 mg, 1.58 mmol, 6 eq). Yield: 85 mg, 74%. Carried forward without characterization.



28. *(S)*-2-amino-*N*-((*R*)-6-benzyl-8-(piperidin-1-ylmethyl)-1,2,3,4-tetrahydroquinolin-4-yl)-3-(4-hydroxy-2,6-dimethylphenyl)propanamide. **28** was synthesized following **General Procedure (G)** from **28-5** (85 mg, 0.19 mmol, 1 eq) and concentrated HCl (0.05 mL, excess). **Step 2:** Performed amide coupling using **28-5** amine salt (37 mg, 0.090 mmol, 1 eq), di-Boc-Dmt (41 mg, 0.099 mmol, 1.1 eq), PyBOP (52 mg, 0.099 mmol, 1.1 eq), 6-Cl HOBt (17 mg, 0.099 mmol, 1.1 eq), and DIPEA (0.16 mL, 0.90 mmol, 10 eq). **Step 3:** Boc-deprotected as described in **General Procedure (G)**. Final yield not calculated. ^1H NMR (500 MHz, Methanol- d_4) δ 7.25 – 7.20 (m, 2H), 7.16 – 7.10 (m, 3H), 7.01 (d, J = 2.0 Hz, 1H), 6.96 (d, J = 2.1 Hz, 1H), 6.47 (s, 2H), 4.93 (dt, J = 7.9, 4.2

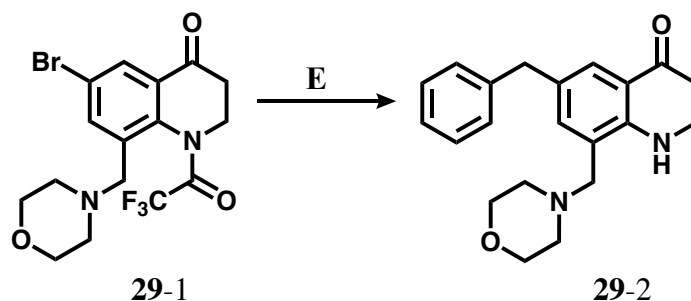
Hz, 1H), 4.15 – 4.02 (m, 2H), 3.88 (dd, $J = 11.6, 5.0$ Hz, 1H), 3.79 (s, 2H), 3.37 (d, $J = 12.4$ Hz, 2H), 3.26 (dd, $J = 13.6, 11.6$ Hz, 1H), 3.07 (dt, $J = 12.4, 4.2$ Hz, 1H), 3.02 (dd, $J = 13.7, 5.1$ Hz, 1H), 2.95 – 2.84 (m, 2H), 2.54 – 2.45 (m, 1H), 2.27 (s, 6H), 1.89 (d, $J = 14.7$ Hz, 2H), 1.80 (d, $J = 12.8$ Hz, 1H), 1.71 (m, 2H), 1.65 (m, 1H), 1.53 (q, $J = 4.2$ Hz, 1H), 1.49 (m, 1H). HPLC (gradient A): retention time = 27.6min. ESI-MS 527.3[M + H]⁺ and 549.3 [M + Na]⁺.

Compound 29 (Notebook reference: AFN-17 or afn-iv-33, notebook 4 p. 33)

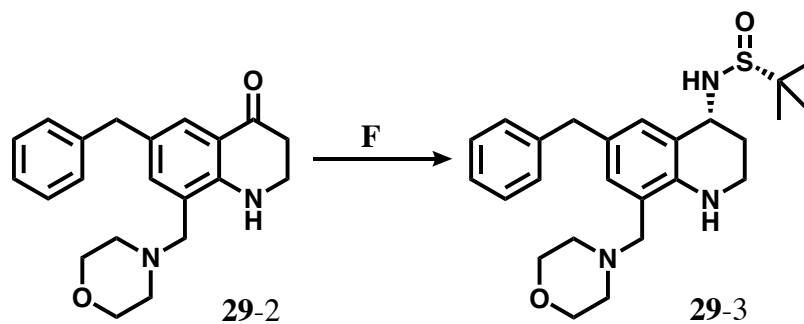


29-1. *6-bromo-8-(morpholinomethyl)-1-(2,2,2-trifluoroacetyl)-2,3-dihydroquinolin-4(1H)-one.*

29-1 was synthesized following **General Procedure (L)** from intermediate **28-2** (250 mg, 0.60 mmol, 1 eq), and morpholine (3 mL, excess.); K₂CO₃ was not used here. No loss of trifluoroacetic protecting group observed. Yield: 160 mg, 63% ¹H NMR (500 MHz, CDCl₃) δ 8.09 (d, $J = 2.4$ Hz, 1H), 7.95 (d, $J = 2.3$ Hz, 1H), 4.53 (d, $J = 14.3$ Hz, 1H), 3.88 (d, $J = 13.8$ Hz, 1H), 3.70 (t, $J = 4.7$ Hz, 4H), 3.41 (s, 2H), 2.96 (ddd, $J = 18.8, 13.4, 5.5$ Hz, 1H), 2.88 (ddd, $J = 18.5, 3.9, 1.7$ Hz, 1H), 2.37 (s, 4H). ¹³C NMR(126 MHz, CDCl₃) δ 191.46, 139.50, 138.53, 130.11, 129.88, 122.18, 77.16, 66.72, 60.08, 53.72, 46.11, 40.04.

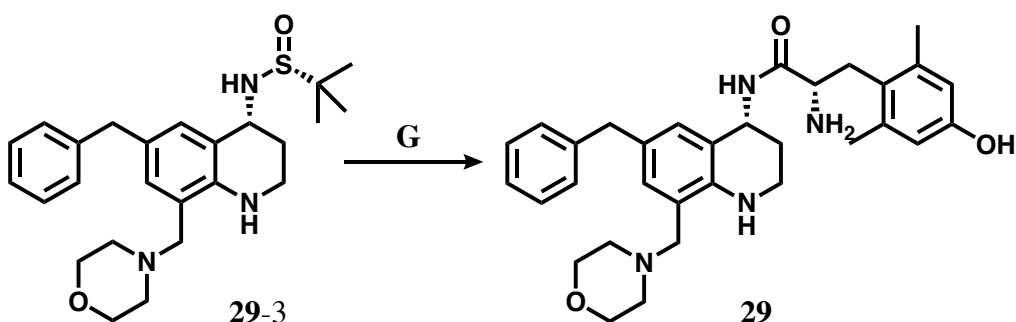


29-2. *6-benzyl-8-(morpholinomethyl)-2,3-dihydroquinolin-4(1H)-one*. **29-2** was synthesized following **General Procedure (E)** from **29-1** (160 mg, 0.38 mmol, 1 eq), benzyl boronic acid pinacol ester (0.13 mL, 0.57 mmol, 1.5 eq), K_2CO_3 (160 mg, 1.14 mmol, 3 eq) and $Pd(dppf)Cl_2$ (30 mg, 0.04 mmol, 0.1 eq). Yield: 75 mg, 60%. 1H NMR (500 MHz, $CDCl_3$) δ 7.68 (d, $J = 2.1$ Hz, 1H), 7.26 (s, 2H), 7.22 – 7.13 (m, 3H), 6.96 (d, $J = 2.2$ Hz, 1H), 3.83 (s, 2H), 3.68 (t, $J = 4.7$ Hz, 4H), 3.56 (p, $J = 5.9$ Hz, 2H), 3.47 (s, 2H), 2.65 (dd, $J = 7.7, 6.5$ Hz, 2H), 2.43 – 2.37 (m, 4H). ^{13}C NMR (126 MHz, $CDCl_3$) δ 194.16, 151.08, 141.36, 136.94, 129.29, 128.78, 128.75, 128.56, 128.53, 128.35, 126.77, 126.14, 119.35, 77.16, 67.10, 62.16, 53.22, 53.15, 41.75, 41.01, 37.83, 24.96.



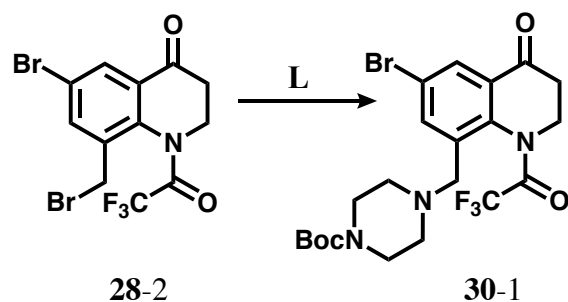
29-3. *(R)-N-((R)-6-benzyl-8-(morpholinomethyl)-1,2,3,4-tetrahydroquinolin-4-yl)-2-methylpropane-2-sulfinamide*. **29-3** was synthesized following **General Procedure (F)** from **29-2** (75 mg, 0.22 mmol, 1 eq), (R)-2-methyl-2-propanesulfinamide (81 mg, 0.66 mmol, 3 eq), and $Ti(OEt)_4$ (0.28 mL, 1.34 mmol, 6 eq), then $NaBH_4$ (51 mg, 1.34 mmol, 6 eq). Yield: 31 mg, 31%.

^1H NMR (500 MHz, CDCl_3) δ 7.26 (s, 2H), 7.18 – 7.13 (m, 3H), 7.07 (d, $J = 2.0$ Hz, 1H), 6.74 (d, $J = 2.1$ Hz, 1H), 4.52 (q, $J = 3.3$ Hz, 1H), 3.81 (d, $J = 3.2$ Hz, 2H), 3.67 (t, $J = 4.7$ Hz, 4H), 3.46 (d, $J = 12.8$ Hz, 1H), 3.36 – 3.33 (m, 1H), 3.32 – 3.23 (m, 2H), 2.37 (t, $J = 10.1$ Hz, 4H), 2.10 – 2.02 (m, 1H), 1.89 – 1.79 (m, 1H), 1.21 (s, 9H). ^{13}C NMR(126 MHz, CDCl_3) δ 143.41, 141.97, 131.00, 129.99, 128.86, 128.79, 128.46, 125.93, 121.35, 120.64, 116.06, 67.17, 62.46, 53.22, 49.92, 41.08, 36.19, 28.37, 22.78.

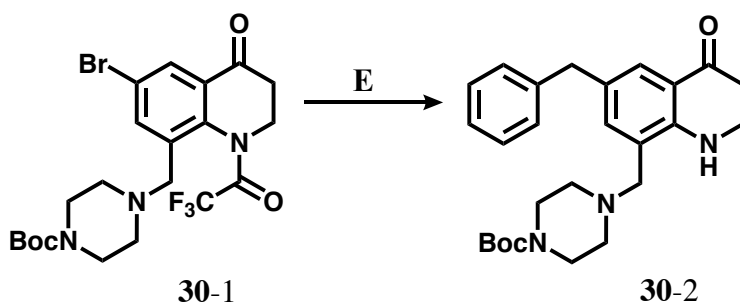


29. *(S)*-2-amino-*N*-((*R*)-6-benzyl-8-(morpholinomethyl)-1,2,3,4-tetrahydroquinolin-4-yl)-3-(4-hydroxy-2,6-dimethylphenyl)propanamide. **29** was synthesized following **General Procedure (G)** from **29-3** (31 mg, 0.070 mmol, 1 eq) and concentrated HCl (0.03 mL, excess). Carried forward without characterization. **Step 2:** Performed amide coupling using **29-3** amine salt (25 mg, 0.068 mmol, 1 eq), di-Boc-Dmt (31 mg, 0.075 mmol, 1.1 eq), PyBOP (39 mg, 0.075 mmol, 1.1 eq), 6-Cl HOBt (13 mg, 0.075 mmol, 1.1 eq), and DIPEA (0.13 mL, 0.70 mmol, 10 eq). **Step 3:** Boc-deprotected as described in **General Procedure (G)**. Final yield not calculated. ^1H NMR (500 MHz, Methanol- d_4) δ 7.24 – 7.17 (m, 2H), 7.15 – 7.09 (m, 3H), 7.01 (d, $J = 2.1$ Hz, 1H), 6.98 (d, $J = 2.1$ Hz, 1H), 6.47 (s, 2H), 4.92 (m, 1H), 4.17 (m, 2H), 3.88 (m, 1H), 3.88 (broad s, 4H), 3.78 (s, 2H), 3.26 (m, 1H), 3.19 (broad s, 4H), 3.07 (dt, $J = 12.3, 4.3$ Hz, 1H), 3.02 (dd, $J = 13.7, 5.1$ Hz, 1H), 2.49 (td, $J = 11.9, 2.9$ Hz, 1H), 2.27 (s, 6H), 1.64 (ddt, $J = 13.0, 11.4, 4.1$ Hz, 1H), 1.55 – 1.47 (m, 1H). HPLC (gradient A): retention time = 24.2 min. ESI-MS 551.3 $[\text{M} + \text{Na}]^+$.

Compound 30 (Notebook reference: AFN-41 or afn-v-113, notebook 5 p. 113)

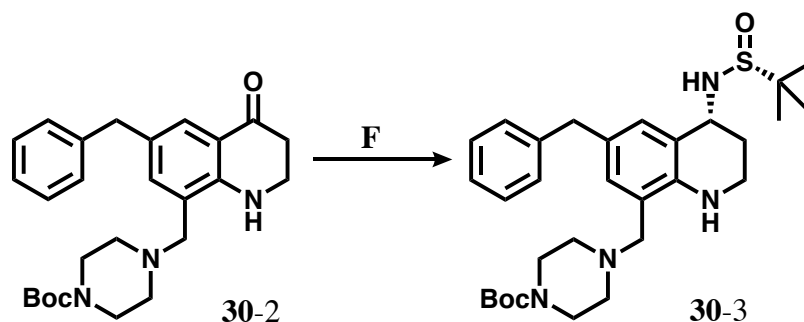


30-1. *tert-butyl 4-((6-bromo-4-oxo-1-(2,2,2-trifluoroacetyl)-1,2,3,4-tetrahydroquinolin-8-yl)methyl)piperazine-1-carboxylate.* **30-1** was synthesized following **General Procedure (L)** from **28-1** (280 mg, 0.67 mmol, 1 eq), K_2CO_3 (251 mg, 1.35 mmol, 2 eq), and monoBoc-piperazine (187 mg, 1.35 mmol, 2 eq). Some loss of trifluoroacetic protecting group observed, but not isolated. Yield: 212 mg, 75%. 1H NMR (500 MHz, $CDCl_3$) δ 7.99 (d, $J = 2.2$ Hz, 1H), 7.85 (d, $J = 2.4$ Hz, 1H), 4.51 – 4.38 (m, 1H), 3.77 (t, $J = 14.0$ Hz, 1H), 3.38 – 3.29 (m, 4H), 2.91 – 2.84 (m, 1H), 2.79 (ddd, $J = 18.6, 3.7, 1.7$ Hz, 1H), 2.21 (t, $J = 5.0$ Hz, 4H), 1.38 (s, 9H). ^{13}C NMR(126 MHz, $CDCl_3$) δ 191.48, 154.81, 139.39, 138.36, 136.59, 130.05, 129.69, 122.08, 119.68, 117.38, 115.09, 79.88, 59.83, 53.09, 46.02, 43.33, 39.99, 28.51.

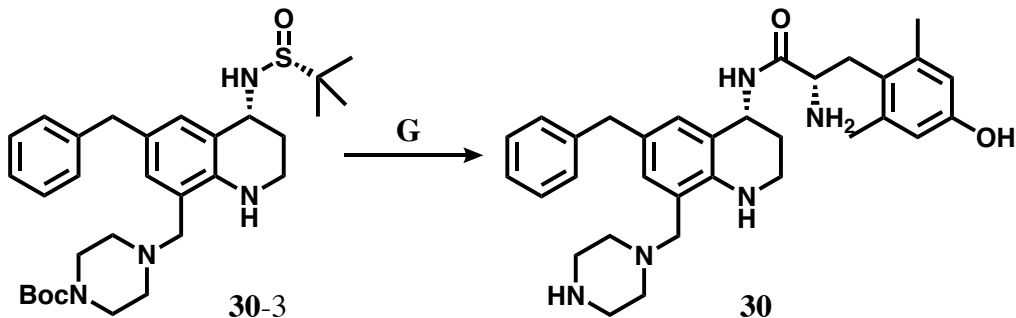


30-2. *tert-butyl 4-((6-benzyl-4-oxo-1,2,3,4-tetrahydroquinolin-8-yl)methyl)piperazine-1-carboxylate.* **30-2** was synthesized following **General Procedure (E)** from **30-1** (212 mg, 0.50

mmol, 1 eq), benzyl boronic acid pinacol ester (0.22 mL, 1.00 mmol, 2 eq), K₂CO₃ (207 mg, 1.50 mmol, 3 eq) and Pd(dppf)Cl₂ (37 mg, 0.05 mmol, 0.1 eq). Yield: 84 mg, 39%. ¹H NMR (500 MHz, CDCl₃) δ 7.69 (d, *J* = 2.1 Hz, 1H), 7.29 – 7.24 (m, 2H), 7.20 – 7.14 (m, 3H), 6.94 (d, *J* = 2.2 Hz, 1H), 6.83 (s, 1H), 3.84 (s, 2H), 3.55 (ddd, *J* = 7.7, 5.3, 2.0 Hz, 2H), 3.48 (s, 2H), 3.45 – 3.36 (m, 4H), 2.68 – 2.61 (m, 2H), 2.35 (s, 4H), 1.45 (s, 9H). ¹³C NMR(126 MHz, CDCl₃) δ 194.18, 178.30, 154.82, 151.11, 141.40, 136.90, 129.39, 128.83, 128.61, 126.84, 126.19, 122.69, 119.45, 80.00, 61.88, 52.54, 41.79, 41.05, 37.88, 28.54.

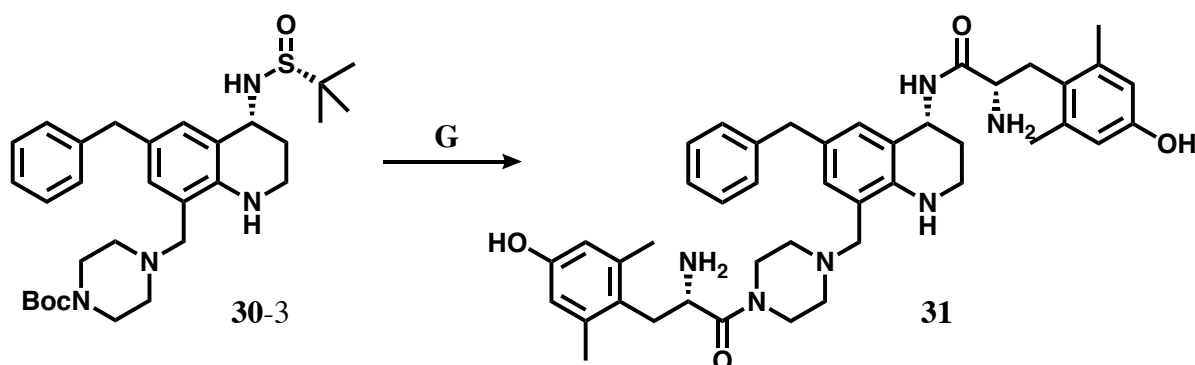


30-3. *tert-butyl 4-(((R)-6-benzyl-4-(((R)-tert-butylsulfinyl)amino)-1,2,3,4-tetrahydroquinolin-8-yl)methyl)piperazine-1-carboxylate.* **30-2** was synthesized following **General Procedure (F)** from **30-2** (84 mg, 0.19 mmol, 1 eq), (R)-2-methyl-2-propanesulfinamide (71 mg, 0.58 mmol, 3 eq), and Ti(OEt)₄ (0.24 mL, 1.16 mmol, 6 eq), then NaBH₄ (44 mg, 1.16 mmol, 6 eq). Yield: 83 mg, 80%. ¹H NMR (500 MHz, CDCl₃) δ 7.27 – 7.23 (m, 2H), 7.20 – 7.12 (m, 3H), 7.07 (d, *J* = 2.0 Hz, 1H), 6.72 (d, *J* = 2.0 Hz, 1H), 4.53 (q, *J* = 3.3 Hz, 1H), 3.82 (d, *J* = 3.3 Hz, 2H), 3.52 – 3.43 (m, 1H), 3.39 (q, *J* = 6.7, 4.9 Hz, 4H), 3.33 (d, *J* = 13.1 Hz, 2H), 3.27 (ddd, *J* = 11.7, 8.1, 3.4 Hz, 1H), 2.35 – 2.30 (m, 4H), 2.13 – 2.02 (m, 1H), 1.85 (tt, *J* = 13.0, 12.5, 4.0 Hz, 1H), 1.45 (s, 9H), 1.22 (s, 9H). ¹³C NMR(126 MHz, CDCl₃) δ 154.87, 143.41, 141.97, 130.94, 129.99, 128.92, 128.81, 128.49, 125.95, 121.54, 120.68, 79.81, 62.11, 55.45, 52.53, 49.92, 41.10, 36.18, 28.52, 28.36, 22.80, 22.63.



30. (*S*)-2-amino-*N*-((*R*)-6-benzyl-8-(piperazin-1-ylmethyl)-1,2,3,4-tetrahydroquinolin-4-yl)-3-(4-hydroxy-2,6-dimethylphenyl)propanamide. **30** was synthesized following **General Procedure (G)** from **30-3** (43 mg, 0.080 mmol, 1 eq) and concentrated HCl (0.015 mL, 0.18 mmol, 2 eq). Reaction was monitored by TLC for disappearance of **30-3**, and solvent was removed after 12 minutes. Recovered 40 mg crude product. Carried forward without characterization. **Step 2:** Performed amide coupling using **30-3** amine salt (40 mg, 0.079 mmol, 1 eq), diBoc-Dmt (36 mg, 0.087 mmol, 1.1 eq), PyBOP (46 mg, 0.087 mmol, 1.1 eq), 6-Cl HOBt (15 mg, 0.087 mmol, 1.1 eq), and DIPEA (0.14 mL, 0.79 mmol, 10 eq). **Step 3:** Boc-protected as described in **General Procedure (G)**. Final yield not calculated. $^1\text{H NMR}$ (500 MHz, Methanol- d_4) δ 7.20 (t, $J = 7.4$ Hz, 2H), 7.14 – 7.07 (m, 3H), 6.88 (s, 1H), 6.74 (s, 1H), 6.48 (s, 2H), 4.94 (s, 1H), 3.84 (d, $J = 10.0$ Hz, 1H), 3.76 (s, 2H), 3.47 – 3.44 (m, 2H), 3.26 (m, 1H), 3.21 – 3.15 (m, 4H), 3.09 (d, $J = 12.5$ Hz, 1H), 3.01 (dd, $J = 13.8, 5.0$ Hz, 1H), 2.53 (m, 1H), 2.28 (s, 6H), 1.66 (t, $J = 12.2$ Hz, 1H), 1.56 – 1.47 (m, 1H), 1.29 (s, 4H). HPLC (gradient A): retention time = 21.7 min. ESI-MS 528.3[M + H] $^+$ and 550.3 [M + Na] $^+$.

Compound 31 (Notebook reference: AFN-14E or afn-iii-301, notebook 3 p. 301)



31. *(S)*-2-amino-*N*-((*R*)-8-((4-((*S*)-2-amino-3-(4-hydroxy-2,6-dimethylphenyl)propanoyl)piperazin-1-yl)methyl)-6-benzyl-1,2,3,4-tetrahydroquinolin-4-yl)-3-(4-hydroxy-2,6-dimethylphenyl)propenamide. **31** was synthesized following **General Procedure (G)** from **30-3** (65 mg, 0.14 mmol, 1 eq) and concentrated HCl (0.05 mL, excess). Boc group likely removed during this step. Carried forward without characterization. **Step 2:** Performed amide coupling using **30-3** amine salt (45 mg, 0.09 mmol, 1 eq), diBoc-Dmt (43 mg, 0.09 mmol, 1.1 eq), PyBOP (52 mg, 0.10 mmol, 1.1 eq), 6-Cl HOBt (17 mg, 0.10 mmol, 1.1 eq), and DIPEA (0.16 mL, 0.91 mmol, 10 eq). **Step 3:** Boc-protected as described in **General Procedure (G)**. Final yield not calculated. ¹H NMR (500 MHz, Methanol-d₄) δ 7.25 – 7.21 (m, 1H), 7.12 (d, J = 6.9 Hz, 2H), 6.99 – 6.95 (m, 1H), 6.91 – 6.83 (m, 1H), 6.55 (d, J = 8.1 Hz, 1H), 6.52 (d, J = 8.0 Hz, 1H), 6.46 (dd, J = 8.4, 5.7 Hz, 3H), 4.91 (d, J = 18.6 Hz, 1H), 4.54 (ddt, J = 12.4, 8.1, 4.6 Hz, 1H), 3.95 – 3.81 (m, 1H), 3.82 – 3.74 (m, 4H), 3.75 – 3.66 (m, 0H), 3.26 – 3.20 (m, 1H), 3.23 – 3.13 (m, 2H), 3.15 – 3.06 (m, 1H), 3.06 – 2.98 (m, 1H), 2.97 – 2.66 (m, 4H), 2.48 (d, J = 12.2 Hz, 1H), 2.31 – 2.19 (m, 12H), 2.04 (d, J = 11.1 Hz, 1H), 1.69 (d, J = 11.5 Hz, 1H), 1.65 – 1.58 (m, 1H), 1.51 (d, J = 17.4 Hz, 1H), 1.49 (s, 1H). HPLC (gradient A): retention time = 25.2 min. ESI-MS 719.3[M + H]⁺ and 741.3 [M + Na]⁺.

Chapter 3: Dual Pharmacophores Explored via SAR Matrix

3.1 Introduction

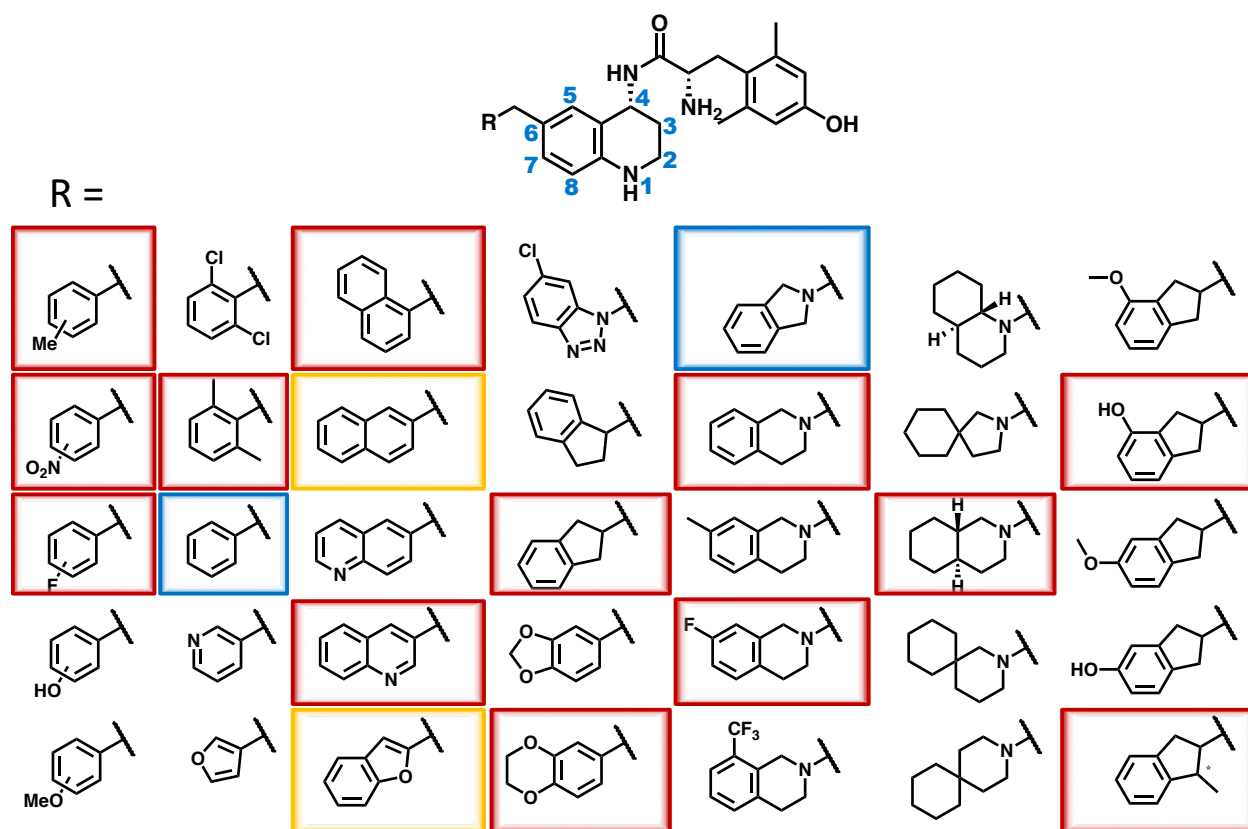
Translating the pharmacophore models derived from bifunctional opioid peptides (described in Chapter 1) required replication of the Tyr¹ and Phe⁴ moieties, separated by a spacer region—the THQ core. While some modifications to the Tyr¹ moiety were investigated, much exploration went into the Phe⁴ binding pocket, which translates to C-6 on our peptidomimetic scaffold. A summary of the C-6 substitutions investigated by our lab is depicted in **Fig. 14**, though this is not a comprehensive listing. Coloring in **Fig. 14** corresponds to *in vivo* activity, where blue indicates full antinociception in the previously described WWTW assay while yellow denotes partial activity and red denotes no activity. Those without any coloration were not tested *in vivo*.

As illustrated in the first column of **Fig. 14**, various substitutions were probed at the *ortho*, *meta*, and *para* positions including methyl, nitro, fluoro, hydroxyl, and methoxy substitutions. The second column depicts other modifications to the monocyclic aryl ring, with the unsubstituted phenyl ring of lead peptidomimetic **1** (referred to as the benzyl pendant henceforth) being the only fully active compound of those tested. By expanding the size of the C-6 pendant to a bicyclic system, the pharmacological profile was improved, as this typically reduced DOR stimulation while generally maintaining MOR efficacy. Some key observations from the C-6 SAR expansion shown in **Fig. 14** are described below.

- 1) Heteroatoms distal to the THQ core reduced MOR efficacy significantly.
- 2) Basic amines near C-6 generally display high affinity and partial efficacy for KOR.
- 3) Saturated rings display lower MOR efficacy and potency than aryl or semi-aryl bicyclics.
- 4) Monocyclic rings sometimes elicited DOR agonism whereas bicyclics did not.
- 5) All analogues displayed 10- to 200-fold MOR selectivity regardless of C-6 substitution.
- 6) Antinociceptive activity was unpredictable and infrequent amongst these substitutions.

These results suggested that aryl or semi-aryl bicyclic pendants offered the optimal MOR agonist/DOR antagonist profile but most displayed high MOR-selectivity and poor bioavailability.

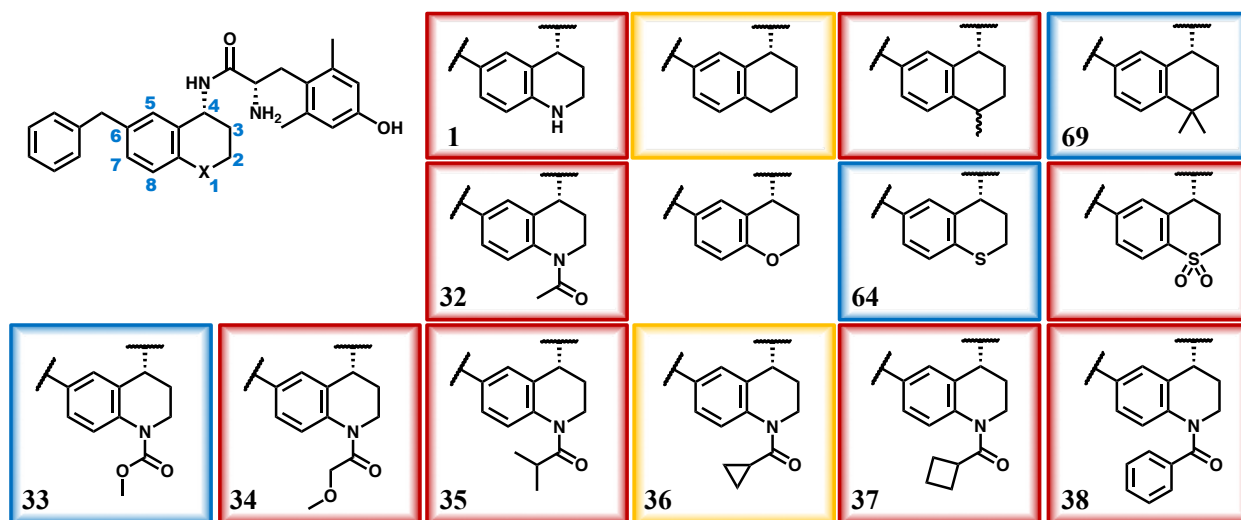
Figure 14. Abbreviated Catalogue of C-6 Substitutions Probing the Phe⁴ Binding Pocket^a



^a Red coloration indicates no significant antinociceptive activity in the mouse WWTW assay. Yellow denotes partial activity whereas blue denotes full antinociception. No color indicates that the compound was not tested in the WWTW assay. Analogues presented here were synthesized primarily by A.M.B. and A.A.H. with help by A.F.N. and D.J.M.

Concurrent with the exploration at C-6, a separate SAR project was aimed at modifying the *N*-1 position of the THQ core. The initial focus of this work was to remove or block the metabolic hotspot at C-2, alpha to the nitrogen atom in the THQ core. First, the nitrogen was replaced with a methylene unit, though this benzylic carbon could undergo radical oxidation and showed only partial *in vivo* activity. Substituting the C-1 position with a methyl group did not improve bioavailability, however a geminal dimethyl substitution (analogue **69**) did achieve full antinociceptive activity. Unfortunately, this scaffold was prohibitively lipophilic (ClogP = 6.3), requiring us to seek out alternative methods of improving bioavailability. The core -NH- was then replaced with -O-, -S-, and -SO₂-. The ether analogue showed 200-fold selectivity for MOR and was not pursued for *in vivo* testing. However, the thioether and sulfone—which showed comparable MOR selectivity to lead peptidomimetic **1**—were carried forward with *in vivo* evaluation. While the thioether was fully efficacious *in vivo*, the sulfone showed no activity.

Figure 15. Substitutions at the 1-Position of the Peptidomimetic Core^a



^a Red coloration indicates no significant antinociceptive activity in the mouse WWTW assay. Yellow denotes partial activity whereas blue indicates full antinociception. No coloration indicates that the compound was not tested in the WWTW assay. Analogues presented here were synthesized by A.A.H. and A.M.B. **69** was synthesized by A.F.N.

Although replacement of the THQ core -NH- with a -CH₂-, -O-, -S-, or -SO₂- gave analogues with 30- to 200-fold selectivity for MOR, it was found that acylating the *N*-1 position significantly improved DOR affinity and reduced MOR selectivity. A selection of the *N*-acyl substitutions investigated are presented in **Table 7**, adapted from Harland et. al., 2016.⁹⁵ These results demonstrated a very promising approach to balanced MOR-/DOR-selective bifunctional ligands. However, while the *N*-acyl series was very effective at balancing affinities between MOR and DOR, all analogues except the *N*-benzoyl analogue showed considerable DOR efficacy.

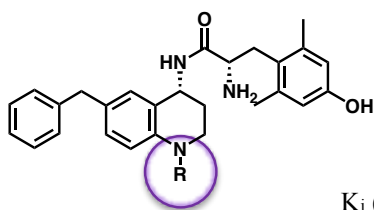


Table 7. *N*-Acyl Analogues with Improved MOR/DOR Affinity Balance, MOR Agonism/DOR Partial Agonism^{a, b}

#	<i>N</i> -1 Substitution	K _i (nM)				DOR K _i /MOR K _i	EC ₅₀ (nM)			% stim		
		MOR	DOR	KOR			MOR	DOR	KOR	MOR	DOR	KOR
1 ^c	H	0.22 (0.02)	9.4 (0.8)	68 (2)	43	1.6 (0.3)	110 (6)	>500	81 (2)	16 (2)	22 (2)	
32 ^d	COCH ₃	0.13 (0.02)	1.8 (0.1)	87 (11)	14	6.0 (1.3)	68 (2)	>500	76 (4)	26 (3)	29 (5)	
33	COOMe	0.19 (0.05)	0.51 (0.19)	29 (8)	2.7	0.78 (0.19)	14 (3)	250 (40)	95 (5)	40 (7)	28 (3)	
34	COCH ₂ OCH ₃	0.15 (0.04)	2.1 (0.7)	34 (4)	14	3.0 (0.5)	67 (22)	>500	91 (1)	47 (8)	38 (4)	
35	CO ^{<i>i</i>} Pr	0.38 (0.10)	0.53 (0.14)	76 (12)	1.7	9.6 (2.6)	25 (16)	>500	95 (4)	52 (2)	41 (4)	
36	CO ^{<i>c</i>} Pr	0.10 (0.03)	0.35 (0.01)	25 (5)	3.5	1.8 (0.3)	10 (2)	>500	88 (3)	69 (6)	32 (1)	
37	CO ^{<i>c</i>} Bu	0.23 (0.07)	0.15 (0.07)	56 (4)	0.7	2.1 (0.2)	5.1 (1.9)	dns	94 (5)	58 (4)	dns	
38	COPh	0.08 (0.03)	0.24 (0.09)	40 (15)	3	2.6 (0.6)	dns	>500	75 (7)	dns	16 (4)	

^a Data table adapted from Harland et. al., 2016 (reference ⁹⁵). ^b Binding affinities (K_i) were obtained by competitive displacement of radiolabeled [³H]-diprenorphine in membrane preparations. Functional data were obtained using agonist induced stimulation of [³⁵S]-GTPγS binding. Potency is represented as EC₅₀ (nM) and efficacy as percent maximal stimulation relative to standard agonist DAMGO (MOR), DPDPE (DOR), or U69,593 (KOR) at 10 μM. All values are expressed as the mean of three separate assays performed in duplicate with standard error of the mean in parentheses. “dns” = does not stimulate (<10% stim). ^c First reported in reference ⁹³. ^d First reported in reference ⁹⁴. Compounds in this table were synthesized by A.A.H. and A.M.B.

The opposing effects of the C-6 and *N*-1 campaigns—MOR-selective MOR agonism/DOR antagonism and balanced MOR agonism/DOR partial agonism—led us to combine these approaches in a small sampling of dually substituted C-6/*N*-1 analogues. Several bicyclic analogues were *N*-acetylated with the hope of retaining both MOR agonism/DOR antagonism as well as high DOR affinity/decreased MOR selectivity. Two *N*-acetylated that succeeded in achieving this goal featured 2-naphthyl and 1-tetrahydroisoquinoliny1 (THIQ) pendants. These were potent MOR agonists, displayed no DOR efficacy, were less than 10-fold selective for MOR, and produced a robust antinociceptive effect *in vivo* with a duration of action twice as long as our lead **1**. More recently, these analogues were demonstrated to show significantly reduced analgesic tolerance compared to morphine. Additionally, the 2-naphthyl analogue showed no dependence (no naloxone-induced withdrawal symptoms) or reward (measured by conditioned place preference), validating this chemotype for the treatment of pain with reduced side effects.⁹⁸

These results suggested a highly promising method for achieving our desired *in vitro* and *in vivo* goals. Following this success, several bicyclic analogues were *N*-acetylated with the aim of reproducing the previously observed boost in bioavailability. However, the subsequent *N*-acetyl analogues were as unpredictable *in vivo* as the unsubstituted analogues in **Fig. 14**, with no others displaying full antinociception. At this time, chemists A.A.H. and A.M.B. left the Mosberg lab, leaving this chemotype open to further development. What follows is a summary of the continued investigation into the C-6/*N*-1 chemotype. At present, a manuscript describing these results in abbreviated form is undergoing editing and resubmission to the *Journal of Medicinal Chemistry*.

3.2 Rationale & Approach

As discussed, the C-6 pharmacophore had been explored fairly extensively in past SAR campaigns. Additionally, while position-1 heteroatom replacement did not improve the pharmacological profile, it was discovered the *N*-1 substitutions could in fact be utilized to modulate DOR affinity (and in some cases bioavailability), establishing this as a second pharmacophore worth exploiting. Prior analogues had established that some combinations of C-6 and *N*-1 substitutions could achieve high-affinity, high-potency, non-selective MOR agonism and DOR antagonism. However, bioavailability was both uncommon and unpredictable. As such, it was hypothesized that more incremental changes to this validated chemotype could both fine-tune our understanding of the SAR resulting from *both* pharmacophore elements and might also deliver more *in vivo* hits around these islands of bioavailability.

Considering most C-6 pendants had been incorporated on the -NH- THQ core, and all *N*-1 substitutions were explored in the context of the benzyl C-6 scaffold, it seemed advantageous to combine promising moieties from both pharmacophores into a series of dually-substituted analogues. In order to most reliably compare across analogues, we identified select substitutions from each pharmacophore and synthesized the dually-substituted analogue resulting from each combination. In doing so, we generated a 2D matrix of compounds, allowing us to observe trends in both the *x* and *y* dimensions corresponding to different C-6 and *N*-1 substitutions. For this 2D matrix, we selected six C-6 substitutions and five *N*-1 moieties, resulting in 30 dual-pharmacophore analogues in the series. The C-6 substitutions were selected based on several criteria. Because of the delay between synthesis of a novel analogue and full pharmacological evaluation, all C-6 substitutions were selected from the list of previously synthesized and characterized analogues in **Fig. 14**. A similar approach was taken for the *N*-1 moieties, however

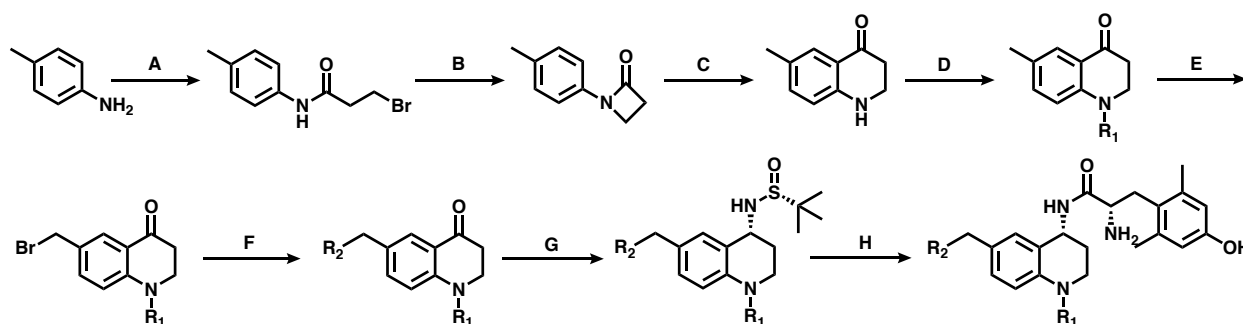
as will be discussed later, an additional (novel) *N*-1 substitution was incorporated into the matrix as well. In order to fully present the pharmacological data, tables are presented with the *N*-1 substitution as the independent variable initially, and matrices of select properties are included later in this chapter. As a follow-up to this study, the C-6 substitutions described below were also incorporated into the thiochromane scaffold (where the THQ -NH- was replaced with -S-), as the initial analogue in that series displayed full *in vivo* activity as depicted in **Fig. 15**. That series will be addressed separately at the end of this chapter along with the bioavailable *gem*-demethyl analogue **69** also found in **Fig. 15**.

Selection of C-6 pendants began with the bioavailable peptidomimetic lead **1**, which featured a benzyl pendant. The 2-naphthyl pendant (the first bicyclic pendant that displayed the desired MOR agonist/DOR antagonist profile *in vitro* and, when *N*-acetylated, showed activity *in vivo*) was the next clear candidate selected for inclusion in this series. In order to decrease the lipophilicity associated with the 2-naphthyl pendant while keeping heteroatoms near the THQ core for reasons discussed previously, a 3-quinolinyl pendant was selected as a naphthyl isostere. Additionally, despite its mild KOR activity, the THIQ pendant showed high MOR efficacy and was known to be bioavailable upon *N*-acetylation. Thus, the first four pendants explored the effects of ring conjugation, lipophilicity, basicity, and planarity in the context of the C-6 pendant. Additionally, the 6-benzo-1,4-dioxanyl pendant and 2-benzofuranyl pendants explored the effects of oxygen incorporation, both into a semi-saturated as well as a fully aromatic bicyclic system. Contrary to prior observations of distal heteroatoms reducing MOR efficacy, it was believed that the ethylenedioxy bridge sufficiently masked these heteroatoms as demonstrated by analogue **41** in **Table 8**. Subsequent analogues featuring the benzodioxanyl pendant would prove that assumption to have been incorrect.

3.3 Synthesis of Analogues 39-69

The synthesis of compounds presented in this work began with the commercially available *p*-toluidine. As described in Chapter 2, this aniline was acylated with a 3-bromopropionyl chloride. Intramolecular cyclization to the β -lactam followed by Fries Rearrangement yielded the THQ core with a C-6 methyl substitution. In step **D** of **Scheme 6**, the *N*-1 position was acylated with Boc anhydride, acetic anhydride, cyclopropyl acyl chloride, or benzoyl chloride. The mesyl group was poorly tolerated for subsequent benzylic bromination, as was the unprotected amine, necessitating use of the Boc group for these syntheses.

Scheme 6. Condensed Synthetic Scheme of C-6/*N*-1 Dual Pharmacophore Ligands^a



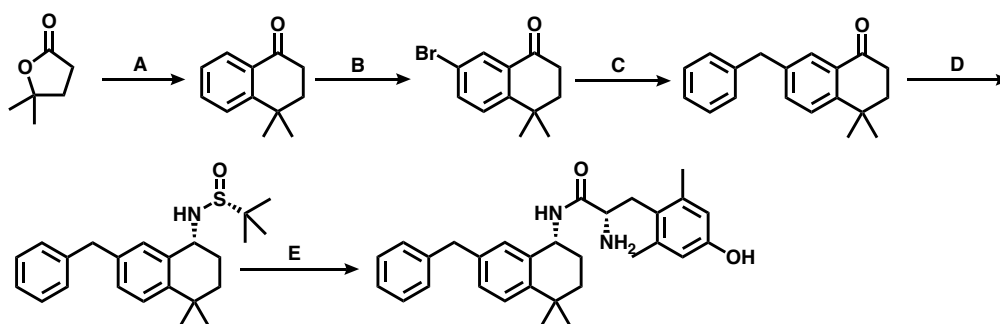
^a **(A)** 3-bromopropionyl chloride & K₂CO₃ in DCM. **(B)** NaOtBu in DMF. **(C)** TfOH in DCE. **(D)** Boc₂O, Ac₂O, cyclopropanecarbonyl chloride, or benzoyl chloride, DIPEA, DCM. **(E)** NBS, benzoyl peroxide, CCl₄, reflux. **(F)** R₂-boronic acid pinacol ester, Pd(dppf)Cl₂, K₂CO₃, 3:1 acetone/water, 80°C, or tetrahydroisoquinoline-HCl, K₂CO₃, DMF, r.t. **(G)** (R)-(+)-2-methyl-2-propanesulfonamide, Ti(OEt)₄, THF, 0°C to reflux, then NaBH₄, THF, -78°C to r.t. **(H)** HCl, 1,4-dioxane, r.t., then diBoc 2,6-dimethyl-L-tyrosine, PyBOP, DIPEA, DMF, r.t., then TFA, DCM, r.t.

The C-6 methyl group of the 6-methyl THQ intermediate underwent radical benzylic bromination in step **E**, catalyzed by benzoyl peroxide and heat. The C-6 pharmacophore then replaced the benzylic bromide by either Suzuki coupling with an aryl boronic acid or via

nucleophilic substitution with THIQ under basic conditions. Reductive amination was performed as described in Chapter 2 using the chiral Ellman auxiliary^{115–117} (R)-(+)-2-methyl-2-propanesulfonamide, Ti(OEt)₄, and NaBH₄ to achieve the desired (*R*) stereochemistry at C-4. The sulfonamide was cleaved with concentrated HCl, leaving an enantiomerically pure amine salt, which was carried forward without further characterization to amide coupling with Boc-protected L-2,6-dimethyltyrosine.^{97,102,118} Boc deprotection with trifluoroacetic acid gave final compounds described in **Tables 8-12**. Final compounds were purified by semi-preparative HPLC. Due to availability of common intermediates, the R₁ group appearing in the final compound was often incorporated at different stages for each compound in a subset. As such, **Scheme 6** offers only a general schematic of the synthetic steps. Full synthetic procedures can be found at the end of Chapter 3.

In addition to the bicyclic analogues presented in this chapter, the synthesis of the *gem*-dimethyl analogue **69** as well as a series of thiochromane analogues **65-68** (presented at the end of this chapter) are included here.

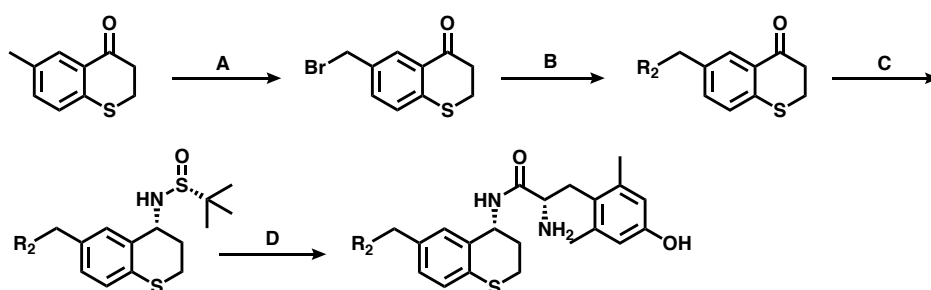
Scheme 7. Synthesis of *Gem*-Dimethyl Analogue **69**^a



^a (A) AlCl₃, benzene, 95°C. (B) NBS, H₂SO₄, 60°C (C) benzyl boronic acid pinacol ester, Pd(dppf)Cl₂, K₂CO₃, 3:1 acetone/water, 80°C (D) (R)-(+)-2-methyl-2-propanesulfonamide, Ti(OEt)₄, THF, 0°C to reflux, then NaBH₄, THF, -78°C to r.t. (E) HCl, 1,4-dioxane, r.t., then diBoc 2,6-dimethyl-L-tyrosine, PyBOP, DIPEA, DMF, r.t., then TFA, DCM, r.t.

The initial steps of **Scheme 7** differ significantly from those of the prior syntheses. In step **A** of **Scheme 7**, a 5-membered lactone undergoes Friedel Crafts acylation with benzene, generating the substituted *gem*-dimethyl tetrahydronaphthalene (THN) core in one step. Due to the electronics of this core, bromination did not proceed under standard conditions (NBS in DCM). As such, this reaction was performed in concentrated sulfuric acid, which facilitated selective C-6 bromination in 53% yield. The following steps were carried out as previously described, utilizing Suzuki, Ellman, and amide coupling reactions to produce final compound **69**.

Scheme 8. Synthesis of Thiochromane Analogues **65-68^a**



^a (A) NBS, benzoyl peroxide, CCl₄, reflux. (B) R₂-boronic acid pinacol ester, Pd(dppf)Cl₂, K₂CO₃, 3:1 acetone/water, 80°C, or tetrahydroisoquinoline-HCl, K₂CO₃, DMF, r.t. (C) (R)-(+)-2-methyl-2-propanesulfonamide, Ti(OEt)₄, THF, 0°C to reflux, then NaBH₄, THF, -78°C to r.t. (D) HCl, 1,4-dioxane, r.t., then diBoc 2,6-dimethyl-L-tyrosine, PyBOP, DIPEA, DMF, r.t., then TFA, DCM, r.t.

Synthesis of the thiochromane analogues in **Scheme 8** followed the same steps outlined in **Scheme 6** from a commercially available 6-methyl thiochromane core. Benzylic bromination of this scaffold gave lower yields than the THQ scaffold, likely due to oxidation of the thioether by benzoyl peroxide. Removal of benzoyl peroxide eliminated some side-reactions, providing better yields. Subsequent steps were carried out as previously described in **Scheme 6**.

3.4 In Vitro Pharmacology of Dual-Pharmacophore Ligands

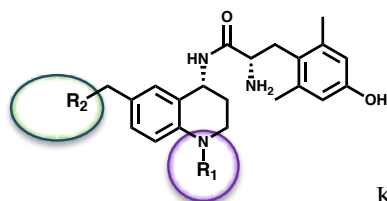


Table 8. Bicyclic C-6 Pendant with Unsubstituted *N*-1 Affords a MOR-Selective, MOR Agonist/DOR Antagonist Profile^a

#	R ₂	R ₁	K _i (nM)			DOR K _i /MOR K _i	EC ₅₀ (nM)			% stim		
			MOR	DOR	KOR		MOR	DOR	KOR	MOR	DOR	KOR
1 ^b			0.22 (0.02)	9.4 (0.8)	68 (2)	43	1.6 (0.3)	110 (6)	>500 (70)	81 (2)	16 (2)	22 (2)
4 ^b			0.08 (0.01)	10 (2)	54 (7)	125	0.53 (0.08)	dns	dns	96 (3)	dns	dns
39 ^c			0.10 (0.02)	1.5 (0.2)	16 (4)	15	2.2 (0.9)	dns	dns	84 (6)	dns	dns
40 ^c			0.03 (0.01)	3.1 (0.2)	2.2 (0.4)	103	0.4 (0.1)	dns	90 (65)	105 (6)	dns	25 (4)
41 ^d			0.35 (0.11)	5.5 (0.8)	116 (65)	16	7.3 (1.8)	dns	dns	88 (8)	dns	dns
42 ^d			0.11 (0.03)	5 (2)	40 (20)	44	1.1 (0.5)	dns	dns	98 (1)	dns	dns

^a Binding affinities (K_i) were obtained by competitive displacement of radiolabeled [³H]-diprenorphine in membrane preparations. Functional data were obtained using agonist induced stimulation of [³⁵S]-GTPγS binding. Potency is represented as EC₅₀ (nM) and efficacy as percent maximal stimulation relative to standard agonist DAMGO (MOR), DPDPE (DOR), or U69,593 (KOR) at 10 μM. All values are expressed as the mean of three separate assays performed in duplicate with standard error of the mean in parentheses. dns = does not stimulate. ^b Reported in reference ⁸³. ^c Reported in reference ⁹⁹. ^d Synthesized by A.M.B. Previously reported analogues were synthesized by those authors.

Bicyclic compounds in **Table 8** featuring no *N*-substitution display the MOR agonist/DOR antagonist profile, though the monocyclic C-6 analogue **1** displays low DOR and KOR efficacy at relatively high concentration of ligand (EC₅₀ = 110 nM). The primary limitation of this subset remains the high degree of MOR selectivity. While compounds **39** and **41** display 15:1 and 16:1 MOR selectivities, the others in this subset are at least 40-fold selective for MOR. This selectivity was combatted by acylation of the *N*-1 position with an acetyl group in **Table 9**.

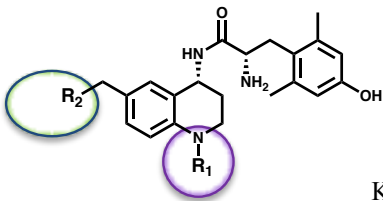


Table 9. *N*-1 Acetylation Reduces MOR Selectivity, Achieves Sub-Nanomolar DOR Affinity with Modest DOR Efficacy^a

#	R ₂	R ₁	K _i (nM)			DOR K _i /MOR K _i	EC ₅₀ (nM)			% stim		
			MOR	DOR	KOR		MOR	DOR	KOR	MOR	DOR	KOR
32 ^b			0.13 (0.02)	1.8 (0.1)	87 (10)	14	6 (1)	68 (2)	>500	76 (4)	26 (3)	29 (5)
43 ^b			0.04 (0.01)	0.23 (0.02)	48 (20)	6	0.9 (0.2)	dns	dns	87 (3)	dns	dns
44			0.15 (0.05)	0.20 (0.08)	53 (14)	1	1.1 (0.3)	5.8 (0.6)	dns	76 (4)	35 (4)	dns
45 ^c			0.19 (0.08)	0.89 (0.21)	0.78 (0.10)	5	6 (2)	dns	190 (30)	96 (4)	dns	41 (6)
46			0.38 (0.11)	0.83 (0.03)	142 (23)	2	13 (5)	dns	dns	45 (3)	dns	dns
47			0.12 (0.03)	0.73 (0.22)	58 (9)	6	1.9 (0.3)	1.6 (0.9)	>500	86 (5)	30 (2)	33 (10)

^a Binding affinities (K_i) were obtained by competitive displacement of radiolabeled [³H]-diprenorphine in membrane preparations. Functional data were obtained using agonist induced stimulation of [³⁵S]-GTPγS binding. Potency is represented as EC₅₀ (nM) and efficacy as percent maximal stimulation relative to standard agonist DAMGO (MOR), DPDPE (DOR), or U69,593 (KOR) at 10 μM. All values are expressed as the mean of three separate assays performed in duplicate with standard error of the mean in parentheses. dns = does not stimulate. ^b Reported in reference ⁹³. ^c Reported in reference ⁹⁹. Previously reported analogues were synthesized by those authors.

N-Acetylation of the THQ core improves binding affinity at DOR for all compounds in this subset. Notably, the five bicyclic analogues **43-47** all display subnanomolar affinity at both MOR and DOR. The drastic reduction in MOR selectivity of compounds **43** and **45** (6:1 and 5:1 respectively) compared to their unsubstituted analogues **4** and **40** (125:1 and 103:1) was consistent throughout this subset, yielding very balanced profiles across **Table 9**. As shown in **Table 7**, *N*-substitutions paired with monocyclic pendants generally caused low-potency, low-efficacy DOR agonism. However, bicyclic analogues **44** and **47** also displayed some low-efficacy DOR agonism but now with nanomolar potency. In fact, compound **44** was a remarkably well-balanced MOR agonist/DOR partial agonist in terms of both affinity and potency.

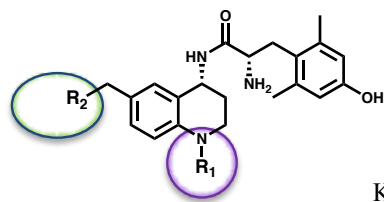


Table 10. Cyclopropyl Acyl *N*-1 Substitution Further Improves MOR and DOR Affinity, Increases DOR Efficacy & Potency^a

#	R ₂	R ₁	K _i (nM)			DOR K _i / MOR K _i	EC ₅₀ (nM)			% stim		
			MOR	DOR	KOR		MOR	DOR	KOR	MOR	DOR	KOR
36 ^b			0.10 (0.03)	0.35 (0.01)	25 (5)	4	1.8 (0.3)	10 (2)	>500	88 (3)	69 (6)	32 (1)
48			0.05 (0.02)	0.37 (0.20)	117 (56)	7	0.42 (0.16)	1.9 (0.9)	>500	85 (7)	32 (4)	38 (3)
49			0.05 (0.01)	0.08 (0.04)	84 (26)	2	0.34 (0.12)	0.71 (0.13)	dns	47 (4)	84 (4)	dns
50			0.12 (0.06)	0.88 (0.23)	40 (10)	7	0.52 (0.22)	dns	dns	95 (5)	dns	dns
51			0.28 (0.08)	0.19 (0.03)	412 (200)	0.7	6 (2)	dns	dns	36 (7)	dns	dns
52			0.05 (0.01)	0.26 (0.07)	98 (9)	5	0.9 (0.3)	3.7 (2.6)	dns	89 (4)	52 (7)	dns

^a Binding affinities (K_i) were obtained by competitive displacement of radiolabeled [³H]-diprenorphine in membrane preparations. Functional data were obtained using agonist induced stimulation of [³⁵S]-GTPγS binding. Potency is represented as EC₅₀ (nM) and efficacy as percent maximal stimulation relative to standard agonist DAMGO (MOR), DPDPE (DOR), or U69,593 (KOR) at 10 μM. All values are expressed as the mean of three separate assays performed in duplicate with standard error of the mean in parentheses. dns = does not stimulate. ^b Reported in reference ⁹³.

The third *N*-1 motif explored in this SAR study was a cyclopropyl acyl moiety, shown in **Table 10**. The bioavailable *N*-acetyl analogues **43** and **45** had each shown significant increases in duration of action. It was hypothesized that by sterically masking the *N*-1 amide bond with a cyclopropyl group, this duration of action and bioavailability might further be improved. Additionally, due to its similarity in size and electronics to the acetyl group, it was hypothesized that the cyclopropyl analogues would display similar increases in DOR affinity. Indeed, all analogues in **Table 10** display subnanomolar affinity at both MOR and DOR. Compounds **49** and **51** displayed the best binding profile yet achieved in this series, with nearly equal binding at MOR and DOR paired with substantial selectivity over KOR. Unfortunately, these highly optimal binding profiles were not paired with the desired MOR agonist/DOR antagonist functional profile.

Both compounds were only partial agonists at MOR while compound **49** was additionally a highly-potent, full DOR agonist (greater than 70% stimulation). In fact, all four planar, aromatic pendants display 30% or greater DOR efficacy. Three of these pendants also showed DOR efficacy in the *N*-acetyl subset. Taken together, these results indicate that while a bicyclic C-6 pendant is sufficient to prevent DOR activation in the context of the unsubstituted THQ core, the DOR-activating propensity of some *N*-1 modifications reverses this trend. As such, the planar bicyclic pendants may revert to displaying DOR agonism, but with the increased potency associated with this bicyclic C-6/*N*-1 series. Notably, the non-planar THIQ and benzodioxanyl pendants both maintained the DOR antagonist profile in analogues **50** and **51** respectively. Analogue **50** combines the favorable binding profile of the cyclopropyl acyl subset with the favorable functional profile of the THIQ pendant, yielding an optimal *in vitro* profile. Compared to its *N*-acetyl analogue, **50** shows significantly better selectivity over KOR, displays no KOR efficacy, and offers a 12-fold improvement in MOR potency, making this a highlight of the cyclopropyl acyl subset.

As illustrated by the analogues in **Tables 9** and **10**, small acyl substitutions at the *N*-1 position do indeed drastically improve the DOR binding for all analogues in this series. Of these 12 compounds, 11 display subnanomolar affinity for both MOR and DOR, while most are highly selective over KOR. However, DOR efficacy does appear in several of the planar pendant analogues, restricting the achievement of an optimal *in vitro* profile to compounds **43** and **50**. Between these two acyl subsets, the cyclopropyl acyl group offers greater MOR potency. In the case of the high-efficacy DOR agonists **36** and **49**, the cyclopropyl group also offers greater DOR potency compared to their *N*-acetyl analogues. For investigators aiming to design highly potent MOR agonist/DOR agonist ligands, one might look to combinations of the 3-quinolinyl pendant with the *N*-1 methyl carbamate, isopropyl acyl, or cyclobutyl acyl groups.

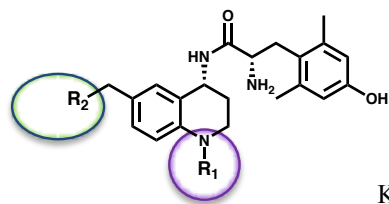


Table 11. Sulfonyl N-1 Moiety Increases MOR Selectivity, MOR Potency & MOR Efficacy; Regains DOR Antagonism^a

#	R ₂	R ₁	K _i (nM)				EC ₅₀ (nM)			% stim		
			MOR	DOR	KOR	DOR K _i /MOR K _i	MOR	DOR	KOR	MOR	DOR	KOR
53			0.06 (0.02)	0.41 (0.16)	8 (4)	7	0.23 (0.06)	12 (1)	121 (24)	98 (1)	22 (2)	60 (9)
54			0.04 (0.01)	0.95 (0.25)	27 (10)	24	0.23 (0.04)	dns	dns	102 (4)	dns	dns
55			0.23 (0.08)	0.64 (0.24)	7 (1)	3	0.26 (0.07)	dns	dns	96 (3)	dns	dns
56			0.11 (0.02)	0.98 (0.13)	1.1 (0.3)	9	0.12 (0.04)	dns	45 (14)	114 (6)	dns	51 (5)
57			0.07 (0.01)	1.5 (0.5)	46 (4)	21	9 (1)	dns	>500	47 (6)	dns	39 (4)
58			0.05 (0.01)	1.0 (0.2)	8 (3)	20	0.34 (0.11)	dns	>500	102 (3)	dns	61 (7)

^a Binding affinities (K_i) were obtained by competitive displacement of radiolabeled [³H]-diprenorphine in membrane preparations. Functional data were obtained using agonist induced stimulation of [³⁵S]-GTPγS binding. Potency is represented as EC₅₀ (nM) and efficacy as percent maximal stimulation relative to standard agonist DAMGO (MOR), DPDPE (DOR), or U69,593 (KOR) at 10 μM. All values are expressed as the mean of three separate assays performed in duplicate with standard error of the mean in parentheses. dns = does not stimulate.

In **Table 11**, the *N*-acyl motif is replaced with a methyl sulfone, or “mesyl” group. This was chosen to mimic the amide functionality while increasing stability toward amidases or peptidases that might otherwise cleave the amide bond. Additionally, the S=O bonds mimic the H-bond accepting capacity of the C=O bond of the acyl analogues. While the compounds in this subset did show improvements in DOR affinity relative to the unsubstituted analogues, the mesyl group does not elicit the same DOR affinity as was observed with the cyclopropyl acyl subset. MOR affinity remained high throughout the series, yielding more MOR-selective compounds than in the previous two subsets. Notably, the mesyl group showed no DOR efficacy amongst the bicyclic analogues, though the monocyclic analogue **53** showed mild DOR efficacy. Additionally, the mesyl group boosted both MOR potency and efficacy. With the exception of **57**, all analogues

in this subset displayed a MOR EC₅₀ of less than 0.4 nM paired with a MOR efficacy of at least 95%. Three analogues displayed over 100% efficacy at MOR. Despite its 24-fold MOR selectivity, analogue **54** offers a highly potent MOR agonist/DOR antagonist profile. Meanwhile, the more balanced 3-quinolinyl pendant maintains its MOR/DOR affinity balance in analogue **55** and also achieves the highly potent MOR agonist/DOR antagonist profile. Additionally, analogues **56** and **58** both display highly potent and efficacious MOR agonism (greater than 100%) with no DOR efficacy, though both also have some KOR agonism at high concentrations of ligand.

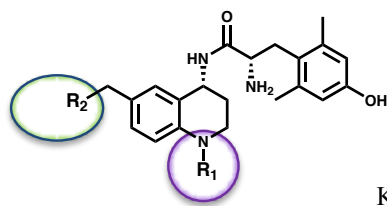


Table 12. Benzoyl *N*-1 Substitution Maintains DOR Antagonism, Reduces MOR Efficacy & Potency^a

#	R ₂	R ₁	K _i (nM)			DOR K _i /MOR K _i	EC ₅₀ (nM)			% stim		
			MOR	DOR	KOR		MOR	DOR	KOR	MOR	DOR	KOR
38^b			0.08 (0.03)	0.24 (0.09)	40 (15)	3	2.6 (0.6)	dns	>500	75 (7)	dns	16 (4)
59^c			0.26 (0.13)	0.46 (0.05)	160 (40)	2	7.9 (3.4)	dns	dns	57 (1)	dns	dns
60^c			0.04 (0.02)	0.74 (0.23)	100 (10)	19	1.0 (0.2)	dns	dns	43 (4)	dns	dns
61^c			0.37 (0.11)	4 (2)	160 (30)	11	4.2 (1.6)	dns	dns	93 (2)	dns	dns
62			1.5 (0.3)	0.22 (0.07)	240 (60)	0.15	dns	dns	>500	dns	dns	60 (16)
63			0.35 (0.13)	0.64 (0.03)	100 (20)	2	12 (2)	dns	dns	64 (4)	dns	dns

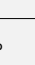
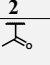
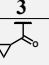
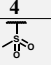
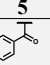
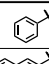
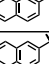
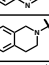
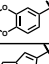
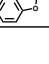

^a Binding affinities (K_i) were obtained by competitive displacement of radiolabeled [³H]-diprenorphine in membrane preparations. Functional data were obtained using agonist induced stimulation of [³⁵S]-GTPγS binding. Potency is represented as EC₅₀ (nM) and efficacy as percent maximal stimulation relative to standard agonist DAMGO (MOR), DPDPE (DOR), or U69,593 (KOR) at 10 μM. All values are expressed as the mean of three separate assays performed in duplicate with standard error of the mean in parentheses. dns = does not stimulate. ^b Reported in reference ⁹³, synthesized by A.A.H. ^c Synthesized by D.J.M.

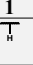
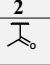
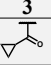
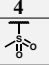
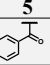
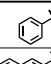
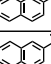
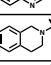
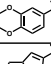
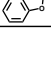

The final substitution explored in this series was the *N*-benzoyl acyl group. Whereas the monocyclic analogues in each of the past subsets (**1**, **32**, **36**, and **53**) displayed some DOR agonism, the monocyclic *N*-benzoyl analogue **38** was a DOR antagonist. Thus, the benzoyl moiety was selected as it was most likely to deliver the MOR agonist/DOR antagonist profile in subsequent bicyclic analogues. Unfortunately, the benzoyl group was also associated with a reduction in efficacy at MOR, as four of the analogues display only partial (less than 70%) efficacy. These analogues were also the least potent at MOR in the series. However, in terms of binding, these compounds were generally well-balanced. Four of the six compounds displayed 3-fold or less MOR selectivity, with one compound (**62**) actually favoring DOR 7-fold. Functionally, compound **62** was an antagonist at both MOR and DOR.

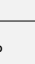
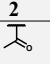
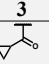
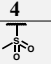
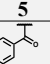
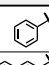
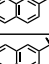
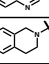
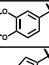
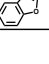

The benzoyl substitution, despite its beneficial effects on balancing MOR/DOR affinity and maintaining DOR antagonism, caused a significant increase in lipophilicity. In fact, compounds such **59** and **63** displayed a ClogP of greater than 5. Due to issues with solubility in aqueous media, the benzoyl moiety was the most lipophilic substitution deemed feasible for this study, considering the possibility of precipitation of the compound *in vivo*.

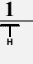
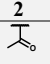
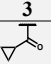
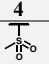
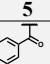
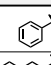
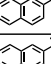
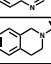
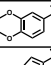
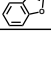

In order to more easily observe trends in SAR relating to both C-6 pendant as well as *N*-1 motif, a series of 2D matrices were constructed highlighting specific trends. In these matrices, *N*-1 substituents are placed on the *x* axis in columns **1-5** while the C-6 pendants are listed on the *y* axis in rows **A-F**. Desirable values are in white, while less favorable values are colored in shades of blue where increasingly darker shades correspond to the least favorable values. Data presented in these matrices are taken from **Tables 8-12**, wherein standard error, original references, and compound numbers can be found; these matrices are designed to more visually display trends in both the C-6 and *N*-1 dimensions.

Figure 16. SAR Matrices Highlight Trends in Potency & Efficacy at MOR & DOR^a

A		MOR Potency, EC ₅₀ (nM)				
		1	2	3	4	5
						
A		1.6	6	1.8	0.23	2.6
B		0.53	0.9	0.42	0.23	7.9
C		2.2	1.1	0.34	0.26	1.0
D		0.4	6	0.52	0.12	4.2
E		7.3	13	6	9	dns
F		1.1	1.9	0.9	0.34	12
		≤ 1.0	1.1 – 5.0	5.1 – 10	> 10	dns

B		MOR Efficacy (% stim)				
		1	2	3	4	5
						
A		81	76	88	98	75
B		96	87	85	102	57
C		84	76	47	96	43
D		105	96	95	114	93
E		88	45	36	47	dns
F		98	86	89	102	58
		≤ 30	31 – 50	51 – 70	71 – 90	> 90

C		DOR Potency, EC ₅₀ (nM)				
		1	2	3	4	5
						
A		110	68	10	12	dns
B		dns	dns	1.9	dns	dns
C		dns	5.8	0.71	dns	dns
D		dns	dns	dns	dns	dns
E		dns	dns	dns	dns	dns
F		dns	1.6	3.7	dns	dns
		≤ 1.0	1.1 – 5.0	5.1 – 10	> 10	dns

D		DOR Efficacy (% stim)				
		1	2	3	4	5
						
A		16	26	69	22	dns
B		dns	dns	32	dns	dns
C		dns	35	84	dns	dns
D		dns	dns	dns	dns	dns
E		dns	dns	dns	dns	dns
F		dns	30	52	dns	dns
		≤ 30	31 – 50	51 – 70	71 – 90	> 90

^aSAR matrices of potency and efficacy at MOR and DOR highlight favorable values (high MOR potency, dns at DOR) in white with low MOR potency and high DOR potency in increasingly darker shades of blue, corresponding to less favorable values. Similarly, high MOR efficacy and no DOR efficacy (dns) are most favorable, rendered in white while low MOR efficacy and high DOR efficacy (unfavorable) are shown in darker shades of blue.

Investigating the effects of C-6 and N-1 substitutions on MOR potency showed that subnanomolar potency was achieved in nine of the twelve analogues in the cyclopropyl acyl and mesyl subsets (**Fig. 16A** columns 3 and 4). Conversely, the N-acetyl and N-benzoyl substitutions (**Fig. 16A** columns 2 and 5) were generally less potent at MOR. Notably, analogues in row E of **Fig. 16A** are consistently the least potent in each subset. Looking at MOR efficacy in **Fig. 16B**, we see that row E is also consistently the least efficacious at MOR. On the other hand, analogues in the row above, row D, were consistently the most efficacious. In the vertical direction, column

4 (the mesyl subset) is the most efficacious subset at MOR. Unsurprisingly, the analogue at the intersection of these two high-efficacy functionalities in square **4-D** (compound **56**) displays the highest MOR efficacy of the series (114%) as well as the best MOR potency (**Fig. 16A**). Compounds in columns **1**, **2**, and **3** were generally full MOR agonists, whereas column **5**—the *N*-benzoyl subset—displayed the lowest efficacy. The compound at the intersection of the lowest-efficacy functionalities in square **5-E** (compound **62**) was the only MOR antagonist throughout the series.

Focusing on DOR potency (**Fig. 16C**) and efficacy (**Fig. 16D**), most analogues in columns **1**, **4**, and **5** are antagonists, as are analogues in rows **B**, **D**, and **E**. Conversely, the monocyclic benzyl pendant of row **A** is most commonly associated with DOR efficacy, though rows **C** and **F** each feature two DOR agonist ligands as well. In the vertical direction, the acetyl and cyclopropyl acyl substitutions (columns **2** and **3**) display some DOR efficacy. Again, the combination of the 3-quinolinyl pendant (row **C**) and cyclopropyl acyl group (column **3**) yield the most potent (**Fig. 16C**) and efficacious (**Fig. 16D**) DOR analogue in the series. In terms of targeting our desired MOR agonist/DOR antagonist profile, column **4** (the mesyl subset) is consistently the most potent and efficacious at MOR while maintaining DOR antagonism. Row **4** analogues **B**, **C**, **D**, and **F** (**54**, **55**, **56**, and **58** respectively) all display high-potency MOR agonism and DOR antagonism with varying selectivity profiles between 3:1 and 24:1 in favor of MOR (see **Table 11**).

SAR analysis of two pharmacophores via 2D matrices provides useful information that may not have been readily apparent from individual SAR campaigns at either C-6 or *N*-1 alone. Based on our initial monocyclic series, it seemed that DOR efficacy would be a consistent issue for most if not all *N*-substituted analogues. However, combining these *N*-1 modifications with bicyclic pharmacophore elements at C-6 has shown that, contrary to initial expectations, some *N*-

substitutions (namely the mesyl group) offer reliable DOR antagonism despite the mild efficacy of the initial analogue in the series. Additionally, the matrix setup allows us to identify intersections of key trends, enhancing our ability to fine-tune specific profiles. Some exemplary intersections are **3-C** (compound **49**), a potent, high-efficacy DOR agonist; **4-D** (compound **56**), a potent, high-efficacy MOR agonist/DOR antagonist; and **5E** (compound **62**), a dual antagonist. Additionally, chemists looking to replicate these results in slightly altered forms could add to remove a carbon atom (THIQ to isoindoline, cyclopropyl to cyclobutyl, ethylenedioxy to methylenedioxy benzodioxane) generating very similar profiles *in vitro* to those reported above. This could be advantageous in expanding the net of optimized *in vitro* candidates for *in vivo* testing. As will be described in the next section, *in vivo* results have thus far been fairly unpredictable with small modifications causing large differences in bioavailability. As such, by incrementally modifying past bioavailable ligands, we may be able to generate novel ligands with optimized *in vitro* profiles and *in vivo* antinociceptive activity.

3.5 *In Vivo* Pharmacology

To determine whether the improved *in vivo* activity achieved by acetylating compounds **43** and **45** translates to other *N*-substituted analogues, all compounds in this series with MOR agonist activity *in vitro* were evaluated for their antinociceptive activity in mice via the WWTW assay. Of the 21 novel analogues presented here, four reached the maximal possible effect (100% MPE) while six others showed partial activity (50-75% MPE); the remaining eleven compounds showed no significant difference from baseline (**Table 13**).

Within the -NH- subset, only the lead compound **1** showed full antinociceptive activity, while two others were partially active (50% MPE). The acetyl and mesyl subsets showed the

greatest *in vivo* efficacy with 2 fully active, 2 partially active, and 2 inactive analogues each. The benzoyl subset also contained 2 fully active analogues, though the remaining 4 analogues had no significant antinociceptive activity. The cyclopropyl acyl subset offered only two partially active analogues (50-60% MPE).

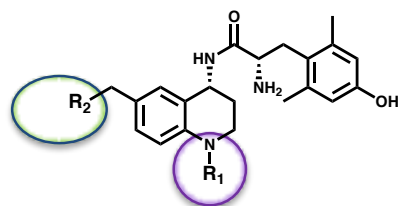


Table 13. Antinociceptive Activity of C-6/N-1 Analogues in WWTW Assay Following Intraperitoneal Administration^a

#	R ₂	R ₁	% MPE	#	R ₂	R ₁	% MPE	#	R ₂	R ₁	% MPE
1 ^b		H	100	36 ^f			50	38 ^f			dns
4 ^b		H	50	48			dns	59 ^g			100
39 ^c		H	dns	49			dns	60 ^g			100
40 ^c		H	dns	50			60	61 ^g			dns
41 ^d		H	dns	51			dns	62			dns
42 ^d		H	50	52			dns	63			dns
Duration of Action (h)											
32 ^e			dns	53			100	43			4.5
43 ^e			100	54			dns	45			4.5
44			60	55			50	53			1.5
45 ^c			100	56			100	56			1.5
46			75	57			70	59			3.0
47			dns	58			dns	60			2.5

^a Results from the mouse WWTW assay after cumulative dosing of test compound up to 10 mg/kg ip. Antinociceptive activity represented as percent maximum possible effect (% MPE), with MPE being a 20 s latency to tail withdrawal. Baseline tail withdrawal latency is ~5 s, or 25% MPE. “dns” indicates no stimulation of an antinociceptive response.

^b Reported in reference ⁸³. ^c Reported in reference ⁹⁹. ^d Synthesized by A.M.B. ^e Reported in reference ⁹⁴. ^f Reported in reference ⁹⁵. ^g Synthesized by D.J.M.

In the bottom right section of **Table 13**, *N*-acetyl analogues **43** and **45** displayed a duration of action greater than 4 hours, whereas the mesyl derivatives **53** and **56** displayed antinociceptive effects lasting less than 2 hours. The benzoyl analogues **59** and **60** showed a duration of action of approximately 3 hours. Of note, **60** displayed only 43% efficacy *in vitro* at MOR, yet elicited a full antinociceptive effect in the WWTW assay, indicating even partial agonists may elicit full activity *in vivo*.

As was the case with the mono-substituted C-6 and *N*-1 campaigns, a clear relationship between structure and *in vivo* activity was not easily detectable. We are still working toward developing more exact predictors of *in vivo* efficacy, however comparison with ClogP does offer some (albeit limited) insight. **Fig. 17** compares ClogP for each compound with its corresponding *in vivo* activity.

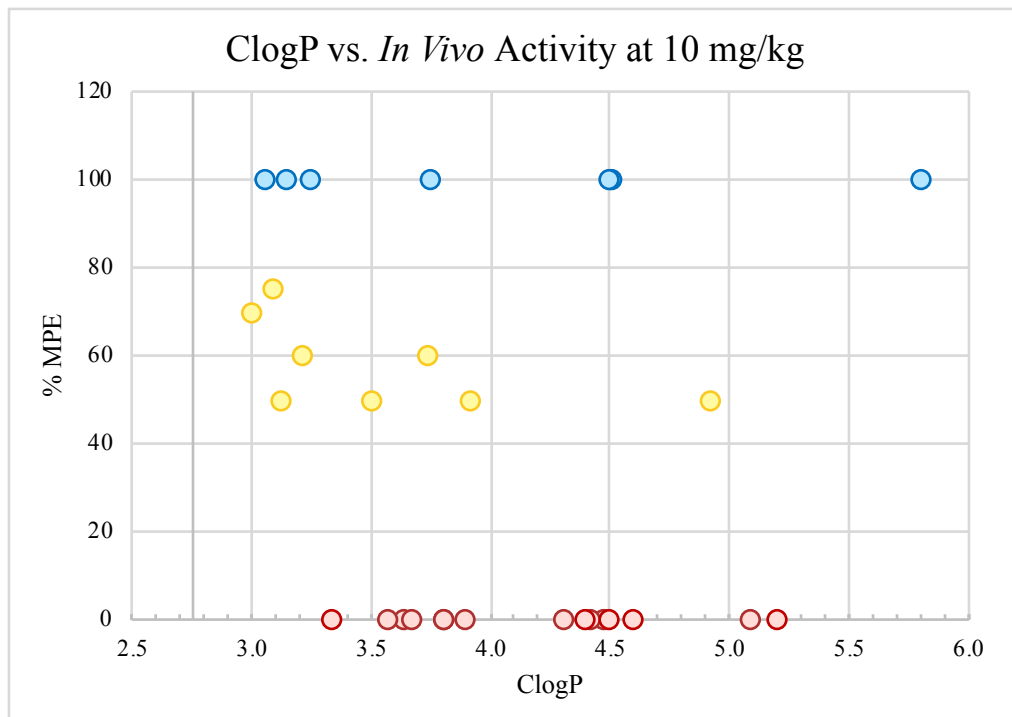
Figure 17. *In Vivo* SAR Matrix Indicates Lower ClogP is Favorable for Bioavailability^a

		ClogP					Antinociceptive Efficacy (% MPE)				
		1	2	3	4	5	1	2	3	4	5
A		3.8	3.4	3.9	3.3 *	4.6	100	dns	50	100 *	dns
B		4.9	4.5	5.1	4.4	5.8	50	100	dns	dns	100
C		3.7	3.2 *	3.8	3.1 *	4.5	dns	60 *	dns	50 *	100
D		3.7	3.2 *	3.8	3.1 *	4.5	dns	100 *	60	100 *	dns
E		3.5	3.1 *	3.7	3.0 *	4.4	dns	75 *	dns	70 *	dns
F		4.3	3.9	4.5	3.8	5.2	50	dns	dns	dns	dns
ClogP		3.0 - 3.4	3.5 - 3.9	4.0 - 4.4	4.5 - 4.9	≥ 5.0					
Active/Total		7/8	3/10	1/3	3/6	1/3	≤ 30	31 - 50	51 - 70	71 - 90	> 90

^a Comparison of Clog P with *in vivo* activity shows that compounds with ClogP of 3.3 or less, denoted by blue stars, are all partially or fully active *in vivo*.

Splitting compounds into bins by their ClogP, we see that seven of eight compounds in the lowest ClogP bin have full or partial antinociceptive activity, where the one outlier is the highest ClogP analogue of the group. However, in the bins with ClogP greater than or equal to 3.5, approximately only one in three (8 of 22) have activity *in vivo*. Those low-ClogP, bioavailable ligands are denoted in **Table 17** with a blue star. These data indicate a greater propensity for *in vivo* activity amongst low-ClogP compounds than those in the higher-ClogP bins. This effect may correspond to greater solubility in blood, and thus a greater ability to reach the target receptors (lower volume of distribution). Conversely, several analogues with high Clog P including **43**, **59** and **60** (ClogP = 4.5, 4.5, and 5.8 respectively) have a much higher ClogP and corresponding volume of distribution yet are still fully active *in vivo*. It is worth noting that the two THIQ compounds **45** and **56** are very similar structurally and differ by only 0.1 ClogP units yet have a 3-hour difference in duration of action. From these data, duration of action seems most correlated to *N*-1 substitution rather than ClogP or C-6 pendant, though more data would be needed to draw a more meaningful conclusion.

Figure 18. Plotting ClogP Against *In Vivo* Activity



While *in vivo* activity does correlate with ClogP generally, the presence of clear outliers to this trend indicates the presence of other contributing factors as well (e.g., efflux, metabolism, distribution, elimination). Nonetheless, chemists looking to develop new, bioavailable analogues of this chemotype would be well-advised to strive for low ClogP, both to improve solubility but also to favor *in vivo* activity.

3.6 SAR of the Thiochromane Analogues of the Bicyclic Series

As discussed previously, an additional subset of analogues built around a thiochromane core instead of the THQ core were designed for inclusion within this study. The thiochromane core replaces the THQ amine (-NH-) with a thioether (-S-). The initial analogue utilizing the

thiochromane core, which featured a monocyclic benzyl pendant at C-6, was one of the few scaffolds that maintained bioavailability *in vivo*. As this series was among the most recently synthesized, many data points are still missing, and *in vivo* testing has not yet been conducted. Nevertheless, the existing data points are included in **Table 14** below. The standalone *gem*-dimethyl tetrahydronaphthalene analogue **69** is also included in **Table 14**.

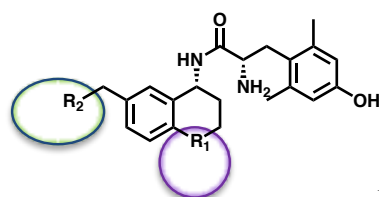


Table 14. Thiochromane and *Gem*-Dimethyl Tetrahydronaphthalene Analogues Show High MOR Selectivity^a

#	R ₂	R ₁	K _i (nM)			DOR K _i /MOR K _i	EC ₅₀ (nM)			% stim		
			MOR	DOR	KOR		MOR	DOR	KOR	MOR	DOR	KOR
64^b		-S-	0.15 (0.04)	4.8 (1.1)	48 (23)	32	1.9 (0.5)	dns [†]	dns	80 (8)	dns [†]	dns
65		-S-	0.20 (0.09)	4.3 [†] (0.6)	---	22	0.8 (0.6)	dns	---	79 (6)	dns	---
66		-S-	0.18 (0.09)	3.1 (0.4)	---	17	0.7 [†] (0.1)	15 [‡] (---)	---	57 [†] (6)	28 [‡] (---)	---
67		-S-	0.07 (0.02)	3.9 (0.7)	14 (4)	56	0.7 (0.4)	dns [†]	85 [‡] (---)	93 (2)	dns [†]	40 [‡] (---)
68		-S-	0.7 (0.2)	6.5 [‡] (---)	---	9	26 [†] (20)	dns [†]	---	25 [†] (1)	dns [†]	---
69		-C(CH ₃) ₂ -	0.36 (0.08)	6.5 (0.7)	27 (5)	2	16 (5)	>500	>500	75 (4)	16 (3)	75 (3)

^a Binding affinities (K_i) were obtained by competitive displacement of radiolabeled [³H]-diprenorphine in membrane preparations. Functional data were obtained using agonist induced stimulation of [³⁵S]-GTPγS binding. Potency is represented as EC₅₀ (nM) and efficacy as percent maximal stimulation relative to standard agonist DAMGO (MOR), DPDPE (DOR), or U69,593 (KOR). Values are expressed as the mean of three separate assays performed in duplicate with standard error of the mean in parentheses. dns = does not stimulate. ^b Synthesized by A.M.B. [†] n=2 [‡] n=1.

Analogues in this series are more MOR-selective than those in the substituted THQ series. This is to be expected, as the acyl C=O (or S=O) bond is critical to achieving subnanomolar DOR affinity. Analogues **64**, **65** and **67** display high MOR potency and efficacy while maintaining the

DOR antagonist profile. As was observed in some 3-quinolinyl analogues in the previous series, analogue **66** displayed low MOR efficacy and partial DOR efficacy. In addition to the high degree of MOR selectivity, a key drawback of this series is lipophilicity. Analogues in this series range in ClogP from 4.6 to 6.0, limiting our ability to test these compounds for antinociception due to solubility issues. At present, only analogue **64** (ClogP = 4.8) has been tested *in vivo*. Based on lipophilicity and *in vitro* profile, compound **67** (ClogP = 4.6) may be a suitable candidate for future *in vivo* screening, though its MOR selectivity could limit the positive effects of DOR antagonism. Due to the limiting factors of lipophilicity and MOR selectivity, this scaffold is unlikely to be utilized for future drug development. The standalone analogue **69** also suffered high MOR selectivity and lipophilicity (and associated solubility issues) while also displaying lower MOR potency. Due to these issues, this scaffold was not further explored despite its *in vivo* activity.

3.7 Conclusions

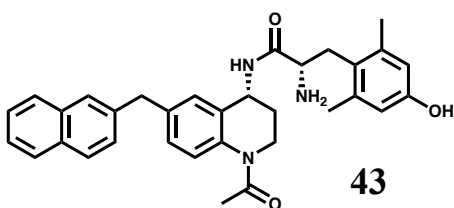
By combining advantageous C-6 and N-1 moieties from past SAR campaigns and expanding those with novel substituents at both positions, we have developed an SAR matrix of 30 analogues that further expand the available toolkit of multifunctional opioid ligands. Although our goal was to explore the C-6/N-1 chemotype with a focus on the MOR agonist/DOR antagonist profile, this SAR study has also yielded strategies for creating highly potent multifunctional MOR agonists/DOR agonists as well. While most compounds in this series displayed the desired DOR antagonist profile, cyclopropyl acyl analogues **36** and **39** (Table 10) showed surprising DOR efficacy and could be useful in the study of the MOR agonist/DOR agonist profile, which also holds promise for reducing opioid-related tolerance while improving analgesic potency and efficacy.^{112,119} Other compounds of note include **50**, **54**, and **55**, which reproduce the desired *in vitro* profile: subnanomolar values for MOR affinity, DOR affinity, and MOR potency as well as

high efficacy at MOR with no DOR or KOR activity. Four novel compounds from this series, **53**, **56**, **59**, and **60** (Table 13), showed full antinociceptive activity in mice, and will be carried forward for evaluation in tolerance and dependence models. Comparing these with the bioavailable bicyclic lead **43** (2-naphthyl/*N*-acetyl, ClogP = 4.5), we observed a significant improvement in aqueous solubility for analogues **53** (ClogP = 3.2) and **56** (ClogP = 3.1), while **59** (ClogP = 5.8) was significantly more lipophilic and **60** (ClogP = 4.5) showed no change. Duration of action *in vivo* was not positively impacted by the *N*-1 substitutions explored in this series, as the previously reported analogues **43** and **45** showed longer-lasting antinociception than **53**, **56**, **59** and **60**.

A key finding of this work is the development compound **56**, which shows the highest efficacy at MOR and displays subnanomolar potency at both MOR and DOR. Additionally, **56** is fully efficacious *in vivo* after peripheral administration and has a drug-like ClogP of 3.1. However, selectivity over KOR and duration of action are significantly reduced compared to **43**, indicating areas in need of further optimization.

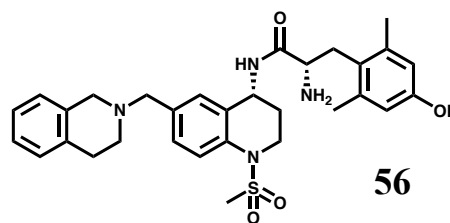
Figure 19. Summary Profiles of 2nd Generation Lead **43** and Optimized Analogue **56**

Previously Reported Bicyclic Lead



MOR agonist (87% stim, EC₅₀ = 0.9 nM)
 DOR antagonist (<10% stim, K_e = 2.0 nM)
 MOR/DOR selectivity: 6:1
 MOR/KOR selectivity: 1200:1
 Full antinociceptive activity (100% MPE)
 Duration of action = 4.5 h; ClogP = 4.5

Optimized Analogue from This Work



MOR agonist (114% stim, EC₅₀ = 0.12 nM)
 DOR antagonist (<10% stim, K_e = 0.85 nM)
 MOR/DOR selectivity: 9:1
 MOR/KOR selectivity: 10:1
 Full antinociceptive activity (100% MPE)
 Duration of action = 1.5 h; ClogP = 3.1

In summary, we have further investigated the bicyclic C-6/*N*-1 chemotype established by **43** and **45**,^{94,99} expanding the published C-6 and *N*-1 chemical space. The various C-6 and *N*-1 modifications reported here have been combined in an SAR matrix to further elucidate the chemical motifs that govern ligand binding and receptor activation in the context of the THQ peptidomimetic core. This SAR study reinforces previous findings and refines our ability to develop potent bifunctional opioid ligands with a range of mixed-efficacy profiles in order to further probe the unique pharmacology of the opioid receptor family. The *N*-acyl and *N*-sulfonyl series—when combined with a bicyclic C-6 pendant—display among the most favorable *in vitro* profiles yet discovered throughout all of our peptidomimetic investigations to date.

3.8 Experimental Procedures

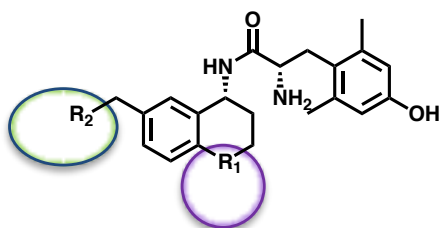


Table 15. Chapter 3 Compound Numbering and Literature References

		R ₁ Moieties						
C-6 Pendants		1^a	32^d	36^e	53	38^e	64	69
		4^b	43^d	48	54	59	65	---
		39^c	44	49	55	60	66	---
		40^c	45^c	50	56	61	67	---
		41	46	51	57	62	68	---
		42	47	52	58	63	---	---

^a Synthesis reported in reference ⁹³. ^b Synthesis reported in reference ⁸³. ^c Synthesis reported in reference ⁹⁹. ^d Synthesis reported in reference ⁹⁴. ^e Synthesis reported in reference ⁹⁵. Syntheses of referenced compounds are not reproduced in this dissertation.

General Procedures	153
Syntheses of Common Intermediates	158
Compound 41 and Preceding Intermediates	165
Compound 42 and Preceding Intermediates	167
Compound 44 and Preceding Intermediates	169
Compound 46 and Preceding Intermediates	172
Compound 47 and Preceding Intermediates	175

Compound 48 and Preceding Intermediates	178
Compound 49 and Preceding Intermediates	182
Compound 50 and Preceding Intermediates	184
Compound 51 and Preceding Intermediates	187
Compound 52 and Preceding Intermediates	190
Compound 53 and Preceding Intermediates	192
Compound 54 and Preceding Intermediates	195
Compound 55 and Preceding Intermediates	197
Compound 56 and Preceding Intermediates	201
Compound 57 and Preceding Intermediates	203
Compound 58 and Preceding Intermediates	206
Compound 59 and Preceding Intermediates	208
Compound 60 and Preceding Intermediates	210
Compound 61 and Preceding Intermediates	212
Compound 62 and Preceding Intermediates	214
Compound 63 and Preceding Intermediates	217
Compound 65 and Preceding Intermediates	219
Compound 66 and Preceding Intermediates	222
Compound 67 and Preceding Intermediates	224
Compound 68 and Preceding Intermediates	226
Compound 69 and Preceding Intermediates	228
Compound 64 was synthesized by A.M.B, the details for which can be found in his dissertation.	

General Procedures

General Procedure (A): Schotten-Bauman Acylation of a Commercially Available Aniline

Starting Material. To a flame-dried round-bottom flask under Ar atmosphere was added aniline starting material (1.00 eq), followed by dichloromethane, then K_2CO_3 (1.2-3.0 eq.). After 10 minutes, 3-bromopropionyl chloride (1.05 eq) was added slowly via syringe. Reaction was monitored by TLC in 40% ethyl acetate, 60% hexanes. Ninhydrin stain was used to help monitor disappearance of aniline starting material. After 1-3 h, reaction was quenched with deionized water. Organics were separated and dried over $MgSO_4$, then filtered and concentrated under vacuum. Product was purified by crystallization or, when necessary, column chromatography.

General Procedure (B): Intramolecular β -Lactam Cyclization.

To a flame-dried round-bottom flask under Ar atmosphere was added sodium *tert*-butoxide (1.05 eq) followed by anhydrous DMF, then stirred 10 min before slowly adding a solution of acyl bromide intermediate from step A (1.00 eq) dissolved in DMF at ambient temperature via syringe. Monitored reaction by TLC in 40% ethyl acetate, 60% hexanes. Desired product showed a moderate decrease in R_f relative to starting material. After stirring 1-3 h, reaction mixture was concentrated under vacuum, then resuspended in dichloromethane or ethyl acetate. Extracted reaction mixture with deionized water and aqueous sodium bicarbonate, then separated organics and dried over $MgSO_4$. Filtered and reconcentrated organics onto silica, then purified by flash chromatography.

General Procedure (C): Fries Rearrangement to Synthesize the THQ Core.

To a round-bottom flask containing β -lactam intermediate (1 eq) dissolved in dichloroethane under inert atmosphere was slowly added TfOH (3 eq). After 1 hour, TLC in 40% ethyl acetate, 60% hexanes showed a decrease in R_f . Reaction was quenched with deionized water and neutralized with

K₂CO₃, then diluted with dichloromethane. Separated organics and dried over MgSO₄, then filtered and concentrated organics onto silica and purified by flash chromatography.

General Procedure (D): *N*-Substitution of the THQ Core

Boc protection of the tetrahydroquinoline (THQ) core. To a flame-dried round bottom flask under Ar was added tetrahydroquinolin-4-one intermediate (1.0 eq), Boc₂O (1.5 eq), and DMAP (0.1 eq). The reaction vessel was placed under vacuum for 5 min, then anhydrous DCM was added via syringe and the solution stirred for 5 min under vacuum. The round bottom flask was flooded with Ar, and DIPEA (1.5 eq) was added via syringe. The reaction vessel was equipped with a condenser and placed in oil bath at 60°C. The reaction stirred at reflux for 12-16 h under Ar and was monitored by TLC. Once significant conversion to product was seen, the reaction was quenched using di H₂O (20 mL) and the layers were separated. The organic layer was washed with sat. NaHCO₃ and sat. NaCl solutions then dried over MgSO₄. Organics were filtered and concentrated under reduced pressure, then purified using silica gel chromatography.

***N*-Acylation or Mesylation of the THQ core.** To a round-bottom flask containing THQ intermediate (1.0 eq) under Ar atmosphere was added DCM. Reaction flask was then cooled to 0°C before adding Et₃N (1.2 eq), followed by acyl or sulfonyl chloride (1.2 eq). When starting material showed complete conversion to product by TLC, solvent was removed under reduced pressure and reaction mixture was purified by silica chromatography.

General Procedure (E): Benzylic Bromination of the C-6 Methyl Group. To a round-bottom flask containing *N*-protected 6-methyl THQ intermediate (1.00 eq) under Ar atmosphere was added degassed, Ar-sparged CCl₄, followed by *N*-bromosuccinimide (1.05 eq) and benzoyl peroxide (0.1 eq). Reaction was then heated to reflux, monitored by TLC. Quantitative conversion

of starting material was generally not observed, so reaction was halted when side-product began to form. Reaction was halted by cooling to -20°C , and precipitate was filtered from solution (washing with additional cold CCl_4). Filtrate was then concentrated onto silica and purified by silica chromatography.

General Procedure (F): Substitution of C-6 Benzylic Bromide with R_2

Suzuki Coupling of Benzylic Bromide to R_2 -Boronic Acid. To a round-bottom flask under Ar atmosphere was added 3:1 acetone/water and stirred under vacuum for 10 minutes. Next, Ar was bubbled through solvent for an additional 10 minutes before adding benzylic bromide intermediate (1.0 eq), boronic acid (1.2-2.0 eq), K_2CO_3 (3 eq) and $\text{Pd}(\text{dppf})\text{Cl}_2$ (0.1 eq). Reaction was heated to 80°C for 6-12 hours, after which the reaction mixture was cooled and diluted with ethyl acetate and aqueous NaHCO_3 . Organics were separated and dried over MgSO_4 , then filtered and concentrated *in vacuo* onto silica. Product was purified by silica chromatography.

Substitution of Benzylic Bromide with Tetrahydroisoquinoline (THIQ). To a round-bottom flask under inert atmosphere was added DMF, followed by K_2CO_3 (1.2 eq) and THIQ (1.2 eq), then benzylic bromide (1.0 eq) stirring at ambient temperature. After 6-12 hours, solvent was removed under reduced pressure and residual oil was resuspended in ethyl acetate and sat. NaHCO_3 . Organics were separated and dried over MgSO_4 , then filtered and concentrated *in vacuo* onto silica. Product was purified by silica chromatography.

General Procedure (G): Reductive Amination of THQ Ketone to Sulfinamide Using Ellman's Sulfinamide. To a round bottom flask already containing desiccated THQ intermediate (1.0 eq) under Ar atmosphere was added (R)-2-methylpropane-2-sulfinamide (3.0 eq). Meanwhile, a reflux condenser was flame-dried under vacuum, and then flooded with Ar. Next, anhydrous THF (5-10

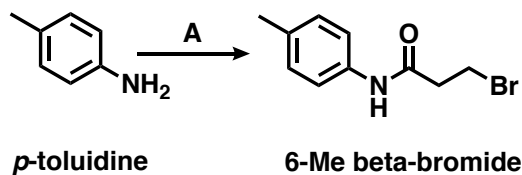
mL) was added to the reaction vessel containing starting reagents via syringe. The round bottom flask was placed in an ice bath and allowed to equilibrate to 0°C. Next, Ti(OEt)₄ (6.0 eq) was added slowly via syringe. Once addition was complete, the reaction vessel was taken out of ice bath and placed in oil bath at 70°C-75°C, affixed condenser, and stirred for 16-48 h under Ar. The reaction was monitored by TLC for loss of ketone. Once sufficient conversion to the tert-butanesulfinyl imine was observed, reaction vessel was taken out of oil bath and cooled to ambient temperature. Meanwhile, an additional round bottom flask was flame-dried under vacuum, then flooded with Ar. NaBH₄ (6.0 eq) was added quickly, and anhydrous THF was added (5-10 mL). The round bottom flask was placed in dry ice/acetone bath and allowed to equilibrate to -78°C. Contents from the round bottom flask containing the imine intermediate were transferred to round bottom flask containing NaBH₄ via cannula. Imine-containing flask was washed twice with minimal THF, which was also transferred to reducing flask via cannula under Ar. Once contents were completely added, the reaction was taken out of dry ice/acetone bath and was allowed to warm to room temperature. The reaction stirred at ambient temperature for 2-3 h. To quench, sat. NaCl solution was added. Reaction mixture was diluted with ethyl acetate and DI H₂O and separated, washing with H₂O until both layers were clear, indicating sufficient removal of titanium oxide by-product. Organics were then isolated and dried over MgSO₄ and filtered through a fritted funnel. Organic extract was then concentrated onto silica and purified by silica chromatography.

General Procedure (H): Conversion of Sulfinamide to Final Compound – Step 1: Sulfinamide Cleavage. To a round bottom flask containing sulfinamide (1.0 eq) was added 1,4-dioxane, followed by conc. HCl (6.0 eq), cleaving the sulfinamide to the primary amine. The reaction stirred at RT for up to 3 h. Solvent was removed under reduced, and residue was re-suspended in Et₂O. The resultant white solid precipitate (the HCl salt of the amine) was isolated

by decanting and washing with Et₂O up to three times. After desiccation, the solid residue was used without further purification. **Step 2: Amide Coupling.** To a pear-shaped flask under inert atmosphere containing amine salt (1.0 eq) was added di-Boc-Dmt (1.1 eq), PyBOP (1.1 eq), and, when specified, 6-Cl HOBt (1.1 eq), followed by DMF (10 mL) and DIPEA (10 eq) at ambient temperature. After stirring for 6 hours, solvent was removed under reduced pressure and residual oil was loaded onto silica. Boc-protected intermediate was purified by silica chromatography but was generally not characterized by NMR. **Step 3: Boc Deprotection.** Boc-protected intermediate was suspended in DCM (10 mL), then TFA (3-5 mL) was added. After 1 hour, solvent was removed under vacuum. Product was resuspended in a solution of 99.9% acetonitrile, 0.1% TFA, then diluted with deionized water. Final products were purified by reverse-phase semi-preparative HPLC. Final yield not calculated.

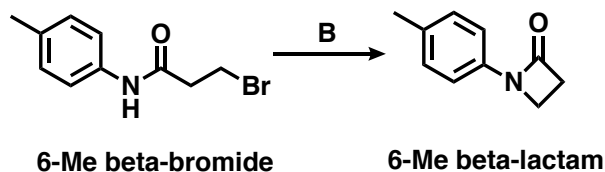
General Procedure (I): Boc-Deprotection Boc-protected intermediate was suspended in DCM (10 mL), then TFA (3-5 mL) was added. After 1 hour, solvent was removed *in vacuo*, resuspended in DCM, then dry-loaded onto silica *in vacuo* and purified by flash chromatography.

Common Intermediates: Step A – 6-Methyl beta-Bromide



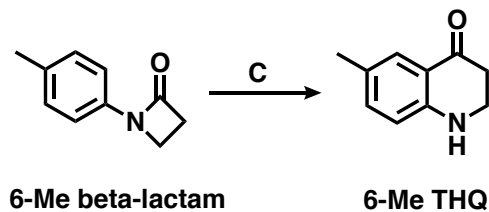
6-Me beta-bromide. *3-bromo-N-(p-tolyl)propanamide.* **6-Me beta-bromide** intermediate was synthesized following **General Procedure (A)** from *p*-toluidine (5.0 g, 46.7 mmol, 1.00 eq), K_2CO_3 (19.4 g, 140.1 mmol, 3.0 eq), and 3-bromopropionyl chloride (4.94 mL, 49.0 mmol, 1.05 eq). Yield: 10.76 g, 95%. 1H NMR (400 MHz, $CDCl_3$) δ 7.33 – 7.28 (m, 2H), 7.05 (d, $J = 8.1$ Hz, 2H), 3.63 (t, $J = 6.6$ Hz, 2H), 2.84 (t, $J = 6.6$ Hz, 2H), 2.24 (s, 3H). ^{13}C NMR (126 MHz, $CDCl_3$) δ 167.85, 134.78, 134.37, 129.49, 120.21, 40.58, 27.17, 20.86.

Common Intermediates: Step B – 6-Methyl Beta-Lactam



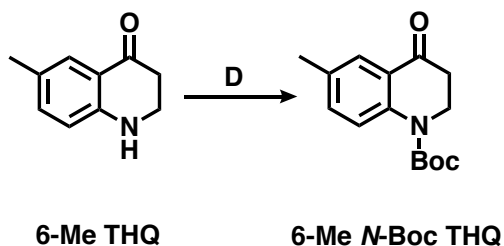
6-Me beta-lactam. *1-(p-tolyl)azetidin-2-one.* **6-Me beta-lactam** intermediate was synthesized following **General Procedure (B)** from **6-Me beta-bromide** (10.76, 44.4 mmol, 1.00 eq) and $NaOtBu$ (4.48 g, 46.7 mmol, 1.05 eq). Yield: 7.07 g, 99%. 1H NMR (400 MHz, $CDCl_3$) δ 7.25 (d, $J = 8.2$ Hz, 2H), 7.13 (d, $J = 8.1$ Hz, 2H), 3.60 (m, 2H), 3.12 – 3.06 (m, 2H), 2.31 (s, 3H). ^{13}C NMR (126 MHz, $CDCl_3$) δ 164.22, 136.12, 133.36, 129.56, 116.03, 37.95, 35.97, 20.87.

Common Intermediates: Step C – 6-Methyl THQ



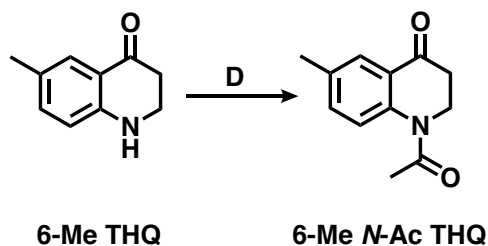
6-Me THQ *6-methyl-2,3-dihydroquinolin-4(1H)-one*. **6-Me THQ** intermediate was synthesized following **General Procedure (C)** from **6-Me beta-lactam** (7.07 g, 43.9 mmol, 1 eq) and TfOH (11.6 mL, 131.6 mmol, 3 eq). Yield: 4.23 g, 60%. ¹H NMR (400 MHz, CDCl₃) δ 7.65 (d, *J* = 2.1 Hz, 1H), 7.13 (dd, *J* = 8.3, 2.1 Hz, 1H), 6.61 (d, *J* = 8.3 Hz, 1H), 3.58 – 3.52 (m, 2H), 2.68 (dd, *J* = 7.5, 6.4 Hz, 2H), 2.24 (s, 3H). ¹³C NMR (126 MHz, CDCl₃) δ 193.85, 149.95, 136.34, 127.41, 127.12, 119.34, 115.92, 42.55, 38.22, 20.24.

Common Intermediates: Step D – *N*-Substituted THQ Cores

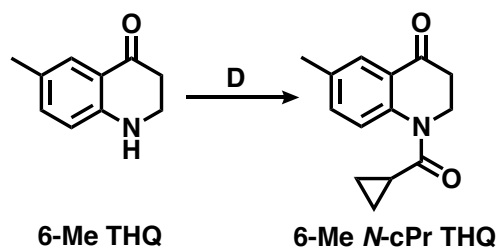


6-Me *N*-Boc THQ *tert-butyl 6-methyl-4-oxo-3,4-dihydroquinoline-1(2H)-carboxylate*. Intermediate **6-Me *N*-Boc THQ** was synthesized following **General Procedure (D)** from **6-Me THQ** (2.25 g, 13.96 mmol, 1.0 equiv), Boc₂O (6.09 g, 27.92 mmol, 2.0 eq), DMAP (171 mg, 1.40 mmol, 0.1 eq), and DIPEA (4.88 mL, 27.92 mmol, 2.0 eq). Yield: 3.06 g, 84%. ¹H-NMR (400 MHz, CDCl₃) δ 8.00 (d, *J* = 2.3 Hz, 1H), 7.80 (d, *J* = 8.7 Hz, 1H), 7.53 (dd, *J* = 8.7, 2.4 Hz, 1H), 4.48 (s, 2H), 4.15 (t, *J* = 6.4 Hz, 2H), 2.77 (t, *J* = 6.4 Hz, 2H), 1.56 (s, 9H); ¹³C-NMR (101 MHz,

CDCl₃) δ 193.66, 152.68, 144.20, 134.70, 133.40, 127.75, 124.87, 124.30, 82.64, 44.36, 38.90, 32.49, 28.40.

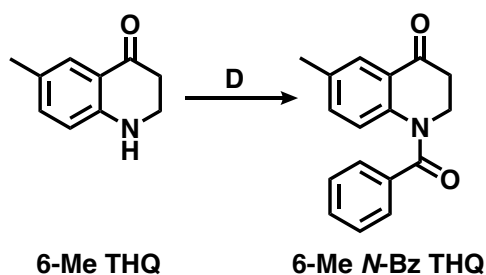


6-Me N-Ac THQ *1-acetyl-6-methyl-2,3-dihydroquinolin-4(1H)-one*. Intermediate **6-Me N-Ac THQ** was synthesized following a modified version of **General Procedure (D)** from intermediate **6-Me THQ**: To a round-bottom flask containing **6-Me THQ** (318 mg, 1.97 mmol, 1.0 eq) under inert atmosphere was added acetic anhydride (10 mL, excess), then reaction was heated to 80°C. After 5 hours, solvent was removed under reduced pressure and reaction mixture was purified by flash chromatography. Yield: 355 mg, 89%. ¹H NMR (500 MHz, Chloroform-*d*) δ 7.81 (s, 1H), 7.36 (dd, *J* = 8.1, 2.2 Hz, 1H), 7.30 (br s, 1H), 4.22 (t, *J* = 6.3 Hz, 2H), 2.78 (t, *J* = 6.2 Hz, 2H), 2.37 (s, 3H), 2.32 (s, 3H). ¹³C NMR (126 MHz, cdcl₃) δ 135.07, 127.87, 124.13, 39.70, 23.21, 20.91.



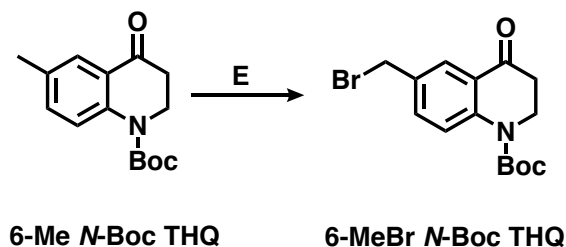
6-Me N-cPr THQ *1-(cyclopropanecarbonyl)-6-methyl-2,3-dihydroquinolin-4(1H)-one*. Intermediate **6-Me N-cPr THQ** was synthesized following **General Procedure (D)** from **6-Me THQ** (950 mg, 5.9 mmol, 1.0 eq), Et₃N (1.64 mL, 11.8 mmol, 2.0 eq), and cyclopropanecarbonyl

chloride (1.07 mL, 11.8 mmol, 2.0 eq). Yield: 1.24 g, 92%. ^1H NMR (500 MHz, Chloroform-*d*) δ 7.81 (d, $J = 2.2$ Hz, 1H), 7.42 (d, $J = 8.3$ Hz, 1H), 7.34 (dd, $J = 8.3, 2.1$ Hz, 1H), 4.26 (t, $J = 6.3$ Hz, 2H), 2.77 (td, $J = 6.3, 1.9$ Hz, 2H), 2.37 (d, $J = 1.9$ Hz, 3H), 2.01 (tt, $J = 8.0, 4.5$ Hz, 1H), 1.19 (ddd, $J = 4.7, 3.0, 1.8$ Hz, 2H), 0.87 (dq, $J = 7.1, 3.8$ Hz, 2H). ^{13}C NMR (126 MHz, cdcl_3) δ 194.71, 173.10, 141.97, 135.28, 134.90, 127.91, 125.85, 123.91, 43.65, 39.82, 20.85, 13.74, 9.80.



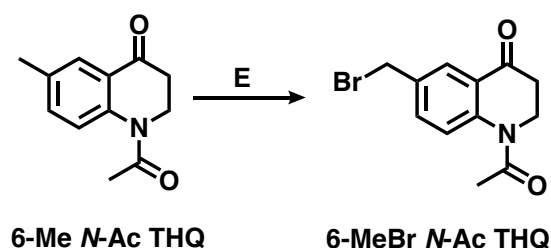
6-Me N-Bz THQ *1-benzoyl-6-methyl-2,3-dihydroquinolin-4(1H)-one*. Intermediate **6-Me N-Bz THQ** was synthesized following **General Procedure (D)** from intermediate **6-Me THQ** (1.0 g, 6.20 mmol, 1.0 eq), Et_3N (0.86 mL, 7.44 mmol, 1.2 eq), and benzoyl chloride (1.25 mL, 7.44 mmol, 1.2 eq). Reaction mixture was purified by silica chromatography. Yield: 1.63 g, 99%. ^1H NMR (500 MHz, Chloroform-*d*) δ 7.81 (d, $J = 2.2$ Hz, 1H), 7.48 (dd, $J = 8.1, 1.3$ Hz, 2H), 7.44 (t, $J = 7.7$ Hz, 1H), 7.35 (t, $J = 7.6$ Hz, 2H), 7.06 (dd, $J = 8.4, 2.1$ Hz, 1H), 6.79 (d, $J = 8.4$ Hz, 1H), 4.31 (t, $J = 6.3$ Hz, 2H), 2.87 (t, $J = 6.3$ Hz, 2H), 2.31 (s, 3H).

Common Intermediates: Step E – Benzyl Bromides



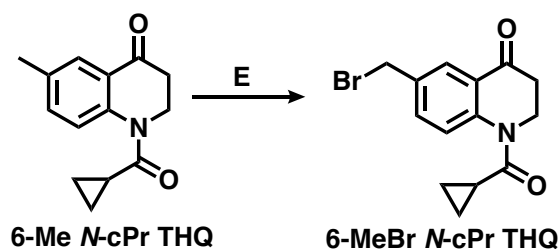
6-MeBr N-Boc THQ *tert-butyl 6-(bromomethyl)-4-oxo-3,4-dihydroquinoline-1(2H)-carboxylate*.

Intermediate **6-MeBr N-Boc THQ** was synthesized following **General Procedure (E)** from intermediate **6-Me N-Boc THQ** (588 mg, 2.25 mmol, 1.00 eq), NBS (420 mg, 2.36 mmol, 1.05 eq) and benzoyl peroxide (55 mg, 0.23 mmol, 0.10 eq). Yield: 596 mg, 78%. ¹H-NMR (400 MHz, CDCl₃) δ 8.49 (d, *J* = 1.5 Hz, 1H), 8.47 (dd, *J* = 4.8, 1.6 Hz, 1H), 7.83 (d, *J* = 1.8 Hz, 1H), 7.72 (d, *J* = 8.6 Hz, 1H), 7.46 (dt, *J* = 7.9, 2.0 Hz, 1H), 7.30 (dd, *J* = 8.6, 2.3 Hz, 1H), 7.21 (ddd, *J* = 7.8, 4.8, 0.9 Hz, 1H), 4.14 (t, *J* = 6.4 Hz, 2H), 3.96 (s, 2H), 2.75 (t, *J* = 6.4 Hz, 2H), 1.55 (s, 9H); ¹³C-NMR (101 MHz, CDCl₃) δ 194.18, 152.79, 150.18, 147.99, 142.84, 136.35, 135.93, 135.56, 134.55, 127.23, 124.98, 124.21, 123.60, 82.33, 44.37, 39.04, 38.37, 28.39.

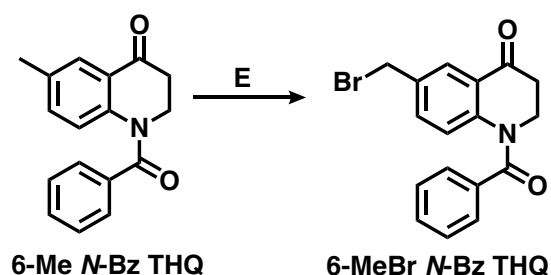


6-MeBr N-Ac THQ *1-acetyl-6-(bromomethyl)-2,3-dihydroquinolin-4(1H)-one*. Intermediate **6-Me N-Ac THQ** was synthesized following **General Procedure (E)** from intermediate **6-MeBr N-Ac THQ** (350 mg, 1.72 mmol, 1.00 eq), NBS (338 mg, 1.89 mmol, 1.10 eq) and benzoyl peroxide (42 mg, 0.17 mmol, 0.10 eq). Reaction was heated at reflux for 2 hours. Yield: 200 mg,

41%. ^1H NMR (500 MHz, Chloroform-*d*) δ 8.00 (d, $J = 2.2$ Hz, 1H), 7.57 (dd, $J = 8.4, 2.3$ Hz, 1H), 7.48 (s, 1H), 4.47 (s, 2H), 4.20 (t, $J = 6.2$ Hz, 2H), 2.78 (t, $J = 6.3$ Hz, 2H), 2.34 (s, 3H). ^{13}C NMR (126 MHz, cdCl_3) δ 193.38, 169.39, 143.77, 135.23, 134.73, 128.06, 126.01, 124.77, 44.20, 39.39, 32.02, 23.33.

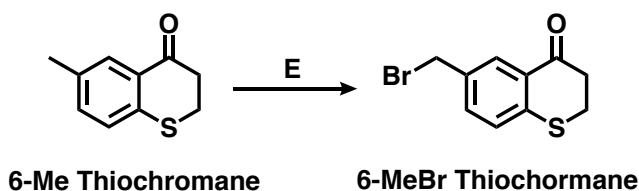


8 *6-(bromomethyl)-1-(cyclopropanecarbonyl)-2,3-dihydroquinolin-4(1H)-one*. Intermediate **8** was synthesized following **General Procedure (C)** from intermediate **4** (836 mg, 3.65 mmol, 1.00 eq), NBS (714 mg, 4.01 mmol, 1.10 eq) and benzoyl peroxide (88 mg, 0.37 mmol, 0.10 eq). Reaction time: 3 hours. Yield: 460 mg, 41%. ^1H NMR (500 MHz, Chloroform-*d*) δ 8.03 (d, $J = 1.9$ Hz, 1H), 7.57 (d, $J = 2.7$ Hz, 2H), 4.50 (s, 2H), 4.29 (t, $J = 6.3$ Hz, 2H), 2.81 (t, $J = 6.4$ Hz, 2H), 2.05 – 1.97 (m, 1H), 1.23 (dt, $J = 6.7, 3.4$ Hz, 2H), 0.93 (dq, $J = 7.1, 3.8$ Hz, 2H). ^{13}C NMR (126 MHz, cdCl_3) δ 193.82, 173.28, 144.23, 134.95, 134.65, 128.30, 125.88, 124.50, 43.69, 39.65, 32.13, 14.07, 10.11.



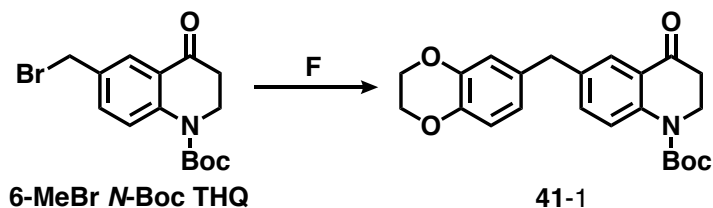
6-MeBr N-Bz THQ *1-benzoyl-6-(bromomethyl)-2,3-dihydroquinolin-4(1H)-one*. Intermediate **6-MeBr N-Bz THQ** was synthesized following **General Procedure (E)** from intermediate **6-Me N-**

Bz THQ (1.20 g, 4.52 mmol, 1.0 eq), *N*-bromosuccinimide (821 mg, 4.61 mmol, 1.02 eq) and benzoyl peroxide (55 mg, 0.23 mmol, 0.05 eq). Reaction was heated for 4 hours at reflux. Yield: 685 mg, 44%. ¹H NMR (500 MHz, Chloroform-*d*) δ 8.02 (s, 1H), 7.53 – 7.47 (m, 2H), 7.47 (dd, *J* = 7.0, 1.5 Hz, 1H), 7.42 – 7.34 (m, 2H), 7.31 (dt, *J* = 8.5, 2.0 Hz, 1H), 6.98 (d, *J* = 8.6 Hz, 1H), 4.43 (d, *J* = 3.7 Hz, 2H), 4.31 (t, *J* = 6.0 Hz, 2H), 2.87 (t, *J* = 6.3 Hz, 2H).

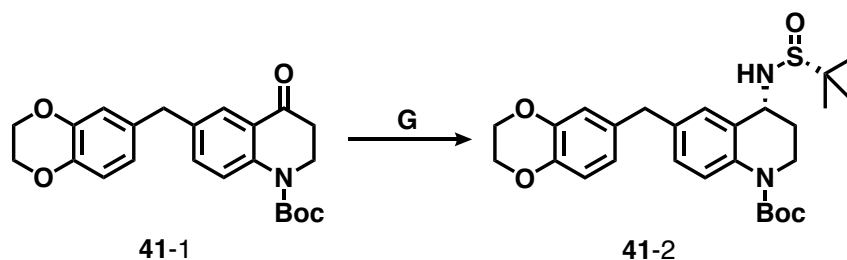


6-MeBr Thiochromane *6-(bromomethyl)thiochroman-4-one*. Intermediate **6-MeBr Thiochromane** was synthesized following **General Procedure (E)** from intermediate **6-Me Thiochromane** (1.00 g, 5.61 mmol, 1.00 eq) and NBS (1.05 g, 5.89 mmol, 1.05 eq). Yield: 559 mg, 39%. ¹H NMR (500 MHz, Chloroform-*d*) δ 8.11 (d, *J* = 1.7 Hz, 1H), 7.42 (dd, *J* = 8.3, 2.1 Hz, 1H), 7.28 (d, *J* = 8.2 Hz, 1H), 4.47 (s, 2H), 3.25 (td, *J* = 6.6, 1.0 Hz, 2H), 2.99 (t, *J* = 6.5 Hz, 2H). ¹³C NMR (126 MHz, cdcl₃) δ 193.67, 133.98, 133.89, 130.34, 129.52, 128.64, 128.48, 39.48, 32.64, 26.69.

Compound 41

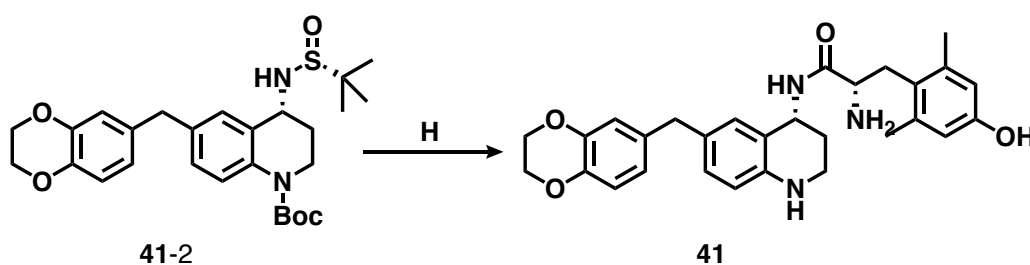


41-1 *tert-butyl 6-((2,3-dihydrobenzo[b][1,4]dioxin-6-yl)methyl)-4-oxo-3,4-dihydroquinoline-1(2H)-carboxylate*. **41-1** was synthesized following **General Procedure (F)** from intermediate **6-MeBr N-Boc THQ** (300 mg, 0.88 mmol, 1.0 eq), 1,4-benzodioxane-6-boronic acid (238 mg, 1.32 mmol, 1.5 eq), K_2CO_3 (365 mg, 2.64 mmol, 3.0 eq) and $Pd(dppf)Cl_2$ (65 mg, 0.09 mmol, 0.1 eq). Reaction was heated 12 hours. Yield: 266 mg, 76%. 1H -NMR (500 MHz, $CDCl_3$) δ 7.81 (d, $J = 2.2$ Hz, 1H), 7.67 (d, $J = 8.6$ Hz, 1H), 7.30 (dd, $J = 8.6, 2.3$ Hz, 1H), 6.76 (d, $J = 8.0$ Hz, 1H), 6.67 – 6.62 (m, 2H), 4.21 (s, 4H), 4.13 (t, $J = 6.3$ Hz, 2H), 3.84 (s, 2H), 2.74 (t, $J = 6.3$ Hz, 2H), 1.54 (s, 9H); ^{13}C -NMR (126 MHz, $CDCl_3$) δ 194.34, 152.86, 143.53, 142.45, 142.12, 137.18, 134.68, 133.86, 127.16, 124.90, 123.93, 121.81, 117.60, 117.34, 82.16, 64.47, 64.39, 44.38, 40.50, 39.10, 28.40.



41-2 *tert-butyl (R)-4-(((R)-tert-butylsulfinyl)amino)-6-((2,3-dihydrobenzo[b][1,4]dioxin-6-yl)methyl)-3,4-dihydroquinoline-1(2H)-carboxylate*. **41-2** was synthesized following **General Procedure (G)** from **41-1** (78 mg, 0.20 mmol, 1.0 eq), (R)-2-methyl-2-propanesulfinamide (72 mg, 0.59 mmol, 3.0 eq), and $Ti(OEt)_4$ (0.31 mL, 1.18 mmol, 6.0 eq), then $NaBH_4$ (45 mg, 1.18 mmol, 6.0 eq). Yield: 60 mg, 61%. 1H -NMR (500 MHz, $CDCl_3$) δ 7.68 (d, $J = 8.5$ Hz, 1H), 7.15

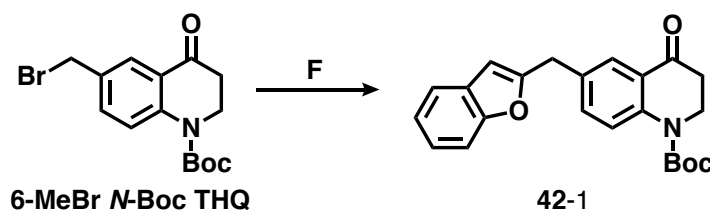
(d, $J = 2.1$ Hz, 1H), 7.06 (dd, $J = 8.6, 2.2$ Hz, 1H), 6.76 (d, $J = 8.1$ Hz, 1H), 6.68 – 6.63 (m, 2H), 4.52 (q, $J = 3.6$ Hz, 1H), 4.22 (s, 4H), 3.94 (dt, $J = 12.9, 4.5$ Hz, 1H), 3.80 (s, 2H), 3.57 (ddd, $J = 12.9, 11.3, 3.9$ Hz, 1H), 3.29 (d, $J = 1.1$ Hz, 1H), 2.20 (dq, $J = 14.0, 4.0$ Hz, 1H), 2.00 – 1.89 (m, 1H), 1.51 (s, 9H), 1.20 (s, 9H); ^{13}C -NMR (126 MHz, CDCl_3) δ 153.68, 143.48, 142.01, 136.92, 136.63, 134.36, 128.99, 128.73, 128.69, 124.15, 121.85, 117.62, 117.25, 81.20, 64.47, 64.41, 55.76, 50.48, 40.54, 40.15, 29.50, 28.46, 22.73.



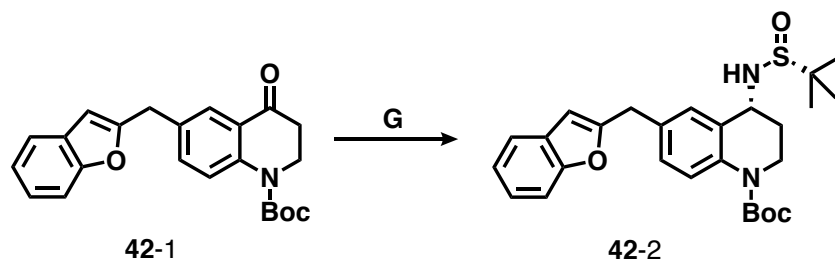
41 *(S)*-2-amino-*N*-((*R*)-6-((2,3-dihydrobenzo[*b*][1,4]dioxin-6-yl)methyl)-1,2,3,4-tetrahydroquinolin-4-yl)-3-(4-hydroxy-2,6-dimethylphenyl)propenamide. **41** was synthesized following **General Procedure (H)** from intermediate **41-2**. **Step 1:** Sulfinamide cleavage was carried out with **41-2** (60 mg, 0.12 mmol, 1.0 eq) and excess concentrated HCl (0.06 mL) precipitating product as a white solid (35 mg total, 23 mg of which was carried forward) which was used without further purification. **Step 2:** Amide coupling was performed with the aminium chloride salt of **41-2** (23 mg, 0.053 mmol, 1.0 eq), di-Boc-Dmt (22 mg, 0.053 mmol, 1.0 eq), PyBOP (28 mg, 0.053 mmol, 1.0 eq), and 6-Cl HOBt (9 mg, 0.053 mmol, 1.0 eq), followed by DIPEA (0.09 mL, 0.53 mmol, 10 eq). After purification by silica chromatography, product was carried forward to **Step 3:** TFA deprotection, followed by purification by reverse-phase semi-preparative HPLC, as described in **General Procedure (H)**. Final yield not calculated. ^1H -NMR (126 MHz, CD_3OD) δ 6.96 (d, $J = 2.0$ Hz, 1H), 6.93 (dd, $J = 8.2, 2.0$ Hz, 1H), 6.67 (dd, $J = 8.1,$

6.8 Hz, 2H), 6.58 – 6.54 (m, 2H), 6.48 (s, 2H), 4.96 (t, $J = 4.6$ Hz, 1H), 4.17 (s, 4H), 3.86 (dd, $J = 11.5, 5.1$ Hz, 1H), 3.69 (s, 2H), 3.25 (dd, $J = 13.6, 11.5$ Hz, 1H), 3.07 (dt, $J = 12.4, 4.5$ Hz, 1H), 3.02 (dd, $J = 13.6, 5.1$ Hz, 1H), 2.58 (td, $J = 11.7, 2.7$ Hz, 1H), 2.27 (s, 6H), 1.83 – 1.74 (m, 1H), 1.58 – 1.50 (m, 1H). Calculated $[M+H]^+$: 488.3. ESI-MS mass observed: 488.3 (M+H). Analytical HPLC retention time: 24.49 min.

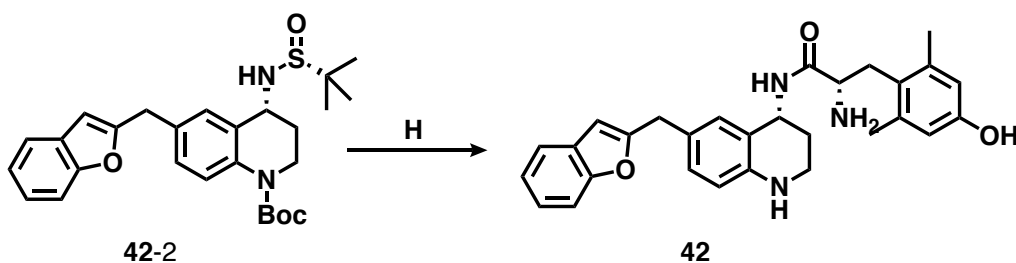
Compound 42



42-1 *tert-butyl 6-(benzofuran-2-ylmethyl)-4-oxo-3,4-dihydroquinoline-1(2H)-carboxylate*. **42-1** was synthesized following **General Procedure (F)** from intermediate **6-MeBr N-Boc THQ** (300 mg, 0.88 mmol, 1.0 eq), 2-benzofuran-2-ylmethylboronic acid MIDA ester (360 mg, 1.32 mmol, 1.5 eq), K_2CO_3 (365 mg, 2.64 mmol, 3.0 eq) and $Pd(dppf)Cl_2$ (65 mg, 0.09 mmol, 0.1 eq). Reaction was heated 12 hours. Yield: 245 mg, 74%. 1H -NMR (500 MHz, $CDCl_3$) δ 7.95 (d, $J = 2.3$ Hz, 1H), 7.75 (d, $J = 8.9$ Hz, 1H), 7.50 – 7.42 (m, 2H), 7.39 (d, $J = 7.7$ Hz, 1H), 7.24 – 7.13 (m, 2H), 6.41 (s, 1H), 4.14 (t, $J = 6.2$ Hz, 2H), 4.08 (s, 2H), 2.76 (t, $J = 6.2$ Hz, 2H), 1.56 (s, 9H); ^{13}C -NMR (126 MHz, $CDCl_3$) δ 194.06, 156.92, 154.98, 152.72, 142.93, 134.55, 132.95, 128.68, 127.37, 124.89, 123.99, 123.56, 122.59, 120.49, 110.91, 103.56, 82.20, 44.27, 38.93, 34.19, 28.30.



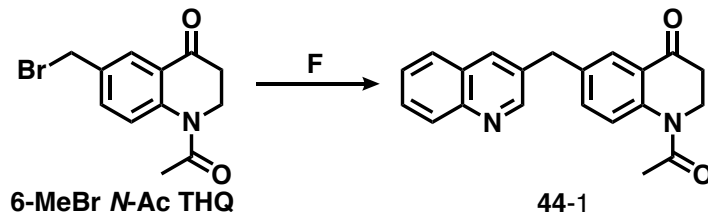
42-2 *tert-butyl (R)-6-(benzofuran-2-ylmethyl)-4-(((R)-tert-butylsulfinyl)amino)-3,4-dihydroquinoline-1(2H)-carboxylate*. **42-2** was synthesized following **General Procedure (G)** from **42-1** (88 mg, 0.23 mmol, 1.0 eq), (*R*)-2-methyl-2-propanesulfinamide (85 mg, 0.70 mmol, 3.0 eq), and Ti(OEt)₄ (0.30 mL, 1.40 mmol, 6.0 eq), then NaBH₄ (53 mg, 1.40 mmol, 6.0 eq). Yield: 78 mg, 70%. ¹H-NMR (500 MHz, CDCl₃) δ 7.74 (d, *J* = 8.5 Hz, 1H), 7.46 (d, *J* = 7.8 Hz, 1H), 7.38 (d, *J* = 8.2 Hz, 1H), 7.30 (s, 1H), 7.22 – 7.12 (m, 3H), 6.41 (s, 1H), 4.55 (q, *J* = 3.7 Hz, 1H), 4.04 (s, 2H), 3.95 (dt, *J* = 13.1, 5.0 Hz, 1H), 3.64 – 3.50 (m, 1H), 3.30 (s, 1H), 2.22 – 2.15 (m, 1H), 2.02 – 1.92 (m, 1H), 1.51 (s, 9H), 1.19 (s, 9H); ¹³C-NMR (126 MHz, CDCl₃) δ 157.38, 154.93, 153.53, 137.16, 132.62, 129.10, 128.78, 128.75, 128.61, 124.16, 123.39, 122.49, 120.42, 110.88, 103.34, 81.22, 55.66, 50.44, 40.12, 34.19, 29.50, 28.33, 22.58.



42 (*S*)-2-amino-*N*-((*R*)-6-(benzofuran-2-ylmethyl)-1,2,3,4-tetrahydroquinolin-4-yl)-3-(4-hydroxy-2,6-dimethylphenyl)propenamide. **42** was synthesized following **General Procedure (H)** from **42-2**. **Step 1:** Sulfinamide cleavage was carried out with **42-2** (78 mg, 0.16 mmol, 1.0 eq) and excess concentrated HCl (0.08 mL), precipitating product as a white solid (79 mg crude yield, 40 mg of

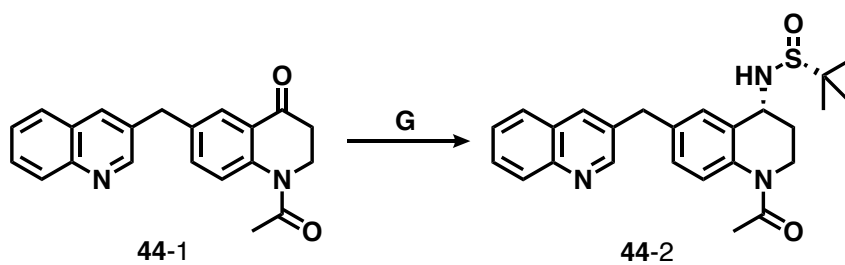
which was carried forward), which was used without further purification. **Step 2:** Amide coupling was performed with the aminium chloride salt of **42-2** (40 mg, 0.096 mmol, 1.0 eq), di-Boc-Dmt (39 mg, 0.096 mmol, 1.0 eq), PyBOP (50 mg, 0.096 mmol, 1.0 eq), and 6-Cl HOBt (16 mg, 0.096 mmol, 1.0 eq), followed by DIPEA (0.17 mL, 0.96 mmol, 10 eq). After purification by silica chromatography, product was carried forward to **Step 3:** TFA deprotection, followed by purification by reverse-phase semi-preparative HPLC, as described in **General Procedure (H)**. Final yield not calculated. ¹H-NMR (500 MHz, CD₃OD) δ 8.13 (d, *J* = 8.0 Hz, 1H), 7.44 (d, *J* = 6.6 Hz, 1H), 7.31 (d, *J* = 7.9 Hz, 1H), 7.20 – 7.10 (m, 2H), 7.00 (s, 1H), 6.98 (d, *J* = 2.1 Hz, 1H), 6.57 (d, *J* = 8.1 Hz, 1H), 6.48 (s, 2H), 6.34 (s, 1H), 4.97 – 4.93 (m, 1H), 3.98 – 3.87 (m, 2H), 3.85 (dd, *J* = 11.5, 5.0 Hz, 1H), 3.25 (dd, *J* = 13.6, 11.6 Hz, 1H), 3.04 – 2.96 (m, 2H), 2.52 (td, *J* = 11.7, 2.5 Hz, 1H), 2.27 (s, 6H), 1.77 – 1.69 (m, 1H), 1.56 – 1.49 (m, 1H). Calculated [M+H]⁺: 469.2. ESI-MS mass observed: 492.2 (M+Na). Analytical HPLC retention time: 30.3 min.

Compound 44

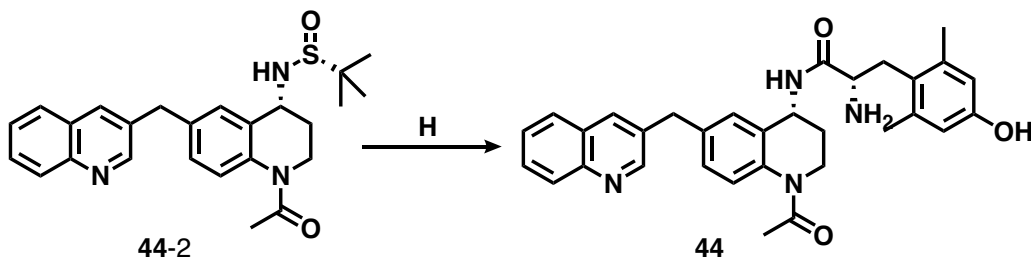


44-1 *1-acetyl-6-(quinolin-3-ylmethyl)-2,3-dihydroquinolin-4(1H)-one*. Intermediate **44-1** was synthesized following **General Procedure (F)** from intermediate **6-MeBr N-Ac THQ** (200 mg, 0.71 mmol, 1.0 eq), 3-quinoline boronic acid (246 mg, 1.42 mmol, 2.0 eq), K₂CO₃ (240 mg, 2.13 mmol, 3.0 eq) and Pd(dppf)Cl₂ (52 mg, 0.07 mmol, 0.1 eq). Reaction was heated 18 hours. Yield:

122 mg, 52%. ¹H NMR (500 MHz, Chloroform-*d*) δ 8.79 (d, *J* = 2.2 Hz, 1H), 8.07 (dt, *J* = 8.5, 1.0 Hz, 1H), 7.93 – 7.89 (m, 2H), 7.75 (dd, *J* = 8.1, 1.4 Hz, 1H), 7.68 (ddd, *J* = 8.4, 6.9, 1.5 Hz, 1H), 7.53 (ddd, *J* = 8.1, 6.9, 1.3 Hz, 1H), 7.42 – 7.38 (m, 1H), 4.22 (t, *J* = 6.2 Hz, 2H), 4.18 (s, 2H), 2.79 (t, *J* = 6.2 Hz, 2H), 2.32 (s, 3H). ¹³C NMR (126 MHz, cdcl₃) δ 169.40, 151.87, 147.16, 142.66, 137.52, 135.10, 134.70, 132.91, 129.35, 129.27, 128.15, 127.88, 127.59, 127.03, 126.26, 124.73, 39.60, 38.72, 23.27.

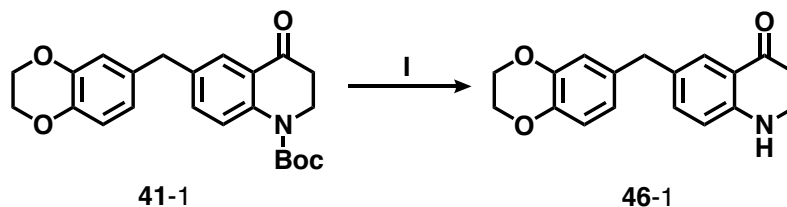


44-2 (*R*)-*N*-((*R*)-1-acetyl-6-(quinolin-3-ylmethyl)-1,2,3,4-tetrahydroquinolin-4-yl)-2-methylpropane-2-sulfonamide. **44-2** was synthesized following **General Procedure (G)** from intermediate **44-1** (112 mg, 0.34 mmol, 1.0 eq), (*R*)-2-methyl-2-propanesulfonamide (123 mg, 1.01 mmol, 3.0 eq), and Ti(OEt)₄ (0.42 mL, 2.03 mmol, 6.0 eq), then NaBH₄ (77 mg, 2.03 mmol, 6.0 eq). Yield: 47 mg, 32%. ¹H NMR (500 MHz, Chloroform-*d*) δ 8.78 (dd, *J* = 6.1, 2.1 Hz, 1H), 8.07 (dd, *J* = 8.6, 4.6 Hz, 1H), 7.96 – 7.92 (m, 1H), 7.76 (t, *J* = 7.9 Hz, 1H), 7.72 – 7.65 (m, 1H), 7.53 (dtd, *J* = 8.1, 6.5, 5.8, 2.5 Hz, 1H), 7.35 (s, 1H), 7.15 (tq, *J* = 5.8, 3.8, 2.9 Hz, 1H), 4.52 (q, *J* = 4.6 Hz, 1H), 4.14 (s, 2H), 3.88 (q, *J* = 6.4 Hz, 1H), 3.75 (td, *J* = 8.9, 4.6 Hz, 1H), 2.22 (s, 3H), 2.18 (dd, *J* = 10.9, 6.1 Hz, 1H), 2.15 – 2.04 (m, 1H), 1.17 (d, *J* = 1.3 Hz, 9H). ¹³C NMR (126 MHz, cdcl₃) δ 169.95, 151.88, 135.02, 134.33, 133.31, 129.08, 128.81, 128.61, 128.09, 127.49, 126.82, 126.43, 125.35, 125.04, 124.71, 55.85, 51.33, 38.72, 30.69, 23.35, 22.55.

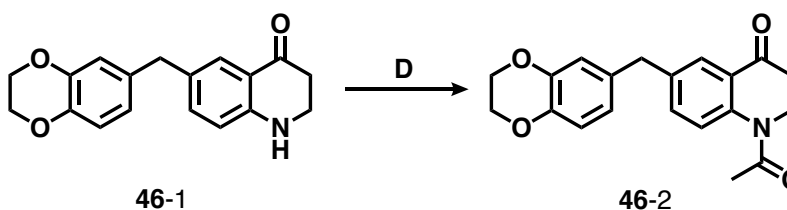


44 *(S)-N-((R)-1-acetyl-6-(quinolin-3-ylmethyl)-1,2,3,4-tetrahydroquinolin-4-yl)-2-amino-3-(4-hydroxy-2,6-dimethylphenyl)propanamide*. **44** was synthesized following **General Procedure (H)** from intermediate **44-2**. **Step 1:** Sulfonamide cleavage was carried out with excess concentrated HCl precipitating product as a white solid which was carried forward without further purification. **Step 2:** Amide coupling was performed with the aminium chloride salt of **44-2** (39 mg, 0.11 mmol, 1.0 eq), di-Boc-Dmt (48 mg, 0.12 mmol, 1.1 eq), PyBOP (60 mg, 0.12 mmol, 1.1 eq), and 6-Cl HOBt (20 mg, 0.12 mmol, 1.1 eq), followed by DIPEA (0.19 mL, 1.06 mmol, 10 eq). After purification by silica chromatography, product was carried forward to **Step 3:** TFA deprotection, followed by purification by reverse-phase semi-preparative HPLC, as described in **General Procedure (H)**. Final yield not calculated. ¹H NMR (500 MHz, Methanol-*d*₄) δ 9.01 (s, 1H), 8.72 (s, 1H), 8.21 (d, *J* = 8.3 Hz, 1H), 8.19 (d, *J* = 8.3 Hz, 1H), 8.15 (t, *J* = 9.1 Hz, 2H), 8.05 (ddd, *J* = 8.3, 6.9, 1.3 Hz, 1H), 8.02 (ddd, *J* = 8.5, 7.0, 1.4 Hz, 1H), 7.89 (t, *J* = 7.6 Hz, 1H), 7.87 – 7.83 (m, 1H), 6.51 (s, 2H), 4.95 (d, *J* = 6.1 Hz, 1H), 4.29 (s, 2H), 3.91 (dt, *J* = 11.3, 5.3 Hz, 2H), 3.30 – 3.27 (m, 1H), 3.27 – 3.22 (m, 1H), 3.03 (ddd, *J* = 25.6, 13.8, 4.7 Hz, 2H), 2.27 (s, 6H), 2.20 (s, 3H), 1.87 (ddt, *J* = 13.5, 8.1, 5.3 Hz, 1H), 1.47 (m, 1H). Calculated [M+H]⁺: 523.3. ESI-MS mass observed: 523.3 (M+H) and 545.3 (M+Na). Analytical HPLC retention time: 20.9 min.

Compound 46

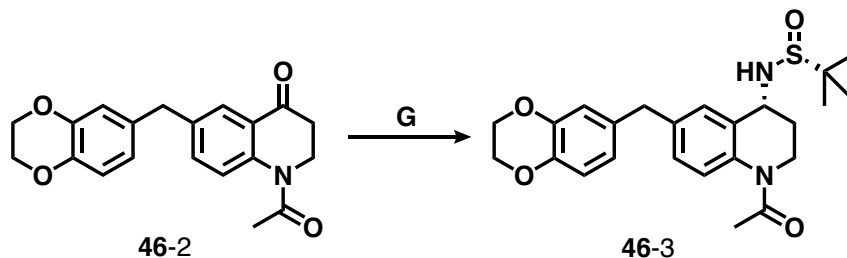


46-1 6-((2,3-dihydrobenzo[b][1,4]dioxin-6-yl)methyl)-2,3-dihydroquinolin-4(1H)-one. **46-1** was synthesized following **General Procedure (I)** from intermediate **41-1** (266 mg, 0.67 mmol, 1.0 eq). Clean product **46-1** crystallized and was not purified by chromatography. Yield: 199 mg, 100%. ¹H NMR (500 MHz, Chloroform-*d*) δ 7.68 (d, *J* = 2.1 Hz, 1H), 7.11 (dd, *J* = 8.4, 2.2 Hz, 1H), 6.75 (d, *J* = 8.1 Hz, 1H), 6.65 – 6.61 (m, 2H), 6.59 (d, *J* = 8.4 Hz, 1H), 4.21 (s, 4H), 3.74 (s, 2H), 3.54 (t, *J* = 7.4, 6.7 Hz, 2H), 2.68 (t, *J* = 7.7, 6.9 Hz, 2H). ¹³C NMR (126 MHz, cdcl₃) δ 193.96, 150.72, 143.47, 141.97, 136.19, 134.75, 131.12, 127.30, 121.75, 119.36, 117.52, 117.28, 116.34, 64.51, 64.43, 42.56, 40.32, 38.31.

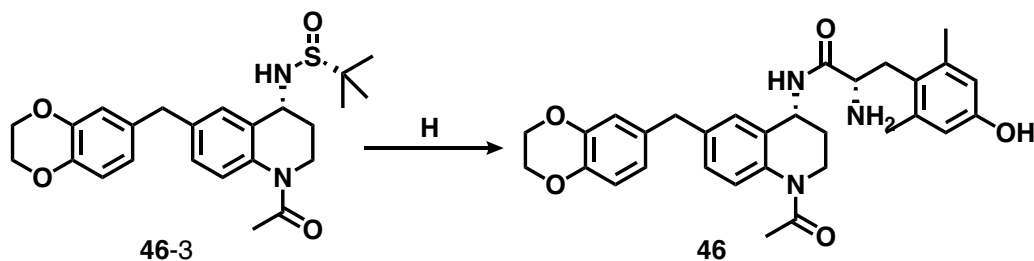


46-2 1-acetyl-6-((2,3-dihydrobenzo[b][1,4]dioxin-6-yl)methyl)-2,3-dihydroquinolin-4(1H)-one. Intermediate **46-2** was synthesized following **General Procedure (D)** from intermediate **46-1** (97 mg, 0.33 mmol, 1.0 eq). After removal of solvent, clean product crystallized and thus was not purified by chromatography. Yield: 107 mg, 98%. ¹H NMR (500 MHz, Chloroform-*d*) δ 7.83 (s, 1H), 7.35 (dt, *J* = 6.0, 2.3, 2.1 Hz, 1H), 7.29 (br s, 1H), 6.78 (d, *J* = 7.9 Hz, 1H), 6.65 (d, *J* = 7.9 Hz, 2H), 4.23 (s, 4H), 4.22 (t, *J* = 5.9 Hz, 2H), 3.87 (s, 2H), 2.77 (t, *J* = 6.2 Hz, 2H), 2.32 (s, 3H).

^{13}C NMR (126 MHz, cdCl_3) δ 169.49, 143.63, 142.29, 134.73, 133.47, 127.71, 124.37, 121.89, 117.66, 117.50, 64.52, 64.44, 40.62, 39.67, 23.22.

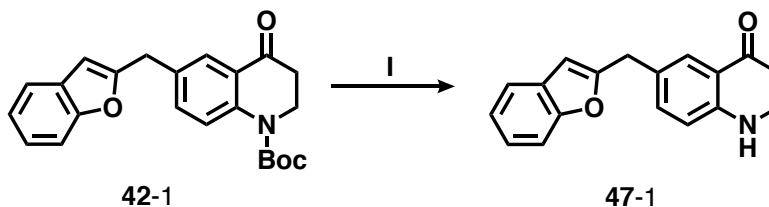


46-3 *(R)-N-((R)-1-acetyl-6-((2,3-dihydrobenzo[*b*][1,4]dioxin-6-yl)methyl)-1,2,3,4-tetrahydroquinolin-4-yl)-2-methylpropane-2-sulfonamide*. Intermediate **46-3** was synthesized following **General Procedure (G)** from **46-2** (102 mg, 0.30 mmol, 1.0 eq), (R)-2-methyl-2-propanesulfonamide (110 mg, 0.91 mmol, 3.0 eq), and $\text{Ti}(\text{OEt})_4$ (0.38 mL, 1.82 mmol, 6.0 eq), then NaBH_4 (69 mg, 1.82 mmol, 6.0 eq). Yield: 103 mg, 77%. ^1H NMR (500 MHz, Chloroform-*d*) δ 7.22 (d, $J = 1.9$ Hz, 1H), 7.09 (dd, $J = 8.2, 2.0$ Hz, 1H), 6.77 (d, $J = 7.9$ Hz, 1H), 6.66 (d, $J = 8.4$ Hz, 2H), 4.52 (q, $J = 4.1$ Hz, 1H), 4.22 (d, $J = 0.8$ Hz, 4H), 3.87 (dt, $J = 11.8, 5.4$ Hz, 1H), 3.83 (s, 2H), 3.76 (ddd, $J = 13.1, 9.4, 5.3$ Hz, 1H), 3.30 (d, $J = 3.2$ Hz, 1H), 2.24 (dt, $J = 13.9, 4.9$ Hz, 1H), 2.21 (s, 3H), 2.07 – 1.96 (m, 1H), 1.19 (d, $J = 0.8$ Hz, 9H). ^{13}C NMR (126 MHz, cdCl_3) δ 170.05, 143.55, 142.15, 133.93, 128.71, 128.66, 124.93, 121.92, 117.66, 117.38, 110.12, 77.16, 64.50, 60.51, 55.87, 40.68, 30.46, 22.70, 22.24.

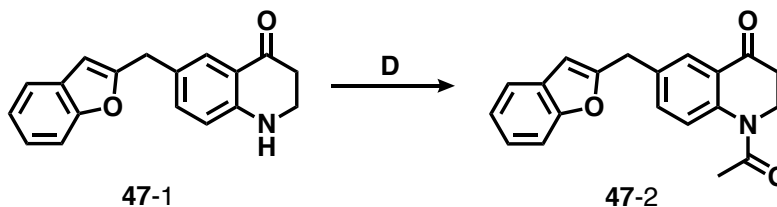


46 *(S)-N-((R)-1-acetyl-6-((2,3-dihydrobenzo[b][1,4]dioxin-6-yl)methyl)-1,2,3,4-tetrahydroquinolin-4-yl)-2-amino-3-(4-hydroxy-2,6-dimethylphenyl)propenamide. **46** was synthesized following **General Procedure (H)** from intermediate **46-3**. **Step 1:** Sulfinamide cleavage was carried out with **46-3** (103 mg, 0.23 mmol, 1.0 eq) and excess concentrated HCl (0.10 mL), precipitating product as a white solid, which was used without further purification. **Step 2:** Amide coupling was performed with the aminium chloride salt of **46-3** (87 mg, 0.23 mmol, 1.0 eq), di-Boc-Dmt (104 mg, 0.26 mmol, 1.1 eq), and PyBOP (132 mg, 0.26 mmol, 1.1 eq), followed by DIPEA (0.41 mL, 2.32 mmol, 10 eq). After purification by silica chromatography, product was carried forward to **Step 3:** TFA deprotection, followed by purification by reverse-phase semi-preparative HPLC, as described in **General Procedure (H)**. Final yield not calculated. ¹H NMR (500 MHz, Methanol-*d*₄) δ 7.37 (s, 1H), 7.12 – 7.09 (m, 1H), 7.04 (d, *J* = 8.3 Hz, 1H), 6.69 (d, *J* = 8.1 Hz, 1H), 6.63 – 6.56 (m, 2H), 6.50 (s, 2H), 4.94 (d, *J* = 6.1 Hz, 1H), 4.16 (d, *J* = 0.8 Hz, 4H), 3.87 (dt, *J* = 11.6, 3.2 Hz, 1H), 3.78 (s, 2H), 3.25 (dd, *J* = 13.7, 11.5 Hz, 1H), 3.03 (dd, *J* = 13.7, 5.1 Hz, 1H), 2.27 (s, 6H), 2.18 (s, 3H), 1.89 – 1.81 (m, 1H), 1.45 (s, 1H). ¹³C NMR (126 MHz, cd₃od) δ 172.54, 157.45, 144.85, 143.43, 140.07, 135.44, 129.28, 125.76, 123.25, 122.55, 118.34, 118.05, 116.48, 111.42, 65.63, 65.53, 53.50, 49.00, 47.07, 41.38, 31.97, 20.43. Calculated [M+H]⁺: 530.3. ESI-MS mass observed: 530.3 (M+H) and 552.3 (M+Na). Analytical HPLC retention time: 31.1 min.*

Compound 47

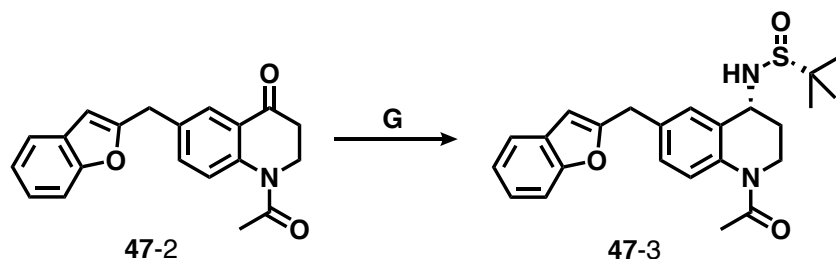


47-1 6-(benzofuran-2-ylmethyl)-2,3-dihydroquinolin-4(1H)-one. Intermediate **47-1** was synthesized follow **General Procedure (I)** from **42-1** (245 mg, 0.65 mmol, 1.0 eq) and 1:1 DCM/TFA (10 mL, excess), yielding clean product **47-1** without further purification. Yield: 180 mg, 100%. ^1H NMR (500 MHz, Chloroform-*d*) δ 7.80 (d, $J = 2.1$ Hz, 1H), 7.46 (dd, $J = 7.3, 1.7$ Hz, 1H), 7.39 (d, $J = 8.2$ Hz, 1H), 7.25 (dd, $J = 6.4, 2.0$ Hz, 1H), 7.20 (td, $J = 7.6, 1.6$ Hz, 1H), 7.16 (td, $J = 7.3, 1.3$ Hz, 1H), 6.64 (d, $J = 8.4$ Hz, 1H), 6.36 (t, $J = 0.9$ Hz, 1H), 3.99 (s, 2H), 3.56 (td, $J = 7.1, 6.2, 1.4$ Hz, 3H), 2.69 (t, $J = 6.9$ Hz, 2H). ^{13}C NMR (126 MHz, cdCl_3) δ 193.78, 157.97, 155.08, 151.10, 136.05, 128.92, 127.71, 123.50, 122.62, 120.53, 116.41, 111.02, 103.32, 42.47, 38.22, 34.14, 28.41.

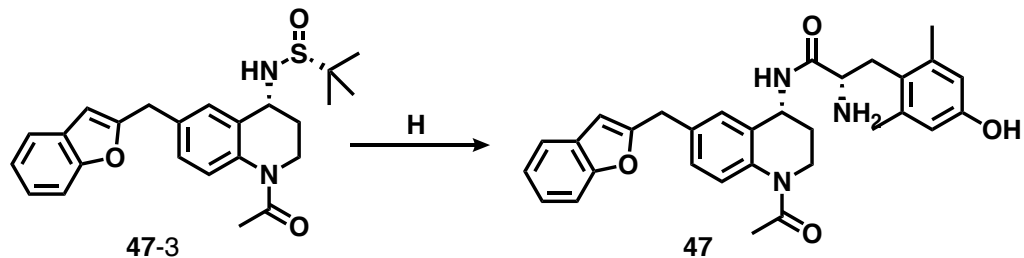


47-2 1-acetyl-6-(benzofuran-2-ylmethyl)-2,3-dihydroquinolin-4(1H)-one. Intermediate **47-2** was synthesized following **General Procedure (G)** from intermediate **47-1** (100 mg, 0.36 mmol, 1.0 eq) and neat Ac_2O (5 mL, excess) yielding clean product **47-1**. Yield: 112 mg, 97%. ^1H NMR (500 MHz, Chloroform-*d*) δ 7.96 (d, $J = 2.1$ Hz, 1H), 7.49 (td, $J = 7.6, 6.8, 1.9$ Hz, 2H), 7.40 (d, $J = 8.0$ Hz, 1H), 7.22 (td, $J = 7.7, 1.6$ Hz, 1H), 7.18 (tt, $J = 7.4, 0.9$ Hz, 1H), 6.44 (t, $J = 0.9$ Hz, 1H), 4.23

(t, $J = 6.3$ Hz, 2H), 4.12 (s, 2H), 2.79 (t, $J = 6.2$ Hz, 2H), 2.33 (s, 3H). ^{13}C NMR (126 MHz, cdCl_3) δ 194.01, 169.46, 156.51, 155.14, 142.81, 134.73, 128.72, 127.98, 124.56, 123.85, 122.82, 120.70, 111.09, 103.88, 39.63, 34.43, 23.27. ^{13}C NMR (126 MHz, cdCl_3) δ 170.08, 157.03, 155.09, 128.79, 125.08, 123.68, 122.73, 120.63, 111.05, 103.68, 60.53, 55.93, 51.06, 34.47, 30.64, 22.70, 22.24.

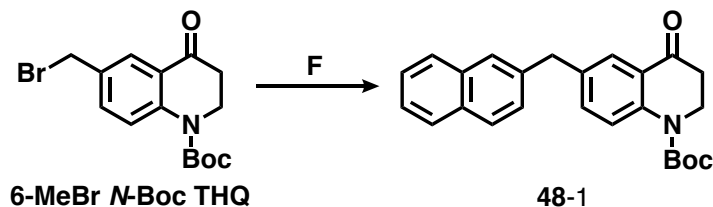


47-3 *(R)-N-((R)-1-acetyl-6-(benzofuran-2-ylmethyl)-1,2,3,4-tetrahydroquinolin-4-yl)-2-methylpropane-2-sulfonamide*. **47-3** was synthesized following **General Procedure (G)** from **47-2** (110 mg, 0.34 mmol, 1.0 eq), (R)-2-methyl-2-propanesulfonamide (125 mg, 1.03 mmol, 3.0 eq), and $\text{Ti}(\text{OEt})_4$ (0.43 mL, 2.07 mmol, 6.0 eq), then NaBH_4 (78 mg, 2.07 mmol, 6.0 eq). Yield: 90 mg, 62%. ^1H NMR (500 MHz, Chloroform-*d*) δ 7.48 (dd, $J = 7.3, 1.7$ Hz, 1H), 7.39 (dd, $J = 8.3, 1.1$ Hz, 1H), 7.38 – 7.37 (m, 1H), 7.23 (dd, $J = 8.2, 2.3$ Hz, 1H), 7.20 (dd, $J = 7.8, 1.8$ Hz, 1H), 7.17 (td, $J = 7.4, 1.3$ Hz, 1H), 6.45 (s, 1H), 4.55 (q, $J = 4.3$ Hz, 1H), 4.08 (s, 2H), 3.90 (dt, $J = 11.7, 5.4$ Hz, 1H), 3.76 (ddd, $J = 12.9, 9.4, 5.3$ Hz, 1H), 3.34 (d, $J = 3.4$ Hz, 1H), 2.23 (s, 3H), 2.28 – 2.18 (m, 1H), 2.11 – 2.00 (m, 2H), 1.19 (s, 9H).



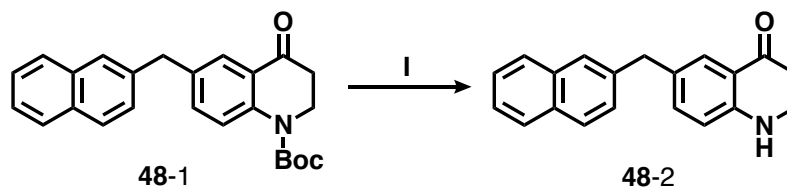
47 (*S*)-*N*-((*R*)-1-acetyl-6-(benzofuran-2-ylmethyl)-1,2,3,4-tetrahydroquinolin-4-yl)-2-amino-3-(4-hydroxy-2,6-dimethylphenyl)propenamide. **47** was synthesized following **General Procedure (H)** from intermediate **47-3**. **Step 1:** Sulfinamide cleavage was carried out with **47-3** (90 mg, 0.21 mmol, 1.0 eq) and excess concentrated HCl (0.10 mL) precipitating product as a white solid, which was used without further purification. **Step 2:** Amide coupling was performed with the aminium chloride salt of **47-3** (76 mg, 0.21 mmol, 1.0 eq), di-Boc-Dmt (94 mg, 0.23 mmol, 1.1 eq), and PyBOP (122 mg, 0.23 mmol, 1.1 eq), followed by DIPEA (0.37 mL, 2.13 mmol, 10 eq). After purification by silica chromatography, product was carried forward to **Step 3:** TFA deprotection, followed by purification by reverse-phase semi-preparative HPLC, as described in **General Procedure (H)**. Final yield not calculated. ^1H NMR (500 MHz, Methanol- d_4) δ 7.46 – 7.43 (m, 1H), 7.32 (dq, $J = 8.4, 0.9$ Hz, 1H), 7.23 (s, 1H), 7.20 (dd, $J = 8.1, 1.8$ Hz, 1H), 7.17 (dd, $J = 7.9, 1.6$ Hz, 1H), 7.14 (td, $J = 7.4, 1.2$ Hz, 1H), 6.51 (s, 2H), 6.42 (d, $J = 1.0$ Hz, 1H), 4.96 (t, $J = 6.1$ Hz, 1H), 4.07 – 4.05 (m, 2H), 3.87 (dd, $J = 11.5, 5.0$ Hz, 1H), 3.78 (s, 1H), 3.25 (dd, $J = 13.7, 11.6$ Hz, 1H), 3.21 – 3.12 (m, 2H), 3.04 (dd, $J = 13.7, 5.1$ Hz, 1H), 2.27 (s, 6H), 2.19 (s, 3H), 1.86 (ddt, $J = 13.5, 8.0, 5.3$ Hz, 1H), 1.46 (s, 1H). ^{13}C NMR (126 MHz, cd_3od) δ 172.56, 158.85, 157.42, 156.35, 140.07, 130.10, 129.34, 125.90, 124.61, 123.67, 123.29, 121.49, 116.46, 111.52, 104.22, 53.50, 49.00, 46.99, 34.99, 31.93, 23.38, 20.42. Calculated $[\text{M}+\text{H}]^+$: 512.2. ESI-MS mass observed: 512.2 (M+H) and 534.2 (M+Na). Analytical HPLC retention time: 35.3 min.

Compound 48



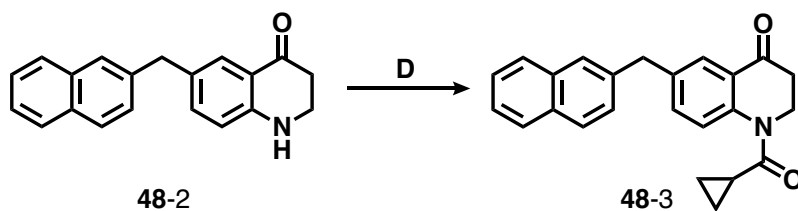
48-1 *tert-butyl 6-(naphthalen-2-ylmethyl)-4-oxo-3,4-dihydroquinoline-1(2H)-carboxylate.*

Intermediate **48-1** was synthesized following **General Procedure (F)** from intermediate **6-MeBr N-Boc THQ** (500 mg, 1.47 mmol, 1.0 eq), naphthalene-2-boronic acid (505 mg, 2.94 mmol, 2.0 eq), K_2CO_3 (609 mg, 0.82 mmol, 3.0 eq) and $Pd(dppf)Cl_2$ (100 mg, 0.15 mmol, 0.1 eq). Reaction was heated 18 hours. Yield: 471 mg, 83%. 1H NMR (500 MHz, Chloroform-*d*) δ 7.90 (d, $J = 2.2$ Hz, 1H), 7.81 – 7.73 (m, 3H), 7.69 (d, $J = 8.7$ Hz, 1H), 7.63 (s, 1H), 7.49 – 7.40 (m, 2H), 7.35 (dt, $J = 8.6, 1.8$ Hz, 1H), 7.30 (dt, $J = 8.4, 1.5$ Hz, 1H), 4.16 – 4.10 (m, 4H), 2.75 (t, $J = 6.4$ Hz, 2H), 1.54 (s, 9H). ^{13}C NMR (126 MHz, $cdCl_3$) δ 194.26, 152.75, 142.47, 137.89, 136.72, 134.71, 133.58, 132.13, 128.24, 127.61, 127.54, 127.35, 127.31, 127.25, 127.08, 126.78, 126.05, 125.46, 124.82, 123.87, 82.12, 77.25, 77.20, 77.00, 76.75, 44.28, 41.33, 38.99, 28.29.



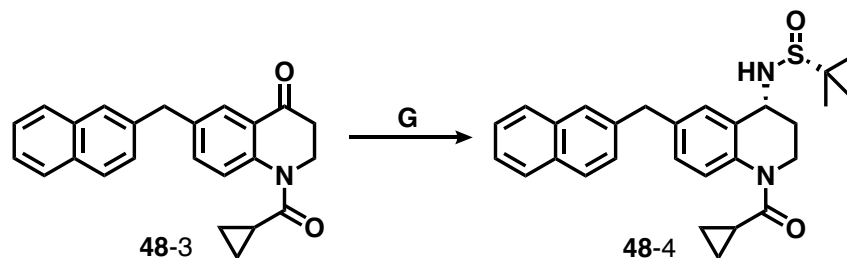
48-2 *6-(naphthalen-2-ylmethyl)-2,3-dihydroquinolin-4(1H)-one.* Intermediate **48-2** was synthesized following **General Procedure (I)** from intermediate **48-1** (220 mg, 0.57 mmol, 1.0 eq) and 1:1 DCM/TFA (10 mL, excess). Yield: 135 mg, 83%. 1H NMR (500 MHz, Chloroform-*d*) δ 7.80 – 7.72 (m, 4H), 7.61 (d, $J = 1.8$ Hz, 1H), 7.47 – 7.39 (m, 2H), 7.30 (dd, $J = 8.4, 1.8$ Hz,

1H), 7.15 (dd, $J = 8.4, 2.2$ Hz, 1H), 6.59 (d, $J = 8.4$ Hz, 1H), 4.31 (s, 1H), 4.02 (s, 2H), 3.59 – 3.51 (m, 2H), 2.72 – 2.66 (m, 2H). ^{13}C NMR (126 MHz, cdCl_3) δ 193.66, 138.64, 136.34, 136.11, 133.56, 132.05, 128.11, 127.58, 127.51, 127.40, 127.36, 127.20, 126.87, 125.95, 125.31, 77.00, 42.41, 41.14, 38.08.

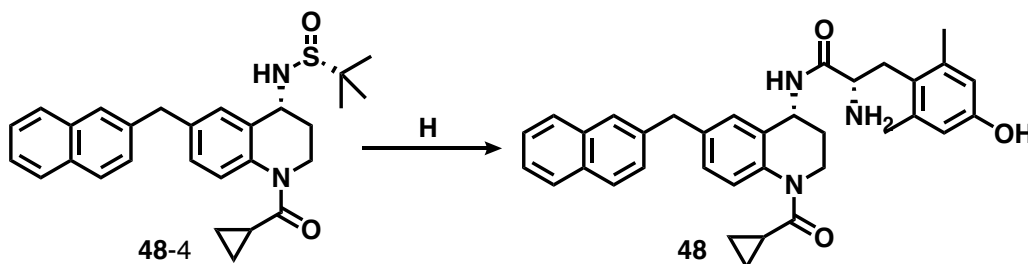


48-3 *1-(cyclopropanecarbonyl)-6-(naphthalen-2-ylmethyl)-2,3-dihydroquinolin-4(1H)-one.*

Intermediate **48-3** was synthesized following **General Procedure (D)** from intermediate **48-2** (100 mg, 0.35 mmol, 1.0 eq), Et_3N (0.10 mL, 0.70 mmol, 2.0 eq), and cyclopropanecarbonyl chloride (0.06 mL, 0.70 mmol, 2.0 eq). Yield: 65 mg, 52%. ^1H NMR (500 MHz, $\text{Chloroform-}d$) δ 7.95 (d, $J = 2.2$ Hz, 1H), 7.83 – 7.76 (m, 3H), 7.65 (s, 1H), 7.49 – 7.42 (m, 3H), 7.38 (dd, $J = 8.3, 2.2$ Hz, 1H), 7.31 (dd, $J = 8.4, 1.8$ Hz, 1H), 4.28 (t, $J = 6.3$ Hz, 2H), 4.15 (s, 2H), 3.48 (s, 1H), 2.78 (t, $J = 6.3$ Hz, 2H), 2.00 (tt, $J = 7.9, 4.6$ Hz, 1H), 1.21 – 1.16 (m, 2H), 0.87 (dq, $J = 7.2, 3.8$ Hz, 2H). ^{13}C NMR (126 MHz, cdCl_3) δ 194.56, 173.16, 142.61, 138.55, 137.69, 134.67, 133.71, 132.30, 128.53, 127.90, 127.78, 127.66, 127.42, 127.31, 126.31, 125.97, 125.73, 124.22, 43.63, 41.56, 39.80, 21.09, 13.85, 9.88, 7.57.



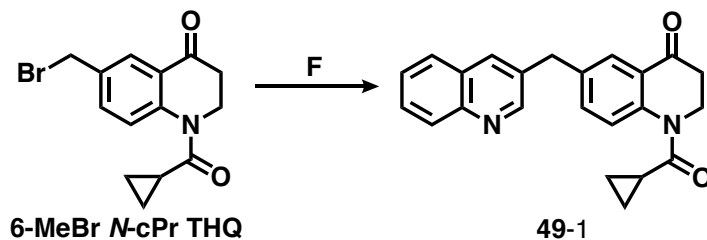
48-4 *(R)-N-((R)-1-(cyclopropanecarbonyl)-6-(naphthalen-2-ylmethyl)-1,2,3,4-tetrahydroquinolin-4-yl)-2-methylpropane-2-sulfonamide*. **48-4** was synthesized following **General Procedure (G)** from intermediate **48-3** (65 mg, 0.18 mmol, 1.0 eq), (R)-2-methyl-2-propanesulfonamide (66 mg, 0.55 mmol, 3.0 eq), and $\text{Ti}(\text{OEt})_4$ (0.23 mL, 1.10 mmol, 6.0 eq), then NaBH_4 (42 mg, 1.10 mmol, 6.0 eq). Yield: 41 mg, 49%. ^1H NMR (500 MHz, Chloroform-*d*) δ 7.79 (td, $J = 8.2, 7.6, 5.7$ Hz, 3H), 7.68 – 7.64 (m, 1H), 7.49 – 7.40 (m, 2H), 7.39 – 7.31 (m, 3H), 7.13 (dd, $J = 8.3, 2.0$ Hz, 1H), 4.56 (q, $J = 4.3$ Hz, 1H), 4.12 (s, 2H), 3.97 (ddd, $J = 12.8, 6.2, 4.9$ Hz, 1H), 3.75 (ddd, $J = 12.9, 9.3, 5.6$ Hz, 1H), 3.32 (d, $J = 3.6$ Hz, 1H), 2.23 (dq, $J = 14.8, 5.1$ Hz, 1H), 2.10 – 1.99 (m, 1H), 1.92 (tt, $J = 7.9, 4.7$ Hz, 1H), 1.65 (s, 2H), 1.18 (s, 9H), 1.16 – 1.04 (m, 2H), 0.80 – 0.73 (m, 2H). ^{13}C NMR (126 MHz, cdCl_3) δ 173.47, 138.51, 138.22, 136.97, 133.74, 132.27, 128.78, 128.63, 128.40, 127.76, 127.69, 127.63, 127.28, 126.23, 125.62, 125.01, 55.94, 51.31, 41.74, 39.93, 30.80, 22.70, 13.70, 9.36.



48 *(R)-N-((R)-1-(cyclopropanecarbonyl)-6-(naphthalen-2-ylmethyl)-1,2,3,4-tetrahydroquinolin-4-yl)-2-methylpropane-2-sulfonamide*. Final compound **48** was synthesized following **General**

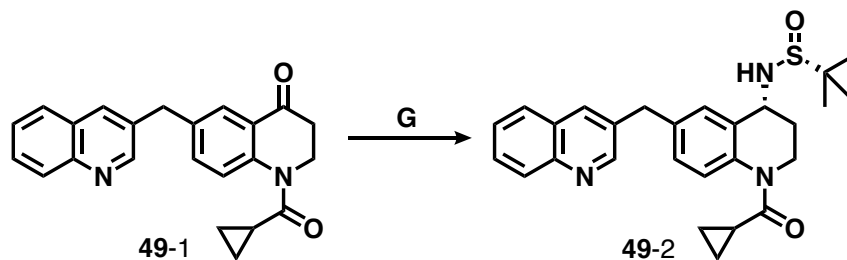
Procedure (H) from intermediate **48-4**. **Step 1:** Sulfinamide cleavage was carried out with **48-4** (41 mg, 0.09 mmol, 1.0 eq) and excess concentrated HCl (0.06 mL) precipitating product as a white solid, which was used without further purification. **Step 2:** Amide coupling was performed with the aminium chloride salt of **48-4** (35 mg, 0.09 mmol, 1.0 eq), di-Boc-Dmt (40 mg, 0.10 mmol, 1.1 eq), PyBOP (51 mg, 0.10 mmol, 1.1 eq), and 6-Cl HOBt (17 mg, 0.10 mmol, 1.1 eq), followed by DIPEA (0.16 mL, 0.89 mmol, 10 eq). After purification by silica chromatography, product was carried forward to **Step 3:** TFA deprotection, followed by purification by reverse-phase semi-preparative HPLC, as described in **General Procedure (H)**. Final yield not calculated. ^1H NMR (500 MHz, Methanol- d_4) δ 7.81 – 7.76 (m, 1H), 7.74 (d, J = 8.1 Hz, 2H), 7.61 (s, 1H), 7.46 – 7.38 (m, 3H), 7.29 (dd, J = 8.4, 1.7 Hz, 1H), 7.24 (d, J = 2.0 Hz, 1H), 7.14 (dd, J = 8.2, 2.1 Hz, 1H), 6.51 (s, 2H), 4.97 (t, J = 6.3 Hz, 1H), 4.10 (s, 2H), 3.94 – 3.83 (m, 2H), 3.30 – 3.21 (m, 2H), 3.04 (dd, J = 13.7, 5.1 Hz, 1H), 2.27 (s, 6H), 1.96 (td, J = 8.2, 4.2 Hz, 1H), 1.86 (dq, J = 13.0, 6.0 Hz, 1H), 1.43 (dq, J = 12.9, 6.4 Hz, 1H), 1.37 (dd, J = 6.7, 4.1 Hz, 2H), 1.09 – 0.91 (m, 1H), 0.91 – 0.78 (m, 2H). Calculated $[\text{M}+\text{H}]^+$: 548.3. ESI-MS mass observed: 548.3 (M+H) and 570.3 (M+Na). Analytical HPLC retention time: 42.9 min.

Compound 49



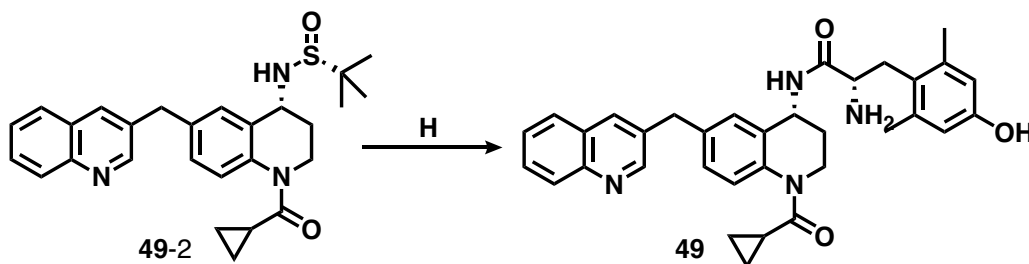
49-1 *1-(cyclopropanecarbonyl)-6-(quinolin-3-ylmethyl)-2,3-dihydroquinolin-4(1H)-one.*

Intermediate **49-1** was synthesized following **General Procedure (F)** from **6-MeBr N-cPr THQ** (85 mg, 0.28 mmol, 1.0 eq), 3-quinoline boronic acid (72 mg, 0.41 mmol, 1.5 eq), K_2CO_3 (113 mg, 0.82 mmol, 3.0 eq) and $Pd(dppf)Cl_2$ (22 mg, 0.03 mmol, 0.1 eq). Yield: 53 mg, 54%. 1H NMR (500 MHz, Chloroform-*d*) δ 8.79 (d, $J = 2.1$ Hz, 1H), 8.08 (d, $J = 8.5$ Hz, 1H), 7.93 (dd, $J = 6.4$, 2.0 Hz, 2H), 7.76 (dd, $J = 8.2$, 1.4 Hz, 1H), 7.68 (ddd, $J = 8.3$, 6.9, 1.4 Hz, 1H), 7.56 – 7.53 (m, 1H), 7.53 – 7.48 (m, 1H), 7.38 (dd, $J = 8.4$, 2.2 Hz, 1H), 7.26 (s, 0H), 4.28 (t, $J = 6.3$ Hz, 2H), 4.19 (s, 2H), 2.79 (t, $J = 6.3$ Hz, 2H), 2.00 (tt, $J = 8.1$, 4.7 Hz, 1H), 1.69 (s, 1H), 1.19 (dt, $J = 6.5$, 3.5 Hz, 2H), 0.88 (dq, $J = 7.1$, 3.9 Hz, 2H). ^{13}C NMR (126 MHz, $cdCl_3$) δ 194.39, 173.17, 151.89, 142.98, 137.18, 135.11, 134.53, 132.99, 129.37, 129.28, 127.99, 127.59, 127.05, 126.09, 124.48, 112.06, 96.17, 43.67, 39.79, 38.75, 13.90, 9.94.



49-2 *(R)-N-((R)-1-(cyclopropanecarbonyl)-6-(quinolin-3-ylmethyl)-1,2,3,4-tetrahydroquinolin-4-yl)-2-methylpropane-2-sulfonamide.* Intermediate **49-2** was synthesized following **General**

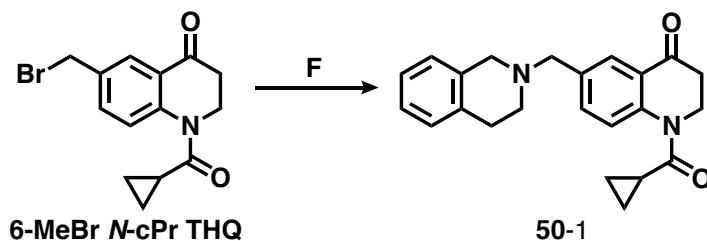
Procedure (G) from intermediate **49-1** (53 mg, 0.15 mmol, 1.0 eq), (R)-2-methyl-2-propanesulfonamide (54 mg, 0.45 mmol, 3.0 eq), and Ti(OEt)₄ (0.19 mL, 0.90 mmol, 6.0 eq), then NaBH₄ (34 mg, 0.90 mmol, 6.0 eq). Yield: 32 mg, 46%. ¹H NMR (500 MHz, Chloroform-*d*) δ 8.09 (d, *J* = 8.4 Hz, 1H), 8.01 (s, 1H), 7.87 (dd, *J* = 8.3, 6.5 Hz, 1H), 7.79 (d, *J* = 8.2 Hz, 1H), 7.73 – 7.66 (m, 1H), 7.58 – 7.51 (m, 1H), 7.44 – 7.37 (m, 2H), 7.12 (dt, *J* = 8.4, 2.6 Hz, 1H), 4.54 (q, *J* = 4.6 Hz, 1H), 4.15 (s, 2H), 3.98 (dt, *J* = 12.1, 5.7 Hz, 1H), 3.75 (ddd, *J* = 13.5, 8.9, 5.8 Hz, 1H), 2.21 (dq, *J* = 15.5, 5.3 Hz, 1H), 2.08 (dq, *J* = 13.9, 5.5, 4.1 Hz, 1H), 1.90 (tq, *J* = 8.3, 4.4 Hz, 1H), 1.18 (s, 9H), 1.13 – 1.07 (m, 2H), 0.78 (dd, *J* = 7.9, 3.0 Hz, 2H). ¹³C NMR (126 MHz, cdcl₃) δ 173.50, 140.00, 136.94, 133.60, 131.75, 129.42, 128.87, 128.82, 128.63, 128.55, 128.46, 128.01, 127.67, 127.13, 125.21, 56.00, 51.62, 40.08, 38.87, 31.01, 22.71, 22.69, 13.72, 9.35.



49 (*S*)-2-amino-*N*-((*R*)-1-(cyclopropanecarbonyl)-6-(quinolin-3-ylmethyl)-1,2,3,4-tetrahydroquinolin-4-yl)-3-(4-hydroxy-2,6-dimethylphenyl)propenamide. Final compound **49** was synthesized following **General Procedure (H)** from intermediate **49-2**. **Step 1:** Sulfonamide cleavage was carried out with **49-2** (32 mg, 0.07 mmol, 1.0 eq) and excess concentrated HCl (0.06 mL) precipitating product as a white solid, which was used without further purification. **Step 2:** Amide coupling was performed with the aminium chloride salt of **49-2** (28 mg, 0.07 mmol, 1.0 eq), di-Boc-Dmt (40 mg, 0.10 mmol, 1.3 eq), PyBOP (47 mg, 0.09 mmol, 1.3 eq), and 6-Cl HOBt (16 mg, 0.09 mmol, 1.3 eq), followed by DIPEA (0.14 mL, 0.81 mmol, 12 eq). Yield not

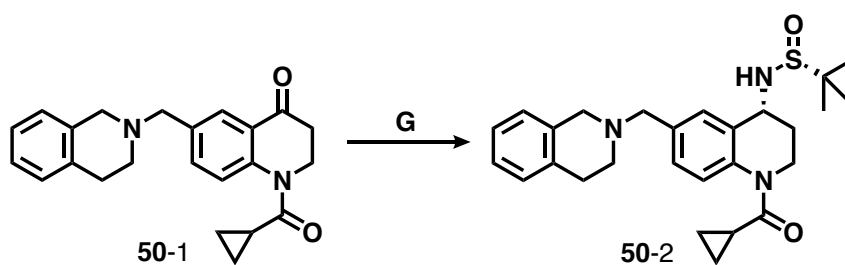
calculated. After purification by silica chromatography, product was carried forward to **Step 3**: TFA deprotection, followed by purification by reverse-phase semi-preparative HPLC, as described in **General Procedure (H)**. Final yield not calculated. ¹H NMR (500 MHz, Methanol-*d*₄) δ 9.02 (d, *J* = 1.8 Hz, 1H), 8.73 (d, *J* = 5.8 Hz, 1H), 8.19 – 8.13 (m, 2H), 8.02 (tq, *J* = 8.4, 7.1, 1.4 Hz, 1H), 7.89 – 7.83 (m, 1H), 7.48 (d, *J* = 8.3 Hz, 1H), 7.32 (d, *J* = 2.0 Hz, 1H), 7.20 (dd, *J* = 8.4, 2.1 Hz, 1H), 6.51 (s, 2H), 4.97 (q, *J* = 6.2 Hz, 1H), 4.30 (s, 2H), 3.96 – 3.87 (m, 2H), 3.30 – 3.22 (m, 2H), 3.07 (dd, *J* = 13.7, 5.0 Hz, 1H), 2.28 (s, 6H), 1.96 (ddd, *J* = 7.8, 6.2, 3.9 Hz, 1H), 1.86 (ddt, *J* = 13.1, 7.3, 5.5 Hz, 1H), 1.44 (tt, *J* = 13.1, 6.2 Hz, 1H), 1.09 – 1.01 (m, 1H), 0.98 – 0.92 (m, 1H), 0.92 – 0.79 (m, 2H). ¹³C NMR (500 MHz, CD₃OD) δ 175.52, 157.43, 140.55, 140.05, 138.42, 137.14, 134.40, 130.61, 130.26, 129.77, 129.41, 126.25, 123.31, 121.22, 118.90, 116.45, 53.57, 47.11, 42.38, 38.73, 31.93, 31.32, 20.42, 14.43, 9.90, 9.48. Calculated [M+H]⁺: 549.3. ESI-MS mass observed: 549.3 (M+H) and 571.3 (M+Na). Analytical HPLC retention time: 24.6 min.

Compound 50

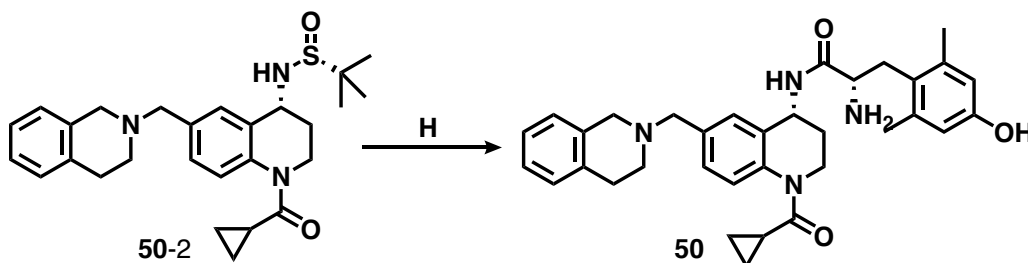


50-1 *1-(cyclopropanecarbonyl)-6-((3,4-dihydroisoquinolin-2(1H)-yl)methyl)-2,3-dihydroquinolin-4(1H)-one*. Intermediate **50-1** was synthesized following **General Procedure (F)** from intermediate **6-MeBr N-cPr THQ** (140 mg, 0.45 mmol, 1.0 eq), K₂CO₃ (76 mg, 0.55 mmol, 1.2 eq) and THIQ (0.07 mL, 0.55 mmol, 1.2 eq). Yield: 145 mg, 88%. ¹H NMR (500 MHz,

Chloroform-*d*) δ 7.99 (d, $J = 2.1$ Hz, 1H), 7.64 (dd, $J = 8.4, 2.1$ Hz, 1H), 7.52 (d, $J = 8.4$ Hz, 1H), 7.14 – 7.07 (m, 3H), 6.99 – 6.95 (m, 1H), 4.30 (t, $J = 6.3$ Hz, 2H), 3.69 (s, 2H), 3.63 (s, 2H), 2.91 (t, $J = 5.9$ Hz, 2H), 2.78 (dt, $J = 16.0, 6.1$ Hz, 4H), 2.07 – 2.00 (m, 1H), 1.24 – 1.19 (m, 2H), 0.90 (dq, $J = 7.1, 3.8$ Hz, 2H). ^{13}C NMR (126 MHz, cdCl_3) δ 194.52, 173.18, 143.40, 135.96, 134.78, 134.65, 134.31, 128.82, 128.12, 126.64, 126.32, 125.75, 125.69, 124.11, 61.92, 56.07, 50.88, 43.67, 39.80, 29.24, 13.90, 9.92.



50-2 (*R*)-*N*-((*R*)-1-(cyclopropanecarbonyl)-6-((3,4-dihydroisoquinolin-2(1H)-yl)methyl)-1,2,3,4-tetrahydroquinolin-4-yl)-2-methylpropane-2-sulfonamide. **50-2** was synthesized following **General Procedure (G)** from **50-1** (120 mg, 0.33 mmol, 1.0 eq), (*R*)-2-methyl-2-propanesulfonamide (121 mg, 1.00 mmol, 3.0 eq), and $\text{Ti}(\text{OEt})_4$ (0.42 mL, 2.00 mmol, 6.0 eq), then NaBH_4 (76 mg, 2.00 mmol, 6.0 eq). Yield: 91 mg, 59%. Characterized by NMR after sulfonamide cleavage in next step (see Final Compound **50** Step 1).



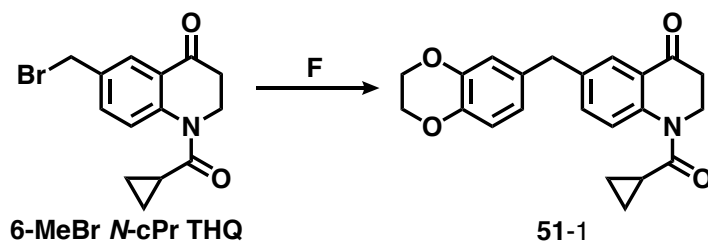
50 *(S)*-2-amino-*N*-((*R*)-1-(cyclopropanecarbonyl)-6-((3,4-dihydroisoquinolin-2(1*H*)-yl)methyl)-1,2,3,4-tetrahydroquinolin-4-yl)-3-(4-hydroxy-2,6-dimethylphenyl)propanamide. Final

compound **50** was synthesized following **General Procedure (H)** from intermediate **50-2**. **Step**

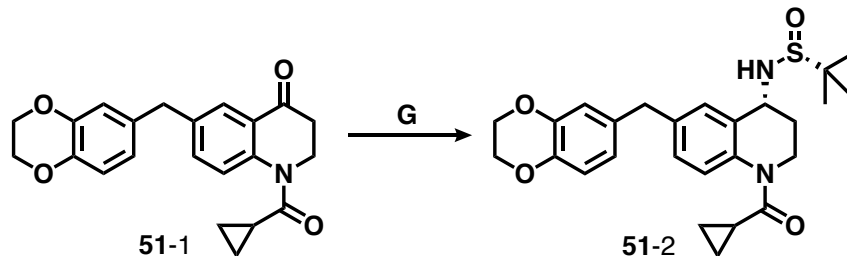
1: Sulfinamide cleavage was carried out with **50-2** (91 mg, 0.20 mmol, 1.0 eq) and excess concentrated HCl, precipitating product as a white solid, which was used without further purification. ¹H NMR (500 MHz, Methanol-*d*₄) δ 7.87 (s, 1H), 7.77 (d, *J* = 8.4 Hz, 1H), 7.69 (td, *J* = 8.1, 2.4 Hz, 1H), 7.32 – 7.27 (m, 1H), 7.28 – 7.23 (m, 2H), 7.21 (t, *J* = 7.5 Hz, 1H), 4.72 (q, *J* = 6.6 Hz, 1H), 4.59 (s, 2H), 4.47 (s, 2H), 4.07 (ddd, *J* = 12.9, 7.6, 5.1 Hz, 1H), 3.99 (ddd, *J* = 13.1, 7.1, 5.1 Hz, 1H), 3.52 – 3.46 (m, 4H), 2.46 (tq, *J* = 12.8, 7.2 Hz, 1H), 2.22 – 2.14 (m, 1H), 2.09 (dtd, *J* = 26.0, 7.8, 4.0 Hz, 1H), 1.09 (dq, *J* = 8.4, 4.7, 4.1 Hz, 2H), 0.95 (qd, *J* = 8.0, 7.3, 3.2 Hz, 2H). ¹³C NMR (126 MHz, cd₃od) δ 175.70, 141.71, 133.22, 132.59, 132.21, 130.39, 129.84, 129.41, 128.84, 128.18, 127.88, 127.02, 126.82, 60.07, 53.91, 53.64, 50.80, 48.20, 41.82, 29.55, 14.80, 10.07. **Step 2:** Amide coupling was performed with the aminium chloride salt of **50-2** (76 mg, 0.17 mmol, 1.0 eq), di-Boc-Dmt (78 mg, 0.19 mmol, 1.1 eq), PyBOP (99 mg, 0.19 mmol, 1.1 eq), and 6-Cl HOBt (32 mg, 0.19 mmol, 1.1 eq), followed by DIPEA (0.30 mL, 1.74 mmol, 10 eq). Yield not calculated. After purification by silica chromatography, product was carried forward to **Step 3:** TFA deprotection, followed by purification by reverse-phase semi-preparative HPLC, as described in **General Procedure (H)**. Final yield not calculated. ¹H NMR (500 MHz, Methanol-*d*₄) δ 7.70 (d, *J* = 8.4 Hz, 1H), 7.47 – 7.40 (m, 2H), 7.34 – 7.29 (m, 1H), 7.29 – 7.24 (m, 2H), 7.16 (d, *J* = 7.6 Hz, 1H), 6.53 (s, 2H), 5.01 (t, *J* = 5.8 Hz, 1H), 4.46 – 4.39 (m, 2H), 4.39 – 4.32 (m, 4H), 3.94 (dt, *J* = 12.6, 5.9 Hz, 1H), 3.88 (dd, *J* = 11.6, 5.0 Hz, 1H), 3.30 – 3.25 (m, 1H), 3.17 (s, 1H), 3.07 (dd, *J* = 13.7, 5.1 Hz, 1H), 2.29 (s, 6H), 2.00 (td, *J* = 8.0, 3.9 Hz, 1H), 1.92 – 1.85 (m, 1H), 1.52 (d, *J* = 7.4 Hz, 1H), 1.28 (d, *J* = 10.3 Hz, 1H), 1.05 (m, 2H), 0.97 – 0.85 (m, 2H).

Calculated $[M+H]^+$: 553.3. ESI-MS mass observed: 553.3 (M+H) and 575.3 (M+Na). Analytical HPLC retention time: 24.6 min.

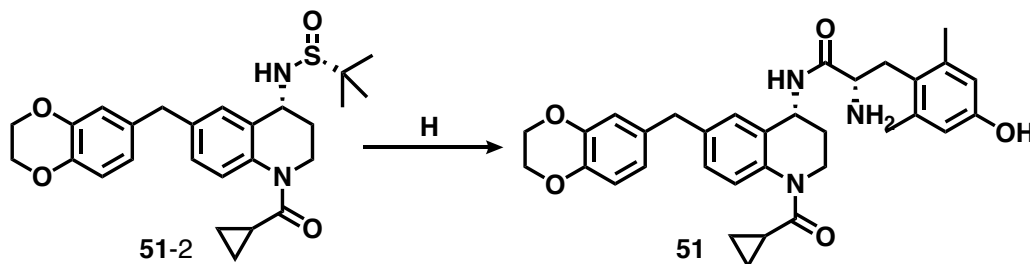
Compound 51



51-1 *1-(cyclopropanecarbonyl)-6-((2,3-dihydrobenzo[b][1,4]dioxin-6-yl)methyl)-2,3-dihydroquinolin-4(1H)-one*. Intermediate **51-1** was synthesized following **General Procedure (F)** from **6-MeBr N-cPr THQ** (100 mg, 0.32 mmol, 1.0 eq), 1,4-benzodioxane-6-boronic acid (88 mg, 0.49 mmol, 1.5 eq), K_2CO_3 (133 mg, 0.96 mmol, 3.0 eq) and $Pd(dppf)Cl_2$ (24 mg, 0.03 mmol, 0.1 eq). Reaction was heated 18 hours. Yield: 109 mg, 92%. 1H NMR (500 MHz, Chloroform-*d*) δ 7.85 (d, $J = 2.2$ Hz, 1H), 7.44 (d, $J = 8.3$ Hz, 1H), 7.34 (dd, $J = 8.4, 2.2$ Hz, 1H), 6.81 – 6.77 (m, 1H), 6.66 (d, $J = 7.5$ Hz, 2H), 4.27 (t, $J = 6.3$ Hz, 2H), 4.23 (s, 4H), 3.87 (s, 2H), 2.77 (t, $J = 6.3$ Hz, 2H), 2.02 (tt, $J = 7.8, 5.2$ Hz, 1H), 1.22 – 1.17 (m, 2H), 0.88 (dq, $J = 7.1, 3.8$ Hz, 2H). ^{13}C NMR (126 MHz, $cdCl_3$) δ 194.61, 173.16, 143.64, 142.53, 142.30, 138.87, 134.56, 133.55, 127.81, 125.98, 124.17, 121.91, 117.66, 117.51, 64.54, 64.44, 43.62, 40.63, 39.84, 13.85, 9.90.



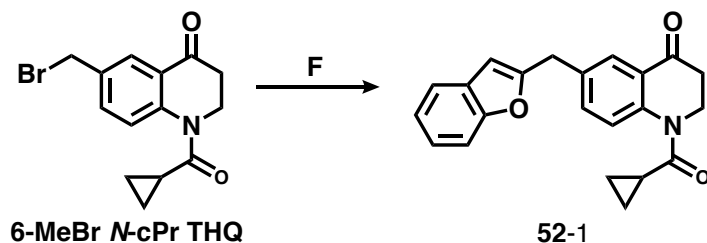
51-2 *(R)-N-((R)-1-(cyclopropanecarbonyl)-6-((2,3-dihydrobenzo[*b*][1,4]dioxin-6-yl)methyl)-1,2,3,4-tetrahydroquinolin-4-yl)-2-methylpropane-2-sulfinamide*. Intermediate **51-2** was synthesized following **General Procedure (G)** from **51-1** (104 mg, 0.29 mmol, 1.0 eq), (R)-2-methyl-2-propanesulfinamide (104 mg, 0.87 mmol, 3.0 eq), and Ti(OEt)₄ (0.36 mL, 1.72 mmol, 6.0 eq), then NaBH₄ (65 mg, 1.72 mmol, 6.0 eq). Yield: 123 mg, 92%. ¹H NMR (500 MHz, Chloroform-*d*) δ 7.34 (d, *J* = 8.2 Hz, 1H), 7.25 (d, *J* = 1.9 Hz, 1H), 7.08 (dd, *J* = 8.1, 2.0 Hz, 1H), 6.78 (dt, *J* = 7.7, 1.1 Hz, 1H), 6.68 (d, *J* = 1.4 Hz, 1H), 4.54 (q, *J* = 4.2 Hz, 1H), 4.22 (d, *J* = 1.5 Hz, 4H), 3.99 – 3.91 (m, 1H), 3.83 (s, 2H), 3.74 (ddd, *J* = 14.9, 10.0, 6.3 Hz, 1H), 3.32 (d, *J* = 3.3 Hz, 1H), 2.24 (dq, *J* = 14.7, 5.1 Hz, 1H), 1.97 – 1.89 (m, 1H), 1.84 (d, *J* = 13.6 Hz, 1H), 1.19 (d, *J* = 1.3 Hz, 9H), 1.12 – 1.08 (m, 2H), 0.80 – 0.74 (m, 2H). ¹³C NMR (500 MHz, cdcl₃) δ 173.43, 143.54, 142.14, 138.74, 136.85, 133.99, 128.61, 128.52, 124.96, 121.92, 117.65, 117.38, 64.50, 64.41, 55.90, 51.18, 40.71, 39.83, 30.60, 22.70, 13.66, 9.31.



51 *(S)-2-amino-N-((R)-1-(cyclopropanecarbonyl)-6-((2,3-dihydrobenzo[*b*][1,4]dioxin-6-yl)methyl)-1,2,3,4-tetrahydroquinolin-4-yl)-3-(4-hydroxy-2,6-dimethylphenyl)propanamide*. Final

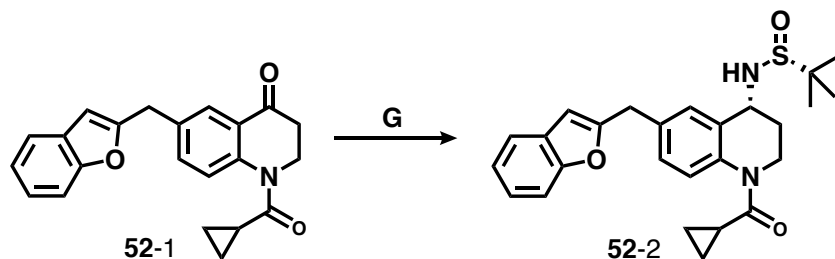
compound **51** was synthesized following **General Procedure (H)** from intermediate **51-2**. **Step 1:** Sulfinamide cleavage was carried out with **51-2** (123 mg, 0.26 mmol, 1.0 eq) and excess concentrated HCl, precipitating product as a white solid, which was used without further purification. **Step 2:** Amide coupling was performed with the aminium chloride salt of **51-2** (105 mg, 0.26 mmol, 1.0 eq), di-Boc-Dmt (118 mg, 0.29 mmol, 1.1 eq), and PyBOP (151 mg, 0.29 mmol, 1.1 eq), followed by DIPEA (0.46 mL, 2.62 mmol, 10 eq). After purification by silica chromatography (Yield: 121 mg, 61%), uncharacterized product was carried forward to **Step 3:** TFA deprotection, followed by purification by reverse-phase semi-preparative HPLC, as described in **General Procedure (H)**. Final yield not calculated. ¹H NMR (500 MHz, Methanol-*d*₄) δ 8.18 (d, *J* = 8.2 Hz, 0H), 7.36 (d, *J* = 8.3 Hz, 1H), 7.15 (d, *J* = 2.0 Hz, 1H), 7.03 (dd, *J* = 8.2, 2.0 Hz, 1H), 6.68 (d, *J* = 8.0 Hz, 1H), 6.60 (dd, *J* = 10.0, 1.6 Hz, 2H), 6.50 (s, 2H), 4.94 (t, *J* = 6.3 Hz, 1H), 4.15 (s, 4H), 3.89 (dt, *J* = 12.9, 5.3 Hz, 2H), 3.78 (s, 2H), 3.29 – 3.21 (m, 2H), 3.06 (dd, *J* = 13.7, 5.1 Hz, 1H), 2.27 (s, 6H), 1.95 (tt, *J* = 8.1, 4.6 Hz, 1H), 1.84 (dq, *J* = 13.1, 5.8 Hz, 1H), 1.40 (dq, *J* = 12.9, 6.8 Hz, 1H), 1.06 – 1.00 (m, 1H), 0.94 (tt, *J* = 9.0, 4.1 Hz, 1H), 0.87 (qd, *J* = 7.6, 6.4, 4.0 Hz, 1H), 0.81 (qd, *J* = 9.0, 8.1, 2.8 Hz, 1H). ¹³C NMR (500 MHz, cd₃od) δ 175.46, 157.41, 144.83, 143.41, 140.05, 137.45, 135.46, 129.25, 129.16, 125.66, 123.27, 122.56, 118.33, 118.04, 116.45, 65.61, 65.51, 53.52, 47.03, 42.23, 41.40, 31.98, 31.51, 20.44, 14.44. Calculated [M+H]⁺: 556.3. ESI-MS mass observed: 556.3 (M+H) and 578.3 (M+Na). Analytical HPLC retention time: 35.8 min.

Compound 52



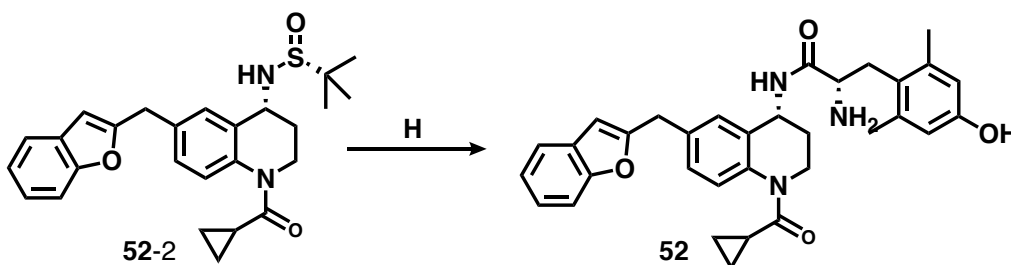
52-1 *6-(benzofuran-2-ylmethyl)-1-(cyclopropanecarbonyl)-2,3-dihydroquinolin-4(1H)-one.*

Intermediate **52-1** was synthesized following **General Procedure (F)** from **6-MeBr N-cPr THQ** (110 mg, 0.36 mmol, 1.0 eq), 2-benzofuranylboronic acid MIDA ester (146 mg, 0.54 mmol, 1.5 eq), K_2CO_3 (149 mg, 1.08 mmol, 3.0 eq) and $Pd(dppf)Cl_2$ (27 mg, 0.04 mmol, 0.1 eq). Reaction was heated 18 hours. Yield: 99 mg, 80%. 1H NMR (500 MHz, Chloroform-*d*) δ 7.98 (d, $J = 2.0$ Hz, 1H), 7.53 – 7.45 (m, 3H), 7.40 (d, $J = 8.0$ Hz, 1H), 7.24 – 7.16 (m, 2H), 6.45 (s, 1H), 4.28 (t, $J = 6.3$ Hz, 2H), 4.13 (s, 2H), 2.79 (t, $J = 6.3$ Hz, 2H), 2.02 (dd, $J = 8.0, 4.2$ Hz, 1H), 1.23 – 1.18 (m, 2H), 0.89 (dq, $J = 7.2, 3.9$ Hz, 2H). ^{13}C NMR (126 MHz, $cdCl_3$) δ 194.34, 173.17, 156.57, 155.13, 143.09, 134.72, 134.52, 128.72, 128.06, 126.03, 124.29, 123.83, 122.81, 120.69, 111.07, 103.85, 43.64, 39.78, 34.40, 13.89, 9.94.



52-2 *(R)-N-((R)-6-(benzofuran-2-ylmethyl)-1-(cyclopropanecarbonyl)-1,2,3,4-tetrahydroquinolin-4-yl)-2-methylpropane-2-sulfonamide.* Intermediate **52-2** was synthesized following **General Procedure (G)** from **52-1** (85 mg, 0.25 mmol, 1.0 eq), (R)-2-methyl-2-

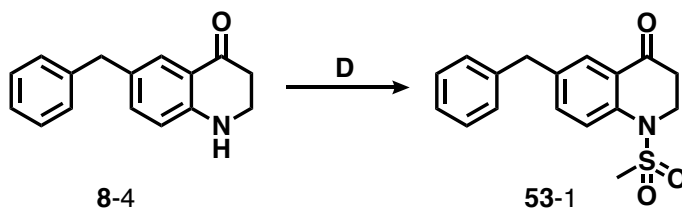
propanesulfinamide (90 mg, 0.74 mmol, 3.0 eq), and Ti(OEt)₄ (0.31 mL, 1.48 mmol, 6.0 eq), then NaBH₄ (56 mg, 1.48 mmol, 6.0 eq). Yield: 90 mg, 81%. ¹H NMR (500 MHz, Chloroform-*d*) δ 7.49 (dd, *J* = 7.3, 1.8 Hz, 1H), 7.43 – 7.39 (m, 3H), 7.23 (dd, *J* = 8.7, 1.9 Hz, 2H), 7.21 – 7.16 (m, 1H), 6.47 (d, *J* = 1.1 Hz, 1H), 4.58 (q, *J* = 4.3 Hz, 1H), 4.10 (s, 2H), 3.99 (ddd, *J* = 12.8, 6.2, 4.9 Hz, 1H), 3.76 (ddd, *J* = 12.9, 9.3, 5.6 Hz, 1H), 3.34 (d, *J* = 3.6 Hz, 1H), 2.25 (dq, *J* = 14.7, 5.1 Hz, 1H), 1.94 (tt, *J* = 7.9, 4.6 Hz, 1H), 1.68 (d, *J* = 11.3 Hz, 1H), 1.20 (s, 9H), 1.17 – 1.08 (m, 1H), 0.79 (dq, *J* = 7.9, 1.8 Hz, 2H). ¹³C NMR (126 MHz, cdcl₃) δ 173.51, 157.10, 155.10, 137.51, 134.63, 128.84, 128.80, 128.61, 125.10, 123.69, 122.75, 120.65, 111.06, 103.67, 55.96, 51.30, 39.95, 34.50, 30.79, 22.71, 13.73, 9.41, 9.37.



52 (*S*)-2-amino-*N*-((*R*)-6-(benzofuran-2-ylmethyl)-1-(cyclopropanecarbonyl)-1,2,3,4-tetrahydroquinolin-4-yl)-3-(4-hydroxy-2,6-dimethylphenyl)propenamide. Final compound **52** was synthesized following **General Procedure (H)** from intermediate **52-2**. **Step 1:** Sulfinamide cleavage was carried out with **52-2** (90 mg, 0.20 mmol, 1.0 eq) and excess concentrated HCl (0.09 mL) precipitating product as a white solid, which was used without further purification. **Step 2:** Amide coupling was performed with the aminium chloride salt of **52-2** (75 mg, 0.20 mmol, 1.0 eq), di-Boc-Dmt (90 mg, 0.22 mmol, 1.1 eq), and PyBOP (114 mg, 0.22 mmol, 1.1 eq), followed by DIPEA (0.34 mL, 1.96 mmol, 10 eq). After purification by silica chromatography, product was carried forward to **Step 3:** TFA deprotection, followed by purification by reverse-phase semi-

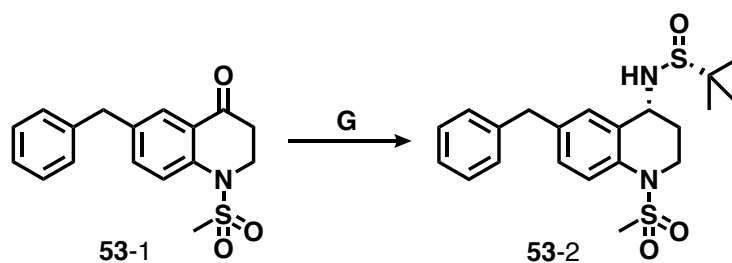
preparative HPLC, as described in **General Procedure (H)**. Final yield not calculated. ^1H NMR (500 MHz, Methanol- d_4) δ 8.21 (d, $J = 8.2$ Hz, 1H), 7.47 – 7.41 (m, 2H), 7.32 (dq, $J = 8.3, 0.9$ Hz, 1H), 7.27 (d, $J = 2.0$ Hz, 1H), 7.21 (dd, $J = 8.3, 2.1$ Hz, 1H), 7.17 (td, $J = 7.7, 1.6$ Hz, 1H), 7.14 (td, $J = 7.4, 1.3$ Hz, 1H), 6.50 (s, 2H), 6.43 (d, $J = 1.0$ Hz, 1H), 4.97 (t, $J = 6.2$ Hz, 1H), 4.07 (s, 2H), 3.93 – 3.86 (m, 2H), 3.29 – 3.22 (m, 2H), 3.05 (dd, $J = 13.7, 5.0$ Hz, 1H), 2.27 (s, 6H), 1.96 (tt, $J = 7.9, 4.7$ Hz, 1H), 1.86 (ddt, $J = 13.1, 7.4, 5.4$ Hz, 1H), 1.42 (tt, $J = 13.0, 6.1$ Hz, 1H), 1.28 (s, 1H), 1.05 (dddd, $J = 9.7, 6.6, 4.6, 3.1$ Hz, 1H), 0.95 (dddd, $J = 9.5, 6.8, 4.7, 3.2$ Hz, 1H), 0.91 – 0.85 (m, 1H), 0.82 (qd, $J = 9.2, 8.3, 3.0$ Hz, 1H). ^{13}C NMR (500 MHz, cd_3od) δ 175.51, 169.39, 158.87, 157.43, 156.35, 140.05, 138.12, 136.00, 130.11, 129.52, 129.26, 125.82, 124.61, 123.67, 123.26, 121.50, 116.45, 111.52, 104.24, 53.55, 47.10, 42.29, 35.02, 31.97, 31.47, 20.43, 14.47, 9.91, 9.50. Calculated $[\text{M}+\text{H}]^+$: 538.3. ESI-MS mass observed: 538.3 (M+H) and 560.3 (M+Na). Analytical HPLC retention time: 40.1 min.

Compound 53

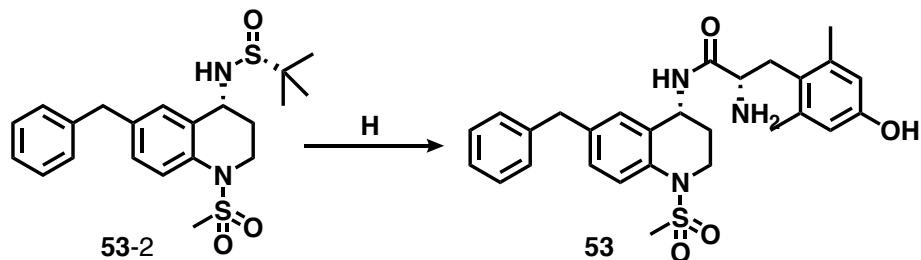


53-1 *6-benzyl-1-(methylsulfonyl)-2,3-dihydroquinolin-4(1H)-one*. Intermediate **53-1** was synthesized from intermediate **8-4**, the synthesis of which can be found in Chapter 2. Intermediate **53-1** was synthesized following **General Procedure (D)** with intermediate **8-4** (200 mg, 0.84 mmol, 1.0 eq), Et_3N (0.23 mL, 1.68 mmol, 2.0 eq), and methanesulfonyl chloride (0.13 mL, 1.68

mmol, 2.0 eq). Yield: 178 mg, 67%. ¹H NMR (400 MHz, Chloroform-*d*) δ 7.91 (d, *J* = 2.3 Hz, 1H), 7.64 (d, *J* = 8.5 Hz, 1H), 7.38 (dd, *J* = 8.5, 2.3 Hz, 1H), 7.30 (tt, *J* = 6.9, 1.0 Hz, 2H), 7.26 (s, 1H), 7.26 – 7.18 (m, 1H), 7.18 (d, *J* = 8.0 Hz, 1H), 4.17 (t, *J* = 6.5 Hz, 2H), 3.98 (s, 2H), 3.04 (s, 3H), 2.84 (dd, *J* = 7.0, 5.9 Hz, 2H). ¹³C NMR (101 MHz, cdcl₃) δ 192.71, 148.67, 140.72, 140.11, 138.45, 135.74, 133.96, 128.95, 128.81, 128.36, 126.60, 124.99, 122.19, 46.12, 41.23, 40.10, 38.16.

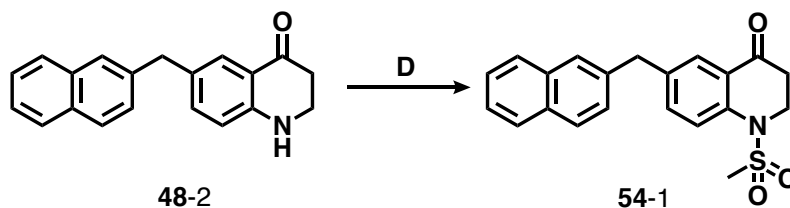


53-2 (*R*)-*N*-((*R*)-6-benzyl-1-(methylsulfonyl)-1,2,3,4-tetrahydroquinolin-4-yl)-2-methylpropane-2-sulfonamide. Intermediate **53-2** was synthesized following **General Procedure (G)** from **53-1** (104 mg, 0.33 mmol, 1.0 eq), (*R*)-2-methyl-2-propanesulfonamide (120 mg, 0.99 mmol, 3.0 eq), and Ti(OEt)₄ (0.42 mL, 1.98 mmol, 6.0 eq), then NaBH₄ (75 mg, 1.98 mmol, 6.0 eq). Yield: 61 mg, 43%. ¹H NMR (400 MHz, Chloroform-*d*) δ 7.70 (d, *J* = 8.8 Hz, 1H), 7.31 – 7.25 (m, 3H), 7.23 – 7.16 (m, 3H), 7.12 (dd, *J* = 8.6, 2.2 Hz, 1H), 4.57 (q, *J* = 3.5 Hz, 1H), 4.09 (dt, *J* = 13.3, 3.7 Hz, 1H), 3.93 (s, 2H), 3.67 (ddd, *J* = 13.6, 11.4, 2.9 Hz, 1H), 2.93 (d, *J* = 0.8 Hz, 3H), 2.18 (dq, *J* = 14.3, 3.9 Hz, 1H), 2.09 – 1.98 (m, 1H), 1.20 (d, *J* = 0.8 Hz, 9H). ¹³C NMR (101 MHz, cdcl₃) δ 140.65, 138.03, 135.31, 130.73, 129.84, 128.95, 128.72, 127.67, 126.42, 121.72, 55.84, 49.91, 41.76, 41.21, 38.88, 28.77, 22.71.

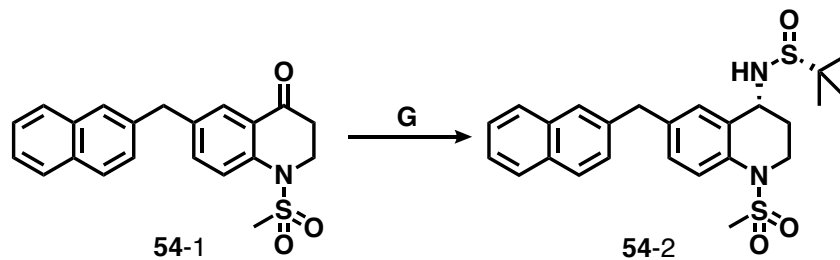


53 *(S)*-2-amino-*N*-((*R*)-6-benzyl-1-(methylsulfonyl)-1,2,3,4-tetrahydroquinolin-4-yl)-3-(4-hydroxy-2,6-dimethylphenyl)propanamide. Final compound **53** was synthesized following **General Procedure (H)** from intermediate **53-2**. **Step 1:** Sulfinamide cleavage was carried out with **53-2** (61 mg, 0.15 mmol, 1.0 eq) and excess concentrated HCl (0.08 mL) precipitating product as a white solid, which was used without further purification. **Step 2:** Amide coupling was performed with the aminium chloride salt of **53-2** (45 mg, 0.13 mmol, 1.0 eq), di-Boc-Dmt (58 mg, 0.14 mmol, 1.1 eq), PyBOP (73 mg, 0.14 mmol, 1.1 eq), and 6-Cl HOBt (24 mg, 0.14 mmol, 1.1 eq), followed by DIPEA (0.23 mL, 1.30 mmol, 10 eq). After purification by silica chromatography, product was carried forward to **Step 3:** TFA deprotection, followed by purification by reverse-phase semi-preparative HPLC, as described in **General Procedure (H)**. Final yield not calculated. ^1H NMR (500 MHz, Methanol- d_4) δ 7.60 (d, J = 8.6 Hz, 1H), 7.27 – 7.21 (m, 2H), 7.18 – 7.11 (m, 4H), 7.06 (dd, J = 8.6, 2.2 Hz, 1H), 6.50 (s, 2H), 4.98 (t, J = 4.9 Hz, 1H), 3.88 (s, 2H), 3.86 – 3.76 (m, 2H), 3.25 (dd, J = 13.6, 11.6 Hz, 1H), 3.02 (dd, J = 13.7, 5.2 Hz, 1H), 2.93 (ddd, J = 13.5, 10.6, 2.7 Hz, 1H), 2.86 (s, 3H), 2.27 (s, 6H), 1.89 (dddd, J = 14.0, 10.6, 5.2, 3.5 Hz, 1H), 1.56 – 1.48 (m, 1H). ^{13}C NMR (500 MHz, cd_3od) δ 140.02, 138.89, 138.40, 136.72, 130.27, 129.76, 129.50, 127.98, 127.20, 122.91, 116.48, 46.65, 43.64, 41.91, 38.82, 31.88, 29.21, 20.45. Calculated $[\text{M}+\text{H}]^+$: 508.3. ESI-MS mass observed: 508.3 (M+H) and 530.3 (M+Na). Analytical HPLC retention time: 34.8 min.

Compound 54

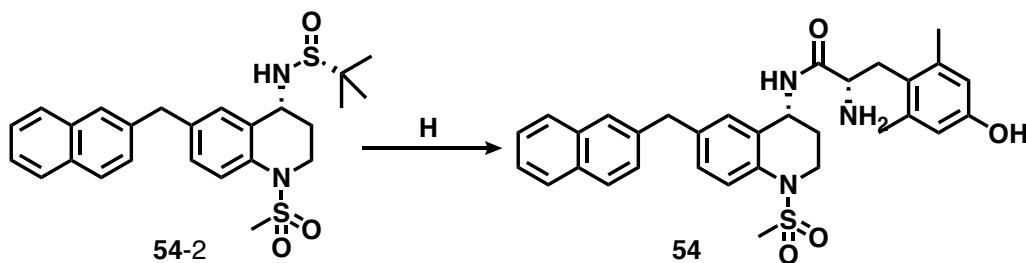


54-1 *1-(methylsulfonyl)-6-(naphthalen-2-ylmethyl)-2,3-dihydroquinolin-4(1H)-one*. Intermediate **54-1** was synthesized following **General Procedure (D)** from intermediate **48-2** (120 mg, 0.42 mmol, 1.0 eq), Et₃N (0.12 mL, 0.84 mmol, 2.0 eq), and methanesulfonyl chloride (0.06 mL, 0.84 mmol, 2.0 eq). Yield: 100 mg, 66%. ¹H NMR (500 MHz, Chloroform-*d*) δ 7.96 (d, *J* = 2.2 Hz, 1H), 7.78 (ddd, *J* = 13.2, 8.0, 2.5 Hz, 3H), 7.67 – 7.62 (m, 2H), 7.49 – 7.40 (m, 3H), 7.29 (dd, *J* = 8.5, 1.7 Hz, 1H), 4.16 (t, *J* = 5.8 Hz, 2H), 4.13 (s, 2H), 3.02 (d, *J* = 1.1 Hz, 3H), 2.83 (t, *J* = 6.5 Hz, 2H). ¹³C NMR (126 MHz, cdcl₃) δ 192.66, 140.80, 138.28, 137.59, 135.80, 133.69, 132.28, 128.52, 128.39, 127.76, 127.66, 127.36, 127.27, 126.31, 125.73, 125.01, 122.21, 46.09, 41.40, 40.05, 38.14.



54-2 *(R)-2-methyl-N-((R)-1-(methylsulfonyl)-6-(naphthalen-2-ylmethyl)-1,2,3,4-tetrahydroquinolin-4-yl)propane-2-sulfonamide*. Intermediate **54-2** was synthesized following **General Procedure (G)** from **54-1** (100 mg, 0.27 mmol, 1.0 eq), (R)-2-methyl-2-propanesulfonamide (100 mg, 0.82 mmol, 3.0 eq), and Ti(OEt)₄ (0.35 mL, 1.64 mmol, 6.0 eq), then

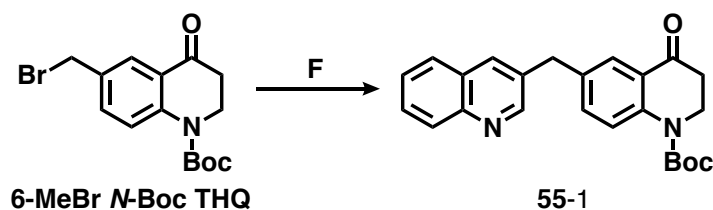
NaBH₄ (62 mg, 1.64 mmol, 6.0 eq). Yield: 74 mg, 57%. ¹H NMR (500 MHz, Chloroform-*d*) δ 7.81 – 7.74 (m, 3H), 7.70 (d, *J* = 8.6 Hz, 1H), 7.65 – 7.63 (m, 1H), 7.47 – 7.40 (m, 2H), 7.33 (d, *J* = 2.2 Hz, 1H), 7.31 (dd, *J* = 8.4, 1.8 Hz, 1H), 7.16 (dd, *J* = 8.6, 2.2 Hz, 1H), 4.57 (q, *J* = 3.7 Hz, 1H), 4.08 (s, 2H), 4.06 (td, *J* = 4.0, 2.0 Hz, 1H), 3.68 (ddd, *J* = 13.2, 11.3, 2.9 Hz, 1H), 3.25 (d, *J* = 2.4 Hz, 1H), 2.92 (s, 3H), 2.18 (dddd, *J* = 14.3, 4.9, 3.8, 2.9 Hz, 1H), 2.08 – 1.99 (m, 1H), 1.18 (s, 9H). ¹³C NMR (126 MHz, cdcl₃) δ 138.16, 137.89, 135.39, 133.71, 132.24, 130.81, 129.87, 128.36, 127.78, 127.73, 127.66, 127.49, 127.17, 126.20, 125.60, 121.75, 55.83, 50.04, 41.84, 41.41, 38.86, 28.88, 22.68.



54 (*S*)-2-amino-3-(4-hydroxy-2,6-dimethylphenyl)-*N*-((*R*)-1-(methylsulfonyl)-6-(naphthalen-2-ylmethyl)-1,2,3,4-tetrahydroquinolin-4-yl)propenamide. Final compound **54** was synthesized following **General Procedure (H)** from **54-2**. **Step 1:** Sulfinamide cleavage was carried out with **54-2** (74 mg, 0.16 mmol, 1.0 eq) and excess concentrated HCl (0.09 mL) precipitating product as a white solid, which was used without further purification. **Step 2:** Amide coupling was performed with the aminium chloride salt of **54-2** (60 mg, 0.15 mmol, 1.0 eq), di-Boc-Dmt (67 mg, 0.16 mmol, 1.1 eq), PyBOP (85 mg, 0.16 mmol, 1.1 eq), and 6-Cl HOBt (28 mg, 0.16 mmol, 1.1 eq), followed by DIPEA (0.26 mL, 1.49 mmol, 10 eq). Yield: 102 mg, 90%. Carried forward without characterization. **Step 3:** TFA deprotection, followed by purification by reverse-phase semi-preparative HPLC, as described in **General Procedure (H)**. Final yield not calculated. ¹H NMR

(500 MHz, Methanol- d_4) δ 7.78 (d, J = 7.8 Hz, 1H), 7.74 (d, J = 8.1 Hz, 2H), 7.65 – 7.59 (m, 2H), 7.46 – 7.38 (m, 2H), 7.28 (dd, J = 8.6, 1.6 Hz, 1H), 7.18 (d, J = 2.0 Hz, 1H), 7.16 – 7.13 (m, 1H), 6.50 (s, 2H), 4.99 (t, J = 5.0 Hz, 1H), 4.06 (s, 2H), 3.80 (td, J = 10.6, 9.7, 4.4 Hz, 2H), 3.24 (dd, J = 13.6, 11.6 Hz, 1H), 3.01 (dd, J = 13.7, 5.3 Hz, 1H), 2.95 (ddd, J = 13.0, 10.5, 2.3 Hz, 1H), 2.87 (d, J = 1.0 Hz, 3H), 2.26 (s, 6H), 1.94 – 1.85 (m, 1H), 1.58 – 1.49 (m, 1H). Calculated $[M+H]^+$: 558.3. ESI-MS mass observed: 558.3 (M+H) and 580.3 (M+Na). Analytical HPLC retention time: 41.4 min.

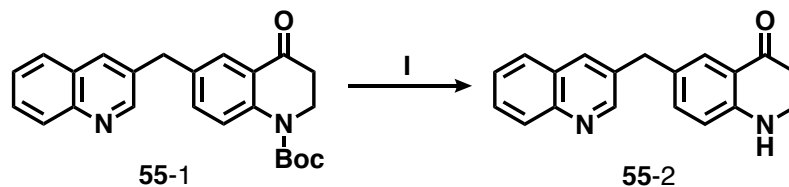
Compound 55



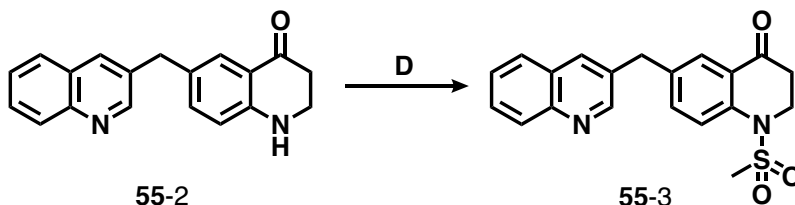
55-1 *tert-butyl 4-oxo-6-(quinolin-3-ylmethyl)-3,4-dihydroquinoline-1(2H)-carboxylate.*

Intermediate **55-1** was synthesized following **General Procedure (F)** from intermediate **6-MeBr N-Boc THQ** (250 mg, 0.73 mmol, 1.0 eq), 3-quinoline boronic acid (190 mg, 1.10 mmol, 1.5 eq), K_2CO_3 (302 mg, 2.19 mmol, 3.0 eq) and $Pd(dppf)Cl_2$ (51 mg, 0.07 mmol, 0.1 eq). Reaction was heated 24 hours. Yield: 248 mg, 87%. 1H NMR (500 MHz, Chloroform- d) δ 8.80 (d, J = 2.2 Hz, 1H), 8.09 – 8.05 (m, 1H), 7.90 – 7.88 (m, 2H), 7.76 – 7.71 (m, 2H), 7.67 (ddd, J = 8.4, 6.9, 1.5 Hz, 1H), 7.52 (ddd, J = 8.0, 6.8, 1.2 Hz, 1H), 7.35 (dd, J = 8.6, 2.3 Hz, 1H), 4.16 (s, 2H), 4.15 (t, J = 6.6, 6.0 Hz, 2H), 2.76 (dd, J = 6.8, 5.8 Hz, 2H), 1.54 (s, 9H). ^{13}C NMR (126 MHz, $cdCl_3$) δ 192.68,

152.86, 152.01, 142.96, 135.01, 134.69, 129.38, 129.14, 127.62, 127.48, 126.94, 125.11, 124.29, 82.42, 44.43, 39.10, 38.66, 28.44.

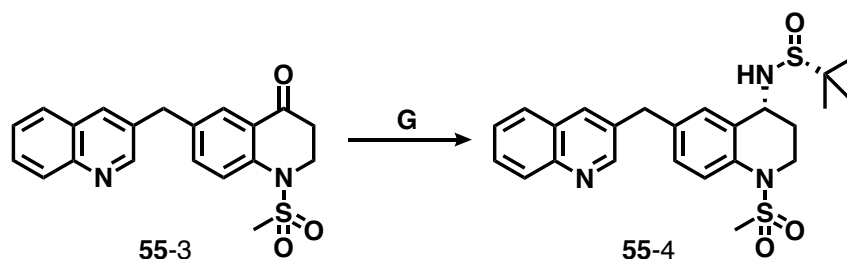


55-2 *6-(quinolin-3-ylmethyl)-2,3-dihydroquinolin-4(1H)-one*. Intermediate **55-2** was synthesized following **General Procedure (I)** from intermediate **55-1** (248 mg, 0.64 mmol, 1.0 eq) and 1:3 TFA/DCM (12 mL, excess). Yield: 184 mg, 100%. ^1H NMR (500 MHz, Chloroform-*d*) δ 8.79 (d, $J = 2.2$ Hz, 1H), 8.08 (dd, $J = 8.5, 1.1$ Hz, 1H), 7.96 (d, $J = 2.2$ Hz, 1H), 7.90 (dd, $J = 2.3, 1.0$ Hz, 1H), 7.80 (s, 1H), 7.75 (dd, $J = 8.2, 1.3$ Hz, 1H), 7.70 – 7.65 (m, 1H), 7.54 (ddd, $J = 8.1, 6.9, 1.2$ Hz, 1H), 7.49 (dd, $J = 8.5, 2.3$ Hz, 1H), 4.24 – 4.20 (m, 4H), 2.89 (t, $J = 6.2$ Hz, 2H). ^{13}C NMR (126 MHz, cdCl_3) δ 192.05, 151.81, 147.24, 135.14, 134.99, 132.64, 129.41, 129.33, 128.15, 127.99, 127.61, 127.08, 126.77, 45.70, 39.40, 38.80.

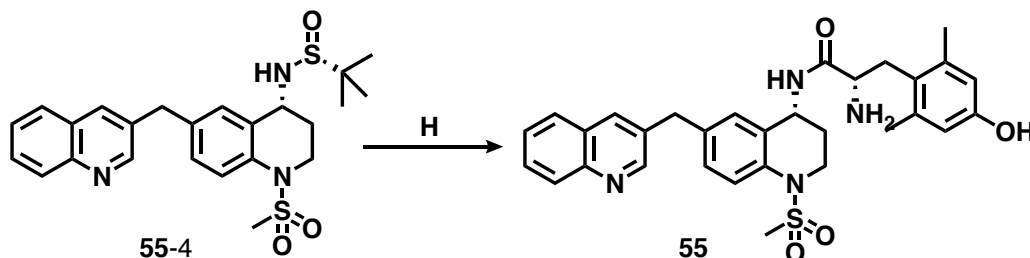


55-3 *1-(methylsulfonyl)-6-(quinolin-3-ylmethyl)-2,3-dihydroquinolin-4(1H)-one*. Intermediate **55-2** was synthesized following **General Procedure (D)** from intermediate **55-2** (184 mg, 0.64 mmol, 1.0 eq), Et_3N (0.27 mL, 1.92 mmol, 3.0 eq), and methanesulfonyl chloride (0.10 mL, 1.28 mmol, 2.0 eq). Yield: 151 mg, 65%. ^1H NMR (500 MHz, Chloroform-*d*) δ 8.76 (t, $J = 1.8$ Hz, 1H), 8.05 (d, $J = 8.4$ Hz, 1H), 7.92 (d, $J = 2.2$ Hz, 1H), 7.88 (d, $J = 2.1$ Hz, 1H), 7.75 – 7.72 (m, 1H), 7.68 –

7.63 (m, 2H), 7.50 (ddt, $J = 7.8, 6.6, 1.5$ Hz, 1H), 7.40 (dt, $J = 8.6, 2.0$ Hz, 1H), 4.14 (t, $J = 6.5$ Hz, 2H), 4.14 (s, 2H), 3.03 (d, $J = 1.6$ Hz, 3H), 2.82 (t, $J = 6.4$ Hz, 2H). ^{13}C NMR (126 MHz, cdCl_3) δ 192.43, 151.77, 147.07, 141.09, 136.82, 135.57, 134.97, 132.85, 129.25, 129.19, 128.37, 128.06, 127.53, 126.96, 125.04, 122.30, 46.01, 40.04, 38.48, 38.06.



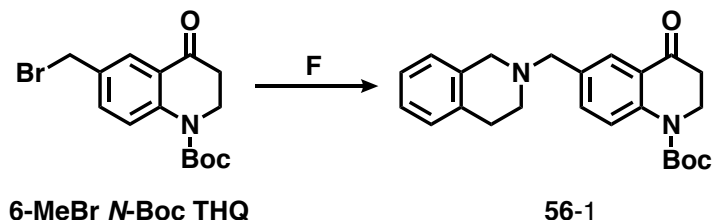
55-4 (*R*)-2-methyl-*N*-((*R*)-1-(methylsulfonyl)-6-(quinolin-3-ylmethyl)-1,2,3,4-tetrahydroquinolin-4-yl)propane-2-sulfonamide. Intermediate **55-4** was synthesized following **General Procedure (G)** from intermediate **55-3** (70 mg, 0.19 mmol, 1.0 eq), (*R*)-2-methyl-2-propanesulfonamide (70 mg, 0.57 mmol, 3.0 eq), and $\text{Ti}(\text{OEt})_4$ (0.24 mL, 1.15 mmol, 6.0 eq), then NaBH_4 (44 mg, 1.15 mmol, 6.0 eq). Yield: 47 mg, 52%. Intermediate **55-4** not characterized by NMR until after sulfonamide cleavage (see Final Compound **55** Step 1).



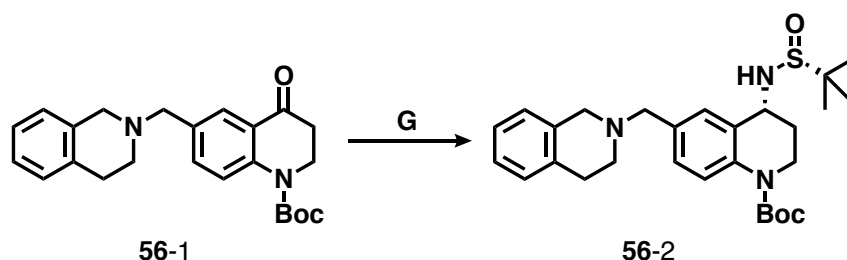
55 (*S*)-2-amino-3-(4-hydroxy-2,6-dimethylphenyl)-*N*-((*R*)-1-(methylsulfonyl)-6-(quinolin-3-ylmethyl)-1,2,3,4-tetrahydroquinolin-4-yl)propanamide. Final compound **55** was synthesized following **General Procedure (H)** from intermediate **55-4**. **Step 1:** Sulfonamide cleavage was carried out with **55-4** (47 mg, 0.10 mmol, 1.0 eq) and excess concentrated HCl (0.06 mL)

precipitating product as a white solid, which was used without further purification. ^1H NMR (500 MHz, Methanol- d_4) δ 9.25 (d, $J = 2.0$ Hz, 1H), 9.14 – 9.11 (m, 1H), 8.35 – 8.32 (m, 1H), 8.26 (d, $J = 8.7$ Hz, 1H), 8.15 (ddd, $J = 8.5, 7.0, 1.3$ Hz, 1H), 7.97 (ddd, $J = 8.1, 7.0, 1.1$ Hz, 1H), 7.79 (d, $J = 8.7$ Hz, 1H), 7.66 – 7.62 (m, 1H), 7.43 (dd, $J = 8.7, 2.2$ Hz, 1H), 4.65 (t, $J = 5.7$ Hz, 1H), 4.44 (s, 2H), 4.03 (ddd, $J = 13.9, 6.9, 3.6$ Hz, 1H), 3.86 – 3.78 (m, 1H), 3.09 (s, 2H), 2.46 – 2.33 (m, 1H), 2.23 – 2.15 (m, 1H). **Step 2:** Amide coupling was performed with the aminium chloride salt of **55-4** (40 mg, 0.10 mmol, 1.0 eq), di-Boc-Dmt (49 mg, 0.12 mmol, 1.2 eq), and PyBOP (63 mg, 0.12 mmol, 1.2 eq), followed by DIPEA (0.18 mL, 1.00 mmol, 10 eq). Yield: 102 mg, 90%. Carried forward without characterization. **Step 3:** TFA deprotection, followed by purification by reverse-phase semi-preparative HPLC, as described in **General Procedure (H)**. Final yield not calculated. ^1H NMR (500 MHz, Methanol- d_4) δ 8.85 (d, $J = 3.9$ Hz, 1H), 8.45 (s, 1H), 8.07 (d, $J = 8.7$ Hz, 1H), 8.02 (d, $J = 9.1$ Hz, 1H), 7.90 (d, $J = 8.6$ Hz, 1H), 7.74 (t, $J = 7.5$ Hz, 1H), 7.66 (d, $J = 8.7$ Hz, 1H), 7.24 (d, $J = 2.2$ Hz, 1H), 7.18 (dd, $J = 8.7, 2.2$ Hz, 1H), 6.50 (s, 2H), 5.01 (t, $J = 5.1$ Hz, 1H), 4.20 (s, 2H), 3.87 – 3.76 (m, 2H), 3.25 (dd, $J = 13.6, 11.6$ Hz, 1H), 3.06 – 2.94 (m, 2H), 2.90 (s, 3H), 2.26 (s, 6H), 1.89 (ddt, $J = 14.2, 9.4, 4.3$ Hz, 1H), 1.53 (dt, $J = 13.8, 7.0$ Hz, 1H). Calculated $[\text{M}+\text{H}]^+$: 559.3. ESI-MS mass observed: 559.3 (M+H) and 581.3 (M+Na). Analytical HPLC retention time: 23.6 min.

Compound 56

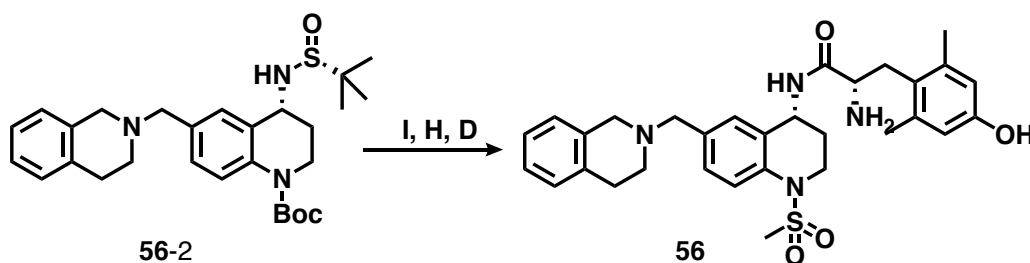


56-1 *tert-butyl 6-((3,4-dihydroisoquinolin-2(1H)-yl)methyl)-4-oxo-3,4-dihydroquinoline-1(2H)-carboxylate*. **56-1** was synthesized following **General Procedure (F)** from intermediate **6-MeBr N-Boc THQ** (500 mg, 1.47 mmol, 1.0 eq), K_2CO_3 (243 mg, 1.76 mmol, 1.2 eq) and THIQ (0.23 mL, 1.76 mmol, 1.2 eq). Yield: 519 mg, 90%. 1H NMR (500 MHz, Chloroform-*d*) δ 7.95 (d, $J = 2.2$ Hz, 1H), 7.75 (d, $J = 8.6$ Hz, 1H), 7.59 (dd, $J = 8.6, 2.2$ Hz, 1H), 7.10 (tdd, $J = 8.8, 4.6, 2.4$ Hz, 3H), 6.97 (dd, $J = 7.8, 1.7$ Hz, 1H), 4.19 – 4.14 (m, 2H), 3.66 (s, 2H), 3.62 (s, 2H), 2.89 (t, $J = 5.9$ Hz, 2H), 2.80 – 2.71 (m, 4H), 1.56 (s, 9H). ^{13}C NMR (126 MHz, $cdCl_3$) δ 194.41, 152.92, 143.39, 134.95, 134.85, 134.43, 128.83, 127.68, 126.70, 126.27, 125.73, 124.70, 123.88, 82.34, 61.97, 56.15, 50.74, 44.48, 39.14, 29.27, 28.46.



56-2 *tert-butyl (R)-4-(((R)-tert-butylsulfinyl)amino)-6-((3,4-dihydroisoquinolin-2(1H)-yl)methyl)-3,4-dihydroquinoline-1(2H)-carboxylate*. Intermediate **56-2** was synthesized following **General Procedure (G)** from **56-1** (244 mg, 0.62 mmol, 1.0 eq), (R)-2-methyl-2-propanesulfonamide (225 mg, 1.86 mmol, 3.0 eq), and $Ti(OEt)_4$ (0.78 mL, 3.73 mmol, 6.0 eq), then $NaBH_4$ (141 mg, 3.73

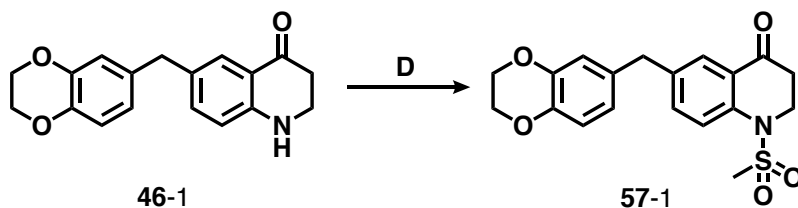
mmol, 6.0 eq). Yield: 281 mg, 91%. ^1H NMR (500 MHz, Chloroform-*d*) δ 7.82 (dd, $J = 12.9, 8.6$ Hz, 1H), 7.43 (dd, $J = 4.8, 2.1$ Hz, 1H), 7.25 – 7.20 (m, 2H), 7.19 – 7.14 (m, 2H), 7.05 – 6.98 (m, 1H), 4.57 (dq, $J = 7.2, 3.7$ Hz, 1H), 4.06 – 3.88 (m, 5H), 3.58 (ddt, $J = 12.8, 11.2, 3.7$ Hz, 1H), 3.30 – 3.19 (m, 2H), 3.15 – 2.94 (m, 2H), 2.21 (tq, $J = 12.5, 4.2$ Hz, 1H), 1.99 (tt, $J = 10.3, 3.2$ Hz, 1H), 1.52 (d, $J = 1.3$ Hz, 9H), 1.22 (d, $J = 4.2$ Hz, 9H). ^{13}C NMR (126 MHz, cdCl_3) δ 139.11, 138.45, 136.54, 134.47, 132.41, 132.18, 131.16, 128.61, 127.28, 126.72, 125.92, 123.11, 63.64, 62.69, 57.30, 54.85, 50.36, 40.26, 29.25, 28.30, 24.72, 22.60.



56 (*S*)-2-amino-*N*-((*R*)-6-((3,4-dihydroisoquinolin-2(*1H*)-yl)methyl)-1-(methylsulfonyl)-1,2,3,4-tetrahydroquinolin-4-yl)-3-(4-hydroxy-2,6-dimethylphenyl)propanamide. **56** was synthesized following **General Procedures (I), (H)** and **(D)** from intermediate **56-2**. Intermediate **56-2** (150 mg, 0.30 mmol) was Boc deprotected with 1:1 TFA/DCM (15 mL) as described in **General Procedure (I)**. Crude product was carried forward without further characterization. **General Procedure (H) Step 1:** Sulfinamide cleavage was carried out with Boc-deprotected **56-2** and excess concentrated HCl, precipitating product as a white solid, a portion of which was used without further purification in subsequent steps. **Step 2:** Amide coupling was performed with the aminium chloride salt of **56-2** (29 mg, 0.08 mmol, 1.0 eq), di-Boc-Dmt (39 mg, 0.10 mmol, 1.2 eq), and PyBOP (50 mg, 0.10 mmol, 1.2 eq), followed by DIPEA (0.14 mL, 0.78 mmol, 10 eq). Product was purified by silica chromatography, yielding 22 mg (0.03 mmol) of amide-coupled

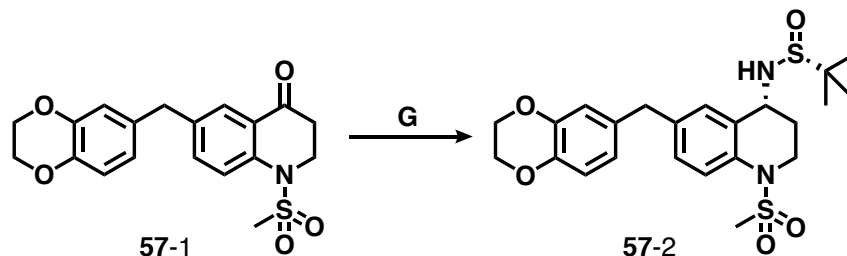
product, which was then sulfonylated following **General Procedure (D)** with methanesulfonyl chloride (0.03 mL, 0.04 mmol, 1.2 eq) and Et₃N (0.06 mL, 0.04 mmol, 1.2 eq). Sulfonylated, di-Boc-Dmt coupled product was then purified by silica chromatography before **Step 3**: Boc-deprotecting with 1:1 TFA/DCM (5 mL). Final compound **56** was purified by reverse-phase semi-preparative HPLC, as described in **General Procedure (H)**. Final yield not calculated. ¹H NMR (500 MHz, Methanol-*d*₄) δ 7.81 (d, *J* = 8.7 Hz, 1H), 7.47 – 7.43 (m, 1H), 7.40 (dd, *J* = 8.7, 2.2 Hz, 1H), 7.33 – 7.28 (m, 1H), 7.28 – 7.23 (m, 2H), 7.15 (d, *J* = 7.7 Hz, 1H), 6.51 (s, 2H), 5.04 (t, *J* = 5.3 Hz, 1H), 4.41 (s, 2H), 4.37 (s, 2H), 3.89 – 3.80 (m, 2H), 3.29 – 3.23 (m, 1H), 3.18 (s, 2H), 3.11 – 3.01 (m, 2H), 3.00 (s, 3H), 2.28 (s, 6H), 1.90 (ddt, *J* = 14.3, 9.3, 4.7 Hz, 1H), 1.60 – 1.52 (m, 1H). Calculated [M+H]⁺: 563.3. ESI-MS mass observed: 563.3 (M+H) and 585.3 (M+Na). Analytical HPLC retention time: 23.9 min.

Compound 57

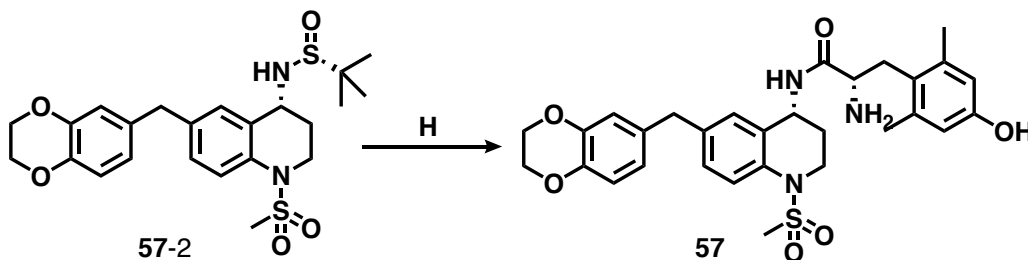


57-1 6-((2,3-dihydrobenzo[*b*][1,4]dioxin-6-yl)methyl)-1-(methylsulfonyl)-2,3-dihydroquinolin-4(1*H*)-one. **57-1** was synthesized following **General Procedure (D)** from **46-1** (100 mg, 0.34 mmol, 1.0 eq), Et₃N (0.10 mL, 0.68 mmol, 2.0 eq), and methanesulfonyl chloride (0.05 mL, 0.68 mmol, 2.0 eq). Yield: 70 mg, 56%. ¹H NMR (500 MHz, Chloroform-*d*) δ 7.88 (d, *J* = 2.3 Hz, 1H), 7.64 (d, *J* = 8.5 Hz, 1H), 7.37 (dd, *J* = 8.6, 2.3 Hz, 1H), 6.78 (d, *J* = 8.9 Hz, 1H), 6.65 (s, 1H), 4.23

(s, 4H), 4.17 (t, $J = 6.4$ Hz, 2H), 3.86 (s, 2H), 3.04 (s, 3H), 2.84 (t, $J = 6.5$ Hz, 2H). ^{13}C NMR (126 MHz, cdCl_3) δ 192.70, 142.31, 140.71, 138.70, 135.76, 133.46, 128.30, 125.03, 122.24, 121.88, 117.65, 117.51, 64.54, 64.45, 46.16, 40.49, 40.11, 38.18.

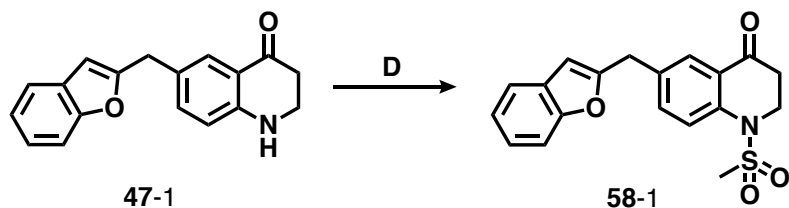


57-2 *(R)-N-((R)-6-((2,3-dihydrobenzo[*b*][1,4]dioxin-6-yl)methyl)-1-(methylsulfonyl)-1,2,3,4-tetrahydroquinolin-4-yl)-2-methylpropane-2-sulfonamide*. Intermediate **57-2** was synthesized following **General Procedure (G)** from **57-1** (70 mg, 0.19 mmol, 1.0 eq), (R)-2-methyl-2-propanesulfonamide (66 mg, 0.56 mmol, 3.0 eq), and $\text{Ti}(\text{OEt})_4$ (0.23 mL, 1.12 mmol, 6.0 eq), then NaBH_4 (42 mg, 1.12 mmol, 6.0 eq). Yield: 65 mg, 72%. ^1H NMR (500 MHz, Chloroform-*d*) δ 7.69 (d, $J = 8.6$ Hz, 1H), 7.23 (d, $J = 2.1$ Hz, 1H), 7.10 (dd, $J = 8.6, 2.2$ Hz, 1H), 6.77 (d, $J = 8.9$ Hz, 1H), 6.68 – 6.62 (m, 2H), 4.57 (q, $J = 4.4$ Hz, 3H), 4.23 (s, 4H), 4.09 (dt, $J = 13.2, 4.3$ Hz, 1H), 3.81 (s, 2H), 3.66 (ddd, $J = 13.6, 11.5, 2.9$ Hz, 1H), 2.93 (s, 3H), 2.23 – 2.14 (m, 1H), 2.09 – 1.98 (m, 1H), 1.21 (s, 9H). ^{13}C NMR (126 MHz, cdCl_3) δ 143.56, 138.19, 135.30, 133.99, 130.66, 129.85, 127.63, 124.34, 121.87, 121.72, 117.62, 117.39, 64.45, 55.85, 49.90, 41.76, 40.43, 38.87, 28.72, 22.74.

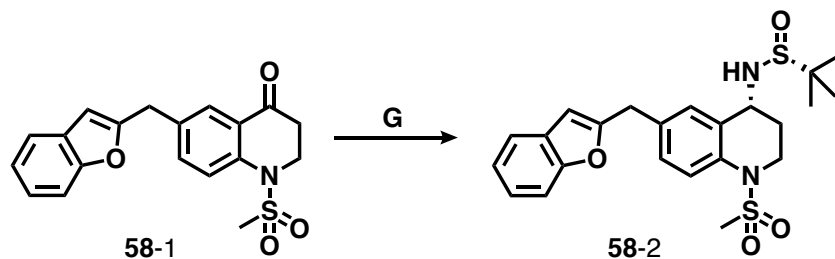


57 *(S)*-2-amino-*N*-((*R*)-6-((2,3-dihydrobenzo[*b*][1,4]dioxin-6-yl)methyl)-1-(methylsulfonyl)-1,2,3,4-tetrahydroquinolin-4-yl)-3-(4-hydroxy-2,6-dimethylphenyl)propenamide. **57** was synthesized following **General Procedure (H)** from intermediate **57-2**. **Step 1:** Sulfinamide cleavage was carried out with **57-2** (65 mg, 0.13 mmol, 1.0 eq) and excess concentrated HCl (0.06 mL) precipitating product as a white solid, which was used without further purification. **Step 2:** Amide coupling was performed with the aminium chloride salt of **57-2** (56 mg, 0.14 mmol, 1.0 eq), di-Boc-Dmt (61 mg, 0.15 mmol, 1.1 eq), and PyBOP (78 mg, 0.15 mmol, 1.1 eq), followed by DIPEA (0.24 mL, 1.36 mmol, 10 eq). After purification by silica chromatography, product was carried forward to **Step 3:** TFA deprotection, followed by purification by reverse-phase semi-preparative HPLC, as described in **General Procedure (H)**. Final yield not calculated. ¹H NMR (500 MHz, Methanol-*d*₄) δ 7.58 (d, *J* = 8.6 Hz, 1H), 7.09 (d, *J* = 2.1 Hz, 1H), 7.02 (dd, *J* = 8.6, 2.2 Hz, 1H), 6.70 – 6.67 (m, 1H), 6.59 (d, *J* = 7.7 Hz, 2H), 6.49 (s, 2H), 4.97 (q, *J* = 5.1 Hz, 1H), 4.16 (s, 4H), 3.85 (dd, *J* = 11.5, 5.1 Hz, 1H), 3.77 (ddd, *J* = 14.0, 6.1, 3.6 Hz, 1H), 3.74 (s, 2H), 3.25 (dd, *J* = 13.6, 11.6 Hz, 1H), 3.04 (dd, *J* = 13.7, 5.2 Hz, 1H), 2.93 (ddd, *J* = 13.5, 10.5, 2.7 Hz, 1H), 2.84 (s, 3H), 2.26 (s, 6H), 1.87 (dddd, *J* = 14.0, 10.6, 5.4, 3.5 Hz, 1H), 1.51 (dddd, *J* = 13.7, 5.9, 4.6, 2.7 Hz, 1H). ¹³C NMR (500 MHz, cd₃od) δ 168.91, 168.83, 157.41, 144.81, 143.40, 140.04, 139.18, 136.58, 135.40, 131.53, 130.15, 127.93, 123.27, 122.83, 122.54, 118.32, 118.05, 116.44, 111.39, 65.60, 65.50, 53.37, 49.00, 46.65, 43.67, 41.13, 38.76, 31.84, 29.18, 20.45. Calculated [M+H]⁺: 566.2. ESI-MS mass observed: 566.2 (M+H) and 588.2 (M+Na). Analytical HPLC retention time: 34.1 min.

Compound 58

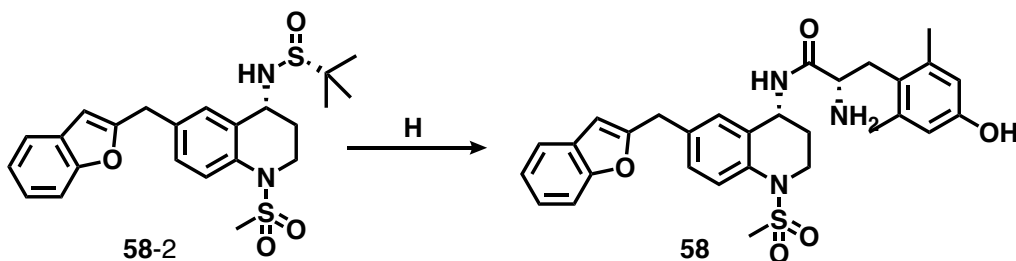


58-1 6-(benzofuran-2-ylmethyl)-1-(methylsulfonyl)-2,3-dihydroquinolin-4(1H)-one. **58-1** was synthesized following **General Procedure (D)** from **47-1** (80 mg, 0.29 mmol, 1.0 eq), Et₃N (0.09 mL, 0.58 mmol, 2.0 eq), and methanesulfonyl chloride (0.05 mL, 0.58 mmol, 2.0 eq). Yield: 31 mg, 30%. ¹H NMR (500 MHz, Chloroform-*d*) δ 8.01 (d, *J* = 2.3 Hz, 1H), 7.70 (d, *J* = 8.6 Hz, 1H), 7.52 (dd, *J* = 8.6, 2.4 Hz, 1H), 7.48 (dd, *J* = 7.7, 1.5 Hz, 1H), 7.39 (d, *J* = 8.3 Hz, 1H), 7.21 (dd, *J* = 7.9, 1.6 Hz, 1H), 7.19 (dd, *J* = 7.4, 1.2 Hz, 1H), 6.44 (s, 1H), 4.19 (t, *J* = 6.3 Hz, 2H), 4.11 (s, 2H), 3.06 (s, 3H), 2.86 (t, *J* = 6.5 Hz, 2H). ¹³C NMR (126 MHz, cdCl₃) δ 192.49, 176.33, 156.49, 141.30, 135.74, 134.54, 128.60, 125.08, 123.86, 122.83, 122.27, 120.71, 111.09, 103.87, 46.15, 40.15, 38.17, 34.31, 28.43.



58-2 (*R*)-*N*-((*R*)-6-(benzofuran-2-ylmethyl)-1-(methylsulfonyl)-1,2,3,4-tetrahydroquinolin-4-yl)-2-methylpropane-2-sulfonamide. **58-2** was synthesized following **General Procedure (G)** from **58-1** (31 mg, 0.09 mmol, 1.0 eq), (*R*)-2-methyl-2-propanesulfonamide (32 mg, 0.26 mmol, 3.0 eq),

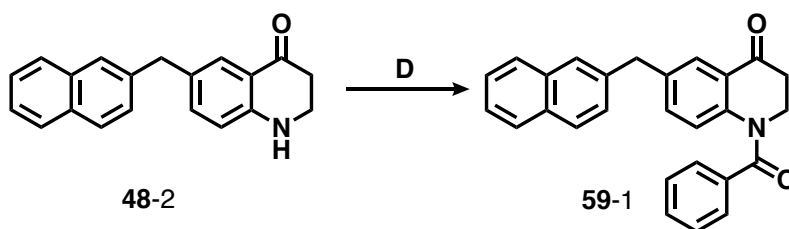
and $\text{Ti}(\text{OEt})_4$ (0.11 mL, 0.52 mmol, 6.0 eq), then NaBH_4 (20 mg, 0.52 mmol, 6.0 eq). Yield: 38 mg, 95%. ^1H NMR (500 MHz, Chloroform-*d*) δ 7.74 (d, $J = 8.6$ Hz, 1H), 7.50 – 7.44 (m, 1H), 7.38 (q, $J = 2.9, 1.7$ Hz, 2H), 7.24 (dd, $J = 8.6, 2.2$ Hz, 1H), 7.20 (td, $J = 7.7, 1.7$ Hz, 1H), 7.18 (dd, $J = 7.4, 1.3$ Hz, 1H), 6.43 (d, $J = 1.0$ Hz, 1H), 4.59 (q, $J = 3.7$ Hz, 1H), 4.09 (dt, $J = 13.3, 4.4$ Hz, 1H), 4.06 (s, 2H), 3.68 (ddd, $J = 13.2, 11.4, 2.9$ Hz, 1H), 2.94 (s, 3H), 2.19 (ddd, $J = 14.3, 7.8, 3.4$ Hz, 1H), 2.05 (ddt, $J = 14.8, 11.1, 4.0$ Hz, 1H), 1.20 (s, 9H). ^{13}C NMR (126 MHz, cdCl_3) δ 157.00, 155.08, 135.93, 134.04, 130.89, 129.88, 128.80, 127.82, 123.69, 122.74, 121.78, 120.64, 115.06, 111.03, 103.60, 77.16, 55.89, 50.03, 41.82, 38.90, 34.23, 28.84, 22.25.



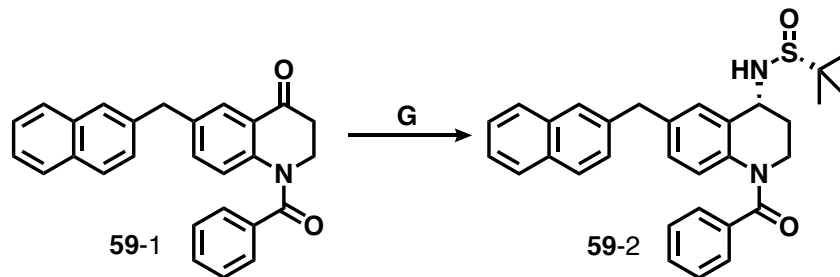
58 (*S*)-2-amino-*N*-((*R*)-6-(benzofuran-2-ylmethyl)-1-(methylsulfonyl)-1,2,3,4-tetrahydroquinolin-4-yl)-3-(4-hydroxy-2,6-dimethylphenyl)propenamide. **58** was synthesized following **General Procedure (H)** from intermediate **58-2**. **Step 1:** Sulfonamide cleavage was carried out with **58-2** (38 mg, 0.08 mmol, 1.0 eq) and excess concentrated HCl (0.05 mL) precipitating product as a white solid, which was used without further purification. **Step 2:** Amide coupling was performed with the aminium chloride salt of **58-2** (32 mg, 0.081 mmol, 1.0 eq), di-Boc-Dmt (37 mg, 0.089 mmol, 1.1 eq), and PyBOP (47 mg, 0.089 mmol, 1.1 eq), followed by DIPEA (0.14 mL, 0.81 mmol, 10 eq). After purification by silica chromatography, product was carried forward to **Step 3:** TFA deprotection, followed by purification by reverse-phase semi-preparative HPLC, as described in **General Procedure (H)**. Final yield not calculated. ^1H NMR (500 MHz, Methanol-*d*₄) δ 7.66

(d, $J = 8.5$ Hz, 1H), 7.48 – 7.43 (m, 1H), 7.32 (d, $J = 8.0$ Hz, 1H), 7.22 (s, 1H), 7.20 (dd, $J = 8.4$, 2.0 Hz, 1H), 7.17 (dd, $J = 7.9$, 1.6 Hz, 1H), 7.14 (td, $J = 7.4$, 1.1 Hz, 1H), 6.49 (s, 2H), 6.43 (d, $J = 1.0$ Hz, 1H), 5.01 (t, $J = 5.0$ Hz, 1H), 4.03 (d, $J = 5.0$ Hz, 2H), 3.81 (td, $J = 10.9$, 10.4, 4.3 Hz, 2H), 3.26 – 3.21 (m, 1H), 3.02 (dd, $J = 13.7$, 5.2 Hz, 1H), 2.96 (ddd, $J = 13.4$, 10.4, 2.7 Hz, 1H), 2.88 (s, 3H), 2.26 (s, 6H), 1.89 (ddd, $J = 14.2$, 9.4, 4.6 Hz, 1H), 1.56 – 1.50 (m, 1H). Calculated $[M+H]^+$: 548.2. ESI-MS mass observed: 548.2 (M+H) and 570.2 (M+Na). Analytical HPLC retention time: 38.7 min.

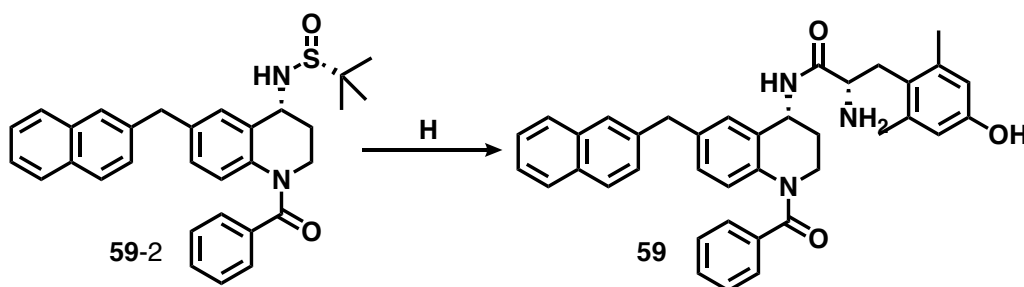
Compound 59



59-1 *1-benzoyl-6-(naphthalen-2-ylmethyl)-2,3-dihydroquinolin-4(1H)-one*. Intermediate **59-1** was synthesized following **General Procedure (D)** from intermediate **48-2** (45 mg, 0.158 mmol, 1.0 eq) and benzoyl chloride (0.04 mL, 0.31 mmol, 2.0 eq). Yield: 38 mg, 62%. ^1H NMR (500 MHz, CDCl_3) δ 7.92 (d, $J = 2.2$ Hz, 1H), 7.79 (dd, $J = 7.5$, 1.7 Hz, 1H), 7.76 (d, $J = 7.9$ Hz, 2H), 7.60 (s, 1H), 7.49 (m, 2H), 7.43 (m, 3H), 7.36 (m, 2H), 7.26 (dd, $J = 8.3$, 2.0 Hz, 1H), 7.13 (dd, $J = 8.5$, 2.2 Hz, 1H), 6.89 (d, $J = 8.5$ Hz, 1H), 4.30 (t, $J = 6.1$ Hz, 2H), 4.09 (s, 2H), 2.85 (t, $J = 6.4$ Hz, 2H). ^{13}C NMR (126 MHz, CDCl_3) δ 193.88, 170.23, 142.81, 138.09, 137.62, 135.18, 134.52, 133.66, 132.26, 131.17, 128.63, 128.61, 128.43, 127.74, 127.63, 127.61, 127.37, 127.26, 126.25, 125.67, 125.00, 124.83, 45.44, 41.43, 39.64.



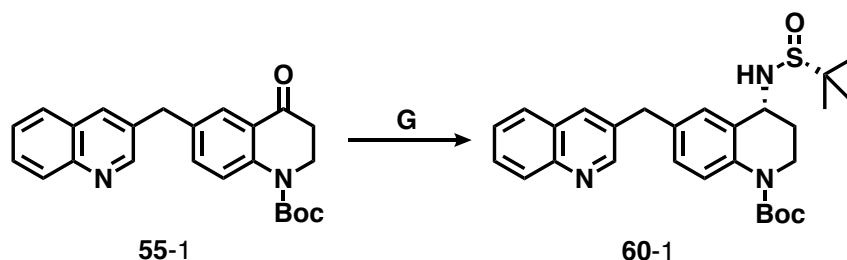
59-2 *(R)-N-((R)-1-benzoyl-6-(naphthalen-2-ylmethyl)-1,2,3,4-tetrahydroquinolin-4-yl)-2-methylpropane-2-sulfonamide*. Intermediate **59-2** was synthesized following **General Procedure (G)** from intermediate **59-1** (38 mg, 0.10 mmol, 1.0 eq), (R)-2-methyl-2-propanesulfonamide (35 mg, 0.29 mmol, 3.0 eq), and $\text{Ti}(\text{OEt})_4$ (0.12 mL, 0.58 mmol, 6.0 eq), then NaBH_4 (15 mg, 0.04 mmol, 4.0 eq). Yield: 25 mg, 52%. ^1H NMR (500 MHz, CDCl_3) δ 7.78 (m, 3H), 7.61 (s, 1H), 7.45 (m, 2H), 7.39 (m, 3H), 7.32 (m, 3H), 7.28 (dd, $J = 8.6, 1.7$ Hz, 1H), 6.89 (m, 2H), 4.62 (q, $J = 4.1$ Hz, 1H), 4.06 (s, 2H), 4.01 (dt, $J = 12.9, 5.1$ Hz, 1H), 3.81 (ddd, $J = 13.0, 10.0, 4.9$ Hz, 1H), 3.45 (m, 1H), 2.29 (dq, $J = 14.0, 4.7$ Hz, 1H), 2.10 (ddt, $J = 14.5, 10.0, 5.1$ Hz, 1H), 1.18 (s, 9H). ^{13}C NMR (126 MHz, CDCl_3) δ 170.44, 138.20, 138.11, 136.95, 136.11, 133.70, 132.22, 130.55, 130.12, 128.98, 128.60, 128.53, 128.43, 128.30, 127.73, 127.66, 127.57, 127.21, 126.81, 125.57, 55.96, 50.88, 41.56, 41.57, 30.41, 22.70



59 *(S)-2-amino-N-((R)-1-benzoyl-6-(naphthalen-2-ylmethyl)-1,2,3,4-tetrahydroquinolin-4-yl)-3-(4-hydroxy-2,6-dimethylphenyl)propenamide*. Final compound **59** was synthesized following

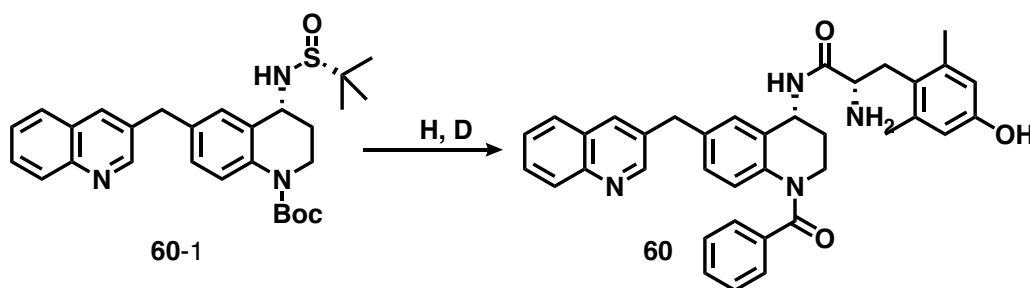
General Procedure (H) from intermediate **59-2**. **Step 1:** Sulfinamide cleavage was carried out with **59-2** (25 mg, 0.05 mmol, 1.0 eq) and excess concentrated HCl, precipitating product as a white solid, which was used without further purification. **Step 2:** Amide coupling was performed with the aminium chloride salt of **59-2** (21 mg, 0.05 mmol, 1.0 eq), di-Boc-Dmt (21 mg, 0.05 mmol, 1.05 eq), 6-Cl HOBt (8 mg, 0.05 mmol, 1.0 eq), and PyBOP (25 mg, 0.05 mmol, 1.0 eq), followed by DIPEA (0.07 mL, 0.49 mmol, 10 eq). After purification by silica chromatography, uncharacterized product was carried forward to **Step 3:** TFA deprotection, followed by purification by reverse-phase semi-preparative HPLC, as described in **General Procedure (H)**. Final yield not calculated. ¹H NMR (500 MHz, Methanol-*d*₄) δ 8.26 (d, *J* = 8.3 Hz, 1H), 7.78 (dd, *J* = 7.6, 1.2 Hz, 1H), 7.73 (d, *J* = 8.8 Hz, 2H), 7.55 (s, 1H), 7.40 (m, 7H), 7.25 (dd, *J* = 8.3, 1.5 Hz, 1H), 7.21 (s, 1H), 6.87 (br. s, 2H), 6.49 (s, 2H), 5.05 (m, 1H), 4.04 (s, 2H), 3.87 (m, 2H), 3.36 (m, 1H), 3.25 (dd, *J* = 13.7, 11.7 Hz, 1H), 3.05 (dd, *J* = 13.7, 5.4 Hz, 1H), 2.27 (s, 6H), 1.94 (m, 1H), 1.50 (m, 1H). Calculated [M+H]⁺: 584.3. ESI-MS mass observed: 584.3. (M+H). Analytical HPLC retention time: 45.0 min.

Compound 60



60-1 *tert-butyl* (*R*)-4-(((*R*)-*tert*-butylsulfinyl)amino)-6-(quinolin-3-ylmethyl)-3,4-dihydroquinoline-1(2*H*)-carboxylate. Intermediate **60-1** was synthesized following **General**

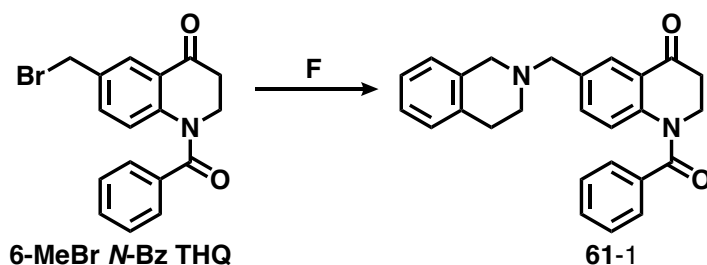
Procedure (G) from intermediate **55-1** (135 mg, 0.35 mmol, 1.0 eq), (R)-2-methyl-2-propanesulfonamide (127 mg, 1.04 mmol, 3.0 eq), and Ti(OEt)₄ (0.44 mL, 2.09 mmol, 6.0 eq), then NaBH₄ (53 mg, 1.39 mmol, 4.0 eq). Yield: 11 mg, 8%. ¹H NMR (500 MHz, Chloroform-*d*) δ 9.05 – 9.01 (m, 1H), 8.90 (d, *J* = 8.9 Hz, 1H), 8.24 (d, *J* = 2.1 Hz, 1H), 7.90 – 7.84 (m, 2H), 7.78 (d, *J* = 8.7 Hz, 1H), 7.69 (ddd, *J* = 8.1, 6.9, 1.1 Hz, 1H), 7.29 (d, *J* = 2.1 Hz, 1H), 7.09 (dd, *J* = 8.6, 2.2 Hz, 1H), 4.54 (q, *J* = 4.0 Hz, 1H), 4.13 (d, *J* = 1.6 Hz, 2H), 3.95 (dt, *J* = 12.9, 4.7 Hz, 1H), 3.61 (ddd, *J* = 13.1, 10.9, 4.0 Hz, 1H), 2.17 (dq, *J* = 13.4, 4.4 Hz, 1H), 2.00 (ddt, *J* = 14.4, 10.0, 4.3 Hz, 1H), 1.52 (s, 9H), 1.19 (s, 9H).



60 (*S*)-2-amino-*N*-((*R*)-1-benzoyl-6-(quinolin-3-ylmethyl)-1,2,3,4-tetrahydroquinolin-4-yl)-3-(4-hydroxy-2,6-dimethylphenyl)propanamide. **60** was synthesized following **General Procedures (H)** and **(D)** from intermediate **60-1**. **Step 1:** Sulfonamide cleavage was carried out with **60-1** (11 mg, 0.028 mmol) and excess concentrated HCl, precipitating product as a white solid, which was used without further purification. **Step 2:** Amide coupling was performed with the aminium chloride salt of **60-1** (9 mg, 0.028 mmol, 1.00 eq), di-Boc-Dmt (12 mg, 0.029 mmol, 1.05 eq), 6-Cl HOBt (5 mg, 0.028 mmol, 1.00 eq), and PyBOP (15 mg, 0.028 mmol, 1.00 eq), followed by DIPEA (0.04 mL, 0.28 mmol, 10 eq). Product was benzoylated as described in **General Procedure (D)**. Crude product was carried forward to **Step 3:** Boc-deprotection with 1:1 TFA/DCM (2 mL), followed by purification by reverse-phase semi-preparative HPLC, as described in **General**

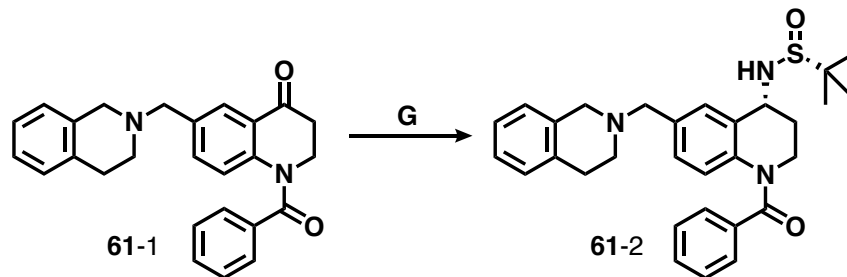
Procedure (H). Final yield not calculated. ^1H NMR (500 MHz, Methanol- d_4) δ 8.70 (s, 1H), 8.15 (s, 1H), 8.00 (d, $J = 8.5$ Hz, 1H), 7.89 (d, $J = 8.2$ Hz, 1H), 7.77 (t, $J = 7.7$ Hz, 1H), 7.64 (t, $J = 7.5$ Hz, 1H), 7.45 (t, $J = 7.0$ Hz, 1H), 7.41 – 7.34 (m, 4H), 7.24 (s, 1H), 6.93 (s, 2H), 6.49 (s, 2H), 5.06 (t, $J = 6.2$ Hz, 1H), 4.14 (s, 2H), 3.86 (dt, $J = 14.1, 6.9$ Hz, 2H), 3.36 (dd, $J = 1.0, 0.5$ Hz, 1H), 3.29 – 3.22 (m, 1H), 3.04 (dd, $J = 13.7, 5.1$ Hz, 1H), 2.27 (s, 6H), 2.00 – 1.90 (m, 1H), 1.49 (dt, $J = 12.9, 6.4$ Hz, 1H). Calculated $[\text{M}+\text{H}]^+$: 584.3. ESI-MS mass observed: 584.3 (M+H). Analytical HPLC retention time: 27.9 min.

Compound 61

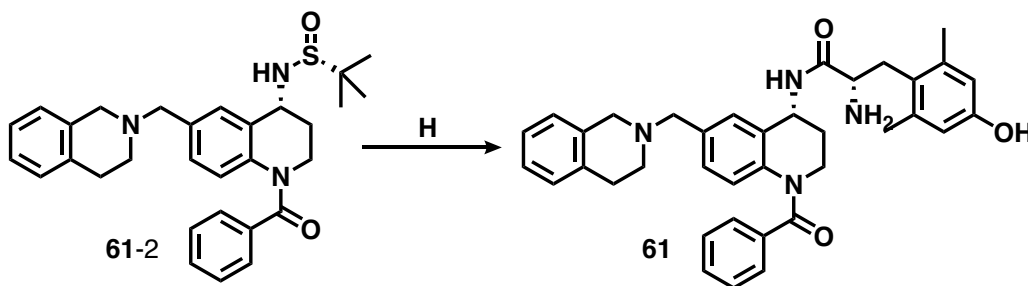


61-1 *1-benzoyl-6-((3,4-dihydroisoquinolin-2(1H)-yl)methyl)-2,3-dihydroquinolin-4(1H)-one.*

Intermediate **61-1** was synthesized following **General Procedure (F)** from intermediate **6-MeBr N-Bz THQ** (100 mg, 0.29 mmol, 1.0 eq), K_2CO_3 (48 mg, 0.35 mmol, 1.2 eq), and THIQ (0.044 mL, 0.35 mmol, 1.2 eq). Yield: 112 mg, 97%. ^1H NMR (500 MHz, Chloroform- d) δ 7.98 (d, $J = 2.0$ Hz, 1H), 7.52 – 7.47 (m, 2H), 7.47 – 7.42 (m, 1H), 7.36 (td, $J = 6.8, 5.7, 3.1$ Hz, 3H), 7.10 (d, $J = 6.4$ Hz, 2H), 6.95 (t, $J = 7.3$ Hz, 2H), 4.32 (td, $J = 6.1, 1.8$ Hz, 2H), 3.61 (d, $J = 25.1$ Hz, 2H), 2.87 (t, $J = 6.2$ Hz, 4H), 2.72 (dd, $J = 6.7, 5.0$ Hz, 2H).



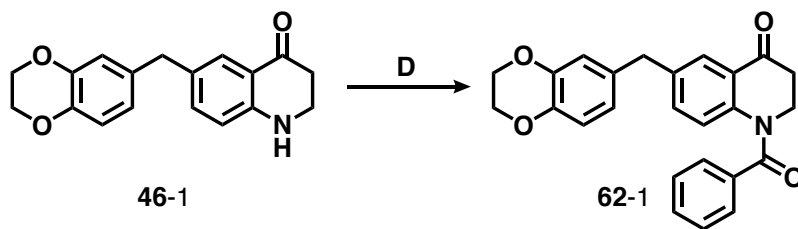
61-2 *(R)-N-((R)-1-benzoyl-6-((3,4-dihydroisoquinolin-2(1H)-yl)methyl)-1,2,3,4-tetrahydroquinolin-4-yl)-2-methylpropane-2-sulfonamide*. Intermediate **61-2** was synthesized following **General Procedure (G)** from intermediate **61-1** (112 mg, 0.28 mmol, 1.0 eq), (R)-2-methyl-2-propanesulfonamide (103 mg, 0.85 mmol, 3.0 eq), and Ti(OEt)₄ (0.36 mL, 1.69 mmol, 6.0 eq), then NaBH₄ (43 mg, 1.13 mmol, 4.0 eq). Yield: 123 mg, 87%. ¹H NMR (500 MHz, Chloroform-*d*) δ 7.43 (d, *J* = 1.9 Hz, 1H), 7.40 – 7.35 (m, 3H), 7.29 (t, *J* = 7.5 Hz, 2H), 7.10 – 7.03 (m, 4H), 6.95 – 6.89 (m, 2H), 4.63 (q, *J* = 4.3 Hz, 1H), 4.01 (dt, *J* = 12.9, 5.2 Hz, 1H), 3.87 – 3.77 (m, 1H), 3.59 (dd, *J* = 23.3, 11.8 Hz, 4H), 2.86 (t, *J* = 5.9 Hz, 2H), 2.71 (q, *J* = 6.0, 4.6 Hz, 2H), 2.27 (dq, *J* = 14.3, 4.9 Hz, 1H), 2.10 (ddt, *J* = 14.3, 9.8, 5.5 Hz, 1H), 1.18 (d, *J* = 1.4 Hz, 9H).



61 *(S)-2-amino-N-((R)-1-benzoyl-6-((3,4-dihydroisoquinolin-2(1H)-yl)methyl)-1,2,3,4-tetrahydroquinolin-4-yl)-3-(4-hydroxy-2,6-dimethylphenyl)propenamide*. Final compound **61** was synthesized following **General Procedure (H)** from intermediate **61-2**. **Step 1:** Sulfonamide cleavage was carried out with intermediate **61-2** (123 mg, 0.25 mmol) and excess concentrated

HCl (0.50 mL), precipitating product as a white solid, a portion of which was used without further purification in subsequent steps. **Step 2:** Amide coupling was performed with the aminium chloride salt of **61-2** (36 mg, 0.077 mmol, 1.00 eq), di-Boc-Dmt (33 mg, 0.081 mmol, 1.05 eq), 6-Cl HOBt (13 mg, 0.77 mmol, 1.00 eq), and PyBOP (40 mg, 0.077 mmol, 1.00 eq), followed by DIPEA (0.11 mL, 0.77 mmol, 10 eq). Crude product was carried forward to **Step 3:** Boc-deprotection with 1:1 TFA/DCM (3 mL), followed by purification by reverse-phase semi-preparative HPLC, as described in **General Procedure (H)**. Final yield not calculated. ¹H NMR (500 MHz, Methanol-*d*₄) δ 7.68 (s, 1H), 7.51 – 7.43 (m, 4H), 7.42 – 7.37 (m, 2H), 7.31 (t, *J* = 7.3, 5.9 Hz, 1H), 7.26 (t, *J* = 7.1 Hz, 2H), 7.20 (t, *J* = 11.6, 10.5 Hz, 1H), 7.14 (t, *J* = 7.4 Hz, 2H), 6.49 (s, 2H), 5.07 (t, *J* = 6.3 Hz, 1H), 4.42 (d, *J* = 25.6 Hz, 2H), 4.35 (d, *J* = 22.3 Hz, 2H), 3.90 (dd, *J* = 11.7, 4.9 Hz, 1H), 3.88 – 3.79 (m, 1H), 3.42 (d, *J* = 17.8 Hz, 1H), 3.26 (d, *J* = 12.2 Hz, 1H), 3.18 (s, 2H), 3.07 (dd, *J* = 13.7, 4.9 Hz, 1H), 2.28 (s, 6H), 1.94 (q, *J* = 7.1, 6.5 Hz, 1H), 1.51 (td, *J* = 12.0, 6.9 Hz, 1H). Calculated [M+H]⁺: 589.3. ESI-MS mass observed: 589.3 (M+H). Analytical HPLC retention time: 27.7 min.

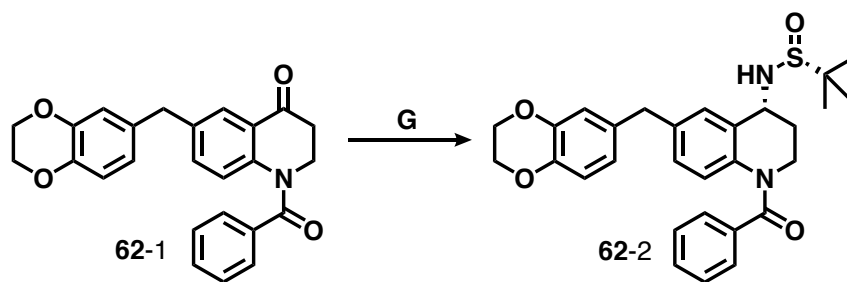
Compound 62



62-1 1-benzoyl-6-((2,3-dihydrobenzo[*b*][1,4]dioxin-6-yl)methyl)-2,3-dihydroquinolin-4(1H)-one.

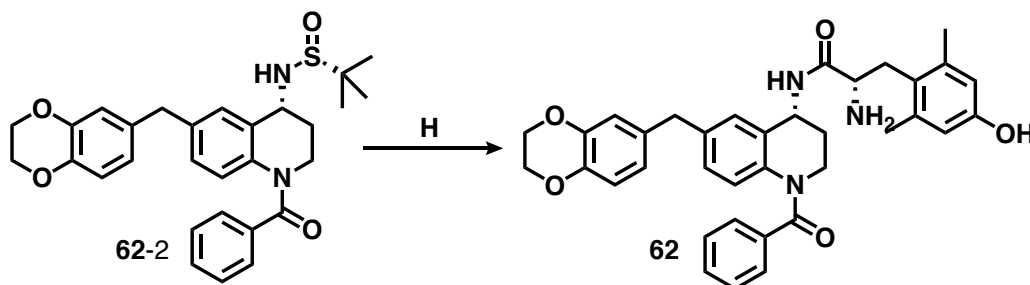
Intermediate **62-1** was synthesized following **General Procedure (D)** from intermediate **46-1** (101

mg, 0.34 mmol, 1.0 eq), Et₃N (0.10 mL, 0.68 mmol, 2.0 eq), and benzoyl chloride (0.08 mL, 0.68 mmol, 2.0 eq). After 12 hours, added additional equivalents of Et₃N (0.15 mL, 1.08 mmol, 3.2 eq) and benzoyl chloride (0.10 mL, 0.86 mmol, 2.5 eq). After another two hours, TLC indicated complete consumption of product. Yield: 128 mg, 94%. ¹H NMR (500 MHz, Chloroform-*d*) δ 7.83 (d, *J* = 2.1 Hz, 1H), 7.49 – 7.46 (m, 2H), 7.44 (t, *J* = 7.6 Hz, 1H), 7.36 (t, *J* = 7.6 Hz, 2H), 7.07 (dd, *J* = 8.5, 2.2 Hz, 1H), 6.85 (d, *J* = 8.5 Hz, 1H), 6.76 (d, *J* = 7.9 Hz, 1H), 6.61 (d, *J* = 8.3 Hz, 2H), 4.30 (t, *J* = 6.3 Hz, 2H), 4.22 (s, 4H), 3.82 (s, 2H), 2.85 (t, *J* = 6.3 Hz, 2H). ¹³C NMR (126 MHz, cdcl₃) δ 193.75, 170.01, 142.61, 142.09, 138.28, 135.12, 134.27, 133.33, 131.00, 128.51, 128.50, 127.33, 124.83, 124.62, 121.71, 117.50, 117.28, 64.36, 64.28, 45.26, 40.36, 39.55.



62-2 *(R)*-*N*-((*R*)-1-benzoyl-6-((2,3-dihydrobenzo[*b*][1,4]dioxin-6-yl)methyl)-1,2,3,4-tetrahydroquinolin-4-yl)-2-methylpropane-2-sulfonamide. **62-2** was synthesized following **General Procedure (G)** from intermediate **62-1** (125 mg, 0.31 mmol, 1.0 eq), (*R*)-2-methyl-2-propanesulfonamide (114 mg, 0.94 mmol, 3.0 eq), and Ti(OEt)₄ (0.39 mL, 1.88 mmol, 6.0 eq), then NaBH₄ (71 mg, 1.88 mmol, 6.0 eq). Yield: 130 mg, 82%. ¹H NMR (500 MHz, Chloroform-*d*) δ 7.39 (td, *J* = 5.4, 4.9, 2.6 Hz, 3H), 7.34 – 7.29 (m, 2H), 7.20 (s, 1H), 6.83 (s, 2H), 6.76 (d, *J* = 7.9 Hz, 1H), 6.62 (d, *J* = 8.4 Hz, 2H), 4.62 (q, *J* = 3.9 Hz, 1H), 4.23 (s, 4H), 4.01 (dt, *J* = 12.8, 5.1 Hz, 1H), 3.85 – 3.79 (m, 1H), 3.79 (s, 2H), 2.30 (dq, *J* = 13.9, 4.6 Hz, 1H), 2.09 (ddt, *J* = 14.5, 10.0, 5.0 Hz, 1H), 1.21 (s, 9H). ¹³C NMR (126 MHz, cdcl₃) δ 170.40, 138.44, 136.89, 136.20, 133.99,

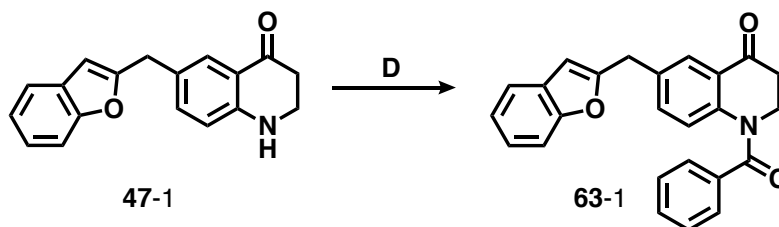
130.52, 130.07, 128.74, 128.54, 128.44, 125.54, 121.91, 117.68, 117.34, 77.16, 64.52, 64.45, 55.91, 50.75, 41.56, 40.59, 30.29, 22.75.



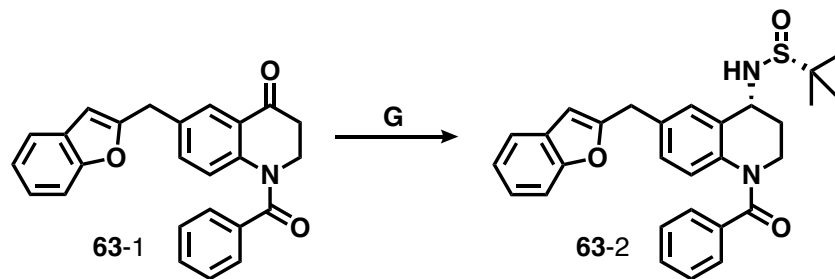
62 (*S*)-2-amino-*N*-((*R*)-6-((2,3-dihydrobenzo[*b*][1,4]dioxin-6-yl)methyl)-1-(methylsulfonyl)-1,2,3,4-tetrahydroquinolin-4-yl)-3-(4-hydroxy-2,6-dimethylphenyl)propenamide. **62** was synthesized following **General Procedure (H)** from intermediate **62-2**. **Step 1:** Sulfinamide cleavage was carried out with **62-2** (130 mg, 0.26 mmol, 1.0 eq) and excess concentrated HCl, precipitating product as a white solid, which was used without further purification. **Step 2:** Amide coupling was performed with the aminium chloride salt of **62-2** (113 mg, 0.26 mmol, 1.0 eq), di-Boc-Dmt (115 mg, 0.28 mmol, 1.1 eq), and PyBOP (146 mg, 0.28 mmol, 1.1 eq), followed by DIPEA (0.45 mL, 2.59 mmol, 10 eq). After purification by silica chromatography, which yielded 99 mg (48% yield), uncharacterized product was carried forward to **Step 3:** TFA deprotection, followed by purification by reverse-phase semi-preparative HPLC, as described in **General Procedure (H)**. Final yield not calculated. ¹H NMR (500 MHz, Methanol-*d*₄) δ 7.44 (tt, *J* = 6.0, 2.7 Hz, 1H), 7.36 (d, *J* = 6.0 Hz, 4H), 7.11 (d, *J* = 1.8 Hz, 1H), 6.78 (t, *J* = 11.4 Hz, 2H), 6.67 (d, *J* = 8.2 Hz, 1H), 6.59 – 6.51 (m, 2H), 6.49 (s, 2H), 5.04 (t, *J* = 6.2 Hz, 1H), 4.16 (s, 4H), 3.88 (dd, *J* = 11.5, 5.2 Hz, 1H), 3.84 (dd, *J* = 7.8, 4.8 Hz, 1H), 3.73 (s, 2H), 3.38 – 3.33 (m, 1H), 3.26 (dd, *J* = 13.7, 11.5 Hz, 1H), 3.05 (dd, *J* = 13.7, 5.1 Hz, 1H), 2.27 (s, 6H), 1.94 (dq, *J* = 13.8, 5.7 Hz, 1H), 1.47 (dtd, *J* = 13.7, 7.2, 4.3 Hz, 1H). ¹³C NMR (126 MHz, cd₃od) δ 157.49, 140.04, 135.41,

131.73, 129.51, 129.40, 128.93, 126.25, 123.17, 122.49, 118.27, 118.01, 116.46, 65.63, 65.53, 53.55, 49.00, 46.87, 41.31, 31.99, 31.43, 20.45. Calculated $[M+H]^+$: 592.3. QTOF high-resolution MS mass observed: 592.2795 (M+H). Analytical HPLC retention time: 38.0 min.

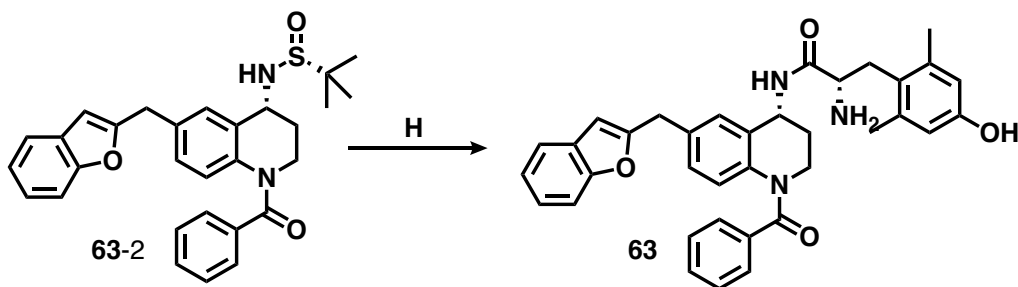
Compound 63



63-1 6-(benzofuran-2-ylmethyl)-1-benzoyl-2,3-dihydroquinolin-4(1H)-one. Intermediate **63-1** was synthesized following **General Procedure (D)** from intermediate **47-1** (87 mg, 0.31 mmol, 1.0 eq), Et₃N (0.09 mL, 0.63 mmol, 2.0 eq), and BzCl (0.07 mL, 0.63 mmol, 2.0 eq). After 12 hours, added additional equivalents of Et₃N (0.15 mL, 1.08 mmol, 3.5 eq) and BzCl (0.10 mL, 0.86 mmol, 2.8 eq). After another two hours, TLC indicated complete consumption of product. Yield: 117 mg, 98%. ¹H NMR (500 MHz, Chloroform-*d*) δ 7.96 (d, $J = 2.2$ Hz, 1H), 7.51 – 7.43 (m, 4H), 7.37 (dt, $J = 8.6, 6.5$ Hz, 3H), 7.21 (ddt, $J = 8.0, 3.6, 2.2$ Hz, 2H), 7.17 (td, $J = 7.4, 1.2$ Hz, 1H), 6.92 (d, $J = 8.5$ Hz, 1H), 6.39 (d, $J = 1.0$ Hz, 1H), 4.31 (t, $J = 6.3$ Hz, 2H), 4.07 (s, 2H), 2.86 (t, $J = 6.3$ Hz, 2H). ¹³C NMR (126 MHz, cdcl₃) δ 193.69, 170.24, 156.60, 155.13, 143.36, 135.19, 134.37, 134.30, 131.26, 128.74, 128.72, 128.68, 127.77, 125.08, 124.93, 123.81, 122.80, 120.67, 111.07, 103.84, 77.16, 45.48, 39.67, 34.35.



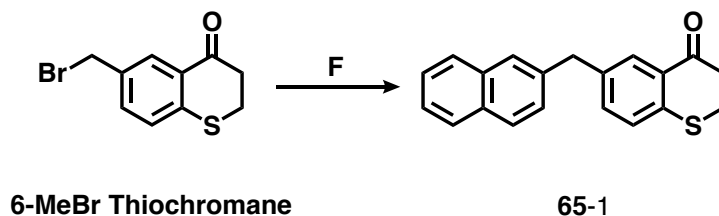
63-2 *(R)-N-((R)-6-(benzofuran-2-ylmethyl)-1-benzoyl-1,2,3,4-tetrahydroquinolin-4-yl)-2-methylpropane-2-sulfonamide*. Intermediate **63-2** was synthesized following **General Procedure (G)** from **63-1** (115 mg, 0.30 mmol, 1.0 eq), (R)-2-methyl-2-propanesulfonamide (110 mg, 0.90 mmol, 3.0 eq), and Ti(OEt)₄ (0.38 mL, 1.80 mmol, 6.0 eq), then NaBH₄ (68 mg, 1.80 mmol, 6.0 eq). Yield: 89 mg, 60%. ¹H NMR (500 MHz, Chloroform-*d*) δ 7.50 – 7.45 (m, 1H), 7.42 – 7.39 (m, 3H), 7.37 (dd, *J* = 8.6, 1.9 Hz, 2H), 7.32 (dd, *J* = 8.4, 6.7 Hz, 2H), 7.19 (dtd, *J* = 18.0, 7.3, 1.3 Hz, 2H), 6.97 (dd, *J* = 8.5, 2.0 Hz, 1H), 6.40 (d, *J* = 1.1 Hz, 1H), 4.65 (q, *J* = 3.8 Hz, 1H), 4.07 – 3.99 (m, 4H), 3.81 (ddd, *J* = 13.1, 10.0, 4.9 Hz, 1H), 2.29 (dq, *J* = 14.1, 4.8 Hz, 1H), 2.11 (ddt, *J* = 14.6, 10.1, 5.1 Hz, 1H), 1.20 (s, 10H). ¹³C NMR (126 MHz, cdcl₃) δ 137.54, 136.09, 134.30, 130.63, 128.95, 128.56, 128.50, 125.67, 123.67, 122.72, 120.62, 111.05, 103.64, 77.16, 64.12, 60.54, 55.95, 50.86, 41.65, 34.43, 30.46, 22.74.



63 *(S)-2-amino-N-((R)-6-(benzofuran-2-ylmethyl)-1-benzoyl-1,2,3,4-tetrahydroquinolin-4-yl)-3-(4-hydroxy-2,6-dimethylphenyl)propanamide*. **63** was synthesized following **General Procedure**

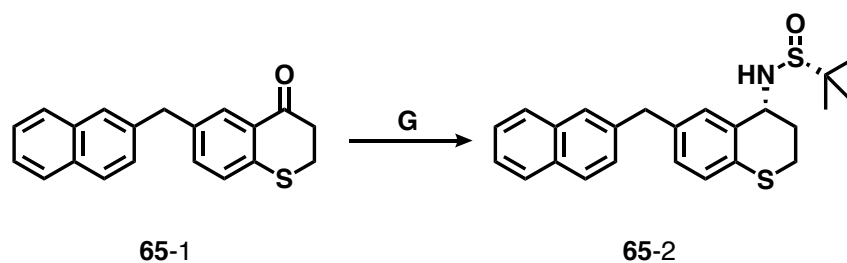
(H) from intermediate **63-2**. **Step 1:** Sulfinamide cleavage was carried out with **63-2** (89 mg, 0.18 mmol, 1.0 eq) and excess concentrated HCl, precipitating product as a white solid, which was used without further purification. **Step 2:** Amide coupling was performed with the aminium chloride salt of **63-2** (77 mg, 0.18 mmol, 1.0 eq), di-Boc-Dmt (82 mg, 0.20 mmol, 1.1 eq), and PyBOP (104 mg, 0.20 mmol, 1.1 eq), followed by DIPEA (0.32 mL, 1.84 mmol, 10 eq). After purification by silica chromatography, which yielded 76 mg (54% yield), uncharacterized product was carried forward to **Step 3:** TFA deprotection, followed by purification by reverse-phase semi-preparative HPLC, as described in **General Procedure (H)**. Final yield not calculated. ¹H NMR (500 MHz, Methanol-*d*₄) δ 7.46 – 7.43 (m, 2H), 7.42 – 7.33 (m, 4H), 7.34 – 7.28 (m, 1H), 7.24 (d, *J* = 1.9 Hz, 1H), 7.18 (td, *J* = 7.7, 1.6 Hz, 1H), 7.14 (td, *J* = 7.4, 1.2 Hz, 1H), 6.95 (d, *J* = 8.2 Hz, 1H), 6.90 (s, 1H), 6.49 (s, 2H), 6.37 (d, *J* = 1.0 Hz, 1H), 5.07 (t, *J* = 6.3 Hz, 1H), 4.01 (d, *J* = 4.2 Hz, 2H), 3.88 (d, *J* = 5.0 Hz, 1H), 3.86 (d, *J* = 5.3 Hz, 1H), 3.34 (h, *J* = 1.7 Hz, 1H), 3.26 (dd, *J* = 13.7, 11.5 Hz, 1H), 3.04 (dd, *J* = 13.7, 5.2 Hz, 1H), 2.27 (s, 6H), 1.98 – 1.91 (m, 1H), 1.53 – 1.45 (m, 1H). Calculated [M+H]⁺: 574.3. QTOF high-resolution MS mass observed: 574.2692 (M+H). Analytical HPLC retention time: 42.1 min.

Compound 65



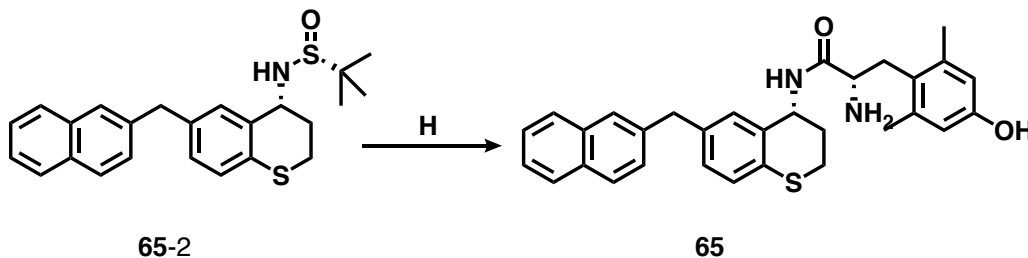
65-1 6-(naphthalen-2-ylmethyl)thiochroman-4-one. Intermediate **65-1** was synthesized following **General Procedure (F)** from **6-MeBr Thiochromane** (103 mg, 0.40 mmol, 1.0 eq), 2-

naphthylboronic acid (138 mg, 0.80 mmol, 2.0 eq), K_2CO_3 (166 mg, 1.20 mmol, 3.0 eq) and $Pd(dppf)Cl_2$ (30 mg, 0.04 mmol, 0.1 eq). Yield: 54 mg, 44%. 1H NMR (500 MHz, Chloroform-*d*) δ 8.04 (d, $J = 1.8$ Hz, 1H), 7.80 – 7.73 (m, 4H), 7.61 (d, $J = 1.8$ Hz, 1H), 7.47 – 7.39 (m, 2H), 7.27 (dd, $J = 8.5, 1.8$ Hz, 1H), 7.22 (dd, $J = 8.2, 2.1$ Hz, 1H), 7.18 (d, $J = 8.1$ Hz, 1H), 4.09 (s, 2H), 3.20 (t, $J = 6.6$ Hz, 2H), 2.95 (t, $J = 6.7, 6.1$ Hz, 2H). ^{13}C NMR (126 MHz, $cdCl_3$) δ 194.31, 140.01, 138.28, 137.96, 134.31, 133.69, 132.26, 131.01, 129.47, 128.41, 128.04, 127.74, 127.67, 127.42, 127.20, 126.21, 125.62, 77.16, 41.60, 39.78, 26.76.



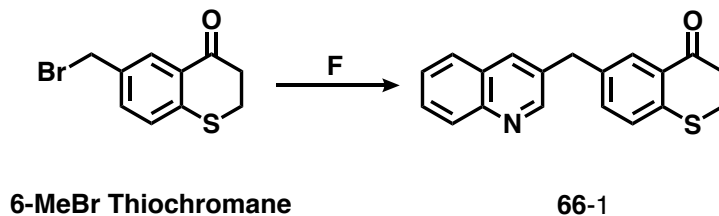
65-2 (*R*)-2-methyl-*N*-((*R*)-6-(naphthalen-2-ylmethyl)thiochroman-4-yl)propane-2-sulfonamide.

65-2 was synthesized following **General Procedure (G)** from intermediate **65-1** (54 mg, 0.18 mmol, 1.0 eq), (*R*)-2-methyl-2-propanesulfonamide (65 mg, 0.53 mmol, 3.0 eq), and $Ti(OEt)_4$ (0.22 mL, 1.06 mmol, 6.0 eq), then $NaBH_4$ (40 mg, 1.06 mmol, 6.0 eq). Yield: 56 mg, 78%. 1H NMR (500 MHz, Chloroform-*d*) δ 7.78 (d, $J = 9.1$ Hz, 1H), 7.74 (d, $J = 8.8$ Hz, 1H), 7.62 (s, 1H), 7.46 – 7.40 (m, 2H), 7.29 (dd, $J = 8.4, 1.8$ Hz, 1H), 7.26 (d, $J = 1.7$ Hz, 1H), 7.26 (s, 1H), 7.04 (d, $J = 8.1$ Hz, 1H), 7.00 (dd, $J = 8.2, 1.9$ Hz, 1H), 4.61 (q, $J = 3.2$ Hz, 1H), 4.05 (s, 2H), 3.28 (td, $J = 12.6, 2.8$ Hz, 1H), 3.18 (s, 1H), 2.79 (dt, $J = 12.5, 4.0$ Hz, 1H), 2.45 (dtd, $J = 14.2, 4.5, 3.0$ Hz, 1H), 2.06 – 1.95 (m, 1H), 1.21 (s, 9H). ^{13}C NMR (126 MHz, $cdCl_3$) δ 138.49, 137.83, 133.73, 132.75, 132.23, 131.90, 131.31, 129.38, 128.29, 127.73, 127.69, 127.57, 127.12, 127.10, 126.13, 125.51, 77.16, 55.76, 50.98, 41.59, 28.22, 22.76, 21.19.

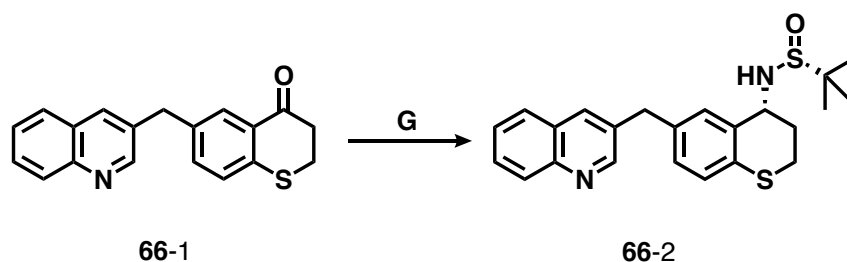


65 *(S)*-2-amino-3-(4-hydroxy-2,6-dimethylphenyl)-*N*-((*R*)-6-(naphthalen-2-ylmethyl)thiochroman-4-yl)propanamide. **65** was synthesized following **General Procedure (H)** from intermediate **65-2**. **Step 1:** Sulfinamide cleavage was carried out with **65-2** (56 mg, 0.14 mmol, 1.0 eq) and excess concentrated HCl, precipitating product as a white solid, which was used without further purification. **Step 2:** Amide coupling was performed with the aminium chloride salt of **65-2** (40 mg, 0.12 mmol, 1.0 eq), di-Boc-Dmt (53 mg, 0.13 mmol, 1.1 eq), and PyBOP (67 mg, 0.13 mmol, 1.1 eq), followed by DIPEA (0.21 mL, 1.20 mmol, 10 eq). Crude product was carried forward to **Step 3:** TFA deprotection, followed by purification by reverse-phase semi-preparative HPLC, as described in **General Procedure (H)**. Final yield not calculated. ^1H NMR (500 MHz, Methanol- d_4) δ 7.77 (dd, $J = 7.9, 1.6$ Hz, 1H), 7.74 – 7.70 (m, 2H), 7.57 (s, 1H), 7.45 – 7.37 (m, 2H), 7.25 (dd, $J = 8.4, 1.7$ Hz, 1H), 7.08 (d, $J = 1.8$ Hz, 1H), 6.99 (dd, $J = 8.2, 1.8$ Hz, 1H), 6.94 (d, $J = 8.1$ Hz, 1H), 6.49 (s, 2H), 5.04 (q, $J = 4.3$ Hz, 1H), 4.00 (s, 2H), 3.85 (dd, $J = 11.6, 5.1$ Hz, 1H), 3.24 (dd, $J = 13.6, 11.6$ Hz, 1H), 3.00 (dd, $J = 13.7, 5.1$ Hz, 1H), 2.52 (dt, $J = 13.3, 4.3$ Hz, 1H), 2.27 (s, 6H), 2.22 (td, $J = 12.7, 2.9$ Hz, 1H), 1.86 (dq, $J = 13.0, 4.4$ Hz, 1H), 1.81 – 1.73 (m, 1H). Calculated $[\text{M}+\text{H}]^+$: 497.2. ESI-MS mass observed: 497.2 (M+H) and 519.2 (M+Na). Analytical HPLC retention time: 45.0 min.

Compound 66

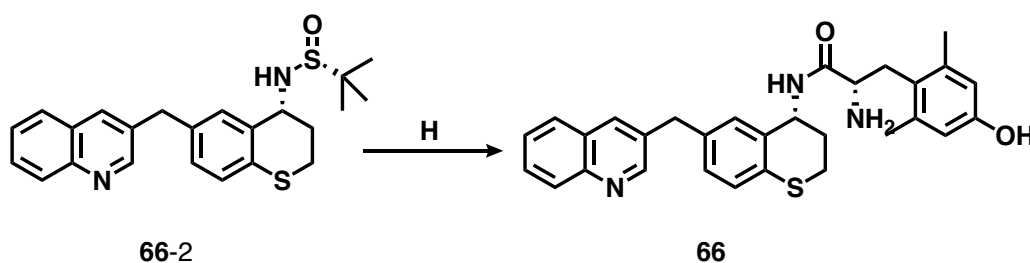


66-1 *6-(quinolin-3-ylmethyl)thiochroman-4-one*. Intermediate **66-1** was synthesized following **General Procedure (F)** from **6-MeBr Thiochromane** (80 mg, 0.31 mmol, 1.0 eq), 3-quinoline boronic acid (107 mg, 0.62 mmol, 2.0 eq), K_2CO_3 (128 mg, 0.93 mmol, 3.0 eq) and $Pd(dppf)Cl_2$ (23 mg, 0.03 mmol, 0.1 eq). Yield: 66 mg, 70%. 1H NMR (500 MHz, Chloroform-*d*) δ 8.78 (d, J = 2.2 Hz, 1H), 8.07 (d, J = 8.6 Hz, 1H), 8.04 (d, J = 1.7 Hz, 1H), 7.89 – 7.86 (m, 1H), 7.74 (dd, J = 8.1, 1.4 Hz, 1H), 7.67 (ddd, J = 8.4, 6.9, 1.4 Hz, 1H), 7.52 (ddd, J = 8.1, 6.8, 1.2 Hz, 1H), 7.24 (d, J = 1.2 Hz, 2H), 4.14 (s, 2H), 3.26 – 3.20 (m, 2H), 3.01 – 2.95 (m, 2H). ^{13}C NMR (126 MHz, $cdCl_3$) δ 151.92, 135.05, 134.13, 129.52, 129.32, 129.19, 128.34, 127.61, 126.97, 77.16, 39.73, 38.79, 26.77.



66-2 *(R)-2-methyl-N-((R)-6-(quinolin-3-ylmethyl)thiochroman-4-yl)propane-2-sulfonamide*. **66-2** was synthesized following **General Procedure (G)** from intermediate **66-1** (66 mg, 0.22 mmol, 1.0 eq), (R)-2-methyl-2-propanesulfonamide (79 mg, 0.65 mmol, 3.0 eq), and $Ti(OEt)_4$ (0.27 mL, 1.30 mmol, 6.0 eq), then $NaBH_4$ (49 mg, 1.30 mmol, 6.0 eq). Yield: 71 mg, 80%. 1H NMR (500

MHz, Chloroform-*d*) δ 8.77 (d, $J = 2.2$ Hz, 1H), 8.06 (d, $J = 8.5, 0.9$ Hz, 1H), 7.90 (s, 1H), 7.75 (d, $J = 8.1$ Hz, 1H), 7.65 (td, $J = 8.2, 1.5$ Hz, 1H), 7.51 (td, $J = 8.1, 1.0$ Hz, 1H), 7.28 (d, $J = 2.0$ Hz, 1H), 7.06 (d, $J = 8.2$ Hz, 1H), 6.99 (dd, $J = 8.2, 2.0$ Hz, 1H), 4.60 (q, $J = 3.3$ Hz, 1H), 4.08 (s, 2H), 3.27 (td, $J = 12.6, 2.8$ Hz, 1H), 3.21 – 3.14 (m, 1H), 2.81 (dt, $J = 12.7, 4.0$ Hz, 1H), 2.44 (dtd, $J = 14.2, 4.6, 3.0$ Hz, 1H), 2.05 – 1.97 (m, 1H), 1.21 (s, 9H).

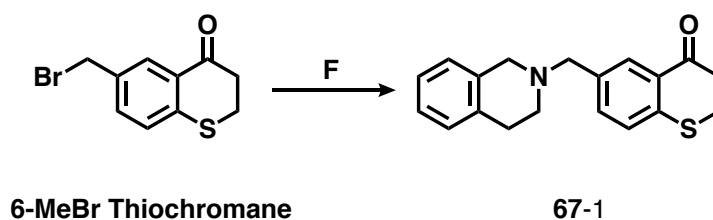


66 (*S*)-2-amino-3-(4-hydroxy-2,6-dimethylphenyl)-*N*-((*R*)-6-(quinolin-3-ylmethyl)thiochroman-4-yl)propanamide. **66** was synthesized following **General Procedure (H)** from intermediate **66-2**.

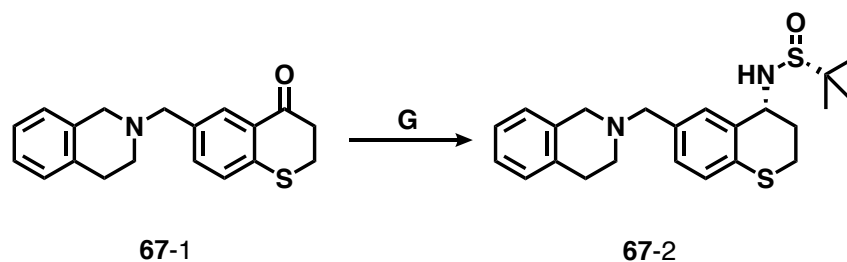
Step 1: Sulfonamide cleavage was carried out with **66-2** (71 mg, 0.17 mmol, 1.0 eq) and excess concentrated HCl, precipitating product as a white solid, which was used without further purification. **Step 2:** Amide coupling was performed with the aminium chloride salt of **66-2** (21 mg, 0.07 mmol, 1.0 eq), di-Boc-Dmt (31 mg, 0.08 mmol, 1.1 eq), and PyBOP (39 mg, 0.08 mmol, 1.1 eq), followed by DIPEA (0.12 mL, 0.69 mmol, 10 eq). Crude product was carried forward to **Step 3:** TFA deprotection, followed by purification by reverse-phase semi-preparative HPLC, as described in **General Procedure (H)**. Final yield not calculated. ^1H NMR (500 MHz, Methanol-*d*₄) δ 8.88 (d, $J = 2.2$ Hz, 1H), 8.54 (s, 1H), 8.29 (d, $J = 8.2$ Hz, 1H), 8.10 (d, $J = 8.7$ Hz, 1H), 8.07 (d, $J = 8.3$ Hz, 1H), 7.95 (t, $J = 7.8$ Hz, 1H), 7.79 (t, $J = 7.7$ Hz, 1H), 7.16 (d, $J = 2.0$ Hz, 1H), 7.05 (dd, $J = 8.2, 1.9$ Hz, 1H), 7.01 (d, $J = 8.1$ Hz, 1H), 6.50 (s, 2H), 5.06 (s, 1H), 4.18 (s, 2H), 3.86 (dd, $J = 11.6, 5.0$ Hz, 1H), 3.26 (dd, $J = 13.6, 11.7$ Hz, 1H), 3.02 (dd, $J = 13.6, 5.0$ Hz, 1H), 2.55 (dt, $J = 13.3, 4.3$ Hz, 1H), 2.28 (s, 6H), 2.25 (d, $J = 12.9$ Hz, 1H), 1.86 (d, $J = 14.3$ Hz, 1H), 1.78

(t, $J = 12.9$ Hz, 1H). Calculated $[M+H]^+$: 498.2. ESI-MS mass observed: 498.2 (M+H) and 520.2 (M+Na). Analytical HPLC retention time: 26.2 min.

Compound 67

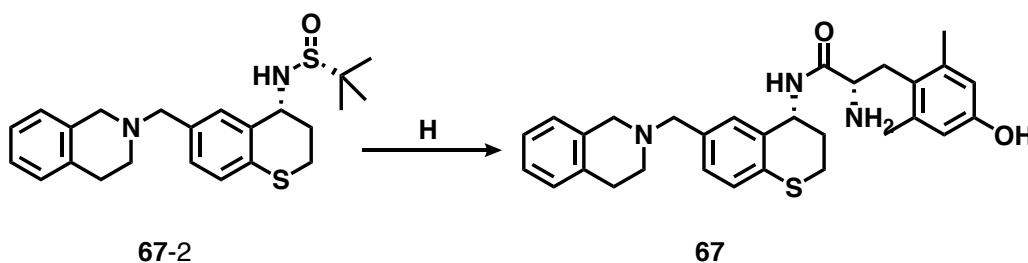


67-1 *6-((3,4-dihydroisoquinolin-2(1H)-yl)methyl)thiochroman-4-one* Intermediate **67-1** was synthesized following **General Procedure (F)** from **6-MeBr Thiochromane** (88 mg, 0.34 mmol, 1.0 eq), THIQ (55 mg, 0.41 mmol, 1.2 eq), and K_2CO_3 (57 mg, 0.41 mmol, 3.0 eq). Yield: 63 mg, 60%. 1H NMR (500 MHz, Chloroform- d) δ 8.07 (d, $J = 2.0$ Hz, 1H), 7.49 (dd, $J = 8.2, 2.0$ Hz, 1H), 7.27 – 7.24 (m, 1H), 7.12 – 7.07 (m, 3H), 6.97 (dd, $J = 7.7, 1.8$ Hz, 1H), 3.65 (s, 2H), 3.61 (s, 2H), 3.24 (t, $J = 6.5$ Hz, 2H), 2.98 (t, $J = 6.5$ Hz, 2H), 2.89 (t, $J = 5.9$ Hz, 2H), 2.73 (t, $J = 5.9$ Hz, 2H). ^{13}C NMR (126 MHz, $cdCl_3$) δ 194.27, 141.00, 135.83, 134.80, 134.39, 134.34, 130.76, 129.64, 128.80, 127.92, 126.67, 126.25, 125.71, 77.16, 62.07, 56.10, 50.72, 39.77, 29.26, 26.78.



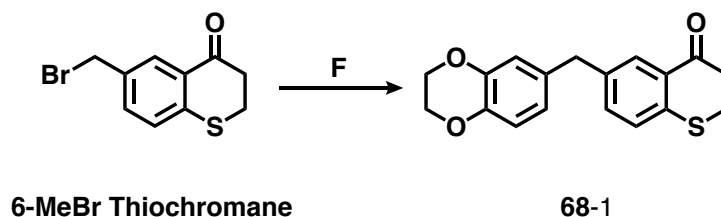
67-2 *(R)-N-((R)-6-((3,4-dihydroisoquinolin-2(1H)-yl)methyl)thiochroman-4-yl)-2-methylpropane-2-sulfonamide*. **67-2** was synthesized following **General Procedure (G)** from

intermediate **67-1** (63 mg, 0.20 mmol, 1.0 eq), (R)-2-methyl-2-propanesulfonamide (74 mg, 0.61 mmol, 3.0 eq), and Ti(OEt)₄ (0.26 mL, 1.22 mmol, 6.0 eq), then NaBH₄ (46 mg, 1.22 mmol, 6.0 eq). Yield: 27 mg, 32%. NMR was taken, but indicated presence of impurity. Carried forward as crude mixture.

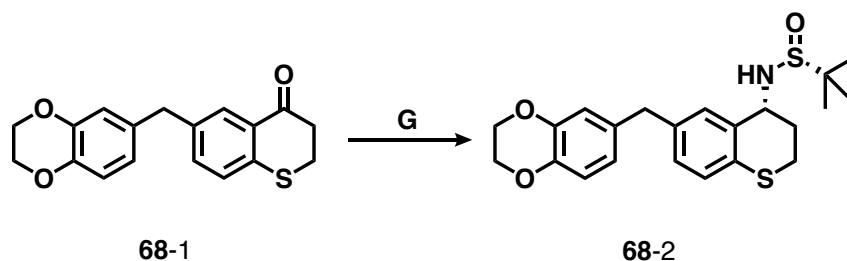


67 (*S*)-2-amino-*N*-((*R*)-6-((3,4-dihydroisoquinolin-2(1*H*)-yl)methyl)thiochroman-4-yl)-3-(4-hydroxy-2,6-dimethylphenyl)propanamide. **67** was synthesized following **General Procedure (H)** from intermediate **67-2**. **Step 1:** Sulfonamide cleavage was carried out with **67-2** (27 mg, 0.07 mmol, 1.0 eq) and excess concentrated HCl, precipitating product as a white solid, which was used without further purification. **Step 2:** Amide coupling was performed with the aminium chloride salt of **67-2** (23 mg, 0.07 mmol, 1.0 eq), di-Boc-Dmt (33 mg, 0.08 mmol, 1.1 eq), and PyBOP (42 mg, 0.08 mmol, 1.1 eq), followed by DIPEA (0.13 mL, 0.74 mmol, 10 eq). Crude product was carried forward to **Step 3:** TFA deprotection, followed by purification by reverse-phase semi-preparative HPLC, as described in **General Procedure (H)**. Final yield not calculated. ¹H NMR (500 MHz, Methanol-*d*₄) δ 7.32 (d, *J* = 5.3 Hz, 1H), 7.32 – 7.27 (m, 1H), 7.29 – 7.22 (m, 3H), 7.17 (d, *J* = 8.2 Hz, 1H), 7.15 (d, *J* = 7.7 Hz, 1H), 6.51 (s, 2H), 5.10 (d, *J* = 4.4 Hz, 1H), 4.36 (q, *J* = 16.6, 14.8 Hz, 4H), 3.86 (dd, *J* = 11.7, 4.9 Hz, 1H), 3.74 (s, 2H), 3.29 – 3.23 (m, 1H), 3.23 – 3.09 (m, 2H), 3.04 (dd, *J* = 13.6, 4.9 Hz, 1H), 2.69 – 2.60 (m, 1H), 2.37 – 2.31 (m, 1H), 1.91 – 1.75 (m, 2H). Calculated [M+H]⁺: 502.3. ESI-MS mass observed: 502.3 (M+H) and 524.3 (M+Na). Analytical HPLC retention time: 26.0 min.

Compound 68

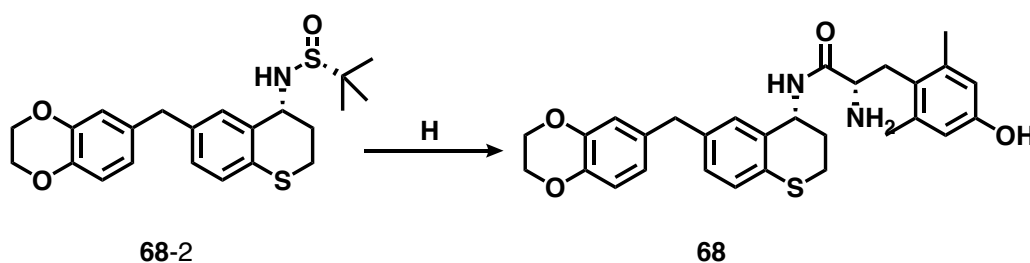


68-1 6-((2,3-dihydrobenzo[*b*][1,4]dioxin-6-yl)methyl)thiochroman-4-one. Intermediate **68-1** was synthesized following **General Procedure (F)** from **6-MeBr Thiochromane** (105 mg, 0.41 mmol, 1.0 eq), 1,4-benzodioxan-6-boronic acid (180 mg, 0.61 mmol, 1.5 eq), K_2CO_3 (168 mg, 1.22 mmol, 3.0 eq) and $Pd(dppf)Cl_2$ (30 mg, 0.04 mmol, 0.1 eq). Yield: 83 mg, 65%. 1H NMR (500 MHz, Chloroform-*d*) δ 7.96 (dt, $J = 1.5, 0.8$ Hz, 1H), 7.20 – 7.18 (m, 2H), 6.79 – 6.75 (m, 1H), 6.63 (dd, $J = 8.9, 1.4$ Hz, 2H), 4.22 (s, 4H), 3.83 (s, 2H), 3.24 – 3.18 (m, 2H), 2.99 – 2.93 (m, 2H). ^{13}C NMR (126 MHz, $cdCl_3$) δ 194.35, 143.58, 142.18, 139.85, 138.63, 134.22, 133.87, 130.99, 129.33, 128.00, 121.83, 117.60, 117.42, 77.16, 64.52, 64.44, 40.69, 39.84, 26.80.



68-2 (R)-N-((R)-6-((2,3-dihydrobenzo[*b*][1,4]dioxin-6-yl)methyl)thiochroman-4-yl)-2-methylpropane-2-sulfonamide. **68-2** was synthesized following **General Procedure (G)** from intermediate **68-1** (82 mg, 0.26 mmol, 1.0 eq), (R)-2-methyl-2-propanesulfonamide (96 mg, 0.79 mmol, 3.0 eq), and $Ti(OEt)_4$ (0.33 mL, 1.57 mmol, 6.0 eq), then $NaBH_4$ (59 mg, 1.57 mmol, 6.0

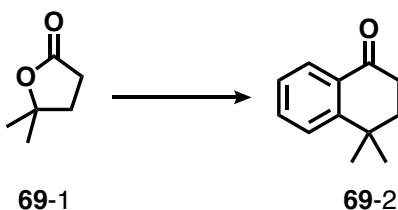
eq). Yield: 42 mg, 39%. ^1H NMR (500 MHz, Chloroform-*d*) δ 7.16 (d, J = 1.9 Hz, 1H), 7.03 (d, J = 8.1 Hz, 1H), 6.96 (dd, J = 8.1, 1.9 Hz, 1H), 6.76 (d, J = 8.0 Hz, 1H), 6.64 (d, J = 8.5 Hz, 2H), 4.60 (q, J = 3.0 Hz, 1H), 4.22 (s, 4H), 3.78 (s, 2H), 3.28 (td, J = 12.6, 2.8 Hz, 1H), 3.16 (s, 1H), 2.78 (dt, J = 12.5, 4.0 Hz, 1H), 2.48 – 2.42 (m, 1H), 2.05 – 1.96 (m, 1H), 1.22 (s, 9H). ^{13}C NMR (126 MHz, cdCl_3) δ 143.50, 142.04, 138.10, 134.36, 132.61, 131.70, 131.14, 129.26, 127.04, 121.81, 117.57, 117.31, 77.16, 64.50, 64.43, 55.74, 50.85, 40.61, 28.09, 22.78, 21.12.



68 (*S*)-2-amino-*N*-((*R*)-6-((2,3-dihydrobenzo[*b*][1,4]dioxin-6-yl)methyl)thiochroman-4-yl)-3-(4-hydroxy-2,6-dimethylphenyl)propanamide. **68** was synthesized following **General Procedure (H)** from intermediate **68-2**. **Step 1:** Sulfonamide cleavage was carried out with **68-2** (42 mg, 0.10 mmol, 1.0 eq) and excess concentrated HCl, precipitating product as a white solid, which was used without further purification. **Step 2:** Amide coupling was performed with the aminium chloride salt of **68-2** (36 mg, 0.10 mmol, 1.0 eq), di-Boc-Dmt (45 mg, 0.11 mmol, 1.1 eq), and PyBOP (57 mg, 0.11 mmol, 1.1 eq), followed by DIPEA (0.18 mL, 1.03 mmol, 10 eq). Crude product was carried forward to **Step 3:** TFA deprotection, followed by purification by reverse-phase semi-preparative HPLC, as described in **General Procedure (H)**. Final yield not calculated. ^1H NMR (500 MHz, Methanol-*d*₄) δ 6.99 (d, J = 1.6 Hz, 1H), 6.92 – 6.90 (m, 2H), 6.70 – 6.66 (m, 1H), 6.56 (d, J = 8.1 Hz, 2H), 6.49 (s, 2H), 5.02 (s, 1H), 4.17 (s, 4H), 3.85 (dd, J = 11.6, 5.1 Hz, 1H), 3.70 (s, 2H), 3.25 (dd, J = 13.6, 11.7 Hz, 1H), 3.01 (dd, J = 13.6, 5.0 Hz, 1H), 2.51 (dt, J = 13.3, 4.4

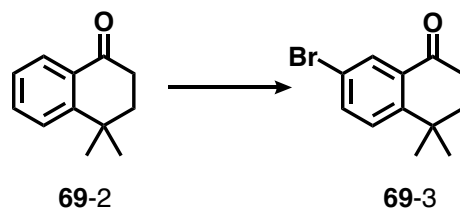
Hz, 1H), 2.27 (s, 6H), 2.21 (td, $J = 12.7, 2.8$ Hz, 1H), 1.85 (dd, $J = 10.4, 5.9$ Hz, 1H), 1.81 – 1.73 (m, 1H). Calculated $[M+H]^+$: 505.2. ESI-MS mass observed: 505.2 (M+H) and 527.2 (M+Na). Analytical HPLC retention time: 38.5 min.

Compound 69

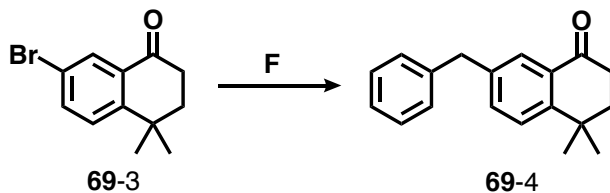


69-2 4,4-dimethyl-3,4-dihydronaphthalen-1(2H)-one (2). Intermediate **69-2** was synthesized by implementation of the following procedure: to a flame-dried reaction vessel was added commercially available lactone **69-1** (500 mg, 4.38 mmol, 1 eq) in anhydrous benzene solvent under inert atmosphere. $AlCl_3$ (2.04 g, 15.3 mmol, 3.0 eq) was then added to a separate flame-dried reaction vessel containing anhydrous benzene under inert atmosphere and was cooled to $0^\circ C$. The solution of lactone was transferred via cannula to the flask containing $AlCl_3$ and heated at reflux ($95^\circ C$) for 2.5 h. Reaction was quenched by pouring over HCl/ice slurry. Reaction mixture was separated with DCM/ H_2O . Product was dried over magnesium sulfate and filtered. Organic solvent was removed under reduced pressure. Purified by silica column in 1:4 ethyl acetate/hexanes. Title compound **69-2** was recovered in 73% yield. 1H NMR (500 MHz, Chloroform- d) δ 8.01 (td, $J = 7.8, 1.7$ Hz, 1H), 7.53 – 7.46 (m, 1H), 7.41 (td, $J = 8.0, 1.3$ Hz, 1H), 7.30 – 7.23 (m, 1H), 2.76 – 2.67 (m, 2H), 2.05 – 1.96 (m, 2H), 1.47 – 1.28 (m, 6H). ^{13}C NMR (126

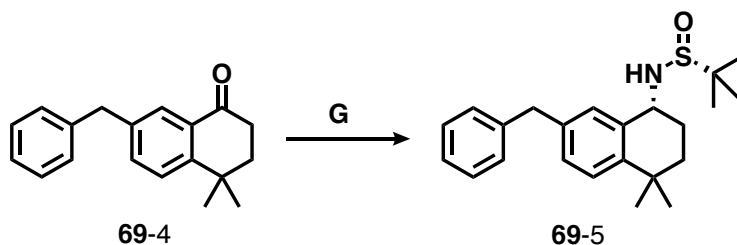
MHz, cdCl_3) δ 198.17, 198.14, 152.12, 133.71, 133.68, 131.04, 127.16, 126.13, 125.70, 77.25, 77.00, 76.98, 76.75, 36.96, 35.00, 33.78, 29.74, 29.62.



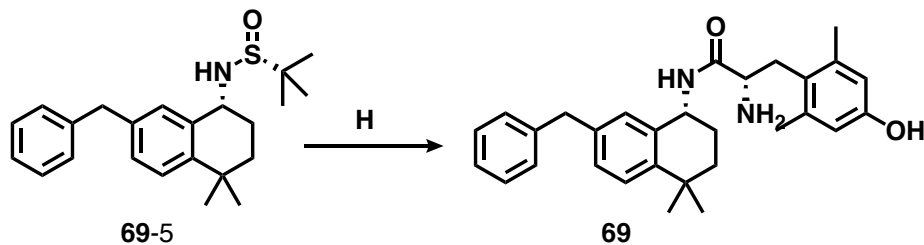
69-3 7-bromo-4,4-dimethyl-3,4-dihydro-1H-naphthalen-1-one. Intermediate **69-3** was synthesized by implementation of the following procedure: Intermediate **69-2** (552 mg, 3.17 mmol, 1 eq) was dissolved in concentrated sulfuric acid, then added NBS (662 mg, 3.80 mmol, 1.2 eq) incrementally. Solution was heated at 60°C until side-product was observed by TLC (30 min). Reaction was quenched reaction with addition of H_2O on ice bath to minimize generation of excess heat. Reaction was extracted with DCM/ H_2O , rinsed with brine, and dried over magnesium sulfate. Filtrate was concentrated under reduced pressure and purified by silica column in 1:9 ethyl acetate/hexanes. Title compound **69-3** was recovered in 53% yield. ^1H NMR (500 MHz, Chloroform- d) δ 8.13 (d, $J = 2.2$ Hz, 1H), 7.62 (ddd, $J = 8.5, 2.3, 1.1$ Hz, 1H), 7.33 – 7.28 (m, 1H), 2.76 – 2.69 (m, 2H), 2.02 (q, $J = 6.9$ Hz, 2H), 1.39 (d, $J = 9.3$ Hz, 6H). ^{13}C NMR (126 MHz, cdCl_3) δ 196.93, 150.97, 136.52, 133.80, 132.68, 130.08, 127.90, 127.27, 126.23, 125.78, 120.48, 77.25, 77.00, 76.75, 37.05, 36.76, 35.09, 34.93, 33.89, 33.79, 29.71, 29.55.



69-4 7-benzyl-4,4-dimethyl-3,4-dihydronaphthalen-1(2H)-one. Intermediate **69-4** was synthesized following a modified form* of **General Procedure (D)** from intermediate **69-3** (100 mg, 0.40 mmol, 1 eq) benzylboronic acid pinacol ester (172 mg, 0.79 mmol, 2.0 eq), K_2CO_3 (164 mg, 1.18 mmol, 3.0 eq) and $Pd(dppf)Cl_2$ (30 mg, 0.04 mmol, 0.1 eq). Yield: 82 mg, 75%. *Modification: reaction was done in microwave reactor at 110°C for 30 minutes. 1H NMR (500 MHz, Chloroform-d) δ 7.33 (t, $J = 1.2$ Hz, 2H), 7.30 – 7.25 (m, 4H), 7.23 – 7.17 (m, 3H), 3.98 (s, 2H), 2.74 – 2.69 (m, 3H), 2.00 (td, $J = 6.9, 1.2$ Hz, 2H), 1.38 (dd, $J = 16.6, 1.0$ Hz, 8H). ^{13}C NMR (126 MHz, $cdCl_3$) δ 198.50, 150.15, 140.57, 139.26, 134.42, 131.13, 128.86, 128.53, 127.31, 127.30, 126.25, 126.21, 126.11, 77.25, 77.00, 76.75, 41.42, 37.10, 37.07, 35.18, 35.11, 33.67, 29.73, 29.72, 24.70.



69-5 (R)-N-((R)-7-benzyl-4,4-dimethyl-1,2,3,4-tetrahydronaphthalen-1-yl)-2-methylpropane-2-sulfonamide. **69-5** was synthesized following **General Procedure (G)** from **69-4** (163 mg, 0.617 mmol, 1 eq), (R)-2-methyl-2-propanesulfonamide (224 mg, 1.85 mmol, 3.0 eq), and $Ti(OEt)_4$ (0.77 mL, 3.70 mmol, 6.0 eq), then $NaBH_4$ (140 mg, 3.70 mmol, 6.0 eq). Yield: 153 mg, 65%. Characterized by NMR after sulfonamide cleavage in next step (see Final Compound **69** Step 1).



69 (*S*)-2-amino-*N*-((*R*)-7-benzyl-4,4-dimethyl-1,2,3,4-tetrahydronaphthalen-1-yl)-3-(4-hydroxy-2,6-dimethylphenyl)propanamide. Final compound **69** was synthesized following **General Procedure (H)** from intermediate **69-4**. **Step 1:** Sulfonamide cleavage was carried out with **69-4** (153 mg, 0.56 mmol, 1 eq) and excess concentrated HCl, precipitating product as a white solid, which was used without further purification. ¹H NMR (500 MHz, Chloroform-*d*) δ 8.76 (s, 4H), 7.48 (d, *J* = 2.1 Hz, 1H), 7.20 (d, *J* = 4.4 Hz, 4H), 7.11 (p, *J* = 4.3 Hz, 1H), 7.09 – 7.04 (m, 1H), 4.33 (d, *J* = 6.2 Hz, 1H), 3.83 (d, *J* = 2.7 Hz, 2H), 2.20 – 2.04 (m, 3H), 1.94 (t, *J* = 12.5 Hz, 1H), 1.54 – 1.46 (m, 1H), 1.32 (s, 3H), 1.18 (s, 3H). **Step 2:** Amide coupling was performed with the aminium chloride salt of **69-4** (46 mg, 0.15 mmol, 1.0 eq), di-Boc-Dmt (69 mg, 0.17 mmol, 1.1 eq), PyBOP (86 mg, 0.15 mmol, 1.0 eq), and 6-Cl HOBt (51 mg, 0.15 mmol, 1.0 eq), followed by DIPEA (0.21 mL, 1.52 mmol, 10 eq). Yield not calculated. After purification by silica chromatography, product was carried forward to **Step 3:** TFA deprotection, followed by purification by reverse-phase semi-preparative HPLC, as described in **General Procedure (H)**. Final yield not calculated. ¹H NMR (500 MHz, Methanol-*d*₄) δ 7.94 (d, *J* = 8.0 Hz, 1H), 7.25 – 7.10 (m, 5H), 7.03 – 6.98 (m, 2H), 6.49 (s, 2H), 3.87 (d, *J* = 14.7 Hz, 3H), 3.26 (dd, *J* = 13.6, 11.5 Hz, 1H), 3.01 (dd, *J* = 13.7, 5.0 Hz, 1H), 2.27 (s, 6H), 1.72 (dddd, *J* = 13.5, 11.0, 4.9, 2.7 Hz, 1H), 1.44 (dddd, *J* = 13.3, 7.8, 5.3, 2.7 Hz, 1H), 1.37 (ddd, *J* = 13.9, 7.4, 2.6 Hz, 1H), 1.24 – 1.18 (m, 1H), 1.17 (d, *J* = 7.2 Hz, 6H). ¹³C NMR (126 MHz, cd₃od) δ 171.84, 168.82, 165.07, 157.40, 145.26, 142.67, 140.04, 139.89, 135.46, 130.38, 129.75, 129.70, 129.38, 128.05, 127.01, 123.16,

116.51, 53.52, 49.83, 49.00, 42.24, 35.88, 34.28, 32.00, 31.71, 31.64, 26.76, 20.49. Calculated [M+H]⁺: 457.3. ESI-MS mass observed: 457.3 (M+H) and 480.3 (M+Na). Analytical HPLC retention time: 45.6 min.

Chapter 4: Additional Projects

The previous chapters have discussed the novel exploration of substitutions at C-8 (Chapter 2) and the effects of combined substitutions at C-6 and *N*-1 (Chapter 3). In the first two sections of Chapter 4, we will investigate cross-over projects, combining C-8 substitutions with each of the Chapter 3 pharmacophores previously explored. In the third section, efforts toward the further development of *in vivo* candidates—including both increasing the scale of synthesis and radiolabeling of analogue **43**—will be discussed. These additional projects involved only a small number of compounds. When relevant, related analogues synthesized by other chemists will be included to provide greater context for these works. The projects discussed in Chapter 4 are in various stages of completion, and as such, have not been published.

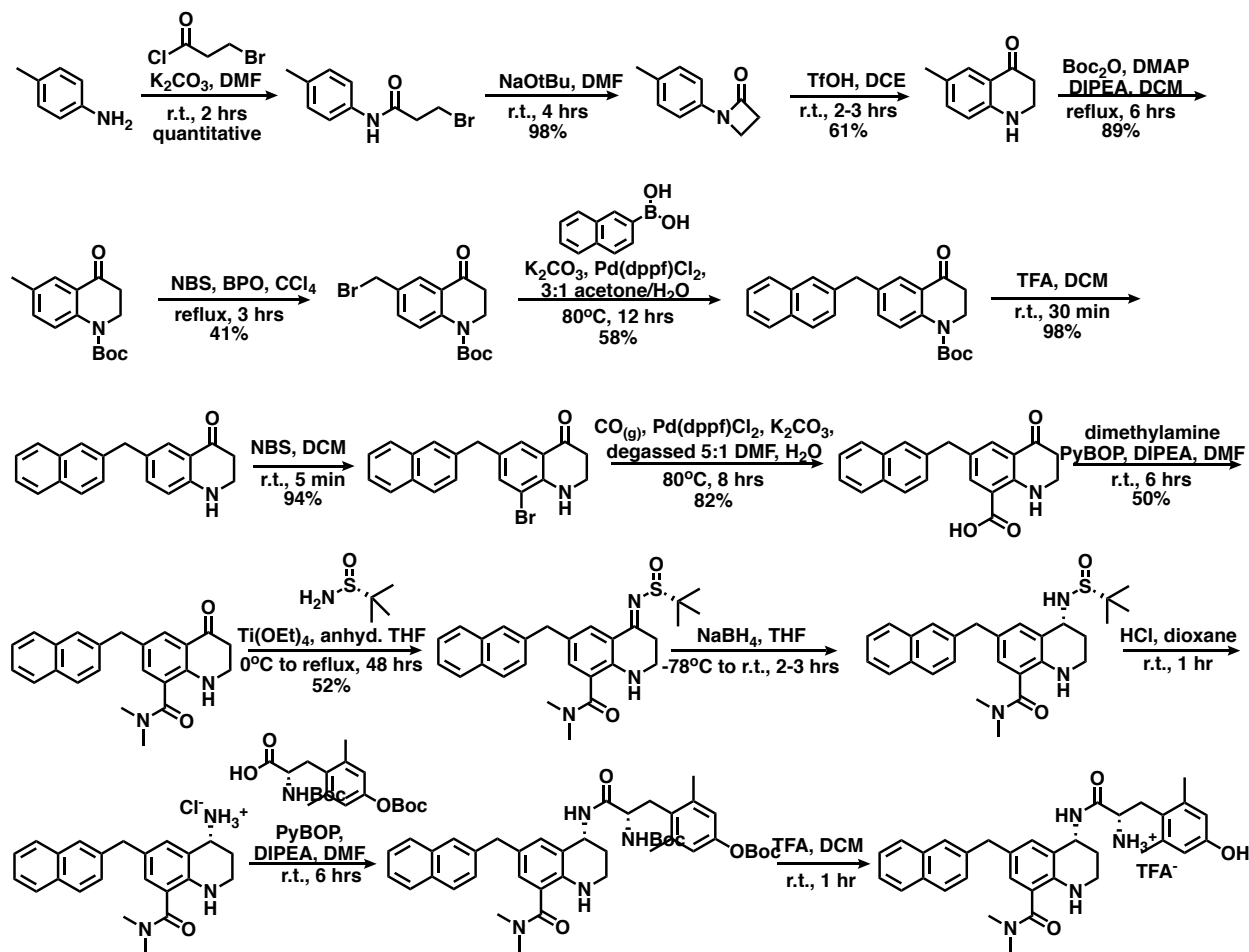
4.1 Bicyclic/C-8 Hybrid Peptidomimetics

As described in greater detail in Chapter 3, it was discovered that bicyclic pendants at the C-6 position of the THQ scaffold proved beneficial toward reducing DOR efficacy. On the other hand, the *N*-acyl and C-8 series—when combined with a monocyclic C-6 THQ core—typically displayed partial DOR agonism. However, when a bicyclic C-6 pendant was combined with an *N*-acyl or *N*-sulfonyl motif, these analogues often maintained the DOR antagonist profile and increased MOR potency to subnanomolar levels. As described previously, some *N*-acyl motifs (namely the acetyl and cyclopropyl) did generate DOR efficacy with single-digit to sub-nanomolar potency. As such, it was inferred that both the C-6 and *N*-1 substitutions could impart effects on *In vitro* pharmacology data obtained by Nicholas Griggs, Thomas Fernandez, Tyler Trask, Jessica Anand, and others in the lab of John Traynor. *In vivo* data were obtained by Jessica Anand and others in the lab of Emily Jutkiewicz.

DOR efficacy. Early on in the C-8 campaign, the idea of combining an advantageous C-8 substitution with a bicyclic C-6 pendant was explored. However, the most advantageous C-8 pendants were also the most bulky and lipophilic. Incorporating two bulky, aryl substitutions at C-6 and C-8 would result in undesirably lipophilic, amphipathic chemical matter. Indeed, compound **8**, which featured benzyl pendants at C-6 and C-8, displayed very poor aqueous solubility. Considering that the benzyl and ethylphenyl were initially our most advantageous substitutions, combining these with a bicyclic C-6 would yield an undesirably lipophilic core. Thus, this idea was shelved at an early stage.

Further synthetic and SAR development at the C-8 position provided renewed interest in combining advantageous C-8 and C-6 substitutions. It was discovered that a small, polar carbonyl-containing motif such as the dimethyl amide moiety found in analogue **20** could not only elicit DOR antagonism, but also reduced ClogP from 3.1 (no C-8 substitution) to 2.2. Furthermore, it had been shown that this low-ClogP analogue (**20**) maintained antinociceptive activity *in vivo*, whereas all other bioactive analogues in the C-8 series increased lipophilicity. Lastly, the carbonyl motif could be incorporated after installation of the C-6 pendant, simplifying the synthesis of this analogue. The first proof-of-concept bicyclic/C-8 hybrid peptidomimetic featured a 2-naphthyl pendant at C-6. The synthesis of this 2-naphthyl/C-8 dimethyl amide analogue **70** can be found in **Scheme 9**. Starting with the commercially available *p*-toluidine, this synthesis involves 15 steps, described in further detail below.

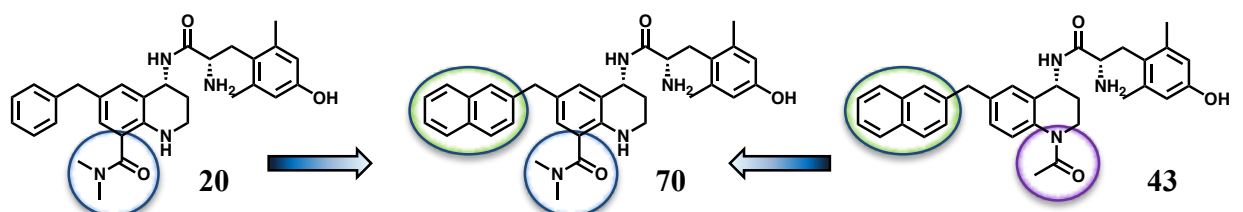
Scheme 9. De Novo Synthesis of Analogue 70



The synthesis of analogue **70** utilized methodologies previously developed and described in Chapters 2 and 3. Acylation, cyclization, and Fries Rearrangement proceed in fairly high yields to give the THQ core, which can be *N*-Boc protected prior to benzylic bromination of the C-6 methyl position. Suzuki coupling and Boc removal give the C-6 naphthyl THQ scaffold, which undergoes facile, selective aryl bromination at the C-8 position with exceptional yields. Palladium-catalyzed carbonylation with carbon monoxide (generated *in situ*) in DMF/H₂O produces the carboxylic acid at C-8. Amide coupling installs the C-8 dimethyl amide prior to reductive

amination. Upon cleaving the sulfinamide, the Dmt moiety is installed through another amide coupling. Final Boc deprotection and HPLC purification yields final compound **70**. While incorporation of the dimethyl amide prior to C-6 substitution would facilitate further diversification, the branched C-8 moiety sterically hinders Boc protection which is necessary for benzylic bromination of the C-6 position. As such, no other analogues have yet been synthesized of this type. However, as **Table 16** indicates, the *in vitro* profile is highly favorable (discussed below) and could merit further research around this chemotype. Further C-6 bicyclic pendants would need to be tolerant of bromination and carbonylation conditions if further analogues are synthesized following **Scheme 9**.

Table 16. Bicyclic/C-8 Hybrid Peptidomimetic **70** Compared to Parent Analogues **20** & **43**^a

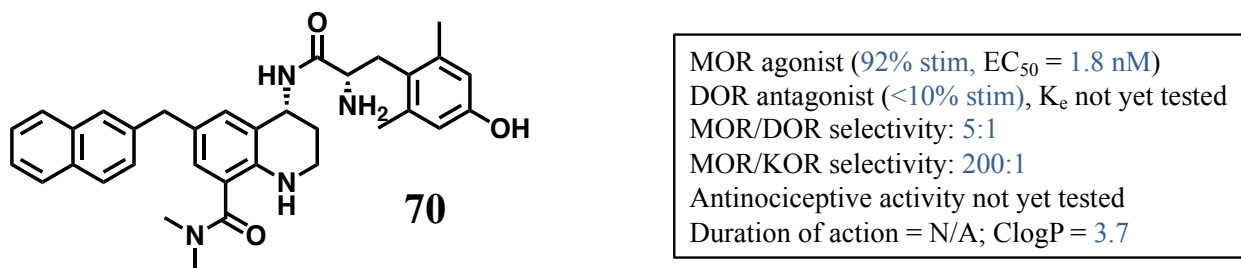


#	K _i (nM)				DOR K _i / MOR K _i	EC ₅₀ (nM)			% stim			ClogP
	MOR	DOR	KOR			MOR	DOR	KOR	MOR	DOR	KOR	
20	0.23 (0.08)	1.3 (0.2)	80 (50)		6	9 (3)	dns	>500	58 (1)	dns	25 (4)	2.2
70	0.15 (0.01)	0.73 (0.03)	28 (3)		5	1.8 (0.7)	dns	dns	92 (8)	dns	dns	3.7
43^b	0.04 (0.01)	0.23 (0.02)	48 (20)		6	0.9 (0.2)	dns	dns	87 (3)	dns	dns	4.5

^a Binding affinities (K_i) were obtained by competitive displacement of radiolabeled [³H]-diprenorphine in membrane preparations. Functional data were obtained using agonist induced stimulation of [³⁵S]-GTPγS binding. Potency is represented as EC₅₀ (nM) and efficacy as percent maximal stimulation relative to standard agonist DAMGO (MOR), DPDPE (DOR), or U69,593 (KOR). Values are expressed as the mean of three separate assays performed in duplicate with standard error of the mean in parentheses. dns = does not stimulate. ^b Synthesized by A.A.H., see reference ⁹⁴.

By translocating and inverting the tertiary amide moiety of analogue **43** from the *N*-1 to the C-8 position, analogue **70** maintains high MOR and DOR affinity but decreases ClogP from 4.5 to 3.7. Additionally, the preferred MOR agonist/DOR antagonist profile is maintained, with only a 2-fold reduction in MOR potency (though the high error associated with this value could negate or amplify this change in potency). Analogue **70** shows subnanomolar affinity for MOR and DOR with 5-fold MOR selectivity, consistent with the parent analogues **20** and **43**. This hybrid shows higher affinity for KOR, though selectivity for MOR over KOR is still approximately 200:1. A profile summary of analogue **70** is provided below in **Fig. 20**.

Figure 20. Profile Summary of Bicyclic/C-8 Hybrid Peptidomimetic **70**



Moving forward, analogue **70** is a prime candidate for further *in vivo* studies, as the *in vitro* profile meets our desired characteristics. However, due to recency of this ligand's synthesis, it still awaits *in vivo* testing.

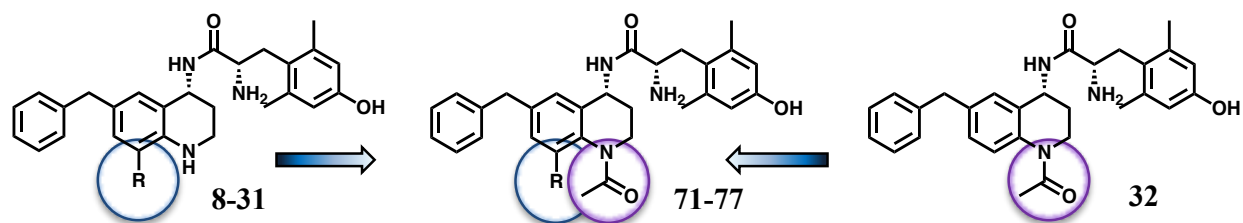
While analogue **70** is the only analogue to date utilizing a bicyclic C-6/carbonyl C-8 substitution pattern, it represents a promising means toward further diversifying the chemical motifs that maintain (or improve) our desired MOR agonist/DOR antagonist profile. Translocating the carbonyl moiety to C-8 and removing the H-bond donating capacity of the amide decreases the

ClogP of **70** relative to **43** while retaining most of the favorable *in vitro* properties. Additional analogues of this type should be further investigated, exploring different modifications to both the bicyclic C-6 and carbonyl C-8 substitutions. Based on the currently available data, analogue **70** represents a novel, if incremental diversification of the THQ-based peptidomimetic series that opens up new opportunities for drug development in the field of bifunctional MOR-/DOR-selective ligands.

4.2 *N*-Acetyl/C-8 Hybrid Peptidomimetics

Prior to the expanded investigation into combined bicyclic C-6/*N*-1 substitutions detailed in Chapter 3, *N*-acetylation of analogues was still a newly identified strategy for increasing DOR affinity and potentially improving bioavailability. This modification could typically be incorporated at a late stage in the synthesis, making these analogues easily accessible synthetically. Following this practice, several C-8 substituted analogues were *N*-acetylated in order to boost DOR affinity and bioavailability. However, given the proximity between the C-8 and *N*-1 substitutions, it was uncertain as to which motif would most strongly influence the pharmacological profile associated with these dually substituted ligands. In order to determine which substitution was most important and whether *N*-acetylation could reliably improve bioavailability, the compounds presented in **Table 17** were synthesized and evaluated *in vitro* and *in vivo*.

Table 17. *N*-Acetyl/C-8 Hybrid Peptidomimetics **71-77** Mimic Parent *N*-Acetyl Analogue **32**^a



#	R	K _i (nM)				DOR K _i / MOR K _i	EC ₅₀ (nM)			% stim		
		MOR	DOR	KOR			MOR	DOR	KOR	MOR	DOR	KOR
32 ^{b,c}	H	0.13 (0.02)	1.8 (0.1)	87 (11)		14	6.0 (1.3)	68 (2)	>500	76 (4)	26 (3)	29 (5)
71 ^b	F	0.15 (0.02)	0.9 (0.4)	30 (6)		6	1.4 (0.2)	77 (8)	>500	98 (2)	48 (5)	47 (3)
72	CH ₃	0.18 (0.04)	1.9 (0.5)	80 (20)		10	7 (2)	24 (1)	>500	85 (3)	31 (3)	31 (2)
73	CF ₃	0.19 (0.02)	1.3 (0.8)	49 (16)		7	11 (5)	30 (12)	>500 [†]	68 (3)	47 (3)	28 (1)
74	Br	0.25 (0.11)	1.2 (0.5)	27 (6)		5	6 [†] (3)	1.0 [†] (0.1)	>500 [‡]	79 (5)	44 (5)	51 [‡] (--)
75 ^b	OCH ₃	0.14 (0.01)	2.2 (1)	45 (17)		15	0.78 (0.2)	5 (2)	>500	96 (10)	45 (4)	16 (6)
76	n-Propyl	0.19 (0.02)	0.9 (0.5)	36 (7)		2	2.9 [†] (0.8)	7 (3)	dns [‡]	103 [†] (6)	29 (4)	dns [‡]
77	Benzyl	0.40 (0.08)	0.39 (0.15)	20 (8)		1	12 (3)	1.5 (0.2)	dns	71 (4)	34 (4)	dns

^a Binding affinities (K_i) were obtained by competitive displacement of radiolabeled [³H]-diprenorphine in membrane preparations. Functional data were obtained using agonist induced stimulation of [³⁵S]-GTPγS binding. Potency is represented as EC₅₀ (nM) and efficacy as percent maximal stimulation relative to standard agonist DAMGO (MOR), DPDPE (DOR), or U69,593 (KOR). Values are expressed as the mean of three separate assays performed in duplicate with standard error of the mean in parentheses. dns = does not stimulate. [†] n=2 [‡] n=1. ^b Synthesized by A.A.H. ^c First reported in reference ⁹⁴.

The analogues in **Table 17** show highly similar *in vitro* profiles to that of the parent analogue **32** featuring an *N*-acetyl moiety and no C-8 substitution. Generally, this series showed 0.1 to 0.2 nM affinity at MOR, 1 to 2 nM affinity at DOR, and double-digit nanomolar affinity at KOR, though KOR affinity varied considerably more than MOR or DOR, ranging between 10 and 100 nM affinity. The C-8 benzyl analogue **77** was somewhat of an outlier, displaying lower MOR

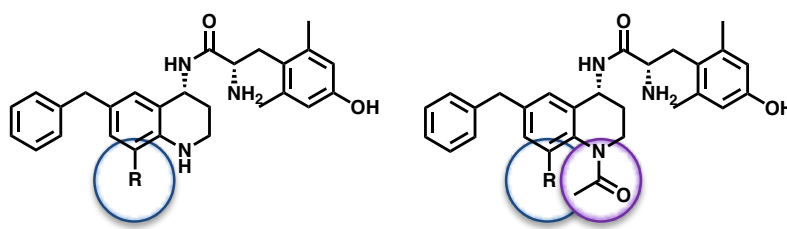
affinity and higher DOR affinity than those general trends previously stated. The decreased MOR affinity and increased DOR affinity combined to yield a perfectly balanced 1:1 MOR/DOR binding profile. Functionally, all analogues displayed MOR agonism with partial DOR agonism. MOR potency typically varied between 1 and 10 nM with no clearly discernible trends. On the other hand, DOR potency did show some dependence on the size of the C-8 substitution, with larger C-8 moieties (analogues **74-77**) displaying single-digit nanomolar potency and smaller C-8 motifs (analogues **32**, **71-73**) showing doubled-digit nanomolar potency. KOR efficacy was only observed at concentrations above 500 nM.

Aside from analogue **77**, all *N*-acetyl/C-8 hybrids in **Table 17** are pharmacologically indistinguishable from the unsubstituted parent analogue **32**. Due to the spatial proximity between C-8 and *N*-1, it appears that any meaningful interaction between these ligands and the opioid receptors are primarily mediated by the *N*-1 acetyl group. However, in the case of the C-8 benzyl analogue **77** where the benzyl group is significantly larger than the *N*-1 moiety, one can observe a departure from the common profile observed for others in this series. Notably, **77** displays more balanced binding and greater potency at DOR compared to most in this series. Additionally, MOR potency is the poorest for **77**, though only by a slight margin. This short series of analogues efficiently answered the question of which motif was most likely to influence the *in vitro* profile of a dually C-8/*N*-1 substituted analogue. This dependence on *N*-1 to dictate pharmacological profile, comparatively independent of C-8, is consistent with the flat binding SAR discussed in the C-8 substituted series of Chapter 2. Because the C-8 moieties likely occupy a flexible or solvent-exposed pocket of the opioid receptors, it is unsurprising that the *N*-1 motif influences ligand binding more strongly. *N*-acetylation of the C-8 ethyl ester analogue **26** was also attempted, seeking to determine whether DOR antagonism could be reestablished despite the masking effect

of the *N*-acetyl moiety. However, synthesis of this analogue was unsuccessful, as acetylation of *N*-1 was sterically occluded by the rigid, branched carbonyl at C-8.

Concerning bioavailability, most analogues in **Table 17** were evaluated *in vivo*, probing whether *N*-acetylation did indeed improve bioavailability for this series. These results are depicted in **Table 18**, where *N*-acetyl analogues are compared with their unacetylated counterparts.

Table 18. Investigating the Effect of *N*-Acetylation on Bioavailability for C-8 Substituted Ligands^a



<i>N</i> -H C-8 Analogues			<i>N</i> -Acetyl C-8 Analogues		
#	C-8 R Group	% MPE	#	C-8 R Group	% MPE
1 ^b	H	100	32 ^{c, d}	H	dns
14 ^c	F	dns	71 ^c	F	dns
9	CH ₃	100	72	CH ₃	100
15	CF ₃	dns	73	CF ₃	50
16	Br	50	74	Br	---
78 ^c	OCH ₃	---	75 ^c	OCH ₃	---
11	n-Propyl	dns	76	n-Propyl	dns
8	Benzyl	dns	77	Benzyl	dns

^a Results from the mouse WWTW assay after cumulative dosing of test compound up to 10 mg/kg ip. Antinociceptive activity represented as percent maximum possible effect (% MPE), with MPE being a 20 s latency to tail withdrawal. Baseline tail withdrawal latency is ~5 s, or 25% MPE. “dns” indicates no stimulation of an antinociceptive response.

^b Reported in reference ⁸³. ^c Synthesized by A.A.H. ^d Reported in reference ⁹⁴.

Of the analogues tested in the WWTW assay for antinociception, only the C-8 methyl analogue **72** (within the *N*-acetyl series) displayed full antinociceptive activity. Correspondingly, the unacetylated C-8 methyl analogue **9** was also fully active *in vivo*. The *N*-acetyl analogue **72** did show a slightly improved duration of action of 2.0 h compared to 1.5 h for **9**. Additionally, the trifluoromethyl analogue went from inactive (analogue **15**) to partially active (**73**) when acetylated. Conversely, *N*-acetylation actually eliminated the bioavailability of the lead peptidomimetic **1** as seen in analogue **32**. It may be informative to evaluate the *N*-acetyl C-8 bromo analogue **74** *in vivo*, as the unacetylated **16** showed partial activity. However, on the whole it can be surmised that while *N*-acetylation may improve bioavailability, it does so only sporadically and unpredictably.

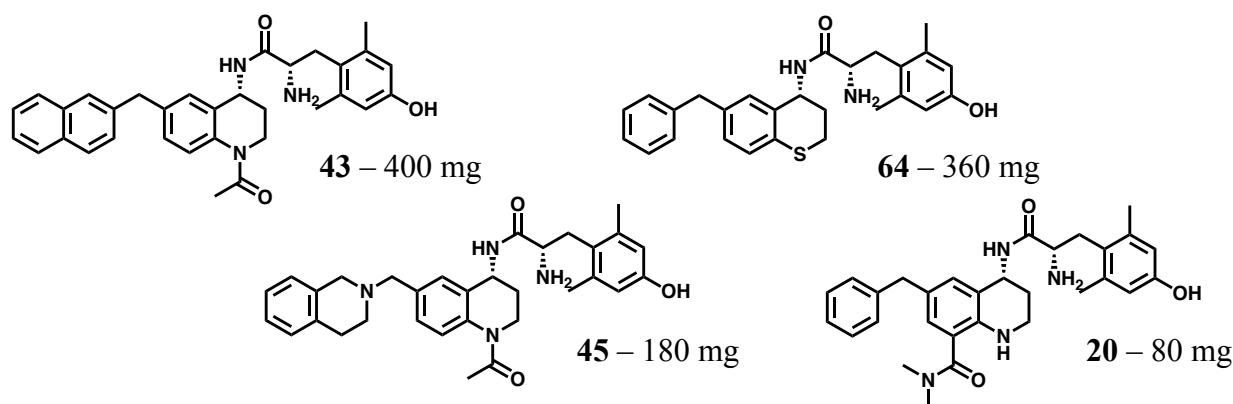
In this short series of analogues, we observed that *N*-acetylation dictates the *in vitro* profile more significantly than the small C-8 substitutions investigated here. However, in the case of the larger benzyl pendant of **77**, the MOR/DOR balancing effect associated with the C-8 benzyl substitution can be observed, as **77** displayed a 1:1 binding ratio at MOR and DOR. Functionally, all ligands in this series were partial DOR agonists. Unfortunately, it was not synthetically tractable to incorporate a C-8 carbonyl substitution as well as an *N*-acetyl substitution, as these branched substitutions caused insurmountable allylic (A^{1,3}) strain. As such, C-8 substitutions evaluated in this series were limited to small or unbranched motifs. Bioavailability for this series of compounds showed no reliable improvement relative to the unsubstituted analogues, consistent with other *N*-acetylated/non-acetylated pairs synthesized previously. From the work presented in this chapter and those preceding, *N*-1 and C-8 substitutions show highly favorable profiles when combined with a C-6 bicyclic pendant. However, when both are implemented in the context of a monocyclic C-6 benzyl pendant, the benefits are minor. While these results support previous observations, this

series did not substantially improve *in vitro* or *in vivo* parameters and is unlikely to be utilized in further ligand design.

4.3 Scaled Syntheses of *In Vivo* Candidates & Radiosynthetic Approaches

The main focus of the preceding chapters has been the design and synthesis of novel ligands to further probe SAR and generate new leads for opioid drug design with the aim of eliminating analgesic tolerance and opioid dependence. In this section, projects focused less on chemical novelty and more on the further evaluation of select candidates *in vivo*. In particular, this section will detail two projects necessitating the increased scale of synthesis of analogues **43**, **45**, **64**, and **20** shown in **Fig. 21**. The first project involved the scaled synthesis of all four aforementioned analogues for evaluation in *in vivo* assays including those for tolerance, dependence, and conditioned place preference (CPP) among others. The second project involved the attempted radiosynthesis of [^{11}C]**43**. The results of the first project were reported in part in a 2018 manuscript published in the *British Journal of Pharmacology*.⁹⁸ Unfortunately, the second project stalled at radiosynthesis and has not been further pursued at present.

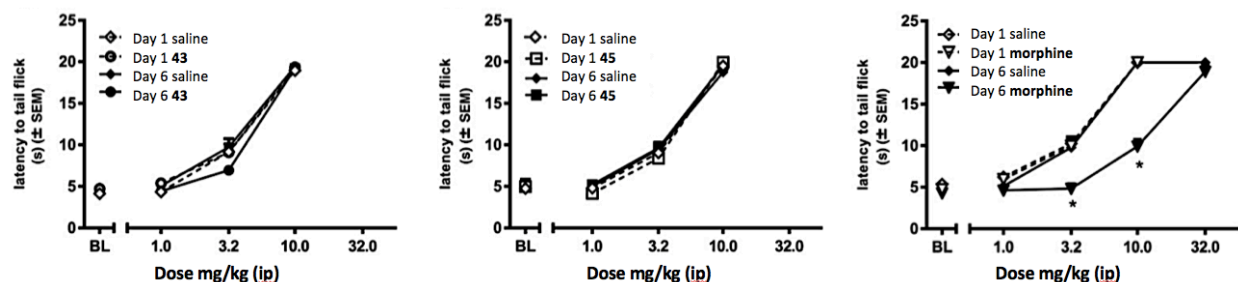
Figure 21. *In Vivo* Candidates and Amounts of Compound Synthesized



Novel peptidomimetic ligands—requiring *in vitro* and in some cases *in vivo* evaluation—are typically synthesized with a target yield of five to ten milligrams of final compound. However, compounds showing robust antinociceptive activity—especially those with a long duration of action and favorable *in vitro* profile—may be selected for further evaluation in chronic antinociceptive tolerance, physical dependence, and CPP models. Descriptions of these assays and the resultant data for compounds **43**, **45**, and **64** are detailed below. Compound **20** has been synthesized but is yet to be evaluated in the assay for chronic tolerance, dependence, or CPP.

To test for chronic tolerance, mice were given twice daily injections ip of saline or test compound at escalating doses, such that on day one, mice received two 10 mg/kg doses of test compound, and by day five, mice received two 50 mg/kg injections of test compound. Following five days of escalating treatment with a test compound, animals were evaluated in the WWTW assay on day six. When using morphine as a test compound, a significant rightward shift in the dose-response curve was observed on day six compared to WWTW dose-response performed prior to chronic drug exposure. However, compounds **43**, **45**, and **64** showed no significant rightward shift in dose-response curve after chronic drug exposure, indicating these compounds produce significantly less antinociceptive tolerance than morphine.⁹⁸ **Fig. 22**, adapted from Anand et. al., 2018, shows the results of the chronic tolerance assay for **43**, **45**, and morphine—**64** was evaluated subsequent to the publication of these results and is not included in **Fig. 22**. Showing no significant analgesic tolerance, **43**, **45** and **64** were then advanced into dependence models.

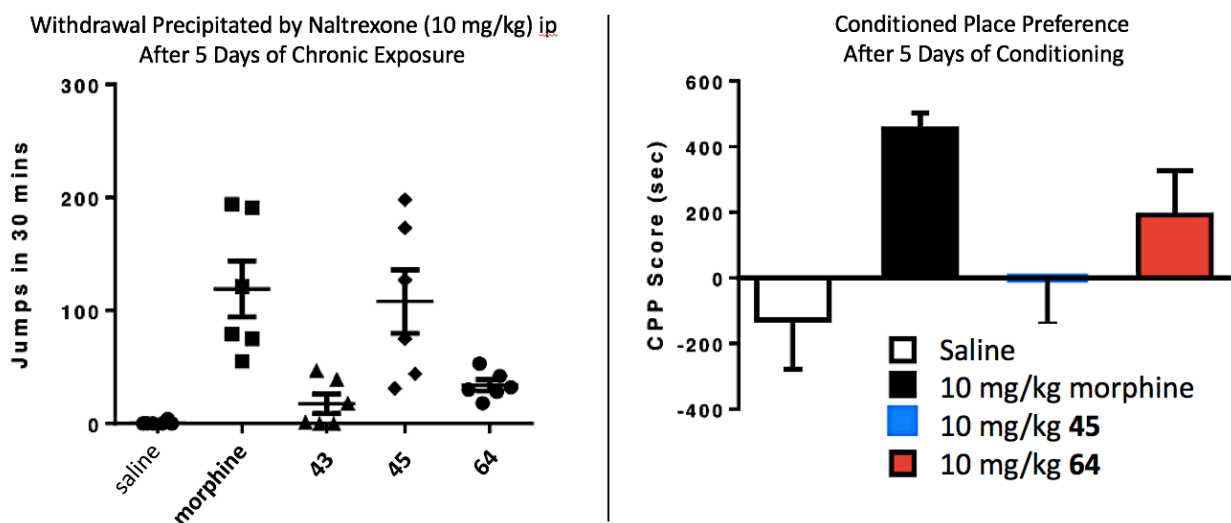
Figure 22. Chronic Antinociceptive Tolerance Evaluation of **43**, **45**, and morphine^a



^a Mice were given test compound or saline in escalating doses over a 5-day regimen and were tested in the WWTW assay using test compound on days 1 and 6. After 5 days of saline, no tolerance is observed for any compound. After 5 days of morphine, tolerance develops indicated by the rightward shift in dose-response curve. No tolerance develops for analogues **43** or **45**. BL = baseline. Figure adapted from Anand et. al., 2018 (reference ⁹⁸).

Dependence models utilized the same escalating dosing regimen as tolerance, where mice were exposed to increasing doses of test compound (or saline) for five days and were evaluated on day six. Following five days of chronic opioid exposure, mice were given naltrexone, an opioid antagonist, to precipitate withdrawal symptoms. Chronic treatment with morphine, followed by naltrexone, induced significant withdrawal jumps compared to chronic saline treatment (baseline). However, compounds **43** and **64** showed no difference in withdrawal jumps compared to saline, suggesting these compounds do not produce significant opioid dependence. On the other hand, compound **45** looked similar to morphine in this assay, indicating **45** did induce physical dependence.⁹⁸ These results, as well as those for CPP evaluation, are displayed below in **Fig. 23**.

Figure 23. Compounds **43** and **64** Show No Physical Dependence; Only **43** Shows No CPP^a



^a To test for physical dependence, mice were given test compound or saline in escalating doses over a 5-day regimen. On day 6, mice were given naltrexone to precipitate opioid-induced withdrawal jumps. Compound **45** showed comparable withdrawal symptoms to morphine while **43** and **64** showed significantly less dependence. In the two-chambered CPP apparatus, mice preferred the morphine-paired side while saline and **45** induced no significant preference. **64** was not significantly different from either saline or morphine. Results adapted from data prepared by J.P.A. and reported in part in reference ⁹⁸.

The final assay discussed here, evaluation of CPP as a proxy for “drug-seeking” or “reward,” uses a two-chambered apparatus. One chamber is paired with test compound whereas the other is paired with saline. After five days of conditioning, mice are free to inhabit either chamber. In this model, rewarding drugs such as morphine cause mice to preferentially occupy the drug-paired side, whereas the negative control (where saline is paired with both chambers) induces no significant preference for either chamber. Only compounds **43** and **64**—which showed significantly less physical dependence than morphine—were evaluated in the CPP assay. Compound **43** showed significantly less CPP than morphine, mimicking the negative control, saline. However, compound **64** showed intermediate levels of CPP, not statistically different from either saline or morphine.⁹⁸ Dr. Jessica Anand (J.P.A.), was the lead pharmacologist who oversaw or performed the aforementioned assays. **Figs. 22** and **23** were adapted from the manuscript⁹⁸ and

data presentations prepared by J.P.A. Compounds for these experiments were synthesized by A.F.N. and D.J.M.

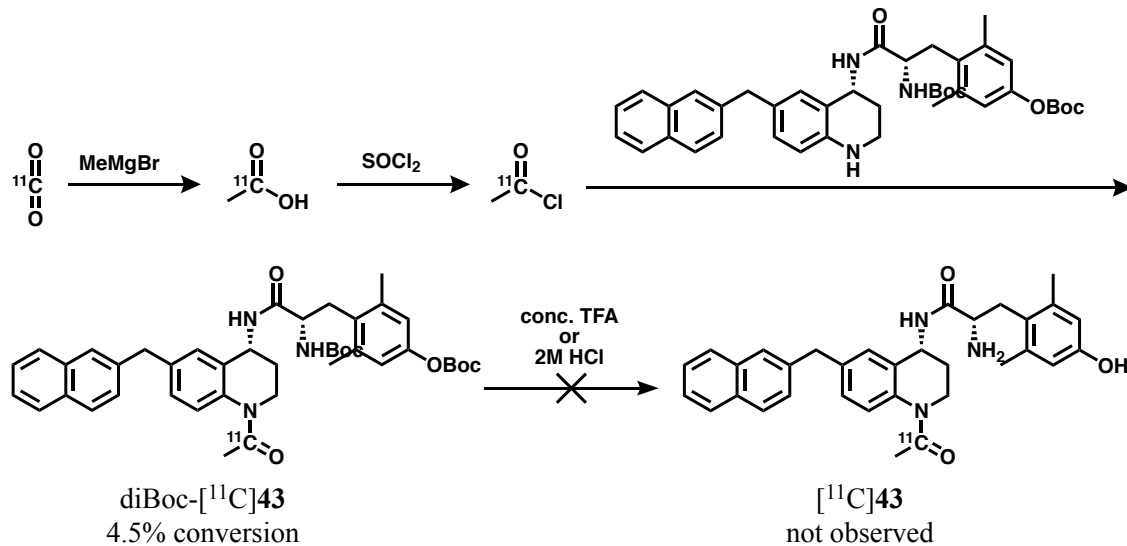
At present, compound **20** is awaiting evaluation in tolerance models to determine whether this analogue should be carried forward with dependence and CPP assays. The twice-daily dosing regimen utilized for morphine, **43**, **45**, and **64** was not suitable for the short-acting analogue **20** (2.0 h), as mice would be below the therapeutic threshold during much of the drug exposure period. As such, methodological development was required in order to evaluate shorter-acting analogues for tolerance, dependence, and CPP. Methods are currently in development using fentanyl—a short-acting MOR agonist known to induce tolerance and dependence—as a positive control. Once these protocols are established and functioning reliably, compound **20** will be evaluated for the aforementioned assays.

Due to the cumulative dosing and number of trials (n=6 mice for each compound), the amount of final compound required for these assays was substantial. As such, the scale of syntheses were increased by one to two orders of magnitude. In addition to tolerance, dependence, and CPP, the *in vivo* candidates shown in **Fig. 21** (as well as others not shown, but also synthesized in lesser, 20 to 60 mg quantities) were required for various other *in vivo* experiments including but not limited to the following: evaluation of antinociception in rats as well as MOR-knockout and PGP-knockout mice, evaluation of antinociception after pretreatment with the non-specific opioid antagonist naltrexone (affirming opioid-mediated antinociception) or the PGP-inhibitor elacridar (to determine if these ligands are PGP substrates), evaluation of DOR antagonism *in vivo* by pretreatment with ligand followed by the DOR agonist SNC-80, evaluation for constipation and locomotion, and various other *in vivo* assays. Because these compounds were synthesized on-demand, the quantities listed in **Fig. 21** represent cumulative totals and not yields synthesized in a

single batch. The largest single batch of compound produced was 280 mg of **43**, followed by two batches of 180 mg each for compound **64**.

Advancement of *in vivo* candidates through preclinical animal models has validated **43** as a bioavailable analgesic with significantly reduced tolerance, dependence and CPP compared to morphine. More generally, these results support the bifunctional MOR agonist/DOR antagonist approach as a viable strategy for reducing side effects associated with classical opioid treatment. Moving forward, the Mosberg lab and collaborators were interested in gathering further data concerning the pharmacokinetics of **43**. In order to track **43** through the phases of absorption, distribution, metabolism and excretion, effort was made toward radiolabeling **43** with a ^{11}C nuclide which can be tracked via positron emission tomography (PET) *in vivo*. Though at longer-lasting nuclide such as ^{18}F would provide more information over a longer duration, no fluorinated analogues of the peptidomimetic series have demonstrated robust *in vivo* activity. Importantly, despite the short half-life of the ^{11}C nuclide, an [^{11}C]**43** ligand could confirm whether or not **43** gains access to the central nervous system (CNS), further substantiating the notion that our peptidomimetic was centrally-acting. In order to bolster the novelty of **43** as a CNS-active opioid devoid of tolerance and dependence, visual demonstration (in addition to pharmacological evidence) of CNS access via PET would be instrumental. With this goal in mind, we aimed to incorporate an ^{11}C nuclide into the acetyl group of **43** as described in **Scheme 10**. The synthesis of unlabeled precursor and HPLC standards was performed by A.F.N., while radiolabeling was performed by Dr. Allan Brooks and Dr. Xia Shao as a collaborative project with Dr. Peter Scott's laboratory.

Scheme 10. Attempted Radiolabeling of [^{11}C]**43**



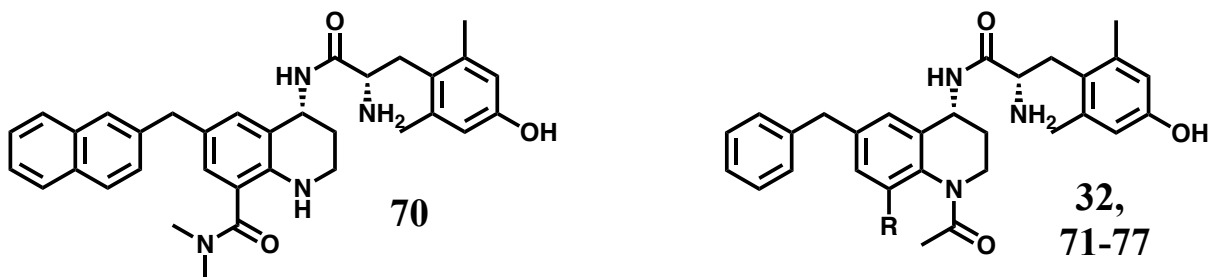
Synthesis of [^{11}C]**43** was attempted using a Boc-protected unacetylated precursor of **43** and [^{11}C]acetyl chloride, derived from [^{11}C]CO₂ which is converted to [^{11}C]acetate by methyl Grignard. Treatment of the acetate with thionyl chloride gives the activated acid chloride, which was successfully incorporated into the peptidomimetic molecule with 4.5% conversion. However, subsequent Boc-deprotection methodologies using TFA or HCl both removed the ^{11}C -labeled acetyl group. This was unexpected, as acetyl removal had not been observed previously with unlabeled compounds. Nonetheless, the desired [^{11}C]**43** product was not observed by HPLC. Due to expense and time constraints, radiosynthesis was not further pursued at this time.

Although the design and synthesis of novel chemical matter is a major focus of any synthetic chemist working in drug development, the importance of resynthesizing or incrementally modifying chemical hits should not be understated. In order to proceed further, or to redirect efforts in more fruitful directions, it is often necessary to halt novel chemical exploration in favor of

deeper exploration of chemical guideposts. In this chapter, considerable effort was dedicated to further evaluating compound **43** for both pharmacological effects as well as pharmacokinetic properties. Through this deeper investigation, it was discovered that not all MOR agonist/DOR antagonist compounds with *in vivo* activity are effective at reducing tolerance and dependence, as was the case of compound **45**. At present, the reason for why some analogues are more effective than others at reducing side-effects is unknown. However, the work detailed in this section provided critical proof-of-concept data in support of the bifunctional MOR agonist/DOR antagonist approach. Furthermore, this work bolsters the bicyclic C-6/N-1 research described in Chapter 3 which builds incrementally from the chemotype of *in vivo* candidates **43** and **45**. Through this collaborative work, we have demonstrated that the bifunctional, bicyclic C-6/N-1 THQ-based peptidomimetics may indeed (but do not necessarily) offer the target pharmacological profile both *in vitro* and *in vivo*. Future directions in this field of research, in the context of the work described in the preceding chapters, will be discussed further in Chapter 5.

4.4 Experimental Procedures

Figure 24. Structures of Analogues 32, 70-77 Discussed in Chapter 4



R=								
	32	71	72	73	74	75	76	77

General Procedures	252
Compound 70 and Preceding Intermediates	254
Compound 72 and Preceding Intermediates	258
Compound 73 and Preceding Intermediates	261
Compound 74 and Preceding Intermediates	263
Compound 76 and Preceding Intermediates	265
Compound 77 and Preceding Intermediates	267

*Analogues 32, 71 and 75 were synthesized by A.A.H. See her thesis for synthetic details.

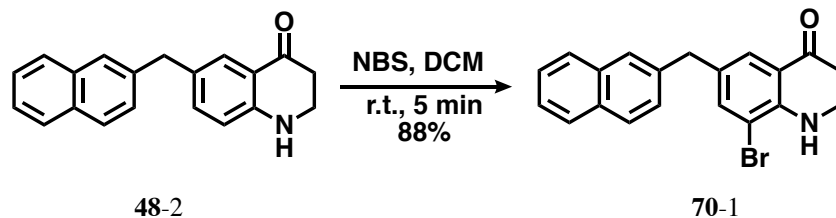
General Procedure (A): *N*-Acylation or Mesylation of the THQ core. To a round-bottom flask containing THQ intermediate (1.0 eq) was added acetic anhydride (excess) and heated to 100°C. When starting material showed complete conversion to product by TLC, solvent was removed under reduced pressure and reaction mixture was purified by silica chromatography. When noted, product was isolated by crystallization and was used without further purification.

General Procedure (B): Reductive Amination of THQ Ketone Intermediate to a Sulfinamide Using Ellman's Chiral Auxilliary. To a round bottom flask already containing desiccated THQ intermediate (1.0 eq) under Ar atmosphere was added (R)-2-methylpropane-2-sulfinamide (3.0 eq). Meanwhile, a reflux condenser was flame-dried under vacuum, and then flooded with Ar. Next, anhydrous THF (5-10 mL) was added to the reaction vessel containing starting reagents via syringe. The round bottom flask was placed in an ice bath and allowed to equilibrate to 0°C. Next, Ti(OEt)₄ (6.0 eq) was added slowly via syringe. Once addition was complete, the reaction vessel was taken out of ice bath and placed in oil bath at 70°C-75°C, affixed condenser, and stirred for 16-48 h under Ar. The reaction was monitored by TLC for loss of ketone. Once sufficient conversion to the tert-butanefulfinyl imine was observed, reaction vessel was taken out of oil bath and cooled to ambient temperature. Meanwhile, an additional round bottom flask was flame-dried under vacuum, then flooded with Ar. NaBH₄ (6.0 eq) was added quickly, and anhydrous THF was added (5-10 mL). The round bottom flask was placed in dry ice/acetone bath and allowed to equilibrate to -78°C. Contents from the round bottom flask containing the imine intermediate were transferred to round bottom flask containing NaBH₄ via cannula. Imine-containing flask was washed twice with minimal THF, which was also transferred to reducing flask via cannula under Ar. Once contents were completely added, the reaction was taken out of dry ice/acetone bath and was allowed to warm to room temperature. The reaction stirred at ambient temperature for 2-3 h.

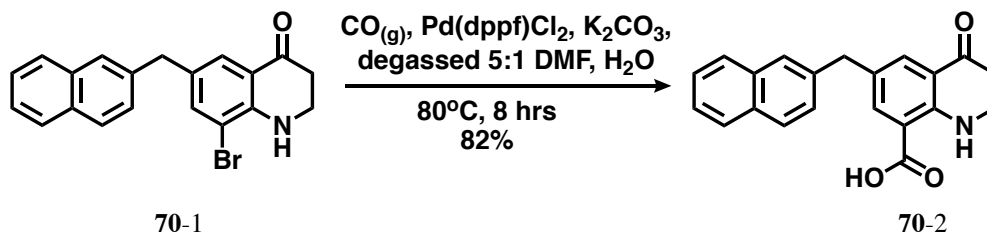
To quench, sat. NaCl solution was added. Reaction mixture was diluted with ethyl acetate and DI H₂O and separated, washing with H₂O until both layers were clear, indicating sufficient removal of titanium oxide by-product. Organics were then isolated and dried over MgSO₄ and filtered through a fritted funnel. Organic extract was then concentrated onto silica and purified by silica chromatography.

General Procedure (C): Conversion of Sulfinamide to Final Compound. Step 1: To a round bottom flask containing sulfinamide (1.0 eq) was added 1,4-dioxane, followed by conc. HCl (6.0 eq), cleaving the sulfinamide to the primary amine. The reaction stirred at RT for up to 3 h. Solvent was removed under reduced, and residue was re-suspended in Et₂O. The resultant white solid precipitate (the HCl salt of the amine) was isolated by decanting and washing with Et₂O up to three times. After desiccation, the solid residue was used without further purification. **Step 2:** To a pear-shaped flask under inert atmosphere containing amine salt (1.0 eq) was added di-Boc-Dmt (1.1 eq), PyBOP (1.1 eq), and, when specified, 6-Cl HOBt (1.1 eq), followed by DMF and DIPEA (10 eq) at ambient temperature. After stirring for 6 hours, solvent was removed under reduced pressure and residual oil was loaded onto silica. Boc-protected intermediate was purified by silica chromatography but was generally not characterized by NMR. **Step 3:** Boc-protected intermediate was suspended in DCM (10 mL), then TFA (3-5 mL) was added. After 1 hour, solvent was removed under vacuum. Product was resuspended in a solution of 99.9% acetonitrile, 0.1% TFA, then diluted with deionized water. Final products were purified by reverse-phase semi-preparative HPLC. Final yield not calculated.

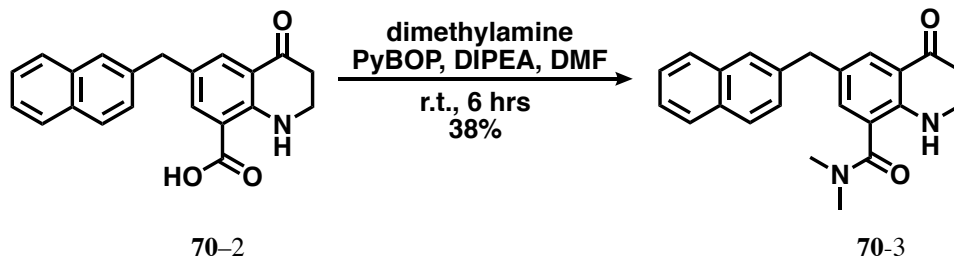
Compound 70



70-1 8-bromo-6-(naphthalen-2-ylmethyl)-2,3-dihydroquinolin-4(1H)-one. Intermediate **70-1** was synthesized from intermediate **48-2**, whose synthesis was described in Section 3.8 Experimental Procedures. To a round-bottom flask containing intermediate **48-2** (275 mg, 0.96 mmol, 1.00 eq), dissolved in dichloromethane under inert atmosphere was added *N*-bromosuccinimide (178 mg, 1.00 mg, 1.05 eq) at ambient temperature. After 5 minutes, TLC in 40% ethyl acetate, 60% hexanes showed complete conversion. Reaction was concentrated onto silica *in vacuo* and was purified by flash chromatography. Yield: 290 mg, 88%. ^1H NMR (500 MHz, Chloroform-*d*) δ 7.79 (d, $J = 8.3$ Hz, 1H), 7.77 (s, 1H), 7.76 (d, $J = 4.9$ Hz, 1H), 7.61 (d, $J = 1.8$ Hz, 1H), 7.48 – 7.41 (m, 3H), 7.43 (s, 1H), 7.28 (dd, $J = 8.4, 1.6$ Hz, 1H), 4.90 (s, 1H), 4.01 (s, 2H), 3.66 – 3.59 (m, 2H), 2.71 (t, $J = 6.9$ Hz, 2H). ^{13}C NMR (126 MHz, cdcl_3) δ 193.14, 147.49, 138.67, 138.14, 133.72, 132.29, 131.25, 128.45, 127.77, 127.71, 127.40, 127.19, 127.13, 126.22, 125.63, 120.35, 110.44, 41.98, 40.99, 37.61.

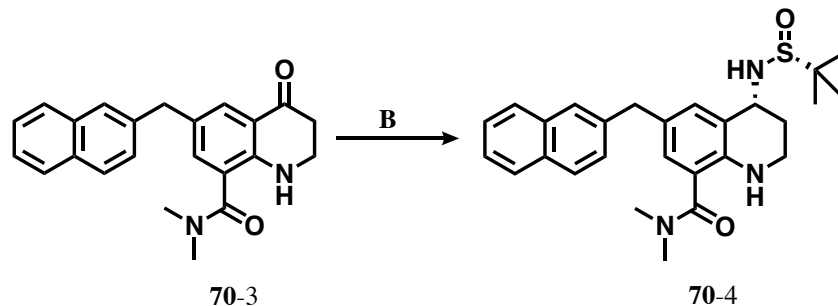


70-2 6-(naphthalen-2-ylmethyl)-4-oxo-1,2,3,4-tetrahydroquinoline-8-carboxylic acid. **70-2** was synthesized using the following procedure: To a flame-dried pear-shaped flask under Ar atmosphere was added intermediate **70-1** (310 mg, 0.85 mmol, 1.0 eq), K₂CO₃ (175 mg, 1.27 mmol, 1.5 eq) and Pd(dppf)Cl₂ (62 mg, 0.09 mmol, 0.1 eq), followed by 5:1 DMF/H₂O (12 mL). To a separate 30 mL pressure tube under Ar atmosphere was added 2M NaOH (15 mL), then evacuated, flushed with Ar, and bubbled Ar through base solution for 15 min. To the bottom of the tube containing stirring base solution was added, via syringe, oxalyl chloride (1 mL in aliquots of 0.1 to 0.2 mL). Carbon monoxide generated *in situ* from the decomposition of oxalyl chloride was cannulated to the reaction mixture. Reaction was heated at 80°C for 8 hours, monitored by TLC. When TLC indicated conversion of starting material to new product, reaction was cooled to ambient temperature and reaction solvents were removed under vacuum. Residual oil was resuspended in ethyl acetate and water, and acid/base extraction was performed. Organics were isolated, dried with MgSO₄, filtered, and reconcentrated onto silica *in vacuo*. Reaction was purified by flash chromatography. Reaction yielded 190 mg pure **70-2**, 82%. An additional 120 mg of impure material containing **70-2** was isolated and was carried forward separately. ¹H NMR (500 MHz, Chloroform-*d*) δ 9.78 (s, 1H), 8.47 (s, 1H), 8.03 (d, *J* = 2.2 Hz, 1H), 7.82 – 7.79 (m, 1H), 7.78 (dd, *J* = 7.8, 2.4 Hz, 2H), 7.65 – 7.61 (m, 1H), 7.52 (d, *J* = 2.3 Hz, 1H), 7.50 – 7.40 (m, 2H), 7.29 (dd, *J* = 8.4, 1.8 Hz, 1H), 4.08 (s, 2H), 3.68 (td, *J* = 7.2, 2.5 Hz, 2H), 2.77 – 2.70 (m, 2H). ¹³C NMR (126 MHz, cdcl₃) δ 193.57, 192.56, 151.31, 143.15, 137.99, 135.06, 133.73, 132.33, 128.57, 128.52, 127.80, 127.70, 127.33, 127.16, 126.32, 125.72, 120.68, 120.15, 77.16, 40.82, 40.68, 37.12.

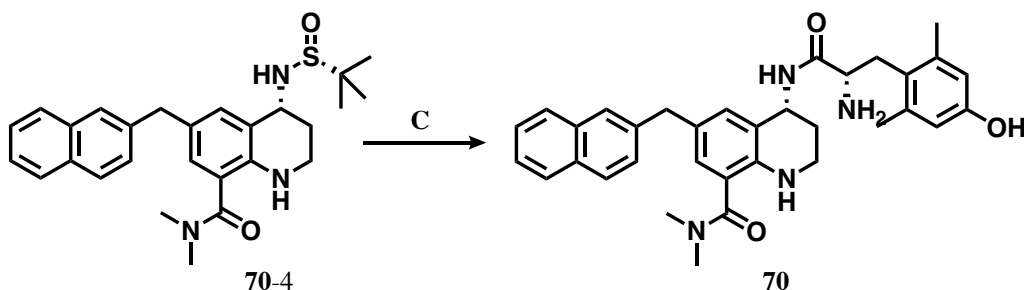


70-3 *N,N*-dimethyl-6-(naphthalen-2-ylmethyl)-4-oxo-1,2,3,4-tetrahydroquinoline-8-carboxamide.

Intermediate **70-3** was synthesized by the following procedure: To a pear-shaped flask containing intermediate **70-2** (91 mg, 0.27 mmol, 1.0 eq) dissolved in DMF under inert atmosphere was added PyBOP (157 mg, 0.30 mmol, 1.1 eq), dimethylamine hydrochloride (45 mg, 0.55 mmol, 2.0 eq) and DIPEA (0.48 mL, 2.74 mmol, 10 eq), then stirred at ambient temperature. Reaction was monitored by TLC. After 5 hours, solvent was removed under reduced pressure and reconcentrated residue onto silica *in vacuo*. Crude reaction mixture was combined with a previously run trial reaction which used impure starting material. The combined reactions were purified by flash chromatography, giving a combined overall yield of 125 mg, or 38% of the theoretical combined yield. ¹H NMR (500 MHz, Chloroform-*d*) δ 7.85 (d, *J* = 2.2 Hz, 1H), 7.79 (dd, *J* = 7.4, 1.8 Hz, 1H), 7.77 – 7.72 (m, 2H), 7.59 (s, 1H), 7.44 (pd, *J* = 6.8, 1.5 Hz, 2H), 7.26 (dd, *J* = 8.4, 1.7 Hz, 1H), 7.08 (d, *J* = 2.2 Hz, 1H), 5.92 (s, 1H), 4.03 (s, 2H), 3.54 (t, *J* = 7.0 Hz, 2H), 2.97 (s, 7H), 2.67 (t, *J* = 7.0 Hz, 2H). ¹³C NMR (126 MHz, cdcl₃) δ 193.60, 170.09, 149.64, 138.42, 134.94, 133.69, 132.24, 129.57, 128.67, 128.36, 127.75, 127.64, 127.43, 127.09, 126.21, 125.58, 120.46, 120.37, 77.16, 46.42, 46.38, 41.59, 41.00, 37.69, 26.50, 26.44.



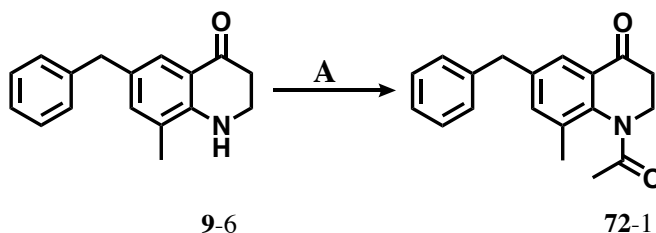
70-4 *(R)*-4-(((*R*)-*tert*-butylsulfinyl)amino)-*N,N*-dimethyl-6-(naphthalen-2-ylmethyl)-1,2,3,4-tetrahydroquinoline-8-carboxamide. Intermediate **70-4** was synthesized following **General Procedure (B)** from intermediate **70-3** (125 mg, 0.35 mmol, 1.0 eq), (*R*)-2-methyl-2-propanesulfonamide (127 mg, 1.05 mmol, 3.0 eq), and $\text{Ti}(\text{OEt})_4$ (0.44 mL, 2.10 mmol, 6.0 eq), then NaBH_4 (80 mg, 2.10 mmol, 6.0 eq). Yield: 45 mg, 23%. ^1H NMR (500 MHz, Chloroform-*d*) δ 7.78 (d, $J = 7.7$ Hz, 2H), 7.74 (dd, $J = 10.7, 8.0$ Hz, 2H), 7.60 (s, 1H), 7.43 (pd, $J = 6.9, 1.6$ Hz, 2H), 7.28 (s, 1H), 7.19 (d, $J = 2.1$ Hz, 1H), 6.82 (d, $J = 2.1$ Hz, 1H), 4.53 (d, $J = 3.0$ Hz, 1H), 3.99 (d, $J = 2.8$ Hz, 2H), 3.37 (td, $J = 11.9, 2.9$ Hz, 1H), 3.22 (td, 1H), 2.96 (s, 6H), 2.05 (dd, $J = 13.7, 3.3$ Hz, 1H), 1.88 (t, $J = 12.9$ Hz, 1H), 1.21 (s, 9H).



70 *(R)*-4-(((*S*)-2-amino-3-(4-hydroxy-2,6-dimethylphenyl)propanamido)-*N,N*-dimethyl-6-(naphthalen-2-ylmethyl)-1,2,3,4-tetrahydroquinoline-8-carboxamide. **70** was synthesized following **General Procedure (C)** from intermediate **70-4**. **Step 1:** Sulfinamide cleavage was carried out with **70-4** (45 mg, 0.10 mmol, 1.0 eq) and excess concentrated HCl, precipitating

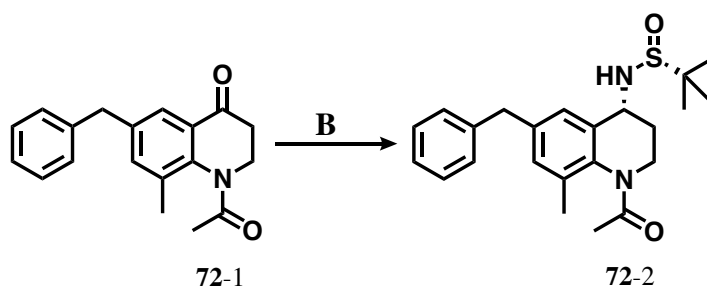
product as a white solid, which was used without further purification. **Step 2:** Amide coupling was performed with the aminium chloride salt of **70-4** (54 mg, 0.14 mmol, 1.0 eq), di-Boc-Dmt (61 mg, 0.15 mmol, 1.1 eq), and PyBOP (78 mg, 0.15 mmol, 1.1 eq), followed by DIPEA (0.24 mL, 1.36 mmol, 10 eq). Crude product was carried forward to **Step 3:** TFA deprotection, followed by purification by reverse-phase semi-preparative HPLC, as described in **General Procedure (C)**. Final yield not calculated. ¹H NMR (500 MHz, Methanol-*d*₄) δ 8.21 (d, *J* = 7.8 Hz, 1H), 7.77 (d, *J* = 7.8 Hz, 1H), 7.75 – 7.69 (m, 2H), 7.57 (s, 1H), 7.44 – 7.37 (m, 2H), 7.25 (dd, *J* = 8.5, 1.8 Hz, 1H), 6.99 (d, *J* = 2.0 Hz, 1H), 6.84 (d, *J* = 2.1 Hz, 1H), 6.47 (d, *J* = 6.8 Hz, 2H), 4.95 – 4.89 (m, 1H), 3.94 (s, 2H), 3.81 (dd, *J* = 11.5, 5.1 Hz, 1H), 3.28 – 3.20 (m, 1H), 3.02 – 2.85 (m, 6H), 2.41 (t, *J* = 12.3 Hz, 1H), 2.26 (s, 6H), 1.70 – 1.61 (m, 1H), 1.51 (dt, *J* = 13.5, 3.7 Hz, 1H). Analytical HPLC retention time: 36.8 min.

Compound 72

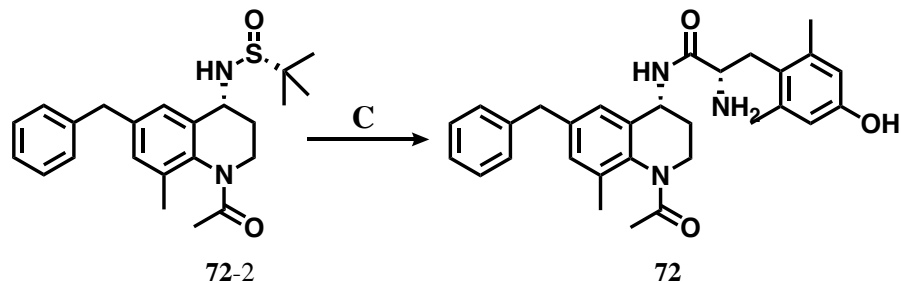


72-1 *1-acetyl-6-benzyl-8-methyl-2,3-dihydroquinolin-4(1H)-one*. Intermediate **72-1** was synthesized following **General Procedure (A)** from intermediate **9-6** (570 mg, 2.27 mmol, 1.0 eq), and Ac₂O (15 mL, excess). Yield not calculated. NMR identified two rotomers, which was supported by HSQC NMR. ¹H NMR (500 MHz, Chloroform-*d*) δ 7.68 (d, *J* = 2.3 Hz, 1H), 7.28 (d, *J* = 7.9 Hz, 3H), 7.18 (d, *J* = 7.2 Hz, 3H), 5.06 (dd, *J* = 13.4, 5.8 Hz, 1H), 4.26 (t, *J* = 9.1 Hz, 0.5H), 3.95 (d, *J* = 10.1 Hz, 2H), 3.88 – 3.77 (m, 0.5H), 3.32 (td, *J* = 13.1, 3.4 Hz, 0.5H), 2.91 (td,

$J = 13.7, 10.4, 4.8$ Hz, 0.5H), 2.89 – 2.80 (m, 0.5H), 2.72 (d, $J = 18.0$ Hz, 0.5H), 2.60 (d, $J = 17.9$ Hz, 0.5H), 2.38 – 2.34 (m, 1.5H), 1.97 (d, $J = 2.5$ Hz, 1.5H). ^{13}C NMR (126 MHz, cdCl_3) δ 195.57, 194.25, 171.04, 168.87, 141.84, 141.11, 140.14, 139.92, 139.45, 137.53, 137.16, 136.98, 135.06, 134.71, 133.11, 131.22, 129.45, 128.87, 128.69, 128.59, 128.08, 127.67, 126.50, 126.32, 125.89, 125.76, 125.05, 115.38, 44.12, 41.32, 40.04, 39.51, 24.83, 22.61, 21.64.

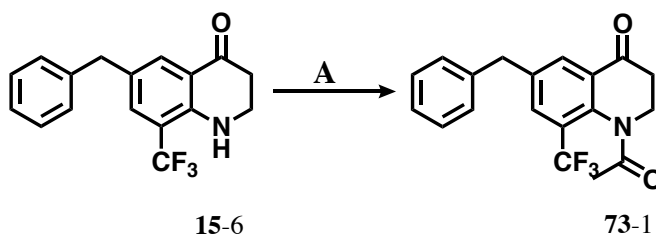


72-2 (*R*)-*N*-((*R*)-1-acetyl-6-benzyl-8-methyl-1,2,3,4-tetrahydroquinolin-4-yl)-2-methylpropane-2-sulfonamide. Intermediate **72-2** was synthesized following **General Procedure (B)** from intermediate **72-1** (90 mg, 0.31 mmol, 1.0 eq), (*R*)-2-methyl-2-propanesulfonamide (112 mg, 0.92 mmol, 3.0 eq), and $\text{Ti}(\text{OEt})_4$ (0.39 mL, 1.84 mmol, 6.0 eq), then NaBH_4 (70 mg, 1.84 mmol, 6.0 eq). Yield: 121 mg, 98%. ^1H NMR (500 MHz, Chloroform-*d*) δ 7.32 – 7.28 (m, 2H), 7.21 (d, $J = 7.0$ Hz, 3H), 7.08 (s, 1H), 6.99 (s, 1H), 4.52 (dt, $J = 4.7, 2.5$ Hz, 1H), 3.94 (d, $J = 20.2$ Hz, 2H), 2.99 (ddd, $J = 13.3, 9.1, 4.4$ Hz, 1H), 2.84 (tt, $J = 10.2, 4.5$ Hz, 1H), 2.54 (dddd, $J = 14.0, 9.4, 4.4, 2.8$ Hz, 1H), 1.88 (d, $J = 1.6$ Hz, 3H), 1.81 (dq, $J = 14.0, 8.8$ Hz, 1H), 1.21 (d, $J = 1.7$ Hz, 9H). ^{13}C NMR (126 MHz, cdCl_3) δ 171.05, 140.13, 137.44, 135.28, 134.08, 131.76, 130.33, 128.96, 128.63, 128.53, 126.37, 126.29, 123.22, 51.71, 41.45, 39.48, 39.11, 28.61, 22.60, 22.12.

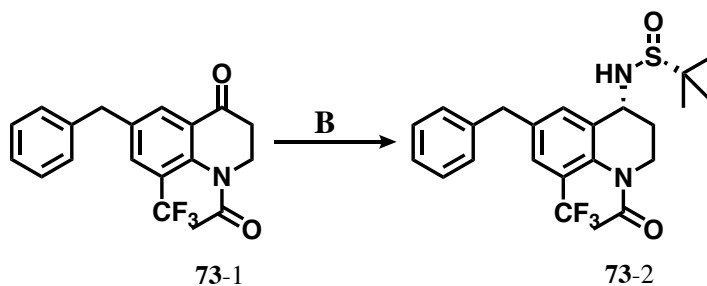


72 (*S*)-*N*-((*R*)-1-acetyl-6-benzyl-8-methyl-1,2,3,4-tetrahydroquinolin-4-yl)-2-amino-3-(4-hydroxy-2,6-dimethylphenyl)propanamide. **72** was synthesized following **General Procedure (C)** from intermediate **72-2**. **Step 1:** Sulfinamide cleavage was carried out with **72-2** (83 mg, 0.21 mmol, 1.0 eq) and excess concentrated HCl, precipitating product as a white solid, which was used without further purification. **Step 2:** Amide coupling was performed with the aminium chloride salt of **72-2** (37 mg, 0.11 mmol, 1.0 eq), di-Boc-Dmt (51 mg, 0.12 mmol, 1.1 eq), and PyBOP (64 mg, 0.12 mmol, 1.1 eq), followed by DIPEA (0.20 mL, 1.12 mmol, 10 eq). Crude product was carried forward to **Step 3:** TFA deprotection, followed by purification by reverse-phase semi-preparative HPLC, as described in **General Procedure (C)**. Final yield not calculated. ¹H NMR (500 MHz, Methanol-*d*₄) δ 7.27 – 7.20 (m, 2H), 7.16 (dq, *J* = 7.5, 4.6, 2.9 Hz, 3H), 7.03 (d, *J* = 6.2 Hz, 1H), 7.01 – 6.96 (m, 1H), 6.94 (s, 0H), 6.52 (d, *J* = 3.3 Hz, 2H), 4.66 – 4.49 (m, 1H), 3.98 (dd, *J* = 11.3, 4.8 Hz, 0.5H), 3.94 (s, 1H), 3.88 (d, *J* = 15.7 Hz, 1H), 3.83 – 3.78 (m, 0.5H), 3.31 (s, 2H), 3.26 (dd, *J* = 13.7, 11.6 Hz, 1H), 3.09 (dd, *J* = 14.0, 4.7 Hz, 1H), 2.72 (ddd, *J* = 13.6, 9.2, 5.2 Hz, 0.5H), 2.33 – 2.26 (m, 6H), 2.02 (d, *J* = 6.3 Hz, 1.5H), 1.88 (d, *J* = 8.3 Hz, 1.5H), 1.48 – 1.28 (m, 0.5H), 1.21 – 1.10 (m, 0.5H). Calculated [M+H]⁺: 486.28. ESI-MS mass observed: 486.3 (M+H) and 508.3 (M+Na). Analytical HPLC retention time: 34.6 min.

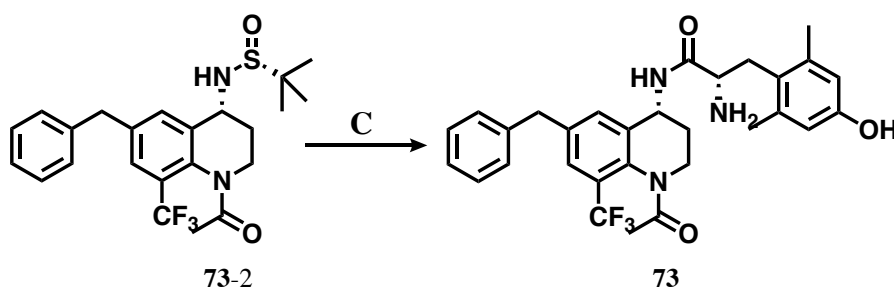
Compound 73



73-1 *1-acetyl-6-benzyl-8-(trifluoromethyl)-2,3-dihydroquinolin-4(1H)-one*. Intermediate **73-1** was synthesized following **General Procedure (A)** from intermediate **15-6** (175 mg, 0.57 mmol, 1.0 eq), and Ac₂O (12 mL, excess). Yield: 45 mg, 23%. NMR identified two rotomers, supported by HSQC NMR. ¹H NMR (500 MHz, Chloroform-*d*) δ 8.01 (d, *J* = 5.8 Hz, 1H), 7.72 – 7.65 (m, 1H), 7.32 (dd, *J* = 11.3, 7.3 Hz, 2H), 7.29 – 7.22 (m, 1H), 7.19 (t, *J* = 6.0 Hz, 2H), 5.08 (dd, *J* = 13.4, 6.2 Hz, 0.5H), 4.32 (dd, *J* = 14.5, 5.4 Hz, 0.5H), 4.05 (d, *J* = 15.3 Hz, 2H), 3.90 (td, *J* = 14.0, 3.9 Hz, 0.5H), 3.40 (td, *J* = 13.2, 3.8 Hz, 0.5H), 2.97 (ddd, *J* = 19.2, 13.1, 6.3 Hz, 0.5H), 2.86 (td, *J* = 13.0, 6.6 Hz, 0.5H), 2.82 – 2.75 (m, 0.5H), 2.64 (dd, *J* = 18.6, 3.7 Hz, 0.5H), 2.37 (s, 1.5H), 1.95 (s, 1.5H). ¹³C NMR (126 MHz, cdCl₃) δ 194.23, 171.41, 141.68, 133.27, 131.63, 131.23, 129.12, 129.00, 127.12, 126.93, 46.69, 44.54, 41.38, 39.88, 39.40, 22.35, 22.06.



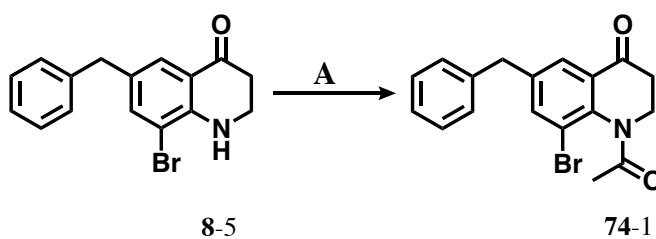
73-2 (*R*)-*N*-((*R*)-1-acetyl-6-benzyl-8-(trifluoromethyl)-1,2,3,4-tetrahydroquinolin-4-yl)-2-methylpropane-2-sulfinamide Intermediate **73-2** was synthesized following **General Procedure (B)** from intermediate **73-1** (45 mg, 0.13 mmol, 1.0 eq), (*R*)-2-methyl-2-propanesulfinamide (47 mg, 0.39 mmol, 3.0 eq), and Ti(OEt)₄ (0.17 mL, 0.78 mmol, 6.0 eq), then NaBH₄ (30 mg, 0.78 mmol, 6.0 eq). Yield: 52 mg, 90%. Carried forward without NMR characterization.



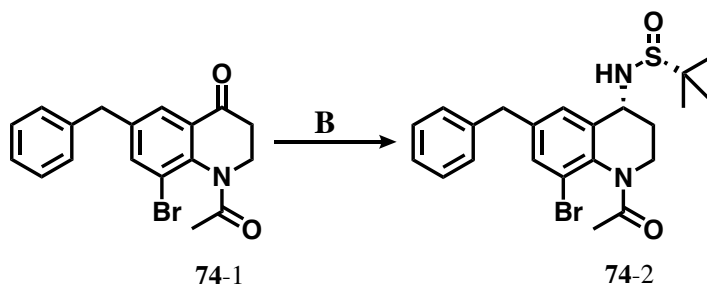
73 (*S*)-*N*-((*R*)-1-acetyl-6-benzyl-8-(trifluoromethyl)-1,2,3,4-tetrahydroquinolin-4-yl)-2-amino-3-(4-hydroxy-2,6-dimethylphenyl)propanamide. **73** was synthesized following **General Procedure (C)** from intermediate **73-2**. **Step 1:** Sulfinamide cleavage was carried out with **73-2** (40 mg, 0.09 mmol, 1.0 eq) and excess concentrated HCl, precipitating product as a white solid, which was used without further purification. **Step 2:** Amide coupling was performed with the aminium chloride salt of **73-2** (32 mg, 0.08 mmol, 1.0 eq), di-Boc-Dmt (38 mg, 0.09 mmol, 1.1 eq), 6-Cl HOBt (16 mg, 0.09 mmol, 1.1 eq), and PyBOP (48 mg, 0.09 mmol, 1.1 eq), followed by DIPEA (0.15 mL, 0.83 mmol, 10 eq). Crude product was carried forward to **Step 3:** TFA deprotection, followed by purification by reverse-phase semi-preparative HPLC, as described in **General Procedure (C)**. Final yield not calculated. ¹H NMR (500 MHz, Methanol-*d*₄) δ 7.46 (d, *J* = 4.2 Hz, 1H), 7.38 (dd, *J* = 20.8, 11.2 Hz, 1H), 7.27 (q, *J* = 6.9 Hz, 3H), 7.18 (d, *J* = 7.3 Hz, 4H), 6.59 (t, *J* = 7.2 Hz, 1H), 6.53 (s, 2H), 4.80 (dd, *J* = 11.9, 6.7 Hz, 0.5H), 4.74 – 4.66 (m, 0.5H), 4.55 (dd, *J* = 11.3, 6.6 Hz, 1H), 4.07 (d, *J* = 5.4 Hz, 2H), 4.02 (s, 1H), 3.99 – 3.93 (m, 1H), 3.25 (d, *J* = 12.0 Hz, 1H), 3.10

(dd, $J = 14.3, 5.4$ Hz, 1H), 2.75 – 2.68 (m, 0.5H), 2.28 (s, 6H), 1.84 (d, $J = 5.2$ Hz, 3H), 1.32 (s, 0.5H), 1.18 (s, 0.5H). Calculated $[M+H]^+$: 540.25. QTOF high-res mass observed: 540.2467 (M+H). Analytical HPLC retention time: 38.1 min.

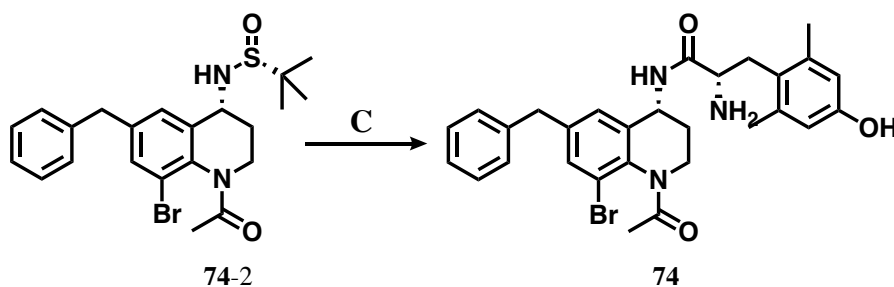
Compound 74



74-1 *1-acetyl-6-benzyl-8-bromo-2,3-dihydroquinolin-4(1H)-one*. Intermediate **74-1** was synthesized following **General Procedure (A)** from intermediate **8-5** (158 mg, 0.50 mmol, 1.0 eq), and Ac₂O (10 mL, excess). Yield: 63 mg, 34%. ¹H NMR (500 MHz, Chloroform-*d*) δ 7.79 (d, $J = 2.0$ Hz, 1H), 7.65 (d, $J = 2.0$ Hz, 1H), 7.32 (t, $J = 7.5$ Hz, 2H), 7.26 (d, $J = 7.2$ Hz, 1H), 7.21 – 7.16 (m, 2H), 5.07 (s, 1H), 3.98 (s, 2H), 3.36 (s, 1H), 2.90 (s, 1H), 2.64 (d, $J = 19.1$ Hz, 1H), 2.14 (s, 2H). ¹³C NMR (126 MHz, cdcl₃) δ 138.98, 128.88, 128.86, 127.19, 126.80, 44.18, 41.06, 39.42, 22.71.



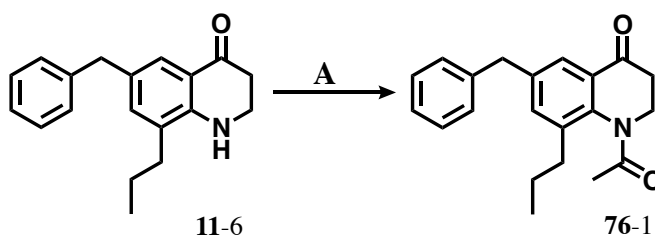
74-2 (*R*)-*N*-((*R*)-1-acetyl-6-benzyl-8-bromo-1,2,3,4-tetrahydroquinolin-4-yl)-2-methylpropane-2-sulfonamide Intermediate **74-2** was synthesized following **General Procedure (B)** from intermediate **74-1** (63 mg, 0.17 mmol, 1.0 eq), (*R*)-2-methyl-2-propanesulfonamide (60 mg, 0.49 mmol, 3.0 eq), and Ti(OEt)₄ (0.21 mL, 0.99 mmol, 6.0 eq), then NaBH₄ (38 mg, 0.99 mmol, 6.0 eq). Yield not calculated. ¹H NMR (500 MHz, Chloroform-*d*) δ 7.45 (d, *J* = 1.9 Hz, 1H), 7.33 (dt, *J* = 10.6, 7.6 Hz, 4H), 7.22 (d, *J* = 8.1 Hz, 2H), 7.12 (d, *J* = 1.8 Hz, 1H), 4.52 (dt, *J* = 4.3, 2.8 Hz, 1H), 3.95 (s, 2H), 3.04 (ddd, *J* = 13.2, 9.2, 4.2 Hz, 0.5H), 2.88 (td, *J* = 10.9, 8.8, 5.2 Hz, 0.5H), 2.61 – 2.53 (m, 0.5H), 2.49 (dt, *J* = 12.5, 6.3 Hz, 0.5H), 2.04 (s, 3H), 1.88 – 1.79 (m, 0.5H), 1.57 (d, *J* = 13.1 Hz, 0.5H), 1.20 (s, 9H). ¹³C NMR (126 MHz, cdcl₃) δ 142.18, 137.57, 133.93, 129.14, 128.97, 128.86, 127.97, 126.87, 126.69, 55.74, 55.30, 52.07, 47.33, 41.29, 39.45, 28.96, 24.97, 22.72, 22.65.



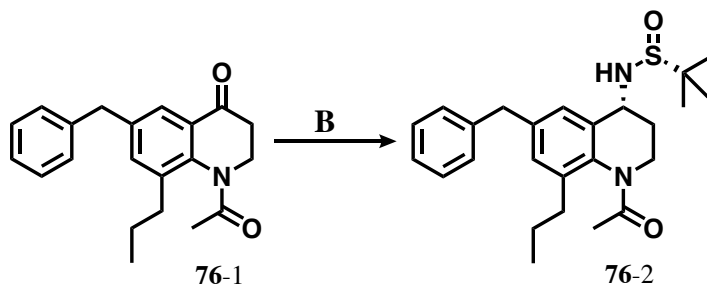
74 (*S*)-*N*-((*R*)-1-acetyl-6-benzyl-8-bromo-1,2,3,4-tetrahydroquinolin-4-yl)-2-amino-3-(4-hydroxy-2,6-dimethylphenyl)propanamide. **74** was synthesized following **General Procedure (C)** from intermediate **74-2**. **Step 1:** Sulfonamide cleavage was carried out with **74-2** and excess concentrated HCl, precipitating product as a white solid, which was used without further purification. **Step 2:** Amide coupling was performed with the aminium chloride salt of **74-2** (58 mg, 0.14 mmol, 1.0 eq), di-Boc-Dmt (57 mg, 0.14 mmol, 1.0 eq), 6-Cl HOBt (26 mg, 0.15 mmol,

1.1 eq), and PyBOP (79 mg, 0.15 mmol, 1.1 eq), followed by DIPEA (0.24 mL, 1.4 mmol, 10 eq). Crude product was carried forward to **Step 3**: TFA deprotection, followed by purification by reverse-phase semi-preparative HPLC, as described in **General Procedure (C)**. Final yield not calculated. Calculated $[M+H]^+$: 550.17. ESI-MS mass observed: 550.2 ($^{79}\text{Br M}+H$), 552.2 ($^{81}\text{Br M}+H$), 572.2 ($^{79}\text{Br M}+\text{Na}$), and 574.2 ($^{81}\text{Br M}+H$). Analytical HPLC retention time: 36.0 min.

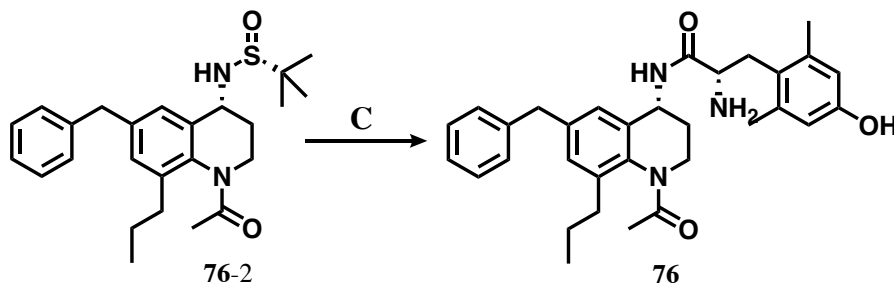
Compound 76



76-1 *1-acetyl-6-benzyl-8-propyl-2,3-dihydroquinolin-4(1H)-one*. Intermediate **76-1** was synthesized following **General Procedure (A)** from intermediate **11-6** (202 mg, 0.72 mmol, 1.0 eq), and Ac_2O (8 mL, excess). Yield: 180 mg, 78%. $^1\text{H NMR}$ (500 MHz, $\text{Chloroform-}d$) δ 7.67 (d, $J = 2.1$ Hz, 1H), 7.33 – 7.29 (m, 2H), 7.27 (d, $J = 13.4$ Hz, 1H), 7.24 – 7.20 (m, 1H), 7.20 – 7.16 (m, 2H), 5.07 (ddd, $J = 12.9, 6.2, 1.2$ Hz, 1H), 3.97 (d, $J = 10.0$ Hz, 2H), 3.31 (td, $J = 13.1, 3.7$ Hz, 1H), 2.92 (ddd, $J = 19.0, 13.2, 6.1$ Hz, 1H), 2.69 – 2.63 (m, 1H), 2.60 (ddd, $J = 18.6, 3.7, 1.3$ Hz, 1H), 2.49 (ddd, $J = 14.3, 8.7, 5.4$ Hz, 2H), 1.95 (s, 3H), 1.69 – 1.44 (m, 2H), 0.87 (t, $J = 7.3$ Hz, 3H). $^{13}\text{C NMR}$ (126 MHz, cdcl_3) δ 195.73, 171.29, 141.67, 140.53, 140.07, 138.03, 136.08, 135.76, 128.95, 128.81, 128.70, 126.60, 126.43, 125.90, 125.32, 44.27, 41.56, 39.55, 33.03, 24.22, 21.98, 13.80.



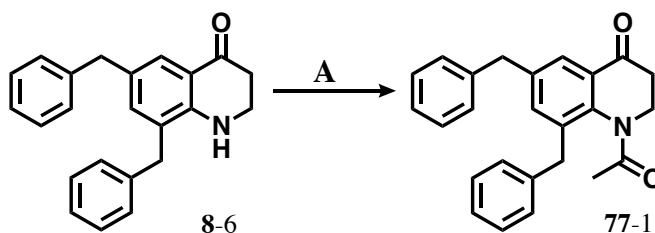
76-2 (*R*)-*N*-((*R*)-1-acetyl-6-benzyl-8-propyl-1,2,3,4-tetrahydroquinolin-4-yl)-2-methylpropane-2-sulfonamide. Intermediate **76-2** was synthesized following **General Procedure (B)** from intermediate **76-1** (180 mg, 0.56 mmol, 1.0 eq), (*R*)-2-methyl-2-propanesulfonamide (204 mg, 1.68 mmol, 3.0 eq), and $\text{Ti}(\text{OEt})_4$ (0.70 mL, 3.36 mmol, 6.0 eq), then NaBH_4 (127 mg, 3.36 mmol, 6.0 eq). Yield not calculated. ^1H NMR (500 MHz, Chloroform-*d*) δ 7.31 (qd, $J = 8.0, 3.8$ Hz, 3H), 7.24 – 7.19 (m, 3H), 7.11 (d, $J = 2.0$ Hz, 1H), 6.99 (d, $J = 2.1$ Hz, 1H), 4.88 – 4.79 (m, 0.5H), 4.76 (ddd, $J = 13.0, 9.0, 6.6$ Hz, 0.5H), 4.52 (dt, $J = 4.6, 2.4$ Hz, 1H), 3.95 (s, 2H), 2.95 (ddd, $J = 13.3, 9.2, 4.5$ Hz, 0.5H), 2.81 (ddd, $J = 13.4, 9.1, 5.2$ Hz, 0.5H), 2.56 (dtdd, $J = 24.1, 11.1, 8.9, 6.2$ Hz, 2H), 2.42 (tdd, $J = 10.9, 5.3, 1.9$ Hz, 1H), 1.87 (s, 3H), 1.85 – 1.78 (m, 0.5H), 1.63 – 1.43 (m, 2H), 1.23 (s, 9H), 0.84 (td, $J = 7.3, 3.2$ Hz, 3H). ^{13}C NMR (126 MHz, cdCl_3) δ 140.42, 138.96, 135.47, 130.71, 129.29, 129.09, 128.76, 128.65, 126.47, 126.32, 55.54, 51.83, 41.71, 39.75, 32.82, 28.76, 24.06, 22.74, 22.68, 22.24, 13.91.



76 (*S*)-*N*-((*R*)-1-acetyl-6-benzyl-8-propyl-1,2,3,4-tetrahydroquinolin-4-yl)-2-amino-3-(4-hydroxy-2,6-dimethylphenyl)propanamide. **76** was synthesized following **General Procedure (C)**

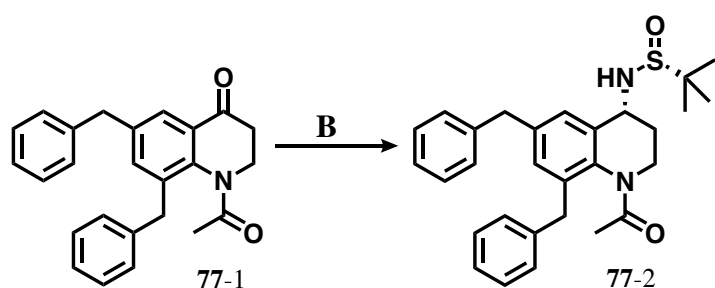
from intermediate **76-2**. **Step 1:** Sulfinamide cleavage was carried out with **76-2** and excess concentrated HCl, precipitating product as a white solid, which was used without further purification. **Step 2:** Amide coupling was performed with the aminium chloride salt of **76-2** (60 mg, 0.17 mmol, 1.0 eq), di-Boc-Dmt (75 mg, 0.18 mmol, 1.1 eq), 6-Cl HOBt (31 mg, 0.18 mmol, 1.1 eq), and PyBOP (93 mg, 0.18 mmol, 1.1 eq), followed by DIPEA (0.29 mL, 1.67 mmol, 10 eq). Crude product was carried forward to **Step 3:** TFA deprotection, followed by purification by reverse-phase semi-preparative HPLC, as described in **General Procedure (C)**. Final yield not calculated. Calculated $[M+H]^+$: 514.31. ESI-MS mass observed: 514.3 (M+H) and 536.3 (M+Na). Analytical HPLC retention time: 39.2 min.

Compound 77

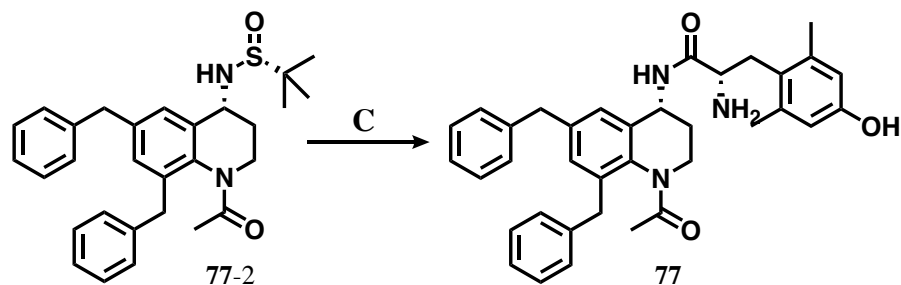


77-1 *1-acetyl-6,8-dibenzyl-2,3-dihydroquinolin-4(1H)-one*. Intermediate **77-1** was synthesized following **General Procedure (A)** from intermediate **8-6** (310 mg, 0.95 mmol, 1.0 eq), and Ac₂O (15 mL, excess). Yield: 158 mg, 45%. NMR identified multiple rotational states. ¹H NMR (500 MHz, Chloroform-*d*) δ 7.70 (dd, *J* = 14.0, 2.2 Hz, 2H), 7.27 (d, *J* = 7.1 Hz, 7H), 7.21 (d, *J* = 6.6 Hz, 4H), 7.15 (d, *J* = 7.7 Hz, 2H), 7.12 (d, *J* = 7.6 Hz, 2H), 7.04 (d, *J* = 7.4 Hz, 4H), 5.00 (dd, *J* = 13.0, 6.1 Hz, 0.5H), 4.01 – 3.94 (m, 0.5H), 3.94 (d, *J* = 3.5 Hz, 4H), 3.49 (td, *J* = 14.1, 3.4 Hz, 0.5H), 3.17 (td, *J* = 13.1, 3.7 Hz, 0.5H), 2.93 (ddd, *J* = 19.2, 13.2, 6.1 Hz, 0.5H), 2.81 (ddd, *J* =

19.2, 13.8, 5.7 Hz, 0.5H), 2.67 (dd, $J = 17.9, 3.8$ Hz, 0.5H), 2.58 (dd, $J = 18.7, 3.6$ Hz, 0.5H), 2.21 (s, 1.5H), 2.05 (s, 1.5H). ^{13}C NMR (126 MHz, cdCl_3) δ 195.16, 193.85, 170.70, 168.53, 141.27, 140.49, 140.33, 139.98, 139.74, 139.52, 139.47, 139.17, 137.86, 136.87, 136.72, 136.56, 128.82, 128.65, 128.60, 128.57, 128.54, 128.48, 128.42, 128.37, 128.31, 128.29, 128.25, 128.16, 128.01, 126.27, 126.19, 126.04, 126.02, 125.85, 125.45, 77.00, 46.34, 43.69, 41.04, 39.60, 39.05, 38.71, 37.04, 22.22, 21.63.



77-2 (*R*)-*N*-((*R*)-1-acetyl-6,8-dibenzyl-1,2,3,4-tetrahydroquinolin-4-yl)-2-methylpropane-2-sulfonamide. Intermediate **77-2** was synthesized following **General Procedure (B)** from intermediate **77-1** (158 mg, 0.43 mmol, 1.0 eq), (*R*)-2-methyl-2-propanesulfonamide (155 mg, 1.28 mmol, 3.0 eq), and $\text{Ti}(\text{OEt})_4$ (0.56 mL, 2.56 mmol, 6.0 eq), then NaBH_4 (98 mg, 2.56 mmol, 6.0 eq). Yield not calculated. H NMR not available.



77 (*S*)-*N*-((*R*)-1-acetyl-6,8-dibenzyl-1,2,3,4-tetrahydroquinolin-4-yl)-2-amino-3-(4-hydroxy-2,6-dimethylphenyl)propanamide. **77** was synthesized following **General Procedure (C)** from

intermediate **77-2**. **Step 1:** Sulfinamide cleavage was carried out with **77-2** and excess concentrated HCl, precipitating product as a white solid, which was used without further purification. **Step 2:** Amide coupling was performed with the aminium chloride salt of **77-2** (63 mg, 0.15 mmol, 1.0 eq), di-Boc-Dmt (69 mg, 0.17 mmol, 1.1 eq), 6-Cl HOBt (26 mg, 0.15 mmol, 1.0 eq), and PyBOP (80 mg, 0.15 mmol, 1.0 eq), followed by DIPEA (0.26 mL, 1.5 mmol, 10 eq). Crude product was carried forward to **Step 3:** TFA deprotection, followed by purification by reverse-phase semi-preparative HPLC, as described in **General Procedure (C)**. Final yield not calculated. Calculated $[M+H]^+$: 562.3. ESI-MS mass observed: 562.3 (M+H) and 584.3 (M+Na). Analytical HPLC retention time: 42.4 min.

Chapter 5: Conclusions & Future Directions

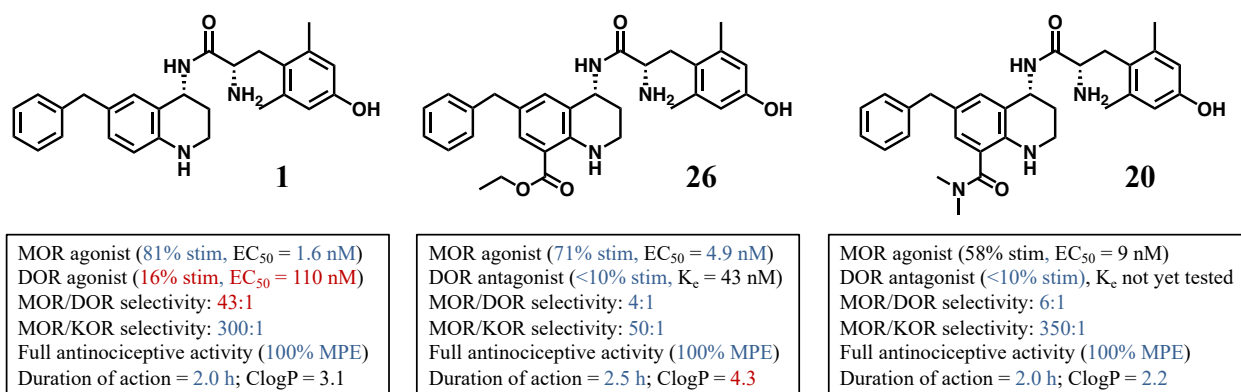
5.1 Observations at C-8

The endogenous opioid peptides such as the enkephalins, endorphins, and dynorphins share the *N*-terminal Tyr¹-Gly²-Gly³-Phe⁴-X⁵ sequence, where X is either Met or Leu, highlighting an importance for the conserved tetrapeptide *N*-terminus. As indicated by pharmacophore models, the di-glycine residues primarily act as a flexible spacer region between two key aryl pharmacophores, Tyr¹ and Phe⁴. The first peptidomimetic series reported by our lab, synthesized by L.Y.M., A.A.H. and A.M.B., exchanged Tyr¹ for the dimethyl analogue Dmt and explored the effects of five aryl Phe⁴ bioisosteres located at the C-6 position of our scaffold. Subsequent work continued to probe C-6, and eventually branched to *N*-1. Recently, that exploration has expanded to include modifications to the C-8 position, which was the focus of Chapter 2. The 24 substitutions investigated here varied widely in length, bulk, lipophilicity, and polarity and included the following motifs: alkanes, halogens, amides, esters, acids, saturated heterocycles, flexible and inflexible aromatics, H-bond donors, H-bond acceptors, as well as nitrile and amino acid substitutions. An intentional emphasis was placed on diversity of chemical matter throughout this SAR campaign so as to thoroughly explore the chemical space with a minimal number of analogues.

One major issue with prior analogues focusing exclusively on C-6 modifications was a high degree of selectivity for MOR over DOR. Though it is not known what specific binding ratio is optimal between MOR and DOR, the 20:1 to 200:1 selectivity for MOR limited the bifunctional aspect of these compounds. Based on the first fifteen compounds synthesized in the C-8 series, the flexible aryl C-8 substitutions of compounds **8** (C-8 = benzyl) and **18** (ethylphenyl) provided the best increase in DOR affinity with a modest decrease in MOR affinity, yielding significantly more balanced profiles (2:1 and 4:1 respectively). However, all analogues in this series also elicited low-potency partial DOR agonism whereas the target had been DOR antagonism.

Subsequent synthetic development allowed access to a C-8 carbonyl motif as in the case of the amides, esters, and acid analogues **20-27**. These carbonyl-featuring analogues consistently displayed the desired DOR antagonist profile. Additionally, the flexible, lipophilic ethyl ester of analogue **26** retained the MOR/DOR affinity balance achieved by the flexible aryl C-8 pendants (4:1 MOR/DOR), achieving a highly favorable *in vitro* profile. This favorability was bolstered by the *in vivo* antinociceptive activity of analogue **26**, solidifying this as a noteworthy improvement over the unsubstituted C-8 lead peptidomimetic **1**. This success was replicated with a less flexible, less lipophilic dimethyl amide analogue **20**. **20** not only retained the optimal functional profile (MOR agonist/DOR antagonist), but also maintained an only 6-fold selectivity for MOR over DOR in terms of binding affinity. Significantly, analogue **20** reduced ClogP to 2.2 compared to 3.1 for the lead **1** and 4.3 for the ethyl ester analogue **26** and maintained antinociceptive activity. These two compounds were featured as highlights of the C-8 series in **Fig. 13**, replicated below with the added comparison to analogue **1** for convenience in **Fig. 25**. The only detraction of **20** is the loss of MOR potency—9 nM compared to 1.6 nM for lead **1** and 4.9 for ethyl ester analogue **26**.

Figure 25. Summary Profiles of Top C-8 *In Vivo* Candidates **20** and **26** Compared to Lead **1**



Based on the library of C-8 substituted compounds **8-31** discussed at length in Chapter 2, the author notes the following observations:

1. C-8 substituted analogues, with the exception of the saturated amino heterocycles, display better binding balance between MOR and DOR (closer to 1:1) than lead peptidomimetic **1**.
2. Most substitutions elicit low-potency DOR agonism, though carbonyl motifs reverse this trend and reliably provide DOR antagonism.
3. Small, non-polar alkyl chains and non-H-bond-donating carbonyl substituents are well-tolerated *in vivo* (i.e. dimethyl amide and esters fully active, secondary amides inactive).
4. Halogens and amines were also poorly tolerated *in vivo* and offered limited benefit *in vitro*.
5. C-8 substituted analogues display 1 to 10 nM MOR potency, though deep, lipophilic n-propyl, n-butyl, ethylphenyl and benzofuranyl substitutions diverge from this trend, displaying double-digit nanomolar potency.
6. DOR and KOR potency is consistently 10 nM or higher, with most in the 100 nM range.
7. Duration of action is not significantly improved by C-8 modifications—the longest-acting analogues display a 2.5 h duration of action compared to 2.0 h for lead peptidomimetic **1**.

Presently, analogue **20** is the only compound from this series under further investigation for *in vivo* tolerance and/or dependence. However, **26** may also be a viable candidate for further evaluation.

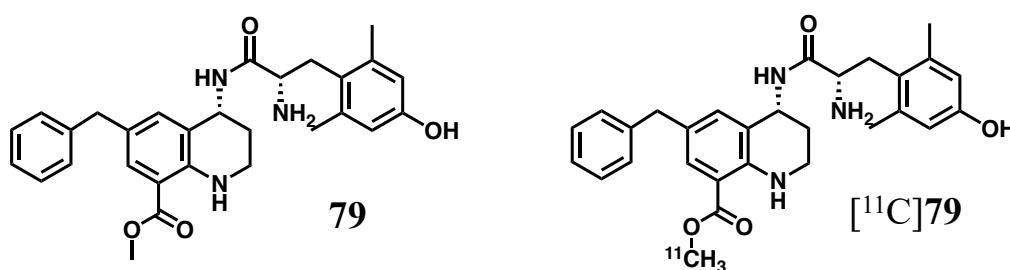
Chapter 4 discussed the combined effects of *N*-acetyl and C-8 moieties, which were evaluated *in vitro* and *in vivo* via a short series of compounds (**71-77**). These analogues all showed highly similar *in vitro* profiles, with MOR affinity between 0.1 and 0.2 nM and DOR affinity ranging from 1 to 2 nM. The one exception, **77**, showed a much more balanced 1:1 binding profile with 0.4 nM affinity at both MOR and DOR. Functionally, all compounds evaluated were MOR agonists/partial DOR agonists. The only analogue showing full antinociceptive activity was the C-8 methyl analogue **72**. Based on this short series of analogues, the pharmacological profile associated with these combined *N*-acetyl/C-8 substitutions is most heavily impacted by the *N*-acetyl motif. All analogues in this series are nearly indistinguishable from the *N*-acetyl/C-8 H lead **32**. As such, these combined substitutions offer no discernible improvement either *in vitro* or *in vivo* relative to the C-8/*N*-H analogues. Furthermore, the *N*-acetyl group sterically precludes a number of advantageous C-8 motifs from being incorporated. Specifically, the carbonyl analogues which showed the most favorable *in vitro* profile could not be incorporated in tandem with an *N*-acetyl motif. As such, it is recommended that further investigations at C-8 be done in the absence of an *N*-1 modification.

5.2 Future Directions for C-8 Utilization

Moving forward, the C-8 position could be an advantageous position to exploit in order to advance various projects yet undeveloped. The first of these potential future directions involves a follow-up to the previously unsuccessful ¹¹C-radiolabeling project discussed in Chapter 4. Based

on the bioavailability of the small, non-H-bonding carbonyl motifs at C-8 tested thus far, the synthesis of a methyl ester at C-8 is suggested (see **Fig. 26**, analogue **79**). Not only will this analogue decrease ClogP relative to the bioavailable ethyl ester (ClogP = 3.7 for **79** vs. 4.3 for **26**), it is predicted that this will maintain bioavailability if existing trends hold true. Furthermore, **79** is likely to maintain the MOR agonist/DOR antagonist profile of the carbonyl series, offering an additional compound with favorable *in vitro* pharmacology.

Figure 26. Structures of Proposed Compound **79** and its Radiolabeled Analogue [^{11}C]**79**

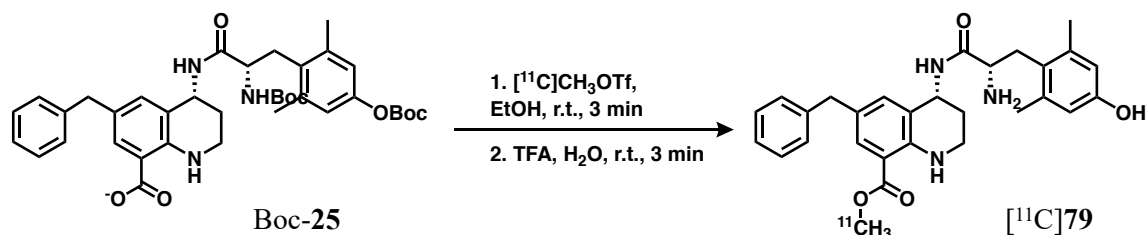


Should analogue **79** demonstrate the predicted *in vivo* activity, a radiolabeled analogue [^{11}C]**79** could then be synthesized and evaluated via PET to observe CNS penetration. An immediately apparent liability of this approach is the positioning of the radiolabel on an ester moiety, as esters are notoriously susceptible to hydrolysis. Hydrolysis of the radiolabel would increase background signal and limit resolution. However, a similar model is currently used in the field of PET for labeling opioid receptors. The radioligand [^{11}C]carfentanil, the synthesis and utilization of which has been widely reported in the literature^{120–131} (including by those in the Peter Scott lab at the University of Michigan^{132–134}), also employs a ^{11}C -labeled methyl ester. Using this radioligand as a model should facilitate the synthesis and evaluation of the methyl ester peptidomimetic [^{11}C]**79**. Additionally, as demonstrated by the wealth of studies utilizing

[¹¹C]carfentanil, hydrolysis of the radioligand is not likely to be a limiting factor in the PET analysis of the proposed peptidomimetic radioligand.

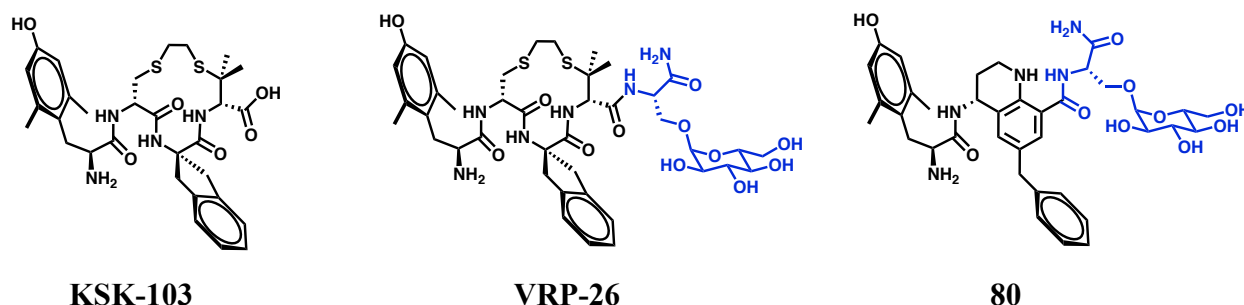
The radiosynthesis of [¹¹C]**79**, outlined in **Scheme 11**, is designed based on the updated [¹¹C]carfentanil radiosynthesis recently reported by members of the Scott lab¹³³ and utilizes input from Dr. Allan Brooks of said research group. The Boc-protected desmethyl precursor (Boc-**25**) has been synthesized in half-gram quantities and is presently available for utilization, should the prerequisite synthesis and pharmacology be executed and yield favorable results.

Scheme 11. Proposed radiosynthesis of [¹¹C]**79**



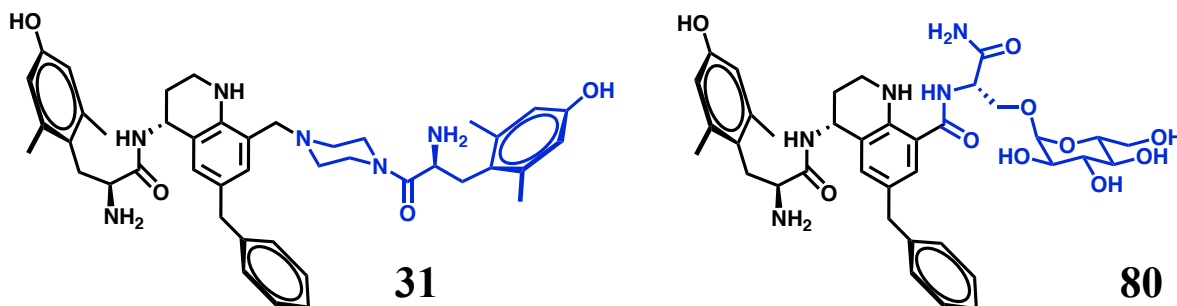
An additional future direction utilizing the C-8 position aims to improve bioavailability by incorporation of a glucoserine moiety. Our lab and others have previously reported on the use of a glycosylated amino acid residue to boost transport into the CNS.^{82,108,111} **Fig. 27** shows the cyclic peptide **KSK-103** developed by our lab, which gained *in vivo* activity via glucoserine attachment (**VRP-26**). By comparison, the unglycosylated peptide showed no activity *in vivo*. In **Fig. 27**, one can see the overlap between the spatial orientation of the glucoserine motif (shown in blue) of **VRP-26** and of the proposed compound **80** in relation to the Tyr¹ and Phe⁴ isosteres.

Figure 27. Structures of the Unglycosylated Peptide **KSK-103**, the Bioavailable **VRP-26**, and **80**



As described in Chapter 2 as well as the above C-8 observations, substitutions at the C-8 position were well-tolerated and had little impact on binding. Despite carbonyl moieties impacting the functional profiles of C-8 substituted compounds, even the larger C-8 substitutions show similar binding profiles to their smaller or unsubstituted counterparts. Highlighted in **Table 19** are the *in vitro* profiles of analogues **1**, **30**, and **31**. The notable similarity between the unsubstituted, piperazine-substituted, and Dmt-piperazine-substituted analogues suggests that even the larger moieties at this position are well-tolerated, as substitutions at this position are likely able to adopt a solvent-accessible conformation. Using this to our advantage, it may be possible to increase BBB permeability and solubility with a similarly-sized glucoserine moiety without significantly impacting binding at MOR and DOR. Additionally, if this analogue should prove promising, the chemistry is presently established to replace the C-6 benzyl pendant with a 2-naphthyl pendant, which may improve the *in vitro* profile.

Table 19. Large, Hydrophilic C-8 Substitution Show Limited Impact on Binding Affinity

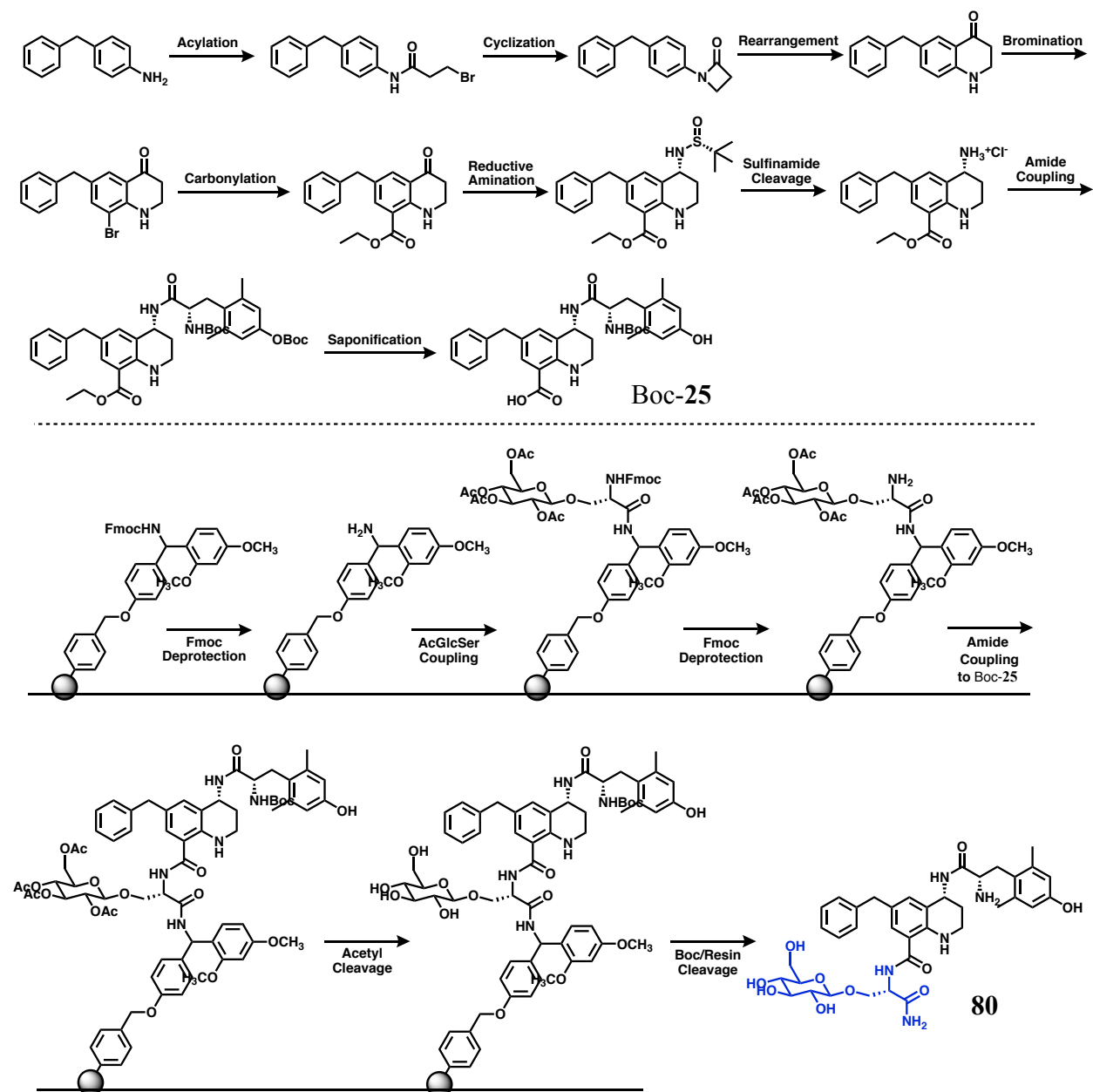


#	C-8 R Group	K _i (nM)			DOR K _i / MOR K _i	EC ₅₀ (nM)			% stim		
		MOR	DOR	KOR		MOR	DOR	KOR	MOR	DOR	KOR
1	H	0.22 (0.02)	9.4 (0.8)	68 (2)	43	1.6 (0.3)	110 (6)	>500	81 (2)	16 (2)	22 (2)
30	piperazine	0.35 (0.18)	15 (3)	1.9 (0.5)	43	8.2 (3.5)	290 (100)	170 (67)	60 (2)	18 (1)	17 (1)
31	piperazine-Dmt	0.31 (0.16)	2.6 (0.5)	7 (2)	20	5.9 (0.7)	dns [†]	dns	86 (8)	dns [†]	dns

^a Binding affinities (K_i) were obtained by competitive displacement of radiolabeled [³H]-diprenorphine in membrane preparations. Functional data were obtained using agonist induced stimulation of [³⁵S]-GTPγS binding. Potency is represented as EC₅₀ (nM) and efficacy as percent maximal stimulation relative to standard agonist DAMGO (MOR), DPDPE (DOR), or U69,593 (KOR) at 10 μM. All values are expressed as the mean of three separate assays performed in duplicate with standard error of the mean in parentheses. dns = does not stimulate. † indicates n=2.

The synthesis of analogue **80** was recently attempted as outlined in **Scheme 12**. However, synthesis stalled at the amide coupling between the peptidomimetic acid and glucoserine amine.

Scheme 12. Full Synthetic Scheme of Glucoserine Conjugated Peptidomimetic **80**



The attempted synthesis of **80** begins as previously described for analogue **25**. The key intermediate **Boc-25** was synthesized in 9 steps as outlined in **Scheme 12**. This key intermediate, useful for both the glucoserine conjugate analogue **80** as well as the proposed radioligand [^{11}C]**79**

described above, has been synthesized in half-gram quantities. The glucoserine component was to be incorporated using resin-bound peptide chemistry. The glucoserine free acid, available on-hand due to the prior synthesis of **VRP-26**, was loaded onto a Rink resin after Fmoc deprotection of the resin. A Rink resin was selected because after ligand cleavage from the resin, the carboxylate is converted to a terminal carboxamide which is more CNS penetrant than the carboxylic acid. Glucoserine loading onto the resin and subsequent Fmoc deprotection proceeded as expected, confirmed by ninhydrin stain and HPLC at each step. Unfortunately, amide coupling between the peptidomimetic carboxylate and glucoserine amine—attempted three times using different coupling reagents—failed to produce the desired product. There was concern that the sterics of the Rink resin could inhibit the amide coupling. Thus, in a fourth attempt, after loading the glucoserine onto the resin and removing the Fmoc group, the glucoserine moiety was cleaved with TFA, yielding the C-terminal carboxamide and free amine. Unfortunately, the attempted solution-phase peptide coupling yielded only a non-volatile oily substance with no relevant peaks in the UV spectrum as observed by HPLC. Again, the peptidomimetic component failed to couple to the glucoserine amine. Due to time constraints as well as the cost of starting materials, a fifth synthesis was not attempted.

Reasons for the lack of success of the synthesis outlined in **Scheme 12** are elusive. The consistent result of an oily substance devoid of any appreciable UV activity is perplexing. This oily substance adhered to the HPLC column and was only removed after excessive washing, limiting the ability to inject higher concentrations of the unidentified substance. Organic/aqueous extraction and vacuum desiccation were unsuccessful at isolating any UV-active product, and TLC showed only uncoupled peptidomimetic fragment. It may be the case that the carboxylic acid, after reductive amination of the ketone, is significantly less reactive than the THQ carboxylate. Amide

couplings were generally low-yielding at the THQ stage and increasing electron density by removal of the ketone may further deactivate the acid. Further synthetic optimization may indeed prove fruitful toward developing analogue **80**, however at present, this project is no longer being actively pursued.

5.3 C-8 Conclusions

A diverse set of substitutions at C-8 have been investigated and reported in part in a 2018 article in the journal *ACS Chemical Neuroscience*. This SAR campaign has demonstrated that C-8 substitutions, with only two exceptions, serve to balance the relative affinities at MOR and DOR, reducing MOR selectivity. Additionally, while most substitutions demonstrate MOR and DOR agonism, carbonyl-substituted ligands decreased efficacy at both receptors yielding MOR agonist/DOR antagonist or, in some cases, MOR partial agonist/DOR antagonist ligands. *In vivo*, 7 of the 24 ligands featuring C-8 modifications demonstrated full antinociceptive activity while two others were partially active. As outlined in section 5.1, some rules governing bioavailability in the context of C-8 substitutions have been observed, though further *in vivo* SAR development is needed to bolster these observations. At present, this SAR campaign has shown the greatest propensity for maintaining bioavailability of any SAR campaigns explored by our lab, with nearly one-third of all compounds showing full antinociceptive activity. The bioavailability of this series, paired with the ability to reduce MOR selectivity *and* to modulate functionality to fit the desired MOR agonist/DOR antagonist profile, sets this campaign apart as a successful area of exploration in the field of THQ-based bifunctional peptidomimetics. Two key analogues to come from the C-8 campaign, **20** and **26**, have been highlighted in **Figs. 13** and **25** noting improvements in several areas of drug development. Moving forward, plans are underway for analogue **20** to be evaluated for antinociceptive tolerance *in vivo*.

Two projects that have been partially developed were outlined in section 5.2, presently in the category of “future directions.” The background and supporting chemical context for both projects are well-founded and both are, by this author’s estimation, high-quality candidates for further research. The C-8 position is additionally viable as a useful chemical handle due to its predicted access to bulk solvent when bound to the opioid receptors. Based on the limited impact of large chemical motifs at C-8 on binding, this position could be utilized in other areas requiring a solvent-exposed handle. C-8 may be further functionalized to design fluorescent, proximity-based (FRET or BRET) probes in an attempt to observe dimerization between opioid receptors and other proposed dimer pairs. Additionally, the C-8 position could serve as a branch for linking two (bifunctional) pharmacophores in a bivalent ligand. Appropriately spaced bivalent peptidomimetics would in theory show increased binding affinity to dimers of opioid receptors compared to monovalent ligands. Furthermore, computational modeling indicates the presence of a conserved lysine residue near C-8 which could be targeted by C-8 substituted lysine-targeting covalent ligands. The need for these chemical probes is not presently well-established; however, these potential applications for C-8 substituted ligands highlights the functionality of this position on the THQ core. Even so, if none of the aforementioned future directions are further pursued, this previously unexplored position has been successfully exploited in a number of bioavailable *in vivo* candidates that may yet provide benefits in the treatment of pain with the promise of reduced side-effects due to their bifunctional nature.

5.4 Observations Based on Combined Bicyclic C-6 and N-1 or C-8 Motifs

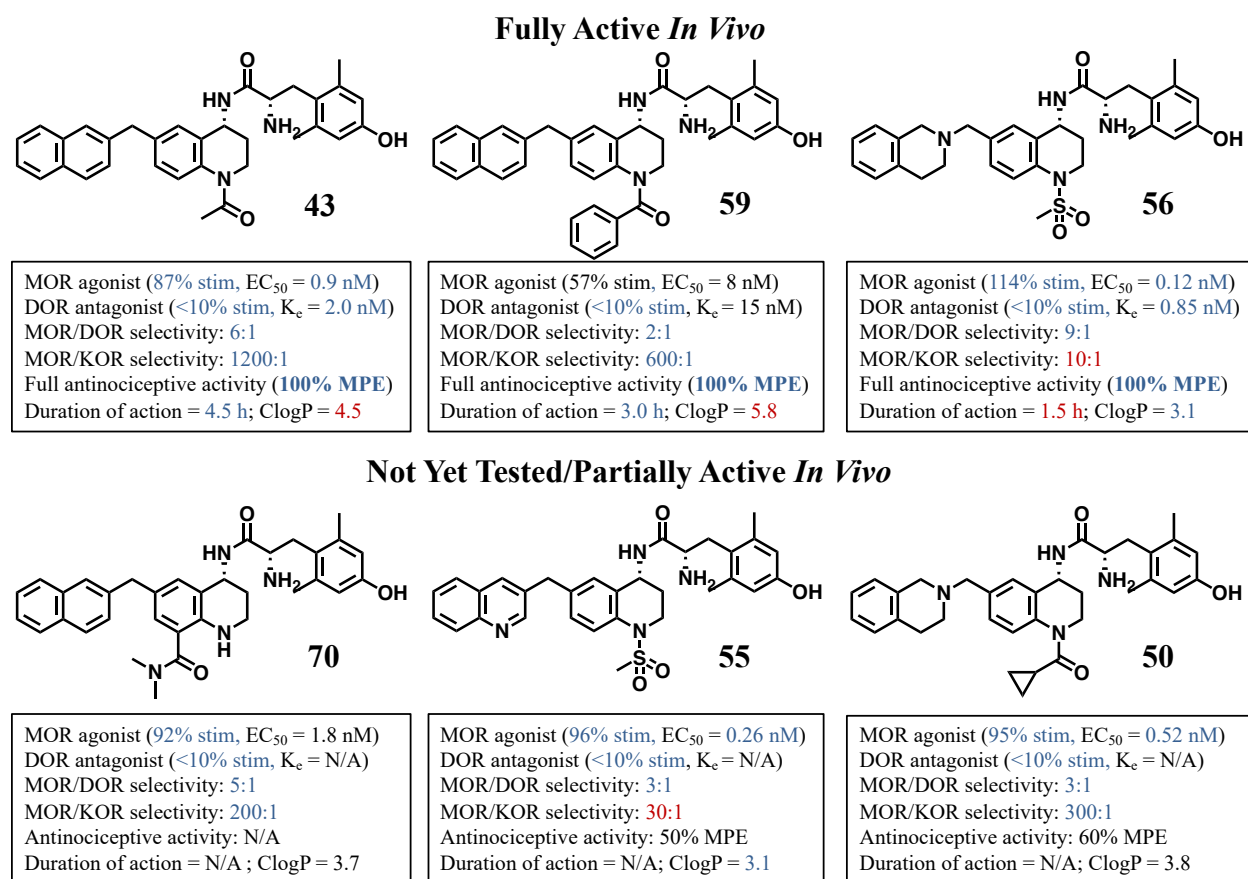
Early peptide-based and peptidomimetic SAR studies had demonstrated that bicyclic substitutions at C-6 (or analogously positioned bicyclics in the peptide series) preferentially bound to the active-state receptor conformation of MOR and to the inactive-state conformation of DOR.

By utilizing a bicyclic C-6 pendant, it was possible to elicit the MOR agonist/DOR antagonist profile which was hypothesized to be advantageous for reducing tolerance and dependence while maintaining antinociceptive activity *in vivo*. A limitation of the C-6 bicyclic approach was the high degree of binding selectivity for MOR over DOR, which limits the bifunctional aspect of these ligands. Chemists previously working on this project (A.A.H. and A.M.B.) had established that *N*-acylation could increase DOR affinity, thereby reducing MOR selectivity and achieving a more optimal *in vitro* profile. Furthermore, two notable *N*-acetylated/bicyclic C-6 analogues (**43** and **45**) had demonstrated a boost in bioavailability whereby both analogues showed robust antinociceptive activity. These promising results were expanded upon as described in Chapter 3 by pairing five bicyclic C-6 pendants with four *N*-acyl and *N*-sulfonyl moieties. The monocyclic benzyl pendant and unsubstituted *N*-H core were included in this series for reference, giving a 6x5 matrix of 30 analogues—20 of which could be classified as bicyclic/*N*-substituted analogues. Of these 20 bicyclic/*N*-substituted analogues, 14 displayed partial or full MOR agonism and DOR antagonism. Based on the results of the study described in Chapter 3, the following observations were made:

1. Subnanomolar affinity at MOR and DOR can be consistently achieved via *N*-substitution.
2. The *N*-mesyl substitution has the most beneficial effect on functional profile, combining DOR antagonism with superior MOR potency and efficacy.
3. *N*-Acetyl and cyclopropyl acyl substitutions provide the best binding profiles (closest to 1:1 between MOR and DOR), but often elicit partial DOR agonism—especially with planar, fully aromatic pendants.
4. Heteroatoms distal to the THQ core are poorly tolerated at MOR (poor potency and efficacy).
5. The THIQ pendant is most effective at achieving the MOR agonist/DOR antagonist profile, but also displays high KOR affinity and sporadic KOR efficacy.
6. Bioavailability is unpredictable, though a ClogP < 3.5 is generally preferred.

The *in vitro* profiles achieved through the combination of C-6 and N-1 substitutions investigated in Chapter 3 are among the most favorable throughout the peptidomimetic series. These typically display less than 10-fold selectivity for MOR over DOR with subnanomolar affinity at both receptors. Additionally, specific motifs (THIQ, *N*-mesyl) could reliably produce the desired MOR agonist/DOR antagonist profile with subnanomolar potency at MOR. Furthermore, clear functional trends showed ways in which both MOR and DOR efficacy could be increased or attenuated. Some highlighted analogues featuring the bicyclic motif at C-6 are displayed in **Fig. 28**.

Figure 28. Bicyclic Leads Displaying MOR Agonism/DOR Antagonism with <10:1 MOR/DOR Selectivity & >10:1 MOR/KOR Selectivity^a



^a Analogues **43** and **59** synthesized by A.A.H. and D.J.M. respectively.

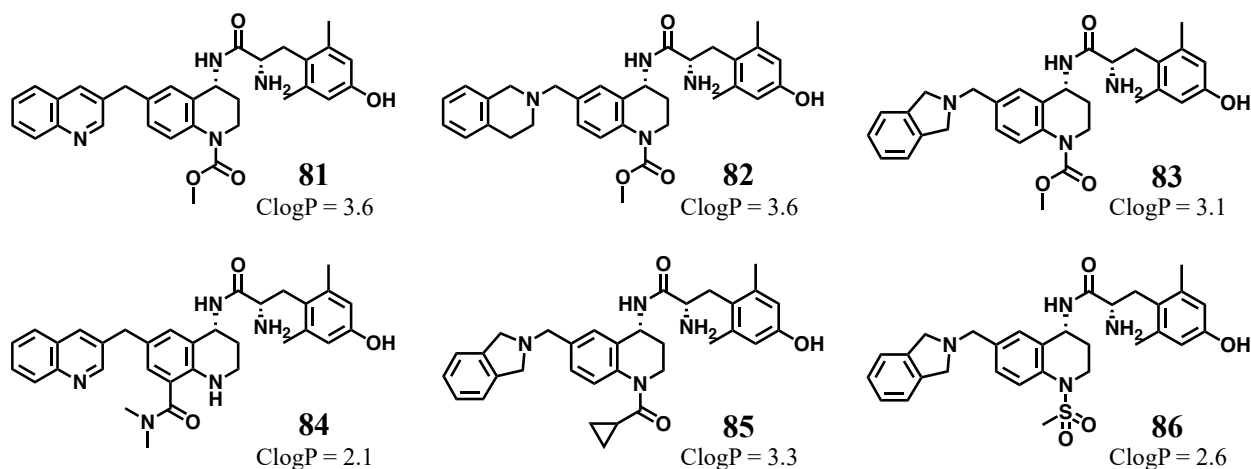
Fig. 28 includes six analogues that display the desired MOR agonist/DOR antagonist profile with less than 10-fold selectivity for MOR over DOR as well as 10-fold or more selectivity for MOR over KOR. Notably, analogue **70** does not incorporate an *N*-1 substitution but features an analogous carbonyl motif at the proximal C-8 position. Analogues **43**, **59**, and **56** all display full antinociceptive activity, but display at least one limiting characteristic. **43** and **59** both display a ClogP of 4.5 or greater, which is associated with poor aqueous solubility. Analogue **56** improves ClogP to 3.1, but shows a diminished duration of action of only 1.5 h. Furthermore, the binding profile of **56** is less optimal than most others included in **Fig. 28**, displaying approximately 10-fold selectivity for MOR over both DOR and KOR. Functionally, **56** is the most efficacious and potent at MOR, and displays a subnanomolar K_e at DOR, indicating high potency as an antagonist. Analogues in the bottom row display highly favorable *in vitro* profiles, but either have not yet been evaluated *in vivo* (**70**) or only show partial activity (**55** and **50**). These three analogues display greater than 90% efficacy at MOR and single-digit to sub-nanomolar potency paired with DOR antagonism. In terms of binding, all show 5:1 or less MOR selectivity over DOR, while **70** and **50** are both 200-fold selective over KOR. These analogues demonstrate the types of favorable *in vitro* profiles achieved through incorporation of bicyclic C-6 pendants in tandem with a carbonyl (or sulfonyl) motif at *N*-1 or C-8. As illustrated in **Fig. 28**, the specific chemical moieties can vary at both positions, however a general pattern of bicyclic C-6 pendant paired with a H-bond acceptor at the bottom face of the THQ core is consistent throughout all six analogues.

5.5 Future Directions of the Bicyclic C-6 Chemotype

Utilizing the insights obtained from the SAR study discussed in Chapter 3 and above, one can re-evaluate past analogues from the C-6 and *N*-1 series to guide future ligand design. Following the success that the THIQ pendant had offered (potent, high-efficacy MOR agonism and DOR

antagonism), an analogous pendant that may afford similar success is the isoindoline pendant shown in **Fig. 29** in analogues **83**, **85** and **86**. Removal of a single carbon is unlikely to drastically affect the pharmacological profile *in vitro*, however as has been demonstrated, even very subtle changes can have significant effects *in vivo*. As such, this pendant may be useful for replicating the *in vitro* profile attained by the THIQ pendant while also increasing bioavailability. Additionally, this pendant was selected for its low lipophilicity. As discussed, existent *in vivo* data indicate a preference for analogues with a ClogP of less than 3.5 (ideally 3.3 or less). Analogues **83**, **85**, and **86** all fit within that optimal window, offering the best opportunity for *in vivo* activity. These three analogues utilize *N*-1 substitutions including the previously unexplored methyl carbamate (**83**) as well as the cyclopropyl acyl moiety (**85**) that showed the greatest benefit in binding as well as the mesyl moiety (**86**) which demonstrated optimal functionality. Similar to **56**, one might predict that **86** will also display high KOR affinity due to the *N*-mesyl group as well as the basic amine at C-6. Nevertheless, synthesis and evaluation of **86** could confirm or aid in the refinement of *in vitro* SAR predictions.

Figure 29. Proposed Bicyclic Analogues **81-86**



The methyl carbamate moiety of **83** has been previously reported by A.A.H. and, in the context of the C-6 benzyl pendant (**33**), showed full antinociceptive activity *in vivo*.⁹⁵ In fact, it was additionally paired with two bicyclic pendants, the 2-naphthyl (**87**) and isoindanyl (**88**) pendants, shown in **Table 20** (all three of which were synthesized by A.A.H.). Unfortunately, the bicyclic analogues were both inactive *in vivo*.

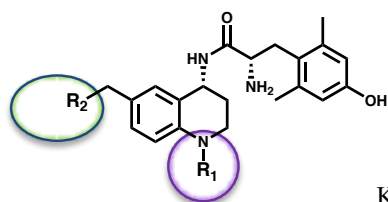


Table 20. *N*-1 Methyl Carbamate Leads **32**, **87**, & **88**, and Proposed C-6 Heterocyclic Analogues **81-83**^a

#	R ₂	R ₁	K _i (nM)			DOR K _i /MOR K _i	EC ₅₀ (nM)			% stim		
			MOR	DOR	KOR		MOR	DOR	KOR	MOR	DOR	KOR
33 ^b			0.19 (0.05)	0.51 (0.19)	29 (8)	3	0.78 (0.19)	14 (3)	250 (40)	95 (5)	40 (7)	28 (3)
87 ^b			0.32 (0.08)	0.46 [†] (0.08)	140 [†] (70)	2	0.39 (0.21)	dns [†]	dns [†]	106 (6)	dns [†]	dns [†]
88 ^b			0.10 (0.02)	0.32 (0.07)	7 [†] (3)	3	0.39 (0.05)	14 [†] (3)	170 [†] (40)	94 (8)	40 [†] (7)	26 [†] (3)
81			---	---	---	---	---	---	---	---	---	---
82			---	---	---	---	---	---	---	---	---	---
83			---	---	---	---	---	---	---	---	---	---

^a Binding affinities (K_i) were obtained by competitive displacement of radiolabeled [³H]-diprenorphine in membrane preparations. Functional data were obtained using agonist induced stimulation of [³⁵S]-GTPγS binding. Potency is represented as EC₅₀ (nM) and efficacy as percent maximal stimulation relative to standard agonist DAMGO (MOR), DPDPE (DOR), or U69,593 (KOR) at 10 μM. All values are expressed as the mean of three separate assays performed in duplicate with standard error of the mean in parentheses. dns = does not stimulate. ^b Synthesized by A.A.H.

The methyl carbamate is comparable in lipophilicity to the cyclopropyl acyl group discussed previously. As such, the bicyclic C-6 pendants proposed for analogues **81-83** are all heterocycles which, can negate some of the added lipophilicity. Analogues **81-83** range in lipophilicity between 3.1 and 3.6 as indicated in **Fig. 28**. These proposed compounds are predicted to display the

favorable profile of the leads **32**, **87**, and **88**, however one might expect **81** to display some DOR agonism, as the 3-quinolinyl pendant was often a partial DOR agonist when paired with the *N*-acetyl and *N*-cyclopropyl acyl moieties. Additionally, **87** shows some DOR agonism suggesting the methyl carbamate may display similar DOR-activating propensity to that of the cyclopropyl acyl motif.

The final analogue proposed in **Fig. 29**, **84**, also incorporates the 3-quinolinyl pendant. However, as observed with prior C-8 carbonyl analogues, it is predicted that the dimethyl amide motif would maintain the DOR antagonist profile. Analogue **84** is largely designed to mimic the 2-naphthyl analogue **70** which has shown promise *in vitro* but displays a ClogP of 3.7 which may be unfavorably high. The 3-quinolinyl analogue **84** displays a lower ClogP (2.1) comparable to that of the C-6 benzyl/C-8 dimethyl amide analogue **20** which previously showed full activity *in vivo*. Analogue **20** displayed a comparatively poor MOR potency of 9 nM, whereas the bicyclic analogue **70** was 5-fold more potent, with an EC₅₀ of 1.8 nM. It is predicted that this increase in potency associated with the bicyclic series would also translate to the 3-quinolinyl analogue **84**.

The proposed analogues above represent incremental changes upon a chemotype proven to display an optimal or near-optimal *in vitro* pharmacological profile. As highlighted in **Fig. 28**, analogues featuring a bicyclic C-6 pendant with a carbonyl moiety at the bottom face (*N*-1/C-8) of the THQ core typically show high-potency MOR agonism and DOR antagonism, though *in vivo* activity and duration of action are less predictable. Thus, the goal of the analogues proposed in **Fig. 29** is to achieve an optimal *in vitro* profile while targeting low (<3.5) ClogP. As the library of analogues displaying related but slightly modified structures and chemical properties expands, it may be possible to better predict which motifs will be favored and which are not. Four novel bicyclic analogues in Chapter 3 displayed full antinociceptive activity. Analogues **81-86** aim to

expand the number of bioavailable ligands so as to better understand correlations between structure, chemical properties, *in vivo* activity, and duration of action. The bicyclic analogues discussed thus far have shown promising result *in vitro* and may yet yield further analogues with *in vivo* profiles comparable to **43**. The data presented above and in the preceding chapters merit further research into compounds of the bicyclic/*N*-1 or bicyclic/*C*-8 carbonyl type.

5.6 Bicyclic C-6 Conclusions

The structural paradigm established by analogues **43** and **45** of two conjugated, aryl or semi-aryl rings at *C*-6 paired with an *N*-1 acetyl moiety has proven widely successful at achieving high affinity at MOR and DOR in tandem with potent, efficacious MOR agonism and DOR antagonism. Several analogues replicating this chemotype have demonstrated optimal or near-optimal *in vitro* profiles spanning a range of characteristics. Following this structural paradigm, efficacious have spanned the range of <10% to 114% at MOR and <10% to 84% at DOR. Furthermore, by strategically pairing sets of *C*-6 and *N*-1 motifs with one another in a 2D matrix setup, trends have emerged that facilitate the design of ligands with tailorable profiles including dual agonists, dual antagonists, and anywhere between. This capacity is instrumental in the continued evaluation of bifunctional opioid profiles and what impact those have *in vivo*. Presently, the duration of antinociceptive activity achieved by **43** and **45** is yet to be rivaled. However, the number of ligands achieving a full antinociceptive effect, albeit for a shorter duration, has increased from 2 to 6, with plans for further analogues detailed above. A reliable predictor of bioavailability based on *in vitro* pharmacology, structural traits, or physicochemical properties remains elusive. Yet, preliminary data within this series indicates low lipophilicity (ClogP < 3.5) is a fair correlate of bioavailability. Further investigation of this chemotype could yield novel analogues that reproduce the *in vitro* and *in vivo* success observed for **43** outlined in Chapter 4.

In addition to combining bicyclic C-6 pendants with *N*-acyl or *N*-sulfonyl motifs, the recent analogue **70** has demonstrated that the carbonyl moiety can effectively be translocated to C-8 (described in Chapter 2), replicating the *in vitro* profile achieved by **43**. Furthermore, by inversion of the tertiary amide moiety of **43** as in analogue **70**, lipophilicity is decreased considerably (ClogP of 4.3 for **43** is reduced to 3.7 for **70**). At present, analogue **70** is a prime candidate for evaluation *in vivo* for antinociception.

5.7 Concluding Remarks

As a result of the work presented here, the number of fully active *in vivo* candidates has been expanded by 11. Seven of the *in vivo* candidates come from the C-8 campaign described in Chapter 2 while four come from the bicyclic project of Chapter 3. It should be noted that credit for the synthesis of two of those bicyclic analogues (**59** and **60**) belongs to chemist D.J.M. who also contributed to the bicyclic project. These analogues cover a range of *in vitro* profiles. The further evaluation of said *in vivo* candidates for tolerance and dependence may aid in the identification of which pharmacological descriptors best predict reductions in tolerance, dependence, and CPP. This work additionally has yielded numerous compounds displaying optimal *in vitro* profiles—potent, efficacious MOR agonism and DOR antagonism with similar affinity at both receptors (and 100-fold selectivity over KOR). The SAR research described here has laid strong foundations for future development of analogues in both the C-8 and bicyclic series. It is now established that carbonyl C-8 moieties and sulfonyl *N*-1 motifs (when combined with bicyclic C-6 pendants) can reliably achieve the desired MOR agonist/DOR antagonist profile. Additionally, compounds of both types of shown robust antinociceptive activity after peripheral administration, suggesting both approaches are viable for the development of future analgesics.

Plans for the continued utilization of C-8, bicyclic C-6/N-1, and C-6/C-8 substitution patterns have been laid out in this chapter. C-8 may serve as a functional handle for radiolabeling and glucoserine conjugation, while proposed C-6/N-1 and C-6/C-8 analogues hold promise for further optimization of physicochemical properties as well as *in vitro* and *in vivo* pharmacology. The work presented here was made possible by foundational SAR work performed by chemists Larisa Yeomans, Aubrie Harland, and Aaron Bender. Should future chemists carry on in this field of research, it is hoped by this author that the work described herein will provide a similarly strong foundation for continued opioid drug discovery.

References

- (1) Merlin, M. D. Archaeological Evidence for the Tradition of Psychoactive Plant Use in the Old World. *Econ. Bot.* **2003**, *57* (3), 295–323.
- (2) Kunzig, R.; Tzar, J. La Marmotta. *Discov. Mag.* **2002**, *23* (11), 34–40.
- (3) Brownstein, M. J. A Brief History of Opiates, Opioid Peptides, and Opioid Receptors. *Proc. Natl. Acad. Sci. U. S. A.* **1993**, *90* (June), 5391–5393.
- (4) Krikorian, A. D. Were the Opium Poppy and Opium Known in the Ancient near East? *J. Hist. Biol.* **1975**, *8* (1), 95–114.
- (5) Kritikos, P. G.; Papadaki, S. P. The History of the Poppy and Opium and Their Expansion in Antiquity in the Eastern Mediterranean Area. *Bull. Narc.* **1967**, *19* (3).
- (6) Day, J. Botany Meets Archaeology: People and Plants in the Past. *J. Exp. Bot.* **2013**, *64* (18), 5805–5816.
- (7) Coxe, J. R. *The Writings of Hippocrates and Galen. Epitomised from the Original Latin Translations.*; Lindsay and Blakiston: Philadelphia, 1846.
- (8) Diniejko, A. Victorian Drug Use
<http://www.victorianweb.org/victorian/science/addiction/addiction2.html> (accessed Aug 15, 2018).
- (9) Foxcroft, L. *The Making of Addiction: The Use and Abuse of Opium in Nineteenth-Century Britain*; Ashgate Publishing, Ltd., 2007.
- (10) Klockgether-Radke, A. P. F. W. Sertürner und die Entdeckung des Morphins TT - F. W. Sertürner and the Discovery of Morphine. *Anästhesiol Intensivmed Notfallmed Schmerzther* **2002**, *37* (05), 244–249.
- (11) Hari, J. *Chasing the Scream : The First and Last Days of the War on Drugs*; Bloomsbury: New York, 2015.
- (12) Quinones, S. *Dreamland: The True Tale of America's Opiate Epidemic*; Bloomberg Press: New York, 2015.
- (13) Macy, B. *Dopesick: Doctors, Dealers, and the Drug Company That Addicted America*, First Edit.; Little, Brown and Company: New York, 2018.

- (14) Beckett, A. H.; Casy, A. F. Synthetic Analgesics: Stereochemical Considerations. *J. Pharm. Pharmacol.* **1954**, *6*, 986–999.
- (15) Portoghese, P. S. A New Concept on the Mode of Interaction of Narcotic Analgesics with Receptors. *J. Med. Chem.* **1965**, *8*, 609–616.
- (16) Snyder, S. H.; Pasternak, G. W. Historical Review: Opioid Receptors. *Trends Pharmacol. Sci.* **2003**, *24* (4), 198–205.
- (17) Pasternak, G. W.; Pan, Y.-X. Mu Opioids and Their Receptors: Evolution of a Concept. *Pharmacol. Rev.* **2013**, *65* (4), 1257–1317.
- (18) Pert, C. B.; Snyder, S. H. Opiate Receptor: Demonstration in Nervous Tissue. *Science* **1973**, *179* (4077), 1011–1014.
- (19) Terenius, L. Stereospecific Uptake of Narcotic Analgesics by a Subcellular Fraction of the Guinea-Pig Ileum: A Preliminary Communication. *Ups. J. Med. Sci.* **1973**, *78* (3), 150–152.
- (20) Appelgren, L.-E.; Terenius, L. Differences in the Autoradiographic Localization of Labelled Morphine-Like Analgesics in the Mouse. *Acta Physiol. Scand.* **1973**, *88* (2), 175–182.
- (21) Simon, E. J.; Hiller, J. M.; Edelman, I. Stereospecific Binding of the Potent Narcotic Analgesic [3H]Etorphine to Rat-Brain Homogenate. *Proc. Natl. Acad. Sci. U. S. A.* **1973**, *70* (7), 1947–1949.
- (22) Hughes, J.; Smith, T. W.; Kosterlitz, H. W.; Fothergill, L. A.; Morgan, B. A.; Morris, H. R. Identification of Two Related Pentapeptides from the Brain with Potent Opiate Agonist Activity. *Nature* **1975**, *258* (5536), 577–579.
- (23) Li, C. H.; Chung, D. Isolation and Structure of an Untriakontapeptide with Opiate Activity from Camel Pituitary Glands. *Proc. Natl. Acad. Sci.* **1976**, *73* (4), 1145–1148.
- (24) Thompson, R. C.; Mansour, A.; Watson, S. Cloning and Pharmacological Characterization of a Rat Mu Opioid Receptor. **1993**, *11*, 903–913.
- (25) Wang, J. I. A. B. E. I.; Imai, Y.; Epplert, C. M.; Gregor, P.; Spivak, C. E.; Uhl, G. R. Mu Opiate Receptor : CDNA Cloning and Expression. **1993**, *90* (November), 10230–10234.
- (26) Evans, C. J.; Keith, D. E.; Morrison, H.; Magendzo, K.; Evans, C. J.; Jr, D. E. K.; Morrison, H.; Magendzo, K.; Edwards, R. H. Cloning of a Delta Opioid Receptor by Functional Expression. *Science* (80-.). **1992**, *258* (5090), 1952–1955.
- (27) Kieffer, B. L.; Befort, K.; Gaveriaux-ruff, C.; Hirtht, C. G. The Delta Opioid Receptor : Isolation of a CDNA by Expression Cloning and Pharmacological Characterization. *Proc. Natl. Acad. Sci.* **1992**, *89*, 12048–12052.

- (28) Meng, F. A. N.; Xie, G.; Thompson, R. C.; Mansour, A.; Goldsteint, A.; Watson, S. J.; Akil, H. Cloning and Pharmacological Characterization of a Rat κ Opioid Receptor. **1993**, *90* (November), 9954–9958.
- (29) Li, S.; Zhu, J.; Chen, C.; Chen, Y.; Deriel, J. K.; Ashby, B. Molecular Cloning and Expression of a Rat κ Opioid Receptor. **1993**, *633*, 629–633.
- (30) Broom, D. C.; Nitsche, J. F.; Pintar, J. E.; Rice, K. C.; Woods, J. H.; Traynor, J. R. Comparison of Receptor Mechanisms and Efficacy Requirements for Delta-Agonist-Induced Convulsive Activity and Antinociception in Mice. *J. Pharmacol. Exp. Ther.* **2002**, *303* (2), 723–729.
- (31) Perrine, S. A.; Hoshaw, B. A.; Unterwald, E. M. Delta Opioid Receptor Ligands Modulate Anxiety-like Behaviors in the Rat. *Br. J. Pharmacol.* **2006**, *147* (8), 864–872.
- (32) Chu Sin Chung, P.; Boehrer, A.; Stephan, A.; Matifas, A.; Scherrer, G.; Darcq, E.; Befort, K.; Kieffer, B. L. Delta Opioid Receptors Expressed in Forebrain GABAergic Neurons Are Responsible for SNC80-Induced Seizures. *Behav. Brain Res.* **2015**, *278*, 429–434.
- (33) Schwarzer, C. 30 Years of Dynorphins - New Insights on Their Functions in Neuropsychiatric Diseases. *Pharmacol. Ther.* **2009**, *123* (3), 353–370.
- (34) Casselman, I.; Nock, C. J.; Wohlmuth, H.; Weatherby, R. P.; Heinrich, M. From Local to Global - Fifty Years of Research on *Salvia Divinorum*. *J. Ethnopharmacol.* **2014**, *151* (2), 768–783.
- (35) Valdés, L. J.; Díaz, J.; Paul, A. G. Ethnopharmacology of Ska María Pastora (*Salvia Divinorum*, Epling AND Játiva-M.). *J. Ethnopharmacol.* **1983**, *7* (3), 287–312.
- (36) Cui, X.; Yeliseev, A.; Liu, R. Ligand Interaction, Binding Site and G Protein Activation of the μ Opioid Receptor. *Eur. J. Pharmacol.* **2013**, *702* (1–3), 309–315.
- (37) Manglik, A.; Kruse, A. C.; Kobilka, T. S.; Thian, F. S.; Mathiesen, J. M.; Sunahara, R. K.; Pardo, L.; Weis, W. I.; Kobilka, B. K.; Granier, S. Crystal Structure of the μ -Opioid Receptor Bound to a Morphinan Antagonist. *Nature* **2012**, *485* (7398), 321–326.
- (38) Koehl, A.; Hu, H.; Maeda, S.; Zhang, Y.; Qu, Q.; Paggi, J. M.; Latorraca, N. R.; Hilger, D.; Dawson, R.; Matile, H.; Schertler, G. F. X.; Granier, S.; Weis, W. I.; Dror, R. O.; Manglik, A.; Skiniotis, G.; Kobilka, B. K. Structure of the μ -Opioid Receptor– G_i Protein Complex. *Nature* **2018**, *558* (7711), 547–552.
- (39) Sounier, R.; Mas, C.; Steyaert, J.; Laeremans, T.; Manglik, A.; Huang, W.; Kobilka, B. K.; Déméné, H.; Granier, S. Propagation of Conformational Changes during μ -Opioid Receptor Activation. *Nature* **2015**, *524*, 375–379.
- (40) Fenalti, G.; Giguere, P. M.; Katritch, V.; Huang, X.-P.; Thompson, A. a; Cherezov, V.; Roth, B. L.; Stevens, R. C. Molecular Control of Delta-Opioid Receptor Signalling. *Nature* **2014**, *506* (7487), 191–196.

- (41) Dror, R. O.; Arlow, D. H.; Maragakis, P.; Mildorf, T. J.; Pan, A. C.; Xu, H.; Borhani, D. W.; Shaw, D. E. Activation Mechanism of the B2 -Adrenergic Receptor. *Proc. Natl. Acad. Sci. USA* **2011**, *108* (46), 18684–18689.
- (42) Nygaard, R.; Zou, Y.; Dror, R. O.; Mildorf, T. J.; Arlow, D. H.; Manglik, A.; Pan, A. C.; Liu, C. W.; Fung, J. J.; Bokoch, M. P.; Thian, F. S.; Kobilka, T. S.; Shaw, D. E.; Mueller, L.; Prosser, R. S.; Kobilka, B. K. The Dynamic Process of B2-Adrenergic Receptor Activation. *Cell* **2013**, *152* (3), 532–542.
- (43) Latorraca, N. R.; Venkatakrishnan, A. J.; Dror, R. O. GPCR Dynamics: Structures in Motion. *Chem. Rev.* **2017**, *117* (1), 139–155.
- (44) Huang, W.; Manglik, A.; Venkatakrishnan, A. J.; Laeremans, T.; Feinberg, E. N.; Sanborn, A. L.; Kato, H. E.; Livingston, K. E.; Thorsen, T. S.; Kling, R. C.; Granier, S.; Gmeiner, P.; Husbands, S. M.; Traynor, J. R.; Weis, W. I.; Steyaert, J.; Dror, R. O.; Kobilka, B. K. Structural Insights into μ -Opioid Receptor Activation. *Nature* **2015**, *524* (7565), 315–321.
- (45) Manglik, A.; Kim, T. H.; Masureel, M.; Altenbach, C.; Yang, Z.; Hilger, D.; Lerch, M. T.; Kobilka, T. S.; Thian, F. S.; Hubbell, W. L.; Prosser, R. S.; Kobilka, B. K. Structural Insights into the Dynamic Process of B2-Adrenergic Receptor Signaling. *Cell* **2015**, *161* (5), 1101–1111.
- (46) Huang, W.; Manglik, A.; Venkatakrishnan, a J.; Laeremans, T.; Feinberg, E. N.; Sanborn, A. L.; Kato, H. E.; Livingston, K. E.; Thorsen, T. S.; Kling, R. C.; Granier, S.; Gmeiner, P.; Husbands, S. M.; Traynor, J. R.; Weis, W. I.; Steyaert, J.; Dror, R. O.; Kobilka, B. K. Structural Insights into Mu-Opioid Receptor Activation. *Nature* **2015**, *524* (7565), 315–321.
- (47) Venkatakrishnan, A. J.; Ma, A. K.; Fonseca, R.; Latorraca, N. R.; Kelly, B.; Betz, R. M.; Asawa, C.; Kobilka, B. K.; Dror, R. O. *Stable Networks of Water-Mediated Interactions Are Conserved in Activation of Diverse GPCRs*; unpublished work accessed 08/28/2018.
- (48) Mason, J. S.; Bortolato, A.; Weiss, D. R.; Deflorian, F.; Tehan, B.; Marshall, F. H. High End GPCR Design: Crafted Ligand Design and Druggability Analysis Using Protein Structure, Lipophilic Hotspots and Explicit Water Networks. *Silico Pharmacol.* **2013**, *1* (23).
- (49) Blankenship, E.; Vahedi-Faridi, A.; Lodowski, D. T. The High-Resolution Structure of Activated Opsin Reveals a Conserved Solvent Network in the Transmembrane Region Essential for Activation. *Structure* **2015**, *23* (12), 2358–2364.
- (50) Breiten, B.; Lockett, M. R.; Sherman, W.; Fujita, S.; Al-Sayah, M.; Lange, H.; Bowers, C. M.; Heroux, A.; Krilov, G.; Whitesides, G. M. Water Networks Contribute to Enthalpy/Entropy Compensation in Protein-Ligand Binding. *J. Am. Chem. Soc.* **2013**, *135* (41), 15579–15584.
- (51) Bortolato, A.; Tehan, B. G.; Bodnarchuk, M. S.; Essex, J. W.; Mason, J. S. Water

- Network Perturbation in Ligand Binding: Adenosine A2A Antagonists as a Case Study. *J. Chem. Inf. Model.* **2013**, *53* (7), 1700–1713.
- (52) Yuan, S.; Palczewski, K.; Peng, Q.; Kolinski, M.; Vogel, H.; Filipek, S. The Mechanism of Ligand-Induced Activation or Inhibition of μ - And κ -Opioid Receptors. *Angew. Chemie - Int. Ed.* **2015**, *54* (26), 7560–7563.
- (53) Yuan, S.; Filipek, S.; Palczewski, K.; Vogel, H. Activation of G-Protein-Coupled Receptors Correlates with the Formation of a Continuous Internal Water Pathway. *Nat. Commun.* **2014**, *5* (May), 1–10.
- (54) Liu, W.; Chun, E.; Thompson, A. A.; Chubukov, P.; Xu, F.; Han, G. W.; Roth, C. B.; Heitman, L. H.; Ijzerman, A. P.; Cherezov, V.; Stevens, R. C. Structural Basis for Allosteric Regulation of GPCRs by Sodium Ions. *Science (80-)*. **2013**, *337* (6091), 232–236.
- (55) Mahoney, J. P.; Sunahara, R. K. Mechanistic Insights into GPCR–G Protein Interactions. *Curr. Opin. Struct. Biol.* **2016**, *41*, 247–254.
- (56) Al-Hasani, R.; Bruchas, M. R. Molecular Mechanisms of Opioid Receptor-Dependent Signaling and Behavior. *Anesthesiology* **2011**, *115* (6), 1.
- (57) Neer, E. J. Heterotrimeric G Proteins: Organizers of Transmembrane Signals. *Cell* **1995**, *80* (2), 249–257.
- (58) Wimpey, T. L.; Chavkin, C. Opioids Activate Both an Inward Rectifier and a Novel Voltage-Gated Potassium Conductance in the Hippocampal Formation. *Neuron* **1991**, *6* (2), 281–289.
- (59) Nagi, K.; Pineyro, G. Kir3 Channel Signaling Complexes: Focus on Opioid Receptor Signaling. *Front. Cell. Neurosci.* **2014**, *8* (July), 1–15.
- (60) Fujita, W.; Gomes, I.; Devi, L. A. Revolution in GPCR Signalling: Opioid Receptor Heteromers as Novel Therapeutic Targets: IUPHAR Review 10. *Br. J. Pharmacol.* **2014**, *171* (18), 4155–4176.
- (61) Jiang, Q.; Mosberg, H. I.; Porreca, F. Selective Modulation of Morphine Antinociception, but Not Development of Tolerance, by Delta Receptor Agonists. *Eur. J. Pharmacol.* **1990**, *186* (1), 137–141.
- (62) Heyman, J. S.; Jiang, Q.; Rothman, R. B.; Mosberg, H. I.; Porreca, F. Modulation of Mu-Mediated Antinociception by Delta Agonists: Characterization with Antagonists. *Eur J Pharmacol* **1989**, *169* (1), 43–52.
- (63) Porreca, F.; Takemori, A. E.; Sultana, M.; Portoghese, P. S.; Bowen, W. D.; Mosberg, H. I. Modulation of Mu-Mediated Antinociception in the Mouse Involves Opioid Delta-2 Receptors. *J. Pharmacol. Exp. Ther.* **1992**, *263* (1), 147–152.

- (64) Abdelhamid, E. E.; Sultana, M.; Portoghese, P. S.; Takemori, A. E. Selective Blockage of Delta Opioid Receptors Prevents the Development of Morphine Tolerance and Dependence in Mice. *J. Pharmacol. Exp. Ther.* **1991**, *258* (1), 299–303.
- (65) Hepburn, M. J.; Little, P. J.; Gingras, J.; Kuhn, C. M. Differential Effects of Naltrindole on Morphine-Induced Tolerance and Physical Dependence in Rats. *J. Pharmacol. Exp. Ther.* **1997**, *281* (3), 1350–1356.
- (66) Zhu, Y.; King, M. a.; Schuller, A. G. P.; Nitsche, J. F.; Reidl, M.; Elde, R. P.; Unterwald, E.; Pasternak, G. W.; Pintar, J. E. Retention of Supraspinal Delta-like Analgesia and Loss of Morphine Tolerance in δ Opioid Receptor Knockout Mice. *Neuron* **1999**, *24* (1), 243–252.
- (67) Kest, B.; Lee, C. E.; McLemore, G. L.; Inturrisi, C. E. An Antisense Oligodeoxynucleotide to the Delta Opioid Receptor (DOR-1) Inhibits Morphine Tolerance and Acute Dependence in Mice. *Brain Res. Bull.* **1996**, *39* (3), 185–188.
- (68) Wells, J. L.; Bartlett, J. L.; Ananthan, S.; Bilsky, E. J. In Vivo Pharmacological Characterization of SoRI 9409, a Nonpeptidic Opioid Mu-Agonist/Delta-Antagonist That Produces Limited Antinociceptive Tolerance and Attenuates Morphine Physical Dependence. *J. Pharmacol. Exp. Ther.* **2001**, *297* (2), 597–605.
- (69) Ananthan, S.; Khare, N. K.; Saini, S. K.; Seitz, L. E.; Bartlett, J. L.; Davis, P.; Dersch, C. M.; Porreca, F.; Rothman, R. B.; Bilsky, E. J. Identification of Opioid Ligands Possessing Mixed μ Agonist / δ Antagonist Activity among Pyridomorphinans Derived from Naloxone , Oxymorphone , and Hydromorphone. *J. Med. Chem.* **2003**, *47*, 1400–1412.
- (70) Ananthan, S.; Kezar, H. S.; Carter, R. L.; Saini, S. K.; Rice, K. C.; Wells, J. L.; Davis, P.; Xu, H.; Dersch, C. M.; Bilsky, E. J.; Porreca, F.; Rothman, R. B. Synthesis, Opioid Receptor Binding, and Biological Activities of Naltrexone-Derived Pyrido- and Pyrimidomorphinans. *J. Med. Chem.* **1999**, *42* (18), 3527–3538.
- (71) Ananthan, S. Opioid Ligands With Mixed Mu / Delta Opioid Receptor Interactions : An Emerging Approach to Novel Analgesics. *AAPS J.* **2006**, *8* (1), 118–125.
- (72) Deekonda, S.; Wugalter, L.; Rankin, D.; Largent-Milnes, T. M.; Davis, P.; Wang, Y.; Bassirirad, N. M.; Lai, J.; Kulkarni, V.; Vanderah, T. W.; Porreca, F.; Hruby, V. J. Design and Synthesis of Novel Bivalent Ligands (MOR and DOR) by Conjugation of Enkephalin Analogues with 4-Anilidopiperidine Derivatives. *Bioorganic Med. Chem. Lett.* **2015**, *25* (20), 4683–4688.
- (73) Lenard, N. R.; Daniels, D. J.; Portoghese, P. S.; Roerig, S. C. Absence of Conditioned Place Preference or Reinstatement with Bivalent Ligands Containing Mu-Opioid Receptor Agonist and Delta-Opioid Receptor Antagonist Pharmacophores. *Eur. J. Pharmacol.* **2007**, *566* (1–3), 75–82.
- (74) Aceto, M. D.; Harris, L. S.; Negus, S. S.; Banks, M. L.; Hughes, L. D.; Akgün, E.; Portoghese, P. S. MDAN-21: A Bivalent Opioid Ligand Containing Mu-Agonist and

- Delta-Antagonist Pharmacophores and Its Effects in Rhesus Monkeys. *Int. J. Med. Chem.* **2012**, *2012*, 1–6.
- (75) Daniels, D. J.; Lenard, N. R.; Etienne, C. L.; Law, P.-Y.; Roerig, S. C.; Portoghese, P. S. Opioid-Induced Tolerance and Dependence in Mice Is Modulated by the Distance between Pharmacophores in a Bivalent Ligand Series. *Proc. Natl. Acad. Sci. U. S. A.* **2005**, *102* (52), 19208–19213.
- (76) Gomes, I.; Fujita, W.; Gupta, A.; Saldanha, S. A.; Negri, A.; Pinello, C. E.; Eberhart, C.; Roberts, E.; Filizola, M.; Hodder, P.; Devi, L. A. Identification of a Mu-Delta Opioid Receptor Heteromer-Biased Agonist with Antinociceptive Activity. *Proc. Natl. Acad. Sci.* **2013**, *110* (29), 12072–12077.
- (77) Schiller, P. W.; Fundytus, M. E.; Merovitz, L.; Weltrowska, G.; Nguyen, T. M.; Lemieux, C.; Chung, N. N.; Coderre, T. J. The Opioid Mu Agonist/Delta Antagonist DIPP-NH(2)[Psi] Produces a Potent Analgesic Effect, No Physical Dependence, and Less Tolerance than Morphine in Rats. *J. Med. Chem.* **1999**, *42* (18), 3520–3526.
- (78) Schiller, P. W. Bi- or Multifunctional Opioid Peptide Drugs. *Life Sci.* **2010**, *86* (15–16), 598–603.
- (79) Salvadori, S.; Trapella, C.; Fiorini, S.; Negri, L.; Lattanzi, R.; Bryant, S. D.; Jinsmaa, Y.; Lazarus, L. H.; Balboni, G. A New Opioid Designed Multiple Ligand Derived from the μ Opioid Agonist Endomorphin-2 and the δ Opioid Antagonist Pharmacophore Dmt-Tic. *Bioorganic Med. Chem.* **2007**, *15* (22), 6876–6881.
- (80) Bender, A. M.; Clark, M. J.; Agius, M. P.; Traynor, J. R.; Mosberg, H. I. Synthesis and Evaluation of 4-Substituted Piperidines and Piperazines as Balanced Affinity μ Opioid Receptor (MOR) Agonist/ δ Opioid Receptor (DOR) Antagonist Ligands. *Bioorganic Med. Chem. Lett.* **2014**, *24* (2), 548–551.
- (81) Turnaturi, R.; Aricò, G.; Ronsisvalle, G.; Parenti, C.; Pasquinucci, L. Multitarget Opioid Ligands in Pain Relief: New Players in an Old Game. *Eur. J. Med. Chem.* **2016**, *108*, 211–228.
- (82) Mosberg, H. I.; Yeomans, L.; Anand, J. P.; Porter, V.; Sobczyk-Kojiro, K.; Traynor, J. R.; Jutkiewicz, E. M. Development of a Bioavailable μ Opioid Receptor (MOPr) Agonist, δ Opioid Receptor (DOPr) Antagonist Peptide That Evokes Antinociception Without Development of Acute Tolerance. *J. Med. Chem.* **2014**, *57* (7), 3148–3153.
- (83) Mosberg, H. I.; Yeomans, L.; Harland, A. a.; Bender, A. M.; Sobczyk-Kojiro, K.; Anand, J. P.; Clark, M. J.; Jutkiewicz, E. M.; Traynor, J. R. Opioid Peptidomimetics: Leads for the Design of Bioavailable Mixed Efficacy μ Opioid Receptor (MOR) Agonist/ δ Opioid Receptor (DOR) Antagonist Ligands. *J. Med. Chem.* **2013**, *56* (5), 2139–2149.
- (84) Purington, L. C.; Pogozeva, I. D.; Traynor, J. R.; Mosberg, H. I. Pentapeptides Displaying Mu Opioid Receptor Agonist and Delta Opioid Receptor Partial Agonist/Antagonist Properties. *J. Med. Chem.* **2009**, *52* (23), 7724–7731.

- (85) Purington, L. C.; Sobczyk-Kojiro, K.; Pogozheva, I. D.; Traynor, J. R.; Mosberg, H. I. Development and in Vitro Characterization of a Novel Bifunctional μ -Agonist/ δ -Antagonist Opioid Tetrapeptide. *ACS Chem. Biol.* **2011**, *6* (12), 1375–1381.
- (86) Harvey, J. H.; Long, D. H.; England, P. M.; Whistler, J. L. Tuned-Affinity Bivalent Ligands for the Characterization of Opioid Receptor Heteromers. *ACS Med. Chem. Lett.* **2012**, *3* (8), 640–644.
- (87) Dietis, N.; Guerrini, R.; Calo, G.; Salvadori, S.; Rowbotham, D. J.; Lambert, D. G. Simultaneous Targeting of Multiple Opioid Receptors: A Strategy to Improve Side-Effect Profile. *Br. J. Anaesth.* **2009**, *103* (1), 38–49.
- (88) Pasternak, G. W.; Pan, Y. X. Mix and Match: Heterodimers and Opioid Tolerance. *Neuron* **2011**, *69* (1), 6–8.
- (89) Anand, J. P.; Purington, L. C.; Pogozheva, I. D.; Traynor, J. R.; Mosberg, H. I. Modulation of Opioid Receptor Ligand Affinity and Efficacy Using Active and Inactive State Receptor Models. *Chem. Biol. Drug Des.* **2012**, *80* (5), 763–770.
- (90) Mosberg, H. I.; Omnaas, J. R.; Medzlhadrsky, F.; Smith, C. B. Cyclic, Disulfide- and Dithioether-Containing Opioid Tetrapeptides: Development of a Ligand with High Delta Opioid Receptor Selectivity and Affinity. **1988**, *43* (1), 1013–1020.
- (91) Anand, J. P.; Boyer, B. T.; Mosberg, H. I.; Jutkiewicz, E. M. The Behavioral Effects of a Mixed Efficacy Antinociceptive Peptide, VRP26, Following Chronic Administration in Mice. *Psychopharmacology (Berl)*. **2016**, *233* (13), 2479–2487.
- (92) Mosberg, H. I.; Montgomery, D.; Bender, A.; Nastase, A.; Henry, S.; Harland, A. Peptidomimetics and Methods of Using the Same. US2018/0072677 A1, 2018.
- (93) Wang, C.; McFayden, I.; Traynor, J. R.; Mosberg, H. I. Design of a High Affinity Peptidomimetic Opioid Agonist from Peptide Pharmacophore Models. *Bioorganic Med. Chem. Lett.* **1998**, *8*, 2685–2688.
- (94) Harland, A. A.; Yeomans, L.; Griggs, N. W.; Anand, J. P.; Pogozheva, I. D.; Jutkiewicz, E. M.; Traynor, J. R.; Mosberg, H. I. Further Optimization and Evaluation of Bioavailable, Mixed-Efficacy Mu-Opioid Receptor (MOR) Agonists/Delta-Opioid Receptor (DOR) Antagonists: Balancing MOR and DOR Affinities. *J. Med. Chem.* **2015**, *58* (22), 8952–8969.
- (95) Harland, A. A.; Bender, A. M.; Griggs, N. W.; Gao, C.; Anand, J. P.; Pogozheva, I. D.; Traynor, J. R.; Jutkiewicz, E. M.; Mosberg, H. I. Effects of N-Substitutions on the Tetrahydroquinoline (THQ) Core of Mixed-Efficacy μ -Opioid Receptor (MOR)/ δ -Opioid Receptor (DOR) Ligands. *J. Med. Chem.* **2016**, *59* (10), 4985–4998.
- (96) Nastase, A. F.; Griggs, N. W.; Anand, J. P.; Fernandez, T. J.; Harland, A. A.; Trask, T. J.; Jutkiewicz, E. M.; Traynor, J. R.; Mosberg, H. I. Synthesis and Pharmacological Evaluation of Novel C - 8 Substituted Tetrahydroquinolines as Balanced-Affinity

- Mu/Delta Opioid Ligands for the Treatment of Pain. *ACS Chem. Neurosci.* **2018**.
- (97) Bender, A. M.; Griggs, N. W.; Gao, C.; Trask, T. J.; Traynor, J. R.; Mosberg, H. I. Rapid Synthesis of Boc-2',6'-Dimethyl-L-Tyrosine and Derivatives and Incorporation into Opioid Peptidomimetics. *ACS Med. Chem. Lett.* **2015**, *6*, 1199–1203.
- (98) Anand, J. P.; Kochan, K. E.; Nastase, A. F.; Montgomery, D.; Griggs, N. W.; Traynor, J. R.; Mosberg, H. I.; Jutkiewicz, E. M. In Vivo Effects of μ Opioid Receptor Agonist/ δ Opioid Receptor Antagonist Peptidomimetics Following Acute and Repeated Administration. *Br. J. Pharmacol.* **2018**.
- (99) Bender, A. M.; Griggs, N. W.; Anand, J. P.; Traynor, J. R.; Jutkiewicz, E. M.; Mosberg, H. I. Asymmetric Synthesis and in Vitro and in Vivo Activity of Tetrahydroquinolines Featuring a Diverse Set of Polar Substitutions at the 6 Position as Mixed-Efficacy μ Opioid Receptor/ δ Opioid Receptor Ligands. *ACS Chem. Neurosci.* **2015**, *6*, 1428–1435.
- (100) Harland, A. A.; Pogozheva, I. D.; Griggs, N. W.; Trask, T. J.; Traynor, J. R.; Mosberg, H. I. Placement of Hydroxy Moiety on Pendant of Peptidomimetic Scaffold Modulates Mu and Kappa Opioid Receptor Efficacy. *ACS Chem. Neurosci.* **2017**, *8* (11), 2549–2557.
- (101) Hansen, D. W. J.; Mazur, R. H.; Clare, M. Peptides: Structure and Function. In *Proceedings of the 9th American Peptide Symposium*; Deber, C. M., Hruby, V. J., Kopple, K. D., Eds.; Pierce Chem. Co.: Rockford, IL: Toronto, 1985; p 491.
- (102) Lazarus, L. H.; Bryant, S. D.; Salvadori, S.; Geurrini, R.; Balboni, G.; Tsuda, Y.; Okada, Y. Dimethyltyrosine, the Viagra of Opioids. *Chem. Res. Chinese U.* **2006**, *22* (2), 258–262.
- (103) Balboni, G.; Marzola, E.; Sasaki, Y.; Ambo, A.; Marczak, E. D.; Lazarus, L. H.; Salvadori, S. Role of 2',6'-Dimethyl-L-Tyrosine (Dmt) in Some Opioid Lead Compounds. *Bioorganic Med. Chem.* **2010**, *18* (16), 6024–6030.
- (104) Manhas, M. S.; Jeng, S. J. Cyclization of Omega-Haloamides to Lactams. *J. Org. Chem.* **1967**, *32* (9), 1246–1248.
- (105) Anderson, K. W.; Tepe, J. J. Trifluoromethanesulfonic Acid Catalyzed Friedel-Crafts Acylation of Aromatics with beta-Lactams. *Tetrahedron* **2002**, *58* (42), 8475–8481.
- (106) Granier, S.; Manglik, A.; Kruse, A. C.; Kobilka, T. S.; Thian, F. S.; Weis, W. I.; Kobilka, B. K. Structure of the δ -Opioid Receptor Bound to Naltrindole. *Nature* **2012**, *485* (7398), 400–404.
- (107) Pettinger, J.; Jones, K.; Cheeseman, M. D. Lysine-Targeting Covalent Inhibitors. *Angew. Chemie - Int. Ed.* **2017**, *56* (48), 15200–15209.
- (108) Zeiadeh, I.; Najjar, A.; Karaman, R. Strategies for Enhancing the Permeation of CNS-Active Drugs through the Blood-Brain Barrier: A Review. *Molecules* **2018**, *23* (6).

- (109) Salameh, T. S.; Banks, W. A. *Delivery of Therapeutic Peptides and Proteins to the CNS*, 1st ed.; Elsevier Inc., 2014; Vol. 71.
- (110) Pardridge, W. M. Drug Transport across the Blood-Brain Barrier. *J. Cereb. Blood Flow Metab.* **2012**, *32* (11), 1959–1972.
- (111) Li, Y.; Lefever, M. R.; Muthu, D.; Bidlack, J. M.; Bilsky, E. J.; Polt, R. Opioid Glycopeptide Analgesics Derived from Endogenous Enkephalins and Endorphins. *Future Med. Chem.* **2012**, *4* (2), 205–226.
- (112) Lowery, J. J.; Raymond, T. J.; Giuvelis, D.; Bidlack, J. M.; Polt, R.; Bilsky, E. J. In Vivo Characterization of MMP-2200, a Mixed Delta/Mu Opioid Agonist, in Mice. **2011**, *336* (3), 767–778.
- (113) Polt, R.; Dhanasekaran, M.; Keyari, C. M. Glycosylated Neuropeptides: A New Vista for Neuropsychopharmacology? *Med. Res. Rev.* **2005**, *25* (5), 557–585.
- (114) Traynor, J. R.; Nahorski, S. R. Modulation by Mu-Opioid Agonists of Guanosine-5'-O-(3-[35S]Thio)Triphosphate Binding to Membranes from Human Neuroblastoma SH-SY5Y Cells. *Mol. Pharmacol.* **1995**, *47* (4), 848–854.
- (115) Liu, G.; Cogan, D. A.; Ellman, J. A. Catalytic Asymmetric Synthesis of Tert - Butanesulfinamide . Application to the Asymmetric Synthesis of Amines. *J. Am. Chem. Soc.* **1997**, *119*, 9913–9914.
- (116) Ellman, J. A. Applications of Tert-Butanesulfinamide in the Asymmetric Synthesis of Amines. *Pure Appl. Chem.* **2003**, *75* (1), 39–46.
- (117) Guan, X. Y. 2-Methyl-2-Propanesulfinamide (Ellmans Sulfinamide): A Versatile Chiral Reagent. *Synlett* **2010**, No. 3, 503–504.
- (118) Hansen, D. W.; Stapelfeld, A.; Savage, M. A.; Reichman, M.; Hammond, D. L.; Haaseth, R. C.; Mosberg, H. I. Systemic Analgesic Activity and Delta-Opioid Selectivity in [2,6-Dimethyl-Tyr1,D-Pen2,D-Pen5]Enkephalin. *J. Med. Chem.* **1992**, *35*, 684–687.
- (119) Stevenson, G. W.; Folk, J. E.; Linsenmayer, D. C.; Rice, K. C.; Negus, S. S. Opioid Interactions in Rhesus Monkeys : Effects of Delta + Mu and Delta + Kappa Agonists on Schedule-Controlled Responding and Thermal Nociception. **2003**, *307* (3), 1054–1064.
- (120) Bice, A. N.; Wagner, H. N.; Frost, J. J.; Natarajan, T. K.; Lee, M. C.; Wong, D. F.; Dannals, R. F.; Ravert, H. T.; Wilson, A. A.; Links, J. M. Simplified Detection System for Neuroreceptor Studies in the Human Brain. *J. Nucl. Med.* **1986**, *27*, 184–191.
- (121) Wagner, H. N. Radiolabeled Drugs as Probes of Central Nervous System Neurons. *Clin. Chem.* **1985**, *31* (9), 1521–1524.
- (122) Nascimento, T. D.; DosSantos, M. F.; Lucas, S.; van Holsbeeck, H.; DeBoer, M.; Maslowski, E.; Love, T.; Martikainen, I. K.; Koeppe, R. A.; Smith, Y. R.; Zubieta, J. K.;

- DaSilva, A. F. μ -Opioid Activation in the Midbrain during Migraine Allodynia – Brief Report II. *Ann. Clin. Transl. Neurol.* **2014**, *1* (6), 445–450.
- (123) Eriksson, O.; Antoni, G. [11C]Carfentanil Binds Preferentially to μ -Opioid Receptor Subtype 1 Compared to Subtype 2. *Mol. Imaging* **2015**, *14* (8), 476–483.
- (124) Dannals, R. F.; Ravert, H. T.; Frost, J. J.; Wilson, A. A.; Burns, H. D.; Wagner, H. N. Radiosynthesis of an Opiate Receptor Binding Radiotracer: [11C]Carfentanil. *Int. J. Appl. Radiat. Isot.* **1985**, *36* (4), 303–306.
- (125) Sadzot, B.; Mayberg, H. S.; Frost, J. J. Imaging Opiate Receptors in the Human Brain with Positron Emission Tomography. Potential Applications for Drug Addiction Research. *Acta psychiatrica Belgica*. 1990, pp 9–19.
- (126) Saji, H.; Tsutsumi, D.; Magata, Y.; Iida, Y.; Konishi, J.; Yokoyama, A. Preparation and Biodistribution in Mice of [11C]Carfentanil: A Radiopharmaceutical for Studying Brain μ -Opioid Receptors by Positron Emission Tomography. *Ann. Nucl. Med.* **1992**, *6* (1), 63–67.
- (127) Endres, C. J.; Bencherif, B.; Hilton, J.; Madar, I.; Frost, J. J. Quantification of Brain μ -Opioid Receptors with [11C]Carfentanil: Reference-Tissue Methods. *Nucl. Med. Biol.* **2003**, *30* (2), 177–186.
- (128) Hirvonen, J.; Aalto, S.; Hagelberg, N.; Maksimow, A.; Ingman, K.; Oikonen, V.; Virkkala, J.; Någren, K.; Scheinin, H. Measurement of Central μ -Opioid Receptor Binding in Vivo with PET and [11C]Carfentanil: A Test-Retest Study in Healthy Subjects. *Eur. J. Nucl. Med. Mol. Imaging* **2009**, *36* (2), 275–286.
- (129) Mick, I.; Myers, J.; Stokes, P. R. A.; Erritzoe, D.; Colasanti, A.; Bowden-Jones, H.; Clark, L.; Gunn, R. N.; Rabiner, E. A.; Searle, G. E.; Waldman, A. D.; Parkin, M. C.; Brailsford, A. D.; Nutt, D. J.; Lingford-Hughes, A. R. Amphetamine Induced Endogenous Opioid Release in the Human Brain Detected with [¹¹C]Carfentanil PET: Replication in an Independent Cohort. *Int. J. Neuropsychopharmacol.* **2014**, *17* (12), 2069–2074.
- (130) Quelch, D. R.; Katsouri, L.; Nutt, D. J.; Parker, C. A.; Tyacke, R. J. Imaging Endogenous Opioid Peptide Release with [11C]Carfentanil and [³H]Diprenorphine: Influence of Agonist-Induced Internalization. *J. Cereb. Blood Flow Metab.* **2014**, *34* (10), 1604–1612.
- (131) DaSilva, A. F.; Nascimento, T. D.; DosSantos, M. F.; Lucas, S.; van Holsbeeck, H.; DeBoer, M.; Maslowski, E.; Love, T.; Martikainen, I. K.; Koeppe, R. A.; Smith, Y. R.; Zubieta, J. K. μ -Opioid Activation in the Prefrontal Cortex in Migraine Attacks – Brief Report I. *Ann. Clin. Transl. Neurol.* **2014**, *1* (6), 439–444.
- (132) Shao, X.; Kilbourn, M. R. A Simple Modification of GE Tracerlab FX C Pro for Rapid Sequential Preparation of [11C]Carfentanil and [11C]Raclopride. *Appl. Radiat. Isot.* **2009**, *67* (4), 602–605.
- (133) Blecha, J. E.; Henderson, B. D.; Hockley, B. G.; VanBrocklin, H. F.; Zubieta, J.-K.;

- DaSilva, A. F.; Kilbourn, M. R.; Koeppe, R. A.; Scott, P. J. H.; Shao, X. An Updated Synthesis of [¹¹C]Carfentanil for Positron Emission Tomography (PET) Imaging of the μ -Opioid Receptor. *J. Label. Compd. Radiopharm.* **2017**, *60* (8), 375–380.
- (134) Saccone, P. A.; Lindsey, A. M.; Koeppe, R. A.; Zelenock, K. A.; Shao, X.; Sherman, P.; Quesada, C. A.; Woods, J. H.; Scott, P. J. H. Intranasal Opioid Administration in Rhesus Monkeys: PET Imaging and Antinociception. *J. Pharmacol. Exp. Ther.* **2016**, *359* (2), 366–373.